

Instrumental Methods for the Analysis and Identification of Bioactive Molecules

ACS SYMPOSIUM SERIES **1185**

**Instrumental Methods for the
Analysis and Identification of
Bioactive Molecules**

Guddarangavvanahally K. Jayprakash, Editor

*Texas A&M University
College Station, Texas*

Bhimanagouda S. Patil, Editor

*Texas A&M University
College Station, Texas*

Federica Pellati, Editor

*University of Modena and Reggio Emilia
Modena, Italy*

**Sponsored by the
ACS Division of Agricultural and Food Chemistry, Inc.**



American Chemical Society, Washington, DC

Distributed in print by Oxford University Press



Library of Congress Cataloging-in-Publication Data

Instrumental methods for the analysis and identification of bioactive molecules /
Guddadarangavvanahally K. Jayprakasha, editor, Bhimanagouda S. Patil, editor, Federica
Pellati, editor ; sponsored by the ACS Division of Agricultural and Food Chemistry, Inc.

p. ; cm. -- (ACS symposium series ; 1185)

Includes bibliographical references and index.

ISBN 978-0-8412-2976-1 (alk. paper)

I. Jayprakasha, Guddadarangavvanahally K., editor. II. Patil, Bhimanagouda S., 1962-
editor. III. Pellati, Federica, editor. IV. American Chemical Society. Division of Agricultural
and Food Chemistry, sponsoring body. V. Series: ACS symposium series ; 1185.

[DNLM: 1. Biological Products--analysis. 2. Chemistry Techniques, Analytical--
methods. QY 90]

QP514.2

572--dc23

2014045847

The paper used in this publication meets the minimum requirements of American National
Standard for Information Sciences—Permanence of Paper for Printed Library Materials,
ANSI Z39.48n1984.

Copyright © 2014 American Chemical Society

Distributed in print by Oxford University Press

All Rights Reserved. Reprographic copying beyond that permitted by Sections 107 or 108
of the U.S. Copyright Act is allowed for internal use only, provided that a per-chapter fee of
\$40.25 plus \$0.75 per page is paid to the Copyright Clearance Center, Inc., 222 Rosewood
Drive, Danvers, MA 01923, USA. Republication or reproduction for sale of pages in this
book is permitted only under license from ACS. Direct these and other permission requests
to ACS Copyright Office, Publications Division, 1155 16th Street, N.W., Washington, DC
20036.

The citation of trade names and/or names of manufacturers in this publication is not to be
construed as an endorsement or as approval by ACS of the commercial products or services
referenced herein; nor should the mere reference herein to any drawing, specification,
chemical process, or other data be regarded as a license or as a conveyance of any right
or permission to the holder, reader, or any other person or corporation, to manufacture,
reproduce, use, or sell any patented invention or copyrighted work that may in any way be
related thereto. Registered names, trademarks, etc., used in this publication, even without
specific indication thereof, are not to be considered unprotected by law.

PRINTED IN THE UNITED STATES OF AMERICA

Foreword

The ACS Symposium Series was first published in 1974 to provide a mechanism for publishing symposia quickly in book form. The purpose of the series is to publish timely, comprehensive books developed from the ACS sponsored symposia based on current scientific research. Occasionally, books are developed from symposia sponsored by other organizations when the topic is of keen interest to the chemistry audience.

Before agreeing to publish a book, the proposed table of contents is reviewed for appropriate and comprehensive coverage and for interest to the audience. Some papers may be excluded to better focus the book; others may be added to provide comprehensiveness. When appropriate, overview or introductory chapters are added. Drafts of chapters are peer-reviewed prior to final acceptance or rejection, and manuscripts are prepared in camera-ready format.

As a rule, only original research papers and original review papers are included in the volumes. Verbatim reproductions of previous published papers are not accepted.

ACS Books Department

Preface

This ACS Symposium Series Book was evolved from the ACS symposium “Instrumental Methods for Analysis of Bioactive Molecules”, sponsored by the Division of Agricultural and Food Chemistry at the 246th American Chemical Society National Meeting & Exposition in Indianapolis, Indiana, September 8-12, 2013. Researchers in this field with common interests in the analysis of natural bioactive compounds were successfully brought together from all over the world to attend this exciting symposium to exchange ideas and results focusing on sample preparation, method development, validation, and application to real samples. A total of 33 scientists from 12 countries participated in this symposium. A World-class group of academic researchers and industrial scientists wrote the chapters published in this book to provide a state-of-the-art review and global perspective on this rapidly changing field.

The main purpose of this book is to discuss cutting-edge research techniques in the field of biologically active compounds derived from plants and foods, and in particular to describe advanced instrumental methods for the identification and quantification of these important compounds. Natural products are used worldwide to prevent and treat various diseases. The efficacy and safety of natural products require the development and application of reliable analytical methods to regulate and control usage. Because of their complex chemical compositions, natural products often require separation techniques for reliable analysis of their constituents. This book provides an integrated approach to address the separation, identification, quantification and chemistry of natural products for their analysis through various instrumental analyses.

Based on the symposium themes, this book contains nineteen chapters and is divided into four sections: 1) Sample Preparation, Separation and Identification 2) Identification by LC-MS and LC-NMR 3) Identification by GC, GC-MS, LC-GC and Spectroscopic Methods and 4). Metabolomic Fingerprinting. The first section covers sample preparation, extraction and rapid flash separation techniques, rapid LC analysis with bioassays and hyphenations to identify active constituents. The second section covers chromatographic separation by LC for active constituents, identification by mass spectra, and LC-NMR for the characterization of specific constituents from species such as *Melia azedarach*, *Sambucus nigra*, Citrus and Pomegranate. The third section covers separation of volatile constituents by GC and GC-MS. In recent years, analysis of volatiles using headspace has become more sensitive and popular, as it does not alter the original composition of volatile chemicals. This section also describes an approach based on solid-phase extraction and on-line LC-GC for the determination of naturally occurring free sterols, stanols and their esters. In addition, non-destructive

methods for the determination of chemical fingerprints and metabolomics profiles of natural products are also described; these methods allow reliable analysis of samples through the rapid acquisition of complex samples using nuclear magnetic resonance spectra. Moreover, Fourier Transform Infrared Photoacoustic Spectroscopy (FTIR-PAS) provides a method to measure resistant starch without separating it from the biological matrix is described. The fourth section includes two chapters on metabolic fingerprinting techniques. Metabolomics involves the study of small molecules from cells, plants, foods, tissues, organisms, or other biological tissues. These small molecules include primary and intermediary metabolites, as well as exogenous compounds, such as secondary metabolites, drugs and other compounds. Metabolic fingerprinting compares patterns, also called signatures or fingerprints of metabolites; these patterns change in response to external stimuli either in different plant varieties or species, or in response to adulteration, toxins, drug exposure, environmental or genetic alterations.

Thus, this book comprehensively describes the basic information presented at the symposium, providing a current review that will be useful for scientists, researchers, teachers, and engineers in general, and is particularly useful for chemists, biochemists, chemical engineers, biochemical engineers, and others in chemistry-related fields.

The editors gratefully acknowledge all authors for their patience, hard work and timely contributions as well as rest of the speakers who gave oral presentations in the three-day symposium. Furthermore, we wish to thank all reviewers for their critical suggestions/comments for making this book possible. Moreover, we thank Autumn Rizzo, Jose Perez and Michael Harries from VFIC, Texas A&M University, for their technical help. The editors also thank ACS Books Division, Bob Hauserman, Tim Marney and Kat Squibb, for their help in the review process as well as individuals from the press especially Mary Calvert and Pamela Kame for publishing this symposium series. The editors acknowledge Wikipedia at http://en.wikipedia.org/wiki/Momordica_charantia and Dr. Rachel Amir, Migal Galilee Technology Center, Israel for providing images for the cover.

G. K. Jayaprakasha, Ph.D, FRSC, FAGFD-ACS
Vegetable and Fruit Improvement Center
Texas A&M University
College Station, TX, 77845

Bhimangouda S. Patil, Ph.D.
Vegetable and Fruit Improvement Center
Texas A&M University
College Station, TX, 77845

Federica Pellati, Ph.D.
Department of Life Sciences
University of Modena and Reggio Emilia
Modena, Italy

Editors' Biographies

Dr. G. K. Jayaprakasha

Dr. G. K. Jayaprakasha is working as Research Professor with 24 years of research and 3 years of industrial experience. His research involves bioassay directed discovery, purification and chemical characterization of natural compounds from fruits, vegetables, spices and herbs using preliminary *in vitro* assays such as anticancer, antimicrobial and antioxidant properties. Isolated and identified more than 90 novel, rare and unstudied bioactive compounds from various natural products. He filed 24 patents in U.S., Europe and India. He published 130 research papers, 140 presentations, and edited three books. He is a fellow of Indian Chemist, Agricultural Food and Food Chemistry and elected Fellow of The Royal Society of Chemistry (FRSC), U.K.

Dr. Bhimu Patil

Dr. Bhimu Patil is the Professor and Director of the Vegetable and Fruit Improvement Center and has published more than 150 peer-reviewed papers. He has been actively involved in both research and educational activities related to global level 'Foods for Health'. He gave more than 120 invited presentations in land grant institutions, professional societies, industry, and learned society organizations including 9 plenary/keynote in several countries including China, Australia, New Zealand, South Korea, Brazil, Sweden, France, India, Israel, Spain, Canada, Portugal, Chile, and different states in the U.S.A. Patil received 17 awards including three "Fellow" recognition by professional societies. He co-founded an international symposium on FAVHealth in 2005. He has chaired or co-chaired 25 symposia. He has been interviewed and/or his work has been published in 135 articles and news media.

Dr. Federica Pellati

Dr. Federica Pellati is an Assistant Professor in Medicinal Chemistry, Dept. Life Sci., UNIMORE, Italy. She is the Coordinator of International Relations and Advisor of the 2nd ACS/AGFD International Student Chapter. Her research activity focuses on the development of innovative techniques for the metabolite fingerprinting of natural products; she is involved in the isolation and characterization of bioactive natural compounds. She is the author of more than 40 scientific papers, 1 patent, 3 book chapters and more than 70 congress communications. She is an editorial board member of 7 international Journals; she is a reviewer for many international Journals.

Chapter 1

Influence of Postharvest Storage, Processing, and Extraction Methods on the Analysis of Phenolic Phytochemicals

Yingjian Lu and Devanand Luthria*

**Beltsville Human Nutrition Research Center, Agricultural Research Service,
U.S. Department of Agriculture, Beltsville, Maryland 20705, United States**

***E-mail: Dave.Luthria@ars.usda.gov.**

This chapter provides an overview of the challenges associated with accurate analysis of phenolic compounds from foods, dietary supplements, and other matrices. It discusses the significance of sample preparation, post-harvest processing, and storage conditions on the assay of phenolic phytochemicals. This chapter is divided into three sections: 1) changes in phenolic contents during postharvest storage, and processing, 2) influence of extraction techniques and conditions, and 3) analytical techniques used for qualitative and quantitative analysis of phenolic compounds.

An Introduction to Phenolics

Plants contain a wide range of phytochemicals, many of which provide potential health benefits. These include vitamins, alkaloids, sterols, polysaccharides, fatty acids, and phenolic compounds. Phenolic compounds can be defined as compounds containing an aromatic ring with one or more hydroxyl groups (*I*). Phenolic phytochemicals are found throughout the plant kingdom. In general, plant phenolics can be broadly classified into multiple subgroups such as phenolic acids, flavonoids (flavones, flavanones, flavonols, etc.), tannins, and miscellaneous group (lignins, lignans, stilbenoids, coumarins, etc.). Phenolic acids can be further divided into two classes, derivatives of hydroxybenzoic acids such as gallic acid, and derivatives of hydroxycinnamic acids including ferulic acid, chlorogenic acid, and caffeic acid. Higher levels of phenolic acids are found in grain crops, while moderate amounts of phenolic acids exist in red wine and

tea (2, 3). Ferulic acid is the primary and most abundant phenolic acid in cereals whereas chlorogenic acid is a major phenolic acid extracted from medicinal plants belonging to *Apocynaceae* and *Asclepiadaceae* families (4).

Flavonoids are the most abundant polyphenols in our daily diets (5). They can be divided into different classes based on the chemical structure of heterocyclic ring as flavones, flavanones, flavonols, etc (6). High concentration of flavones are found in dietary plants, like herbs (parsley 4503 mg/100 g of edible portion), fruits (blueberries 163 mg/100 g of edible portion), and vegetables (mustard greens, flavonols 63 mg/ 100 g of edible portion) (7). The common flavones include, luteolin, apigenin, baicalein, chrysin, and their glycosides. These compounds are distributed in common foods such as parsley, tea, olives, thyme, cherries, and broccoli (8).

Tannins are another major subgroup of polyphenols in our diets. They are further divided into two categories hydrolyzable tannins and condensed tannins (1). Hydrolyzable tannins are complex polyphenols, which can be degraded into sugars and phenolic acids through either pH changes or enzymatic or non-enzymatic hydrolysis. Condensed tannins are oligomeric or polymers of flavan-3-ol linked through an interflavan carbon bond. Many common fruits and vegetables such as chickpeas, strawberries, apples, and black-eyed peas contain high amounts of hydrolyzable and condensed tannins (9).

The health effects of dietary phenolics have drawn attention of healthcare professionals and consumers in recent years. Phenolics are known to exhibit bioactivities like antioxidant, antimicrobial, anti-inflammatory, and antitumor. For instance, some flavonoid components in green tea or apples could effectively inhibit cancer or induce mechanisms that may kill cancer cells and inhibit tumor invasion (10, 11). Furthermore, a lignan component called podophyllotoxin initially identified from *Podophyllum peltatum*, could be used as an anti-tumor drug (12).

Hence, understanding the influence of postharvest storage, sample preparation, processing, and different analysis methods of bioactive phenolic compounds is of significant interest to nutrition and food processing professionals. Accurate quantification is also of significant importance for establishing dietary intake and safety guidelines. Although the phenolic content of food is generally considered to be reduced during postharvest and some processing methods, there are some examples where chemical reactions that release more free or bound components during processing that can result in an increase in concentration of bioactive phenolics (13, 14).

Factors Influencing the Analysis of Phenolic Compounds

Sampling

As phenolic phytochemicals are not uniformly distributed uniformly in fruits and vegetables. Both the concentration and the composition of the phenolic phytochemicals vary significantly depending on how the fruits and vegetables are sampled. For example, the mean concentration of anthocyanidins, flavan-3-ols, flavonols in apple skin were 5.5 mg, 36.1 mg, and 19.4 mg, respectively, per 100

g of edible portion. However, the concentration of anthocyanidins, flavan-3-ols, flavonols in apple Fuji with skin were significantly lower as 0.8 mg, 9.6 mg, and 2.4mg respectively per 100 g of edible portion (7). In another recent example, Zainudin et al. (15) investigated the variation of total phenolic content (TPC), total flavonoid content (TFC), total carotenoid content (TCC), and antioxidant activity of carambola fruit at different ripening stages. The authors showed that TCC increased as ripening progressed, however, TPC, TFC, and antioxidant activity decreased with ripening. The USDA database list several other examples where both the composition and concentration of the phenolics vary significantly based on the part analyzed and the ripening stage of the food sample (7).

Postharvest and Storage

Postharvest storage and processing (such as grinding and drying) can influence the quantity of phenolic phytochemicals present in food. Most plant materials are ground into fine powder with varying particle size prior to extraction and analysis. Kuang et al. (16) investigated the effect of grinding time, which influenced particle size of cinnamon and clove on antibacterial activity. The results indicated that the ultrafine powders had strong antibacterial activity which increased with the decrease in particle size. The optimal sizes of cinnamon and clove powders on antibacterial activity was determined as 11.2 and 14.4 μm , respectively. However, with dried parsley flakes, the yield of phenolic compounds was marginally reduced between 5-20% with an increase in particle size (17). This small decrease as compared to corn and soybean can be attributed to the thin flake type nature of parsley as compared to solid hard physical property of corn and soybean.

Several drying processes, including thermal (sun, oven, or microwave) drying, freeze drying, and cool-wind drying are commonly used in preparing plant samples for analysis. Generally, freeze-drying, cool-wind drying, and vacuum oven drying retain greater levels of phenolics content in plant samples as compared to air, thermal, microwave, or sun drying (18–20). For example, Chan et al. (18) compared the influence of five drying methods on the antioxidant activities of leaves and tea of ginger species. They found that freeze-dried leaves had higher amounts in total phenolic contents (TPC) (6440 mg GAE/ 100g) and ferric-reducing antioxidant power (FRAP)(31 mg GAE/g) as compared to those of (275 mg GAE/100g and 1.1 mg GAE/g, respectively) by commercial drying methods (microwave, oven, and sun drying). In addition, Lin, Sung, and Chen (19) examined the effect of cold-wind drying (30 °C), vacuum freeze drying, and hot air drying (40, 55, 70 °C) on caffeic acid derivatives (cichoric and caftaric acids) and total phenolics of *Echinacea purpurea* grown in Taiwan. They showed that cold-wind drying was a good drying method as compared to hot-air drying. However, in a recent study with *Artemisia annua* leaves, we observed that drying methods (freeze, oven, shade, and sun drying), drying time, and light intensity had significant influence on the concentration of artemisinin, dihydroartemisinic acid, artemisinic acid, and the leaf antioxidant capacity. The results showed that the freeze- and oven-dried samples had similarly high antioxidant activities, which declined significantly in the shade- and sun-dried samples (20).

Table 1. Influence of Postharvest Processing and Storage on Plant Phenolics

<i>Serial No.</i>	<i>Postharvest processing and storage</i>	<i>Results</i>	<i>Changes in levels of phenolics^a</i>	<i>References</i>
	<i>Grinding</i>			
1	Ultra-fine grinding	With the ball-milled time increasing, the reduction rates of the particle sizes can be divided into four stages: quick at the start, gradually reached a steady state, decreased sharply, and finally became tiny particles.	*	(16)
	<i>Drying</i>			
2	Freeze-drying	Freeze-dried leaves had significant amounts in total phenolic contents and antioxidant activities.	+	(18)
3	Thermal(microwave, oven, or sun) drying	Thermal drying resulted in significant decrease of total phenolic contents and antioxidant activities.	-	(18)
4	Cool-wind drying	Cool-wind drying was a good drying method as compared to hot-air drying.	+	(19)
	<i>Storage</i>			
5	Temperature	Higher storage temperature (30oC) would decrease the levels of cichoric acid and caftaric acid in dried <i>E. purpurea</i> samples.	-	(19)
6	Temperature	Results showed that storage of wild blueberry at room temperature reduced less content of anthocyanins as compared to other higher storage temperatures.	-	(21)

<i>Serial No.</i>	<i>Postharvest processing and storage</i>	<i>Results</i>	<i>Changes in levels of phenolics^a</i>	<i>References</i>
7	Temperature	Cold storage of potatoes at 4 oC for six months significantly affected the levels of total anthocyanins (TAC) differently in different varieties.	+/*/-	(22)
8	Time	Total phenolics of apples showed an increase after 3 months of storage at 1 oC in a controlled atomosphere, followed by a decrease as under all storage period (6 and 9 months).	+/-	(23)

^a (+) increase, (-) decrease or (*) no significant changes in levels of phenolic phytochemicals.

Table 2. Influence of Extraction Methods on Analysis of Phenolic Compounds from Plants

Serial No.	Extraction	Results	Changes in levels of phenolics ^a	References
1	Solid-phase extraction (SPE)	The optimized SPE method can detect and quantify a large amount of phenolic acids and flavonols with better recoveries from honey.	+	(99)
2	SPE	The proposed SPE method could quantify at least 33 individual phenolic compounds. It is a rapid technique with less total sample preparation time.	+	(100)
3	Microwave-assisted extraction (MAE)	There was little difference of levels of phenolic acids in distillers dried grains with solubles (DDGS) between heating with microwave irradiation and the same conditions using a regular water bath as the heat source.	+	(101)
4	MAE	The optimized microwave-assisted extraction conditions for soy isoflavones were: 0.5 g of sample, 50 °C, 20 min and 50% ethanol as extracting solvent. No degradation of the isoflavones was observed during MAE and a high reproducibility was achieved (>95%).	+	(31)
5	MAE	It has been concluded that all the phenolic compounds studied are stable up to 100 °C, whereas at 125 °C there is significant degradation of epicatechin, resveratrol, and myricetin during MAE.	+	(32)
6	MAE	The extraction yield of <i>trans</i> -resveratrol in <i>Rhizma polygoni cuspidati</i> was 92.8% and the recovery rate ranged from 94-102%. The MAE technique was a simple and effective extraction method for separation of <i>trans</i> -resveratrol from Chinese herb.	+	(33)

Serial No.	Extraction	Results	Changes in levels of phenolics ^a	References
7	Ultrasonic-assisted extraction (UAE)	The total amount of rosmarinic acid extracted by the microwave-assisted (MAE) and ultrasonic-assisted extractions (UAE) processes was greater than those obtained by other extraction methods.	+	(102)
8	UAE	The UAE has been shown to be an efficient method for the extraction of phenolic compounds and vitamin C from acerola fruit in comparison of EAE.	+	(51)
9	UAE	The optimized ultrasonic extraction conditions found were: 70% aqueous ethanol; solvent: sample ratio 40:1 (v/w); extraction time 3 x 30 min. The UAE showed high efficiency in the extraction of rutin and quercetin from <i>E. alatus</i> (Thunb.) Sieb compared to conventional methods.	+	(36)
10	UAE	The UAE method produced similar or higher recoveries for phenolic compounds in grapes under different conditions by significantly shorter time (6 min) as compared to the regular extraction method for phenolics.	+/*	(37)
11	Ultrasonic and microwave assisted extraction (UMAE)	The yields of phenolic compounds including caffeic acid and quercetin obtained by ILUMAE were greater than those by using regular UMAE. In addition, ILUMAE obtained higher extraction yields and significantly reduced extraction time.	+	(38)
12	Pressurized liquid extraction (PLE)	Among the three different extraction methods, pressurized liquid extraction (PLE) using ethanol as solvents achieved the highest extraction yields of antioxidants.	+	(42)

Continued on next page.

Table 2. (Continued). Influence of Extraction Methods on Analysis of Phenolic Compounds from Plants

<i>Serial No.</i>	<i>Extraction</i>	<i>Results</i>	<i>Changes in levels of phenolics^a</i>	<i>References</i>
13	PLE	The yields of phenolic compounds extracted by PLE were comparable to or better than those of four classical extraction procedures. Optimum extraction efficiency with PLE was obtained when extractions were performed with four extraction cycles using ethanol-water (50:50, v/v).	+	(41)
14	Supercritical fluid extraction (SFE)	Supercritical fluid extraction (SFE) using CO ₂ was a capable extraction method for extracting phenolic antioxidants, however, the SFE is somehow limited given relatively low extraction yields as compared to PLE method.	+	(42)
15	SFE	Optimized extraction conditions using SFE were: 20% v/v ethanol, 60°C, 250 bars and flow rate 2 mL/min. Under these conditions, the extraction of the five polyphenols by using SFE is quantitative and robust.	+	(46)
16	Enzyme-assisted extraction (EAE)	Rhamnosidase has been used to increase polyphenols such as flavonoids release from citrus peel. This might be a significant improvement for citrus processing industry.	+	(50)

<i>Serial No.</i>	<i>Extraction</i>	<i>Results</i>	<i>Changes in levels of phenolics^a</i>	<i>References</i>
17	EAE	The use of cell wall degrading enzymes increased the mass transfer of total phenols, with proteases having a particular increasing effect on the yield of chlorogenic acid. This study showed that phenols can be selectively extracted by adding cell wall degradation enzymes.	+	(49)
18	EAE	EAE took about 2 hours to reach the efficient concentration of enzymatic extraction. Though the extraction time of EAE was significantly longer than that of UAE, it is still a potential biocatalyst to obtain antioxidant-rich fruit juice.	+	(51)

^a (+) increase, (-) decrease or (*) no significant changes in levels of phenolic phytochemicals.

Storage temperature and time also influence the concentration of phenolic compounds in plant samples. Fracassetti et al. (21) investigated the influence of storage time and temperature on anthocyanin content and total antioxidant property in wild blueberry (*Vaccinium angustifolium*) powder. Results showed that significant degradation (at 25 °C, 3% reduction after 2 weeks; at 60 °C, 60% reduction after 3 days; at 80 °C, 85% reduction after 3 days) in the anthocyanin content during storage. The authors showed that as the storage temperature increased, the rate of degradation of anthocyanin increased. The value of the half life for anthocyanin in blueberry was determined as 139, 39, and 12 days at 25, 42, and 60 °C, respectively. However, the same group observed no significant effect in total antioxidant activity with the increase in storage temperature. Lin, Sung, and Chen (19) evaluated the effect of storage temperature on caffeic acid derivatives and total phenolics in fresh flower, leaves, stems, and root of *Echinacea purpurea*. The results showed that freeze dried samples stored between 10-20 °C with 40-60% relative humidity in seal bags/aluminum foil retained the highest content of bioactive phenolic acids. Lachman et al. (22) also studied on the impact of storage temperature on the content of anthocyanins in colored-flesh potatoes. The response of individual cultivars to storage varied significantly. The total anthocyanin content of Violette and Highland Burgundy Red cultivars increased by around 20%, while Valfi cultivar decreased by 36% and the remaining two potato cultivars (Blaue St. Galler and Blue Congo) did not show any significant change. Interestingly, Kevers et al. (23) studied the influence of long-term storage time (3-9 months) on the total phenolics in apples under three different conditions (1 °C in the air, 1°C in controlled atmosphere (0.9% O₂; 1.2% CO₂), and 1°C in controlled atmosphere after treatment with 1-methylcyclopropene). The authors found that the levels of phenolics in apples increased by 75% after 3 months of storage at 1 °C in a controlled atmosphere, followed by a decrease under all storage conditions tested in that study (6 and 9 months) (Table 1).

Extraction

After the above post-harvest processing steps such as drying and grinding, samples are subjected to extraction. This step concentrates the bioactive phytochemicals in extraction solvents. The concentrated extracts are analyzed by different chromatographic methods coupled to various detectors. Samples are often extracted using supercritical fluids, or solvents. Solvent extractions are the most commonly used methods to prepare extracts from plant materials based on their low-cost, ease of use, and general applicability. Generally, it is known that the efficiency of the extraction depends on the polarity of the analyte and its association with sample matrix, polarity of solvents, extraction time, extraction temperature, and techniques used. Thus, the phytochemical contents in different plant extracts vary significantly based on extraction techniques and conditions. The complexity of developing a single optimized extraction procedure for all phenolic compounds is practically not possible as over 8000 different phenolics have been reported in scientific literature (24). In addition phenolics are known

to occur in multiple forms such as simple aglycons, conjugated with single or multiple units of other phytochemicals and compounds. Thus, optimization of extraction process is important for accurate quantification of phytochemicals to establish proper dietary intake and safety guidelines. Several aqueous- organic solvent mixtures have been described in peer-reviewed scientific literature for extraction of phytochemicals from plant sources. The conventional extraction methods such as stirring, shaking, and Soxhlet procedures often require long extraction time and use a large amount of organic solvents. The separation and enrichment of phenolics from plant samples is also achieved by solid-phase extraction (SPE) (Table 2).

SPE is a rapid and easy sample preparation technique that is often used prior to the analysis step. Several authors have carried out SPE procedures to isolate and pre-concentrate of phenolics from plants (Table 2). Spietelun et al. (25) recently published a review article on SPE where he describes a comprehensive discussion of advantages and disadvantages of some new SPE techniques including solid-phase microextraction (SPME), stir bar sorptive extraction (SBSE) and magnetic solid phase extraction (MSPE). The authors concluded that the advantages of using solid-phase microextraction such as SPME and SBSE are 1) simple operation, 2) adaptability, 3) low cost, 4) quick extraction, 5) easy coupling to detection systems. Plutowska et al. (26) used SPME as extraction method and GC-MS as detection method to identify around 200 compounds such as phenols, aromatic acid, and terpenoids in Polish honeys. The authors concluded that SPME with GC-MS method provided great efficiency in isolation and determination of a large number of aromatic compounds in different honeys. Diez et al. (27) determined four volatile phenols (4-ethylguaiaicol, 4-ethylphenol, 4-vinylguaiaicol, and 4-vinylphenol) in wines using SBSE method coupled with GC-MS. The authors found that SBSE provided better recovery (90-100%) for the four volatile phenols than regular SPE, and needed a small sample volume for extraction.

In recent years, many new extraction techniques, such as microwave-assisted (MAE), ultrasound-assisted extractions (UAE), and their combination (UMAE), subcritical water extraction (SWE), supercritical fluid extraction (SFE), pressurized liquid extraction (PLE) and enzyme-assisted extraction (EAE) have been developed to automate and increase sample extraction efficiency and accuracy. The new methods can perform automated serial or batch extractions for multiple samples.

Microwave-assisted extraction (MAE) is a process utilizing microwave energy to extract the phytochemicals from the plant matrix into the solvent. The advantages of MAE include reduction of extraction time and reduced solvent usage (28). However, Wang and Weller (29) showed that the efficiency of microwave extraction can be poor when either the target compounds or the solvents are non-polar, or volatile. In another study, Xue et al. (30) showed that microwave heating caused gelatinization of starch in wheat flour. This may potentially impact the extraction of phytochemicals from grain products. MAE has been recently used for the extractions of phenolic compounds which were stable under microwave-assisted heating conditions. Rostagno et al. (31) pointed out that the optimized microwave-assisted extraction conditions for soy

isoflavones were: 0.5 g of sample, 50 °C, 20 min and 50% ethanol as extracting solvent. No degradation of the isoflavones was observed during MAE and a high reproducibility was achieved (>95%). In addition, Lizard et al. (32) concluded that all 22 phenolic compounds studied were stable up to 100 °C, while there was significant degradation of epicatechin, resveratrol, and myricetin at 125 °C during MAE. Du et al. (33) reported that improved extraction yield of *trans*-resveratrol (93%) and high recovery rate (ranged from 94-102%) in *Rhizma Polygoni Cuspidati* were found using MAE. Other similar study using MAE for extraction of phenolic compound from plant material is summarized in Table 2.

Ultrasonic-assisted extraction (UAE) is a useful and low-cost technology. The mechanism for ultrasonic treatment is based on the collapse of bubbles generated by acoustic waves that produce physical, chemical and mechanical effects, which leads to the disruption of biological membranes to facilitate the release of extractable compounds from plant materials (34, 35). However, the dispersed phase contributes to the ultrasound wave attenuation and the active part of ultrasound inside the extractor is restricted to a zone located in the ultrasonic emitter. Thus, these two factors should be considered seriously in ultrasound-assisted extractors (29). Recently, UAE has been widely used in extracting different phenolic compounds from various plant materials. Yang and Zhang (36) concluded that the developed UAE showed high recoveries for rutin (99%) and quercetin (100%) from *E. alatus* (Thunb.) Sieb compared to conventional methods. The optimal conditions for the extraction were: 70% aqueous ethanol and sample ratio 40:1 (v/w) with three cycles of extraction for 30 min. Carrera et al. (37) also showed that the UAE method produced similar or higher recoveries for phenolic compounds including total phenolic, total anthocyanins and condensed tannins from grapes in shorter extraction time (6 min) as compared to the regular extraction method with 60 minutes of extraction time. Additional studies using UAE to extract phenolic compounds from plant materials are summarized in Table 2. Lou et al. (38) developed a combination extraction method using ionic liquids with simultaneous ultrasonic and microwave assisted extraction (IL-UMAE) to extract compounds from burdock leaves. The authors found that the yields of caffeic acid (0.281 mg/g) and quercetin (0.272 mg/g) obtained by IL-UMAE were greater than those of using regular (0.256 and 0.242 mg/g, respectively) UMAE. In addition, IL-UMAE obtained higher extraction yields (8%-17% increased) and significantly reduced extraction time (from 5 hours to 30 seconds) as compared to the regular heat-reflux extraction method, suggesting that IL-UMAE was a rapid and highly effective extraction method.

Pressurized liquid extraction (PLE) is a relative new method that uses high temperature and pressure for extraction. Benthin et al. (39) conducted a comprehensive study on the feasibility of applying PLE to medicinal herbs after its emergence in the mid-1990s. By using PLE, the temperature of extraction solvent is greater than its normal boiling point because of high pressure. The combined use of high pressures (20.3 MPa) and temperatures (200 °C) provides faster extraction processes that require small amounts of solvents (40). The major disadvantages with newer technologies is higher equipment cost as compared to classical stirring and solvent extraction methods. Luthria et al. (41) investigated

the influence of extraction methods and polarity of solvents on the assay of phenolic compounds from parsley. The authors pointed out that the yields of total phenolic compounds extracted by PLE (15.5 mg GAE/g) were comparable or better than those of four classical extraction procedures (shaking, vortex mixing, sonication, and stirring) The optimum extraction efficiency with PLE was performed with four extraction cycles using ethanol - water (50:50, v/v). In addition, Herrero et al. (42) investigated the performance of three different processes for the extraction of antioxidants from rosemary. The PLE using ethanol as solvents at 200 °C achieved the highest extraction yields (38.6%) of antioxidants among all extraction methods. Similar to PLE, high-pressure extraction (HPE), which usually works under the high pressure ranging from 100 to 800 MPa, has been also used to extract phenolic compounds from green tea and Litchi fruit pericarp (43–45). Prasad et al. indicated that HPE provided higher extraction yield (29.3%) and required less time (2.5 min) as compared to conventional extraction method for extraction of total phenolic contents in Litchi fruit pericarp, but there were no significant differences in the total phenolic content in Litchi fruit pericarp of among these various extractions (44). The same group also found that HPE provided higher extraction yield of flavonoids (30%) in comparison to conventional extraction method (45).

Supercritical fluid extraction (SFE) is an extraction process that uses supercritical fluids such as CO₂ as the extracting solvent. The advantage of using SFE is that less organic solvents are needed as compared to traditional solvent extraction techniques. However, SFE is not suitable for polar compounds and has higher equipment cost (29). Chafer et al. (46) determined polyphenolic compounds in grape skins by using SFE and HPLC, and found that the extraction of the five polyphenols (catechin, epicatechin, rutin, quercetin and *trans*-resveratrol) by SFE is quantitative and robust under the optimized extraction conditions (Solvent: 20% v/v ethanol as a modifier of supercritical CO₂; Temperature: 60°C; Pressure: 250 bars; Flow rate: 2 mL/min). In addition, Herrero et al. (42) reported that SFE using CO₂ at 400 bars pressure obtained the highest extraction (330 ug/mg extract) of total phenolic antioxidants from rosemary. SFE is a commonly preferred extraction procedure of nonpolar compounds.

Many enzyme-assisted extraction (EAE) procedures are used to accelerate the release of bound phenolics. Enzymes widely used in the food industry catalyze a variety of hydrolytic reactions and a high percentage act on cell wall polymers improving extraction yield of phenolic compounds in fruits and juices, but the main limitation for using these enzymes in industrial processes has been their high cost (47). Puri et al. (48) published a review article on enzymatic assisted extraction of bioactive compounds from plants where the authors concluded that EAE provided better recovery with lower extraction time and reduced solvent usage compared to non-enzymatic methods because enzymes enhance the release of bound bioactive compounds from plants. In the study by Pinelo et al. (49), the authors reported that the use of cell wall degrading enzymes such as pectinase and protease increased the mass transfer of total phenols. Proteases had a significant effect on the yield of chlorogenic acid. The author concluded that phenols can be selectively extracted by adding cell wall degradation enzymes. In addition, Kaur et al. (50) found that rhamnosidase increased naringin release

(greater than 77%) from citrus while minimizing the uses of energy and solvents. Other studies using EAE to isolate phenolic compounds from plant matrix are summarized in detail in Table 2 (51).

Processing

Processing including fermentation, enzymatic treatment, thermal, and non-thermal treatments have significant influence on the yield of phenolic compounds extracted from food materials. Generally, the phenolic content is considered to decrease during processing (52, 53), but some studies showed that chemical or enzymatic reactions from fermentation or thermal treatment can release more bound components during processing, which can result in an increase of phenolic content (54, 55).

Solid-state fermentation (enzymatic procedures) has been widely developed and used to enhance the release of phenolic compounds from fruits and nuts (56–58). Ajila et al. (56) determined the changes in phenolic compounds and antioxidant activities in apple pomace using fungi (*Phanerochaete chrysosporium*) during the solid-state fermentation. The authors observed that the polyphenolic content was increased in fermented apple pomaces as compared to unfermented samples (from 4.6 to 16.1 mg GAE/g dry weight), and the antioxidant activity was correlated with the increase in polyphenolic content. In another study, Mateo Anson et al. (54) studied the bioaccessibility of phenolics in wheat-bran breads using fermentation and/or enzymatic treatments. The authors found that the combination of enzyme treatments and fermentation increased the bioaccessibility of ferulic acid from 1.1% to 5.5% (Table 3).

Thermal processing, including baking, cooking, and microwaving, change the levels of phenolics in plant materials. There appears to be a common consensus about the loss of phenolics when exposed to heat (53). Mulinacci et al. (55) investigated the influence of cooking on the anthocyanins and phenolic acids content in two pigmented potatoes. The authors reported that cooking did not change the phenolic acids content but decreased anthocyanins in pigmented potatoes by 16-29%. In another study, Lachman et al. (22) investigated the impact of cooking and baking on the total anthocyanin content in colored-flesh potatoes. The authors found that there was a significant increase in total anthocyanin content (TAC) (3.3 folds increase) in baked colored potatoes as compared to their respective unbaked samples, while cooking increased the TAC over four times than the uncooked potato samples. However, Brown et al. (59) reported that the TAC of four potato varieties remained either unchanged or increased (0.7-1.7 mg/g DW) after microwave cooking as compared to the raw potato samples (0.6-1.8 mg/g DW)(Table 3).

Different from thermal processing, non-thermal treatments such as high hydrostatic pressure (HHP), ultraviolet (UV) light treatments, pulsed electric field (PEF), and others have also been used during processing of foods. Recent studies have investigated the effect of these non-thermal technologies on the levels of phenolic compounds in plant materials (60–62).

Table 3. Influence of Secondary Processing on Analysis of Phenolic Compounds

<i>Serial No.</i>	<i>Secondary Processing</i>	<i>Results</i>	<i>Changes in levels of phenolics^a</i>	<i>References</i>
	<i>Wet-fractionation</i>			
1	Enzymatic treatment	The most effective treatment was the combination of enzymes and fermentation that increased the bioaccessibility of ferulic acid.	+	(54)
2	Solid state Fermentation	The phenolic content was increased in fermented apple pomace than fresh ones, and the antioxidant activity was correlated with the increase in polyphenolic content.	+	(56)
	<i>Thermal processing</i>			
3	Baking	There was a significant increase of total anthocyanin content (TAC) in baked colored potatoes as compared to unbaked ones.	+	(22)
4	Cooking	Total anthocyanin contents (TAC) found in cooked potatoes was higher than uncooked potatoes.	+	(22)
5	Cooking	Cooking did not change the phenolic acids content, while it decreased anthocyanins content in pigmented potatoes.	*/-	(55)
6	Microwaving	Thermal processing such as microwaving and boiling reserved more TAC than frying or baking treatment.	+	(59)
	<i>Non-thermal processing</i>			

Continued on next page.

Table 3. (Continued). Influence of Secondary Processing on Analysis of Phenolic Compounds

<i>Serial No.</i>	<i>Secondary Processing</i>	<i>Results</i>	<i>Changes in levels of phenolics^a</i>	<i>References</i>
7	High hydrostatic pressure (HHP)	The levels of phenols in strawberry and blackberry purees increased significantly as compared to unprocessed samples during HHP treatment. In addition, the anthocyanins were well retained at all HHP treatment levels.	+	(63)
8	HHP	Greatest stability of the anthocyanins (cyanidin-3-glucoside and cyanidin-3-sophoroside) was found when raspberries were pressured under 200 and 800 MPa and stored at 4 °C.	*	(64)
9	Atmospheric pressure plasma (APP)	In lamb's lettuce, phenolic acids are slowly decreased and flavonoids are fast degraded when exposed to atmospheric pressure plasma jet.	-	(60)
10	UV light	Phenolic acids and antioxidant capacity of minimally processed Satsuma mandarin were not greatly influenced by UV-C treatments. Flavonoids and total phenolics were significantly increased by 1.5 and 3.0kJ/m ² treatment after 3 days storage.	+	(66)
11	UV light	No significant changes of total phenolics and antioxidant activity in a blend of apple and cranberry juice were found during UV and high intensity light pulses (HILP).	*	(61)
12	Pulsed electric field (PEF)	The anthocyanins in strawberry juice increased significantly from 80% to 90% when pulse width raised from 1 to 7 μ s at 50 Hz.	+	(69)

<i>Serial No.</i>	<i>Secondary Processing</i>	<i>Results</i>	<i>Changes in levels of phenolics^a</i>	<i>References</i>
13	PEF	The contents of chlorogenic, caffeic and other phenolic acids increased dramatically at 1.2 kV/cm and 30 pulses, while the contents of α -carotene, 9- and 13- <i>cis</i> -lycopene increased by around 100% at 1.2 kV/cm and 5 pulses as PEF test conditions.	+	(70)
14	Vacuum	Different phenolic acids in red beet seem to be more stable with vacuum treatment, especially by using high vacuum treatments.	+	(62)
15	Germination	With germination there was up to 21% increase in antioxidant activity when compared to control extract from red beet plant.	+	(62)
16	Sonication	The amount of anthocyanins in pomegranate juices slightly increased (0.5-7.3%) as compared to unprocessed samples at 50% sonication intensity. Total phenolic content in some juices increased about 5.4-42.5% at 100% sonication intensity and 9 min.	+	(71)

^a (+) increase, (-) decrease or (*) no significant changes in levels of phenolic phytochemicals.

Table 4. Techniques Used for the Nalysis of Phenolic Compounds

<i>Serial No.</i>	<i>Analysis</i>	<i>Results</i>	<i>References</i>
1	Fast Blue BB method	A new method is based on interactions of phenolics with Fast Blue BB diazonium salt in alkali pH, forming azo complexes, with the absorbance measured at 420 nm after 60 min.	(73)
2	High performance liquid chromatography (HPLC)-electrochemical detection (ECD)	Highly efficient separation and sensitive analysis of five phenolic acids in Xuebijing by using high performance liquid chromatography (HPLC)-electrochemical detection (ECD) were observed.	(79)
3	ECD	ECD provides great resolution of all analytes in quantification of eight selected phenolic compounds in olive oil as compared to published methods.	(80)
4	HPLC-electro-array detection (EAD)	EAD was reliable and accurate for quantification of flavonoids in plant materials.	(81)
5	HPLC- mass spectrometric (MS/MS)	Comprehensive MS analysis of the phenolic compounds in <i>Chrysanthemum</i> flower would be significant for the quality control for this herb and its products. 25 phenolic compounds were firstly found.	(89)
6	LC-MS	Luteolin 7-O-glucuronide, apigenin 7-O-glucuronide, and chrysoerisol 7-O-glucuronide in extract of <i>Cardiospermum halicacabum</i> by UPLCMS/MS analysis.	(90)
7	LC-MS	The bioactive phenolic compound from crude extracts of <i>Humulus lupulus</i> L. by LC-MS/MS was determined.	(103)
8	LC-MS	The phenolic acids and their methylates, glucuronides, sulfates and lactones metabolites in human plasma by using LC-MS/MS after ingestion of soluble coffee were analyzed.	(91)

<i>Serial No.</i>	<i>Analysis</i>	<i>Results</i>	<i>References</i>
9	Gas chromatography (GC)-MS	The bioactive phenolic compound from crude extracts of <i>Humulus lupulus</i> L. by GC-MS was determined.	(103)
10	GC-MS	The phenolic compounds in aromatic plants by GC-MS after silylation were studied.	(104)
11	Nuclear magnetic resonance (NMR)	The process of phenolic compound biodegradation by yeast <i>Candida tropicalis</i> NCIM 3556 in liquid medium by ¹ H, ¹³ C, and DOSY NMR techniques was investigated.	(95)
12	NMR	The ³¹ P NMR analysis of ³¹ P-labeled samples allowed the unprecedented quantitative and qualitative structural characterization of phenolics.	(94)
13	HPLC-NMR	LC-NMR can be used to analyze several minor compounds, such as <i>cis</i> isomers PET- and PEO-(6- <i>p</i> -coumaroyl)-5-diglucoside in the skins of four grape species.	(92)
14	LC-NMR	LC-NMR, NMR, and LC-MS have great performance in identification of major flavonoids, ellagic acid derivatives, and some minor compounds in <i>Drosera peltata</i> .	(93)
15	LC-MS/NMR	LC-MS/NMR PDS combined with an incomplete separation strategy has the potential to expedite the structure identification of natural products in crude extracts.	(105)
16	LC-MS/NMR	LC//MS/NMR analysis of ethyl acetate extract led to the structure determination of three new isomeric products from the root of <i>Fagara zanthoxyloides</i> Lam.	(106)

Continued on next page.

Table 4. (Continued). Techniques Used for the Nalysis of Phenolic Compounds

<i>Serial No.</i>	<i>Analysis</i>	<i>Results</i>	<i>References</i>
17	Fingerprints	Six analytical instruments significantly discriminated broccoli samples of different variety and growing environments by PCA analysis.	(96)
18	Fingerprints	Organic basil sample contained greater levels of almost all the major compounds than its conventional counterpart.	(97)
19	Fingerprints	Organic sage samples were significantly differentiated by using the combinations of chromatographic and mass spectrometric fingerprints.	(98)

Patras et al. (63) investigated the effect of HHP on phenolic content and antioxidant capacity of strawberry and blackberry purees. The results showed that the levels of phenols in strawberry purees increased significantly (9.8%, $p < 0.05$) as compared to unprocessed samples during HHP treatment. The same trend was observed with blackberry purees. Suthanthangjai et al. (64) also studied the impact of HHP on the levels of anthocyanins in raspberry. The results showed that the highest stability of the anthocyanins (cyanidin-3-glucoside and cyanidin-3-sophoroside) was found when the raspberries were pressured under 200 and 800 MPa and stored at 4 °C. Another pressure-based non-thermal treatment was used in the study of Grzegorzewski et al. (60), the authors investigated the effect of atmospheric pressure plasma jet at varying operating conditions on the concentration of selected flavonoids and phenolic acids in lamb's lettuce. The results showed that phenolic acids in lamb's lettuce are slowly decreased while flavonoids are rapidly degraded when exposed to atmospheric pressure plasma jet. Similarly, Uckoo et al. (65) determined the influence of HHP (400 MPa for 2 mins) on the the levels of flavonoids in grapefruit juice. The authors indicated that HPP processing significantly decrease the levels of narirutin, naringin, didymin, and poncirin, which was most distinct at 7 days after storage.

UV irradiation is an easy-to-use technique which produces no contamination, and has been proved to have efficiency in controlling microbial growth, delaying ripening and extending the shelf-life of various fruits and vegetables. Shen et al. (66) investigated the impact of UV irradiation on phenolic compounds and antioxidant capacity of *Satsuma mandarin* during refrigerated storage. They found that phenolic acids and antioxidant capacity of *Satsuma mandarin* were not greatly influenced by UV-C treatments. The authors also found that flavonoids and total phenolics were significantly increased by 1.5 and 3.0kJ/m² treatment after 3 days storage. Similarly, Caminiti et al. (61) investigated the impact of non-thermal processing technologies, including UV, high intensity light pulses (HILP), and high-voltage pulsed electric fields (PEF) on the phenolic levels and antioxidant activity of apple and cranberry juice blend. No significant changes of total phenolics and antioxidant activity in a blend of apple and cranberry juice were detected during UV and HILP treatments. In addition, electro beam irradiation might be used as a preservation technology based on its safety, less cost, and ability to ensure hygienic and sensory quality. Fernandes et al. (67) investigated the effect of gamma irradiation on the levels of phenolic acids in fresh, dried and frozen mushroom. The results showed that gamma irradiation (1.0 kGy dose) exerted a protective effect on total phenolic acids content in dried mushroom.

PEF processing is based on using brief pulses of a strong electric field to inactivate microorganism in food product (68). In the study of Odriozola-Serrano et al. (69), more than 80% of the anthocyanin content of strawberry juice treated with high-voltage PEF was maintained. Especially, the anthocyanins in strawberry juice increased significantly from 80% to 90% when pulse width raised from 1 to 7 μ s at 50 Hz. In another study, Vallverdu-Queralt et al. (70) determined the phenolic and carotenoid contents in tomatoes after treating with moderate-intensity PEF, and they found that the contents of chlorogenic, caffeic and other phenolic

acids increased dramatically by around 150% at 1.2 kV/cm and 30 pulses, while the contents of α -carotene, 9- and 13-*cis*-lycopene increased by around 100% at 1.2 kV/cm and 5 pulses as PEF test conditions. The authors explained that these increases might be attributed to the physiological responses to induced-stress brought by PEF.

Furthermore, the effects of vacuum and germination on the phenolic compounds of plants was reported by Ravichandran et al. (62). The authors studied the effect of vacuum and germination on the phenolic acid content and antioxidant activity of red beet. The results showed that different phenolic acids in red beet seem to be stable under high vacuum treatments. The authors also pointed out that high vacuum treatment raised the levels of 4-hydroxy benzoic acid (from 23.3 to 24.9 $\mu\text{mol/g DM}$) and vanillic acid (from 8.9 to 9.15 $\mu\text{mol/g DM}$) in red beet. In addition, red beet with the germination obtained higher levels of *p*-coumaric acid (0.77 $\mu\text{mol/g}$) as compared to that of fresh red beet (0.53 $\mu\text{mol/g}$). Thus, with germination there was up to 21% increase in antioxidant activity when compared to control extract from the red beet plant. Ionizing radiation is commonly used to inactivate foodborne pathogens and extend the shelf-life of many fresh fruits and vegetables. Furthermore, sonication has shown its importance in food processing in the industry for last few years. In the study of Alighourchi et al. (71), the amount of anthocyanins slightly increased (0.5-7.3%) as compared to unprocessed samples at 50% wave amplitude during sonication. The authors also found that the total phenolic content in pomegranate juices increased about 5.4-42.5% at 100% wave amplitude for 9 minutes during sonication (Table 3).

Analytical Techniques Used for Qualitative and Quantitative Analysis

The analytical methods used for determination of the phenolics in plant materials primarily depend on the resources available and the research objectives. The rapid assays usually are different colorimetric methods that are also sometimes referred to as antioxidant assays. The most commonly procedure for measuring the total phenolic contents (TPC) is Folin-Ciocalteu method (FC) developed by Singleton et al. One of the disadvantages of using FC assay is that some reducing agents such as amino-acids, proteins, sugars may interfere with the analysis of TPC content. In addition, lipophilic phenolic compounds are not analyzed. Recently, Berker et al. (72) developed a modified FC assay to include non-polar antioxidants using NaOH added isobutanol-water medium. Several other modifications have also been recently reported. For example, Medina (73) developed a rapid and simple method for phenolics determination which is mainly based on the reaction between phenolic and Fast Blue BB diazonium salt in alkali pH.

Furthermore, multiple antioxidant assays such as DPPH or oxygen radical absorbing capacity (ORAC), ferric-reducing antioxidant power (FRAP), Trolox equivalent antioxidant capacity (TEAC), total radical trapping antioxidant parameter (TRAP), 2, 2-diphenyl-1-picrylhydrazyl (DPPH•) are used for indirect estimation for the analysis of phenolic compounds. Apak et al. (74) utilized QUENCHER-CUPRAC method for assaying total antioxidant

capacity whereas Serpen et al. (75) measured antioxidant capacity in insoluble portion of the food by QUENCHER procedure using ABTS• (2, 2-azino-bis (3-ethylbenzthiazoline-6-sulfonic acid), or DPPH• However, some studies showed that there was no significant correlation between TPC, different antioxidant assays and phenolic compounds as analyzed by HPLC (76, 77).

Chromatographic techniques such as high performance liquid chromatography (HPLC) and gas chromatography (GC) have extensively been used for separation, identification, and quantification of phenolic compounds. Thousands of studies utilized HPLC or GC for determination of phenolic compounds from various plant materials have been reported in peer-reviewed publications (78). HPLC is the most popular and reliable technique for separation and quantification of phenolic compounds and is commonly preferred over GC technique which frequently requires an additional derivatization step. These chromatographic separation methods are commonly coupled to wide array of detection methodologies such as ultraviolet/visible spectrometric detectors, electrochemical detectors (ECD) (79–81), mass spectrometry (MS) (82–84) and nuclear magnetic resonance (NMR) detection methods (85, 86). Some of the recent applications are summarized in Table 4.

Electrochemical detection (ECD) provides an accurate detection of trace amounts of electroactive compounds such as phenolics. Due to its extreme sensitivity, high specificity, low detection limits and enhanced resolving power, ECD coupled to HPLC has been widely used for the analysis of phenolic compounds in herbs and vegetables (87, 88). Mattila et al. (81) determined the levels flavonoids and compositions in plant material by HPLC-EAD. The limits of detection (LOD) range was 4.0-250.0 ng/mL. The authors concluded that EAD was reliable and accurate for quantification of flavonoids in plant materials. Jia et al. (79) observed high efficient separation and sensitive analysis of five phenolic acids in Xuebijing by using HPLC-ECD utilizing ionic liquid of 1-butyl-3-methylimidazolium bromide and an additive gold nanoparticles. This method was successfully used for pharmacokinetics study using Xuebijing injection. The limits of quantification (LOQ) range were 3.7–8.5 ng/mL. Bayram et al. (80) also developed a validated method for the determination of phenolics in olive oil using HPLC-ECD, and pointed out that ECD provides great resolution of all analytes in quantification of eight selected phenolic compounds in olive oil as compared to other published methods. The LOQ ranged from 0.3 to 15.3 ng/mL while the LOD range was 0.03-1.70 ng/mL (Table 4).

MS and NMR detections are commonly used for structural elucidation rather than for quantification. Several studies have been published on the applications of MS for the analysis of phenolics in herbs and spices. Lin and Harnly (89) identified 46 flavonoids and 17 caffeic acid derivatives in the extract of *Chrysanthemum morifolium* Ramat by LC-MS. Twenty five phenolic compounds were separated and identified in *Chrysanthemum* flower. The authors pointed out that the comprehensive MS analysis of the phenolic compounds in *Chrysanthemum* flower would be significant for the quality control for this herb and its products. In another study, Jeyadevi et al. (90) identified phenolic profile, including luteolin 7-O-glucuronide, apigenin 7-O-glucuronide, and chrysoerisol 7-O-glucuronide in the extract of *Cardiospermum halicacabum* by

ultra performance liquid chromatography (UPLC) coupled with MS/MS detection procedure. In addition, in the study of Marmet et al. (91), phenolic acids and their methylates, glucuronides, sulfates and lactones metabolites in human plasma after ingestion of soluble coffee were analyzed using LC-MS/MS. The authors concluded that the LC-MS/MS method was found to be sensitive, selective, accurate and repeatable for the quantification of dietary phenolic compounds. More recent applications of MS were summarized in Table 4.

Usually compounds are purified by classical chromatographic methods and then assayed by NMR. However, in recent years LC-NMR has often used for structural confirmation of phytochemicals. Cruz et al. (92) determined the chemical profile and levels of anthocyanins in the skins of four grape species by LC-NMR. Combination of analytical data generated by LC-MS and LC-NMR aided authors in identifying 33 anthocyanins from four grape species. The author indicated that LC-NMR information was vital for identification of several minor compounds, such as *cis* isomers petunidin- and peonidin-(6-*p*-coumaroyl)-5-diglucoside. In another recent study, Branberger et al. (93) determined flavonoids and ellagic acid derivatives from the herb *Drosera peltata* by LC-NMR, and LC-MS analysis. Melone et al. (94) recently developed a new ³¹P NMR analysis for structural elucidation of tannins on the basis of tannin model compounds by *in situ* labeling of all labile H-groups (aliphatic and phenolic –OH, carboxylic acids) with phosphorous reagent. The ³¹P NMR analysis of labeled samples allowed the quantitative and qualitative structural characterization of hydrolyzable tannins, proanthocyanidins, and catechin tannin model compounds. Phalgune et al. (95) studied the process of phenolic compound biodegradation by yeast using ¹H, ¹³C, and DOSY NMR techniques.

The LC-MS was used to determine the molecular mass of the phenolic compounds and the LC-NMR provided the necessary structural information to unambiguously assign the structure of phenolics. The combination of these two techniques provides unique ways for structural elucidation of phenolic compounds.

Fingerprinting is a characteristic profile or pattern which chemically represents the sample composition. In general, fingerprints can be obtained using both chromatographic and spectrometric techniques. Recently, several analytical strategies to obtain and analyze fingerprints of herbs and other plant material have already been investigated. We recently utilized different (Fourier transform infrared (FT-IR), Fourier transform near-infrared (NIR) spectrometry, UV, visible (VIS) regions and mass spectrometry with negative (MS⁻) and positive (MS⁺) ionization) spectral fingerprints to differentiate broccoli and bean samples belonging to different cultivars and/or grown under different environmental conditions (96). The spectral fingerprints were analyzed using nested one-way analysis of variance (ANOVA) and principal component analysis (PCA) to statistically evaluate the quality of discrimination. In another study from our group, we differentiated adulterated Ginkgo biloba supplements from authentic samples by UV spectral fingerprints and HPLC analysis. In addition, the combinations of chromatography and mass spectrometric fingerprints have been successfully used to differentiate organic and conventional botanicals (97, 98). Lu et al. (97) found that the organic basil sample contained greater concentrations

of almost all the major compounds than its conventional counterpart. Similar results were observed in the study of Gao et al. (98), organic sage samples were significantly differentiated by using the combinations of HPLC and flow-injection MS fingerprints (Table 4).

In conclusions, this chapters provides an overview of methodologies used from sample preparation to extraction and analysis of phenolic compounds. It also provides information on the recent advances in the methodologies used for qualitative, quantitative and detail structural elucidation methods for analysis of phenolic compounds form wide array of matrices.

References

1. Cai, Y. Z.; Luo, Q.; Sun, M.; Corke, H. *Life Sci.* **2004**, *74*, 2157–2184.
2. Liyana-Pathirana, C. M.; Shahidi, F. *J. Agric. Food Chem.* **2006**, *86*, 477–485.
3. Goncalves, B.; Falco, V.; Moutinho-Pereira, J.; Bacelar, E.; Peixoto, F.; Correia, C. *J. Agric. Food Chem.* **2009**, *57*, 265–273.
4. Huang, W. Y.; Cai, Y. Z.; Xing, J.; Corke, H.; Sun, M. *Econ. Bot.* **2007**, *61*, 14–30.
5. D'Archivio, M.; Filesi, C.; Vari, R.; Scazzocchio, B.; Masella, R. *Int. J. Mol. Sci.* **2010**, *11*, 1321–1342..
6. Ghasemzadeh, A.; Jaafar, H. Z. E.; Rahmat, A. *Molecules* **2010**, *15*, 7907–7922.
7. Bhagwat, S.; Haytowitz, D. B.; Holden, J. M. *USDA Database for the Flavonoid Content of Selected Foods*; http://www.ars.usda.gov/SP2UserFiles/Place/12354500/Data/Flav/Flav_R03-1.pdf, 2014.
8. Fresco, P.; Borges, F.; Diniz, C.; Marques, M. P. M. *Med. Res. Rev.* **2006**, *26*, 747–766.
9. Han, X. Z.; Shen, T.; Lou, H. X. *Int. J. Mol. Sci.* **2007**, *8*, 950–988.
10. Park, S. J.; Myoung, H.; Kim, Y. Y.; Paeng, J. Y.; Park, J. W.; Kim, M. J.; Hong, S. M. *J. Korean Assoc. Oral Maxillofac. Surg.* **2008**, *34*, 1–10.
11. Veeriah, S.; Kautenburger, T.; Habermann, N.; Sauer, J.; Dietrich, H. *Mol Carcinogen.* **2006**, *45*, 164–174.
12. Effterth, T.; Li, P.; Konkimalla, V.; Kaina, B. *Trends Mol. Med.* **2007**, *13*, 353–361.
13. Moore, J.; Luther, M.; Cheng, Z.; Yu, L. *J. Agric. Food Chem.* **2009**, *57*, 832–839.
14. Abdel-Aal, E. S. M.; Rabalski, I. *J. Cereal Sci.* **2013**, 312–318.
15. Zainudin, M. S. M.; Hamid, A. A.; Anwar, F.; Osman, A.; Saari, N. *Sci. Hortic. (Amsterdam, Neth.)* **2014**, *172*, 325–331.
16. Kuang, X.; Li, B.; Kuang, R.; Zheng, X.; Zhu, B.; Xu, B.; Ma, M. *J. Food Saf.* **2011**, *31*, 291–296.
17. Luthria, D. L. *Food Chem.* **2008**, *107*, 745–752.
18. Chan, E. W. C.; Lim, Y. Y.; Wong, S. K.; Lim, K. K.; Tan, S. P.; Lianto, F. S.; Yong, M. Y. *Food Chem.* **2009**, *113*, 166–172.
19. Lin, S.; Sung, J.; Chen, C. *Food Chem.* **2011**, *125*, 226–231.

20. Ferreira, J. F. S.; Luthria, D. L. *J. Agric. Food Chem.* **2010**, *58*, 1691–1698.
21. Fracassetti, D.; Del Bo, C.; Simonetti, P.; Gardana, C.; Klimis-Zacas, D.; Ciappellano, S. *J. Agric. Food Chem.* **2013**, *61*, 2999–3005.
22. Lachman, J.; Hamouz, K.; Orsak, M.; Pivec, V.; Hejtmankova, K.; Pazderu, K.; Dvorak, P.; Cepl, J. *Food Chem.* **2012**, *133*, 1107–1116.
23. Kevers, C.; Pincemail, J.; Tabart, J.; Defraigne, J.; Dommès, J. *J. Agric. Food Chem.* **2011**, *59*, 6165–6171.
24. Bravo, L. *Nutr. Rev.* **1998**, *56*, 317–333.
25. Spietelun, A.; Marcinkowski, L.; Guardia, M.; Namiesnik, J. *J. Chromatogr. A* **2011**, *1321*, 1–13.
26. Plutowska, B.; Chmiel, T.; Dymerski, T.; Wardencki, W. *Food Chem.* **2011**, *126*, 1288–1298.
27. Diez, J.; Dominguez, C.; Guillen, D. A.; Veas, R.; Barroso, C. G. *J. Chromatogr. A* **2004**, *1025*, 263–267.
28. Eskilsson, C. S.; Bjorklund, E. *J. Chromatogr. A* **2000**, *902*, 227–250.
29. Wang, L.; Weller, C. L. *Trends Food Sci. Technol.* **2006**, *17*, 300–312.
30. Xue, C.; Fukuoka, M.; Sakai, N. *J. Food Eng.* **2010**, *97*, 40–45.
31. Rostagno, M. A.; Palma, M.; Barroso, C. G. *Anal. Chim. Acta* **2007**, *588*, 274–282.
32. Liqid, A.; Palma, M.; Brigui, J.; Barroso, C. G. *J. Chromatogr. A* **2007**, *1140*, 29–34.
33. Du, F. Y.; Xiao, X. H.; Li, G. K. *J. Chromatogr. A* **2007**, *1140*, 56–62.
34. Vinatoru, M. *Ultrason. Sonochem.* **2001**, *8*, 303–313.
35. Mason, T. J.; Paniwnyk, L.; Lorimer, J. P. *Ultrason. Sonochem.* **1996**, *3*, 253–260.
36. Yang, Y.; Zhang, F. *Ultrason. Sonochem.* **2008**, *15*, 308–313.
37. Carrera, C.; Ruiz-Rodriguez, A.; Palma, M.; Barroso, C. G. *Anal. Chim. Acta* **2012**, *732*, 100–104.
38. Lou, Z.; Wang, H.; Zhu, S.; Chen, S.; Zhang, M.; Wang, Z. *Anal. Chim. Acta* **2012**, *716*, 28–33.
39. Benthin, B.; Danz, H.; Hamburger, M. Pressurized liquid extraction of medicinal plants. *J. Chromatogr. A* **1999**, *837*, 211–219.
40. Mendiola, J. A.; Herrero, M.; Cifuentes, A.; Ibanez, E. *J. Chromatogr. A* **2007**, *1152*, 234–246.
41. Luthria, D. L.; Mukhopadhyay, S.; Kwansa, A. L. *J. Sci. Food Agric.* **2006**, *86*, 1350–1358.
42. Herrero, M.; Plaza, M.; Cifuentes, A.; Ibanez, E. *J. Chromatogr. A* **2010**, *1217*, 2512–2520.
43. Zhang, S.; Zhu, J.; Wang, C. *Int. J. Pharm.* **2004**, *78*, 471–474.
44. Prasad, N. K.; Yang, B.; Zhao, M.; Wang, B.; Chen, F.; Jiang, Y. *Int. J. Food Sci. Technol.* **2009**, *44*, 960–966.
45. Prasad, N. K.; Yang, B.; Zhao, M.; Ruenroengklin, N.; Jiang, Y. *J. Food Process Eng.* **2009**, *32*, 828–843.
46. Chafer, A.; Pascual-Marti, M. C.; Salvador, A.; Berna, A. *J. Sep. Sci.* **2005**, *28*, 2050–2056.
47. Laroze, L.; Soto, C.; Zuniga, M. E. *Electron. J. Biotechnol.* **2010**, *13*, 1–11.
48. Puri, M.; Sharma, D.; Barrow, C. J. *Trends Biotechnol.* **2012**, *30*, 37–44.

49. Pinelo, M.; Zornoza, B.; Meyer, A. S. *Sep. Purif. Technol.* **2008**, *63*, 620–627.
50. Kaur, A.; Singh, S.; Singh, R. S.; Schwarz, W. H.; Puri, M. *J. Chem. Technol. Biotechnol.* **2010**, *85*, 1419–1422.
51. Le, H. V.; Le, V. V. M. *Int. J. Food Sci. Technol.* **2012**, *47*, 1206–1214.
52. Zilic, S.; Mogol, B. A.; Akillioglu, G.; Serpen, A.; Babic, M.; Gokmen, V. *J. Cereal Sci.* **2013**, *58*, 1–7.
53. Chen, Y.; Yu, L. J.; Rupasinghe, H. *J. Sci. Food Agric.* **2013**, *93*, 981–986.
54. Mateo Anson, N.; Van den Berg, R.; Havenaar, R.; Bast, A.; Haenen, G. R. *J. Agric. Food Chem.* **2008**, *56*, 5589–5594.
55. Mulinacci, N.; Ieri, F.; Giaccherini, C.; Innocenti, M.; Andrenelli, L.; Canova, G.; Saracchi, M.; Casiraghi, M. C. *J. Agric. Food Chem.* **2008**, *56*, 11830–11837.
56. Ajila, C. M.; Brar, S. K.; Verma, M.; Tyagi, R. D.; Valero, J. R. *Food Chem.* **2011**, *126*, 1071–1080.
57. Lopez, C.; Torrado, A.; Guerra, N. P.; Pastrana, L. *J. Agric. Food Chem.* **2005**, *53*, 989–995.
58. Zheng, Z.; Shetty, K. *J. Agric. Food Chem.* **2000**, *48*, 895–900.
59. Brown, C. R.; Durst, R. W.; Wrolstad, R.; De Jong, W. *Potato Res.* **2008**, *51*, 259–270.
60. Grzegorzewski, F.; Ehlbeck, J.; Schluter, O.; Kroh, L. W.; Rohn, S. *LWT- Food Sci. Technol.* **2011**, *44*, 2285–2289.
61. Caminiti, I. M.; Noci, F.; Munoz, A.; Whyte, P.; Morgan, D. J.; Cronin, D. A.; Lyng, J. G. *Food Chem.* **2011**, *124*, 1387–1392.
62. Ravichandran, K.; Ahmed, A. R.; Knorr, D.; Smetanska, I. *Food Res. Int.* **2012**, *48*, 16–20.
63. Patras, A.; Brunton, N.; Pieve, S. D.; Butler, F. *Innovative Food Sci. Emerging Technol.* **2009**, *10*, 308–313.
64. Suthathangjai, W.; Kajda, P.; Zabetakis, L. *Food Chem.* **2005**, *90*, 193–197.
65. Uckoo, R. M.; Jayaprakasha, G. K.; Somerville, J. A.; Balasubramaniam, V. M.; Pinarte, M.; Patil, B. S. *Innovative Food Sci. Emerging Technol.* **2013**, *18*, 7–14.
66. Shen, Y.; Sun, Y.; Qiao, L.; Chen, J.; Liu, D.; Ye, X. *Postharvest Biol. Technol.* **2013**, *76*, 50–57.
67. Fernandes, A.; Barros, L.; Antonio, A. L.; Barreira, J. C.; Oliveira, M.; Martins, A.; Ferreira, I. *Food Bioprocess Technol.* **2014**, *7*, 3012–3021.
68. Jeyamkondan, S.; Jayas, D. S.; Holly, R. A. *J. Food Prot.* **1999**, *62*, 1088–1096.
69. Odriozola-Serrano, I.; Soliva-Fortuny, R.; Martin-Belloso, O. *LWT- Food Sci. Technol.* **2009**, *42*, 93–100.
70. Vallverdu-Queralt, A.; Oms-Oliu, G.; Odriozola-Serrano, I.; Lamuela-Raventos, R. M.; Martin-Belloso, O.; Elez-Martinez, P. *Food Chem.* **2013**, *136*, 199–205.
71. Alighourchi, H. R.; Barzegar, M.; Sahari, M. A.; Abbasi, S. *Int. Food. Res. J.* **2013**, *20*, 1703–1709.
72. Berker, K. I.; Olgun, F. A. O.; Ozyurt, D.; Demirata, B.; Apak, R. *J. Agric. Food Chem.* **2013**, *61*, 4783–4791.

73. Medina, M. *J. Agric. Food Chem.* **2011**, *59*, 1565–1571.
74. Apak, R.; Guclu, K.; Demirata, B.; Ozyurek, M.; Celik, S. E.; Bektasoglu, B.; Berker, K. L.; Ozyurt, D. *Molecules* **2007**, *12*, 1496–1547.
75. Serpen, A.; Capuano, E.; Fogliano, V.; Gokmen, V. *J. Agric. Food Chem.* **2007**, *55*, 7676–7681.
76. Atanackovic, M.; Aleksandar, P.; Jovic, S.; Gojkovic-Bukarica, L.; Bursac, M.; Cvejic, J. *Food Chem.* **2012**, *131*, 531–518.
77. Farvin, K. H. S.; Jacobsen, C. *Food Chem.* **2013**, *138*, 1670–1681.
78. Ignat, I.; Volf, I.; Popa, V. *Food Chem.* **2011**, *126*, 1821–1835.
79. Jia, P.; Wang, S.; Meng, X.; Lan, W.; Luo, J.; Liao, S.; Xiao, C.; Zheng, X.; Li, L.; Liu, Q.; Zheng, J.; Zhou, Y.; Zheng, X. *Talanta* **2013**, *107*, 103–110.
80. Bayram, B.; Ozcelik, B.; Schultheiss, G.; Frank, J.; Rimbacha, G. *Food Chem.* **2013**, *138*, 1663–1669.
81. Mattila, P.; Astola, J.; Kumpulainen, J. *J. Agric. Food Chem.* **2000**, *48*, 5834–5841.
82. Harris, C. S.; Burt, A. J.; Saleem, A.; Le, P. M.; Martineau, L. C.; Haddad, P. S.; Bennett, S. A.; Arnason, J. T. *Phytochem. Anal.* **2007**, *18*, 161–169.
83. Oh, Y. S.; Lee, J. H.; Yoon, S. H.; Oh, C. H.; Choi, D. S.; Choe, E.; Jung, M. Y. *J. Food Sci.* **2008**, *73*, 378–389.
84. Cavaliere, C.; Foglia, P.; Gubbiotti, R.; Sacchetti, P.; Samperi, R.; Lagana, A. *Rapid Commun. Mass Spectrom.* **2008**, *22*, 3089–3099.
85. Pawlowska, A. M.; Oleszek, W.; Braca, A. *J. Agric. Food Chem.* **2008**, *56*, 3377–3380.
86. Christophoridou, S.; Dais, P. *Anal. Chim. Acta.* **2009**, *633*, 283–292.
87. Svendsen, C. N. *Analyst* **1993**, *118*, 123–129.
88. Guo, C.; Cao, G.; Sofic, E.; Prior, R. L. *J. Agric. Food Chem.* **1997**, *45*, 1787–1796.
89. Lin, L.; Harnly, J. M. *Food Chem.* **2010**, *120*, 319–326.
90. Jeyadevi, R.; Sivasudha, T.; Rameshkumar, A.; Harnly, J. M.; Lin, L. *J. Funct. Foods* **2013**, *5*, 289–298.
91. Marmet, C.; Actis-Goretta, L.; Renouf, M.; Giuffrida, F. *J. Pharmaceut. Biomed.* **2014**, *88*, 617–625.
92. Cruz, A.; Hilbert, G.; Riviere, C.; Mengin, V.; Ollat, N.; Bordenave, L.; Decroocq, S.; Delaunay, J.; Delrot, S.; Merillon, J.; Monti, J.; Gomes, E.; Richard, T. *Anal. Chim. Acta* **2012**, *732*, 145–152.
93. Braunberger, C.; Zehl, M.; Conrad, J.; Fischer, S.; Adhami, H.; Beifuss, U.; Krenn, L. *J. Chromatogr. B* **2013**, *932*, 111–116.
94. Melone, F.; Saladino, R.; Lange, H.; Crestini, C. *J. Agric. Food Chem.* **2013**, *61*, 9307–9315.
95. Phalgune, U. D.; Rajamohanam, P. R.; Gaikwad, B. G.; Varma, R. J.; George, S. *Appl. Biochem. Biotechnol.* **2012**, *169*, 2029–2037.
96. Luthria, D. L.; Mukhopadhyay, S.; Lin, L.; Harnly, J. *Appl. Spectrosc.* **2011**, *65*, 250–259.
97. Lu, Y.; Gao, B.; Chen, P.; Charles, D.; Yu, L. *Food Chem.* **2014**, *154*, 262–268.
98. Gao, B.; Lu, Y.; Sheng, Y.; Chen, P.; Yu, L. *J. Agric. Food Chem.* **2013**, *61*, 2957–2963.

99. Michalkiewicz, A.; Biesaga, M.; Pyrzynska, K. *J. Chromatogr. A* **2008**, *1187*, 18–24.
100. Perez-Magarino, S.; Ortega-Heras, M.; Cano-Mozo, E. *J. Agric. Food Chem.* **2008**, *56*, 11560–11570.
101. Inglett, G. E.; Rose, D.; Stevenson, D. G.; Chen, D.; Biswas, A. *Cereal Sci.* **2009**, *86*, 661–664.
102. Rodriguez-Rojo, S.; Visenti, A.; Maestri, D.; Cocero, M. J. *J. Food Eng.* **2012**, *109*, 98–103.
103. Onder, F. C.; Ay, M.; Sarker, S. D. *J. Agric. Food Chem.* **2013**, *61*, 10498–10506.
104. Proestos, C.; Komaitis, M. *Foods* **2013**, *2*, 90–99.
105. Dai, D.; He, J.; Sun, R.; Zhang, R.; Aisa, H. A.; Abliz, Z. *Anal. Chim. Acta* **2009**, *632*, 221–228.
106. Ouattara, B.; Angenot, L.; Guissou, P.; Fondu, P.; Dubois, J.; Frederich, M.; Jansen, O.; Van Heugen, J. C.; Wauters, J. N.; Tits, M. *Phytochemistry* **2004**, *65*, 1145–1151.

Chapter 2

Innovative Methods for the Extraction and Chromatographic Analysis of Honey Bee Products

Federica Pellati*

Department of Life Sciences, University of Modena and Reggio Emilia,
Via G. Campi 183, 41125 Modena, Italy
*E-mail: federica.pellati@unimore.it.

The aim of this study was to provide an overview of recent techniques developed for the chemical characterization of raw propolis, based on the determination of polyphenols and volatile compounds, which are responsible for the biological activity of the extracts widely used in apitherapy. The analysis of polyphenols, including phenolic acids and flavonoids, was performed by RP-HPLC coupled with UV/DAD and MS detection. As regards the extraction of polyphenols from raw propolis, microwave-assisted extraction (MAE) was carried out for these constituents and its parameters were optimized by means of response surface experimental design methodology. The characterization of propolis volatile compounds was based on GC coupled with MS detection. In this ambit, a suitable HS-SPME extraction procedure was developed using a PDMS fiber. These chromatographic techniques were applied to raw propolis samples collected from different Italian regions to determine their fingerprinting, thus providing new and reliable tools for the complete chemical characterization of this biologically active material.

Introduction

Propolis (also known as bee glue) is a resinous material collected and processed by honeybees (*Apis mellifera* L.) from several tree species (*I*). In regions with temperate climate, the resin is collected mainly from buds and cracks

in the bark of *Populus* species (2); then, it is enriched with bee salivary and enzymatic secretions (1). The resulting product is used by bees to seal holes in their hives, to exclude draught and to make the entrance of the hive weather tight or easier to defend (1). Another advantage for bees is the capacity of this material to reduce the incidence of bacteria and moulds within the hive (2).

Propolis is a chemically complex mixture composed of 50% resin (containing polyphenols), 30% wax, 10% essential oil, 5% pollen and 5% other organic compounds (1). A series of biological properties have been described for propolis extracts, such as antibacterial, antifungal, antiviral, antioxidant, anti-inflammatory, antiproliferative and immunostimulant (3). Typical applications of propolis include herbal products for cold syndrome and dermatological preparations (4). Propolis extracts are also used to prevent and treat oral inflammation (4).

Several methods have been described in the literature for the analysis of polyphenols in propolis, based either on non-separation or on separation techniques (1). Spectrophotometric methods are considered to be useful especially for the routine control of propolis samples (1, 5). In the ambit of chromatographic techniques, HPLC is a very powerful tool for the chemical analysis of complex matrices, such as propolis, since it provides a reliable determination of individual phenolic compounds (1, 6–8). In particular, HPLC in combination with spectroscopic and spectrometric detection has significantly improved the analysis of phenolic compounds in natural products derived from bees, providing definitive information for the identification and quantification of these biologically active constituents (1).

In addition to phenolics, another important class of propolis constituents is represented by volatile compounds (4). Previous studies performed on propolis volatile fraction have been focused on the gas chromatographic (GC) analysis of the essential oil extracted by hydrodistillation (HD) (4, 9–11). In this ambit, the composition of propolis essential oil from different countries has been described (4, 9–11). In some of these studies, propolis essential oil has demonstrated antimicrobial activity mainly against Gram-positive bacteria, but it is also active on Gram-negative bacteria and fungi (4).

Due to the complex chemical composition of propolis, innovative and reliable methods for comprehensive multi-component analysis of this biologically active apiary product have been recently developed. In particular, this review summarizes the results of recent studies aimed at the determination of propolis polyphenols by means of HPLC-UV/DAD, HPLC-ESI-MS and MS/MS techniques (13); a HS-SPME-GC-MS method is also described for the determination of volatile compounds (14).

HPLC-UV/DAD and ESI-MS Analysis of Propolis Polyphenols on a Conventional Fully-Porous Stationary phase

Regarding propolis polyphenols, a HPLC method was firstly developed on a conventional fully-porous reversed-phase stationary phase to provide a complete chemical profiling (12). Figure 1 shows a representative HPLC-UV/DAD chromatogram obtained at 290 nm for propolis polyphenols, using an Ascentis

C₁₈ column (250 mm × 4.6 mm I.D., 5 μm, Supelco) (12). A mobile phase composed of 0.1% formic acid in water and acetonitrile was selected in order to be compatible with ESI-MS. The other chromatographic parameters, such as gradient elution, flow-rate and column temperature were also optimized.

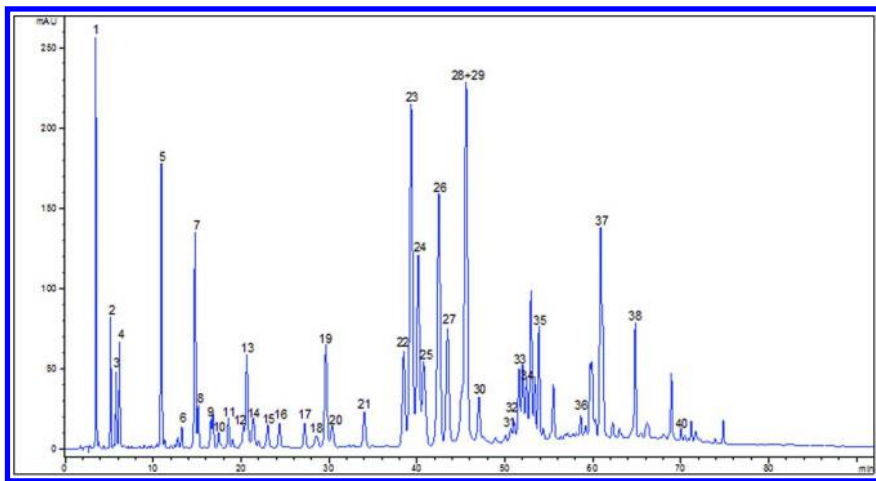


Figure 1. Representative HPLC-UV/DAD chromatogram of a propolis hydroalcoholic extract at 290 nm on a conventional fully-porous stationary phase. For peak identification, see Tables 1-3.

The chromatographic data and UV spectra, in comparison with reference standards, allowed the assignment of the main classes of polyphenols occurring in propolis, such as phenolic acids and flavonoids, since each class exhibits a characteristic UV/Vis spectrum. However, retention time data and UV spectra alone did not provide sufficient information for the correct identification of the constituents in such a complex matrix. For this reason, HPLC-ESI-MS experiments were performed, using the same conditions previously described for HPLC-UV/DAD. The performance of two types of mass analyzers, including an ion trap and a triple quadrupole, was compared (12). For both mass analyzers, MS data were collected in the full-scan positive and negative ion modes. For the ion trap mass analyzer, MS² spectra were automatically performed with helium as the collision gas (12). For the triple quadrupole mass analyzer, the product ion scan (PIS) mode was carried out using nitrogen as the collision gas (12); in this case, the collision energy was optimized for phenolic acids and flavonoids.

MS and MS/MS data allowed the identification of 40 phenolic compounds (12), whose fragmentation pathways were evaluated by both mass analyzers. When the reference standards were available, the identification was further confirmed by comparison of the MS and MS/MS data with those of the standard compounds. Under the applied conditions, the triple quadrupole mass analyzer provided a higher fragmentation degree of the target analytes in comparison with the ion trap and, therefore, more structural information (12).

Table 1 shows the chemical structures of phenolic acids identified in propolis extracts (12). Five caffeic acid derivatives were also detected in propolis, together with four *p*-coumaric acid esters (12). For all these compounds, the negative ion mode provided a higher level of sensitivity if compared with the positive one.

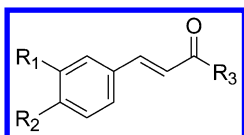


Table 1. Structures of Phenolic Acids and Derivatives Identified in Propolis Extracts^a

<i>Compound</i>	<i>Peak number</i>	<i>R</i> ₁	<i>R</i> ₂	<i>R</i> ₃
Caffeic acid	1	OH	OH	OH
<i>p</i> -Coumaric acid	2	H	OH	OH
Ferulic acid	3	OCH ₃	OH	OH
Isoferulic acid	4	OH	OCH ₃	OH
3,4-Dimethyl-caffeic acid (DMCA)	5	OCH ₃	OCH ₃	OH
Cinnamic acid	9	H	H	OH
Caffeic acid prenyl ester	22/25	OH	OH	
Caffeic acid benzyl ester	24	OH	OH	
Caffeic acid phenylethyl ester (CAPE)	28	OH	OH	
<i>p</i> -Coumaric acid prenyl ester	31/34	H	OH	
<i>p</i> -Coumaric acid benzyl ester	32	H	OH	
Caffeic acid cinnamyl ester	33	OH	OH	
<i>p</i> -Coumaric acid cinnamyl ester	36	H	OH	
<i>p</i> -Methoxy cinnamic acid cinnamyl ester	40	H	OCH ₃	

^a Compounds are in order of elution time on the conventional fully-porous stationary phase.

Source: Reproduced with permission from reference (12). Copyright (2011) Elsevier.

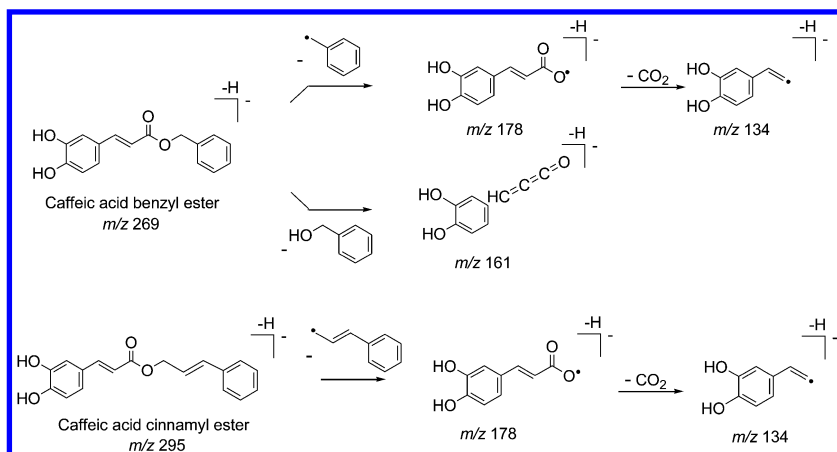


Figure 2. Fragmentation pathways of caffeic acid benzyl and cinnamyl esters in the negative ion mode.

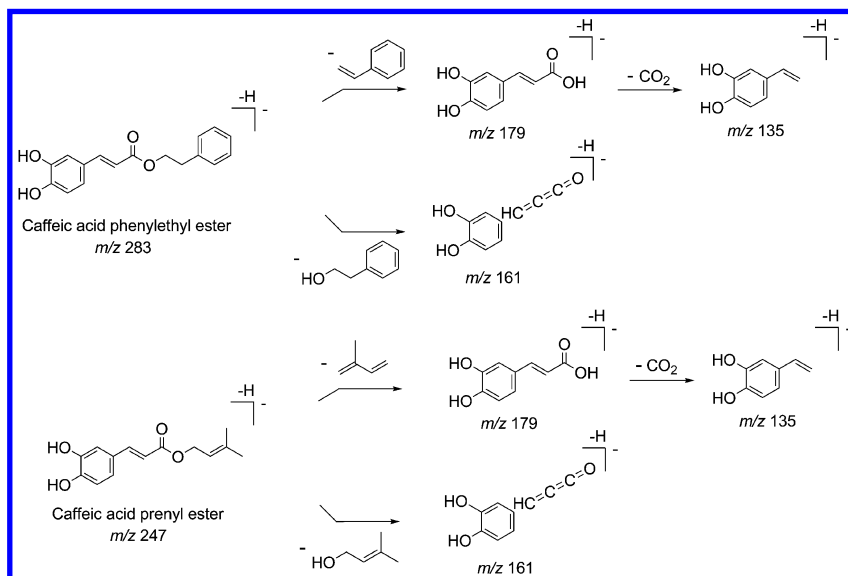


Figure 3. Fragmentation pathways of caffeic acid phenylethyl and prenyl esters in the negative ion mode.

As shown in Figures 2 and 3, the main fragmentation mechanism for caffeic acid derivatives in the negative mode with both mass analyzers was based on the homolytic and heterolytic cleavages of the bonds with the benzyl, cinnamyl, phenylethyl and prenyl groups, which generated an odd electron product ion at m/z 178 and a negative product ion at m/z 179, respectively, which, after the loss of a CO_2 molecule, originated further fragments at m/z 134 and 135, respectively (12). More specifically, the first mechanism was observed for the benzyl and the cinnamyl caffeate derivatives (Figure 2), while the second pattern occurred for the phenylethyl (CAPE) and the prenyl caffeate derivatives (Figure 3). In the MS/MS spectra obtained by triple quadrupole mass analyzer in the negative mode, the benzyl, phenylethyl and prenyl caffeate derivatives showed also a common negative fragment at m/z 161, due to the heterolytic cleavage of the C–O ester bond of the deprotonated molecule (12).

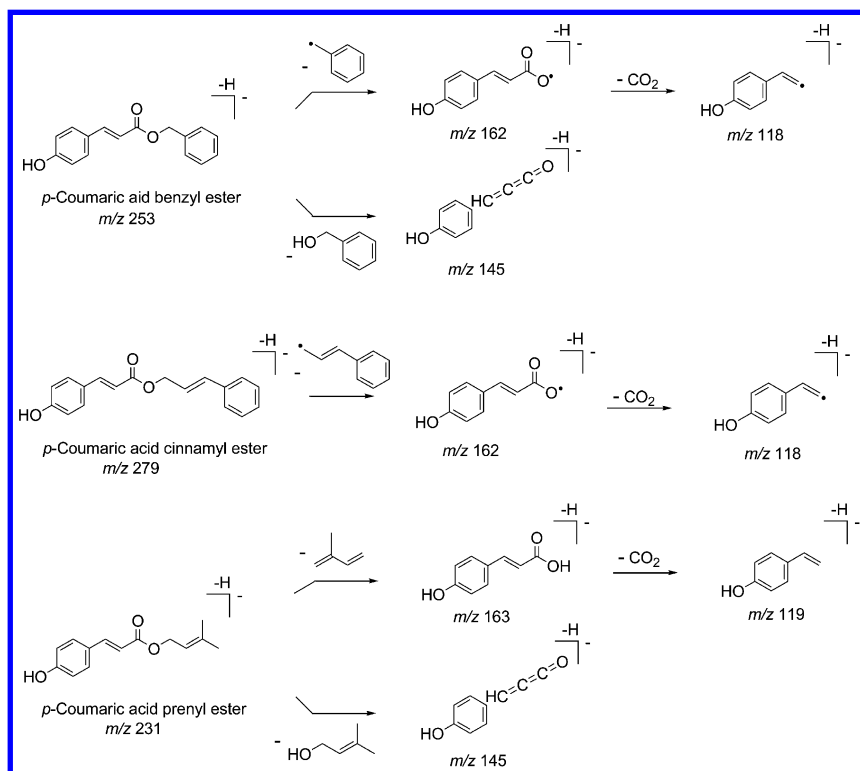


Figure 4. Fragmentation pathways of *p*-coumaric acid benzyl, cinnamyl and prenyl esters in the negative ion mode.

In analogy with caffeate derivatives, the MS/MS spectra of *p*-coumaric acid derivatives in the negative mode with both mass analyzers indicated a fragmentation pattern based on the homolytic and heterolytic cleavages of the bonds with the benzyl, cinnamyl and prenyl groups (Figure 4), which generated a

radical product ion at m/z 162 and a negative product ion at m/z 163, respectively, which, after the loss of a CO_2 molecule, originated further fragments at m/z 118 and 119, respectively (12). In particular, the first mechanism was observed for the benzyl and the cinnamyl coumarate derivatives, while the second pattern occurred in the case of the prenyl coumarate derivative. Another negative product ion at m/z 145 was obtained for the benzyl and the prenyl coumarate derivatives, originated from the heterolytic breakdown of the C–O ester bond of the deprotonated molecule (12).

All flavonoids occurring in the samples of propolis analyzed showed protonated and deprotonated molecules of good intensity in the positive and in the negative ion mode, respectively. In this way, it was possible to individuate flavones, flavonols, flavanones and dihydroflavonols (Tables 2 and 3) (12), either as free form or as ether or ester derivatives.

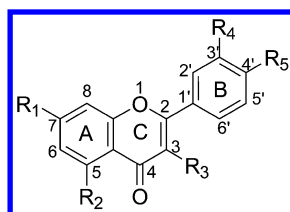


Table 2. Structures of flavones and flavonols identified in propolis extracts^a. Source: Reproduced with permission from reference (12). Copyright (2011) Elsevier.

<i>Compound</i>	<i>Peak number</i>	R_1	R_2	R_3	R_4	R_5
Quercetin	6	OH	OH	OH	OH	OH
Quercetin-3-methyl-ether	8	OH	OH	OCH_3	OH	OH
Chrysin-5-methyl-ether	10	OH	OCH_3	H	H	H
Apigenin	11	OH	OH	H	H	OH
Kaempferol	12	OH	OH	OH	H	OH
Isorhamnetin	14	OH	OH	OH	OCH_3	OH
Galangin-5-methyl-ether	17	OH	OCH_3	OH	H	H
Quercetin-7-methyl-ether	20	OCH_3	OH	OH	OH	OH
Chrysin	23	OH	OH	H	H	H
Galangin	27	OH	OH	OH	H	H

^a Compounds are in order of elution time on the conventional fully-porous stationary phase.

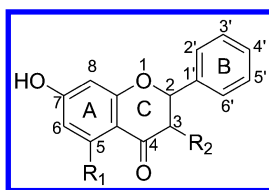


Table 3. Structures of flavanones and dihydroflavonols identified in propolis extracts^a. Source: Reproduced with permission from reference (12). Copyright (2011) Elsevier.

<i>Compound</i>	<i>Peak number</i>	<i>R₁</i>	<i>R₂</i>
Pinobanksin-5-methyl-ether	7	OCH ₃	OH
Pinobanksin	13	OH	OH
Pinobanksin-5-methyl-ether-3- <i>O</i> -acetate	18	OCH ₃	OCOCH ₃
Pinocebrin	26	OH	H
Pinobanksin-3- <i>O</i> -acetate	29	OH	OCOCH ₃
Pinobanksin-3- <i>O</i> -propionate	35	OH	OCOC ₂ H ₅
Pinobanksin-3- <i>O</i> -butyrate ^b	37	OH	OCOC ₃ H ₇
Pinobanksin-3- <i>O</i> -pentanoate ^b	38	OH	OCOC ₄ H ₉
Pinobanksin-3- <i>O</i> -hexanoate ^b	39	OH	OCOC ₅ H ₁₁

^a Compounds are in order of elution time on the conventional fully-porous stationary phase. ^b Or positional isomers.

MS/MS spectra were recorded to study the fragmentation pathways of the different classes of flavonoids. It is well-known that the most useful fragmentations in terms of flavonoid identification are those that require the cleavage of two C–C bonds of the C-ring, due to retro-Diels-Alder (RDA) reactions, resulting in structurally informative ions containing the A or B ring (Figure 5) (12). In particular, the 1/3 position was involved in the RDA reactions of all flavonoid classes present in propolis extracts in the positive ion mode, originating an $[^{1,3}A]^+$ ion, which was observed for all flavonoid groups and usually occurred at m/z 153 for un-substituted compounds. In the negative ion mode, different mechanisms and structures have been proposed for retro-Diels-Alder reactions of flavonoids (Figure 6) (12). The $[^{1,3}A]^-$ ions of flavones, flavonols and flavanones were found at m/z 151 in the negative mode.

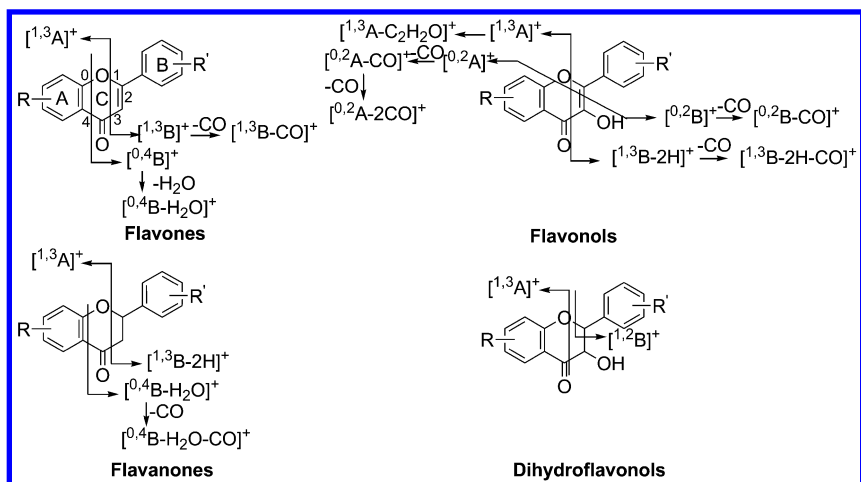


Figure 5. Fragmentation pathways of propolis flavonoids in the positive ion mode.

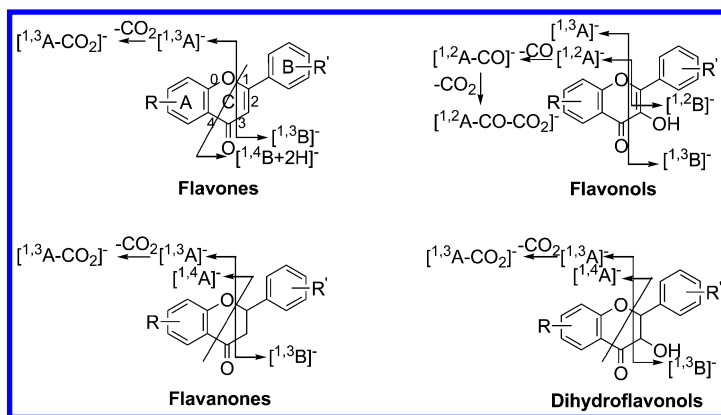


Figure 6. Fragmentation pathways of propolis flavonoids in the negative ion mode.

Among dihydroflavonols, pinobanksin esters deserve a specific comment. The first fragmentation observed for these compounds was the loss of the acyl group, which in turn underwent the loss of one H₂O molecule (Figure 7) (12). All subsequent fragmentation steps of pinobanksin esters followed the pathways proposed for flavones, both in the positive and negative ion modes. In this way, pinobanksin-3-*O*-acetate, propionate, butyrate (or isomer), pentanoate (or isomer) and hexanoate (or isomer) were identified (12).

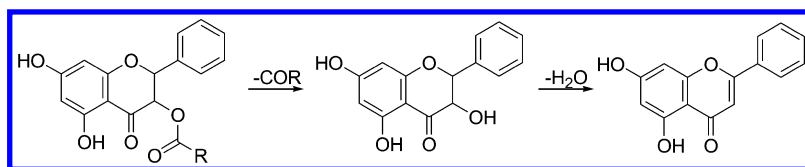


Figure 7. General fragmentation pattern of pinobanksin esters.

HPLC-UV/DAD and ESI-MS Analysis of Propolis Polyphenols on a Fused-Core Stationary Phase

Due to the long analysis time of propolis components on a conventional fully porous stationary phase, the fused-core technology was evaluated (13). A fused-core support is characterized by 2.7 μm particles, which comprise a solid 1.7 μm diameter silica core that is encapsulated in a 0.5 μm thick layer of porous silica gel (15). Compared with fully porous particles, the fused-core ones have a much shorter diffusion path because of the solid core (15). This tends to reduce the axial dispersion of solutes and minimizes peak broadening (15). Several studies have shown that fused-core columns offer good chromatographic performance, such as narrow peaks, high resolution and a short analysis time (16). This type of support can provide speed and efficiency similar to column packed with sub-2 μm particles, but with reduced backpressure (15). This allows fused-core columns to be applied to conventional HPLC equipment, operating within the 400 bar pressure limit.

In particular, the method initially developed on the fully porous stationary phase was transferred to a fused-core Ascentis Express C₁₈ column (150 mm \times 3.0 mm I.D., 2.7 μm , Supelco) (13), but the flow rate was decreased from 1.2 to 0.6 mL/min to avoid the risk of excessive backpressure. A parallel careful adaptation of the mobile phase gradient was performed. As regards column temperature, the best separation was obtained by setting this parameter at 30 $^{\circ}\text{C}$. In this way, the total analysis time was decreased from 92 to 65 min, with a consequent advantage in terms of time and solvent usage. Under these conditions (13), the highest observed backpressure was about 300 bar, within the previously mentioned pressure limit of conventional HPLC systems.

The HPLC-UV/DAD analysis at 290 nm of a hydroalcoholic extract obtained from a representative sample of raw propolis is shown in Figure 8 (13). Considering the complexity of the sample, the chromatographic separation can be considered satisfactory. The elution order of propolis polyphenols on the fused-core column was slightly different if compared with the fully porous one. It should also be pointed out that the peaks corresponding to pinobanksin-3-*O*-acetate (29) and caffeic acid phenylethyl ester (CAPE) (28), that were completely overlapped on the conventional fully porous column, were well-resolved using the fused-core stationary phase. Peaks were narrower with the fused-core column and also more symmetric.

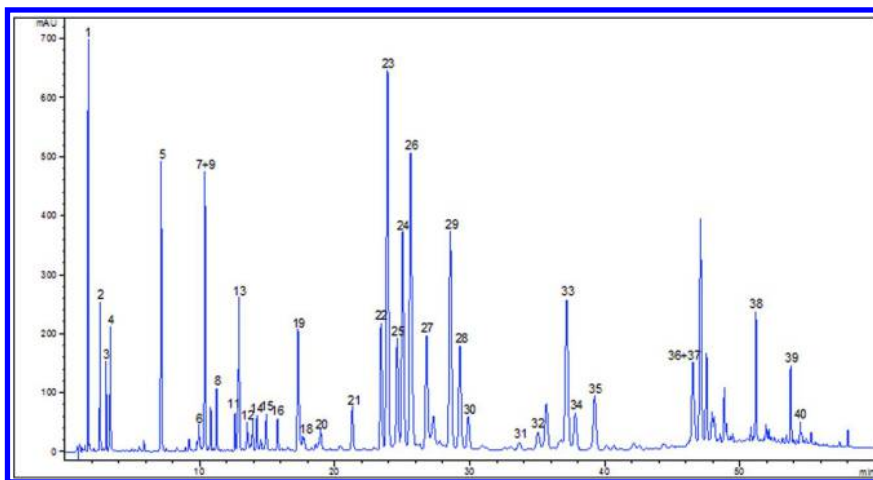


Figure 8. Representative HPLC-UV/DAD chromatogram of a propolis hydroalcoholic extract at 290 nm on a fused-core stationary phase. For peak identification, see Tables 1-3. Adapted with permission from reference (13). Copyright (2013) Elsevier.

Methods for the Extraction of Polyphenols from Raw Propolis

As for the extraction of polyphenols from raw propolis, four methods were evaluated in order to obtain an efficient and rapid extraction of these compounds (13). The comparison was carried out between conventional extraction methods (including maceration, heat-reflux extraction (HRE) and ultrasound-assisted extraction (UAE)) and microwave-assisted extraction, which represents a more innovative extraction procedure (13). The applied sample-to-solvent ratio was 1:10 (w/v). EtOH-H₂O (80:20, v/v) was used as the extraction solvent for maceration, HRE and UAE.

Traditional methods of optimization evaluate the effect of one variable at a time, keeping all the others constant during the experiments with the exception of the one being studied. However, this type of experiment does not allow to determine what it would happen if the other variables also change. The experimental design enables the effects of several variables to be estimated simultaneously: following a sequential approach, it allows firstly to obtain information on the significance of the factors and secondly to explore more thoroughly the most promising variables. In particular, response surface experimental design methodology coupled with central composite design (CCD) is a useful tool to optimize procedures depending on several variables (17).

The experimental parameters, selected to optimize the extraction of polyphenols from raw propolis by means of closed-vessel MAE, included solvent composition, extraction temperature and time (13). The results of the CCD indicated that the linear and the quadratic term of the extraction time, as well

as its interaction with the other factors, did not show a significant influence on the efficiency of the extraction process. In the light of this, a second CCD was set up, focusing on solvent composition and extraction temperature, and keeping the extraction time constant (13). As a confirmation of what was observed with the previous CCD, the solvent composition showed a strong influence on the extraction yield of phenolics from raw propolis. The interaction between solvent composition and extraction temperature was also found to be significant in the extraction procedure.

The analysis of the second CCD was performed by response surface methodology (13); this surface represents a good description of the relationship between the experimental variables and the response within a limited experimental domain. Figure 9 shows the response surface plot for the total amount of the extracted compounds *versus* solvent composition and extraction temperature, with an extraction time equal to 15 min (13). The experimental results showed that the best global response, within the range studied, was reached when the extraction temperature was set at 106 °C, the extraction solvent close to EtOH-H₂O 80:20 (v/v), with an extraction time of 15 min (13). These values were therefore selected for the extraction of polyphenols from raw propolis in all the subsequent analyses.

The total amount of representative propolis phenolic compounds extracted under optimized MAE conditions was then compared with those obtained by maceration, HRE and UAE. It was found that the MAE technique allowed to obtain the yield of other methods in only 15 min (13). With the assistance of the fast heating of microwave irradiation, the extraction with MAE was improved by a reduced extraction time and half volume of solvent needed.

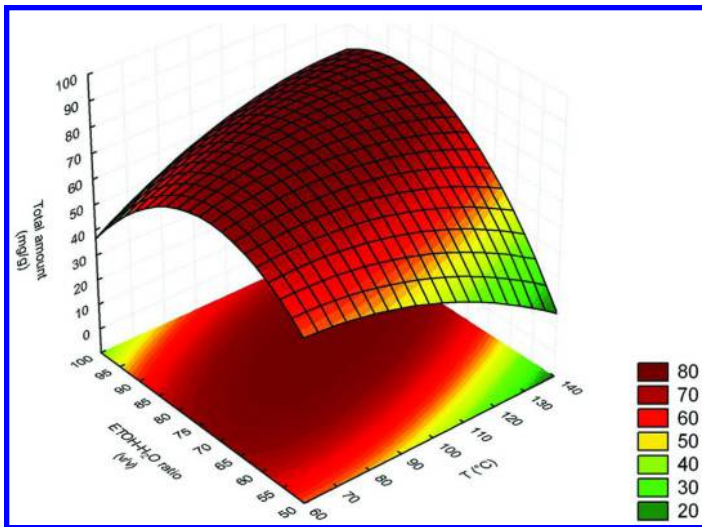


Figure 9. Response surface plot for total amount (mg/g) of six representative polyphenolic compounds extracted from raw propolis versus solvent composition and extraction temperature, with a constant extraction time equal to 15 min. Reproduced with permission from reference (13). Copyright (2013) Elsevier.

Analysis of Polyphenols in Raw Propolis Samples

The optimized MAE procedure and RP-HPLC method on the fused-core column were validated and applied to the analysis of nine Italian samples of raw propolis (13). The overall chemical composition was the same in all the samples analyzed, including phenolic acids, flavones, flavonols, flavanones and dihydroflavonols. This polyphenol composition was found to be in agreement with what has been described for bud extracts from *Populus* (18, 19).

As regards quantitative data, a significant variability in the content of total phenolics, including both phenolic acids and flavonoids, was observed in these samples, as shown in Figure 10 (13). Data are expressed as mg/g. On the basis of total flavonoid content (expressed as percentage) (6), propolis with a value lower than 11% should be considered of low quality, while that with a value of 11-14% or 14-17% should be classified as acceptable or good, respectively. In this context, samples RP-1, RP-2, RP-3, RP-5, RP-7 and RP-9 can be considered as low quality; sample RP-4 as acceptable; samples RP-6 and RP-8 as good (13). In the samples analyzed, the most abundant flavonoids were chrysin, pinocembrin, galangin and pinobanksin-3-*O*-acetate. Regarding phenolic acids, caffeic acid, *p*-coumaric acid and ferulic acid were the most abundant ones. As for phenolic acid derivatives, 3,4-dimethyl caffeic acid (DMCA), caffeic acid prenyl, benzyl, phenylethyl (CAPE) and cinnamyl esters were the most representative compounds.

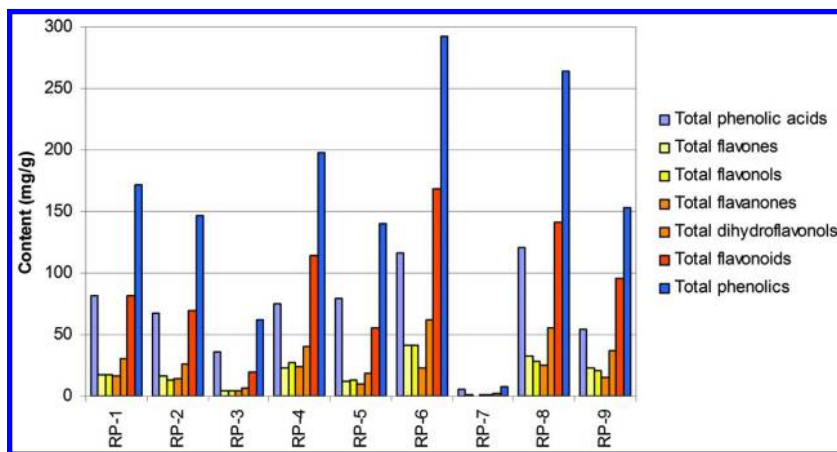


Figure 10. Content (expressed as mg/g) of polyphenols in Italian samples of raw propolis. Adapted with permission from reference (13). Copyright (2013) Elsevier.

HS-SPME-GC-MS Analysis of Propolis Volatile Compounds

Regarding the analysis of propolis volatile fraction, a novel and efficient method based on headspace solid-phase microextraction (HS-SPME), followed by gas chromatography-mass spectrometry (GC-MS), has been recently developed (14). Even if volatile compounds are present at low concentration in propolis, their

aroma and biological activity make them of importance for the characterization of this product. In addition, the volatile composition can give valuable information about the origin of samples. In particular, after the optimization of the extraction conditions, comparative studies on the typical HS-SPME-GC-MS profiles of raw propolis samples collected from different Italian regions were performed with the aim of confirming the applicability of the method developed for the chemical characterization of their volatile compounds (14).

HS-SPME is a multistage equilibrium sampling method which is known to be influenced by many parameters (20, 21). In this ambit, the first step of the method optimization was the selection of the best fiber coating for HS-SPME (14). To obtain the optimal HS-SPME conditions, additional variables were chosen, including sample amount, extraction temperature, equilibrium time and extraction time. Other parameters, such as salt addition and sample agitation during the equilibrium time, were also studied.

The fiber screening was carried out using two fiber types, including a polydimethylsiloxane (PDMS, 100 μm) and a divinylbenzene-carboxen-polydimethylsiloxane (DVB-CAR-PDMS, 50/30 μm) (14). Of these two fibers, the DVB-CAR-PDMS showed a strong extraction affinity for carboxylic acids and, in particular, for benzoic acid; in samples where benzoic acid was present at high level, this caused a significant peak broadening and tailing, with the consequent overlapping of adjacent compounds (14). The PDMS fiber was finally selected, because it allowed to obtain a better profile for all classes of propolis volatile compounds (Figure 11) and a composition more similar to the essential oil processed by HD (14).

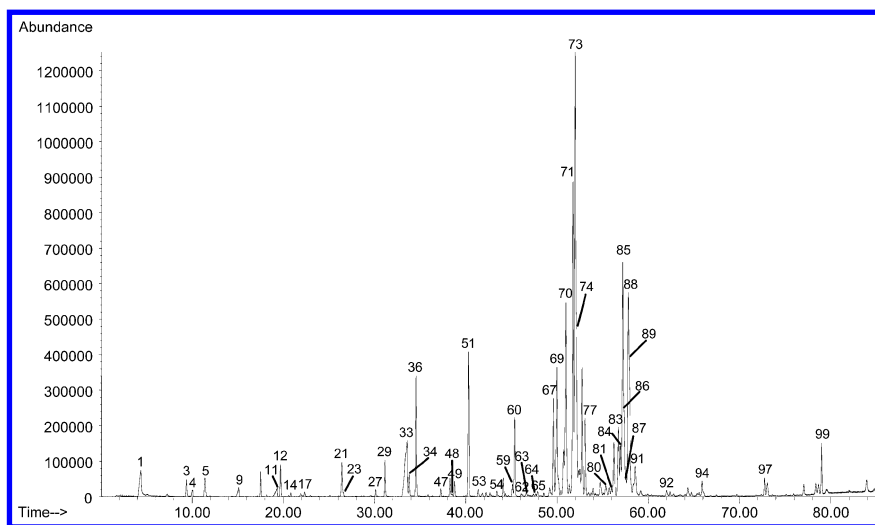


Figure 11. Representative total ion current (TIC) chromatogram obtained by HS-SPME-GS-MS analysis of propolis volatile compounds, using a 100 μm PDMS fiber. For peak identification, see reference (14).

Qualitative and semi-quantitative analysis of propolis volatile compounds was performed by GC-MS on a HP-5 MS cross-linked 5% diphenyl-95% dimethyl polysiloxane capillary column (30 m × 0.25 mm I.D., 1.00 μm film thickness, Agilent Technologies) (14). Ninety-nine constituents were identified using this technique in raw propolis collected from different Italian regions (14). Figure 12 shows the distribution of the main classes of propolis volatile compounds in the samples analyzed; data are expressed as % peak area values.

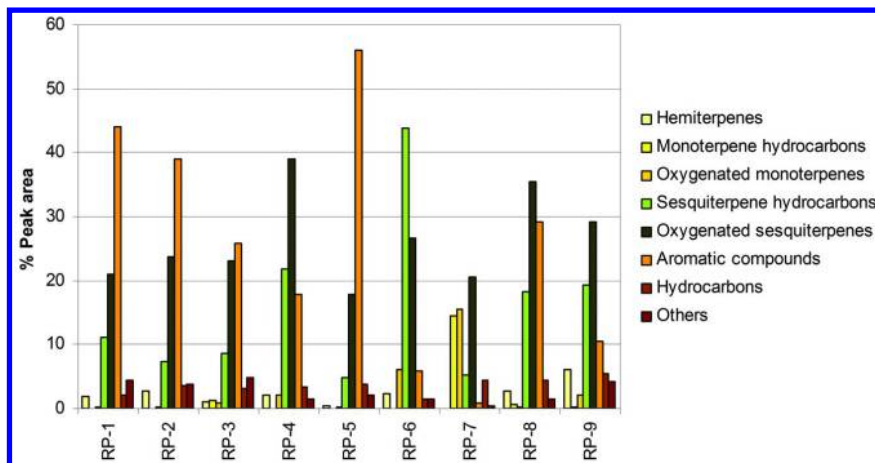


Figure 12. Semi-quantitative data (expressed as % peak area) of the main classes of volatile compounds in Italian samples of raw propolis. Adapted with permission from reference (14). Copyright (2013) Elsevier.

Among propolis volatile compounds, the most abundant constituents include aromatic compounds, such as benzoic acid and its esters (benzyl benzoate, benzyl salicylate and benzyl cinnamate) (14). Another relevant class is represented by sesquiterpene hydrocarbons, such as δ -cadinene, γ -cadinene and α -muurolene, and oxygenated sesquiterpenes, such as β -eudesmol, T-cadinol and α -cadinol (14). Regarding monoterpene hydrocarbons, they were found to be present at low level in the samples analyzed in this study, with the exception of one sample from Southern Italy, where α -pinene was the most abundant constituent (14). As for oxygenated monoterpenes, menthol was determined mainly in sample RP-6 and thymol in samples RP-4 and RP-6 (14). Hemiterpenes were detected at low percentages in all the samples and were absent in sample RP-7 (14). The presence of naphthalene in sample RP-5 was attributed to unexpected material collected by bees or to inappropriate environmental storage conditions of propolis (14) and confirms a previous observation that propolis could be used as a marker of pollution (10).

The volatile composition of the Italian samples of raw propolis investigated in this work indicates a close relationship with bud extracts of *Populus* species (18, 22). In the case of sample RP-7, originated from a region of Southern Italy (the Adriatic coast) where poplars are not present, the high percentage of α -pinene suggests that the botanical source of bee glue may be attributed to *Pinus* species (14).

Summary

An efficient closed-vessel MAE process was developed and optimized by response surface experimental design for the fast extraction of phenolic acids and flavonoids from raw propolis. The proposed RP-HPLC method using the fused-core technology allowed a satisfactory separation of propolis constituents and a reduction of total analysis time and solvent usage. The combination of UV/DAD detection with ESI-MS and MS/MS provided a reliable identification of propolis phenolic compounds.

A new, rapid and simple HS-SPME-GC-MS method was developed for the analysis of propolis volatile compounds.

Both these methods were applied to raw propolis samples collected from different Italian regions to determine their metabolite fingerprinting, thus providing new and reliable tools for the complete chemical characterization of this biologically active apiary product.

References

1. Gómez-Caravaca, A. M.; Gómez-Romero, M.; Arráez-Román, D.; Segura-Carretero, A.; Farnández-Gutiérrez, A. *J. Pharm. Biomed. Anal.* **2006**, *41*, 1220–1234.
2. Salatino, A.; Fernandes-Silva, C. C.; Righi, A. A.; Salatino, M. L. F. *Nat. Prod. Rep.* **2011**, *28*, 925–936.
3. Sforcin, J. M.; Bankova, V. J. *Ethnopharmacol.* **2011**, *133*, 253–260.
4. Xu, Y.; Luo, L.; Chen, B.; Fu, Y. *Front. Biol. China* **2009**, *4*, 385–391.
5. Bankova, V. J. *Ethnopharmacol.* **2005**, *100*, 114–117.
6. Gardana, C.; Scaglianti, M.; Pietta, P.; Simonetti, P. *J. Pharm. Biomed. Anal.* **2007**, *45*, 390–399.
7. Medana, C.; Carbone, F.; Aigotti, R.; Appendino, G.; Baiocchi, C. *Phytochem. Anal.* **2008**, *19*, 32–39.
8. Falcão, S.; Vilas-Boas, M.; Estevinho, L. M.; Barros, C.; Domingues, M. R. M.; Cardoso, S. M. *Anal. Bioanal. Chem.* **2010**, *396*, 887–897.
9. Petri, G.; Lemberkovic, E.; Foldvari, F. In *Flavors and Fragrances: A World Perspective*; Lawrence, B. M., Mookherjee, B. D., Willis, B. J., Eds.; Elsevier Science Publishers B.V.: Amsterdam, 1988; pp 439–446.
10. Borčić, I.; Radonić, A.; Grzunov, K. *Flavour Fragrance J.* **1996**, *11*, 311–313.
11. Melliou, E.; Stratis, E.; Chinou, I. *Food Chem.* **2007**, *103*, 375–380.

12. Pellati, F.; Orlandini, G.; Pinetti, D.; Benvenuti, S. *J. Pharm. Biomed. Anal.* **2011**, *55*, 934–948.
13. Pellati, F.; Prencipe, F. P.; Bertelli, D.; Benvenuti, S. *J. Pharm. Biomed. Anal.* **2013**, *81-82*, 126–132.
14. Pellati, F.; Prencipe, F. P.; Benvenuti, S. *J. Pharm. Biomed. Anal.* **2013**, *84*, 103–111.
15. Guillarme, D.; Ruta, J.; Rudaz, S.; Veuthey, J.-L. *Anal. Bioanal. Chem.* **2010**, *397*, 1069–1082.
16. Ali, I.; AL-Othman, Z. A.; Al-Za'abi, M. *Biomed. Chromatogr.* **2012**, *26*, 1001–1008.
17. Bezerra, M. A.; Santelli, R. E.; Oliveira, E. P.; Villar, L. S.; Escaleira, L. A. *Talanta* **2008**, *76*, 965–977.
18. Rubiolo, P.; Casetta, C.; Cagliero, C.; Brevard, H.; Sgorbini, B.; Bicchi, C. *Anal. Bioanal. Chem.* **2013**, *405*, 1223–1235.
19. Isidorov, V. A.; Szczepaniak, L.; Bakier, S. *Food Chem.* **2014**, *142*, 101–106.
20. Belliardo, F.; Bicchi, C.; Cordero, C.; Liberto, E.; Rubiolo, P.; Sgorbini, B. *J. Chromatogr. Sci.* **2006**, *44*, 416–429.
21. Jeleń, H. H.; Majchera, M.; Dziadas, M. *Anal. Chim. Acta* **2012**, *738*, 13–26.
22. Jerković, I.; Mastelić, J. *Phytochemistry* **2003**, *63*, 109–113.

Chapter 3

Separation and Identification of Cucurbitane-Type Triterpenoids from Bitter Melon

Jose Luis Perez, G. K. Jayaprakasha, and Bhimanagouda S. Patil*

Vegetable and Fruit Improvement Center, Department of Horticultural Sciences, Texas A&M University, College Station, Texas 77845-2119

*E-mail: b-patil@tamu.edu.

Epidemiological data have demonstrated a dramatic increase in the incidence of diabetes worldwide. Bitter melon (*Momordica charantia*), a vegetable native to Asia, has been traditionally used in the management of hyperglycemic conditions. The health-promoting molecules in bitter melon have been described as cucurbitane-type triterpenoids. Recent advances in purification and identification techniques have identified several of these molecules from various parts of the bitter melon plant. This chapter describes the different classes of molecules that have been isolated from bitter melon to-date, and the various purification and identification techniques employed in these endeavors.

Introduction

Currently, the incidence of diabetes, principally type-2 diabetes, is growing at an alarming rate in developed and developing nations. Projections indicate that by 2050, if current trends persist, one in three Americans will be diabetic (1). Type-2 diabetes is a metabolic disorder characterized by sub-optimal regulation of glucose in the body, as a result of the malfunction of several tissues in the body, including the liver, muscle, adipose, and pancreatic tissues (2). The etiology of diabetes is very complex and its causation has been linked to factors such as genetics, high calorie consumption, low levels of physical activity, and general nutrition. Recent

studies have reported that routine consumption of fruits and vegetables is inversely correlated with the development of several chronic diseases, including diabetes and cancer (3–5). The health benefits of such diets have been attributed to the effects of several classes of bioactive compound in dietary fruits and vegetables.

In traditional medicine, bitter melon (*Momordica charantia*) has been used as a natural treatment to manage several diseases, including type-2 diabetes (6, 7). Recently, several studies have evaluated these claims using various animal, cell and enzymatic assays, particularly illustrating promising antidiabetic and anti-cancer activities. Animal studies using different bitter melon extracts have reported that bitter melon can suppress prostate cancer progression, enhance insulin signaling, and favorably influence blood glucose and blood pressure regulation (8–10). Furthermore, various cell culture models have reported that bitter melon extracts can induce apoptosis of human pancreatic carcinoma cells, have reparative effects on pancreatic β -cells, inhibit adipocyte differentiation, and increase insulin sensitivity in muscle cells (11–14). With the recent accumulation of data on bitter melon and its positive health benefits, an increasing interest in identifying its possible bioactive components has emerged.

Studies have reported that bitter melon contains several health-benefiting compounds, such as vitamin C, carotenoids, flavonoids, and other polyphenols, but current interest has focused on the isolation and purification of cucurbitane-type triterpenoids (CTMs) found in the various parts of the bitter melon plant (15–18). These CTMs typically occur in plants of the *Cucurbitaceae* family, which includes bitter melons (19). CTMs have a tetracyclic nucleus, principally 9 β -methyl-19-nor-lanosta-5-ene, with various oxygenated functionalities throughout their structures (19). Furthermore, CTMs may be present in various aglycone and glycosidic forms leading to a vastly diverse pool of compounds found in bitter melon. To date, over 250 cucurbitane-type molecules have been identified from various parts of the bitter melon plant (20).

Extraction of Cucurbitane-Type Molecules

A. Solvent Extractions

Cucurbitane type molecules (CTMs) have diverse polarities due to the variation of substitutions to the side chain or glucose moieties. Historically, all parts of the bitter melon plant, from the roots to fruit to seeds, have been used to ameliorate various health conditions; hence, several studies have isolated and characterized CTMs from different parts of the plant. In most previously published reports, extraction of these molecules from plant material was usually carried out using alcohol or an aqueous/alcoholic mixture (21–30). The extractions were typically performed at room temperature on a mechanical shaker for a period of a day to several weeks (31–33). In a few reports, methanol was refluxed for several hours through the plant tissue to extract the molecules of interest (30). The resulting extracts were dried under reduced pressure and subsequently suspended in water and partitioned with hexane, petroleum ether, ethyl acetate, or n-butanol (21, 26, 34). For example, in 1990, Fatope identified three new CTMs isolated from leaves of bitter melon, along with momordicine

I and II. The extraction procedure consisted of mechanical shaking of 420 g of dried leaf material and the removal of solvent under vacuum. The resulting residue was then dissolved in 300 ml of 90% methanol and extracted three times with 300 ml of hexane. Subsequently, water was added to the methanol layer to make it 80% methanol and it was extracted three times with carbon tetrachloride. The remaining methanolic layer was then further extracted with chloroform, in a similar fashion as the hexane and carbon tetrachloride extractions. The organic extracts were then used for purification using silica gel (35). Murakami et al. used a similar approach to extract cucurbitane and oleanane type triterpenoids, goyaglycosides and goyasaponins from Japanese bitter melon fruits. Dried fruit material was extracted using methanol at high temperature. The resulting extract was concentrated under reduced pressure and partitioned into ethyl acetate: water (1:1). The water phase was further partitioned with n-butanol. The ethyl acetate and butanol soluble fractions were used for purification by open column chromatography (36). The same group later used a similar extraction procedure with methanol to isolate karavilagenins and karavilosides (37). Similarly, eight CTMs were isolated from dried bitter melon stems (25). The stems (18 kg) were extracted in methanol (3 x 30 L) at room temperature for 7 days for each extraction. The resulting pooled extracts were concentrated and re-suspended in water. The extracts were sequentially partitioned with ethyl acetate and n-butanol. The organic extracts were then subjected to open column chromatography. Furthermore, Chen et al. isolated fourteen kuguacins and six previously-reported analogs from vines and leaves of bitter melon (27). Air-dried plant material (30kg) was extracted three times with 100 L of ethanol under reflux conditions. Similarly, the extracts were concentrated, dissolved in water and partitioned by ethyl acetate. The resulting extract was used for purification.

B. Pressurized Extractions

Earlier extraction methods used mechanical mixing or refluxing of alcohols for the isolation of CTMs. These methods are simple and effective, but they consume vast amount of organic solvents. The use of pressurized liquid extraction has several advantages that may increase the extraction efficiencies from sample matrices. In 2007, Pitipanapong et al. explored the use of pressurized liquid extraction to obtain charantin (38). Among the parameters they evaluated were solvent type, temperature, pressure, flow rate, and composition of the extract in ethanol (0, 20, 50, 80, and 100%) (38). From the solvents evaluated, ethanol was used for further evaluation of the extraction parameters, due to its cost and wide industrial use. The efficiency of charantin extraction was compared to Soxhlet extraction using ethanol as the extracting solvent. Results from this study indicated that acetone and ethanol led to higher efficiency compared with dichloromethane and water. Furthermore, from the range of extraction temperature evaluated (50, 80, 100, 120, 150°C) temperatures from 100-150°C were the optimal extraction temperatures for ethanol. The results of this study indicated that pressurized liquid extraction could be a viable alternative to Soxhlet extraction, due the reduced use of toxic solvents such as chloroform and dichloromethane, and the reduced extraction time.

Ji et al., explored the use of ultrahigh pressure extraction of momordicosides by ethanol, using a high pressure chamber (39). The temperature within the chamber was maintained at 30°C and the extraction was carried out for 3-9 min under a pressure of 300-500 MPa. The various extraction parameters were compared with the conventional reflux extraction method to compare extraction efficiency. Results from these studies indicate that total momordicosides were higher in the high pressure extraction system than in the conventional method. Levels of momordicosides were evaluated by colorimetry, and ranged from 2-3.2 g/100 g of material, with the highest extraction efficiency observed at 400 MPa for 9 min.

Purification Techniques

A. Open Column Chromatography

The first curcubitane-type molecules isolated from bitter melon were identified as momordicosides A and B (Fig. 1) (40). In this initial study, seeds were extracted in methanol as described above and chromatographed on silica. Momordicosides A and B were eluted using chloroform: methanol: water (70:25:3). Various compounds have been isolated from bitter melon extracts by separations involving several chromatographic steps. In fact, methanol extracts have been re-chromatographed over thirteen times using normal phase silica and chromatorex octadecyl or ODS, yielding nineteen compounds (37). Several of the molecules that were initially identified from bitter melon were isolated in a similar fashion (36, 41, 42). In 2007, Li et al. isolated several CTMs from an ethanol extract, but this study used the adsorptive resin Diaion HP-20 (43). This marked one of the first cases where an absorptive resin was used for the purification of more polar CTMs. Fractions were eluted with water and ethanol as the mobile phase. Fractions were then re-chromatographed on silica to separate the molecules of interest. Another commonly-reported resin used for the separation of CTMs is Sephadex LH-20 (33, 44, 45). After an initial purification through silica, the resulting extracts were then subjected to various chromatographic techniques using LH-20 and other resins, but principally silica gel (23, 25, 26, 34). Fractions collected from the various chromatographic runs were further separated by high-performance liquid chromatography (HPLC) and molecules were identified based on ultraviolet (UV), infrared (IR), nuclear magnetic resonance (NMR), and mass spectrometry (MS) to elucidate their structures (22, 23, 27, 29). Current research has focused on biological activities from extracts instead of isolated bioactives, possibly because the purification steps reported in the literature to date consist of slow open column purification methods. Typically, these purification methods use copious amounts of solvents and large amounts of raw materials. Furthermore, in several cases the semi-purified extracts are repeatedly chromatographed, possibly leading to a loss of the desired compound. These steps can be extremely time-consuming and expensive.

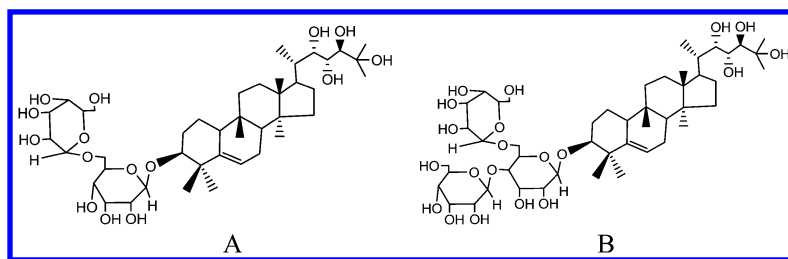


Figure 1. Momordicoside A and B.

Varietal differences have been observed in the biochemical composition and health benefits of bitter melon. Although the health benefits of these triterpenoids might be attractive to consumers, we currently have very limited information on the levels of these triterpenoid molecules in the different varieties of bitter melon available. The levels of polyphenolics, proteins, amino acids, and other chemical constituents have also been reported to vary among different varieties (46–49). Similar results have been observed in other studies on varietal effects on health-promoting properties of bitter melon, ranging from antioxidant activity to hypoglycemia (46, 50, 51). Therefore, further studies will be required to measure the levels of these triterpenoid molecules and their variation among varieties.

B. Preparative HPLC

Guevara et al. reported the preparative-scale purification of bitter melon methanol extracts. After initial purification using an open silica column, a subfraction was subjected to LH-20 chromatography and re-chromatographed by HPLC using an ODS RP-18 column. The fractions were monitored using UV and RI detectors, resulting in the purification of two compounds (32). Similarly, in other studies alcohol extracts were pre-purified before preparative chromatography, which was typically monitoring via UV at 204–210 nm (43). Typical mobile phases used for preparative-scale purification include various ratios of acetonitrile:water; methanol:water with the occasional addition of modifiers such as acetic acid or phosphoric acid. These mobile phases were used with flow rates ranging from 1–4 mL/min (21, 23, 26, 42, 52, 53). Several cucurbitane-type triterpenoids have been isolated via preparative HPLC, but with low yields of pure compounds. For example, in one study 167 kg of fresh fruit were seeded and juiced to yield 61 kg of material. After ethanol extraction, the extract was partitioned and subjected to open column chromatography and preparative HPLC to obtain momordicoside L (9 mg), M (11 mg), N (15 mg), and O (11 mg) (43). Similarly, when 75 kg of freeze-dried material was extracted with 80% ethanol, dried and partitioned with chloroform and butanol, the butanol layer

yielded 800 g of material to use for further purification. Initial purification was carried out by a series of columns using macroporous resins, adsorptive resins, and silica gel as stationary phases. Several fractions were then further purified by preparative HPLC to yield four novel molecules, momordicoside Q, R, S, and T (80, 18, 160, and 220 mg, respectively) (21). Preparative-scale HPLC purification have the added advantage of monitoring the purification process via various detectors. Recent technological advances have thus improved the purification techniques for a more precise and efficient results.

C. Flash Chromatography

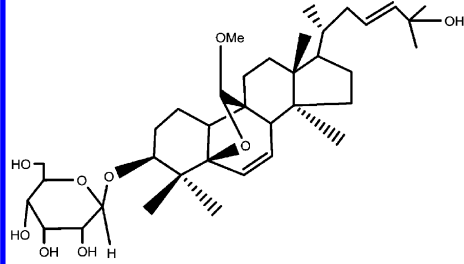
Although flash chromatography has been used to purify several bioactives from a variety of botanicals, few studies have used flash chromatography to purify cucurbitanes from bitter melon. The first report on flash chromatography for the purification of cucurbitane-type molecules from bitter melon was reported by Liu et al (33). In this study, powdered bitter melon fruit was extracted with methanol at room temperature, followed by evaporation of the methanol. The residue was then re-suspended in water and partitioned with petroleum ether, ethyl acetate, and butanol. The ethyl acetate layer was then subjected to silica gel chromatography to give six fractions, resulting in the purification of momordicoside A. This molecule was purified by subjecting fraction 2 (1.2 g) to flash chromatography using a Biotage 40+M cartridge with chloroform and methanol as mobile phases, yielding 201 mg of momordicoside A. Similarly momordicoside F2, goyaglycoside-d, momordicoside K, momordicoside L, momordicoside G, goyacycoside-c, momordicoside F1, 7 β ,25-dimethoxycucurbita-5(6),23(E)-dien-19-al 3-O- β -D-allopyranoside, 25-methoxycucurbita-5(6),23(E)-dien-19-ol 3-O- β -D-allopyranoside, but these were subjected to open column chromatography using Sephadex LH-20 or RP-18 and using either a silica flash column or a Biotage 40+M cartridge to complete the purification. This initial study demonstrated the effectiveness of flash chromatography over previously-reported preparative HPLC methods, resulting in high yields of bioactive molecules from less starting material. While this study reported good yields of bioactives from bitter melon fruit, there was no mention of a monitoring method during the flash purification step. Current flash chromatography systems use various detectors such as UV or evaporative light scattering detectors or ELSD detectors to monitor the separation.

Ma et al. reported the purification of various molecules using 24 g of defatted methanol extracts (54). Initially, the extract was subjected to silica gel column chromatography with chloroform and methanol at a flow rate of 100 mL/min. The fractions from this initial run were pooled according to their thin layer chromatography (TLC) profiles, resulting in five principal fractions. These fractions were subsequently used for repeated flash purification using silica and RP-18 columns, depending on the polar nature of the fraction evaluated. The purification process was monitored using a UV detector at 205 nm. CTM yields from this study ranged from 21-636 mg.

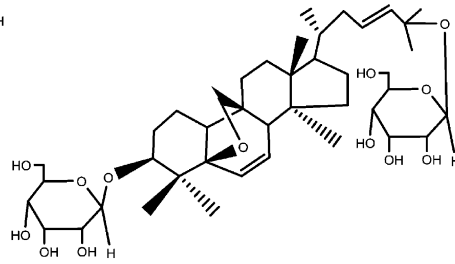
Recently, we reported the separation and identification of several CTMs from bitter melon fruit and seeds (55). Using flash chromatography, dried bitter melon chloroform extracts were chromatographed on silica cartridges and monitored at 210 and 254 nm. The molecules were separated using hexane and acetone as mobile phases with a flow rate of 20 mL/min. The adjustment of threshold settings for peak height allowed for the automatic collection of fractions. After the chromatographic run, fractions were analyzed by TLC and HPLC. Fractions displaying pure molecules were then analyzed by LC-MS or NMR. Charantin, 25,26,27-trinorcucurbit-5-ene-3,7,23 trione, momordicoside Q, and kuguaglycoside D were identified in this study.

Identification of CTMs

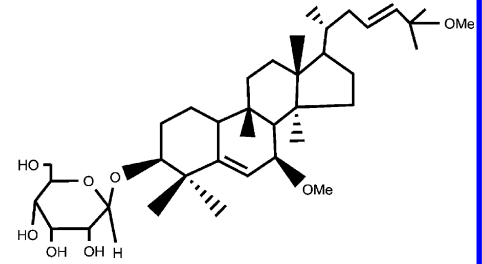
Triterpenoids isolated from bitter melon have a basic tetracyclic nucleus with substitutions of methyl, hydroxyl, or sugar moieties contributing to the diversity of reported structures. The reported molecular weights of the various CTMs ranged from 300 to 1500. Furthermore, in several of the reported compounds, the principal difference between structures was mainly conformational. Therefore, an array of equipment is required to properly identify and study the triterpenoids isolated from bitter melon. The first molecules isolated from bitter melon were reported in 1980 (40). Identification of momordicoside A and B (Fig. 1) from bitter melon seeds was performed by the use of mass spectrometry (MS), NMR (proton and carbon NMR), and X-ray crystallography. After purification, samples were hydrolyzed to give aglycone and sugar moieties. MS and X-ray studies were used to confirm the cucurbitane framework. Additionally, circular dichroism spectrometry revealed the presence of a double bond between carbons 5 and 6 and the presence of a 10 α -hydrogen. Similarly, digital polarimetry has also helped in the elucidation of optical rotational isomers of various CTMs. Additionally, the use of IR spectroscopy has also been implemented for the identification of various functional groups on the cucurbitane triterpenoid structure (56). While many initial studies used 1D proton and carbon NMR to elucidate the structures of CTMs isolated from bitter melon, advances in spectroscopy equipment greatly improved the identification of novel compounds. With the employment of more sophisticated 1D and 2D NMR experiment such as H-H correlation spectroscopy (COSY) to elucidate coupled protons, more CTMs from bitter melon have been identified (35). Further studies also used NMR techniques such as distortionless enhancement by polarization transfer (DEPT, used to distinguish between CH₃, CH₂, and CH groups), heteronuclear multiple quantum coherence (HMQC), which eliminates long range proton carbon coupling and increases sensitivity, heteronuclear multiple bond coherence (HMBC), which details two- and three-bond coupling, nuclear Overhauser and exchange spectroscopy (NOESY), and rotating frame Overhauser effect spectroscopy (ROSEY) for spatially close protons, for the elucidation of over 250 triterpenoids from bitter melon (27, 36, 52, 57, 58).



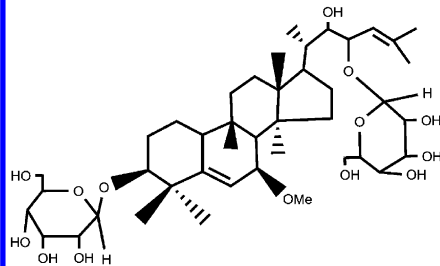
Goyaglycoside A



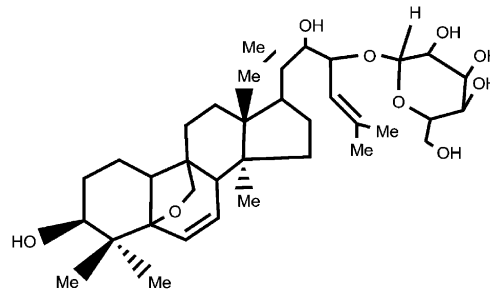
Goyaglycoside A



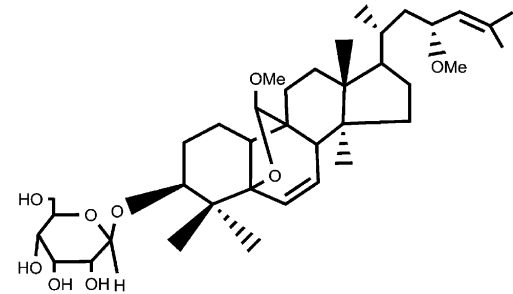
Karaviloside I



Karaviloside V



Karaviloside VIII



Charantoside II

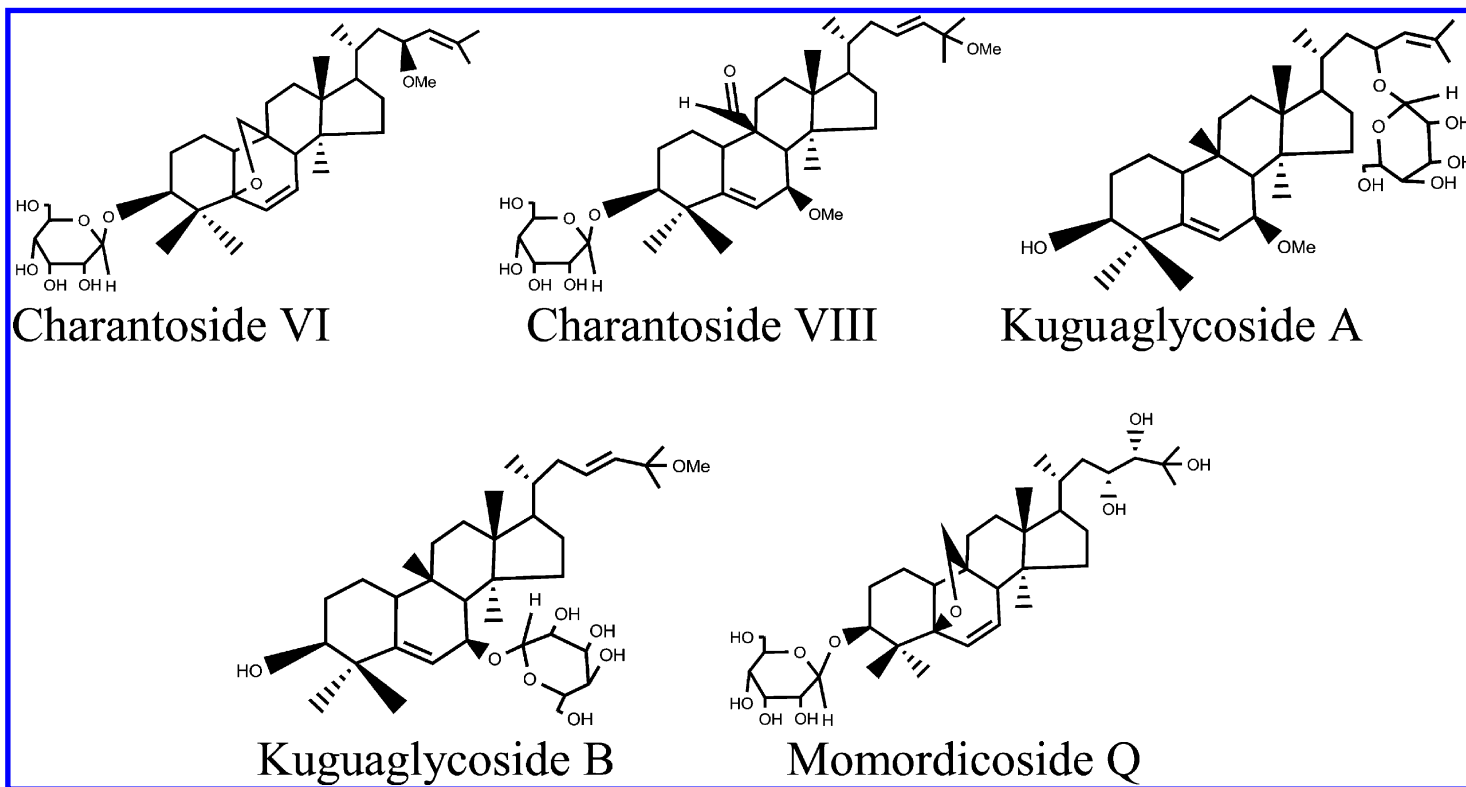


Figure 2. Structures of triterpenoid glucosides isolated from bitter melon.

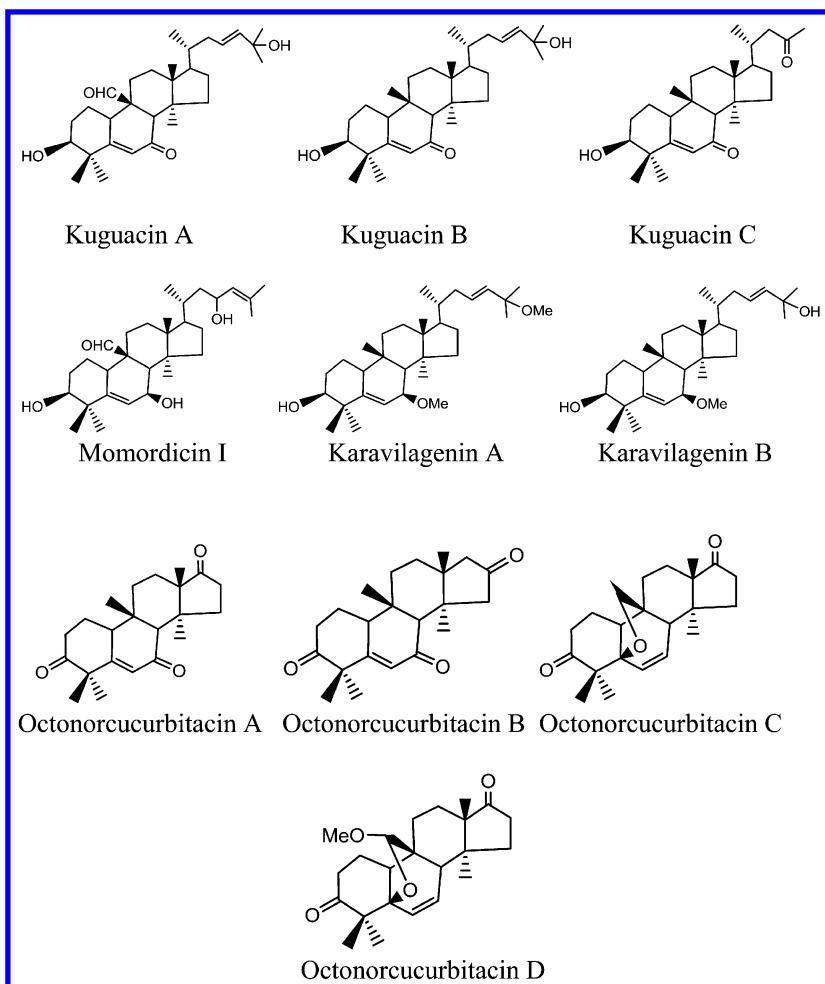


Figure 3. Structures of selected CTM aglycones reorted from bitter melon.

Reported ^{13}C NMR chemical shifts from selected CTM glucosides (Fig. 2) and aglycones (Fig. 3) are listed in Tables 1 and 2 to illustrate the characteristic signals. Additional spectral analysis, such as MS data, has also been a valuable tool for the identification of bitter melon triterpenoids yielding molecular weight and fragmentation information, with the added benefit that the analysis requires material of minimal quantity (21, 57).

Table 1. ¹³C NMR of Compounds A-K^a Isolated from Bitter Melon

<i>Position</i>	<i>A</i>	<i>B</i>	<i>C</i>	<i>D</i>	<i>E</i>	<i>F</i>	<i>G</i>	<i>H</i>	<i>I</i>	<i>J</i>	<i>K</i>
1	18.7	18.9	22.6	22.6	17.8	18.7	18.9	22.2	21.9	21.8	18.9
2	27.4	27.6	28.9	28.8	27.8	27.4	27.6	29.3	30.3	30.2	27.6
3	83.8	85.1	87.8	87.7	76.1	83.4	85.1	86.9	76.2	76.1	85.4
4	39.2	39.0	42.1	42.0	37.4	39.1	39.0	42.1	42.1	42.0	39.1
5	85.5	86.0	148.0	148.0	87.5	85.5	85.9	147.5	148.2	148.4	85.8
6	133.2	134.1	119.2	119.2	132.4	133.1	134.2	120.7	119.7	121.0	134.2
7	131.6	130.0	77.7	77.7	131.2	131.6	130.0	75.7	77.7	72.4	130.0
8	42.3	52.3	48.9	48.9	52.1	42.2	52.3	45.8	48.4	48.4	52.3
9	48.2	45.3	34.4	34.4	45.6	48.2	45.3	50.2	35.1	34.5	45.3
10	41.7	40.2	39.4	39.3	39.2	41.6	40.1	36.8	39.4	39.3	40.1
11	23.3	23.8	32.8	32.9	23.7	23.4	23.8	22.6	28.1	28.0	23.9
12	30.9	31.1	30.4	30.6	31.1	31.1	31.2	29.3	33.1	33.0	31.2
13	45.3	45.5	46.3	46.6	45.6	45.4	45.5	45.8	46.5	46.3	45.6
14	48.4	48.9	48.3	48.0	48.4	48.4	48.9	47.9	48.4	48.2	48.9
15	33.9	33.5	35.0	35.3	33.5	33.8	33.4	35.0	34.5	34.5	33.3
16	28.2	28.2	27.9	27.8	27.9	28.4	28.6	27.6	30.7	30.5	28.5
17	50.4	50.5	50.3	46.6	46.5	51.4	51.3	50.2	51.5	50.3	51.6

Continued on next page.

Table 1. (Continued). ¹³C NMR of Compounds A-K^a Isolated from Bitter Melon

<i>Position</i>	<i>A</i>	<i>B</i>	<i>C</i>	<i>D</i>	<i>E</i>	<i>F</i>	<i>G</i>	<i>H</i>	<i>I</i>	<i>J</i>	<i>K</i>
18	14.9	15.1	15.6	15.1	14.4	14.8	14.9	15.0	15.6	15.7	15.0
19	112.4	80.2	29.2	29.2	79.8	112.4	79.7	207.0	29.3	29.5	80.1
20	36.6	36.5	36.5	40.9	40.6	32.9	33.8	36.3	32.9	36.5	32.7
21	18.9	19.1	19.1	15.0	14.6	19.0	19.9	19.0	19.7	19.1	18.9
22	39.6	39.8	39.8	76.9	76.5	43.4	43.0	39.7	44.0	39.8	43.3
23	124.4	128.4	128.5	81.2	80.9	74.8	76.4	128.4	75.7	128.5	67.7
24	141.7	138.5	137.7	124.8	124.6	127.9	127.9	137.7	129.2	137.6	79.9
25	69.7	77.6	74.9	135.4	135.3	134.4	135.8	74.8	132.3	74.9	73.6
26	30.9	28.7	26.1	26.2	26.0	25.8	25.9	26.1	26.0	26.5	28.0
27	30.9	27.7	26.5	18.6	18.5	18.1	18.5	26.4	18.4	26.5	27.0
28	21.2	21.1	28.9	28.8	20.8	24.8	25.6	27.8	26.4	26.1	21.1
29	24.9	25.6	25.9	25.9	24.5	21.3	21.1	25.8	28.5	28.4	25.6
30	20.0	20.3	18.1	18.1	20.1	20.0	20.2	18.1	18.2	18.0	20.2
7-OMe			56.3	56.2				55.9	56.3		
19-OMe	57.6					57.6					
23-OMe			50.2			55.6	55.3				
25-OMe								50.1		50.2	
1'	105.3	103.8	107.6	104.8	103.4	102.3	103.7	107.3	104.3	101.2	106.7

<i>Position</i>	<i>A</i>	<i>B</i>	<i>C</i>	<i>D</i>	<i>E</i>	<i>F</i>	<i>G</i>	<i>H</i>	<i>I</i>	<i>J</i>	<i>K</i>
2'	76.2	73.1	75.2	72.1	72.9	73.8	73.1	75.2	75.5	75.3	75.8
3'	78.6	72.4	78.7	73.3	72.8	71.7	72.4	78.8	79.0	78.9	78.3
4'	72.1	69.3	71.8	69.3	68.9	69.2	69.3	71.7	72.0	72.0	71.9
5'	78.0	76.1	78.2	75.9	75.7	76.5	76.2	78.3	78.3	78.8	78.4
6'	63.1	63.4	63.2	63.4	62.9	63.3	63.4	63.1	63.0	63.0	63.1
1"		99.8		103.6							
2"		75.3		73.1							
3"		78.8		73.0							
4"		71.9		69.1							
5"		78.0		75.6							
6"		63.0		63.1							
REF	(36)	(36)	(37)	(37)	(59)	(42)	(42)	(42)	(45)	(45)	(21)

^a A-goyaglycoside A, B- goyaglycoside E, C-karaviloside I, D- karaviloside V, E-karavilosideVIII, F- charantoside II, G-charantoside VI, H-charantoside VIII, I-kuguaglycoside A, J-kuguaglycoside B, K- momordicoside Q. The structures of the compounds are illustrated in Figure 2.

Table 2. ¹³C NMR of Nonglycosylated Compounds L-U^a Isolated from Bitter Melon

<i>Position</i>	<i>L</i>	<i>M</i>	<i>N</i>	<i>O</i>	<i>P</i>	<i>Q</i>	<i>R</i>	<i>S</i>	<i>T</i>	<i>U</i>
1	21.6	20.8	20.8	21.2	21.0	21.0	24.2	23.7	24.8	24.5
2	28.7	29.7	28.6	29.4	28.4	28.5	38.0	38.0	35.9	35.5
3	76.1	76.6	76.7	75.4	76.8	76.5	210.8	210.9	213.9	212.7
4	43.6	42.8	42.8	41.6	41.6	41.6	51.6	51.5	48.4	49.5
5	168.1	169.0	169.0	145.4	146.7	146.8	167.9	168.1	89.8	89.5
6	127.1	125.9	125.9	123.6	120.7	120.6	124.9	125.0	133.0	48.9
7	199.4	202.8	202.7	65.5	77.1	77.1	200.7	201.3	129.4	211.5
8	51.2	59.8	59.7	49.1	47.8	47.7	58.1	57.1	51.0	52.2
9	51.2	35.8	35.8	50.9	33.9	33.8	37.4	36.9	46.3	49.8
10	37.9	40.3	40.2	36.3	38.5	38.6	41.8	41.7	40.1	42.9
11	22.3	31.3	31.2	22.2	32.5	32.6	30.6	30.7	22.9	22.6
12	28.4	28.6	29.8	29.0	29.9	29.9	23.1	27.9	23.9	23.5
13	45.3	45.7	45.8	45.2	46.0	46.1	53.1	41.8	52.2	52.7
14	48.2	48.5	48.5	48.1	47.7	47.7	43.8	44.4	43.8	43.7
15	34.5	34.5	34.5	34.3	34.6	34.6	31.8	50.6	30.1	31.9
16	27.4	27.8	28.0	27.6	27.5	27.5	33.6	217.8	33.4	33.4
17	49.5	49.5	49.8	50.6	49.8	49.8	217.4	49.6	217.5	217.6
18	14.9	15.4	15.4	14.5	15.3	15.3	17.3	22.7	16.9	17.5

Position	L	M	N	O	P	Q	R	S	T	U
19	203.4	27.8	27.8	207.5	28.5	28.8	27.6	27.6	79.9	110.0
20	36.2	36.2	32.8	32.4	36.1	36.1				
21	18.8	18.7	19.8	18.6	18.0	18.6				
22	39.0	39.0	51.1	44.9	39.5	39.0				
23	124.9	125.1	209.1	64.9	128.4	125.0				
24	139.8	139.6	30.5	131.5	136.6	139.4				
25	70.7	70.7		130.5	74.7	70.5				
26	29.9	29.9		17.7	26.0	29.8				
27	30.0	29.9		25.7	25.7	29.7				
28	24.9	24.8	24.8	25.3	27.7	27.6	28.6	28.5	24.8	25.0
29	27.2	27.8	27.8	26.8	25.3	25.3	22.8	23.0	16.7	17.2
30	18.3	18.0	18.0	17.6	17.8	17.9	19.1	19.1	19.7	20.3
7-OMe					56.1	56.1				
19-OMe										57.6
25-OMe					50.1					
REF	(44)	(44)	(44)	(60)	(37)	(37)	(61)	(61)	(61)	(61)

^a L-kuguacin A, M-kuguacin B, N-kuguacin C, O-momordicine I, P- karavilegenin A, Q-karavilogenin B, R- octonorcucurbitacin A, S- octonorcucurbitacin B, T- octonorcucurbitacin C, U- octonorcucurbitacin D. The structures of the compounds are illustrated in Figure 3.

Reported CTMs

Momordicosides (A and B) were first isolated in 1980 from bitter melon seeds (40). CTMs from other fruits have been previously reported, but the novelty in these molecules was the absence of oxygen at the C 11 position (Figure 1). The molecules were identified as 3-*O*- β -gentiobioside and 3-*O*- β -D-xylopyranosyl(1 \rightarrow 4)[β -D-glucopyranosyl(1 \rightarrow 6)]- β -D-glucopyranoside of cucurbit-5-ene-3 β , 22(*S*), 23(*R*), 24(*R*), 25-pentol. In subsequent publications, an additional twenty-one momordicosides (C-X) were identified from fruits, seeds, vines, and roots of the bitter melon plant (21, 22, 43, 54, 56, 62–66). Similarly, several other triterpenoids have been identified and named from the bitter melon plant, including momordicine (I-VIII), (58, 60, 67–71), goyaglycosides (A-H) and goyasaponins (I-III) (36), karavilagenin (A-F) and karavilosides (I-XII) (37, 59, 72), charantosides (I-VIII, and A-G) (30, 42, 73, 74), kuguacin (A-S) (27, 44), kuguaglycosides A-H (45), neokuguaglucoiside (75), kuguaosides (A-D) (76), kuguasaponins (A-H) (77), and octonorcucurbitacins (A-D) (61). Additionally, two novel pentanorcucurbitane triterpenes, 22-hydroxy-23,24,25,26,27-pentanorcucurbit-5-en-3-one and 3,7-dioxo-23,24,25,26,27-pentanorcucurbit-5-en-22-oic acid, together with a new trinorcucurbitane triterpene, 25,26,27-trinorcucurbit-5-ene-3,7,23-trione, were isolated from bitter melon stem methanolic extracts (78). Selected structures of these triterpenoids are shown in Figures 1, 2, and 3. Additionally, a summary of named CTMs and related information is presented in Table 3.

Table 3. Various Triterpenoids Reported from Bitter Melon, Their Molecular Formulas, and Exact Masses

<i>Name</i>	<i>Source</i>	<i>Formula</i>	<i>Exact Mass</i>	<i>ref</i>
Charantosides				
I	Fruit	C ₃₇ H ₅₈ O ₈	630.4131	(42)
II	Fruit	C ₃₈ H ₆₂ O ₉	662.4393	(42)
III	Fruit	C ₃₆ H ₅₆ O ₇	600.4026	(42)
IV	Fruit	C ₃₆ H ₅₆ O ₇	600.4026	(42)
V	Fruit	C ₃₇ H ₆₀ O ₈	632.4288	(42)
VI	Fruit	C ₃₇ H ₆₀ O ₈	632.4288	(30, 42)
VII	Fruit	C ₃₆ H ₅₄ O ₈	614.3818	(42)
VIII	Fruit	C ₃₈ H ₆₂ O ₉	662.4393	(42)
A	Fruit	C ₃₇ H ₆₀ O ₉	648.4237	(73)
B	Fruit	C ₃₆ H ₅₈ O ₉	634.4080	(73)

Continued on next page.

Table 3. (Continued). Various Triterpenoids Reported from Bitter Melon, Their Molecular Formulas, and Exact Masses

<i>Name</i>	<i>Source</i>	<i>Formula</i>	<i>Exact Mass</i>	<i>ref</i>
C	Fruit	C ₃₇ H ₅₈ O ₉	646.4080	(73)
D	Fruit	C ₃₇ H ₅₉ O ₉	647.4165	(74)
E	Fruit	C ₃₇ H ₅₉ O ₉	647.4165	(74)
F	Fruit	C ₃₇ H ₅₉ O ₇	615.4266	(74)
G	Fruit	C ₃₆ H ₅₅ O ₈	615.3902	(74)
Goyaglycosides				
A	Fruit, Leaves	C ₃₇ H ₆₁ O ₉	648.4237	(36, 79)
B	Fruit, Leaves	C ₃₇ H ₆₀ O ₉	648.4237	(30, 36, 37, 73, 76, 79)
C	Fruit	C ₃₈ H ₆₂ O ₉	662.4393	(33, 36, 37, 42)
D	Fruit	C ₃₈ H ₆₂ O ₉	662.4393	(30, 33, 36, 37, 42, 76)
E	Fruit	C ₄₂ H ₆₈ O ₁₃	780.4659	(36, 80)
F	Fruit	C ₄₂ H ₆₈ O ₁₃	780.4659	(36, 80)
G	Fruit	C ₄₃ H ₇₀ O ₁₄	810.4765	(36)
H	Fruit	C ₄₂ H ₇₀ O ₁₅	814.4714	(36, 80)
Goyasaponins				
I	Fruit, Seed	C ₆₅ H ₁₀₂ O ₃₁	1378.6405	(36, 81)
II	Fruit, Feed	C ₇₀ H ₁₁₀ O ₃₅	1510.6827	(36, 81)
III	Fruit	C ₄₉ H ₇₆ O ₁₉	968.4980	(36)
Karavilagenin				
A	Fruit	C ₃₂ H ₅₄ O ₃	486.4072	(37)
B	Fruit	C ₃₁ H ₅₂ O ₃	472.3916	(37)
C	Fruit	C ₃₁ H ₅₂ O ₃	472.3916	(37)
D	Leaves, Vines, Fruit	C ₃₀ H ₄₆ O ₄	470.3396	(27, 59, 79, 82)
E	Fruit	C ₃₀ H ₄₈ O ₃	456.3603	(59)
F	Leaves, Stems	C ₃₁ H ₅₀ O ₅	502.3647	(72)
Karavilosides				
I	Fruit	C ₃₈ H ₆₄ O ₈	648.4601	(37, 42)
II	Fruit	C ₃₈ H ₆₄ O ₈	648.4601	(29, 37, 73)

Continued on next page.

Table 3. (Continued). Various Triterpenoids Reported from Bitter Melon, Their Molecular Formulas, and Exact Masses

<i>Name</i>	<i>Source</i>	<i>Formula</i>	<i>Exact Mass</i>	<i>ref</i>
III	Fruit, Root	C ₃₇ H ₆₂ O ₈	634.4444	(29, 37, 45)
IV	Fruit	C ₃₇ H ₆₂ O ₉	650.4393	(37)
V	Fruit, Root	C ₄₃ H ₇₂ O ₁₄	812.4922	(37, 45)
VI	Leaves, Fruit	C ₃₇ H ₅₈ O ₉	646.4080	(59, 79)
VII	Fruit	C ₃₇ H ₆₀ O ₈	632.4288	(59)
VIII	Vine, Leaves, Fruit	C ₃₆ H ₅₈ O ₉	634.4080	(31, 59)
IX	Fruit	C ₄₂ H ₆₈ O ₁₄	796.4609	(59)
X	Vine, Leaves, Fruit	C ₄₂ H ₆₈ O ₁₄	796.4609	(31, 59)
XI	Fruit, Root, Vine, Leaves	C ₃₆ H ₆₀ O ₁₀	652.4186	(21, 31, 45, 59)
XII	Leaves, Stems	C ₃₈ H ₆₀ O ₉	660.4237	(72)
XIII	Leaves, Stems	C ₃₆ H ₅₈ O ₈	618.4123	(72)
Kuguacin				
A	Roots	C ₃₀ H ₄₆ O ₄	470.33961	(44)
B	Roots	C ₃₀ H ₄₈ O ₃	456.360345	(44)
C	Roots	C ₂₇ H ₄₂ O ₃	414.313395	(44)
D	Roots	C ₂₇ H ₄₀ O ₄	428.29266	(44)
E	Roots	C ₂₇ H ₄₂ O ₄	430.30831	(27, 44)
F	Leaves, Vines	C ₃₀ H ₄₂ O ₅	482.303225	(27)
G	Leaves, Vines	C ₃₀ H ₄₄ O ₆	500.31379	(27)
H	Leaves, Vines	C ₃₀ H ₄₄ O ₅	484.318875	(27)
I	Leaves, Vines	C ₃₁ H ₄₆ O ₅	498.334525	(27)
J	Leaves, Vines	C ₃₀ H ₄₆ O ₃	454.344695	(27)
K	Leaves, Vines	C ₂₅ H ₃₄ O ₆	430.23554	(27)
L	Leaves, Vines	C ₂₅ H ₃₆ O ₄	400.261359	(27)
M	Leaves, Vines	C ₂₂ H ₂₈ O ₄	356.19876	(27)
N	Leaves, Vines	C ₃₀ H ₄₆ O ₄	470.33961	(27, 61)
O	Leaves, Vines	C ₃₀ H ₄₂ O ₄	466.30831	(27)
P	Leaves, Vines	C ₂₇ H ₄₀ O ₄	428.29266	(7)
Q	Leaves, Vines	C ₂₉ H ₄₄ O ₅	472.318875	(27)

Continued on next page.

Table 3. (Continued). Various Triterpenoids Reported from Bitter Melon, Their Molecular Formulas, and Exact Masses

<i>Name</i>	<i>Source</i>	<i>Formula</i>	<i>Exact Mass</i>	<i>ref</i>
R	Leaves, Stems	C ₃₀ H ₄₈ O ₄	472.35526	(27, 72)
S	Leaves, Vines	C ₃₀ H ₄₄ O ₄	468.32396	(27)
Kuguaglycosides				
A	Root	C ₃₇ H ₆₂ O ₈	634.4444	(45)
B	Fruit, Root	C ₃₇ H ₆₂ O ₈	634.4444	(45, 83)
C	Leaves, Fruit, Root	C ₃₆ H ₅₆ O ₈	616.3975	(30, 45, 77, 79, 84)
D	Root, Leaves, Vines	C ₃₆ H ₆₀ O ₉	636.4237	(31, 45)
E	Root	C ₄₂ H ₇₀ O ₁₄	798.4765	(45)
F	Root	C ₄₃ H ₇₂ O ₁₃	796.4972	(45)
G	Root	C ₄₂ H ₇₀ O ₁₃	782.4816	(11, 45, 85)
H	Root	C ₄₈ H ₈₀ O ₁₈	944.5344	(45)
Kuguaoside				
A	Fruit	C ₃₆ H ₅₈ O ₈	618.4131	(76)
B	Fruit	C ₃₇ H ₆₀ O ₉	648.4237	(76)
C	Fruit	C ₃₆ H ₅₈ O ₉	634.4080	(76)
D	Fruit	C ₃₇ H ₆₀ O ₉	648.4237	(76)
Kuguasaponins				
A	Fruits	C ₃₆ H ₅₆ O ₈	616.3975	(77)
B	Fruits	C ₃₈ H ₆₂ O ₉	662.4393	(77)
C	Fruits	C ₃₈ H ₆₂ O ₉	662.4393	(77)
D	Fruits	C ₃₈ H ₆₂ O ₉	662.4393	(77)
E	Fruits	C ₃₈ H ₆₂ O ₉	662.4393	(77)
F	Fruits	C ₄₂ H ₆₆ O ₁₄	794.4452	(77)
G	Fruits	C ₄₂ H ₆₉ O ₁₃	781.4738	(77)
H	Fruits	C ₃₆ H ₆₀ O ₉	636.4237	(77)
Momocharaside				
A	Seed	C ₄₂ H ₇₂ O ₁₅	816.4871	(81)
B	Seed, Fruit	C ₃₆ H ₆₂ O ₁₀	654.4343	(21, 81)

Continued on next page.

Table 3. (Continued). Various Triterpenoids Reported from Bitter Melon, Their Molecular Formulas, and Exact Masses

<i>Name</i>	<i>Source</i>	<i>Formula</i>	<i>Exact Mass</i>	<i>ref</i>
Momordicine				
I	Leaves, Vine, Fruit, Root	C ₃₀ H ₄₈ O ₄	472.3552	(11, 27, 31, 44, 58, 60, 67, 69, 77, 86)
II	Leaves, Vine Fruit	C ₃₆ H ₅₈ O ₉	634.4080	(11, 31, 58, 67–69, 86, 87)
III	Leaves, Vine	C ₃₆ H ₅₆ O ₁₀	648.3873	(67)
IV	Leaves	C ₃₆ H ₅₈ O ₉	634.4080	(31, 87, 88)
V	Leaves	C ₃₉ H ₆₀ O ₁₂	720.4084	(71)
VI	Leaves, Stem	C ₃₁ H ₅₀ O ₄	486.3709	(72)
VII	Leaves, Stem	C ₃₄ H ₅₂ O ₇	572.3703	(72)
VIII	Leaves, Stem	C ₃₅ H ₅₄ O ₇	586.3862	(72)
Momordicosides				
A	Seed, Fruit	C ₄₂ H ₇₂ O ₁₅	816.4871	(21, 29, 33, 36, 40, 73, 80)
B	Seed, Fruit	C ₄₇ H ₈₀ O ₁₉	948.5293	(21, 29, 40)
C	Seed, Fruit	C ₄₂ H ₇₂ O ₁₄	800.4922	(36, 62, 73, 81)
D	Seed	C ₄₂ H ₇₀ O ₁₃	782.4816	(62, 80)
E	Seed	C ₃₇ H ₆₀ O ₁₂	696.4080	(62, 81)
F1	Fruit	C ₃₇ H ₆₀ O ₈	632.4288	(33, 36, 37, 42, 63, 73, 76)
F2	Fruit	C ₃₆ H ₅₈ O ₈	618.4130	(33, 37, 42, 63, 73, 76, 80)
G	Fruit, Leaves	C ₃₇ H ₆₀ O ₈	632.4288	(33, 37, 63, 73, 79)
I	Fruit	C ₃₆ H ₅₈ O ₈	618.4130	(33, 37, 63, 73, 76, 80)
K	Fruit, Leaves	C ₃₇ H ₆₀ O ₉	648.4237	(30, 31, 33, 36, 37, 45, 63, 76, 79, 87)

Continued on next page.

Table 3. (Continued). Various Triterpenoids Reported from Bitter Melon, Their Molecular Formulas, and Exact Masses

<i>Name</i>	<i>Source</i>	<i>Formula</i>	<i>Exact Mass</i>	<i>ref</i>
L	Fruit, Leaves	C ₃₆ H ₅₈ O ₉	634.4080	(29, 31, 33, 37, 43, 63, 76, 79)
M	Fruit	C ₄₂ H ₆₈ O ₁₄	796.4609	(29, 43, 73)
N	Fruit	C ₄₂ H ₆₈ O ₁₄	796.4609	(29, 43)
O	Fruit	C ₄₂ H ₆₈ O ₁₅	812.4558	(43)
P	Fruit	C ₃₆ H ₅₈ O ₉	634.4080	(22)
Q	Fruit	C ₃₆ H ₆₀ O ₁₀	652.4186	(21)
R	Fruit	C ₄₂ H ₇₀ O ₁₅	814.4714	(21)
S	Fruit	C ₄₈ H ₈₂ O ₂₀	978.5399	(21, 29)
T	Fruit	C ₅₃ H ₉₀ O ₂₄	1110.5822	(21)
U	Fruit	C ₃₈ H ₆₄ O ₉	648.4237	(66, 76)
V	Fruit	C ₃₆ H ₅₈ O ₈	618.4131	(66)
W	Fruit	C ₃₆ H ₅₉ O ₉	634.4080	(66)
X	Whole Plant	C ₃₆ H ₅₈ O ₉	634.4080	(54)
Octonorcucurbitacin				
A	Stem	C ₂₂ H ₃₀ O ₃	342.2192	(61)
B	Stem	C ₂₂ H ₃₀ O ₃	342.2191	(61)
C	Stem	C ₂₂ H ₃₀ O ₃	342.2205	(61)
D	Stem	C ₂₃ H ₃₂ O ₅	388.2240	(61)
Taiwacin				
A	Stem, Fruit	C ₄₄ H ₆₈ O ₁₄	820.4609	(89)
B	Stem, Fruit	C ₂₅ H ₃₆ O ₄	400.2613	(89)

Additional CTMs reported from *Momordica charantia*

A. Fruits

In addition to the above-mentioned molecules, several other compounds, principally triterpenoids, have been identified from various parts of the bitter melon plant. For example, in 2005, Kimura et al. isolated three new CTMs from fruits of Japanese bitter melon. The newly-identified molecules were: (19*R*,23*E*)-5β,19-epoxy-19-methoxycucurbita-6,23,25-trien-3β-ol,

(23*E*)-3 β -hydroxy-7 β -methoxycucurbita-5,23,25-trien-19-al, and (23*E*)-3 β -hydroxy-7 β ,25-dimethoxycucurbita-5,23-dien-19-al (52). Other studies have also identified several CTMs from Chinese bitter melon fruit. Methanol extracts of fruit were used to isolate three new triterpenes (83). Other CTMs isolated from Chinese bitter melon include: (23*E*)-5 β ,19-epoxycucurbita-6,23,25-triene-3 β -ol, (19*R*, 23*E*)-5 β ,19-epoxy-19-ethoxycucurbita-6,23-diene-3 β ,25-diol and 5 β ,19-epoxy-cucurbita-6,22*E*,24-trien-3 β -ol (90, 91). Additional CTMs isolated from Taiwanese wild bitter melon were identified as: cucurbita-6,22(*E*),24-trien-3 β -ol-19,5 β -olide, 5 β ,19-epoxycucurbita-6,22(*E*),24-triene-3 β ,19-diol, 3 β -hydroxycucurbita-5(10),6,22(*E*),24-tetraen-19-al, 19-dimethoxycucurbita-5(10),6,22(*E*),24-tetraen-3 β -ol, and 19-nor-cucurbita-5(10),6,8,22(*E*),24-pentaen-3 β -ol (92). Other studies have also identified CTMs from fruit material, but the origin of the fruit material was not clearly stated. Among the CTMs identified were: 3 β ,25-dihydroxy-7 β -methoxycucurbita-5,23(*E*)-diene, 3 β -hydroxy-7,25-dimethoxycucurbita-5,23(*E*)-diene, and 3-*O*- β -D-allopyranosyl-7 β ,25-dihydroxycucurbita-5,23(*E*)-dien-19-al, 7 β ,25-dimethoxycucurbita-5(6),23(*E*)-dien-19-al 3-*O*- β -D-allopyranoside, and 25-methoxycucurbita-5(6),23(*E*)-dien-19-ol 3-*O*- β -D-allopyranoside (32, 33). While the exocarp of the bitter melon fruit is commonly consumed, one study evaluated the content of the fruit pulp for the content of CTMs and identified two novel compounds as 25-methoxycucurbita-5,23(*E*)-diene-3 β -19-diol and 7 β -ethoxy-3 β hydroxy-25-methoxycucurbita -5,23(*E*)-din-19al (93).

B. Leaves

Similarly, several CTMs have been isolated from leaves of the bitter melon plant. For example, 3 β ,7 β ,23-trihydroxycucurbita-5,24-diene-7-*O*- β -D-glucoside, 3 β ,7 β ,25-trihydroxycucurbita-5,23(*E*)-dien-19-al, were identified from leaves of bitter melon, along with previously identified momordicin and momordicosides (35). Triterpenoids isolated from the leaves of bitter melon plants have also been found to have potent biological activities. For example, Japanese bitter melon methanol leaf extracts yielded 11 previously-isolated and six new compounds, (23*E*)-3 β ,25-dihydroxy-7 β -methoxycucurbita-5,23-dien-19-al, (23*S**)-3 β -hydroxy-7 β ,23-dimethoxycucurbita-5,24-dien-19-al, (23*R**)-23-*O*-methylmomordicine IV, (25 ξ)-26-hydroxymomordicoside L, 25-oxo-27-normomordicoside L, and 25-*O*-methylkaravilagenin D (79). In another study, lanost-5, 23(*Z*)-diene-3 β ,7 β ,25-triol-30a-carbaldehyde, known as charantal, was isolated from leaves of bitter melon and was shown to have strong antitubercular activity (94). CTMs with similar structural characteristics, such as (19*R*,23*E*)-5 β ,19-epoxy-19,25-dimethoxycucurbita-6,23-dien-3 β -ol and (19*R*,23*E*)-5 β ,19-epoxy-19-methoxycucurbita-6,23-diene-3 β ,25-diol, were also identified in other *Momordica* species (57).

Recently, sixteen CTMs were isolated from leaves and vines of bitter melon, of which six were newly-identified compounds. These novel compounds were identified as: (3 β ,7 β ,15 β ,23*E*)-3,7,15,25-tetrahydroxycucurbita-5,23-dien-19-al, (3 β ,7 β)-3,7,22,23-tetrahydroxycucurbita-5,24-dien-19-al, (3 β ,7 β)-3,7,23,24-

tetrahydroxycucurbita-5,25-dien-19-al, (3 β ,7 β ,23 S)-3,7,23-trihydroxycucurbita-5,24-dien-19-al 7- β -D-glucopyranoside, (3 β ,7 β ,23 E)-cucurbita-5,23-diene-3,7,19,25-tetrol 7- β -D-glucopyranoside, and (3 β ,7 β ,23 E)-3,7-dihydroxy-25-methoxycucurbita-5,23-dien-19-al 3- β -D-allopyranoside (31).

C. Stems

Further studies focusing on the identification of CTM from bitter melon ethanol stem extracts led to the discovery of several molecules. In a study by Chang et al., five new cucurbitane-type triterpenes, (23 E)-25-methoxycucurbit-23-ene-3 β ,7 β -diol, (23 E)-cucurbita-5,23,25-triene-3 β ,7 β -diol, (23 E)-25-hydroxycucurbita-5,23-diene-3,7-dione, (23 E)-cucurbita-5,23,25-triene-3,7-dione, and (23 E)-5 β ,19-epoxycucurbita-6,23-diene-3 β ,25-diol were isolated from bitter melon stems and characterized, along with a previously-identified molecule (41). Similarly in 2008, stems were used for isolation of four new compounds: cucurbita-5,23(E)-diene-3 β ,7 β ,25-triol, 3 β -acetoxy-7 β -methoxycucurbita-5,23(E)-dien-25-ol, cucurbita-5(10),6,23(E)-triene-3 β ,25-diol, and cucurbita-5,24-diene-3,7,23-trione (95). Additional isolation efforts yielded triterpenoids from stems, identified as 3 β -hydroxymultiflora-8-en-17-oic acid, cucurbita-1(10),5,22,24-tetraen-3 α -ol and 5 β ,19 β -epoxycucurbita-6,22,24-trien-3 α -ol, which were also shown to possess antioxidant properties (96).

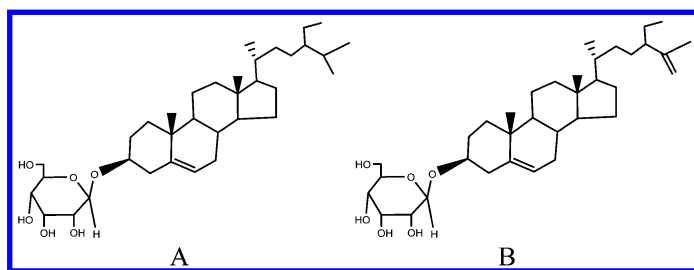


Figure 4. Charantin, a mixture of sitosteryl glucoside (A) and stigmasteryl glucoside (B).

Sterols from *Momordica charantia*

Several acylglucosyl sterol have been isolated from the immature *Momordica charantia* fruit, but many were in such low concentrations that their characterization was not performed. The major acylglucosyl sterol was 3-O-[6'-O-palmitoyl- β -d-glucosyl]-stigmasta-5,25(27)-diene while the minor component was 3-O-[6'-O-stearyl- β -d-glucosyl]-stigmasta-5,25(27)-diene (97). Another group of sterols that received considerable attention was a group of molecules known as charantin (Fig.4). Charantin is composed of a 1:1 mixture of sitosteryl

glucoside and stigmasteryl glucoside. Early studies have proposed charantin as the basis of bitter melon's antidiabetic properties (38). Additional sterols have been identified from fruits including 24(R)-stigmastan-3 β ,5 α ,6 β -triol-25-ene 3-O- β -glucopyranoside, 25 ξ -isopropenylchole-5,(6)-ene-3-O- β -D-glucopyranoside and 7-oxo-stigmasta-5,25-diene-3-O- β -D-glucopyranoside (30, 83, 98).

Summary

Decades of research have elucidated the structures and potential functions of various CTMs isolated from bitter melon. Advances in purification technology have also afforded powerful tools to continue exploring bitter melon in order to pinpoint the compound or compounds responsible for its bioactivities. While most purification efforts have focused on alcohol extracts, some future efforts should focus on exploring non-polar extracts. Additionally, optimization of extraction and purification procedures should be undertaken to avoid the excess use of solvents and reduce extraction times.

Acknowledgments

The current report is based on work supported by the "Designing Foods for Health" through United States Department of Agriculture – National Institute of Food and Agriculture (USDA-NIFA) # 2010-34402-20875 and through the Vegetable & Fruit Improvement Center, Texas AgriLife Research.

References

1. Turner, L. W.; Nartey, D.; Stafford, R. S.; Singh, S.; Alexander, G. C. *Diabetes care* **2013**, *37*, 985–992.
2. Sjöholm, Å.; Nyström, T. *Diabetes/Metab. Res. Rev.* **2006**, *22*, 4–10.
3. Jung, S.; Spiegelman, D.; Baglietto, L.; Bernstein, L.; Boggs, D. A.; van den Brandt, P. A.; Buring, J. E.; Cerhan, J. R.; Gaudet, M. M.; Giles, G. G. *J. Natl. Cancer Inst.* **2013**, *105*, 219–236.
4. Chan, J. M.; Giovannucci, E. L. *Epidemiol. Rev.* **2013**, *23*, 82–6.
5. Clifton, P. M.; Petersen, K. S.; Blanch, N.; Keogh, J. B. *Curr. Opin. Lipidol.* **2014**, *25*, 155–156.
6. Patil, B. S.; Jayaprakasha, G.; Vikram, A. *HortScience* **2012**, *47*, 821–827.
7. Chaturvedi, P. *J. Med. Food* **2012**, *15*, 101–107.
8. Pitchakarn, P.; Ogawa, K.; Suzuki, S.; Takahashi, S.; Asamoto, M.; Chewonarin, T.; Limtrakul, P.; Shirai, T. *Cancer Sci.* **2010**, *101*, 2234–2240.
9. Wang, Z. Q.; Zhang, X. H.; Yu, Y.; Poulev, A.; Ribnicky, D.; Floyd, Z. E.; Cefalu, W. T. *J. Nutr. Biochem.* **2011**, *22*, 1064–1073.
10. Cloutre, D. L.; Rao, S. N.; Preuss, H. G. *J. Med. Food* **2011**, *14*, 1496–1504.
11. Kaur, M.; Deep, G.; Jain, A. K.; Raina, K.; Agarwal, C.; Wempe, M. F.; Agarwal, R. *Carcinogenesis* **2013**, *34*, 1585–1592.
12. Nerurkar, P. V.; Lee, Y.-K.; Nerurkar, V. R. *BMC Complementary Altern. Med.* **2010**, *10*, 34.

13. Xiang, L.; Huang, X.; Chen, L.; Rao, P.; Ke, L. *Asia Pac. J. Clin. Nutr.* **2007**, *16*.
14. Sridhar, M.; Vinayagamoorthi, R.; Arul Suyambunathan, V.; Bobby, Z.; Selvaraj, N. *Br. J. Nutr.* **2008**, *99*, 806–812.
15. Myojin, C.; Enami, N.; Nagata, A.; Yamaguchi, T.; Takamura, H.; Matoba, T. *J. Food Sci.* **2008**, *73*, C546–C550.
16. Tuan, P. A.; Kim, J. K.; Park, N. I.; Lee, S. Y.; Park, S. U. *Food Chem.* **2011**, *126*, 1686–1692.
17. Wu, S.-J.; Ng, L.-T. *LWT–Food Sci. Technol.* **2008**, *41*, 323–330.
18. Lee, S. Y.; Eom, S. H.; Kim, Y. K.; Park, N. I.; Park, S. U. *J. Med. Plants Res.* **2009**, *3*, 1264–1269.
19. Chen, J. C.; Chiu, M. H.; Nie, R. L.; Cordell, G. A.; Qiu, S. X. *Nat. Prod. Rep.* **2005**, *22*, 386–399.
20. Singh, J.; Cumming, E.; Manoharan, G.; Kalasz, H.; Adeghate, E. O. *Open Med. Chem. J.* **2011**, *5*, 70.
21. Tan, M.-J.; Ye, J.-M.; Turner, N.; Hohnen-Behrens, C.; Ke, C.-Q.; Tang, C.-P.; Chen, T.; Weiss, H.-C.; Gesing, E.-R.; Rowland, A.; James, D. E.; Ye, Y. *Chem. Biol.* **2008**, *15*, 263–273.
22. Li, Q. Y.; Liang, H.; Chen, H. B.; Wang, B.; Zhao, Y. Y. *Chin. Chem. Lett.* **2007**, *18*, 843–845.
23. Zhang, J.; Huang, Y.; Kikuchi, T.; Tokuda, H.; Suzuki, N.; Inafuku, K.; Miura, M.; Motohashi, S.; Suzuki, T.; Akihisa, T. *Chem. Biodiversity* **2012**, *9*, 428–440.
24. Chang, C. I.; Chen, C. R.; Liao, Y. W.; Shih, W. L.; Cheng, H. L.; Tzeng, C. Y.; Li, J. W.; Kung, M. T. *Chem. Pharm. Bull.* **2010**, *58*, 225–229.
25. Chang, C. I.; Chen, C. R.; Liao, Y. W.; Cheng, H. L.; Chen, Y. C.; Chou, C. H. *J. Nat. Prod.* **2008**, *71*, 1327–1330.
26. Hsu, C.; Hsieh, C. L.; Kuo, Y. H.; Huang, C. *J. Agric. Food Chem.* **2011**, *59*, 4553–4561.
27. Chen, J.-C.; Liu, W.-Q.; Lu, L.; Qiu, M.-H.; Zheng, Y.-T.; Yang, L.-M.; Zhang, X.-M.; Zhou, L.; Li, Z.-R. *Phytochemistry* **2009**, *70*, 133–140.
28. Liu, C.-H.; Yen, M.-H.; Tsang, S.-F.; Gan, K.-H.; Hsu, H.-Y.; Lin, C.-N. *Food Chem.* **2010**, *118*, 751–756.
29. Liu, J. Q.; Chen, J. C.; Wang, C. F.; Qiu, M. H. *Molecules* **2009**, *14*, 4804–4813.
30. Wang, X.; Sun, W.; Cao, J.; Qu, H.; Bi, X.; Zhao, Y. *J. Agric. Food Chem.* **2012**, *60*, 3927–3933.
31. Cheng, B. H.; Chen, J. C.; Liu, J. Q.; Zhou, L.; Qiu, M. H. *Helv. Chim. Acta* **2013**, *96*, 1111–1120.
32. Harinantenaina, L.; Tanaka, M.; Takaoka, S.; Oda, M.; Mogami, O.; Uchida, M.; Asakawa, Y. *Chem. Pharm. Bull.* **2006**, *54*, 1017–1021.
33. Liu, Y.; Ali, Z.; Khan, I. A. *Planta Med.* **2008**, *74*, 1291–1294.
34. Chen, J.; Tian, R.; Qiu, M.; Lu, L.; Zheng, Y.; Zhang, Z. *Phytochemistry* **2008**, *69*, 1043–1048.
35. Fatope, M. O.; Takeda, Y.; Yamashita, H.; Okabe, H.; Yamauchi, T. *J. Nat. Prod.* **1990**, *53*, 1491–1497.

36. Murakami, T.; Emoto, A.; Matsuda, H.; Yoshikawa, M. *Chem. Pharm. Bull.* **2001**, *49*, 54–63.
37. Nakamura, S.; Murakami, T.; Nakamura, J.; Kobayashi, H.; Matsuda, H.; Yoshikawa, M. *Chem. Pharm. Bull.* **2006**, *54*, 1545–1550.
38. Pitipanapong, J.; Chitprasert, S.; Goto, M.; Jiratchariyakul, W.; Sasaki, M.; Shotipruk, A. *Sep. Purif. Technol.* **2007**, *52*, 416–422.
39. Ji, H.; Zhang, L.; Li, J.; Yang, M.; Liu, X. *Int. J. Food Eng.* **2010**, *6*.
40. Okabe, H.; Miyahara, Y.; Yamauchi, T.; Miyahara, K.; Kawasaki, T. *Chem. Pharm. Bull.* **1980**, *28*, 2753–2762.
41. Chang, C.-I.; Chen, C.-R.; Liao, Y.-W.; Cheng, H.-L.; Chen, Y.-C.; Chou, C.-H. *J. Nat. Prod.* **2006**, *69*, 1168–1171.
42. Akihisa, T.; Higo, N.; Tokuda, H.; Ukiya, M.; Akazawa, H.; Tochigi, Y.; Kimura, Y.; Suzuki, T.; Nishino, H. *J. Nat. Prod.* **2007**, *70*, 1233–1239.
43. Li, Q. Y.; Chen, H. B.; Liu, Z. M.; Wang, B.; Zhao, Y. Y. *Magn. Reson. Chem.* **2007**, *45*, 451–456.
44. Chen, J.; Tian, R.; Qiu, M.; Lu, L.; Zheng, Y.; Zhang, Z. *Phytochemistry* **2008**, *69*, 1043–1048.
45. Chen, J. C.; Lu, L.; Zhang, X. M.; Zhou, L.; Li, Z. R.; Qiu, M. H. *Helv. Chim. Acta* **2008**, *91*, 920–929.
46. Horax, R.; Hettiarachchy, N.; Islam, S. *J. Food Sci.* **2005**, *70*, C275–C280.
47. Islam, S.; Jalaluddin, M.; Hettiarachchy, N. S. *Funct. Foods Health Dis* **2011**, *2*, 61–74.
48. YongKyoung, K.; Hui, X. *J. Med. Plants Res.* **2009**, *3*, 894–897.
49. Ullah, M.; Chy, F. K.; Sarkar, S. K.; Islam, M. K.; Absar, N. *Asian J. Agric. Res.* **2011**, *5*, 186–193.
50. Sathishsekar, D.; Subramanian, S. Antioxidant properties of Momordica Charantia (bitter gourd) seeds on Streptozotocin induced diabetic rats. *Asia Pac. J. Clin. Nutr.* **2005**, *14*, 153–158.
51. Fonseka, R.; Wickramasinghe, P.; Kumara, P.; Wickramarachchi, W.; Fonseka, H.; Chandrasekara, A. In *1st International Conference on Indigenous Vegetables and Legumes. Prospectus for Fighting Poverty, Hunger and Malnutrition 752*; International Society for Horticultural Science: Leuven, Belgium, 2006; pp 131–136.
52. Kimura, Y.; Akihisa, T.; Yuasa, N.; Ukiya, M.; Suzuki, T.; Toriyama, M.; Motohashi, S.; Tokuda, H. *J. Nat. Prod.* **2005**, *68*, 807–809.
53. Guevara, A. P.; Lim-Sylianco, C.; Dayrit, F.; Finch, P. *Mut. Res.* **1990**, *230*, 121–126.
54. Ma, J.; Whittaker, P.; Keller, A. C.; Mazzola, E. P.; Pawar, R. S.; White, K. D.; Callahan, J. H.; Kennelly, E. J.; Krynitsky, A. J.; Rader, J. I. *Planta Med.* **2010**, *76*, 1758–1761.
55. Perez, J. L.; Jayaprakasha, G.; Patil, B. S. Separation of cucurbitane-type triterpenoids from bitter melon using flash chromatography. In *246th ACS National Meeting*, Indianapolis, IN, 2013.
56. Okabe, H.; Miyahara, Y.; Yamauchi, T. *Chem. Pharm. Bull.* **1982**, *30*, 4334–4340.
57. Mulholland, D. A.; Sewram, V.; Osborne, R.; Pegel, K. H.; Connolly, J. D. *Phytochemistry* **1997**, *45*, 391–395.

58. Abe, M.; Matsuda, K. *Appl. Entomol. Zool.* **2000**, *35*, 143–149.
59. Matsuda, H.; Nakamura, S.; Murakami, T.; Yoshikawa, M. *Heterocycles* **2007**, *71*, 331–341.
60. Mekuria, D. B.; Kashiwagi, T.; Tebayashi, S.-i.; Kim, C.-S. *Biosci., Biotechnol., Biochem.* **2005**, *69*, 1706–1710.
61. Chang, C.-I.; Chen, C.-R.; Liao, Y.-W.; Shih, W.-L.; Cheng, H.-L.; Tzeng, C.-Y.; Li, J.-W.; Kung, M.-T. *Chem. Pharm. Bull.* **2010**, *58*, 225–229.
62. Miyahara, Y.; Okabe, H.; Yamauchi, T. *Chem. Pharm. Bull.* **1981**, *29*, 1561–1566.
63. Okabe, H.; Miyahara, Y.; Yamauchi, T. *Tetrahedron Lett.* **1982**, *23*, 77–80.
64. Okabe, H.; Miyahara, Y.; Yamauchi, T. *Chem. Pharm. Bull.* **1982**, *30*, 3977–3986.
65. Donya, A.; Hettiarachchy, N.; Liyanage, R.; Lay, J.; Chen, P.; Jalaluddin, M. *J. Agric. Food Chem.* **2007**, *55*, 5827–5833.
66. Nhiem, N. X.; Kiem, P. V.; Minh, C. V.; Ban, N. K.; Cuong, N. X.; Ha, L. M.; Tai, B. H.; Quang, T. H.; Tung, N. H.; Kim, Y. H. *Magn. Reson. Chem.* **2010**, *48*, 392–396.
67. Yasuda, M.; Iwamoto, M.; Okabe, H.; Yamauchi, T. *Chem. Pharm. Bull.* **1984**, *32*, 2044–2047.
68. Chandravadana, M.; Chander, M. *Indian J. Exp. Biol.* **1990**, *28*, 185–186.
69. Yasui, H. *Jpn. Agric. Res. Q.* **2002**, *36*, 25–30.
70. Yasui, H.; Kato, A.; Yazawa, M. *J. Chem. Ecol.* **1998**, *24*, 803–813.
71. Kashiwagi, T.; Mekuria, D. B.; Dekebo, A.; Sato, K.; Tebayashi, S.-i.; Kim, C. *Z. Naturforsch.* **2007**, *62*, 603.
72. Zhao, G.-T.; Liu, J.-Q.; Deng, Y.-Y.; Li, H.-Z.; Chen, J.-C.; Zhang, Z.-R.; Zhou, L.; Qiu, M.-H. *Fitoterapia* **2014**, *95*, 75–82.
73. Nhiem, N. X.; Kiem, P. V.; Minh, C. V.; Ban, N. K.; Cuong, N. X.; Tung, N. H.; Ha, L. M.; Ha, D. T.; Tai, B. H.; Quang, T. H. *Chem. Pharm. Bull.* **2010**, *58*, 720–724.
74. Yen, P. H.; Dung, D. T.; Nhiem, N. X.; Anh, H. T.; Hang, D.; Yen, D.; Cuc, N.; Ban, N. K.; Van Minh, C.; Van Kiem, P. *Nat. Prod. Commun.* **2014**, *9*, 383–386.
75. Liu, J.-Q.; Chen, J.-C.; Wang, C.-F.; Qiu, M.-H. *Eur. J. Chem.* **2010**, *1*, 294–296.
76. Hsiao, P.-C.; Liaw, C.-C.; Hwang, S.-Y.; Cheng, H.-L.; Zhang, L.-J.; Shen, C.-C.; Hsu, F.-L.; Kuo, Y.-H. *J. Agric. Food Chem.* **2013**, *61*, 2979–2986.
77. Zhang, L.-J.; Liaw, C.-C.; Hsiao, P.-C.; Huang, H.-C.; Lin, M.-J.; Lin, Z.-H.; Hsu, F.-L.; Kuo, Y.-H. *J. Funct. Foods* **2014**, *6*, 564–574.
78. Chen, C.-R.; Liao, Y.-W.; Wang, L.; Kuo, Y.-H.; Liu, H.-J.; Shih, W.-L.; Cheng, H.-L.; Chang, C.-I. *Chem. Pharm. Bull.* **2010**, *58*, 1639–1642.
79. Zhang, J.; Huang, Y.; Kikuchi, T.; Tokuda, H.; Suzuki, N.; Inafuku, K. i.; Miura, M.; Motohashi, S.; Suzuki, T.; Akihisa, T. *Chem. Biodiversity* **2012**, *9*, 428–440.
80. Popovich, D. G.; Lee, Y.; Li, L.; Zhang, W. *J. Med. Food* **2011**, *14*, 201–208.
81. Ma, L.; Yu, A.-H.; Sun, L.-L.; Gao, W.; Zhang, M.-M.; Su, Y.-L.; Liu, H.; Ji, T.-F.; Li, D.-Z. *J. Asian Nat. Prod. Res.* **2014**, 1–7.

82. Cao, J. Q.; Zhang, Y.; Cui, J. M.; Zhao, Y. Q. *Chin. Chem. Lett.* **2011**, *22*, 583–586.
83. Liu, J.-Q.; Chen, J.-C.; Wang, C.-F.; Qiu, M.-H. *Molecules* **2009**, *14*, 4804–4813.
84. Tabata, K.; Hamano, A.; Akihisa, T.; Suzuki, T. *Cancer Sci.* **2012**, *103*, 2153–2158.
85. Keller, A. C.; Ma, J.; Kavalier, A.; He, K.; Brillantes, A.-M. B.; Kennelly, E. J. *Phytomedicine* **2011**, *19*, 32–37.
86. Ling, B.; Wang, G.-C.; Ya, J.; Zhang, M.-X.; Liang, G.-W. *Agric. Sci. China* **2008**, *7*, 1466–1473.
87. Zhang, Y.-B.; Liu, H.; Zhu, C.-Y.; Zhang, M.-X.; Li, Y.-L.; Ling, B.; Wang, G.-C. *J. Asian Nat. Prod. Res.* **2014**, *16*, 358–363.
88. Mekuria, D. B.; Kashiwagi, T.; Tebayashi, S.-i.; Kim, C.-S. *Z. Naturforsch., C: J. Biosci.* **2006**, *61*, 81–86.
89. Lin, K.-W.; Yang, S.-C.; Lin, C.-N. *Food Chem.* **2011**, *127*, 609–614.
90. Cao, J. Q.; Zhang, Y.; Cui, J. M.; Zhao, Y. Q. *Chin. Chem. Lett.* **2011**, *22*, 583–586.
91. Cao, J.-Q.; Zhang, B.-Y.; Zhao, Y.-Q. *Chin. Herb. Med.* **2013**, *5*, 234–236.
92. Hsu, C.; Hsieh, C.-L.; Kuo, Y.-H.; Huang, C.-J. *J. Agric. Food Chem.* **2011**, *59*, 4553–4561.
93. Liao, Y. W.; Chen, C. R.; Chuu, J. J.; Huang, H. C.; Hsu, J. L.; Huang, T. C.; Kuo, Y. H.; Chang, C. I. *J. Chin. Chem. Soc.* **2013**.
94. Panlilio, B. G.; Macabeo, A. P. G.; Knorn, M.; Kohls, P.; Richomme, P.; Kouam, S. F.; Gehle, D.; Krohn, K.; Franzblau, S. G.; Zhang, Q. *Phytochem. Lett.* **2012**.
95. Chang, C.-I.; Chen, C.-R.; Liao, Y.-W.; Cheng, H.-L.; Chen, Y.-C.; Chou, C.-H. *J. Nat. Prod.* **2008**, *71*, 1327–1330.
96. Liu, C.-H.; Yen, M.-H.; Tsang, S.-F.; Gan, K.-H.; Hsu, H.-Y.; Lin, C.-N. *Food Chem.* **2010**, *118*, 751–756.
97. Guevara, A. P.; Lim-Sylianco, C. Y.; Dayrit, F. M.; Finch, P. *Phytochemistry* **1989**, *28*, 1721–1724.
98. Liu, P.; Lu, J.-F.; Kang, L.-P.; Yu, H.-S.; Zhang, L.-J.; Song, X.-B.; Ma, B.-P. *Chin. J. Nat. Med.* **2012**, *10*, 88–91.

Chapter 4

Fast Analysis of Bioactive Compounds by Reverse Phase Liquid Chromatography

**Gislaine C. Nogueira, Mauricio A. Rostagno,*
M. Thereza M. S. Gomes, and M. Angela A. Meireles**

LASEFI/DEA (Department of Food Engineering)/FEA (School of Food Engineering)/UNICAMP (University of Campinas), Rua Monteiro Lobato, 80; Campinas, SP; CEP: 13083-862, Brazil

***E-mail: rostagno@fea.unicamp.br; mauricio.rostagno@gmail.com.
Tel: +55-19-35210100. Fax: +55 19 35214027.**

The analysis of bioactive compounds in raw bioactive materials by liquid chromatography can prove to be a very difficult task and usually require extended times to adequately separate all components from such complex matrices. Currently there is a great interest in the development of new technology to improve chromatographic performance and reduce the necessary time to achieve the separation between components. Liquid chromatography has seen great improvements in the last decades, especially in stationary phase technology. New stationary phase technologies include sub-2 μm particles, partially porous and porous monolithic polymers. These new packing materials are taking the chromatographic performance of separations to a much higher level. Liquid chromatography systems are also seen improvements in term of pressure limits, precision, reproducibility and overall quality of the results. The use of these advanced systems and materials allied to the adoption of carefully planned strategies under optimized conditions can produce excellent chromatographic results with speeds that were thought to be impossible a few years ago. In this context, this chapter discusses current technology available that can be explored to reduce analysis time of bioactive compounds in natural products. It also discusses the influence of most important operational parameters (column

temperature, mobile phase composition and flow rate/ linear velocity in the chromatographic system and how these variables can be adjusted in order to produce the greatest potential for performing separations.

Keywords: Bioactive compounds; liquid chromatography; fast analysis; Sub-2 μm particles; partially porous particles; monolithic columns; temperature; mobile phase; flow rate

1. Introduction

Raw bioactive materials are complex matrixes which contain innumerable chemical compounds with great structural diversity and functional versatility. Several of these compounds are of great interest because they are capable of modulating metabolism and altering gene expression and cellular signaling, among other biological processes. The biological activity of these compounds is closely related to the lead of raw bioactive materials as the most productive source for potential drugs, veterinary and agricultural products (1, 2). Several important compounds have been identified in natural sources, such as phenolic compounds in mushrooms (3), isoflavones in soybeans and derivatives (4), coffeoylquinic acid in artichokes (5), polyphenols and alkaloids in tea and coffee (6, 7), besides other chemical sources for anti-inflammatory (8) and novel drugs (2).

Although some of these compounds are found in relatively high amounts in raw bioactive materials, their concentration varies enormously due to many factors. Concentration and distribution of several compound classes in plants, for example, may be influenced by the plant variety, agricultural practices used, environmental conditions, site of cultivation, attack by microorganisms and pests, among others. In this aspect, the variation of the concentration of compounds present in raw bioactive materials combined with other factors causes great difficulties when identifying the biological potential and efficiency of these compounds for the prevention and treatment of several diseases. Understanding the complexities of the bioactivity of compounds present in raw material through extensive laboratory analysis is fundamental for proper utilization of their potential uses.

Considering the importance of having reliable information about their concentration, it is not surprising that several techniques were used and explored to develop methods for the analysis of bioactive compounds over the years (9). Obviously the characteristics of the molecule and the characteristics of sample, including the components present and their profile and concentration, will determine best technique and method conditions. However, liquid chromatography (LC) is one of the most used techniques due to its advantages which include high separation achievements, method reliability, method sensitivity and compound specificity (10). In this aspect, High Performance LC (HPLC) provides high resolution results, accuracy, data management, security features, reports and instrument validation. For many years, researchers have

been concerned about speeding up LC assays and reducing sample amount as well as solvent spent in an effort, not only to diminishing costs, but also to provide more environment friendly techniques.

2. Fast LC Separations

There is always been a great interest in the development of fast LC methods for the analysis of bioactive compounds in raw bioactive materials. Fast methods can provide several advantages not only in terms of the number of samples that can be processed in a given amount of time, but also in terms of reduction of cost, by increasing the life span of detector lamps and reducing amounts of solvents used (which may also provide environmental benefits). Moreover, fast methods are convenient for samples which are evolving continuously in a short period such as products containing enzymes. Several strategies have been used to increase the speed of LC separations, including shorter columns with new stationary phases and exploring method conditions (temperature, solvent and flow rate) to reduce analysis time (Figure 1).

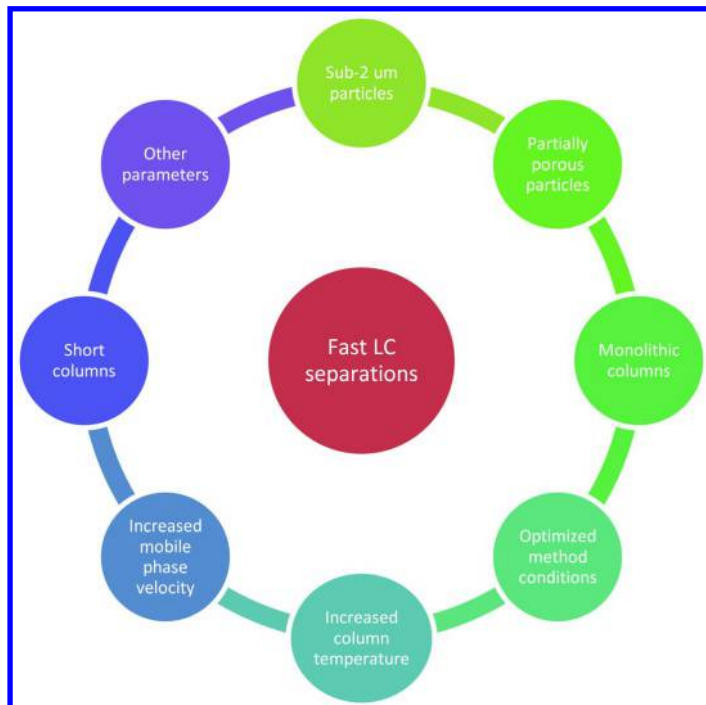


Figure 1. Strategies used to improve and speed-up LC separations.

Table 1. Selection of Recent Applications of Fast LC Strategies for the Analysis of Bioactive Compounds in Raw Materials

<i>Analytes / Sample</i>	<i>Sample preparation</i>	<i>Instrumental analysis</i>	<i>Ref.</i>
Phenolic compounds/ Edible mushrooms	Pre-treatment: freeze-dried and finely milled Extraction: by stirring with methanol at 65°C for 24 h. Then, the mixture was centrifugated at 3000 rpm for 10 min. The residue was re-extracted twice and the methanolic extracts were combined and evaporated to dryness under vacuum	Technique: HPLC-DAD Column: Symmetry reverse phase C ₁₈ (75mmX4.6 mm, 3.5µm) Solvent: Acetonitrile /water/acetic water Column temperature: 25°C Flow rate: 1.0 mL.min ⁻¹ Analysis time: 16 min Detector: UV at 280nm	(3)
Phenolic acids/ Beverages (White wine, grapefruit juice and leaves of green tea)	Pre-treatment: Internal standard of deuterium-labeled 4-hydroxybenzoic and salicylic acids were added to all beverage samples. The samples were filtered by centrifugation through 0.2µm nylon membrane microfilters Extraction: not available	Technique: UPLC-MS/MS Column: BEH C ₈ (2.1mmX150mm, 1.7µm) Solvent: Acetonitrile /water/formic acid Column temperature: 30°C Flow rate: 0.25 mL.min ⁻¹ Analysis time: 12 min Detector: PDA at 230nm	(14)
21 Polyphenols and Alkaloids/ Teas, mate, instant coffee, soft drink and energetic drink	Pre-treatment: not available Extraction: Extraction: with 15mL of 50% methanol, than with 75% methanol, and finally with 100% methanol for 20 min at 60 °C assisted by ultrasound. After, the sample was centrifuged, than the solid was submitted to another extraction using a multi-frequency ultrasonic bath operating at 25 kHz at 100% intensity output.	Technique: HPLC-DAD-FI Column: Kinetex™ C ₁₈ (100mm×4.6mm, 2.6µm) Solvent: Acetonitrile /water/phosphoric acid Column temperature: 55°C Flow rate: 2.2 mL.min ⁻¹ Analysis time: 5.0 min Detector: UV at 260-320nm	(7, 15)

<i>Analytes / Sample</i>	<i>Sample preparation</i>	<i>Instrumental analysis</i>	<i>Ref.</i>
Catechin derivatives/Tea samples	Pre-treatment: not available Extraction: Infusion in water with boiling water	Technique: UHPLCUV and UHPLCMS/MS Column: Hypersil Gold C ₁₈ (50mm×2.1mm, 1.9µm); Acquity BEH C ₁₈ (50mm×2.1mm, 1.7µm); Acquity BEH Shield RP ₁₈ (50, 100 and 150mm×2.1mm, 1.7µm); Acquity BEH phenyl (50mm×2.1mm, 1.7µm) Solvent: Acetonitrile /water/formic acid Column temperature: 30°C Flow rate: 0.6 mL.min ⁻¹ Analysis time: between 2 and 24 min Detector: UV at 265nm	(16)
Resveratrol/Red wines	Pre-treatment: red wine was diluted with methanol and filtered through a 0.22µm membrane filter. Extraction: not available	Technique: SPE-LC-MS Column: Halo fused-core silica (50mmX2.1mm, 2.7 µm) Solvent: Acetonitrile /water/formic acid Column temperature: not provided Flow rate: 0.4 mL.min ⁻¹ Analysis time: 6.0 min Detector: MS	(17)
15 structurally related components/ Natural products mixtures	Pre-treatment: dissolving final product in MeOH Extraction: not available	Technique: HPLC and UPLC Column: Ascentis Express C ₁₈ (100mm4.6mm, 2.7µm), Atlantis T3 C ₁₈ (150mmX4.6mm, 3.0µm); Acquity UPLC BEH C ₁₈ (100mmX2.1mm, 1.7µm) Solvent: Acetonitrile /Methanol/potassium phosphate Column temperature: 35°C Flow rate: 0.4 and 2.0 mL.min ⁻¹ Analysis time: 10-31 min Detector: UV at 250nm	(1)

Continued on next page.

Table 1. (Continued). Selection of Recent Applications of Fast LC Strategies for the Analysis of Bioactive Compounds in Raw Materials

<i>Analytes / Sample</i>	<i>Sample preparation</i>	<i>Instrumental analysis</i>	<i>Ref.</i>
12 Isoflavones/ soybeans and derived foods	Pre-treatment: ground into a fine powder in a coffee grinder. Extraction: solid samples were extracted under sonication with 25mL of 50% EtOH (in water) for 20 min at 60 °C. 10mL of MeOH were added to 40mL of liquid samples before extraction under the same conditions. After extraction, 0.5mL of the internal standard was added to the extracts which were then centrifuged.	Technique: HPLC-PDAD Column: Chromolith RP-18e Monolithic Solvent: Methanol/water/acetic acid Column temperature: 35°C Flow rate: 5.0 mL.min ⁻¹ Analysis time: 10 min Detector: UV at 254nm	(4)
12 Isoflavones/ Soy	Pre-treatment: The soy protein sample was ground in a coffee grinder into a fine powder. Extraction: with methanol during 20 min at 60 °C using a ultrasonic bath operating at 25 kHz at 100% intensity output.	Technique: HPLC-UV Column: Xbridge™ C ₁₈ (150mm×4.6 mm, 3.5µm); Kinetex™ fused-core C ₁₈ (100mm×4.6 mm, 2.6µm); Chromolith® Performance monolithic RP-18 (100mm×3mm) Solvent: Mixtures of water and methanol or acetonitrile Column temperature: 25 and 35°C Flow rate: 0.8 and 1.2 mL.min ⁻¹ Analysis time: 6.0 min Detector: UV at 254nm	(18)

<i>Analytes / Sample</i>	<i>Sample preparation</i>	<i>Instrumental analysis</i>	<i>Ref.</i>
12 Isoflavones/ Soy	Pre-treatment: The soy protein sample was ground in a coffee grinder into a fine powder. Extraction: with ethanol during 20 min at 60 °C using a ultrasonic bath operating at 25 kHz at 100% intensity output.	Technique: HPLC-UV Column: Kinetex™ fused-core C ₁₈ (100mm×4.6mm, 2.6µm) Solvent: Methanol/water or Acetonitrile/water Column temperature: 25-50°C Flow rate: 1.2-2.7 mL.min ⁻¹ Analysis time: 11 min Detector: UV at 254nm	(19)
Flavonoids/ <i>Passiflora incarnata</i> L.	Pre-treatment: not available Extraction: The sample were macerated with ethanol 60% for 8 days and the ethanol solution was filtered obtaining the tincture at 20% title, which was evaporated to dryness at reduced pressure (0.1mmHg, T=40°C) and the dried residue dissolved in H ₂ O/MeOH mixture.	Technique: UPLC and HPLC Column: Ascentis® Express (150mm×2.1mm, 2.7µm); Acquity® BEH C ₁₈ (100mm×2.1mm, 1.7µm); Chromolit-RP18e (100mm×4.6mm) Solvent: water/Methanol/ Acetonitrile / tetrahydrofuran and acetic acid Column temperature: 30°C Flow rate: 0.1-0.3 mL.min ⁻¹ Analysis time: 60-22 min Detector: PDA at 299nm	(20)
Caffeoylquinic acid derivatives/artichoke heads and leaves.	Pre-treatment: powdered to a homogeneous size by a grinder, sieved through a No. 40 mesh sieve. Extraction: the sample were mixed with 100 mL 50% aqueous ethanol. The mixture was placed on a thermostatic water bath and incubated at 50°C for 2 h. After, it was centrifuged and the supernatant solution was transferred and the dregs were re-extracted.	Technique: LC-ESI-MS/MS Column: Halo fused core C ₁₈ -silica (50mmX2.1mm, 2.7µm) Solvent: Acetonitrile /water/formic acid Column temperature: 25°C Flow rate: 0.8 mL.min ⁻¹ Analysis time: 4 min Detector: MS/MS	(5)

Currently, columns packed with sub-2 μm particles in ultra-high performance liquid chromatography (UHPLC) systems, columns packed with partially porous particles and monolithic columns are the three main competing approaches for fast liquid chromatography (11, 12). Other strategies include the use of short columns with reduced internal diameter and optimization of the method conditions to improve separation and allow higher flow rates/ linear velocity of the mobile phase. The use of columns packed with smaller particles (totally or partially porous) allows obtaining better resolution, increased efficiency, and increased sensitivity due to sharper and higher peaks, which can be explored to achieve faster chromatographic separations (10).

UHPLC employs columns packed with particles of drastically reduced size (in the sub-2 μm scale), resulting in high column backpressure, which demanded the development of specific instrument capable of operating at pressures over 1.500 bar. More recently, partially porous particles were developed and due to the reduced diffusion path for analytes, they are expected to have superior mass transfer properties compared with fully porous particles and therefore provide similar separation efficiencies compared to sub-2 μm totally porous particles but at much lower pressures (11). In this case, partially porous particles can be used in both conventional HPLC and UHPLC systems. On the other hand, monolithic silica columns are usually used in HPLC systems and due to their characteristics and structure they allow very high flow rates (up to 10 mL/min) to be used in the pressure range of conventional HPLC systems (<200 bar). The high flow rate and the relative high efficiency allow reducing analysis time but also may increase solvent usage (although this will depend of the duration of the method). Another main strategy used to reduce analysis time is the optimization of analysis conditions (temperature, mobile phase composition, flow rate, among others).

One of the key parameters of fast LC separations is column temperature. Since temperature affects both the kinetics and thermodynamics of the chromatographic process, changes in this parameter can help to speed up LC separations. Higher temperatures can reduce solvent viscosity leading to a lower column backpressure which can be explored to increase flow rate (13). The limitations of this strategy can be considered to be the system pressure and column temperature limits. Solvent choice has been another positive gain with fast HPLC development. The reduction of the backpressure allows the use of viscous solvents instead non-viscous solvents which enable the replacement of toxic solvents by ethanol and water, for example (13). The lower viscosity also allows the use of higher of the mobile phase linear velocity which can be explored to reduce analysis time. Each one of those subjects will be more extensively discuss hereafter. Table 1 summarizes recent applications of fast LC separations for the analysis of bioactive compounds.

3. Column Characteristics

One of the main factors affecting separation in LC is the column's dimensions and characteristics. Stationary phase technology has seen amazing developments in the last decades with advances in several key characteristics

(21). Developments in stationary phase particle technology allowed reducing the particle size to less than 2 μm with the associated increase in efficiency and chromatographic performance. On the other hand, partially porous particles with excellent packing allow expanding the ability of conventional HPLC systems to use smaller particles without a great impact on the system pressure. Other types of columns, made of materials such as monolithic silica, are also becoming widely available commercially, which present several advantages over conventional columns. By using modern stationary phases, which are already available, it is possible to improve existing methods in terms of speed, resolution, reproducibility and also to reduce analysis and disposal costs due to the reduced solvent usage.

3.1. Sub-2 μm Particles Columns

The long analysis time resulted from low diffusion coefficients in the liquid phase, as well as analyte in the stationary phase led to the reduction in the size of the packing materials. As the size of the packing decreased, the efficiency, resolution, and the ability to work with short analysis time increased (10). Sensitivity and separation can be greatly improved with these very small particles, due to narrow peaks results (22). As can be seen in Figure 2 (23), as particle size decreases from 5 to 2.6, 1.7 and 1.3 μm , there is a great improvement in column efficiency which can be observed in the form of a lower height equivalent to a theoretical plate (HETP).

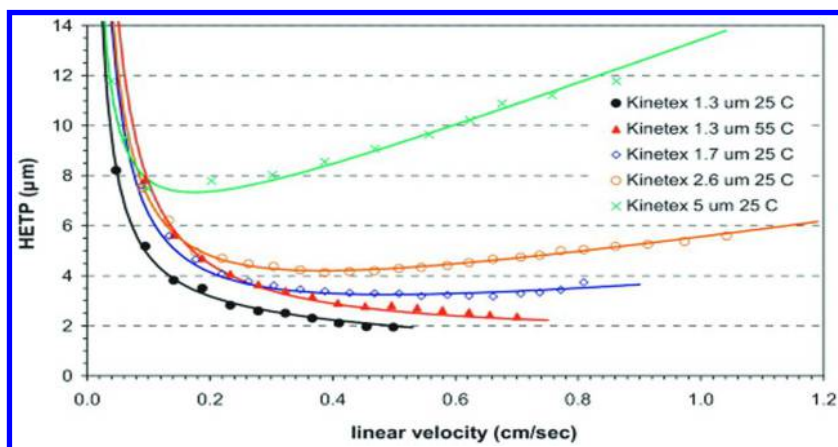


Figure 2. Experimental HEPT (μm) plots of columns packed with 1.3, 1.7, 2.6 and 5 μm partially porous particles (peak widths were corrected for the extra-column band broadening). The test solution was eluted with water/acetonitrile 63/37 on the Kinetex 1.3 μm column. The mobile phase consists of water/ACN 62/38 (v/v) for the 1.7 μm and 2.6 μm columns, and a mixture of water/ACN 60/40 (v/v) for the 5 μm column, to keep the same retention factors for the test solutes on the different columns. The column efficiency of butylparaben was considered. The mobile phase ensured a retention between $k = 6-7$. Reproduced with permission from reference (23). Copyright 2013 Elsevier.

However, smaller particles sizes produce very high operating pressures (10). Conventional HPLC systems reaches its upper pressure limit at 400-600 bar, whereas for the good operation of columns with such small size particles, pressures over 1.000 bar may be required (24). This is because the mobile linear velocity is limited by pressure and if a low velocity is used the column may not provide optimal performance (i.e. high HETP) as seen in Figure 2.

Only the development of new and advanced systems can provide the appropriate operating conditions to columns packed with sub-2 μm totally porous particles. UHPLC systems were designed to withstand very high pressure limits (up to 1.500 bar). Even though UHPLC systems have a very high pressure limit, UHPLC stationary phases generate so much pressure in small diameter columns that implies that a low operational flow rate must be used, which is usually below 1 mL/min. The good part is that the smaller particles are more efficient and therefore require less stationary phase to perform the same separation than achieved with larger particles and thus shorter columns can be used. With shorter columns the path that molecules need to permeate is smaller which will eventually reduce the analysis time if sufficient efficiency is provided. Another advantage of shorter columns is that they generate lower back pressure than longer ones, which can be explored alone or combined with other strategies to further reduce particle size or to increase mobile linear velocity.

However, as column's dimensions are reduced and mobile phase linear velocity is increased, the characteristics of the equipment start to increase its effects in the separation. The system dead volume influences the chromatographic performance of the separation and this factor increases its importance as the dimensions of the column are reduced. However, judicious selection of the column dimensions can alleviate the situation. Short columns are demanding since they generate peaks with very small volume and the effect of extra column volume will be less pronounced as the volume (both length and i.d.) of the column is increased (25). In this context, UHPLC columns are usually available with reduced internal diameter (i.e. 2.1. μm). Tubing length and internal diameter and several components (such as the volume of the detector cell) were also optimized in UHPLC systems to minimize the dead volume of the system and improve the chromatographic performance.

There are several examples of the application of UHPLC for the fast analysis of bioactive compounds in raw bioactive materials, such as phenolic compounds, which are one of the most studied compounds classes (Table 1). Overall, the extreme efficiencies that may be achieved by UHPLC are translated into methods that take only a few minutes to perform the analysis (rather than hours) while being able to separate dozens of compounds on a single run. Such high performance is setting a new standard in LC separations in terms of speed, efficiency and solvent consumption. Surely recent HPLC owners did not find all good in this perspective because their equipment is expected to last for several years without becoming obsolete.

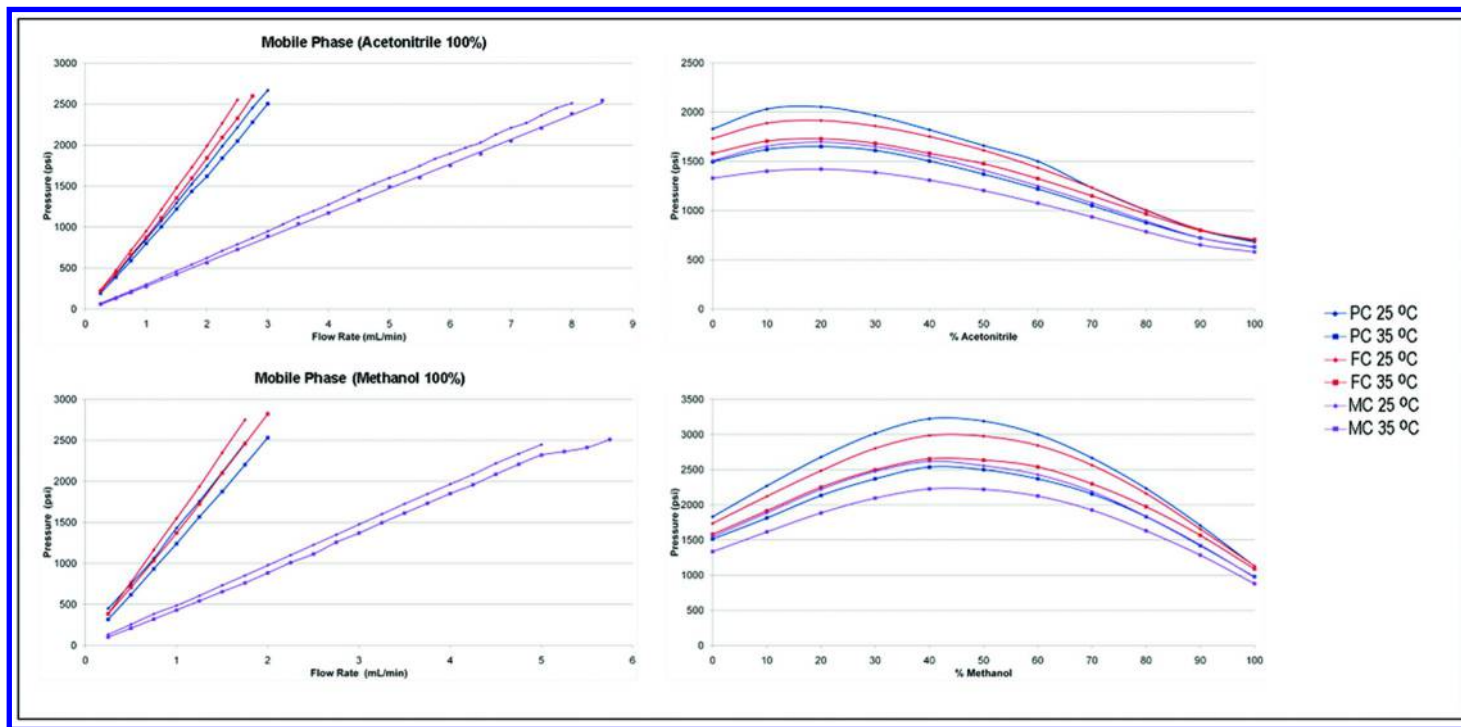


Figure 3. System pressure using different types of columns at different temperatures, flow rates, and mobile phase composition in a conventional HPLC. CP conventional particle column, FC fused-core column, MC monolithic column. Reproduced with permission from reference (18). Copyright 2011 Elsevier.

3.2. Columns Packed with Partially Porous (Fused-Core) Particles

Another emerging technology to improve LC separations is based on columns packed with partially porous particles. In contrast to the totally porous particles used in conventional LC columns, partially porous particles (also termed fused-core, core-shell or porous-shell) are high-purity silica particles with a solid core and a thin porous outer shell (26). The size of the partially porous particles commercially available starts at 1.2 μm solid core and 0.25 μm porous silica surface layer (22). They present a small diffusion path (0.5 μm) compared to fully porous particles (e.g., 1.8 μm), which provides superior mass transfer kinetics and better performance at high mobile phase velocities (27). The sub 3 μm partially porous stationary phases have lower eddy diffusion and higher mass transfer resistance for small analytes than sub 2 μm totally porous stationary phases.

The columns packed with this new type of stationary phase present high performance because of its very narrow particle size distribution and their higher particle density when compared to totally porous stationary phases, which results in very homogeneous, efficient packed beds. Due to their characteristics, columns packed with partially porous particles usually provide better efficiency than columns packed with totally porous particles of the same size. For a typical HPLC column well-packed with 5 μm totally porous particles present HETP values usually between 10 and 15 μm while columns packed with partially porous particles of the same diameter can have HETP values close to 7 μm . It is possible to have HEPT values lower than 2 μm with columns packed with 1.3 μm partially porous particles (Figure 2).

On the other hand, as particle size decreases from 5 to 2.6, 1.7 and 1.3 μm , the maximum linear velocity of the mobile phase that can be achieved without exceeding the system pressure limits also decreases. While columns with particles of 5 μm allowed velocities higher than 1.2 cm/sec (although with very high HETP values), columns packed with particles of 1.3 μm are not able to exceed 0.6 cm/sec, but they are capable of maintaining excellent efficiency.

It is important to highlight that columns packed with partially porous particles packed with 2.7 μm particles produces approximately half of the backpressure of sub-2 μm totally porous particles due to their relatively high specific permeability, which makes it possible to use sub 3 μm columns on conventional HPLC systems. For example, the specific permeability of columns packed with sub 3 μm core-shell particles ranges between $K_0 = 4.6 \times 10^{-11} \text{cm}^2$ and $6.4 \times 10^{-11} \text{cm}^2$, while the permeability of a column packed with 1.7 μm totally porous stationary phase is $\sim 2.5 \times 10^{-11} \text{cm}^2$ (28–30).

The relatively high permeability of partially porous stationary phases also allow the use of the same mobile linear velocity of columns packed with larger totally porous particles while providing significant gains in chromatographic performance due to the smaller particle size. For example, under the same conditions, a column packed with 2.7 μm partially porous particles provide similar pressure to a column of the same dimensions packed with 3.5 μm totally porous particles, especially at lower mobile phase linear velocity (Figure 3).

In this case, with both columns (100 x 4.6 mm) is possible to have flow rate higher than 2.5 mL/min, although the column packed with partially porous particles can take better advantage of the higher mobile phase linear velocity due to a more efficient Van Deemter curve. In addition, columns packed with 2.7 μm fused-core particles can use the same inlet frits typically used on columns with 3–5 μm particles, which makes these columns less susceptible to the plugging problems that are sometimes evident with most sub-2 μm columns, especially for samples from complex matrices such as raw bioactive materials, where several impurities may be present.

However, partially porous stationary phases and sub 2 μm totally porous stationary phases produce peaks with low retention volume, which means that the chromatographic performance might be severely compromised by extra volume from the equipment. Therefore, in order to fully explore their potential, it is also necessary to improve the characteristics of the system, especially dead volume, by optimizing tubing length and internal diameter, and using low volume components.

There number of studies using columns packed with partially porous for the fast analysis of bioactive compounds is steadily increasing in the last years and several applications for the analysis of compounds present in tea, wine, coffee and soybeans, among other raw bioactive materials can be found in the literature (Table 1).

3.3. Monolithic Columns

Monolithic columns are made of a single piece of porous cross-linked polymer or porous silica. The monoliths were developed based on a sol-gel process, which includes the hydrolysis and polycondensation of alkoxy silanes (e.g. tetramethoxysilane or tetraethoxysilane) in the presence of water-soluble polymers (e.g. poly(ethylene) oxide or polyethylene glycol) (31). Silica based material is the most popular substrate for HPLC columns due to its unique properties such as inertness to a wide variety of analytes, mechanical strength to withstand relatively high pressures, and high efficiency (32). The rods formed, containing both macro and mesopores, are highly porous material (Figure 4).

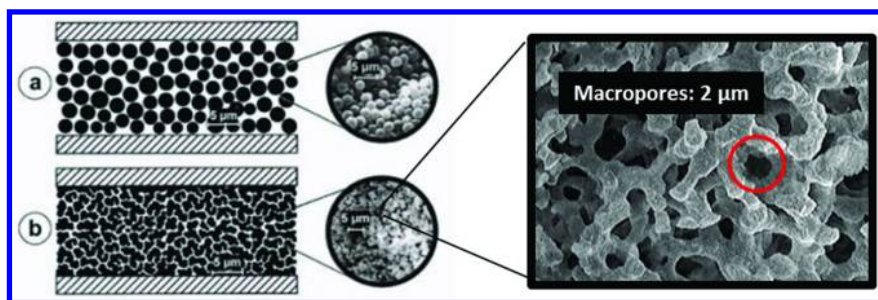


Figure 4. Comparison of the structure of a column packed with conventional particles (a) and monolithic column (b). Reproduced with permission from reference (33). Copyright 2002 Elsevier.

The conceptual design of these columns is to reduce analysis time through low column backpressure and high efficiency, allowing high flow rates, and faster transfer kinetics. Using monolithic columns it is possible to explore flow rates that are 2 to 3 times higher than those allowed with columns of the same dimensions packed with totally porous particles of 3.5 μm or with partially porous particles of 2.7 μm (Figure 3) (18). In this case, the large pores (2 μm) allow the application of high eluent flow rates due to the low flow resistance while the small pores (about 12nm) provide higher separation efficiency because of the high surface area (9, 10). The large through-pore size/skeleton size ratios and high porosities with a small diffusion path result in high permeability and a large number of theoretical plates per unit pressure drop which allows for faster separations with “conventional” HPLC instrumentation. It is important to notice that a relative comparison of the chromatographic performance of monolithic silica columns and particle packed columns suggested that the mass transfer properties of the monolithic columns in the mesopores is equivalent to a column with particle diameter of 3 μm , while the through pore system is equivalent to an interstitial pore system of a packed bed with a particle diameter of 15 μm (34).

Another chromatographic characteristic of monolithic columns is that they are very responsive to changes in flow rate. The flow rate may be modified during analysis (flow gradient) to improve peak definition of a given compound or to reduce total separation time once the target compounds have successfully eluted (34). Thus, fast equilibration times can be achieved and total analysis time will be reduced.

The drawbacks of the monolithic columns include limited chemistries (C_{18} , C_{18} endcapped, C_8) and suppliers, impossibility of directly transfer methods between conventional HPLC and monolithic supports, limited resistance to pressure (<200bar), pH (2<pH<8) and temperature (< 45°C) (24). However, with hybrid chemistry, both silica and polymeric columns have been produced to provide enhanced mechanical stability, high efficiency, and extended pH range (10)

There are some applications of monolithic columns for the analysis of bioactive compounds that can be found in the recent literature (Table 1). In general, it is possible to achieve very fast separations (less than 10 minutes) of complex mixtures while obtaining good resolution. Although it is possible to develop relatively fast methods the high flow rates used may result in excessive solvent usage, which can result in an economical and environmental concern in the case of expensive and toxic solvents.

4. Chromatographic Conditions

Besides of the LC “hardware” (column, system configuration, detector, etc.), operational conditions used for the analysis (column temperature, mobile phase composition, flow rate, etc.) can greatly influence the results obtained in any chromatographic separation. Ideal conditions provide a good balance between resolution of the sample components and the analysis time necessary to achieve the separation. When developing fast methods for LC separations is important to

consider this aspect since there will be several instances where resolution can be sacrificed for speed or where speed can be traded for resolution. This is especially true in samples from raw bioactive materials, where there may be several similar components present (not all may be bioactive) and achieving good separation between peaks can be a challenge.

4.1. Column Temperature

The increase of the column temperature can provide some advantages to chromatographic methods such as speed, efficiency, resolution, selectivity, reduction of the solvents consumption and improved detection and quantitation levels (13, 15, 19). Temperature influences all aspects of the separation, from the mobile phase and the stationary phase to the target analytes themselves. However, one of the most interesting effects of temperature in chromatographic separation is on the mobile phase viscosity.

To illustrate the effect of temperature on the solvent viscosity and pressure we can consider the mixture of water and acetonitrile, which is one of the most used HPLC mobile phases. The viscosity of a mixture of 10% acetonitrile and 90% water mixture (v/v) at 25 °C is approximately 1.0 cP, while at 50 °C it is approximately 0.6 cP (35). As column temperature increases, mobile phase viscosity is reduced which results in lower column backpressure. (Figure 5) (19).

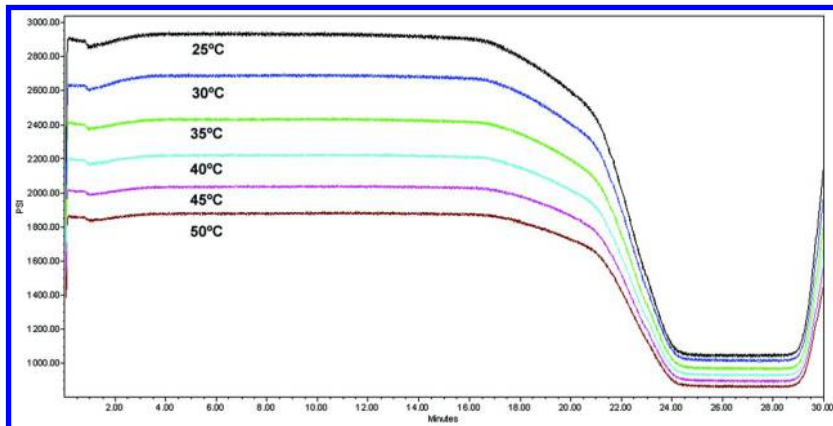


Figure 5. System pressure profile produced by different column temperatures during a gradient separation with acetonitrile and water as mobile phase on a column packed with partially porous particles of 2.7 μm . Initial conditions are 92% water and 8% acetonitrile. Reproduced with permission from reference (19). Copyright 2010 Elsevier.

Although the reduction of the column backpressure is not proportional to the increase in the temperature, the pressure difference can be sufficiently high to allow a great increase in mobile phase flow rate to reduce analysis time. Additionally,

due to the reduction of solvent viscosity caused by the increased temperature, the use ethanol and/or water as mobile phase also may become practical alternatives (13). Moreover, faster separations may lead to lower solvent usage. Besides the advantage of less toxicity, the use of larger amount of water as mobile phase enhances its transparency for UV detection (13).

Another important parameter affecting the separation of compounds which is greatly influenced by the temperature is the transfer rate of the solute from the mobile phase to the stationary phase (9). The B term of Van Deemter's equation represents the contribution to band dispersion from longitudinal diffusion, the C term is the mass transfer parameter (36). The diffusion coefficient is directly proportional to the absolute temperature and inversely proportional to the viscosity. The lower viscosity and higher diffusivity of a mobile phase at high temperatures produce much lower mass transfer resistance, thereby decreasing the peak width (9, 19) and producing a much more "flat" curve.

The effect of temperature on the chromatographic efficiency of columns at different temperatures can be observed in Figure 2. By comparing the Van Deemter curves of the column with 1.3 μm at 25 and 55 $^{\circ}\text{C}$ it is clear that at lower temperatures higher efficiency is achieved (lower HETP values) but at increased temperatures the curve is extended due to expanded limit of achievable linear velocity caused by the lower pressure (i.e. "flatter" curve). Therefore, if column temperature is increased there will be a loss of efficiency but higher linear velocity may be achieved. Additionally, it can be noted in Figure 2 that the increase in mobile phase linear velocity may further reduce the efficiency of the column, especially with columns packed with particles of larger diameter ($> 5\mu\text{m}$). Therefore, it is also necessary to consider a balance between increasing flow rate and reducing analysis time and being able to afford the loss of resolution that the increase in flow rate may cause.

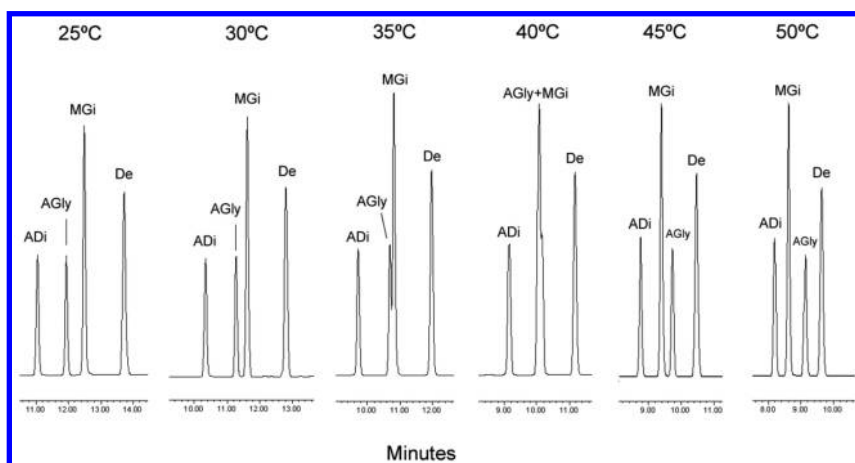


Figure 6. Effect of column temperature in elution order of isoflavones. Reproduced with permission from reference (19). Copyright 2010 Elsevier.

As the linear velocity of the mobile phase increases, mass transfer rates (not column efficiency!) also increases. Consequentially there is a reduction of the retention of the compounds by the column, which implies that dispersion of analytes inside the column, will be reduced and faster analysis may be achieved. This aspect is seen in Figure 6, where the separation of a series of soybean isoflavones is performed at different column temperatures. The retention time of compounds is greatly reduced with the increase of the column temperature from 25 to 50 °C, even though the gradient was maintained constant.

However, temperature may not affect all compounds the same way, and even similar compounds such as some soy isoflavones, can see selectivity changes depending of the temperature used (Figure 6). In this case, it can be observed that elution order of some isoflavones (acetyl glycitin – AGly- and malonyl genistin – MG_i) is different between 25-30 °C and at temperatures above 45 °C. It is also important to note that between 35 and 40 °C, both isoflavones co-eluted which may affect their correct quantitation. On the other hand, it is possible to take advantage of these changes in elution order according to temperature to overcome co-elution problems.

Nevertheless, the use of higher temperatures can be limited due to the lack of thermally resistant stationary phases and of unstable solutes (36). Temperature limits of commercially available stationary phases range from 45 °C (examples: Chromolith C₁₈, XSelect CSH C₁₈) to 90 °C (example: BEH C₁₈ UHPLC 1.7 μm). However, it is noteworthy that increasing column temperature may reduce column life, especially with aggressive conditions (extreme pH, linear velocity and high pressure, among others) and at the temperature limit of the column.

In this context, temperatures close to 60°C (HPLC) or 90 °C (UHPLC) can be used to perform rapid analysis, since mobile phase viscosity and consequentially column backpressure, are greatly decreased, which can be explored to increase flow rate and reduce analysis time. There are several examples where elevated column temperature was used for analysis of bioactive compounds in raw bioactive materials (Table 1).

There are a few columns packed with stationary phases that can withstand extreme temperatures (> 150 °C) that are being developed and, with the proper system, they may allow further exploring the advantages of high temperature for chromatographic analysis. Due to the excellent results obtained with changes in temperature it is expected that this strategy will be further explored in the future which can lead to a whole new age of separations with a new technique which is being defined as high temperature chromatography.

4.2. Mobile Phase Composition

Besides the column temperature, the solvent used in mobile phase is another important parameter that can heavily influence the potential to speed-up a given separation. This is because the solvent viscosity is one of the main responsible for the backpressure generated by column. As mobile phase viscosity increases so does the resistance offered by the column and thus the backpressure generated. In reversed phase separations water is usually the polar solvent while other less polar solvent that is miscible in water is used as secondary component to elute

compounds from the column. Common examples of the secondary mobile phase component include methanol, acetonitrile, and tetrahydrofuran. Each solvent has its own characteristics and may be more suitable for the separation of certain compounds and sample types than other. Nevertheless, it does not imply that other solvents and solvent combinations cannot be used and achieve adequate or even superior results.

Considering fast separations, it is interesting the selection of a mobile phase with low viscosity so that the lower backpressure generated is explored to increase flow and that way reduce the necessary analysis time. Among most used solvents in reversed phase LC separations, methanol and acetonitrile are the most effective and used ones. They are moderately polar solvents that are widely used for the separation of a great number of bioactive compounds present in raw bioactive materials (Table 1). Aside the environmental and toxic aspects of these two solvents they present several different characteristics. Acetonitrile present lower viscosity than methanol and therefore generate a lower column backpressure which in turn allows the use of higher flow rates. This aspect can be observed in Figure 3, where the allowed flow rate by the mobile phase composed by acetonitrile was almost 30% higher than the flow rate allowed by the mobile phase composed by methanol (18).

Another aspect to consider when selecting the appropriate solvent for gradient separations is the pressure profile of the mixture between mobile phase solvents. This is important because strongly associating solvent mixtures such as water/acetonitrile, and water/methanol mixtures show anomalous variations in viscosity with composition. For example, mixtures of water/acetonitrile show maximum viscosity at 35% (v/v) while water/methanol show the highest viscosity near 50% of each component (35). Furthermore, as can be observed in Figure 3, water/acetonitrile mixture produce a much lower difference in the pressure when compared to mixtures of water/ methanol (18). Nevertheless, acetonitrile is convenient for HPLC/MS methods because of the lower level of total volume of gases generated related to methanol based methods.

4.3. Flow Rate and Mobile Phase Linear Velocity

When considering fast LC separations, one of the most important method parameters which can be explored to reduce analysis time is the mobile phase flow rate. The basic concept of this strategy is that increasing mobile phase flow rate increases mass transfer rates between the analytes, the stationary phase and the mobile phase, which reduces the retention of analytes by the stationary phase, thereby reducing analysis time.

In isocratic separations this strategy is fairly simple to implement. In contrast, in gradient separations it is necessary to adjust the gradient and the method may not be adaptable depending of the conditions and stationary phase used (see Figure 7). In this case, it is usually necessary to reduce the gradient time proportionally to the increase in flow rate while maintaining the concentration of the mobile phase components constant (19).

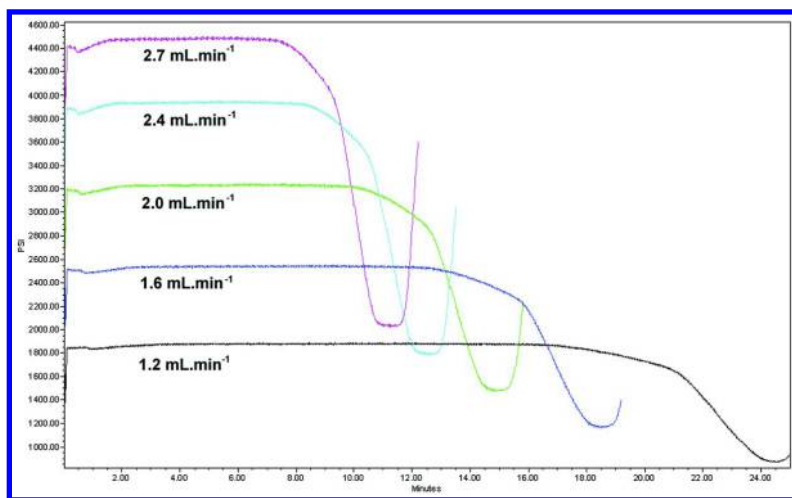


Figure 7. System pressure profile of a separation performed using different flow rates with adjusted gradient conditions. Reproduced with permission from reference (19). Copyright 2010 Elsevier.

To illustrate the principle an example is provided in Table 2

Table 2. Hypothetical Gradient Example Considering a Mixture between Two Solvents (A and B) under Normal Conditions (0.5 mL/min) and the Adjusted Gradient under Elevated Flow Rate Conditions (1.0 mL/min)

	<i>0.5 mL/min</i>		<i>1.0 mL/min</i>		
<i>Time (min)</i>	<i>% solvent A</i>	<i>% solvent B</i>	<i>Time (min)</i>	<i>% solvent A</i>	<i>% solvent B</i>
0	100	0	0	100	0
10	80	20	5	80	20
20	60	40	10	60	40
40	40	60	20	40	60
60	0	100	30	0	100

Considering that resolution is a function of the difference of retention time between two components of the sample, the increase in flow rate will definitely reduce resolution, which is not detrimental to separation as long as compounds are adequately separated from each other. When trying to speed-up methods using this strategy, the maximum usable flow rate is that where the complete separation of target components (or target resolution) is not yet being compromised in order to reduce analysis time. In this sense is advisable to determine the lowest acceptable resolution for specific compounds.

There is a lot of discussion about the economic and environmental implications of adopting the strategy of increasing flow-rate to speed-up LC separations, especially when toxic solvents are used. The negative argument to this discussion is simple: as flow rate increases solvent consumption increases proportionally. And if solvent consumption increases, so does costs and environmental impact.

In order to correctly evaluate the impact of this strategy on costs and environmental impact it is necessary not only to consider flow-rate and solvent consumption but also to evaluate the amount of solvent used. If the mobile phase flow rate is increased and the solvent consumption increases in the same proportion as the reduction of the analysis time of the separation, then the amount of solvent will remain the same but with the advantages of the separation being achieved faster. For example, if a given separation is achieved in 60 minutes at 0.5 mL/min and consumes 30 mL of solvent, doubling flow rate to 1.0 mL/min will reduce analysis time to 30 minutes while consuming the same 30 mL of solvent.

However, since the increase in flow rate affects mobile phase velocity which may reduce column efficiency, it is implied that the reduction in analysis time may not be proportional to the increase in flow rate, inevitably leading to a higher amount of solvent used. In this context, it is important to define mobile phase linear velocity and flow rate. Mobile phase linear velocity refers to the velocity of the mobile phase inside the column (or tubing) while flow rate indicates the volumetric amount of solvent pumped per unit of time. In this sense, we can have two different mobile phase linear velocities for the same flow rate if the same flow rate is used on columns with different inner diameter. This is caused by fluid dynamics. According to Bernoulli's principle, reducing the diameter of the column will reduce the area and consequently the velocity will increase by the same factor that the area is decreased. Each column responds differently to the increase in flow rate because they have their own Van Deemter Curve. And these curves are also affected by temperature (Figure 2).

Therefore, the difference in the amount of solvent consumed and the efficiency achieved (and thus the separation) will depend of the columns dimensions and characteristics as well as of the conditions of the method and the separation achieved. But is important to highlight that in some cases, the resolution loss caused by the lower column efficiency promoted by the implementation of higher flow rates may not affect the separation (considering that may be acceptable loss of resolution). Therefore, there may not be important differences in the amount of solvent used and in the separation even if lower column efficiency is achieved.

5. Conclusions

The analysis of bioactive compounds in raw bioactive materials can be a challenging task because some sample may be very complex matrices, where besides of the target analytes there are several other interfering components. LC technology is rapidly evolving and new systems, materials and strategies are constantly being developed and advances in this area are likely to continue. The need of faster analysis methods is clear and as technology advances the

developments are applied for the analysis of bioactive compounds in raw bioactive materials. Among the new packing materials, sub 2 μ m particles and partially porous particles are currently the cutting edge technology in LC separations. Partially porous particles were only recently developed and still are being subject of intensive research in several fields of liquid chromatography, including raw bioactive materials. It is expected that it can improve separations actually being carried out by conventional HPLC systems to a performance level close to UHPLC separations with columns packed with totally porous sub 2 μ m particles. However, as the number of available partially porous stationary phases for UHPLC increases, it can be anticipated that UHPLC combined with partially porous particles will definitely set a new standards in LC separations. Overall, the combination of these highly efficient stationary phases (partially porous sub 2 μ m particles) packed in short columns with reduced internal diameter, operating at elevated temperature and flow rate with adequate solvents that present low viscosity under optimized conditions can provide huge improvements in the speed of LC separations. Only by adopting an integrated effort where several favourable conditions are used that it will be possible to take full advantage of their characteristics to produce ultra-fast LC separation methods.

Acknowledgments

The authors acknowledge funding from FAPESP (Projects 2012/10685-8 and 2013/04304-4) and from CNPq (Projects 470916/ 2012-5 and 560914/2010-5). Authors are also thankful for scholarships provided by FAPESP (2013/15049-5) and CNPq (163699/2012-7, 140282/2013-0 and 151165/2010-6).

References

1. Yang, P.; Litwinski, G. R.; Pursch, M.; McCabe, T.; Kuppanan, K. *J. Sep. Sci.* **2009**, *32*, 1816–1822.
2. Cragg, G. M.; Newman, D. J. *Biochim. Biophys. Acta, Gen. Subj.* **2013**, *1830*, 3670–3695.
3. Palacios, I.; Lozano, M.; Moro, C.; D'arrigo, M.; Rostagno, M.; Martínez, J.; García-Lafuente, A.; Guillamón, E.; Villares, A. *Food Chem.* **2011**, *128*, 674–678.
4. Rostagno, M. A.; Palma, M.; Barroso, C. G. *Anal. Chim. Acta* **2007**, *597*, 265–272.
5. Shen, Q.; Dai, Z.; Lu, Y. *J. Sep. Sci.* **2010**, *33*, 3152–3158.
6. Fanali, C.; Rocco, A.; Aturki, Z.; Mondello, L.; Fanali, S. *J. Chromatogr., A* **2012**, *1234*, 38–44.
7. Manchon, N.; Mateo-Vivaracho, L.; D'Arrigo, M.; Garcia-Lafuente, A.; Guillamón, E.; Villares, A.; Rostagno, M. A. *Czech J. Food Sci.* **2013**, *2013*, 31.
8. Strömstedt, A. A.; Felth, J.; Bohlin, L. *Phytochem. Anal.* **2013**, *25*, 13–28.
9. Nováková, L.; Vlčková, H. *Analytica Chimica Acta* **2009**, *656*, 8–35.

10. Gumustas, M.; Kurbanoglu, S.; Uslu, B.; Ozkan, S. *Chromatographia* **2013**, *76*, 1365–1427.
11. El Deeb, S. *Chromatographia* **2011**, *74*, 681–691.
12. Natishan, T. K. *J. Liq. Chromatogr. Relat. Technol.* **2011**, *34*, 1133–1156.
13. Vanhoenacker, G.; Sandra, P. *Anal. Bioanal. Chem.* **2008**, *390*, 245–248.
14. Gruz, J.; Novák, O.; Strnad, M. *Food Chem.* **2008**, *111*, 789–794.
15. Rostagno, M.; Manchon, N.; D'Arrigo, M.; Guillamon, E.; Villares, A.; Garcia-Lafuente, A.; Ramos, A.; Martinez, J. *Anal. Chim. Acta* **2011**, *685*, 204–211.
16. Guillarme, D.; Casetta, C.; Bicchi, C.; Veuthey, J.-L. *J. Chromatogr., A* **2010**, *1217*, 6882–6890.
17. Lu, Y.; Shen, Q.; Dai, Z. *J. Agric. Food Chem.* **2010**, *59*, 70–77.
18. Manchón, N.; D'Arrigo, M.; García-Lafuente, A.; Guillamón, E.; Villares, A.; Martínez, J.; Ramos, A.; Rostagno, M. *Anal. Bioanal. Chem.* **2011**, *400*, 1251–1261.
19. Manchón, N.; D'Arrigo, M.; García-Lafuente, A.; Guillamón, E.; Villares, A.; Ramos, A.; Martínez, J.; Rostagno, M. *Talanta* **2010**, *82*, 1986–1994.
20. Pietrogrande, M. C.; Dondi, F.; Ciogli, A.; Gasparrini, F.; Piccin, A.; Serafini, M. *J. Chromatogr., A* **2010**, *1217*, 4355–4364.
21. Gritti, F.; Guiochon, G. *J. Chromatogr., A* **2012**, *1228*, 2–19.
22. Fekete, S.; Oláh, E.; Fekete, J. *J. Chromatogr., A* **2012**, *1228*, 57–71.
23. Fekete, S.; Guillarme, D. *J. Chromatogr., A* **2013**, *1308*, 104–113.
24. Guillarme, D.; Ruta, J.; Rudaz, S.; Veuthey, J.-L. *Anal. Bioanal. Chem.* **2010**, *397*, 1069–1082.
25. Wu, N.; Bradley, A. C.; Welch, C. J.; Zhang, L. *J. Sep. Sci.* **2012**, *35*, 2018–2025.
26. Kirkland, J. J.; Schuster, S. A.; Johnson, W. L.; Boyes, B. E. *J. Pharm. Anal.* **2013**, *3*, 303–312.
27. Abraham, A.; Al-Sayah, M.; Skrdla, P.; Berezniński, Y.; Chen, Y.; Wu, N. *J. Pharm. Biomed. Anal.* **2010**, *51*, 131–137.
28. Gritti, F.; Guiochon, G. *J. Chromatogr., A* **2012**, *1252*, 31–44.
29. Gritti, F.; Guiochon, G. *J. Chromatogr., A* **2012**, *1252*, 45–55.
30. Gritti, F.; Guiochon, G. *J. Chromatogr., A* **2012**, *1252*, 56–66.
31. Štatinský, D.; Solich, P.; Chocholouš, P.; Karliček, R. *Anal. Chim. Acta* **2003**, *499*, 205–214.
32. Zheng, J.; Patel, D.; Tang, Q.; Markovich, R. J.; Rustum, A. M. *J. Pharm. Biomed. Anal.* **2009**, *50*, 815–822.
33. Oberacher, H.; Huber, C. G. *TrAC, Trends Anal. Chem.* **2002**, *21*, 166–174.
34. Rostagno, M. A.; Villares, A. *Monolithic Chromatogr. Its Mod. Appl.* **2010**, 339.
35. Snyder, L. R.; Kirkland, J. J.; Dolan, J. W. *Introduction to Modern Liquid Chromatography*; John Wiley & Sons: New York, 2011.
36. Heinisch, S.; Rocca, J.-L. *J. Chromatogr., A* **2009**, *1216*, 642–658.

Chapter 5

Chromatography Combined with Bioassays and Other Hyphenations – The Direct Link to the Compound Indicating the Effect

Gertrud E. Morlock*

Justus Liebig University Giessen, Interdisciplinary Research Center (IFZ),
Institute of Nutritional Science, Chair of Food Science,
Heinrich-Buff-Ring 26-32, 35392 Giessen, Germany
*E-mail: gertrud.morlock@ernaehrung.uni-giessen.de.

An actual interesting branch is effect-directed analysis. Recent progress in the field of the application of bioassays in direct combination with chromatography (direct bioautography) led to reliable characterization of unknown samples with regard to their activity profile. Planar chromatograms were directly immersed into bioassays, followed by incubation on the plate for up to 2 hours and visualization of the activity profile *via* a color substrate reaction. Despite the long incubation time in the aqueous media, sharp high-performance thin-layer chromatography (HPTLC) zones were obtained, allowing quantitation. Also instant bioluminescent bioassays were employed. Bacteria, yeast cells or enzymes specifically and sensitively detect bioactive compounds in complex samples according to their distinct effect. HPTLC in combination with bioassays, derivatization reagents, spectroscopic and high-resolution mass spectrometric detections led to a fast activity profiling and the direct link to the bioactive compounds of interest in complex raw samples. All these tools, inclusive of structure elucidating methods like NMR, FTIR, SERS and HRMS, were performed at the analytical level directly from the bioactive zone of interest on the HPTLC plate, optionally via the versatile TLC-MS Interface. The image-giving chromatographic system with an open, planar stationary phase and the post-chromatographic evaporation of the mobile phase eased the performance of various kinds of hyphenations.

Effect-Directed Analysis (EDA)

Over 80 million simple compounds are registered in Chemical Abstracts Service (CAS). Even if less than one-per-mil of all these chemicals are discussed as potential contaminants, multi-methods can not cope with it. Their capacity is limited and can not cover the relevant group and scope of substances. This is evident for residue analysis of food and feed. Coming from all over the world due to the global food/feed chain, over 1000 pesticides could be considered as highly relevant. Additionally, metabolites and breakdown products of the residues have to be integrated into such multi-residue methods. However, often this is difficult because of their mostly unknown nature or the unavailability of reference compounds. Target analysis is powerless and can not notice such effective compounds present. The same situation is apparent for the search for effective compounds in highly complex samples, like given for the field of bioactive natural product search (1) or the analysis of antibiotic residues in food of animal origin. Even validated multi-residue methods (2, 3) are not able to cope with the wealth of potential residue candidates.

Opposite to it, *detecting everything* is also limited (4), as it requires complex analytical systems with an extensive capacity for data handling, generates high costs, and takes a great effort and database for detection and identification of several thousands of substances. High-sophisticated, hyphenated and comprehensive online methods in combination with a considerable database are not the key and panacea method for routine food safety (5) and search for bioactive molecules. High sophisticated online systems are complex and the whole analysis chain is interrupted and forced to stop, in case of troubles at a small link.

To conclude, the most appropriate solution for each task should be chosen, irrespective of the prevailing trend. However, this requires a profound knowledge on analytical methods, inclusive of advantages and disadvantages. Other methodologies solve this challenge of the unknown bioactivity and relevance of samples differently, even in a more simple way. Such a workflow is the so-called effect-directed analysis (EDA (6–8);), in which mostly a bioassay is used for specific detection of an effect. In combination with chromatography, single effective compounds can directly be assigned.

Chromatography Directly Combined with Bioassays

Actual bioassays used, e.g. cuvette (9), Petri dish or microtiterplate assays, can characterize complex samples in the whole. A sum parameter is obtainable, but it is not found out, which compounds are responsible for the bioactivity itself. Sum parameter results can be falsified due to matrix interferences, antagonistic or synergistic effects, as there is no chromatographic separation and differentiation.

Hence, it is advisable to combine bioassays with chromatography. This will directly link to the bioactive compound itself and show the distinct bioactivity of single compounds, depending on the bioassays selected. EDA in combination with chromatography leads to targeted answers in a comprehensive context and range

of potentially relevant compounds. All compounds are detected in the complex sample that generate the effect indicated by the bioassay. Thus, thousands of compounds in a complex mixture are reduced to few important bioactive ones. Apart from analytes in the focus, unknown metabolites, side products, (process) contaminants, degradation products, adulterants, migration products, or residues were detectable. Often compounds not detected with the standard techniques, like UV, Vis and fluorescence detection (FLD), are discovered not until with the bioassay. These compounds being bioactive, but not in the analytical focus, are important, but overlooked.

The importance of a comprehensive screening is triggered by the growing global threat to ecosystems due to the profuse release of anthropogenic compounds despite fruitful regulation. Also food safety is concerned due to the global food chain. For example, screening of antimicrobial substances in food of animal origin is mainly performed with biological assays, *e.g.*, 4-plate test, 5-plate test, also called STAR protocol (10–14). In the last two decades, hyphenation of HPLC with MS/MS seemed to be the analytical panacea in the field of veterinary drug residue analysis. Regarding residues of antimicrobial drugs, the intention was to confirm the measured biological effect through the detection and identification of the drug by HPLC-MS/MS (15). This fruitful approach revealed its limits as only about 70 % of the positive biological screening tests could be confirmed. In other words, about 30 % of the food samples detected as positive by a biological assay were not confirmed by MS, as the targeted antibiotic compounds of the multi-residue method were not detected and identified in the samples (private communication with an EU Reference Laboratory). However, it is necessary to obtain information concerning such unknown bioactive substances contained in these food samples with regard to food safety and the increasing resistance of pathogens against antibiotics leading to risky human infections. As recently demonstrated in a proficiency test (16), the false negative rate was 73 % for microbial methods, 50 % for biochemical and 22 % for instrumental methods. It was concluded that substantial effort is needed to improve microbiological screening and instrumental analysis, inclusive of LC/MS/MS. Bioassays in direct combination with chromatography can solve this lack in information and complement existing methodologies.

Drawbacks for Hyphenation of Bioassays with HPLC

The term *hyphenation* (17), and in an excessive understanding jocularly termed *hypernation* (meaning super-hyphenation) (18), comprises chromatographic methods that place *all of the required* detectors into a single system so that all of the mostly spectroscopic and spectrometric information is obtained in a single run. With this hyphenation strategy the most relevant information is obtained out of a single separation (chromatographic run). Although mainly spectroscopic/-metric information is gathered by such hyphenated techniques, the integration of other useful information like effect-directed bioassay detection is of high interest, too.

As HPTLC has been overlooked in analytical chemistry for decades and HPTLC-bioassay was considered as not relevant, the different approaches were based on either direct HPLC flow systems (19–22) or on intermediate parking of HPLC fractions on a carrier (23, 24). Problems associated with column-derived hypernations are capital cost and the complexity of the instrumentation difficult to operate in a routine way. Concepts for dealing with the large amounts of data produced by such systems are challenging, and a single eluent that is optimal for all detectors is difficult to find, especially with regard to differences in sensitivity between spectroscopic techniques and spectrometers (18, 25). The attempts to couple HPLC in flow with bioassay detection showed intrinsic drawbacks:

- After use, the flow system had to be rinsed by disinfectants to prevent the growth of biofilms. Before system re-use, all traces of disinfectants had to be removed, otherwise the bioassay was killed directly.
- The HPLC eluent was restricted to a physiological composition or needed a post-chromatographic aqueous dilution to a mixture with a minor organic ratio, tolerable for the bioassay. This dilution step should not impair peak performance. High salt concentrations of the bioassay media did interfere with online MS detection.
- Only fast bioassay reaction times avoided dramatic peak broadening. The blowing in of air bubbles did mitigate diffusion effects during the relevant interaction time with the bioassay, however, impaired later detection, and thus had to be removed again before the detector cell.
- The instrumental set-up was laborious and complex. The whole online system was forced to stop in case of troubles with a small link.
- Sequential sample analysis limited the online system in the sample throughput. Analysis time was limited by the successive online bioassay duration, also for rapid HPLC separations. Sample preparation had to be adjusted to the requirements of HPLC, as sample matrix may not remain on the column.
- Time-depending effects on the bioassays cannot be studied in the flow-system. For example, *Aliivibrio Fischeri* contact times of 5 min, 15 min, 30 min with the sample components are crucial according to ISO 11348.
- The limit of detection (LOD) was worse in HPLC-enzyme inhibition (EI), e.g. by a factor of 5500 for analysis of paraoxon: LOD was 7.4 ng/peak by HPLC-EI (20) versus 1.3 pg/zone by HPTLC-EI (26).

Various disadvantages of a direct flow-system were circumvented by intermediate parking of HPLC fractions on a carrier. Two microtiter plates were used for collection and parking of HPLC fractions (23). One 96-well plate was subjected to the bioassay (24) and another was intended for later transfer of critical fractions to HPLC-HRMS.

Concluding, the challenges associated with column-based hypernations were the instrumental complexity, capital costs, eluent flexibility with regard to different detectors as well as their different detectabilities and strategies for handling the large data amounts produced. Despite of these clear facts, research funding was spend on such not ideal mainstream approaches.

Challenges for Hyphenation Less Critical for HPTLC-EDA

These challenges are less critical in HPTLC-based hyphenations. The profound knowledge of boundaries between analytical methods makes it evident: The most streamlined option for coupling chromatography with bioassays was *via* planar chromatography. The open, offline and planar format of TLC/HPTLC did not generate all these drawbacks of the column-derived approaches. In contrast to mainstream techniques, planar chromatography was mostly not supported by funding due to lack of understanding.

Screening of samples and tracking of relevant constituents therein can be performed on the same plate with less effort and data handling. The open planar system is adjustable to different detectabilities, remains simple by its modular instrumentation, and is producing low data amounts due to its targeted detection. Whereas in HPLC the online system forces specified pre-settings applied for every run independent on matrix interferences, the modular offline HPTLC instrumentation (fully automated in its single steps) facilitates a flexible mode of hyphenation. HPTLC-EDA can be used at any time for any project and bioassay without additional capital costs, whereas a hyphenated online HPLC system is devoted solely to a single specified task (bioassay). As chromatography is separated from the detection step, one major advantage is the eluent-free detection. After chromatography the eluent is evaporated and an optimal solvent with regard to the detector can be selected. The latter is extremely relevant for EDA using bioassays, which are prone to be killed or inactivated by small organic solvent portions in the eluent.

After HPLC separation, the sample is normally in the waste, whereas in HPTLC the whole sample is stored on the plate after chromatography. This means that unknown samples and their constituents can be evaluated first with regard to their bioactivity profile. After bio-profiling of unknown samples, only relevant zones – discovered to be bioactive compounds – were subjected to further characterization and finally structure elucidation.

Hyphenations for Identification and Structure Elucidation

The next step in the analytical chain was characterization and structure elucidation of the unknown, but bioactive compounds (Figure 1). Hyphenations can be selected as required to reach the relevant information about the sample. Attenuated total reflection (ATR)-FTIR spectra were recorded from zones of interest via the versatile TLC-MS Interface (27, 28) and analogously to that and after detailed discussion with a college (29), the recording of NMR spectra was demonstrated in the same way by this group (30), all at the analytical scale. Diffuse reflectance infrared Fourier transform (DRIFT (31–33),) spectra, and surface-enhanced Raman spectroscopy (SERS (34),) spectra were demonstrated by reflectance measurements directly from the analytical plate. Only what is effective and thus important is selected and directed to MS (35) or high resolution MS (HRMS) (36, 37), and so further characterized through the sum formula. To conclude, the non-target bioassay is followed by a targeted characterization of the effective compounds.

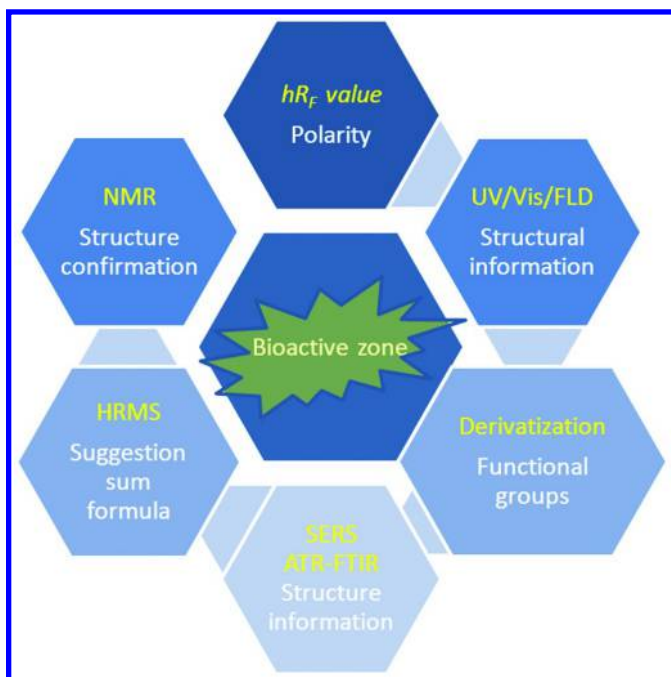


Figure 1. From the bioactive zone to the structure: HPTLC hyphenations for effect-directed analysis at an analytical level. (Reproduced with permission from reference (38). Copyright 2014 G. Morlock.)

HPTLC-UV/Vis/FLD-EDA-HRMS/NMR/SERS/ATR-FTIR provides all relevant information from the bioactive zone to the structural information obtained from a single HPTLC plate, meaning chromatographic run. It is the utmost streamlined analytical approach:

1. HPTLC is matrix-robust and sample preparation can be kept simple, which allows a more comprehensive view on the sample. The sample extract can be applied in a raw or crude nature.
2. In contrast to other high throughput systems, a simple matrix-tolerant planar separation divides analytes from matrix to avoid matrix suppression of the effect-directed detection *etc.* (known from cuvette tests and microtiterplate assays). The UV/Vis/fluorescence detection (FLD) images can be captured.
3. All samples on the plate were simultaneously subjected to the respective bioassay. The bioassay is homogeneously applied onto the chromatogram and indicates single bioactive compounds. The bioassay image is compared with the information obtained from the UV/Vis/FLD images, which provide basic structural information. The polarity of bioactive compounds is estimated based on the chromatographic data.
4. Only bioactive compounds are further characterized by structure elucidating methods at the analytical scale. Bioactive zones of interest

are collected by online elution and subjected to NMR and ATR FTIR or directly introduced into the mass spectrometer. Optionally, a derivatization reaction can be performed with a separate plate section.

An updated recent overview on HPTLC-MS (Figure 2 (39),) divided the approaches in elution and desorption-based approaches (40). Thanks to the hype of ambient mass spectrometry, various options got commercially available in the last 5 years, such as LESA, DART, DESI, MALDI and the TLC-MS Interface. Practical information on the performance of HPTLC-MS was recently given (41) with detailed discussion of background signals (42).

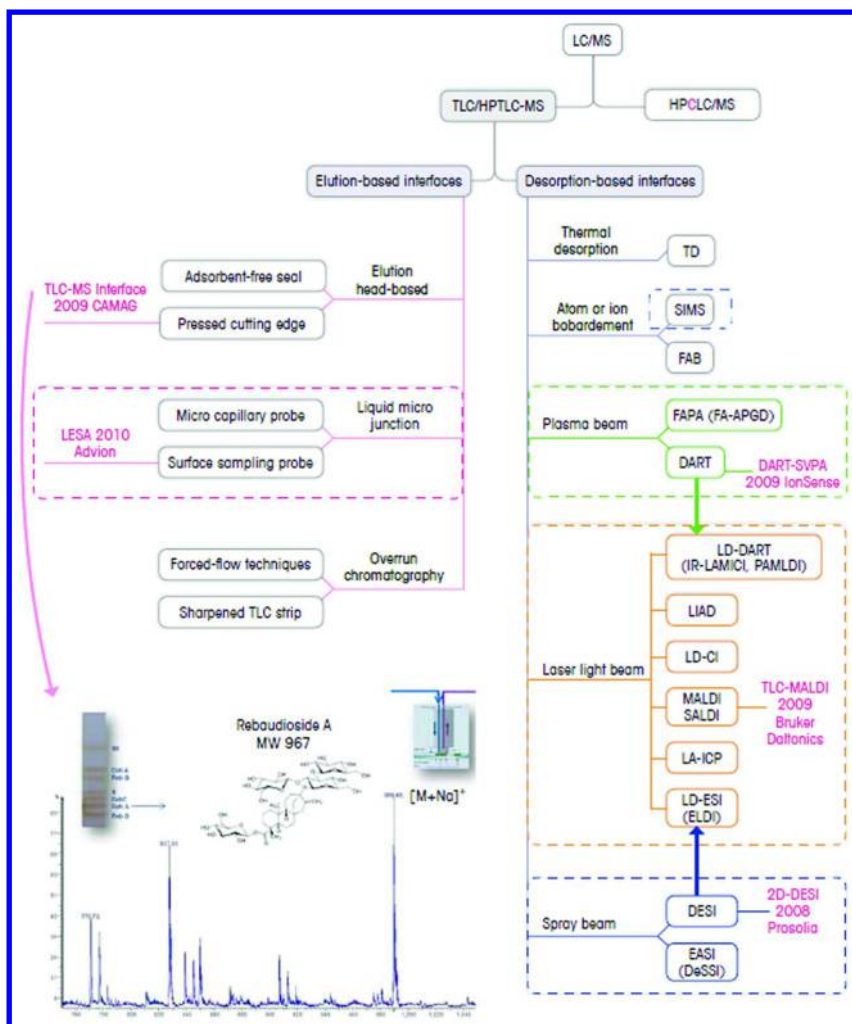


Figure 2. Elution and desorption based HPTLC-MS approaches; scanning MS with dashed frames. (Reproduced with permission from reference (38) and modified according to reference (39), Elsevier, 2014.)

Improvement of the Protocol for Bioassay Detection To Obtain Sharply-Bounded Zones and Optimal Detectabilities

Coupling microbiological assays with planar chromatography (bioautography) has a long tradition for almost 70 years (40). Bioautography plays a key role for screening of complex, mainly botanical samples for specific natural constituents (44–46). In direct bioautography (DB), a developed plate is immersed into a microorganism suspension broth and incubated to let the microorganisms directly grow and react on it. Separation, incubation and visualization are performed directly on the plate. TLC-DB seemed to be an old technique with minor contribution with regard to the broad, diffuse spots obtained after incubation with the aqueous media for hours. However, due to recent combination of knowledge on the individual steps and its factors of influence, a substantial improvement in the efficiency was reached, leading to sharply-bounded zones, even after hours of incubation on the plate (47). This improvement could have been invented since four decades. But not until now it was discovered, leading to a performance level of TLC/HPTLC-DB being not anymore what it was used to be (Figure 3). Even quantifications by HPTLC-DB were performed and led to reliable correlation coefficients (47). Advantages of better detectability, of the direct link to single compounds and of reduced matrix interferences are evident if compared to commonly used microtiterplate, Petri dish or cuvette assays.

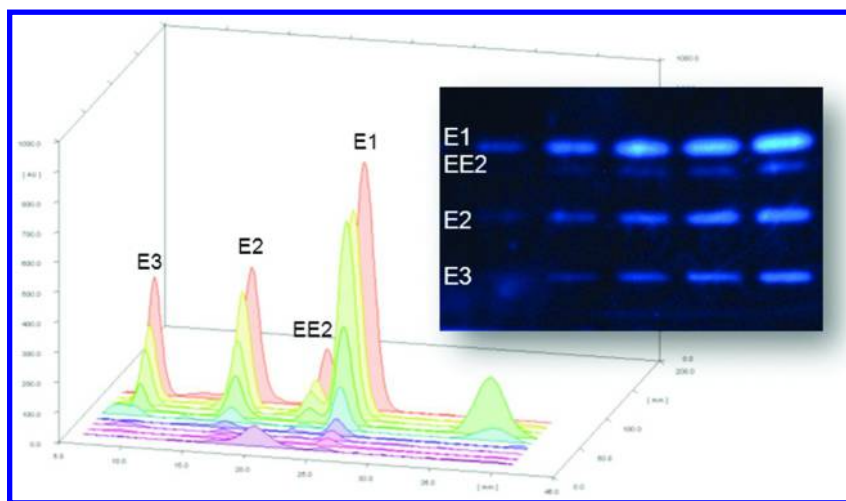


Figure 3. Substantial improvement of the planar yeast estrogen screen (pYES): sharply-bounded zones were obtained even after 2 hours of incubation with aqueous media on the HPTLC plate (E1: Estron, E2: Estradiol, EE2: Ethinylestradiol, E3: Estriol; E1/E3: 250 - 1500 pg/band, E2/EE2: 5 - 30 pg/band).

Additionally, HPTLC was demonstrated to be a highly matrix-robust and rugged chromatographic method (48). The single use of the stationary phase can omit a tedious sample cleanup. The sample preparation was reduced to a minimum and thus the sample extract was as raw and natural as possible (49). Especially rectangular application was shown to cope with a high matrix load (49–51). A focusing step followed for some seconds, if the elution power of the mobile phase mixture was not strong enough to front-elute the analytes out of the rectangular start zone (matrix should remain as rectangle). Thus, the layer was used both for sample preparation and separation (49–53). Matrix left at the start zone does not interfere with the chromatographic separation in HPTLC, but would be enriched in a column chromatographic system and would interfere with successive runs.

HPTLC-EDA allowed the localization of the activity even in a complex matrix and allowed a targeted isolation of the effective constituents. Tedious pointless single compound screening was avoided. The improved HPTLC-pYES method showed very good detectabilities with detection limits down to the fg- or pg-range, depending on the analyte (47). As demonstrated in many projects in the trace and ultra-trace analysis range (49–51), rectangular application substantially lowered the detectability. For a reported LOD of 500 fg/zone for 17 β -estradiol (E2) using the modified HPTLC-pYES method (47), LOD in water can be reduced to 1 ng per liter for an application volume of 500 μ L water sample, being rectangularly applied in 10 min. Hence, without any prior enrichment or clean-up step, this specific HPTLC-EDA method directly worked in the low ng/L-range. The image with the sharply-bounded effective zones can be used for quantification using digital image evaluation systems or densitometric scanning.

HPTLC allowed a comprehensive view on the as far as possible raw sample due to the reduced sample preparation, matrix-tolerance and high application volumes, which, all in all, supported the profound search for new compounds. It can be concluded that HPTLC developed further to a unique chromatographic method for direct combination with bioassays of many samples in parallel. Thereby, DB - performed as a simple immersion - is much more convenient than agar-overlay or agar-diffusion assays.

Performance of HPTLC-EDA

Effect-directed detection can be performed starting from the bioactive zone of a sample and leading to its structure. On one HPTLC plate, the sample can be applied multifold. After chromatography, the plate is cut into sections, and the different sections of the same plate can be subjected to the various detection modes (Figure 4). Comprehensive information is obtained by the different detections, successively employed for a single chromatographic separation.

A first impression of many separated samples in parallel is rapidly got by UV/Vis/FLD inspection of the plate image. Information is obtained on UV absorbance, fluorescence and Vis absorbance of single compounds at UV 254 nm, UV 366 nm and white light illumination, respectively (Figure 5 (54)). But also a more comprehensive and detailed multiwavelength scan from UV 190 nm to Vis 900

nm can be performed or UV/Vis spectra or fluorescence excitation spectra can be recorded. Subsequently, the same plate section was immersed into the *Aliivibrio fischeri* bioassay and distinct bioactive zone were observed.

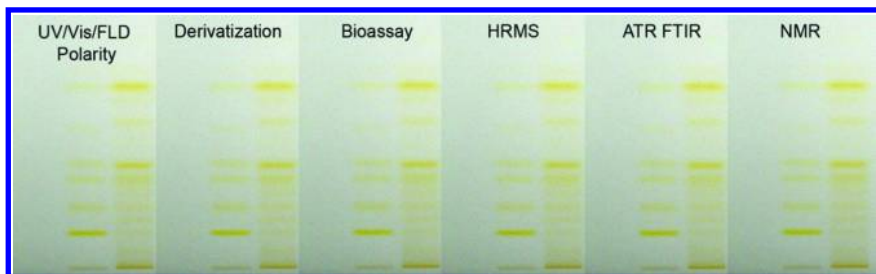


Figure 4. Scheme of one HPTLC plate with two different propolis samples applied multifold and cut into sections after chromatography for subsection to the different detection modes.

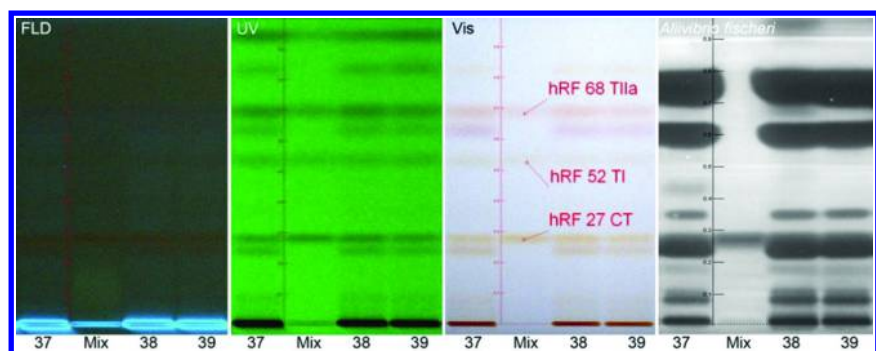


Figure 5. FLD/UV/Vis inspection of the same plate section with *Salvia* extract samples (no. 37-39) and a standard mixture of three tanshinones (TI, TIIa, and CT); bioactive zones were evident after immersion of the same plate section into the *Aliivibrio fischeri* bioassay.

Thereafter further information can be gathered, still on the same plate section, by recording of mass spectra from bioactive zones of interest. The mass spectrum was recorded directly after the use of the bioassay on the same plate section (Figure 6 (54)). In the positive ionization mode, sodium, potassium or any other medium salt adducts are dominant in the mass spectra of such a bioassay plate, if compared to recordings directly after chromatography (without immersion into the bioassay), which showed the protonated molecule as a basepeak. All this information was obtained for three sample extracts on one small plate section (5 cm x 10 cm). Using the three residual plate sections of the 20 x 10 cm plate from the same chromatographic run, further investigations may follow such as ATR-FTIR, NMR and HRMS.

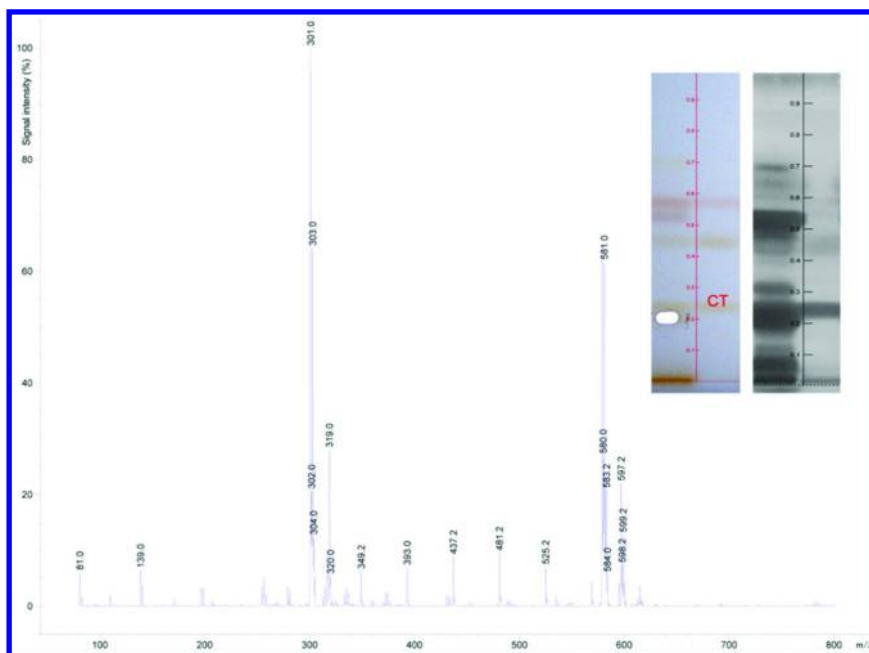


Figure 6. HPTLC-ESI-MS of an unknown bioactive *Salvia* sample zone below cryptotanshinone (CT): the mass spectrum was recorded still on the same plate section after immersion into the bioassay.

On the one hand, one HPTLC plate section (after UV/Vis/FLD evaluation) was immersed into the bioassay to get information about a distinct effect related to single compound zones, on the other hand structurally more profound spectral information (e.g. FTIR, SERS, NMR, and HRMS) and structure confirmation with regard to functional groups by derivatization reactions can be obtained from other plate sections of the same chromatographic run. For a newly discovered, unknown bioactive component, a HRMS is employed to get information about the sum formula. Hence, a wealth of information was rapidly gained with regard to these three *Salvia* sample extracts. From a single chromatographic run and even for several samples in parallel, comprehensive information can be obtained such as identifying bioactive compounds in complex samples, information on polarity, multifold spectral characterization and sum formulae.

On the other hand, parallel information about several response mechanisms can readily be obtained for samples applied multifold on the same plate. The plate divided into plate sections (according to Figure 4) can be subjected to five different bioassays after chromatography.

For a high sample throughput, up to 30 samples per plate can simultaneously be screened for bioactive products (36). The sample throughput can even be doubled using anti-parallel developments from both sides. The most bioactive

samples can be investigated further. Also this is a highly streamlined process: only such samples, identified as the most bioactive, are focused on and characterized further. The bioactivity intensities can easily be compared on the tracks side by side, chromatographed and bio-detected under strict identical conditions. These are decisive advantages of the image-giving HPTLC-EDA technique.

Although HPTLC lacks in as high separation power as given for HPLC or GC, the high specificity and detectability of the bioassays compensate for it. The analysis of thousands of peaks in a complex sample is simplified to few manageable effective zones. Concerns about potential coelution with regard to complex mixtures are defanged using either (1) the elution head-based TLC-MS Interface with an integrated HPLC column or (2) comprehensive HPTLC.

- (1) Assumedly co-eluting substances can be separated via a short HPLC column integrated in the outlet capillary line of the TLC-MS Interface. For example, if a short monolithic RP18 column is integrated in the interface outlet line and transfer line to MS, a normal phase system (HPTLC) is orthogonally coupled to a reversed phase system (HPLC). For such a heart cut HPTLC-HPLC combination, an aqueous-organic elution solvent has to be used. The aqueous part assures a high elution power on HPTLC silica gel plates (front elution) and a sharp transfer of the zone of interest onto the head of the RP column. In RP-HPLC, water has no (if endcapped material) or less elution power and thus a retention and consequently orthogonal separation is enabled by a high water ratio in the eluent. Through an additional valve after the RP column, which guides the first run seconds into the waste, the polar ionic bioassay media can easily be removed and separated from the analytes eluting later, which are transferred online to HRMS.
- (2) Alternatively, comprehensive HPTLC (HPTLC x HPTLC) can readily be employed without instrumental effort in contrast to HPLC or GC. Only a small plate side has to be modified, *e.g.* by immersion of a 2 x 10 cm edge section of a 10 x 10 cm plate into a modifier solution followed by drying, and then a 2-D development has to be performed. For this, the plate is turned 90° after the first separation on the edge section and the second separation with a differing separation mechanisms follows on the non-modified plate part.

These options discussed show the high flexibility of HPTLC-EDA inclusive of all its hyphenations. The system can readily be adapted to a specific need and the utmost streamlined process can be chosen to get the information.

HPTLC-EDA - The Direct Link to the Effective Compound

EDA means effect-directed analysis and comprises all detection means indicating an effect that can affect biological systems. Thus, aside biological assays also microchemical reactions can be included in case of bio-related mechanisms (Figure 7).

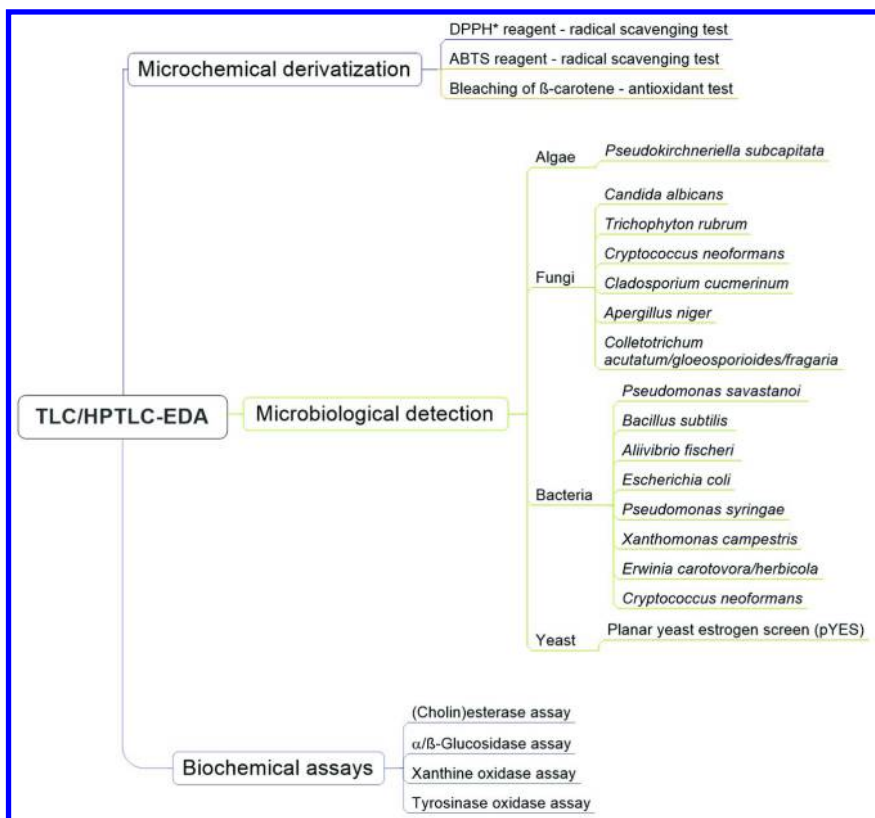


Figure 7. Categorization of TLC/HPTLC-EDA and some examples.

Although enzymes are neither a living organism nor an isolated organelle, biochemical detections are increasingly grouped into bioassays. HPTLC-EDA using the modified DB protocol is the preferred technique as recently shown for pYES (47) leading to sharply-bounded bioactive zones. Bioassays can be carried out highly selective and sensitive down to the pg-per-zone and even fg-per-zone range.

Biological Assays for Effect-Directed Detections

A wealth of microbiological and biochemical assays could be transferred to HPTLC. This field is extremely underexplored, however, the advantage is evident: it links directly to the bioactive compound. Especially cell test systems showing distinct toxicological effects will be an interesting subject of practical importance. Such cell systems will be explored and transferred in the near future, as the benefit of the direct hyphenation with chromatography is extraordinary. So far only some bioassays out of a wealth of possible bioassays using bacteria, fungi, yeasts or algae were transferred to HPTLC.

- Bacterial assays for detection of bioactive compounds in complex samples were described using the directly bioluminescent, marine *Vibrio Fischeri* bacteria ((19, 35, 36, 55, 56); review in (57)), newly classified and termed *Aliivibrio fischeri* in 2007. The direct luminescence enabled a very fast protocol. HPTLC in combination with the *Aliivibrio fischeri* bioassay is highly convenient in practical use, especially if compared to cuvette or microtiterplate assays.

The bacterial detection of antibiotic compounds in environmental and food samples was reported using *Bacillus subtilis* (58) or in natural products and in plants using *Pseudomonas savastanoi* (59, 60). Vitamin B12 was detected in food using *Escherichia coli* 215 (61). Antimicrobial compounds in essential oils were detected using *Xanthomonas campestris* pv. *Vesicatoria*, *Pseudomonas syringae* pv. *Phaseolicola* (62) or *Serratia marcescens* (63). The latter bacteria were red-colored and directly visible, however, for location and visualization of other antibacterials mostly tetrazolium salt solutions were used as a substrate for visualization of the vitality. Respective tetrazolium salts were converted by intact dehydrogenases in living bacteria to colored formazans. However, antimicrobial compound zones killed the bacteria and white zones were obtained on a homogeneously colored background (Figure 8).

An alternative to visualization via tetrazolium salt solutions or instant bioluminescence, was demonstrated for inhibitors of the plant pathogens *Erwinia carotovora* and *Erwinia herbicola*. Plate incubation with esculin, which was hydrolyzed to esculetin by living bacteria and reacted with ferric ion to form a brown complex, led to a brown plate background, whereas inhibitors of the plant bacteria were detected as white zones (64). Many other enzyme-substrate reactions that indicate the vitality of living microorganisms are suited for use in HPTLC-bioassay detection.

- Algae assays were used for detection of algicides like shown for *Pseudokirchneriella subcapitata* (67). White inhibition zones were visible on a colored background.
- Fungi assays were used for detection of antifungal compounds, like suspensions of *Candida albicans*, *Trichophyton rubrum*, *Cryptococcus neoformans*, *Cladosporium cucumerinum*, *Colletotrichum* species, *Penicillium* species or *Aspergillus niger* ((65–70) review in (71)). The developed plate was immersed into a fungal suspension and the fungi grow directly on the plate (visible as grey background with white inhibition zones) until stopped by immersion into ethanol.
- Tailor-made bacteria strains or genetically engineered luminescent (72) or specified microorganisms, so-called reporter gene assays, show strong effects. For example, genetically modified yeast cells were used for detection of estrogens (73) and further endocrine disrupting compounds. The genetically engineered yeast cells contained the human estrogen receptor DNA sequence (YES assay). In the last review (25), YES was indicated to be a hot assay candidate. Meanwhile it was transferred to HPTLC (74, 75), but still showed diffuse, broad zones after the long

incubation time on the plate. Not until now (47, 76), the HPTLC-pYES method was substantially improved to obtain sharply-bounded zones with improved detectabilities (Figure 3). An international pYES expert group is developing this new assay further (interested scientists are invited to participate).

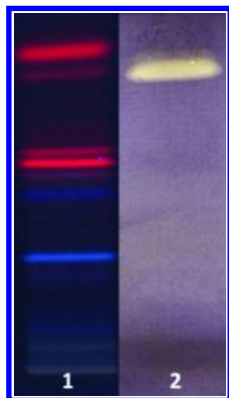


Figure 8. HPTLC-EDA of a bioactive Salvia sample detected with Bacillus subtilis (track 2; compared to fluorescence detection on track 1). (Reproduced with permission from reference (38). Copyright 2014 G. Morlock.)

Biochemical Assays for Effect-Directed Detections

Aside immuno-staining of gangliosides (77, 78), glycosphingolipids (79, 80) or antiphospholipid antibodies (81, 82), enzyme assays were applied for selective detection. So far only few biochemical assays were transferred to the plate.

- The esterase inhibition (EI) by anti-cholinesterase compounds like organo-phosphates, thiophosphates or carbamates (83–85) was demonstrated to be selective and sensitive down to the pg-per-zone range (26, 86). Visualization was performed with Fast Blue Salt B coupled to α - or β -naphthol, which was enzymatically released from the respective acetate substrate. Densitometric evaluation was performed via absorbance measurement at 533 nm. Alternatively, the Ellman reagent forms a pale yellow background within 5 min. AChE inhibitors appear as white spots, which are generally more difficult to visualize than the diazo dye method mentioned before.
- Previously performed as agar overlay and detected using esculin as substrate to produce esculetin reacting with ferric ion to form a brown complex (87, 88), screening for glucosidase inhibitors was employed as TLC-DB (89). Visualization was performed by spraying with a mixture of naphthyl-glucopyranoside solution and Fast Blue Salt B, in a ratio of 1:1 for the α -D-glucosidase and in a ratio of 1:4 for the β -D-glucosidase

assay. Using automated immersion instead of manual spraying would improve the background homogeneity.

- Xanthine oxidase (XO) catalyses the oxidation of hypoxanthine and xanthine to uric acid. Enzymatic oxidation of xanthine produces hydrogen peroxide and superoxide radicals, which reduce the pale yellow tetrazolium salt to a purple formazan. The XO inhibition zones, visible as pale zones on a purple background, may reduce oxidative stress and can have an effect on inflammation, arteriosclerosis, cancer, aging, reduction of gout and kidney stones *etc.* Previously applied as agar overlay (90), detection was recently performed by dipping into a xanthine oxidase solution, followed by incubation, dipping into a xanthine-nitrotetrazolium mixture and followed by a second incubation (91).
- For tyrosinase inhibition, the TLC layer was sprayed with tyrosinase and L-tyrosine solutions successively. Tyrosinase inhibiting zones are detected as white spots against a brownish-purple background down to the low ng-per-zone range (92). Again, using automated immersion instead of manual spraying would improve the background homogeneity.

Microchemical Effect-Directed Detections

Microchemical derivatizations can also link to an effect. Especially assays for antioxidant and radical scavenging properties are often applied.

- Bleaching under white light illumination or UV 366 nm (93) after spraying of a developed plate with β -carotene solution, or better immersion into it, led to antioxidative yellow-orange zones remained on a white background.
- Free-radical scavenging properties of single compounds in complex mixtures can be detected using the microchemical reaction with the stable 2,2-diphenyl-1-picrylhydrazyl radical (DPPH \cdot ,). This reaction is widely used, but instead of application by manual spraying, automated immersion of the developed HPTLC plate into the methanolic DPPH \cdot solution should be preferred to obtain a homogeneous background. The absorption maximum of the purple DPPH \cdot dye decreases upon reduction by a radical scavenger. The revealing yellow-white zones against a purple background are evaluated best under white light illumination in the transmission mode. After 30 min or a longer period, the images captured are more intense in signal gain if compared to the directly captured image.
- Another test with regard to free-radical scavenging properties is the 2,2'-azino-bis(3-ethylbenzthiazoline-6-sulphonic) acid radical (ABTS \cdot) assay. The developed plate is immersed into the ABTS \cdot solution and radical scavengers are observed as colorless or pink spots on a green background. If compared, the performance of the DPPH \cdot reagent is superior with regard to stability and zone differentiation (45).

EDA detects according to its effect depending on the assay selected, and thus additional information different to spectral detections is obtained. For example, the effective zone, previously not detectable with mainstream detection techniques (UV/Vis/FLD), was first revealed with the bioassay (Figures 5 and 8). Microchemical derivatization reactions (for confirmation of functional groups) and further spectroscopic-/metric techniques may follow for further characterization of unknown effective zones discovered (Figure 1). For detailed analysis of newly discovered chiral compounds, chiral HPTLC stationary phases or a chiral agent added to the mobile phase have to be employed. Or the effective zone has to be online eluted into a vial (using the TLC-MS Interface) and subjected to further analysis, *e.g.*, by multi-dimensional gas chromatography with chiral columns.

Conclusions

The field of HPTLC-EDA and its hyphenations attracts ongoingly interest. Comprehensive information about effective compounds in a complex sample is gained, all at the analytical scale. The experience gathered so far suggests HPTLC as highly effective complementary and orthogonal method to column-derived techniques. This hyphenated, flexible strategy HPTLC-UV/Vis/FLD-EDA-HRMS/NMR/ATR-FTIR/SERS has three decisive benefits and substantial advantages: (1) the absolutely direct comparison of samples, run and bio-detected in parallel under identical conditions, (2) the direct correlation of single sample components to biological activities, and (3) the immediate reference to sum formulae, especially of newly discovered bioactive components. This hyphenated strategy will support researcher to recognize effective adulterations and falsifications with regard to food safety, but also to streamline natural product search or residue analysis, as it directly links to effective compounds, depending on the bioassay selected. This strategy reduces the number of compounds in a complex mixture (>1000 to be analyzed, all of potential interest) to a reasonable number and supports effective and comprehensive decisions. Thanks to the combination of chromatography and bioassay, it can rapidly be decided on samples whether there are relevant compounds in. Potential matrix interferences of a sample are substantially reduced thanks to the chromatographic separation, even if it is not the best. The analysis times are substantially reduced, if compared to cuvette, Petri dish or microtiterplate assays. The recently modified bioassay protocol (47, 76) led to sharply-bounded zones, even after long incubation times with aqueous media. This substantial improvement was shown for HPTLC-pYES and its general applicability was demonstrated by transfer to the *Bacillus subtilis* bioassay, for which also sharply-bounded zones were obtained (47). Thus, clear compound assignments are now possible, additionally to structure elucidating techniques at the analytical scale. Both together make HPTLC-EDA attractive for many application fields (76) and new avenues are opened through these substantial improvements.

References

1. Sticher, O. *Nat. Prod. Rep.* **2008**, *25*, 517–554.
2. Bousova, K.; Senyuva, H.; Mittendorf, K. *J. Chromatogr., A* **2013**, *1274*, 19–27.
3. Reemtsma, T.; Alder, L.; Banasiak, U. *J. Chromatogr., A* **2013**, *1271*, 95–104.
4. Reemtsma, T. *J. Chromatogr., A* **2009**, *1216*, 3687–3701.
5. Wright, C. *J. Chromatogr., A* **2009**, *1216*, 316–319.
6. Brack, W. *J. Verbraucherschutz Lebensmittelsicherh.* **2006**, *1*, 301–309.
7. Brack, W. *Anal. Bioanal. Chem.* **2003**, *377*, 397–407.
8. Boehmler, G.; Brack, W.; Gareis, M.; Goerlich, R. *J. Verbraucherschutz Lebensmittelsicherh.* **2006**, *1*, 294–300.
9. Farre, M.; Asperger, D.; Kantiani, L.; Gonzalez, S.; Petrovic, M.; Barcelo, D. *Anal. Bioanal. Chem.* **2008**, *390*, 1999–2007.
10. Gaudin, V.; Hedou, C.; Rault, A.; Verdon, E. *Food Addit. Contam., Part A* **2010**, *27*, 935–952.
11. Gaudin, V.; Hedou, C.; Verdon, E. *Food Addit. Contam., Part A* **2009**, *26*, 1162–1171.
12. Laurentie, M.; Gaudin, V. *J. Chromatogr. B: Anal. Technol. Biomed. Life Sci.* **2009**, *877*, 2375–2379.
13. Gaudin, V.; Hedou, C.; Rault, A.; Sanders, P.; Verdon, E. *Food Addit. Contam., Part A* **2009**, *26*, 427–440.
14. Gaudin, V.; Juhel-Gaugain, M.; Moretain, J. P.; Sanders, P. *Food Addit. Contam., Part A* **2008**, *25*, 1451–1464.
15. Gaugain-Juhel, M.; Delepine, B.; Gautier, S.; Fourmond, M. P.; Gaudin, V.; Hurtaud-Pessel, D.; Verdon, E.; Sanders, P. *Food Addit. Contam., Part A* **2009**, *26*, 1459–1471.
16. Berendsen, B. J. A.; Pikkemaat, M. G.; Stolker, L. A. M. *Anal. Chim. Acta* **2011**, *685*, 170–175.
17. Hirschfeld, T. *Anal. Chem.* **1980**, *52*, 297A–312A.
18. Wilson, D.; Brinkman, U. A. T. *Trends Anal. Chem.* **2007**, *26*, 847–854.
19. Eberz, G.; Rast, H. G.; Burger, K.; Kreiss, W.; Weisemann, C. *Chromatographia* **1996**, *43*, 5–9.
20. Fabel, S.; Niessner, R.; Weller, M. G. *J. Chromatogr., A* **2005**, *1099*, 103.
21. Schebb, N. H.; Heus, F.; Saenger, T.; Karst, U.; Irth, H.; Kool, J. *Anal. Chem.* **2008**, *80*, 6764–6772.
22. Schebb, N. H.; Faber, H.; Maul, R.; Heus, F.; Kool, J.; Irth, H.; Karst, U. *Anal. Bioanal. Chem.* **2009**, *394*, 1361–1373.
23. Nielen, M. W. F.; Bovee, T. F. H.; van Engelen, M. C.; Rutgers, P.; Hamers, A. R. M.; Van Rhijn, J. A.; Hoogenboom, L. A. P. *Anal. Chem.* **2006**, *78*, 424–431.
24. Bovee, T. F. H.; Helsdingen, R. J. R.; Hamers, A. R. M.; Duursen, M. B. M.; Nielen, M. W. F.; Hoogenboom, R. L. A. P. *Anal. Bioanal. Chem.* **2007**, *389*, 1549–1558.
25. Morlock, G.; Schwack, W. *J. Chromatogr., A* **2010**, *1217*, 6600–6609.
26. Akkad, R.; Schwack, W. *J. Planar Chromatogr.* **2008**, *21*, 411–415.

27. Misra, K.; Tulsawani, R.; Shyam, R.; Meena, D. K.; Morlock, G. *J. Liq. Chromatogr. Relat. Technol.* **2012**, *35*, 1364–1387.
28. Dytkiewitz, E.; Morlock, G. E. *J. AOAC Int.* **2008**, *91*, 1237–1243.
29. Morlock, G. *HPTLC-MS in Pharmaceutical Analysis and Food Analysis (in German)*; Lecture, University of Applied Sciences Northwestern (FHNW), Basel, Switzerland, 2010.
30. Gössi, A.; Scherer, U.; Schlotterbeck, G. *Chimia* **2012**, *66*, 347–349.
31. Stahlmann, S.; Herkert, T.; Roseler, C.; Rager, I.; Kovar, K. A. *Eur. J. Pharm. Sci.* **2001**, *12*, 461–465.
32. Brandt, C.; Kovar, K. A. *J. Planar Chromatogr.* **1997**, *10*, 348–352.
33. Morlock, G. Doctorial thesis, University of Saarland, Saarbrücken, Germany, 1995.
34. Brosseau, C. L.; Gambardella, A.; Casadio, F.; Grzywacz, C. M.; Wouters, J.; Van Duyne, R. P. *Anal. Chem.* **2009**, *81*, 3056–3062.
35. Cretu, S.; Morlock, G. *Food. Chem.* **2014**, *146*, 104–112.
36. Kloepfel, A.; Grasse, W.; Bruemmer, F.; Morlock, G. E. *J. Planar Chromatogr.* **2008**, *21*, 431–436.
37. Kloepfel, A.; Kolm, A.; Brümmer, F.; Morlock, G. *CAMAG Bibliogr. Service CBS* **2009**, *102*, 2–3.
38. Morlock, G. *Q&more* **2014**, *1*, 42–47.
39. Morlock, G. In *Reference Module in Chemistry, Molecular Sciences and Engineering*; Reedijk, J., Ed.; Elsevier Reference Module in Chemistry, Molecular Sciences and Chemical Engineering; Elsevier: Waltham, MA, 2014; (07-Aug-14 doi: 10.1016/B978-0-12-409547-2.10736-X)
40. Morlock, G.; Schwack, W. *Trends Anal. Chem.* **2010**, *29*, 1157–1171.
41. Morlock, G. In *Applied Mass Spectroscopy, Handbook*; Lee, M., Ed.; John Wiley and Sons: Hoboken, NJ, 2012; pp 1181–1206.
42. Morlock, G. E. *J. Liq. Chromatogr. Relat. Technol.* **2014**, *37*, 2892–2914.
43. Goodall, R. R.; Levi, A. A. *Nature* **1946**, *158*, 675–676.
44. Choma, I. M.; Grzelak, E. M. *J. Chromatogr., A* **2011**, *1218*, 2684–2691.
45. Marston, A. *J. Chromatogr., A* **2011**, *1218*, 2676–2683.
46. Hostettmann, K.; Marston, A. *Pure Appl. Chem.* **1994**, *66*, 2231–2234.
47. Klingelhöfer, I.; Morlock, G. *J. Chromatogr. A* **2014**, *1360*, 288–295.
48. Eberz, G.; Rast, H. G.; Burger, K.; Kreiss, W.; Weisemann, C. *Chromatographia* **1996**, *43*, 5–9.
49. Morlock, G. E.; Morlock, L. P.; Lemo, C. *J. Chromatogr., A* **2014**, *1324*, 215–223.
50. Morlock, G. E.; Schuele, L.; Grashorn, S. *J. Chromatogr., A* **2011**, *1218*, 2745–2753.
51. Hošťálková, A.; Klingelhöfer, I.; Morlock, G. E. *Anal. Bioanal. Chem.* **2013**, *405*, 9207–9218.
52. Vega-Herrera, M. A.; Morlock, G. E. *J. Planar Chromatogr.* **2007**, *20*, 411–417.
53. Morlock, G. E.; Prabha, S. *J. Agric. Food Chem.* **2007**, *55*, 7217–7223.
54. Morlock, G. E.; Sung, Y. H.; Yan, F.; Honermeier, B. in preparation.
55. Krüger, S.; Urmann, O.; Morlock, G. *J. Chromatogr., A* **2013**, *1299*, 105–118.

56. Baumgartner, V.; Schwack, W. *J. Liq. Chromatogr. Relat. Technol.* **2010**, *33*, 980–995.
57. Sherma, J. *Studia Universitatis Babe-Bolyai, Chemia, Liv* **2009**, *2*, 5–13.
58. Nagy, S.; Kocsis, B.; Koszegi, T.; Botz, L. *J. Planar Chromatogr.* **2002**, *15*, 132–137.
59. Molnar, V.; Billes, F.; Tylhak, E.; Ott, P. G. *J. Planar Chromatogr.* **2008**, *21*, 423–426.
60. Moricz, A. M.; Adanyi, N.; Horvath, E.; Ott, P. G.; Tyihak, E. *J. Planar Chromatogr.* **2008**, *21*, 417–422.
61. Nishioka, M.; Kanosue, F.; Miyamoto, E.; Yabuta, Y.; Watanabe, F. *J. Liq. Chromatogr. Relat. Technol.* **2009**, *32*, 1175–1182.
62. Horvath, G.; Jambor, N.; Vegh, A.; Boszormenyi, A.; Lemberkovics, E.; Hethelyi, E.; Kovacs, K.; Kocsis, B. *Flavour Fragrance J.* **2010**, *25*, 178–182.
63. Williams, L.; Bergersen, O. *J. Planar Chromatogr.* **2001**, *14*, 318–321.
64. Lund, B. M.; Lyon, G. D. *J. Chromatogr.* **1975**, *110*, 193–196.
65. Garo, E.; Wolfender, J. L.; Hostettmann, K.; Hiller, W.; Antus, S.; Mavi, S. *Helv. Chim. Acta* **1998**, *81*, 754–763.
66. Nagy, S.; Kocsis, B.; Koszegi, T.; Botz, L. *J. Planar Chromatogr.* **2007**, *20*, 385–389.
67. Baumann, U.; Brunner, C.; Pletscher, E.; Tobler, N. *Umweltwiss. Schadst.-Forsch.* **2003**, *15*, 163–167.
68. Hostettmann, K.; Potterat, O. *ACS Symp. Ser.* **1997**, *658*, 14–26.
69. Schmourlo, G.; Mendonca-Filho, R. R.; Alviano, C. S.; Costa, S. S. *J. Ethnopharmacol.* **2005**, *96*, 563–568.
70. Altintas, A.; Tabanca, N.; Tyihák, E.; Ott, P. G.; Móricz, Á. M.; Mincsovcics, E.; Wedge, D. E. *J. AOAC Int.* **2013**, *96*, 1200–1208.
71. Favre-Godal, Q.; Queiroz, E. F.; Wolfender, J. *J. AOAC Int.* **2013**, *96*, 1175–1188.
72. Moricz, A. M.; Tyihak, E.; Ott, P. G. *J. Planar Chromatogr.* **2010**, *23*, 180–183.
73. Mueller, M. B.; Dausend, C.; Weins, C.; Frimmel, F. H. *Chromatographia* **2004**, *60*, 207–211.
74. Buchinger, S.; Spira, D.; Bröder, K.; Schlösener, M.; Ternes, T.; Reifferscheid, G. *Anal. Chem.* **2013**, *85*, 7248–7256.
75. Schönborn, A.; Grimmer, A. *J. Planar Chromatogr.* **2013**, *26*, 402–408.
76. Morlock, G. E.; Klingelhöfer, I. *Anal. Chem.* **2014**, *86*, 8289–8295.
77. Popa, J.; Portoukalian, J.; Pernin, M.; David, M. *CAMAG Bibliogr. Service CBS* **2005**, *94*, 11–13.
78. Portoukalian, J.; Bouchon, B. *J. Chromatogr.* **1986**, *380*, 386–392.
79. Kushi, Y.; Ogura, K.; Rokukawa, C.; Handa, S. *J. Biochem.* **1990**, *107*, 685–688.
80. Muething, J.; Cacic, M. *Glycoconjugate J.* **1997**, *14*, 19–28.
81. Alessandri, C.; Sorice, M.; Bombardieri, M.; Conigliaro, P.; Longo, A.; Garofalo, T.; Manganelli, V.; Conti, F.; Degli Esposti, M.; Valesini, G. *Arthritis Res. Ther.* **2006**, *8*, R180 (11 pages).

82. Sorice, M.; Circella, A.; Misasi, R.; Pittoni, V.; Garofalo, T.; Cirelli, A.; Pavan, A.; Pontieri, G. M.; Valesini, G. *Clin. Exp. Immunol.* **2000**, *122*, 277–284.
83. Ackermann, H.; Lexow, B.; Plewka, E. *Arch. Toxikol.* **1969**, *24*, 316–324.
84. Hamada, M.; Wintersteiger, R. *J. Planar Chromatogr.* **2003**, *16*, 4–10.
85. Vashkevich, O. V.; Gankina, E. S. *J. Planar Chromatogr.* **1990**, *3*, 354–356.
86. Akkad, R.; Schwack, W. *J. Chromatogr., B* **2011**, *1218*, 2775–2784.
87. Salazar, M. O.; Furlan, R. L. E. *Phytochem. Anal.* **2007**, *18*, 209–212.
88. Lund, B. M.; Lyon, G. D. *J. Chromatogr.* **1975**, *110*, 193–196.
89. Simões-Pires, C. A.; Hmicha, B.; Marston, A.; Hostettmann, K. *Phytochem. Anal.* **2009**, *20*, 511–515.
90. Ramallo, I. A.; Zacchino, S. A.; Furlan, R. L. E. *Phytochem. Anal.* **2006**, *17*, 15–19.
91. Su, X.; Li, X.; Tao, H.; Zhou, J.; Chou, G.; Cheng, Z. *J. Sep. Sci.* **2013**, *36*, 3644–3650.
92. Wangthong, S.; Tonsiripakdee, I.; Monhaphol, T.; Nonthabenjawan, R.; Wanichwecharungruang, S. P. *Bio. Chromatogr.* **2008**, *21*, 94–100.
93. Pratt, D. E.; Miller, E. E. *J. Am. Oil Chem. Soc.* **1984**, *61*, 1064–1067.
94. Pozharitskaya, O. N.; Ivanova, S. A.; Shikov, A. N.; Makarov, V. G. *Phytochem. Anal.* **2008**, *19*, 236–243.

Chapter 6

Standardization of Analytical Methodology and Procedures for Purity Assessment of Small Molecules in Drug Discovery

Aránzazu Marín,¹ Gary Sharman,² Marie Burgess,²
Christopher Reutter,³ and Alfonso Espada^{*,1}

¹Analytical Technologies, DCR&T Alcobendas, Lilly S.A.,
Avda. de la Industria 30, 28108 Alcobendas, Spain

²Analytical Technologies, Eli Lilly and Company Limited,
Lilly Research Centre, Erl Wood Manor, Sunninghill Road,
Windlesham, Surrey GU206PH, U.K.

³Analytical Technologies, Lilly Research Laboratories, A Division of Eli Lilly
and Company, Lilly Corporate Center, Indianapolis, Indiana 46285, U.S.A.

*E-mail: espada_alfonso@lilly.com.

Purity assessment of pharmaceutical compounds is a key part of ensuring data integrity for any biological assay carried out on such materials. Purity requirements and analytical procedures are different according to the drug discovery stage from chemical synthesis to compound selection for development. In the current climate of globalization and externalization, analytical laboratories should have the ability to deliver high quality levels of a service and to directly develop optimal methods and processes to be able to translate them into effective practices. For this, standardization in drug discovery laboratories working with external partners is of paramount importance to deliver consistent data and procedures, independent of the research site. This chapter reports the implementation and standardization of LC-MS methods and analytical procedures in Lilly research sites to deal with purity assessment and related substances determination in different stages of drug discovery.

Introduction

The purity assessment of a compound in pharmaceutical research is a key part of ensuring data integrity for any biological assay carried out on such materials (1). However purity requirements and analytical procedures differ according to the drug discovery stage from chemical synthesis to compound selection for development (2, 3). Whereas in later stages of pharmaceutical development, individually validated methods for each active pharmaceutical ingredient (API) are necessary and required by regulators, such an approach is not practical in earlier stages of discovery and generic methods applicable to a range of compounds must be used to deliver acceptable analysis rates.

Demands on analytical support for drug discovery have increased in the past few years. As a result, new analytical techniques are being continually developed to meet these challenges. The use of well established methodologies is being enhanced by incremental improvements in technology and protocols (4). Hyphenation of analytical techniques (5, 6) is an approach adopted in drug discovery laboratories to satisfy the compound quality requirements of today's pharmaceutical industry. Herein, liquid chromatography combined with mass spectrometry (LC-MS) has proven to be the analytical technique of choice to assess the purity of drug compounds in various stages of drug discovery (3, 7-9). In addition, reversed-phase is clearly the most prominent and valuable LC separation mode in analytical sciences for its long tradition in quantification and identification of synthesized compounds (3, 10, 11). The benefits of orthogonal reversed-phase LC-MS-based methods, to accurately determine the identity and purity of drug discovery compounds have been recently discussed by our group (3). Additionally, an approach for improving the speed and effectiveness of orthogonal low and high pH LC-MS for routine purity assessment on a single system was demonstrated and standardized across two different sites within Lilly Research Laboratories (12).

In the current climate of globalization and externalization, analytical laboratories should have the ability to deliver high quality levels of a service and to directly develop optimal methods and processes to be able to translate them into effective practices. For this, standardization in drug discovery laboratories working with external partners is of paramount importance to deliver consistent data and procedures, independent of the research site. This chapter reports the implementation and standardization of LC-MS methods and analytical procedures in Lilly research sites to deal with purity assessment and related substances determination in different stages of drug discovery.

We have continued our previous strategy for developing LC-MS methods (3, 12) with the evaluation of different chromatographic approaches for improving the speed and effectiveness of orthogonal LC-MS methods for routine purity assessment under an open access environment (analysis carried out by chemists with minimum training on sample submission). Starting with our optimized 7 min LC-MS gradients (12), more effective and faster methods with higher resolution power were projected to reduce the analysis cycle time without sacrificing data quality. Advantages and disadvantages of 4 column technologies (Gemini

NX C18, XTerra MS C18, Atlantis dC18 and Kinetex C18) were evaluated in comparison with conventional Gemini C18 and XBridge C18 columns.

In relation to the analytical procedure, there are different approaches to determine the purity level and to carry out the quantification/identification of the related substances that can accompany a pre-clinical candidate. Related substances (RS) are defined as impurities derived from the drug candidate structurally related to the compound of interest. The origin of these impurities may be due to the synthesis, degradation of the compound, or some other process occurring during the storage of the material (13–15). They do not include process contaminants such as inorganic impurities, solvents, or water.

The most common approaches for purity assessment and related substances determination are (16):

- The **area percent** approach is one of the simplest ways particularly important through the early phase in drug discovery. This approach does not require a reference standard and calculates the percentage of a specific RS based on the area of this in comparison with the total area by normalisation. It presents some limitations such as the linearity over a wide range of concentration, the sample concentration (method sensitivity) and the response factor that should be similar to that of the drug substance. Due to its simplicity, this approach in combination with the use of LC-MS was the preferred procedure by the pharmaceutical industry (13) and chosen in Lilly laboratories for routine analysis of compounds by synthetic chemists (e.g. monitoring chemical reactions or rapid purity assessment). In this case, the area percentage obtained by UV is used for the quantitative analysis and the MS spectrum obtained is used for the qualitative analysis (17). In addition, due to the robustness of LC-MS, this approach has been adopted as a user friendly open access service (18).
- In the **external standard** approach, the % of RS is calculated using a standard curve. The concentration of RS is determined by the response and the calibration curve. It offers several advantages over the area percent method such as the reduced linear range and improved method sensitivity, but its main limitation is that a well-characterized reference standard is essential and this is not typically the case in drug discovery laboratories.
- In the **high-low approach** (19)], the limitation of the linear range is overcome. The HPLC method relies on the assumptions that impurities will elute from the column, and that they have a UV response that is similar to the main component at that wavelength. These are not always good assumptions; however, the resulting error is minimized as impurity levels decrease. Samples are prepared at two concentrations and related substances are estimated using HPLC techniques by comparing the chromatograms from a pair of sample solutions. Chemical amplification is achieved by comparing the chromatograms from a concentrated solution (high) and an appropriate dilution (low). Based on the area of the target compound in the diluted sample and the area of all the

impurities in the concentrated sample at the maximum wavelength of the target compound, the % of related substances is determined by Equation 1. It is important that the accuracy and precision gains from the improved signal to noise are not offset by new sources of error in the procedure and therefore reproducible injection volumes and accurate dilution are essential to achieve the highest quality results with this high-low approach.

$$\% \text{ TOTAL Related Substances} = A_{\text{High IMP}} / A_{\text{Low CPD}} * 100\% / \text{DF}$$

Where:

$A_{\text{Low CPD}}$ = Area of the target compound in the diluted sample

$A_{\text{High IMP}}$ = Total area of the impurities in the concentrated sample

DF = Dilution factor

Equation 1: % TOTAL Related Substances (%TRS)

Note: The percentage TRS is not directly comparable to the area percent. The area percent is normalised i.e. all peaks summed to 100% whereas the TRS is a percentage of the main component.

Due to the high sensitivity and the absence of a reference standard, this approach was chosen to carry out the analysis of more advanced compounds, such as the pre-clinical candidates, which demand more accurate information. Within our laboratories, compound purity levels must generally be greater than 97%, with no single impurity higher than 2%, and the identification/quantification of the related substances must be performed by analytical scientists. To ensure data consistency across different sites, a global validation exercise was carried out to estimate the error for the individual and total related substances determination.

Experimental

Instrumentation

Experiments were performed on an Agilent 1200 Series Rapid Resolution LC/MSD SL system or Agilent 1100 Series LC/MSD equipped with a solvent degasser, binary pump, auto sampler, column compartment and a diode array detector (Agilent Technologies, Waldbronn, Germany). The UV wavelength was set at 214 nm, band width 16 nm for the area percentage approach and at the maximum wavelength of the compounds of interest for the high-low approach. Electrospray mass spectrometry measurements were performed on a MSD quadrupole mass spectrometer (Agilent Technologies, Palo Alto, CA, USA) interfaced to the HP1200 or HP1100 HPLC system. MS measurements

were acquired simultaneously in both positive and negative ionization modes (fragmentor 120 V, threshold spectral abundance 150, MS peak width 0.09 minutes) over the mass range of 100-800 (12). Data acquisition and integration for LC-UV and MS detection were collected using Chemstation software (Agilent Technologies). HPLC 1100 instruments were optimized with the Agilent Rapid Resolution HT1100 Series LC modification Kit (part number 5188-5328) or a low volume mixer to minimize the system dead volume and gradient delay. Connections between the injector, the column, and detectors were made using 0.17 mm i.d. stainless steel or PEEK tubing.

Reagents and Columns

Water, acetonitrile (ACN) and methanol (MeOH) were HPLC grade from Lab Scand (Dublin, Ireland). Formic acid (FA) and ammonium hydrogencarbonate were from Sigma-Aldrich (Steinheim, Germany).

Propranolol HCl (pKa: 9.2, logP: 3.1), verapamil HCl (pKa: 9.0, logP: 3.9), terfenadine (pKa: 9.5 and 13.3, logP: 6.5) and niflumic acid (pKa: 1.7 and 4.7, logP: 4.9) (20) were the components of the test mix for the studies carried out with low pH mobile phases. Diltiazem HCl (pKa: 8.9, logP: 3.6) was used instead of propranolol for the mixture employed for high pH analyses. The drug compounds were obtained from Sigma-Aldrich. 5 mg of each compound were weighted and dissolved in 30 ml of acetonitrile and made up to 100 ml in a volumetric flask with water. The resulting concentration equaled 50 µg/mL per component. The injection volume was 2 µL.

The columns used in this work were Gemini C18 and Gemini NX C18 50 x 2.0 mm, 3 µm, Kinetex C18 50 x 2.1, 2.6 µm (Phenomenex), XTerra MS C18 and XBridge C18 50 x 2.1 mm, 3.5 µm and Atlantis dC18 50 x 2.1 mm, 3 µm (Waters). The characteristics of the columns given by the manufactures are listed in Table 1. The acidic mobile phases were water (solvent A) and acetonitrile (solvent B), both containing 0.1% formic acid (FA). Meanwhile, the alkaline mobile phases were water (solvent A) with 10 mM ammonium hydrogencarbonate (NH₄HCO₃) adjusted to pH 9 with ammonium hydroxide (NH₄OH) and acetonitrile (solvent B). The flow rate prior to the mass spectrometer was 1 ml/min, which was split at a ratio of 3:1 in order to deliver 250 µL/min into the electrospray interface and 750 µL/min to the waste reservoir.

Results and Discussion

Defining Chromatographic Methods for Purity Assessment: Column and Gradient Time

Starting with our optimized 7 min standard LC-MS gradients (12) for the analysis of final products with low pH (from 5 to 100%B in 7 min, stays at 100%B for 1 min, and then 0.5 min to initial conditions) and high pH mobile phases (from 10 to 100% B in 7 min, holds at 100%B for 1 min, and then 0.5 min to initial

conditions) in the Gemini and XBridge columns respectively (at a flow rate of 1 ml/min and 50°C of column temperature), we focused on a strategy for improving the speed and effectiveness of orthogonal methods for routine purity assessment. A systematic study using the above conditions but modifying the gradient time of our standard methods from 7 min to 4.0, 3.0, 2.5, 2.0 and 1.0 min holding at 0.4 min at 100%B was carried out on both columns. Taking into account the low column volume (0.2 mL), the time taken for the injection step (1 min) was found to be more than enough to equilibrate the column, therefore both the post-time and the re-equilibration time (1.5 min and 0.5 min respectively) which were employed in the previous 7 min gradient were removed.

A test mix containing 4 drug compounds (three amines and one acid) was used to check the performance of these studies (12). Five consecutive injections of this test mix were carried out for each of the conditions tested. Peak capacity was the default chromatographic parameter employed to define the resolution power of each LC method (3, 21). Peak capacity is calculated according to Equation 2. Figure 1 shows the results of this study on the Gemini and XBridge columns for low and high pH, respectively.

$$\text{Peak Capacity} = (\text{TGT} - \text{T}_0) / \text{W}_{10\%}$$

Where:

TGT= Total gradient time in min

T₀= Dead time in min

W_{10%}= Peak width at 10%

Equation 2: Peak capacity.

It is well known that longer gradient times yield higher peak capacity values. Peak capacity of our current 7 min gradients, 162 and 125 for the Gemini and XBridge columns respectively, was lowered when gradient time was decreased. However, the relationship is not linear and an appropriate and optimal balance between analysis time and peak capacity can be found. To this end, a 3 min gradient for the analysis under open access and 4 min gradient for TRS determination were chosen as the best compromise. Peaks capacities with these new methods (3-4 min gradients) were 115-132 for low pH on the Gemini and 80-92 for high pH on the XBridge column. For the final methods of 3 min gradients, the time for washing the column at 100% of mobile phase B was increased from 0.4 to 0.75 min to ensure that all retained compounds elute from the column. Thus, the total analysis time was reduced from 8.5 min to 3.75 min (3 min gradient) for open access analysis, giving more than 50% time reduction. Also note that the new methods still showed good performance in both UV and MS signal detection as is depicted in Figure 2.

Table 1. Physico-Chemical Properties of the Columns Used in This Study

<i>Column Technology</i>	<i>Pore Size (Å)</i>	<i>Surface Area (m²/g)</i>	<i>Coverage μmol/m²</i>	<i>Carbon Load (%)</i>	<i>pH Stability</i>
Gemini® C18 Twin ¹ :	110	375		14	1.0-12.0
Gemini® NX C18	110	375		14	1.0-12.0
XTerra® MS C18 HPT ² :	125	175	2.2	15.5	1.0-12.0
XBridge® C18 BEH ³ :	135	185	3.2	18	1.0-12.0
Atlantis® dC18	100	330		12	3-7
Kinetex® C18	100	200		12	1.5-10

¹: Two-In-One Technology. ²: HPT: Hybrid Particle Technology. ³: BEH: Bridged Ethyl Hybrid Technology.

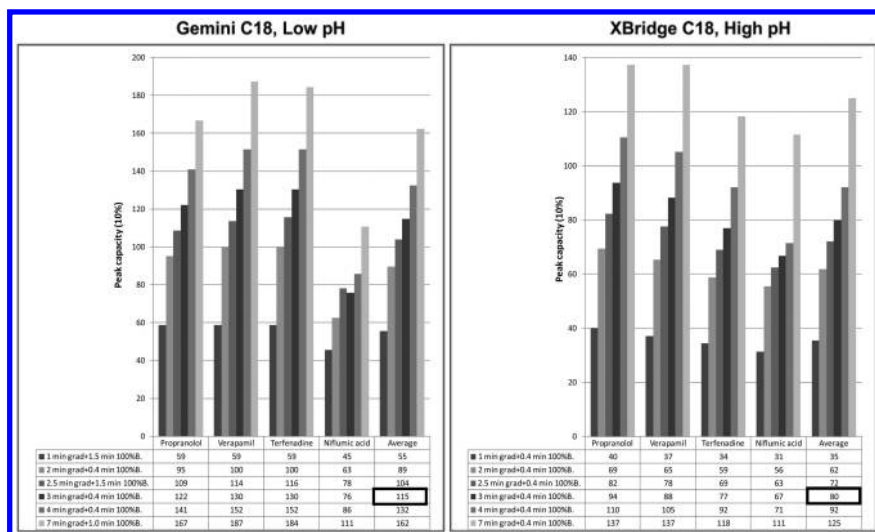


Figure 1. Comparison of peak capacity versus gradient time on the Gemini C18 at low pH and the XBridge C18 at high pH according to the gradient time.

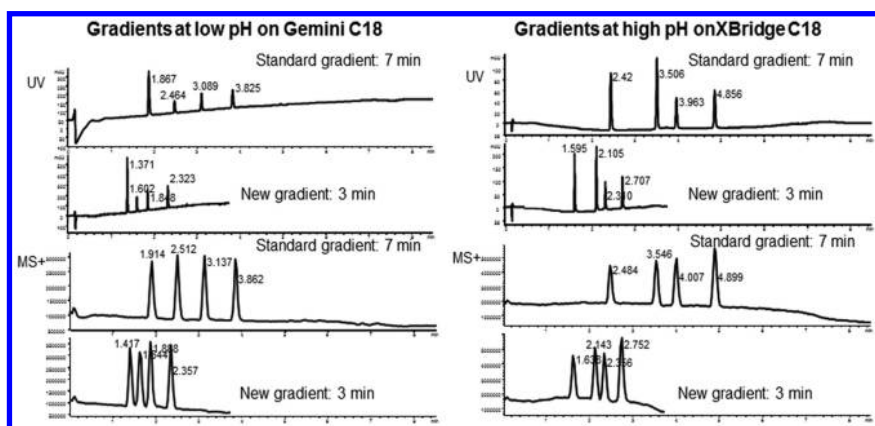


Figure 2. Comparison of the UV and MS response for the standard gradient of 7 min and new gradient of 3 min at low pH on a Gemini C18 column and at high pH on a XBridge C18 column. Elution order at low pH: 1. Propranolol, 2. Verapamil, 3. Terfenadine, 4. Niflumic acid. Elution order at high pH: 1. Niflumic acid, 2. Propranolol, 3. Verapamil, 4. Terfenadine.

An evaluation of the chemical stability of the Gemini and XBridge stationary phases was also performed. In our experience over several years, the tri-functionally bonded C18 ligand of the XBridge BEH C18 sorbent, which can be used in the entire range of mobile phase pH (1-12) and exhibits ultra-low column bleed, showed a good stability during the evaluated time, allowing more than 2000 analyses at high pH and elevated temperature without any loss in efficiency. In contrast, in our hands the Gemini column showed lower stability at low pH, giving a typical life time of 400-700 injections. For this reason, evaluation of modern column technologies such as Gemini NX C18, Kinetex C18 or well-known column chemistries in our laboratories such as XTerra MS C18 or Atlantis dC18, in comparison with Gemini C18 at low pH, was carried out. A summary of the main properties of these columns is described in Table 1.

The Gemini-NX phase is purported to deliver a significant increase in column stability over the original Gemini product, more predictable separations and longer column life, in addition to strong hydrophobic selectivity and high loading capacity. The new phase features advanced TWIN-NX (Two-in-One) technology, which grafts additional silica-organic layers on the surface of the internal base silica. The advanced NX process uses ethane cross-linked groups that resist high pH attacks and multi-point ligand attachments that resist low pH ligand cleavage, to reinforce the silica and extend the performance to a pH range of 1 to 12. The extended pH range allows greater flexibility in mobile phase modifications and more control over retention and selectivity of ionizable compounds (22).

The XTerra MS C18 column is an endcapped, hybrid-based reversed-phase C18 column that provides superior pH stability compared to a silica-based column and is designed to be compatible with mass spectrometry applications (23).

The Atlantis dC18 column is a universal, silica-based, reversed-phase C18 column that is most frequently used for polar compound retention. The Atlantis dC18 column features di-functionally bonded C18 ligands that have been optimized for use with highly aqueous mobile phases, including 100% water. Due to its optimized physical attributes such as endcapping, silica pore size (100Å), bonded phase ligand density and ligand type, this LC-MS compatible column exhibits superior peak shape for all compounds, low pH stability, resistance to dewetting (hydrophobic collapse) and enhanced polar compound retention (23).

Kinetex core-shell column, first introduced in the fall of 2009 have a TMS endcapping phase which offers the hydrophobic retention and methylene selectivity expected from a C18 column. Kinetex core-shell 2.6 µm and 1.7 µm particles (porous shell: 0.35 µm and pressure stability: 600 Bar) were engineered to provide increased efficiencies and improved performance compared to traditional fully porous particles (22).

Due to the above characteristics, these stationary phases have a wide range of applications in drug discovery from analytical method development to purification purposes. A comparison of the peak capacity on these columns with a 3 min gradient time at low pH is presented in Figure 3.

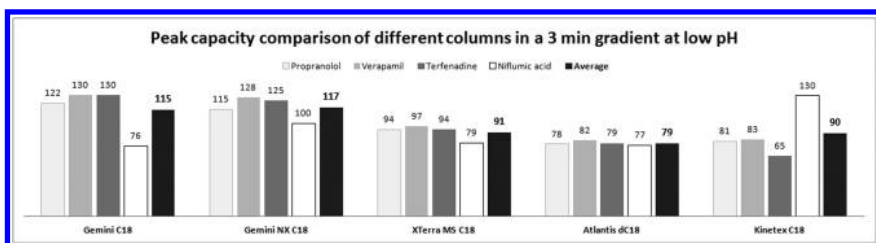


Figure 3. Peak capacity comparison of Gemini C18, Gemini NX C18, XTerra MS C18, Atlantis dC18 and Kinetex C18 in a 3 min gradient at low pH. Average PC in bold.

The results demonstrated that the Gemini NX column exhibited the highest peak capacity (117), with a similar value in comparison with the Gemini (115). However, the column stability was somewhat lower than other phases tested. In contrast, XTerra MS exhibited a medium peak capacity (91) but with a better column life time of more than 5000 injections in routine work without any decrease of peak capacity. The Kinetex showed a similar peak capacity to the XTerra MS (90 and 91 respectively), but with better results for acid compounds than basic compounds. The Atlantis gave the lowest peak capacity, but it was the column that exhibited higher retention times as demonstrated in our overloading comparative study between this column and Gemini NX with 10 different compounds chosen randomly from different projects. The results show no single column offers optimal characteristics for all our criteria. The column that offered the best compromise was chosen (Gemini NX for the OA approach and Atlantis for the high-low approach, both at low pH). In this study, the high-low approach was followed for these 10 research samples. For the high concentration, samples were prepared between 0.9-1.7 mg/mL, 30:70 ACN:H₂O was the preferred option, 50:50 ACN:H₂O, ACN 100% or mixture of ACN:DMSO were used in that order of preference where solubility was an issue. For the diluted samples, a dilution 1:100 was made, using the same solvent. Samples at both concentrations and a blank (prepared with the same solvent mixture) were analysed under identical chromatographic conditions in both Gemini NX and Atlantis using 4 min gradients (from 5 to 100%B in 4 min, holding at 100%B for 0.5 min) with an injection volume of 15 µL as default, with the exception of sample 7 in which one of the impurities presented a UV signal higher than 1000 mAU and this was repeated with 4 µL of injection volume. A summary of this study is presented in Table 2.

Table 2. Comparative Study on the Gemini NX C18 and Atlantis dC18 Columns Using the High-Low Approach for the Determination of %TRS (Calculated Following Equation 1)

Sample	Conc (mg/mL)	Solvent	Injec. Vol (uL)	Ret. Time (min) Gemini C18	Ret. Time (min) Atlantis dC18	% TRS Low pH (Gemini C18)	% TRS Low pH (Atlantis dC18)	UV λ (nm)
1	1.70	30:70 ACN:H ₂ O	15	Solvent front	1.500	NC	15.72	222
2	1.50	30:70 ACN:H ₂ O	15	Solvent front	1.322	NC	4.79	220
3	1.21	50:50 ACN:H ₂ O	15	Solvent front	2.122	NC	3.06	220
4	0.94	83:17 ACN:DMSO	15	2.063	2.132	2.66	3.83 (peak with fronting)	224
5	1.07	50:50 ACN:H ₂ O	15	2.106	2.215	0.08	0.06	212
6	1.40	50:50 ACN:H ₂ O	15	2.05	2.17	0	0	294
7	1.07	50:50 ACN:H ₂ O	4	2.492	2.574	6.88	5.6	246
8	1.07	30:70 ACN:H ₂ O	15	Solvent front	1,519	NC	1.6	220
9	1.00	100% ACN	15	2.358	2.471	1.32	1.13	224
10	1.60	30:70 ACN:H ₂ O	15	2.693	2.803	1.46	0.8	220

*NC: Value not calculated due to part of the compound eluted with the solvent front.

Notes: 1) retention times refer to the retention of the parent. 2) UV λ refers to the wavelength corresponding to the maximum in the UV spectrum with the highest intensity.

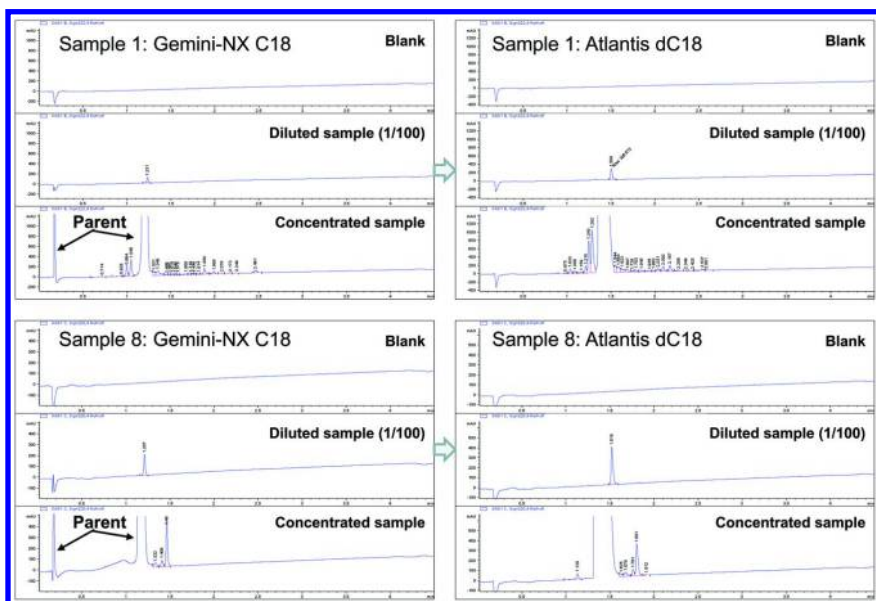


Figure 4. Comparison of the study with Gemini NX C18 and Atlantis dC18 columns of the pre-clinical candidates with the high-low approach methodology. Identical chromatographic conditions in both columns using 4 min gradient time (from 5 to 100%B in 4 min holding at 100%B for 0.5 min. A:H₂O-0.1% FA and B:ACN-0.1% FA) and injecting 15 uL as default.

Interestingly, the Gemini NX column displayed poor retention for four of the ten basic compounds (samples 1, 2, 3 and 8), showing partial elution at the start of the chromatogram (sample solvent mismatch effect) when samples at high concentration were tested (not observed in diluted samples) as illustrated in Figure 4. On the contrary, all the compounds including the most polar analytes (samples 1, 2, 3 and 8) showed good retention on the Atlantis with excellent chromatography performance at high concentration (see Figure 4). This data was of paramount importance for the selection of the column for the high-low approach. Thus, the Atlantis was chosen as the first option for the TRS screening, operated and managed by experts. However, the percentage of total related substances (%TRS) values of the Atlantis were significantly lower than in the Gemini NX column with the exception of sample 4, in which the fronting of the target compound peak, observed in Atlantis, could be the cause of an incorrect quantification. This fact can be understood by comparing the large differences in peak capacities of both columns (117 for Gemini NX and 79 for Atlantis). This meant that a number of impurities co-eluting in the Atlantis could not be resolved. To counteract the low peak capacity of this column, longer gradient times were tested (see Figure 5A). In terms of resolution and time, an 8 min gradient with a peak capacity of 115 was considered optimum. With this gradient, quantification of the related substances was possible without issue.

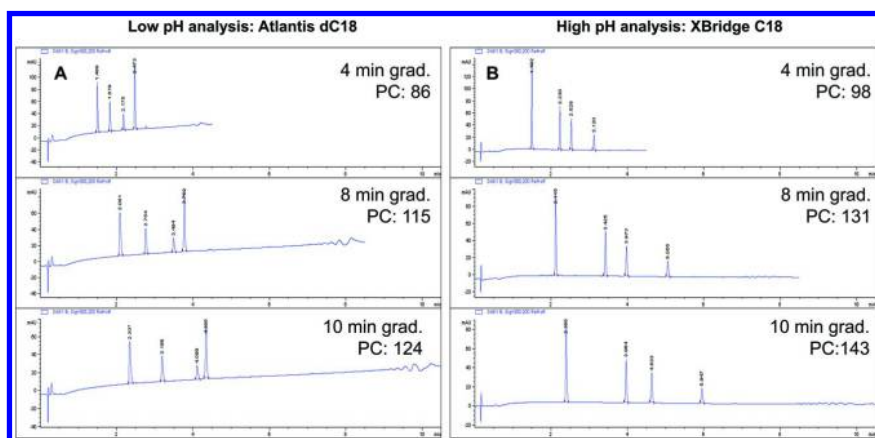


Figure 5. Comparison of gradients of 4, 8 and 10 min on an Atlantis dC18 column for low pH (5A) and on a XBridge C18 column for high pH (5B). Elution order at low pH: 1. Propranolol, 2. Verapamil, 3. Terfenadine, 4. Niflumic acid. Elution order at high pH: 1. Niflumic acid, 2. Propranolol, 3. Verapamil, 4. Terfenadine.

At high pH, comparison of the XBridge and the Gemini NX columns was carried out in terms of peak capacity for a 3 min gradient. Figure 6 showed that both columns gave similar results (80 and 87, respectively). The XBridge was chosen based on the results of column stability with high pH mobile phases. Thus,

two gradients were defined: 3 min gradient for standard open access analysis with a peak capacity of 80 and an 8 min gradient for the analysis of the pre-clinical candidates with a peak capacity of 131, after comparison with gradients of 4, 8 and 10 min (see figure 5B).

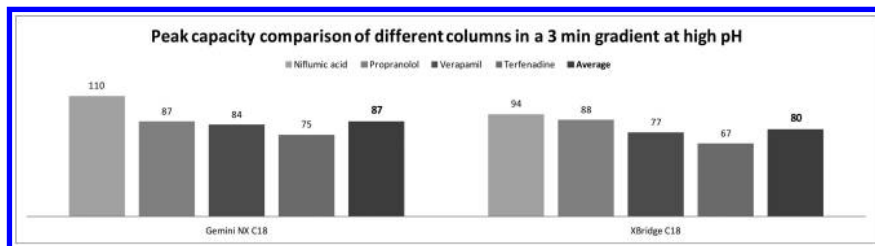


Figure 6. Peak capacity comparison of Gemini NX C18 and XBridge C18 in a 3 min gradient at high pH. Average PC in bold.

Variability in the Methods and Procedures for Purity Assessment

Once the purity assessment (3 min gradients on the Gemini NX and XBridge columns) and TRS methods (8 min gradients on the Atlantis and XBridge columns) were put into practice, the next step was to optimise and standardise the parameters related to the analytical method and analytical procedure. Other factors to minimise the analysis' variability were also considered.

The following points were found to be critical:

- Related to the analytical method:
 - o Selection of the wavelength
 - o Integration parameters
- Related to the analytical procedure:
 - o Solvent for sample preparation
 - o Sample concentration
- Other considerations:
 - o Homogeneity
 - o Stability

Optimization of Analytical Method: Selection of the UV Wavelength

Diode array detectors (DAD) are one the simplest analytical tools of preference for pharmaceutical compound quantification. These highly sensitive detectors monitor the response of eluting compounds across the UV and visible spectrum, and provide both a sensitive and linear response, and qualitative information regarding the UV-vis chromophore of analytes.

For LC-DAD-MS open access analysis it was critical to choose a standard UV wavelength in order to give a percentage of purity based on the area percent approach. In our laboratories, 214 nm was established as a standard wavelength for our 3 min gradients at low and high pH, since most of the drug discovery compounds present a good response at this low wavelength. This procedure presents some limitations such as the linearity over a wide range of concentrations. Overly diluted samples can lead to an over-estimation of purity due to small peaks not being detected. Conversely, overly concentrated samples may give an under-estimated purity due to the main peak being outside the linear range. It was found that the height of the maximum peak at 214 nm should be between 400 and 1200 mAU to avoid these issues. If the height of the maximum peak is lower than 400 mAU, the LC-MS analyses should be repeated with a more concentrated sample or more diluted if the height is higher than 1200 mAU.

For LC-DAD-MS related substances analysis using the high-low approach (19), overcame the limitation of the linear range. This procedure was used to improve the detectability of trace impurities. Enhanced chemical detectability was achieved by comparing the detector response of trace-impurity peaks from a concentrated sample solution with the detector response for the peak in a quantitatively diluted sample solution. Since the HPLC method relies on the assumptions that impurities have a UV response that is similar to the main component at that wavelength, a previous study of the UV spectrum is required. Wavelengths have to be selected to analyze each compound at its highest sensitivity. The optimum wavelength of detection is the λ_{\max} that gives the highest sensitivity, resulting in the largest %TRS in order to over estimate impurity levels. This typically occurs at the lower wavelength.

To evaluate the wavelength influence in the TRS results, the same 10 previous compounds chosen randomly from different projects were used. %TRS were calculated at low and high pH at the maximum UV wavelength ($\lambda_{\max 1}$) and at the second maximum UV wavelength ($\lambda_{\max 2}$) for those compounds that presented more than one. Figure 7 shows the UV spectrum of some of these compounds at low and high pH and the $\lambda_{\max 1}$ chosen in each case. Results in Table 3 clearly showed that using the UV wavelength with the high intensity ($\lambda_{\max 1}$) (for example samples 2, 3 and 9 at low pH or samples 9 and 10 at high pH), gave a %TRS higher than at $\lambda_{\max 2}$, although in other cases similar results were obtained (for example samples 1, 2 or 5 at high pH). Because of this, it was evident that running open access LC-DAD-MS analysis at low and high pH to choose the $\lambda_{\max 1}$ for which the sample concentration is in the linear range was an important step prior to TRS analysis.

Table 3. Percentages of TRS at Low and High pH at the Maximum UV Wavelength ($\lambda_{\max 1}$) and at the 2nd Maximum UV Wavelength ($\lambda_{\max 2}$) for Those Compounds with More than One

<i>Sample</i>	<i>UV λ_{\max} Low pH</i>	<i>% TRS Low pH</i>	<i>UV λ_{\max} High pH</i>	<i>% TRS at high pH</i>
1	$\lambda_{\max 1}$ 218±4	Sig=222,4: 15.72	$\lambda_{\max 1}$ 236±4 $\lambda_{\max 2}$ 318±4	Sig=236,4: 11.23 Sig=318,4: 11.12
2	$\lambda_{\max 1}$ 218±4 $\lambda_{\max 2}$ 254±4	Sig=220,4: 4.79 Sig=258,4: 2.03	$\lambda_{\max 1}$ 250±4 $\lambda_{\max 2}$ 220±4	Sig=250,4: 5.77 Sig=220,4: 5.79
3	$\lambda_{\max 1}$ 226±4 $\lambda_{\max 2}$ 258±4	Sig=226,4: 3.19 Sig=258,4: 1.79	$\lambda_{\max 1}$ 258±4	Sig=258,4: 2.09
4	$\lambda_{\max 1}$ 228±4	Sig=224,4: 3.83	$\lambda_{\max 1}$ 224±4	Sig=224,4: 4.87
5	$\lambda_{\max 1}$ 214±4 $\lambda_{\max 2}$ 248±4	Sig=248,4: 0 Sig=212,4: 0.06	$\lambda_{\max 1}$ 248±4 $\lambda_{\max 2}$ 212±4	Sig=248,4: 0 Sig=212,4: 0.07
6	$\lambda_{\max 1}$ 294±4	Sig=294,4: 0	$\lambda_{\max 1}$ 294±4	Sig=294,4: 0
7	$\lambda_{\max 1}$ 248±4	Sig=246,4: 5.6	$\lambda_{\max 2}$ 248±4	Sig=246,4: 7.23
8	$\lambda_{\max 1}$ 218±4 $\lambda_{\max 2}$ 290±4	Sig=220,4: 1.6 Sig=290,4: 1.54	$\lambda_{\max 1}$ 290±4	Sig=290,4: 1.64
9	$\lambda_{\max 1}$ 224±4 $\lambda_{\max 2}$ 282±4	Sig=224,4: 1.13 Sig=282,4: 0.49	$\lambda_{\max 1}$ 232±4 $\lambda_{\max 2}$ 282±4	Sig=232,4: 1.11 Sig=282,4: 0.72
10	$\lambda_{\max 1}$ 222±4	Sig=220,4: 0.8	$\lambda_{\max 1}$ 210±4 $\lambda_{\max 2}$ 258±4	Sig=210,4: 1.77 Sig=258,4: 1.33

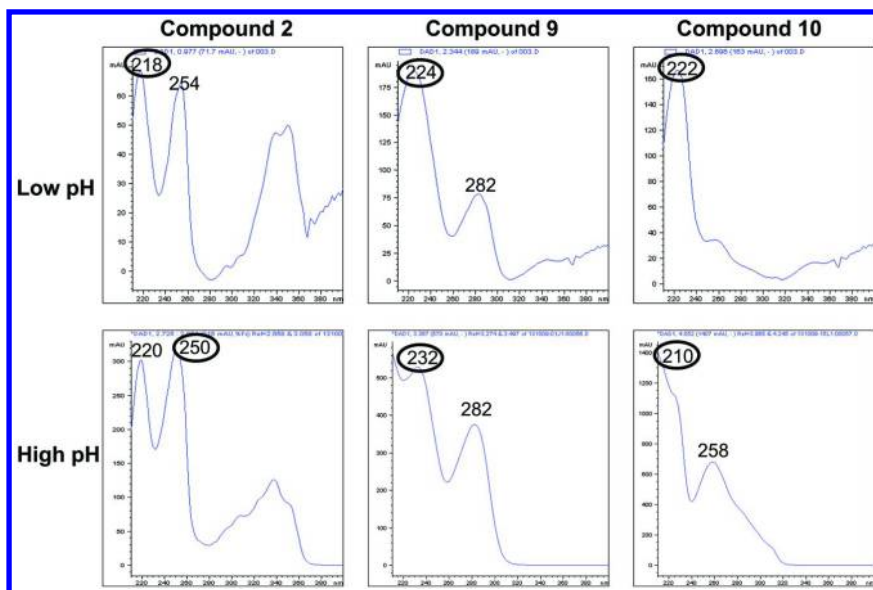


Figure 7. UV spectrum and λ_{max1} chosen for compounds 2, 9 and 10 at low and high pH.

Optimization of the Analytical Method: Integration Parameters

Little attention is typically paid to integration parameters in method development but they can have an important influence on results (24). For example a small change to a parameter such as threshold can result in a disproportionate change in integral values. This can mean that two experiments undergoing the same procedure but processed with different integration parameters may give widely different results. Such changes are exacerbated for small peaks, and could easily result in a change from a pass to a fail based on some purity specification. This was tested with an internal experiment in which 3 samples were analysed in three different laboratories and results were re-analysed by all laboratories following their own criteria (data not shown).

After observing some discrepancies in the final data, an evaluation of the acquired raw data through mathematical integration was carried out. The integration algorithms identify peaks which are characterized by position on the time scale, height, area, width at half-height, symmetry, etc. The integration sensitivity can be adjusted by three integration parameters: threshold (slope), area/height rejects and peak width. Having this in mind, the parameters listed in Table 4 were globally defined in order that all analysts followed the same criteria, by integrating at the base line.

Table 4. Integration Parameters

<i>Integration parameter</i>	<i>Value</i>
Slope sensitivity	60
Peak width	0.005
Area reject	15
Height reject	5

Figure 8 illustrates how the above integration parameters in conjunction with the longer 8 min method are particularly important for obtaining accurate results.

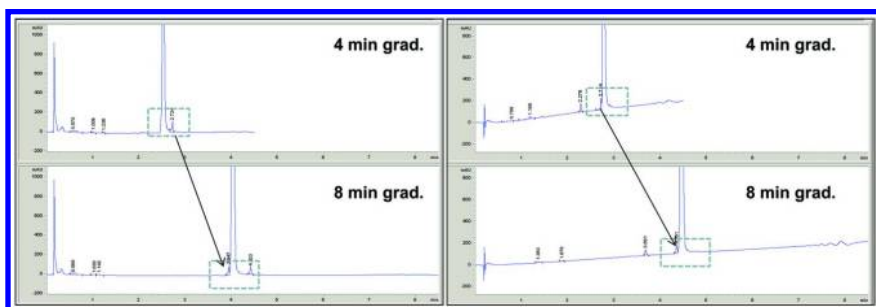


Figure 8. Importance of 8 min gradient for TRS, instead of 4 min gradients.

Optimization of Analytical Procedure: Solvent and Sample Concentration

As a general rule, the sample should be dissolved in the eluent to be used (HPLC mobile phase). The sample solvent must be no stronger than the mobile phase. Making an injection in a stronger solvent causes the sample band to spread out rapidly as it starts migrating down the column. However, it is equally important that the sample must be soluble in an eluent to avoid precipitation problems and the sample solvent must be totally and rapidly miscible with the eluent. Taking into account these general rules, the following sample solvents and concentrations were established:

Standard Open Access Analysis

For our 3 min gradients with water-acetonitrile as mobile phases, a mixture of 80:20 ACN:H₂O was chosen as the first option to prepare the samples for purity assessment. If solubility was a problem, other solvents such as 100% acetonitrile, 100% MeOH or the addition of small traces of DMSO were used as a second choice. Sample concentration was typically between 0.5-0.7 mg/mL to ensure the UV response of the compounds was between 400-1200 mAU.

In the high-low approach or high-low chromatography, described as an HPLC sampling procedure used to improve the detection limits of trace components (19), samples were prepared at two concentrations. For the concentrated sample, 1.5 mg \pm 0.1 was weighed. This was dissolved in 300 μ L ACN. The sample was sonicated and finally, 700 μ L water added to obtain a 1.5 mg/mL solution in a mixture of ACN:H₂O 30:70. Although, compounds can be dissolved in the salt form with high percentages of water, at least 30% acetonitrile is necessary to ensure total solubility. The influence of the percentage of acetonitrile in the sample preparation as well as the wavelength selection for a sample as the salt form in the percentage of TRS is shown in Table 5. In case of solubility problems, the percentage of acetonitrile can be increased from 30% to 50% or the sample can be prepared in pure acetonitrile, pure methanol or mixture of acetonitrile-DMSO or pure DMSO as last option. For the diluted sample: 100 μ L of the concentrated sample are made up to 10 mL in a volumetric flask with the same solvent or mixtures of solvents used for the preparation of the concentrated sample. A blank with the same solvent or mixtures of solvents used for the preparation of the concentrated and diluted samples is required.

Table 5. Influence of the Acetonitrile Percentage in the Sample Preparation as Well as the Wavelength Selection for a Sample as the Salt Form in the Percentage of TRS

<i>Sample Preparation</i>	<i>Injec. Vol (uL)</i>	<i>Lambda (nm)</i>	<i>% TRS</i>
1.6 mg/mL 30:70 ACN:H ₂ O	15	1st maximun: 224 nm	4.09
1.6 mg/mL 100 % H ₂ O	15	1st maximun: 224 nm	2.5
1.6 mg/mL 30:70 ACN:H ₂ O	15	2nd maximun: 300 nm	2.31
1.6 mg/mL 100 % H ₂ O	15	2nd maximun: 300 nm	1.5

Other Considerations

Other important considerations to deliver comparable results between different laboratories were the homogeneity and the stability of the sample. Obviously, a specific quantity of material produced in a process or series of processes should be homogeneous within specified limits. Unfortunately, this is not always true and can cause variability in the results depending of the selected fraction or batch. For this reason, it is critical to use homogeneous samples to investigate the precision of the method. On the other hand, the stability of the sample must be tested if it is possible that measurements are susceptible to variations due to the analytical method and/or procedure. For example, if a

compound is not stable in solution or can be degraded with the mobile phase pH, the final results may not be consistent (25). Overlaid chromatograms on Figure 9 show the TRS analysis of 3 different fractions of an inhomogeneous sample.

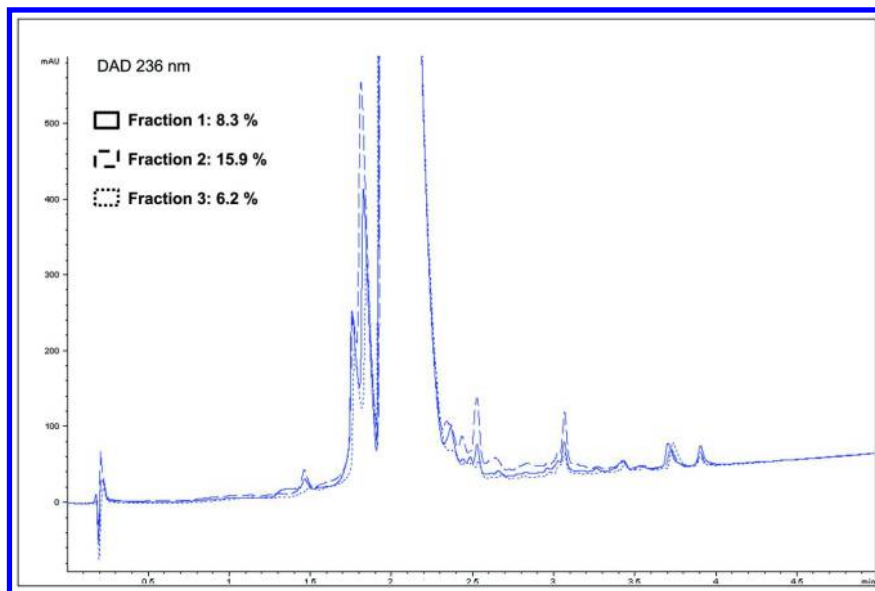


Figure 9. Analysis of 3 different fractions of an inhomogeneous sample.

Global Validation

For open access analysis, due to the high volume of samples analysed, and the numbers of users and instruments in different sites, a globally defined automatic suitability test to check the performance of the columns and systems was established. The previously described test mix containing 4 drug compounds was analysed weekly (5 consecutive injections) for each of the methods at low and high pH. Parameters such as symmetry, tailing and peak capacity were monitored. The same protocol was also applied before running a TRS analysis to check the performance of the LC-MS systems as a whole.

The purity assessment of pre-clinical candidates for in vivo studies can be affected by low level impurities through a number of mechanisms (potential teratogenic, mutagenic or carcinogenic effects) (26). As such accurate and reproducible assessment of impurity levels is paramount, we therefore carried out a global validation pilot study for the TRS test. Three samples known to be stable and homogeneous were chosen for this study to remove these sources of variation. All samples were analysed in duplicate using the previously defined procedures and shipped to the other laboratories to repeat the same procedure. The results of this study are summarized in Table 6. For the %TRS calculations, RS with a percentage below <0.05% were not included because of according to ICH Q3A (R2) (27), reporting threshold is > 0.05%.

Table 6. Results of the TRS at Low and High pH in the 3 Laboratories as Well as the Sample Concentration, Solvent and UV Wavelength Selected and the Injection Volume

Sample	Site	Sample	Weight (mg)	Total Vol. (mL)	Conc (mg/mL)	Solvent	Injec. Vol (uL)	Lambda AC	Lambda BA	% TRS low pH:	% TRS high pH:	% TRS low pH		% TRS high pH		
												Average (n=2)	SD	Average (n=2)	SD	
A	LAB 1	1	1.4	1.4	1.00	50:50 ACN:H2O	15	248±4	248±4	1.75	1.84	1.67	0.11	1.78	0.08	
		2	1.4	1.4	1.00	50:50 ACN:H2O	15	248±4	248±4	1.59	1.72					
	LAB 2	1	1.68	1.12	1.50	30:70 ACN:H2O	15	248±4	248±4	1.42	1.51	1.47	0.07	1.61	0.13	
		2	1.65	1.1	1.50	30:70 ACN:H2O	15	248±4	248±4	1.52	1.7					
	LAB 3	1	1.24	1	1.24	30:70 ACN:H2O	15	248±4	248±4	1.38	1.47	1.41	0.04	1.52	0.07	
		2	1.25	1	1.25	30:70 ACN:H2O	15	248±4	248±4	1.43	1.57					
	Average												1.52	0.14	1.64	0.14
	B	LAB 1	1	1.4	1.4	1.00	50:50 ACN:H2O	15	266±4	266±4	3.59	4.53	3.61	0.02	4.46	0.11
			2	1.5	1.4	1.07	50:50 ACN:H2O	15	266±4	266±4	3.62	4.38				
		LAB 2	1	1.59	1.06	1.50	30:70 ACN:H2O	15	266±4	266±4	3.90	3.89	4.10	0.28	3.99	0.13
2			1.56	1.04	1.50	30:70 ACN:H2O	15	266±4	266±4	4.29	4.08					
LAB 3		1	2.6	1.5	1.73	30:70 ACN:H2O	15	266±4	266±4	3.41	3.31	3.39	0.03	3.54	0.33	
		2	2.5	1.5	1.67	30:70 ACN:H2O	15	266±4	266±4	3.37	3.77					
Average												3.70	0.35	3.99	0.44	
C		LAB 1	1	1.6	1	1.60	30:70 ACN:H2O	15	218±4	214±4	0.16	0.16	0.16	0.00	0.16	0.00
			2	1.6	1	1.60	30:70 ACN:H2O	15	218±4	214±4	0.16	0.16				
		LAB 2	1	1.57	1.05	1.50	30:70 ACN:H2O	5, 15	218±4	214±4	0.13	0.18	0.13	0.01	0.20	0.02
	2		1.5	1	1.50	30:70 ACN:H2O	5, 15	218±4	214±4	0.12	0.21					
	LAB 3	1	2.4	1.5	1.60	30:70 ACN:H2O	15	218±4	214±4	0.24	0.12	0.21	0.04	0.12	0.01	
		2	2.3	1.5	1.53	30:70 ACN:H2O	15	218±4	214±4	0.18	0.11					
	Average												0.17	0.04	0.16	0.04

The good correlation and consistency of the 3 laboratories data showed the ability to reproduce the optimized analytical methods and procedures.

Error Estimation

The final objective of this work was to define the errors for the related substances determination test, taking into account the data generated in the global pilot. The error was defined as $SD * t_{Student} (n-1) / n^{1/2}$ where SD is the standard deviation, t is the $t_{Student}$ for n-1 degrees of freedom and 95% of confidence interval and n is the number of replicates (28).

Table 7. Estimation of the Error or Confidence Interval as a Function of the Total RS %

<i>For Total RS %</i>	<i>Error</i>
0.2	0.05
0.5	0.09
1.0	0.16
1.5	0.23
2.0	0.30
2.5	0.38
3.0	0.45
3.5	0.52
4.0	0.59
4.5	0.66
5.0	0.73

Table 8. Estimation of the Error or Confidence Interval as a Function of the Specific RS %

<i>For Total RS %</i>	<i>Error</i>
<0.2	0.11
$\geq 0.2 - < 0.5$	0.28

The errors estimated for both total related substances and individual related impurities were calculated from the experimental values (n = 6). Tables 7 and 8 show how the error varies for total related substances and individual compounds.

Quality Control of Bioactive Compounds from Natural Sources

It is well known that natural products (i.e. bioactive secondary metabolites from microbial, plant and marine sources) have been a very productive source of leads for the development of new drugs (29). In recent decades, medicinal plant materials and herbal drugs have gained popularity to prevent or treat illness or to act as dietary supplements. Standardization and quality control of herbal medicines is clearly of paramount importance, a fact that is recognised by the World Health Assembly who have discussed the need for using modern analytical techniques and applying suitable standards to ensure the quality of medicinal plant products (30). In this context, LC-MS plays a crucial role for routine analysis of bioactive substances. LC-MS is important for the characterization of unknown impurities and for the quantification of the target analytes. For instance, Tang, et al. described the use of LC-MS-QTOF for the quantitative and qualitative analysis of flavonoids in leaves and roots of *Scutellaria baicalensis* by enhancing UV-B radiation (31). More recently, a LC-UV tandem mass spectrometry (LC-MS/MS) method for the determination of six flavonoids in a dietary supplement plant Citre Reticulatae Pericarpium (CRP) was developed and validated by Liu et al. The authors claimed that this LC-MS/MS method in combination with hierarchical cluster analysis might be used as a quality control method for CRP (32). Without a doubt the advances in analytical tools, combined with multivariate data analysis is paying a pivotal role in the standardization and quality control of herbal products (33).

The analytical methods for natural products analysis typically comprise two stages: extraction and purification of the analytes from the matrix and the chromatography separation method for the detection/identification of the target analytes. Due to the complexity of natural products matrixes, the development of orthogonal separation methods is an essential part in this process. A case in point is the hyphenation of solid phase extraction (SPE) and LC-MS for the isolation of hydrophilic bioactive metabolites in a short timeframe by Espada et al (34). The described simple, fast and low cost approach was found to be highly reproducible and was successfully applied to different type of metabolites. Bearing in mind the wide diversity of analytes present in an organic extract (microbe, plant or marine source) the use of LC-MS base methods with orthogonal stationary and mobile phases will increase the quality of the bioactive substance. A methodology illustrating the advantage of running orthogonal LC-MS methods to confirm the purity and quality of natural bioactive sample was described by our group (35). In this example, a single peak exhibiting a purity level of >97% was detected by reversed-phase LC-MS. However, analysis under hydrophilic interaction LC-MS revealed the presence of two peaks with a 4:6 purity ratio in the same sample. Orthogonal LC-MS analysis allowed assigning the correct purity level as well as the detection and identification of impurities in bioactive products.

The LC-MS methods and analytical procedures described in this chapter for synthetic compounds might therefore be successfully implemented and applied in the field of bioactive compounds from natural sources, providing an appropriate level of analysis for the stage of development of such products.

Conclusions

Delivering reproducible and consistent data in pharmaceutical laboratories has typically been a long, labour-intensive task involving medicinal chemists, analytical scientists, knowledge-base and LC-MS instrument performance. In order to ensure the quality of drug discovery compounds in an efficient way, we have standardized and implemented LC-MS methods and analytical procedures according to drug discovery stage across global research sites. Sample preparation, optimum chromatography separation and resolution, data analysis and interpretation, and LC-MS system suitability tests were the key parameters evaluated and standardized in this study. A compromise between optimum resolution power and analysis time has been reached resulting in the standardization of new and short generic LC-MS methods (3 min gradients) for routine purity assessment in an open access environment. Finally, analytical methods and procedures to deal with TRS analysis were systematically validated and implemented. Global protocols were put in place and are currently being used in our discovery research laboratories. We have largely discussed the analysis of synthetic pharmaceutical compounds, but the methodologies presented could be straightforwardly implemented for the quality control of bioactive compounds from natural sources as briefly discussed in the last section of this chapter.

References

1. Argentine, M. D.; Owens, P. K.; Olsen, B. A. Strategies for the investigation and control of process-related impurities in drug substances. *Adv. Drug Delivery Rev.* **2007**, *59* (1), 12–28.
2. Kassel, D. B. The spanning role of HPLC in drug discovery. In *HPLC for Pharmaceutical Scientists. Part 2: HPLC in the Pharmaceutical Industry*; Kazakevich, Y., LoBrutto, R., Eds.; Wiley-Interscience: New York, 2007, pp 535–576.
3. Molina-Martín, M.; Marín, A.; Rivera-Sagredo, A.; Espada, A. Liquid chromatography-mass spectrometry and related techniques for purity assessment in early drug discovery. *J. Sep. Sci.* **2005**, *28*, 1742–1750.
4. Koh, H. L.; Yau, W. P.; Ong, P. S.; Hegde, A. Current trends in modern pharmaceutical analysis for drug discovery. *Drug Discovery Today* **2003**, *8* (19), 889–897.
5. Sweedler, J. V. The continued evolution of hyphenated instruments. *Anal. Bioanal. Chem.* **2002**, *373*, 321–322.
6. Singh, S.; Handa, T.; Narayanam, M.; Sahu, A.; Junwal, M.; Shah, R. P. A critical review on the use of modern sophisticated hyphenated tools in the characterization of impurities and degradation products. *J. Pharm. Biomed. Anal.* **2012**, *69*, 148–173.
7. Zhao, J.; Zhang, L.; Yang, B. In *Analysis and Purification Methods in Combinatorial Chemistry*; Yang, B., Ed.; Wiley & Sons, New Jersey, 2004; pp 225–280.
8. Shi, Y.; Xiang, R.; Horvath, C.; Wilkins, J. A. The role of liquid chromatography in proteomics. *J. Chromatogr. A* **2004**, *1053*, 27–36.

9. Korfmacher, W. A. Foundation review: Principles and applications of LC-MS in new drug discovery. *Drug Discovery Today* **2005**, *10* (20), 1357–1367.
10. Lim, C. K.; Lord, G. Current developments in LC-MS for pharmaceutical analysis. *Biol. Pharm. Bull.* **2002**, *25*, 547–557.
11. Biswas, K. M.; Olsen, B. A.; Risley, D. S.; Skibic, M. J.; Wright, P. B. A simple and efficient approach to reversed-phase HPLC method screening. *J. Pharm. Biomed. Anal.* **2009**, *49* (3), 692–701.
12. Marín, A.; Byrne, C.; Goodwin, L.; White, C.; Sharman, G.; Burton, K.; Rivera-Sagredo, A.; Espada, A. Optimization and Standardization of Liquid Chromatography-Mass Spectrometry Systems for the Analysis of Drug Discovery Compounds. *J. Liq. Chromatogr. Relat. Technol.* **2008**, *31*, 2–22.
13. Wiberg, K.; Andersson, M.; Hagman, A.; Jacobsson, S. P. Peak purity determination with principal component analysis of high-performance liquid chromatography–diode array detection data. *J. Chromatogr. A* **2004**, *1029* (1-2), 13–20.
14. Wadekar, K. R.; Bhalme, M.; Rao, S. S.; Reddy, K. V.; Kumar, L. S.; Balasubrahmanyam, E. Evaluating impurities in Drugs- Part I. *Pharm. Technol. Eur.* **2012**, *24* (2).
15. Wadekar, K. R.; Ravi, P.; Bhalme, M.; Rao, S. S.; Reddy, K. V.; Kumar, L. S.; Balasubrahmanyam, E. Evaluating impurities in Drugs- Part III. *Pharm. Technol. Eur.* **2012**, *24* (4).
16. Lee, Y. C. Method validation for HPLC analysis of related substances in pharmaceutical drugs products. In *Analytical Method Validation and Instrument Performance Verification*; Chan, C. C., Lam, H., Lee, Y. C., Zhan X. M., Ed.; Wiley-InterScience: New York, 2004; pp 27–50.
17. Deng, G.; Sanyal, G. Applications of mass spectrometry in early stages of target based drug discovery. *J. Pharm. Biomed. Anal.* **2006**, *40*, 528–538.
18. Espada, A.; Molina-Martin, M.; Dage, J.; Kuo, M. S. Application of LC/MS and related techniques to high-throughput drug discovery. *Drug Discovery Today* **2008**, *13* (9-10), 417–423.
19. Inman, E. L.; Tenbarge, H. J. High-Low Chromatography: Estimating Impurities in HPLC Using a Pair of Sample Injections. *J. Chromatogr. Sci.* **1988**, *26* (3), 89–94.
20. pKa and log P values calculated using the ACD Labs programs.
21. Neue, U. D. Theory of peak capacity in gradient elution. *J. Chromatogr. A* **2005**, *1079* (1–2), 153–161.
22. Phenomenex Home Page. <http://www.phenomenex.com> (accessed June 2012).
23. Waters Home Page. <http://www.waters.com> (accessed June 2012).
24. Grize, Y. L.; Schmidli, H.; Born, J. Effect of integration parameters on high-performance liquid chromatographic method development and validation. *J. Chromatogr. A* **1994**, *686* (1), 1–10.
25. Jedynek, Ł.; Puchalska, M.; Zezula, M.; Łaszcz, M.; Łuniewski, W.; Zagrodzka, J. Stability of sample solution as a crucial point during HPLC determination of chemical purity of temozolomide drug substance. *J. Pharm. Biomed. Anal.* **2013**, *83*, 19–27.

26. Wadekar, K. R.; Bhalme, M.; Rao, S. S.; Reddy, K. V.; Kumar, L. S.; Balasubrahmanyam, E.; Ravi, P. Evaluating impurities in Drugs- Part II. *Pharm. Technol. Eur.* **2012**, *24* (3).
27. ICH Q3A (R2): *Impurities in new Drug Substances* (October 2006).
28. Box, G. E.; Hunter, W. G.; Hunter, J. S. *Statistic for Experimenters. Design, Innovation and Discovery*, 2nd ed.; John Wiley: New York, 2005.
29. Li, J. W.-H.; Vederas, J. C. Drug discovery and natural products: end or an era or an endless frontier? *Science*. **2009**, *325* (5937), 161–165.
30. Shinde, V. M.; Dhalwal, K.; Potdar, M.; Mahadik, K. R. Application of quality control principles to herbal drugs. *Int. J. Phytomed.* **2009**, *1* (1), 4–8.
31. Tang, W. T.; Fang, M-F.; Liu, X.; Yue, M. Simultaneous quantitative and qualitative analysis of flavonoids from ultraviolet-B radiation in leaves and roots of *Scutellaria baicalensis*. *J. Anal. Methods Chem.* **2014**, *2014*, 1–9.
32. Liu, E-H.; Zhao, P.; Duan, L.; Zheng, G-D.; Guo, L.; Yang, H.; Li, P. Simultaneous determination of six bioactive flavonoids in Citri Reticulatae Pericarpium by rapid resolution liquid chromatography coupled with triple quadrupole electrospray tandem mass spectrometry. *Food Chem.* **2013**, *141* (4), 3977–3983.
33. van der Kooy, F.; Maltese, F.; Choi, Y. H.; Kim, H. K.; Verpoorte, R. Quality control of herbal material and phytopharmaceuticals with MS and NMR based metabolic fingerprinting. *Planta Med.* **2009**, *75* (07), 763–775.
34. Espada, A.; Anta, C.; Bragado, A.; Rodriguez, J.; Jimenez, C. An approach to speed up the isolation of hydrophilic metabolites from natural sources at semipreparative level by using hydrophilic-liphophobic balanced/mixed mode strong cation exchange-high performance liquid chromatography/mass spectrometry system. *J. Chromatogr. A* **2011**, *1218* (13), 1790–1794.
35. Espada, A.; Stregge, M. Hydrophilic interaction chromatography (HILIC) for drug discovery. In *Hydrophilic Interaction Chromatography a Guide for Practitioners*; Olsen, B. A., Pack, B. W., Eds.; Wiley: New York, 2013; pp 169–193.

Chapter 7

Biofunctional Properties of *Melia azedarach* Extracts

N. G. Ntalli* and P. Caboni

Department of Life and Environmental Sciences, University of Cagliari,
Via Ospedale 72, 09124 Cagliari, Italy

*E-mail: nntali@agro.auth.gr.

Melia azedarach is a botanical species on the focus of global research for its biological properties. It is usually used for its timber as well as a shade tree. This deciduous tree is a Meliaceae species that, unlike *Azadirachta indica*, adapts in various tropical and warm temperate regions around the world and has thus gradually gained scientific interest. The secondary metabolites it contains exhibit various biological properties, belong to different chemical categories and can be extracted from various plants parts. The appliance of such knowledge is of interest in medicine and agriculture, while analytical methods and extraction procedures serve as tools for identification and quantification of similar substances in other complex botanical matrixes. To date the discovery of novel alternative methods for diseases and pest control are mandatory, due to resistance problems and toxicity management to non target organisms.

Introduction

Melia azedarach L. (Sapindales: Meliaceae) is indigenous in India where for the natives has been known for quite long time, and has been used as a good source of folk medications. To date many scientists around the world have focused their research on *M. azedarach* for its promising properties of interest to agriculture and medicine (1, 2). As continue of our last report on the biological activity of *M. azedarach*, herein we review the bibliography reported since 2010.

We finally make a short report on the different chemical groups of *M. azedarach* bioactive substances, together with the extraction methods and identification analytical procedures.

M. azedarach also known as Alanzalaket, Alsabahebah, Chinaberry, Paraiso and Persian lilac, has long been recognized for its insecticidal properties (3). *M. azedarach* is native in Asia but it is naturalised in most of the tropics and subtropics such as Australia, and southern China. It has been introduced in the United States, Brazil, Argentina and Africa, because of its considerable climatic tolerance (3) and in the recent years gains much interest for its biological properties. Together with *Azadirachta indica* it belongs to the Meliaceae family which is famous due to the high contents in limonoids, rich in biological properties (4). *M. azedarach* is used for medicinal (5), ornamental and timber purposes (6) and it affords many different and biologically interesting secondary metabolites such as limonoids, triterpenoids, sterioids, flavonoid glycosides and simple phenolics.

Medicinal Uses/Controlling Diseases

Unfortunately the traditional knowledge involving medicinal plants to treat diseases, used for thousands of years in various parts of the world, is in danger of being lost because it is documented only to a limited extent (7). At the same time there are potentially many important pharmaceutical applications of plants to be exploited since to date approximately only 10,000 species have been studied for medicinal use (8), out of the 420,000 total species that exist in nature (9).

Plant derived natural compounds play an important role in anticancer drug therapy and may thus be promising lead compounds for developing effective preparations. Recent cytotoxicity test results revealed that 12-*O*-acetylazedarachin B (Table 1), isolated from the fruit extract of *M. azedarach*, was found cytotoxic against leukemia (HL-60) ($IC_{50}=0.016 \mu M$) and stomach (AZ521) ($IC_{50}=0.035 \mu M$) cancer cell lines, making it promising as a lead compound for developing an effective drug. 12-*O*-acetylazedarachin B induces apoptosis *via* both the mitochondrial and death receptor-mediated pathways in leukemia cells (10). Also Akihisa and coworkers tested various *M. azedarach* fruits extracts as well as the contained trichilin, vilasinin, salannin, nimbin (Table 1), nimbolinin and tirucallane-type limonoids on various cancer cell lines like HL60 (leukemia), A549 (lung), AZ521 (stomach), and SK-BR-3 (breast) cells against two reference anticancer drugs, cisplatin and 5-fluorouracil. The activities revealed that some of these limonoid compounds may be valuable anticancer lead compounds. It was demonstrated that meliarachin C ($IC_{50}=0.65 \mu M$) and 3-*O*-deacetyl-4-*O*-demethyl-28-oxosalannin ($IC_{50}=2.8 \mu M$) exhibited potent cytotoxic activity against HL60 cells, inducing apoptosis observed by flow cytometry. Western blot analysis proved as above stated by Kikuchi that the limonoids induced apoptosis *via* both the mitochondrial and death receptor-mediated pathways (11). In another study, the seed kernel extract of *M. azedarach* has been found highly selective as well as cytotoxic against HT-29, A-549, MCF-7 and HepG-2 and MDBK cell lines (IC_{50} range of 8.18- 60.10 μg

mL⁻¹), while the flavonols rich methanol leaf fraction was found safer in terms of cytotoxicity. Interestingly, in the same study in comparison with Persian lilac, the neem samples were more toxic on normal cell line, which indicated that neem is more harmful and thus its prescription in high doses needs more caution (12). *M. azedarach*, together with *Asclepias sinaica*, *Urginea maritima*, *Nerium oleander* and *Catharanthus roseus*, was one of the most active out of the 61 total botanical species screened on active human lymphoma cell line U-937 GTB on a 9 year research on medicinal plants from the Sinai desert in collaboration with Bedouin herbalists (13). Yuan reports on some limonoids, triterpenoids, steroids, and sesquiterpenoids found to exhibit cytotoxicity against five human tumor cell lines (HL-60, SMMC-7721, A-549, MCF-7, and SW480) (14), while Kim reports on the hexane layer of *M. azedarach* bark extract was found of anti-cancer activity on A549 human adenocarcinoma cells (15).

Biological methods for synthesis of nanoparticles (NPs) are of great advantage due to their non-toxic and large scale synthesis. Silver nanoparticles can be used in preventing and controlling HIV infection to treat infection against burn and open wounds and they also have antimicrobial activity. Nanoparticles, in comparison to conventional antibiotics, provide more chemical, catalytic, physical and thermal activities due to larger surface area to volume ratio. Interestingly, leaves extract of *M. azedarach* was used as a reducing agent of silver ions to silver nanoparticles, which were additionally highly active as antibacterial agent (*E. coli*, *K. pneumonia*, *S. aureus*, *P. Aeruginosa* and *Proteus* spp.) (16). Similarly, a first synthesis characterization and cytotoxicity of biosynthesized AgNPs from *M. azedarach* against *in vitro* HeLa cells and *in vivo* Dalton's ascites lymphoma mice model, revealing the application of AgNPs and together *M. azedarach* in cancer therapy (17).

The methanolic leaf extract of *M. azedarach* was proved of significant hepatoprotective activity since it maintained the activity of antioxidant enzymes (GPx, GST, SOD and CAT) in liver and the serum enzymes (SGOT, SGPT and Alkaline phosphate), to the normal level if compared to paracetamol effect. Over dosing of paracetamol creates disorders in the concentrations levels of the before mentioned enzymes that in turn causes hepatic damage. Interestingly, the acute oral toxicity test of *M. azedarach* on rats showed no mortality up to 610 mg/kg, revealing the extract's low toxicity to mammals (18).

Topical corticosteroids and antivirals, being the current therapy for *Herpes simplex virus* type 1 (HSV-1) infections, increase in recurrence and severity of disease in treated patients, and additionally provoke intraocular pressure, glaucoma and cataracts (19). Meliacine as a constituent compound of the partially purified leaf extracts of *M. azedarach* was found to reduce virus load and to abolish the inflammatory reaction and neovascularization during the development of herpetic stromal keratitis in mice. On the other hand, 1-cinnamoyl-3,11-dihydroxymeliacarpin (Table 1), displayed anti-herpetic and immunomodulatory activities *in vitro* (20). 1-cinnamoyl-3,11-dihydroxymeliacarpin, isolated from leaf extracts of *M. azedarach* was also found to exhibit antiherpetic effect in epithelial cells and in specific to inhibit Herpes Simplex Virus type 2 (HSV-1) multiplication in Vero cells but not to affect its replication in macrophages which were not permissive to HSV infection (21).

M. azedarach leaf extract was proved of antioxidant activity and protective effect against H₂O₂-induced cellular damage in cultured lymphocytes, thus this botanical species can be developed as an effective antioxidant during oxidative stress (22).

Various crude extracts of *M. azedarach* seeds, produced with different solvents, were tested on 18 hospital isolated human pathogenic gram positive and gram negative bacterial strains (e.g *Staphylococcus*, *Streptococcus*, *Enterococcus*, *Escherichia*, *Edwardsiella*, *Klebsiella*, *Pseudomonas*, *Salmonella* and *Shigella* spp.). All extracts showed antibacterial activity and the inhibition was strain specific and concentration dependent. Interestingly, the water extract showed moderate activity against all tested pathogenic bacteria, while the most active crude extract was that of ethyl acetate (23). 7-cinnamoyl toosendanin isolated from *M. azedarach*, showed activity against the gram-positive bacteria *Micrococcus luteus* ATCC 9341 and *Bacillus subtilis* ATCC 6633 with minimum inhibition concentrations (MICs) of 6.25 and 25 mg/ml, respectively. 21b-methylmelianodiol exhibited respective activities of 12.5 and 25 mg/ml. The antibacterial agent magnolol was used as the positive control showing a MIC value of 12.5 mg/mL against the both bacteria (24). The aerial parts of *M. azedarach* yield two limonoids that exhibit antimicrobial activity. In specific, meliarachin D showed weak activities against *Staphylococcus aureus* (MIC 50 mg/ml) and *Bacillus subtilis* (MIC 50 mg/ml), while meliarachin H exhibited moderate activity against *Bacillus subtilis* (MIC 25 mg/ml) (25). Orhan and co workers have studied the fruit and leaf extracts of *M. azedarach* antimicrobial activity against gram (+) and (-) bacteria *Candida* species, and they showed higher antibacterial effect against gram (-) strains (26).

M. azedarach was also proved of antimicrobial activity against dermatophytic fungus and in specific *Trichophyton rubrum*, *Epidermophyton floccosum* and *Microsporum gypseum* (27).

The methanolic extract of *M. azedarach* was found to exhibit antimalarial activity against *Plasmodium falciparum* with an IC₅₀ of 37 µg/mL (28). Controlling malaria is threatened by the emergence of drug-resistant strains of the malaria parasite, *Plasmodium* (29), so new antimalarial agents need to be exploited. Some of the already existing drugs such as quinine and artemisin originating in plants could serve as examples of further investigating plant species for antimalarial properties.

Trypsin belongs to the serine proteases playing a key role in the normal physiological functions of the cells. Deficiency in the normal activity of this proteolytic enzyme, provokes pathological disorders and therefore the cure by protease inhibitors from natural sources, provides an attractive target for pharmaceutical research. Vanillin extracted from crude ethanolic extract from *M. azedarach* together with other phenolic compounds was found to inhibit trypsin (30).

Last, *M. azedarach* is at place 5 out of the 15 top listed plants for controlling type II diabetes mellitus and thus it has a hopeful prospect for drug discovery in that area (31).

Medicinal Uses/Controlling Insects Vectors of Diseases and Animal Parasites

Rapidly emerging insect vector's resistance to the chemicals threatens the sustainability of synthetic insecticides treatments. Botanical preparations can be locally available, are cheap to produce and thus can be effective in reducing disease vector abundance.

Malaria is an important disease and cause of death in the tropical countries and it is transmitted by the mosquito vector *Anopheles* spp. The botanical family Meliaceae is one of the six of greatest potential as mosquitoes control botanical agents (32). *M. azedarach* aerial part extract exhibits an LC₅₀ value of 5.5 µg/L against *Anopheles stephensi* (33). As mentioned previously *M. azedarach* controls malaria parasite, *Plasmodium* spp. thus by also controlling its vector *Anopheles* spp. it provides with an overall control, reducing malaria incidence and prevalence. *M. azedarach* was also found significantly growth-inhibiting and of larvicidal effects on the malaria vector *Anopheles arabiensis*, which is the most abundant malaria vector in Ethiopia and much of Africa (34). Therefore the use of *M. azedarach* can contribute to an integrated, completely sustainable, approach to combat malaria. Besides malarial vectors *M. azedarach* shows efficacy also against the tick *Rhipicephalus* (B.) *microplus* (35), the dengue vector, *Aedes aegypti* and the human lice *Pediculus humanus capitis* (1). Further, Sousa and co-workers have also studied the synergistic effects of *M. azedarach* extracts and *Beauveria bassiana* (a biological control agent for mites), which makes a nice match with the below mentioned analogous situation with *B. thuringensis* (35, 36). On the other hand, worth mentioning is the fact that *M. azedarach* extracts were not active against other tick, *Amblyomma cajennense* (37).

On the other hand, *M. azedarach* extracts are active against *Culex* spp (38, 39). Interestingly, considerable synergism is presented when *M. azedarach* extract is combined with *Bacillus thuringiensis israelensis* (Bti) and *Bacillus sphaericus* 2362 (Bs) against *Culex pipiens* adults (39). Identifying synergism in mixtures may lead to more effective mosquitocides and to the use of smaller amounts in the mixture to achieve satisfactory levels of efficacy (39). *M. azedarach* may also be sought as potential extract for the sake of synergic combinations against *Aedes aegypti* (40). In insects the effect of *M. azedarach* extracts could be related to the inhibition of NADPH-cytochrome c reductase and cholinesterase (1). Application of *M. azedarach* oils was proved to be a safe and low-cost means of personal protection against sand fly bites in endemic areas of Ethiopia (41).

Gastrointestinal nematodes cause serious economic losses and are the most important factor limiting sheep production worldwide. *Haemonchus contortus* is one of the most important nematode parasites of both sheep and goats as adult worms suck blood, causing loss of plasma and protein in the host. Incorrect and indiscriminate use of synthetic anthelmintics has led to the evolution of resistance in *H. contortus* and therefore to the current need for alternative control measures. In addition, low-cost phytotherapeutic alternatives are extremely needed in small ruminants by family farmers. Interestingly ethanol extracts of *M. azedarach* tested at 10, 20 and 30 % controlled at 48.1, 62.9 and 66.7 % *H. contortus* larvae in sheep

(42). On the other hand, the hexane extract of *M. azedarach* fruits, was found of LC₅₀ 572.2 µg/mL and LC₉₉ 1137.8 µg/mL in the hatch test, and of LC₅₀ 0.7 µg/mL and LC₉₉ 60.8 µg/mL in the larval development test against sheep gastrointestinal nematodes (43). Last, also Ben Ghnaya and coworkers have demonstrated the anthelmintic properties of *M. azedarach* together with its astringent and properties (44).

Agricultural Uses/Controlling Pest Organisms and Pathogens

To date, in Europe pest management is mostly performed under the frame of integrated pest management schemes for low-residue, efficient and cost-effective management of pest populations. Efforts to reduce synthetic pesticides use can be beneficial to the environment, therefore new tools of pest management are needed, and plant-derived semiochemicals are among the lead alternatives towards this ecofriendly direction. *M. azedarach* has fertilizer and herbicide quality (44) as well as pesticidal properties as described here after.

M. azedarach fruits extracts have been found to provoke growth retardation, reduced fecundity, moulting disorders, morphogenetic defects and changes in insects. Yaseen and co-workers (45) proved that *M. azedarach* aqueous extract exerted a significant inhibitory effect on the growth and development of ovaries and ovarian follicles of the *Musca domestica* adult flies and that it also affected the histological structure of the alimentary canal of the midgut (45). Recently the senescent leaf extract has been proved of antifeedant and growth regulation activities to armyworm larvae (*Spodoptera* sp.) when present in the food. A synergistic effect with cypermethrin in topical assays was also evident and in particular to have some inhibitor activity against detoxification enzymes and acetylcholinesterase like piperonyl butoxide (46). This finding is of particular interest since the prospect of using the extract as a botanical insecticide, effective in reducing pest resistance (3), was then compared with the possibility of using it instead as cheaper price synergist, contrary to piperonyl butoxide. In agreement with Al-Rubae (1) also Breuer reported that *M. azedarach* extract has a NADPH-cytochrome *c* reductase and cholinesterase activity in *Spodoptera frugiperda* (47). Farag and co-workers have demonstrated that the oil of *M. azedarach* recorded high insecticidal potential against *Spodoptera littoralis* (48). Interestingly an antagonistic effect was observed concerning efficacy of combined use of *M. azedarach* aqueous extracts and *Bacillus thurigiensis* against *Oryzophagus oryzae* and *S. frugiperda*. Only when tested alone *Bacillus thurigiensis* 1958-2 isolates were effective against *S. frugiperda* and *Bt* 2014-2 isolate or the purified Cry3 proteins controlled *Oryzophagus oryzae* larvae. Also *M. azedarach* aqueous extracts was toxic to both the pests (*O. oryzae* and *S. frugiperda*) when used alone (49). Nonetheless, the activity of *M. azedarach* products on *Spodoptera* spp. is biased as many reports may be conflicting and therefore they deserve a further critical study (50, 51). The difference in species studied could be a possible explanation and perhaps no generalization can be done yet.

M. azedarach alcohol extract at 10% showed insecticidal potential against leaf-cutting ants (*Atta laevigatta* Smith) of planted forests in Brazil (52).

The methanolic extracts of the leaves of *M. azedarach* (0.5 to 2.5 g/mL) were proved of activity against *Alternaria alternata* and decreased the fungal biomass to 83–96% (53). On the other hand, the aqueous extract of *M. azedarach* was highly effective and inhibited zoospore germination of *Phytophthora colocasiae* by >94.0% (54). Last, when the aqueous extract of *M. azedarach* was tested on *Elsinoe ampelina*, the causal agent of grapevine anthracnose, there was a negative linear effect of extract concentrations on disease severity (55).

Among factors that are responsible for the deterioration of the quality and nutrient content of wheat is *Rhizoglyphus tritici*. Initially the damage is restricted to the wheat embryo, and then it leads to a negligible reduction in grain weight and seeds losing their viability. When infestation takes place in the later stages, the entire grain content may be consumed and only the seed might be left. The leaf extract of *M. azedarach* caused 14.8%–74.8%, 42.7%–80.5%, 47.9%–85.2%, and 48.5%–86.6% efficacy at the concentrations of 6.25%, 12.5%, 25%, 50%, and 100%, under exposure for 7, 14, 21, and 28 days against *Rhizoglyphus tritici*. *M. azedarach* can therefore be of further study as natural grain protectant, alternative to toxic synthetic miticides (56). Other reports on the acaricidal activity of extracts of *M. azedarach* include the species *Oligonychus coffeae*, *Eutetranychus orientalis*, *Tetranychus urticae* (57–59).

M. azedarach leaves ethanolic extract was found of larvicidal activity against the cucurbit fly, *Dacus ciliatus* (Diptera: Tephritidae), suggesting that the extract could possibly be used as a sustainable method for controlling this insect pest (60).

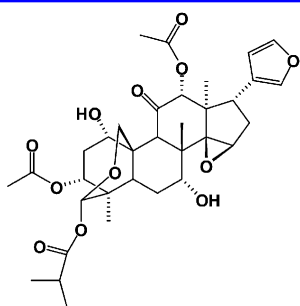
M. azedarach both green and mature fruit extracts, significantly reduced the population of Citrus leafminer, *Phyllocnistis citrella*, and could thus be promising of use in sustainable agriculture approaches (61, 62).

Interestingly, *M. azedarach* has been found friendly against beneficial organisms, thus implying that it could easily be incorporated into IPM programs. *Eriopsis connexa* is a native predator from the Neotropical Region and it feeds on soft-bodies pests such as aphids, whiteflies and thrips. When extracts from unripe fruits of *M. azedarach* were tested no detrimental effects were observed on hatching, development time, adult emergence, pre-oviposition period, fecundity and fertility (63). Extracts of mature and immature *M. azedarach* fruits were combined with the use of the parasitoid *Diglyphus isaea* against the vegetable leafminer *Liriomyza sativae* and were found compatible and not toxic to the beneficial (64). The effect of *M. azedarach* on beneficial fauna has also been demonstrated in field conditions (65).

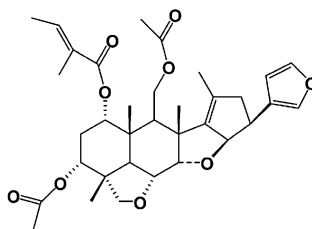
Finally, aphids and whiteflies are included in the range of species taxa against which *M. azedarach* efficacy is evidenced, being these two important pests for the variety of crops they threaten (65–68).

Last, *M. azedarach* was interestingly found to possess a favorable forage quality and of the ability to reduce methane formation at simultaneously acceptable nutritional quality, due to its phenolic fraction (69).

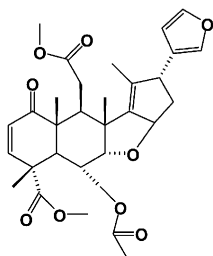
Table 1. Some of the Most Active Compounds Isolated from *Melia azedarach*



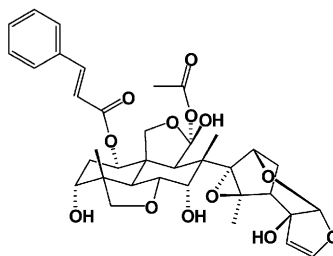
12-*O*-acetylazedarachin B



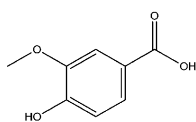
salannin



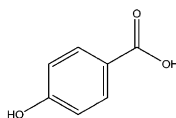
nimbin



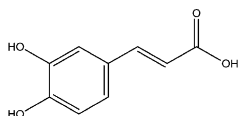
1-cinnamoyl-3,11-dihydroxymeliacarpinin



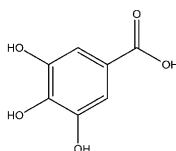
vanillic acid



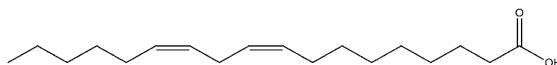
p-hydroxybenzoic acid



caffeic acid



gallic acid



linoleic acid

General Extraction Methods and Chemical Composition Analysis

Limonoids are the most biologically active chemical group of *M. azedarach* constituents. Previously we have reported on the various limonoids that have been isolated from *M. azedarach* (4). In fact, chemical composition studies have taken place to evaluate the effect of crafting *Azadirachta indica* on *M. azedarach* adapted to cool climates, regarding limonoids contents. Interestingly, it was proved that salannin could have been translocated from the *M. azedarach* rootstock to the *A. indica* graft, while meliatoxins were confirmed to be absent in graft fruits (70). Limonoids are usually isolated from alcoholic soluble fractions of plant parts extracts obtained after partitioning with high polarity solvents such as water or butanol. A typical extraction and limonoids isolation procedure was reported by Akihisa and coworkers that used dried and powdered *M. azedarach* fruits for extraction with n-hexane, and then the defatted residue they obtained for extraction with MeOH. Then they fractionated it into EtOAc-, n-BuOH-, and H₂O-soluble fractions. The EtOAc-soluble fraction was subjected to successive column chromatography on silica gel and octadecyl silica gel columns, and to reversed-phase HPLC which led to the isolation of thirty-one limonoids. The structures of the isolated compounds are usually elucidated by 2D NMR spectroscopy and mass spectrometry (11). Similar procedures are undertaken by others (14, 24, 71).

The other than limonoids constituent compounds of *M. azedarach*, usually of lower molecular masses, are screened by gas chromatography-mass spectrometry (GC-MS). In that context analysis of the fatty oils obtained after defatting with non polar solvents like n-hexane or petroleum ether reveals caproic, lauric, myristic, palmitic, stearic, oleic, linoleic (Table 1) and linolenic acid (27). Also Farag and co-workers have demonstrated that linoleic acid methyl ester, oleic acid methyl ester, and free oleic acid as the main components of the oil of *M. azedarach*, together with hexadecanol, palmitic acid, methyl esters of stearic acid and myristic acid (48). Other chemical compounds identified by GC/MS in *M. azedarach* extracts were flavonoids, phytosterols, diterpenes, alkane hydrocarbon, n-alkanoic acid, vitamin-E and tri-terpene as well as terpene alcohol (72). The phenolic composition of the extracts is elucidated by high performance liquid chromatography (HPLC) and gallic, protocatechic, p-hydroxy-benzoic, vanillic, caffeic, chlorogenic, syringic and p-coumaric acid are revealed (27). p-coumaric acid and p-hydroxybenzoic acid (Table 1) were detected in *M. azedarach* as major nematicidal components by Aoudia et al., 2012 (73).

Conclusions

“Natural alternatives” to synthetic formulates and preparations gain increasingly more ground in agriculture and medicine for pests and diseases treatment. Botanicals, as naturally occurring chemicals extracted or derived from plants, are often eco-friendly and appropriate to resistance management schemes. *M. azedarach* is a plant species of particular interest for its biological properties

and the development of analytical methods for its chemical characterisation is thus mandatory. If secondary metabolites of botanical extracts are to be commercially exploited, their identification and quantitation in complex matrices should be further exploited.

References

1. Al-Rubae, A. Y. *Am.-Eurasian J. Sustainable Agric.* **2009**, *3*, 185–194.
2. Carpinella, M. C.; Defagó, M. T.; Valladares, G.; Palacios, S. M. *Adv. Phytomed.* **2006**, *3*, 81–123.
3. Koul, O.; Walia, S. *CAB Rev.* **2009**, *4*, 1749–8848.
4. Caboni, P.; Ntalli, N. G.; Bueno, C. E.; Alchè, L. E. In *Emerging Trends in Dietary Components for Preventing and Combating Disease*; Patil, B., et al.; ACS Symposium Series 1093; American Chemical Society: Washington, DC, 2012; Chapter 4.
5. Kataria, H. C. *Orient. J. Chem.* **1994**, *10*, 178–180.
6. Carpinella, M. C.; Giorda, L. M.; Ferrayoli, C. G.; Palacios, S. M. *J. Agric. Food Chem.* **2003**, *51*, 2506–2511.
7. Parveen; Upadhyay, B.; Roy, S.; Kumar, A. *J. Ethnopharmacol.* **2007**, *113*, 387–399.
8. McChesney, J. D.; Venkataraman, S. K.; Henri, J. T. *Phytochemistry* **2007**, *68*, 2015–2022.
9. Vuorela, P.; Leinonen, M.; Saikku, P. *Curr. Med. Chem.* **2004**, *11*, 1375–1389.
10. Kikuchi, T.; Pan, X.; Ishii, K.; Nakamura, Y.; Ogihara, E.; Koike, K.; Tanaka, R.; Akihisa, T. *Biol. Pharm. Bull.* **2013**, *36*, 135–139.
11. Akihisa, T.; Pan, X.; Nakamura, Y.; Kikuchi, T.; Takahashi, N.; Matsumoto, M.; Ogihara, E.; Fukatsu, M.; Koike, K.; Tokuda, H. *Phytochemistry* **2013**, *89*, 59–70.
12. Jafari, S.; Saeidnia, S.; Hajimehdipoor, H.; Ardekani, M. R. S.; Faramarzi, M. A.; Hadjiakhoondi, A.; Khanavi, M. *J. Pharm. Sci.* **2013**, 21–37.
13. El-Seedi, H. R.; Burman, R.; Mansour, A.; Turki, Z.; Boulos, L.; Gullbo, J.; Goransson, U. *J. Ethnopharmacol.* **2013**, *145*, 746–757.
14. Yuan, C.-M.; Zhang, Y.; Tang, G.-H.; Li, Y.; He, H.-P.; Li, S.-F.; Hou, L.; Li, X.-Y.; Di, Y.-T.; Li, S.-L.; Hua, H.-M.; Hao, X.-J. *Planta Med.* **2013**, *79*, 163–168.
15. Kim, H. W.; Kang, S. C. *Toxicol. Res.* **2012**, *79*, 163–168.
16. Mehmood, A.; Murtaza, G.; Bhatti, T. M.; Kausar, R. *Arabian J. Chem.* **2013**, in press.
17. Sukirthaa, R.; Priyanka, K. M.; Antony, J. J.; Kamalakkannana, S.; Thangamb, R.; Gunasekaran, R.; Krishnana, M.; Achiramana, S. *Process Biochem.* **2012**, *47*, 273–279.
18. Ahmed, M. F.; Rao, A. S.; Thayyil, H.; Ahemad, S. R.; Ibrahim, M. *Pharmacogn. J.* **2011**, *3*, 60–64.
19. Knickelbein, J. E.; Hendricks, R. L.; Charukamnoetkanok, P. *Surv. Ophthalmol.* **2009**, *54*, 226–234.

20. Bueno, C. A.; Lombardi, M. G.; Sales, M. E.; Alché, L. E. *Microvasc. Res.* **2012**, *84*, 235–241.
21. Petrera, E.; Coto, C. E. *Phytother. Res.* **2013**, *28*, 104–109.
22. Marimuthu, S.; Balakrishnan, P.; Nair, S. *Pharm. Biol.* **2013**, *51*, 1331–1340.
23. Khan, A. V.; Ahmed, Q. U.; Mir, M. R.; Shukla, I.; Khan, A. A. *Asian Pac. J. Trop. Biomed.* **2011**, *1*, 452–455.
24. Liu, H. B.; Zhang, C. R.; Dong, S. H.; Dong, L.; Wu, Y.; Yue, J. M. *Chem. Pharm. Bull.* **2011**, *59*, 1003–1007.
25. Su, Z. S.; Yang, S. P.; Zhang, S.; Dong, L.; Yue, J. M. *Helv. Chim. Acta* **2011**, *94*, 1515–1526.
26. Orhan, I. E.; Guner, E.; Ozcelik, B.; Senol, F. S.; Caglar, S. S.; Emecen, G.; Kocak, O.; Sener, B. *Int. J. Food Sci. Nutr* **2012**, *63*, 560–565.
27. Orhan, I. E.; Guner, E.; Ozturk, N.; Senol, F. S.; Erdem, A.; Kartal, M.; Sener, B. *Ind. Crops Prod.* **2012**, *37*, 213–218.
28. Kamaraj, C.; Kaushik, N. K.; Mohanakrishnan, D.; Elango, G.; Bagavan, A.; Zahir, A. A.; Rahuman, A. A.; Sahal, D. *Parasitol. Res.* **2012**, *111*, 703–715.
29. Craft, J. C. *Curr. Opin. Microbiol.* **2008**, *11*, 428–433.
30. Shahwar, D.; Raza, M. A.; Shafiq-Ur-Rehman; Abbasi, M. A.; Rahman, A. *U. Nat. Prod. Res.* **2012**, *26*, 1087–1093.
31. Gu, J.; Chen, L.; Yuan, G.; Xu, X. *Evidence-Based Complementary and Alternative Medicine*; 2013, Article ID 203614, 7 pages, <http://dx.doi.org/10.1155/2013/203614>.
32. Shahi, M.; Hanafi-Bojd, A. A.; Iranshahi, M.; Vatandoost, H.; Hanafi-Bojd, M. Y. *J. Vector Borne Dis.* **2010**, *47*, 185–188.
33. Kumar, S.; Nair, G.; Singh, A. P.; Batra, S.; Wahab, N.; Warikoo, R. *Asian Pac. J. Trop. Dis.* **2012**, *2*, 395–400.
34. Trudel, R. E.; Bomblies, A. *Parasites Vectors* **2011**, *4*, 72.
35. Sousa, L. A. D.; Rocha, T. L.; Sabaia-Morais, S. M. T.; Borges, L. M. F. *Rev. Bras. Parasitol.* **2013**, *22*, 339–345.
36. Sousa, L. A. D.; Pires Junior, H. B.; Soares, S. F.; Ferri, P. H.; Ribas, P.; Lima, E. M.; Furlong, J.; Bittencourt, V. R. E. P.; Perinotto, W. M. D. S.; Borges, L. M. F. *Vet. Parasitol.* **2011**, *175*, 320–324.
37. Soares, S. F.; Borges, L. M. F.; de Sousa Braga, R.; Ferreira, L. L.; Louly, C. C. B.; Tresvenzol, L. M. F.; de Paula, J. R.; Ferri, P. H. *Vet. Parasitol.* **2010**, *167*, 67–73.
38. Al-Mehmadi, R. M.; Al-Khalaf, A. A. *J. King Saud Univ.* **2010**, *22*, 77–85.
39. Mansour, S. A.; Foda, M. S.; Aly, A. R. *Ind. Crop Prod.* **2012**, *35*, 44–52.
40. Grzybowski, A.; Tiboni, M.; da Silva, M. A. N.; Chitolina, R. F.; Passos, M.; Fontana, J. D. *Braz. J. Pharmacogn.* **2012**, *22*, 549–557.
41. Kebede, Y.; Gebre-Michael, T.; Balkew, M. *Acta Trop* **2010**, *113*, 145–150.
42. Ahmed, M.; Laing, M. D.; Nsahlai, I. V. *J. Helminthol.* **2013**, *87*, 174–179.
43. Cala, A. C.; Chagas, A. C. S.; Oliveira, M. C. S.; Matos, A. P. L.; Borges, M. F.; Sousa, L. A. D.; Souza, F. A.; Oliveira, G. P. *Exp. Parasitol.* **2012**, *130*, 98–102.
44. Ben Ghnaya, A.; Hamrouni, L.; Hanana, M. *Phytotherapie* **2013**, *11*, 284–288.

45. Yaseen, A. T. S. M.; Mahmood, S. M.; Gorgees, N. S. *Iraqi J. Vet. Sci.* **2008**, *2*, 149–51.
46. Bullangpoti, V.; Wajnberg, E.; Audant, R.; Feyereisen, R. *Pest. Manage. Sci.* **2012**, *68*, 1255–1264.
47. Breuer, M.; Hoste, B.; De Loof, A.; Naqvi, S. N. H. *Pestic. Biochem. Physiol.* **2003**, *76*, 99–103.
48. Farag, M.; Ahmed, M. H. M.; Yousef, H.; Abdel-Rahman, A. A.-H. *Z. Naturforsch., C: J. Biosci.* **2011**, *66*, 129–135.
49. Berlitz, D. L.; de Azambuja, A. O.; Sebben, A.; de Oliveira, J. V.; Fiuza, L. M. *Braz. Arch. Biol. Technol.* **2012**, *55*, 725–731.
50. Li, W. Q.; Liu, Y. Q.; Zhao, Y. L.; Zhou, X. W.; Yang, L.; Feng, G.; Kou, L. *Curr. Bioact. Compd.* **2012**, *8*, 291–295.
51. Díaz, M.; Castillo, L.; Díaz, C. E.; González-Coloma, A.; Rossini, C. *Nat. Prod. J.* **2012**, *2*, 36–44.
52. Jung, P. H.; da Silveira, C.; Nieri, E. M.; Potrich, M.; da Silva, E. R. L.; Refatti, M. *Floresta e Ambiente* **2013**, *20*, 191–196.
53. Javaid, A.; Samad, S. *Nat. Prod. Res.* **2012**, *26*, 1697–1702.
54. Sugha, S. K.; Gurung, K. *J. Trop. Agric. Sci.* **2006**, *83*, 95–100.
55. da Silva, C. M.; Botelho, R. V.; Faria, C. M. R. D. *Summa Phytopathol.* **2012**, *38*, 312–318.
56. Bashir, M. H.; Gogi, M. D.; Ashfaq, M.; Afzal, M.; Khan, M. A.; Ihsan, M. *Turk. J. Agric. For.* **2013**, *37*, 585–594.
57. Roy, S.; Mukhopadhyay, A. *Int. J. Acarol.* **2012**, *38*, 79–86.
58. Gonzalez-Zamora, J. E.; Lopez, C.; Avilla, C. *Exp. Appl. Acarol.* **2011**, *55*, 389–400.
59. Yanar, D.; Kadioglu, I.; Gokce, A. *Afr. J. Biotechnol.* **2011**, *10*, 11745–11750.
60. Fetohab, B. E. A.; Asiryb, K. A. *Tox. Environ. Chem.* **2012**, *94*, 1350–1356.
61. Mckenna, M. M.; Abou-Fakhr Hammad, E. M.; Farran, M. T. *Springerplus* **2013**, *2*, 144.
62. Abou-Fakhr Hammad, E. M.; Hammad, M. M. M.; Farran, M. T. *Springerplus* **2013**, *2* doi:10.1186/2193-1801-2-144.
63. Haramboure, M.; Mirande, L.; Smagghe, G.; Piñeda, S.; Schneider, M. I. *Commun. Agric. Appl. Biol. Sci.* **2010**, *75*, 373–378.
64. Abou-Fakhr Hammad, E. M.; Heather, J.; McAuslane, H. *J. Food Agric. Environ.* **2010**, *8*, 1247–1252.
65. Kibrom, G.; Kebede, K.; Weldehaweria, G.; Dejen, G.; Mekonen, S.; Gebreegziabher, E.; Nagappan, R. *Arch. Phytopathol. Plant Prot.* **2012**, *45*, 1273–1279.
66. Cichon, L. I.; Garrido, S. A. S.; Lago, J. D.; Menni, M. F. *Acta Hort.* **2013**, *1001*, 115–120.
67. Dehghani, M.; Ahmadi, K. *Arch. Phytopathol. Plant Prot.* **2013**, *46*, 1127–1135.
68. Bezerra-Silva, G. C. D.; Silva, M. A.; Vendramim, J. D.; Dias, C. T. D. S. *Fla. Entomol.* **2012**, *95*, 743–751.
69. Jayanegara, A.; Wina, E.; Soliva, C. R.; Marquardt, S.; Kreuzer, M.; Leibner, F. *Anim. Feed Sci. Technol.* **2011**, *163*, 231–243.

70. Forim, M. R.; Cornélio, V. E.; Da Silva, M. F. D. G. F.; Rodrigues-Filho, E.; Fernandes, J. B.; Vieira, P. C.; Matinez, S. S.; Napolitanoc, M. P.; Yostc, R. A. *Phytochem. Anal.* **2010**, *21*, 363–373.
71. Ntalli, N. G.; Cottiglia, F.; Bueno, C. A.; Alché, L. E.; Leonti, M.; Vargiu, S.; Bifulco, E.; Menkissoglu-Spiroudi, U.; Caboni, P. *Molecules* **2010**, *15*, 5866–5877.
72. Sen, A.; Batra, A. *Asian J. Pharm. Clin. Res.* **2012**, *5*, 42–45.
73. Aoudia, H.; Oomah, B. D.; Zaidi, F.; Zaidi-Yahiaoui, R.; Drover, J. C. G.; Harrison, J. E. *J. Agric. Food Chem.* **2012**, *60*, 11675–11680.

Chapter 8

Characterization of *Sambucus nigra* L. Infusions Using Capillary Electrophoresis and Liquid Chromatography-Tandem Mass Spectrometry

Petr Česla,* Petra Dinisová, Jana Váňová, Lenka Česlová,
and Jan Fischer

Department of Analytical Chemistry, Faculty of Chemical Technology,
University of Pardubice, Pardubice, Czech Republic

*E-mail: Petr.Cesla@upce.cz.

Herbs, herbal teas and infusions are widely used as natural medicines with important biological effects caused by the presence of plant metabolites. One of the major groups of such compounds are polyphenolic compounds including both phenolic acids and flavonoidic natural antioxidants. For separation and determination of the content of (poly)phenolic compounds in herb samples, the liquid chromatographic method (based on a reversed-phase system employing columns packed with porous shell particles coupled to the tandem mass spectrometry) and the capillary electrophoretic method have been developed. The utility of both methods for characterization and quantification of polyphenolic compounds is demonstrated on *Sambucus nigra* L. infusion samples. The quantitative parameters, i.e. the sensitivity, repeatability and linearity of calibrations, limits of detection and the correlation between the concentrations of polyphenolic compounds determined using both methods are compared in this work with the aim of providing a tool for the comprehensive characterization of the herbal infusion samples.

Introduction

In recent years, there is increased interest in the analysis of wild plants rich in polyphenolic compounds due to their possible beneficial effects on human health. Some flowers from wild species such as *Sambucus nigra* L. have been traditionally used for medicinal applications. Due to their diaphoretic properties infusions prepared from the inflorescences of *Sambucus nigra* L. have been used to treat the symptoms of influenza, colds and sinusitis (1). Further, the infusion, poultices or ointments prepared from elderflower can be used for treatment of skin injuries, diabetic wounds or as a blood cleanser (2).

The main constituents reported for elder species are phenolic compounds, triterpenes, essential oils (3) and other compounds such as acyl spermidines (1). Phenolic compounds (also often known as polyphenols) are secondary metabolites synthesized in the plants depending on their development stages. The main classes of phenolic compounds are phenolic acids and flavonoids, which are very often present in the plant material in the glycosylated form. Due to their health benefits, the analytical techniques for the characterization and quantitation of these compounds are required in order to support the steady progress of the medicinal sciences. As the herb infusions are usually complex mixtures containing tens of compounds, the methods possessing high peak capacities are usually required for their analysis.

For the separation and quantification of phenolic compounds in complex samples such as herbal extracts and infusions, reversed-phase liquid chromatography (RP-LC) is a widely used technique (1, 3–13). The mobile phase usually consists of an aqueous solution of acetonitrile or methanol with the addition of formic or acetic acid for suppressing the dissociation of the phenolic acids in acidic *pH*. Octadecyl silica gel columns are used in almost all cases for the separation of polyphenols in herbs, however other special stationary phases were also tested, e.g. poly-(carboxylic acid)-coated silica phase, which is stable in low *pH* and can be used for the fast separation of flavonoids (4). Recently, the RP-LC method for determination of polyphenols in elderflower samples on-line coupled with the assay for determination of their antioxidant capacity have been introduced (14).

The polyphenolic profile of the *Sambucus nigra* L. strongly depends on the genotype, the place of origin (including altitudinal variations) and processing conditions (2, 5, 6). Usually, water infusions, hydromethanolic or hydroethanolic extracts of elderflower are used for quantitative analysis of phenolic compounds. The common extraction techniques like maceration and Soxhlet extraction are time consuming and, consequently, in recent years an effort has been made to develop faster extraction procedures. The comparison of different extraction techniques with the accelerated solvent extraction was performed for rutin and isoquercitrin (7) and other flavonoids glycosides and anthocyanins (5). The application of the accelerated extraction techniques improved the total extraction time more than ten times in comparison with the maceration technique. The method suitable for decreasing the extraction time of preparation of extracts from elder is pressurized liquid extraction (8).

Besides the RP-LC, spectroscopic techniques (3, 15) and various modes of capillary electrophoresis (capillary zone electrophoresis, isotachopheresis, micellar electrokinetic chromatography) can be used for the quantitative analysis of the phenolic compounds (3, 9, 16–18). Recently, the benefits of two-dimensional separation techniques have been recognized for the analysis of polyphenolic compounds of herbs. Thus the two-dimensional liquid chromatography based either on the combination of reversed-phase systems (19, 20) or on the combination of hydrophilic interaction chromatography with reversed-phase system (21, 22) is suitable for characterization of the profile of polyphenolic compounds. The application of capillary electrophoresis in a two-dimensional system with liquid chromatography (23) can further improve the overall peak capacity yielding better separation of the polyphenols.

Quantitative determination of polyphenols presented in herb extracts and infusions performed using different methods should ideally provide the same results. In this work we have therefore focused on the comparison of quantitative parameters of the two most widely applied methods, i.e. reversed-phase liquid chromatography coupled with tandem mass spectrometry and capillary electrophoresis. Both optimized methods were used for the characterization and determination of the 18 physiologically most important polyphenolic compounds in three *Sambucus nigra* L. infusion samples.

Materials and Methods

Chemicals

Standards of phenolic acids (caffeic, chlorogenic, cryptochlorogenic, ferulic, gallic, neochlorogenic, *p*-hydroxybenzoic, *p*-coumaric), flavonoid aglycones (hesperetin, kaempferol, naringenin, quercetin) and glycosides (hesperidin, isoquercitrin, kaempferol-3-*O*-rutinoside, rutin) were purchased from Sigma-Aldrich (St. Louis, MO, USA), as well as the chemicals for the preparation of mobile phases (methanol, LC/MS purity) and background electrolyte components (boric acid, sodium tetraborate). Standards of isorhamnetin-3-*O*-glucoside and isorhamnetin-3-*O*-rutinoside were obtained from Extrasynthese (Genay, France). Background electrolyte additives sodium decyl sulfate, β -cyclodextrin, heptakis(6-*O*-sulfo)- β -cyclodextrin and heptakis(2,6-di-*O*-methyl)- β -cyclodextrin were also from Sigma-Aldrich. Deionized ultra-pure water with conductivity of 0.055 μ S/cm was prepared by Ultra CLEAR UV apparatus (SG, Hamburg, Germany). Formic acid, sodium hydroxide and thiourea were purchased from LachNer (Neratovice, Czech Republic).

Sample Preparation

The three series of samples of *Sambucus nigra* L. infusions were used for the analyses. At first series, the five infusions were prepared using five elderflower tea bags, obtained in a local store. The weight of each bags was 1.6804 g, 1.6277 g, 1.6600 g, 1.6102 g and 1.6803 g, respectively. The second series of infusions was

prepared by homogenization of 20 tea bags (from the same brand like in the first series) and by weighting the elderflower samples. The samples weighted 1.6009 g, 1.6007 g, 1.6074 g, 1.6096 g and 1.6022 g, respectively. The third series of infusions was prepared from the dried inflorescence of wild-growing *Sambucus nigra* L. plant, collected in Veltruby, Czech Republic (location 50° 4.3219' N, 15° 10.8356' E) on June 2013. The samples weighted 1.6076 g, 1.6072 g, 1.6176 g, 1.6218 g and 1.6024 g, respectively. The sample infusions were prepared by keeping the bags or inflorescence samples in 200 mL of 95 °C hot water for 5 min and cooling to the laboratory temperature. Before injection, the infusions were filtered using Millipore 0.45 µm polytetrafluoroethylene syringe filter (Bedford, MA, USA).

Capillary Electrophoresis Method

Electrophoretic analyses with micellar electrokinetic chromatography were performed using an Agilent CE 7100 capillary electrophoresis instrument (Agilent, Palo Alto, CA, USA). Fused silica capillaries were used, 50 µm i.d., 48 cm total length, 40 cm to the detector with 150 µm extended light path cell (also obtained from Agilent). Before the first use, new capillaries were preconditioned by rinsing with 0.5 mol/L sodium hydroxide following by ultra-pure water for 10 min each. The analyses were carried out in background electrolyte (BGE) consisted of 25 mmol/L borate buffer *pH* 9.3 with the addition of 36 mmol/L sodium decyl sulfate. The *pH* of the BGE was adjusted using Metrohm 827 laboratory *pH* meter equipped with Unitrode electrode (Metrohm, Herisau, Switzerland), calibrated using Metrohm standard buffer solutions, *pH* 7.00 and 9.00. The temperature of the capillary was 25 °C and applied voltage was 20 kV. The samples were introduced into the separation capillary hydrodynamically by applying overpressure of 100 mBar for 10 s at the inlet sample vial. The detection wavelengths of the CE instrument were set to 214, 254 and 280 nm.

Liquid Chromatography-Tandem Mass Spectrometry Method

The elderflower infusions were analyzed using a Shimadzu modular liquid chromatograph consisting of two LC-20ADXR pumps, DGU-5 degassing unit, SIL-20ADXR autosampler, SPD-20A UV detector (all Shimadzu, Kyoto, Japan) and LCO-102 column thermostat (ECOM, Prague, Czech Republic) coupled with QTRAP 4500 mass spectrometer operated in electrospray mode (AB SCIEX, Framingham, MA, USA). The tandem mass spectrometric (MS/MS) detection in multiple reactions monitoring mode (MRM) was used for the quantitative analysis. The detection conditions i.e. the MRM transitions, declustering potential, collision energy and collision cell exit potential were optimized for all compounds using direct infusion of the standards into the mass spectrometer. The optimal parameters used for quantitative analysis are indicated in the Table I. Other settings of the ionization source common to all compounds were as follows: curtain gas 25, collision gas – medium, ion spray voltage -4500 V, temperature 400 °C, ion source gases 50/60, entrance potential -10 V.

Table I. Conditions of Liquid Chromatography/Tandem Mass Spectrometric Detection of Phenolic Acids and Flavonoids

<i>Compound</i>	<i>Retention time [min]</i>	<i>MRM transitions</i>	<i>Declustering potential [V]</i>	<i>Collision energy [V]</i>	<i>Collision Cell Exit Potential [V]</i>
Gallic acid	2.12	169/125 ^a	-60	-22	-1
Neochlorogenic acid	3.80	353/179	-70	-26	-7
		353/191 ^a	-70	-30	-5
<i>p</i> -Hydroxybenzoic acid	5.76	137/93 ^a	-40	-18	-5
Chlorogenic acid	6.02	353/135	-60	-46	-11
		353/191 ^a	-60	-35	-5
Cryptochlorogenic acid	6.80	353/173 ^a	-50	-26	-5
		353/179	-50	-26	-9
Caffeic acid	7.23	179/89	-60	-44	-25
		179/135 ^a	-60	-24	-7
<i>p</i> -Coumaric acid	9.84	163/93	-40	-34	-5
		163/119 ^a	-40	-16	-7
Ferulic acid	10.71	193/117	-65	-20	-5
		193/134	-65	-20	-5
Isoquercitrin	13.87	463/271	-140	-60	-3
		463/301	-140	-42	-1

Continued on next page.

Table I. (Continued). Conditions of Liquid Chromatography/Tandem Mass Spectrometric Detection of Phenolic Acids and Flavonoids

<i>Compound</i>	<i>Retention time [min]</i>	<i>MRM transitions</i>	<i>Declustering potential [V]</i>	<i>Collision energy [V]</i>	<i>Collision Cell Exit Potential [V]</i>
Rutin	13.90	609/271	-160	-80	-7
		609/301 ^a	-160	-48	-9
Hesperidin	14.31	609/164	-115	-72	-7
		609/301 ^a	-115	-42	-9
Kaempferol-3- <i>O</i> -rutinoside	16.10	593/255	-150	-72	-9
		593/285 ^a	-150	-48	-11
Isorhamnetin-3- <i>O</i> -glucoside	16.26	477/243	-150	-56	-5
		477/314 ^a	-150	-38	-7
Isorhamnetin-3- <i>O</i> -rutinoside	16.55	623/299	-175	-62	-9
		623/315 ^a	-175	-40	-5
Quercetin	18.90	301/151 ^a	-100	-30	-7
		301/179	-100	-26	-15
Naringenin	19.20	271/119	-85	-34	-9
		271/151 ^a	-85	-24	-9
Hesperetin	20.28	301/151	-75	-34	-5
		301/164 ^a	-75	-34	-5

<i>Compound</i>	<i>Retention time [min]</i>	<i>MRM transitions</i>	<i>Declustering potential [V]</i>	<i>Collision energy [V]</i>	<i>Collision Cell Exit Potential [V]</i>
Kaempferol	21.89	285/117	-135	-58	-11
		285/185 ^a	-135	-36	-7

^a Multiple Reaction Monitoring (MRM) transition used for quantitative analysis.

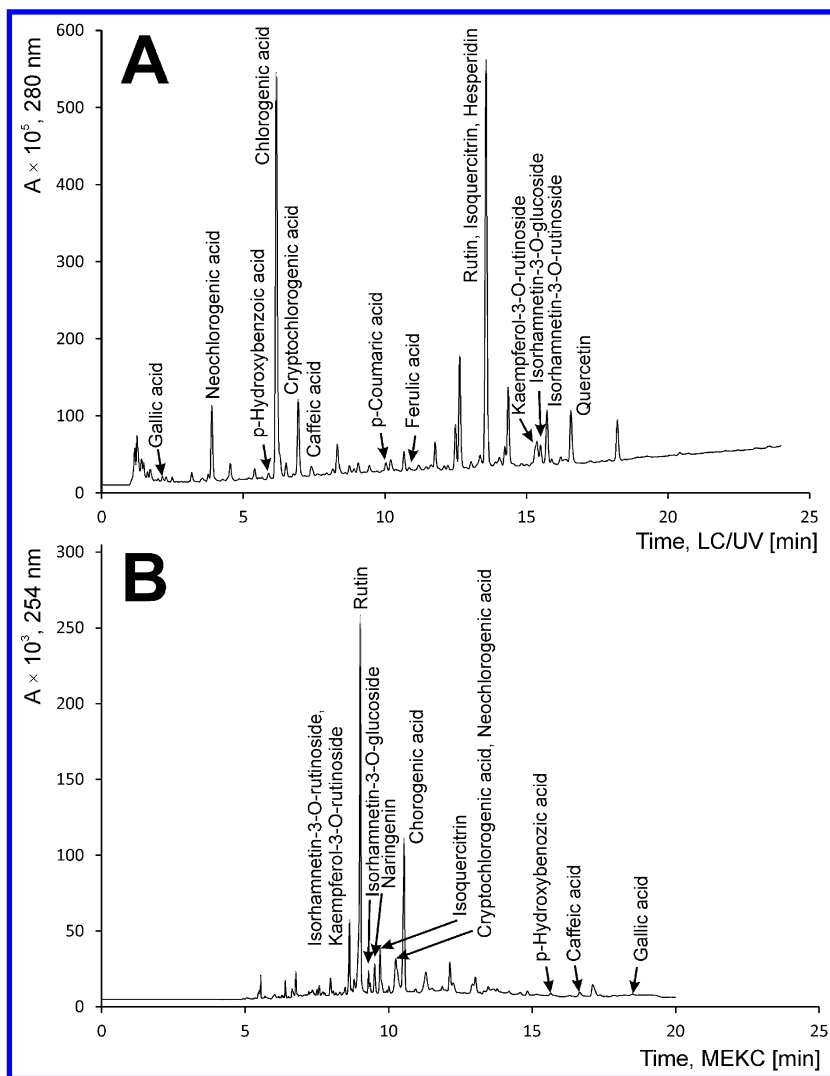


Figure 1. Separation of the elderflower infusion. Liquid chromatography (A) Ascentis Express C18 column (150 x 3.0 mm, 2.7 μ m porous shell particles); gradient elution of methanol/water with 0.1 % (v/v) formic acid, 0.5 mL/min, 30 $^{\circ}$ C. Capillary electrophoresis (B) capillary 48(40) cm x 50 μ m i.d. with 150 μ m light path cell, 25 mmol/L borate buffer pH 9.3 with 36 mmol/L sodium decyl sulfate, 20 kV, 25 $^{\circ}$ C. For other experimental conditions, see Materials and Methods.

In this work, several columns were tested for the separation of (poly)phenolic compounds. Thus Zorbax Eclipse XDB-C18, Luna PFP (both 250x4.6 mm, 5 μ m) and ACE3 C18-PFP (150x3.0 mm, 3 μ m) columns packed with the fully porous particles were compared with the porous shell columns Ascentis Express C8, C18

and phenyl-hexyl (all 150x3.0 mm, 2.7 μm particle size, 1.7 μm core size). The quantitative analysis was performed using Ascentis Express C18 column. The mobile phase A consisted of ultra pure water, mobile phase B was methanol. Formic acid (0.1 %, v/v) was added to both mobile phases. Flow rate of the mobile phase was 0.5 mL/min, temperature of the column 30 °C, injection volume 1 μL . The optimized gradient profile was 0 min – 15 % B, 8 min – 35 % B, 22 min – 59 % B, 24 min – 80 % B. The MS/MS data were acquired with the cycle time 0.6 s at scheduled MRM mode with MRM detection window of 160 s. The UV signal was recorded at 280 nm.

Statistical Evaluation of the Data

The results of the quantitative analysis were evaluated using Statistica 10 software (StatSoft, Inc., 2011, www.statsoft.com). The calibrations for both LC/MS/MS and MEKC methods were measured at least at seven concentration levels with three replicates ($n = 3$). The first, fourth and seventh calibration standards were replicated five times ($n = 5$). The calibration data were fitted using the least square linear regression at a significance level of 95 % ($\alpha = 0.05$). The significance of the regression parameters was tested using Student's t -test and the linearity was checked by inspecting the residuals. Each elderflower infusion was analyzed three times ($n = 3$) and the concentrations of phenolic compounds were calculated together with the standard deviations. Analysis of variance (ANOVA) was used for the determination of the significance of differences between the analyses, the infusions and the methods used.

Results and Discussion

Liquid Chromatography-Tandem Mass Spectrometry Method

For the chromatographic analysis of the polyphenolic compounds presented in *Sambucus nigra* L. infusions, the various reversed-phase columns were tested including octadecyl-, octyl-, phenylhexyl- and pentafluorophenyl silica gel columns. The columns used in the study were packed with both, fully porous and superficially porous (porous shell) particles. Porous shell material reduces the band broadening and allows the attainment of high efficiencies for fast separation similar to sub-2 μm fully porous particles. The advantage of such columns lies predominantly in reduction of longitudinal and eddy diffusion (B and A term of van Deemter plot) (24). The retention and the selectivity of separation for glycosylated flavonoids was higher using the medium-polarity and polar stationary phases (pentafluorophenyl silica gel column). The phenolic acids and flavonoid aglycones were better separated using octadecyl silica gel column. The separation of the elderflower infusion under optimized gradient conditions is presented on Figure 1A.

Polyphenols presented in the elder infusions were identified by comparing the retention times with the standards and by using tandem mass spectrometric detection. Thus two MRM transitions were used for the detection of the compounds, where one transition with higher intensity was used for quantification and the second one for the confirmation of the target compound.

The MRM transitions were optimized using direct infusion of the standards of polyphenols into the mass spectrometer and are shown in Table I. The most intense fragment ions of phenolic acids correspond to the decarboxylation. For the caffeoylquinic acids, either the deprotonated quinic acid (neochlorogenic and chlorogenic acids; Figure 2A) or the loss of caffeic acid from the deprotonated molecule was observed in the tandem mass spectra (cryptochlorogenic acid). The loss of sugar moiety was observed for flavonoid glycosides as the most intense fragments and for the aglycons, both bonds between carbon and oxygen in the central ring (1-2 and 3-4 bonds in C ring) are cleaved yielding characteristic fragment ions m/z 151 (Figure 2B). In case of hesperetin, the central ring can be cleaved in different position (1-2 and 2-3 bonds in C ring). The tandem mass spectra of kaempferol strongly depend on the experimental conditions and many fragment ions are observed. For the conditions used, the transition m/z 285/185 was the most intense, which corresponds to the double decarbonylation and one decarboxylation of the molecular ion and is in agreement with the literature (25).

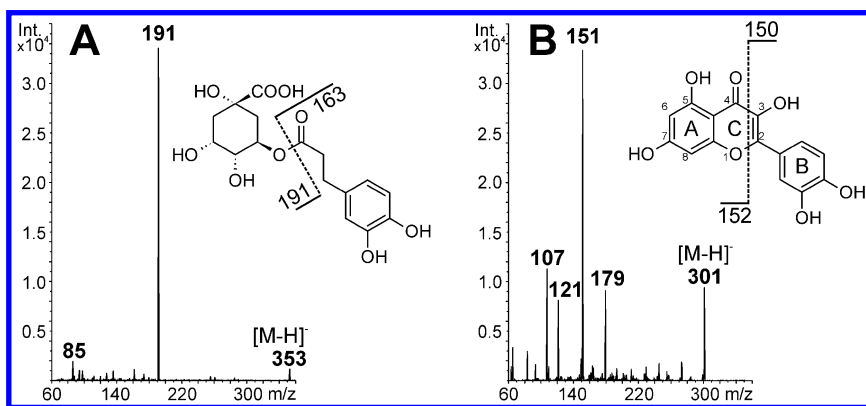


Figure 2. Tandem mass spectra and fragmentation of (A) chlorogenic acid and (B) quercetin. Electrospray ionization in the negative ion mode. For experimental conditions, see Materials and Methods.

Capillary Electrophoresis Method

In contrast to the RP-LC separation of polyphenols, the ionization of the compounds is beneficial for the separation using capillary electrophoresis. The dissociation constants (pK_a values) range from 3.91 to 4.65 for the studied set of phenolic acids (calculated using ACD/Labs Software V11.02; data obtained from SciFinder database). The values of pK_a of flavonoid glycosides and aglycones are even higher (6.17 – 7.52). Therefore, we have selected the borate background electrolyte with alkaline pH 9.3 for the separation of polyphenolic compounds using capillary electrophoresis. To improve the separation of the polyphenols from other compounds presented in *Sambucus nigra* L. infusions, the sodium decyl sulfate surfactant in concentration 36 mmol/L was added to the background electrolyte forming negatively charged micellar pseudostationary phase. The critical micelle concentration for the sodium decyl sulfate under the applied conditions is 25.4 ± 0.9 mmol/L (26, 27), and, thus, the concentration of micelles is approx. 10 mmol/L. In addition to electrophoretic migration, the analyzed compounds are separated also by partitioning between the micellar phase and bulk electrolyte. The separation of the elderflower infusion with the identified polyphenols is shown in Figure 1B. In comparison to the RP-LC analysis (Figure 1A), the separation order is reversed due to the ionization of the compounds as the effective electrophoretic mobilities are directed towards the anodic end of the capillary, which is on the injection side. Some pairs of structurally similar phenolic compounds were not resolved under these conditions (glycosides isorhamnetin- and kaempferol-3-*O*-rutinodise and neo- and cryptochlorogenic acids). To improve the separation of the critical pairs, neutral β -cyclodextrin, heptakis(2,6-di-*O*-methyl)- β -cyclodextrin and negatively charged heptakis(6-*O*-sulfo)- β -cyclodextrin were tested as the additives to the BGE. The application of neutral cyclodextrins led to the slightly improved resolution of the isomers of chlorogenic acids, however, the resolution of other compounds (*p*-coumaric acid / quercetin, isorhamnetin-3-*O*-rutinoside / isorhamnetin-3-*O*-glucoside) decreased. Negatively charged cyclodextrin also has not improved the overall separation of polyphenols in the samples of elderflower infusions. Therefore, we have used the BGE without cyclodextrins for the determination of polyphenols and the comigrating compounds were quantified as the sums.

Comparison of Quantitative Results

The quantitative analysis of *Sambucus nigra* L. infusions was performed using both developed methods, i.e. liquid chromatography-tandem mass spectrometry and capillary electrophoresis. The calibration solutions were prepared in the range of 0.5 ng/mL – 10 μ g/mL for chromatographic method and in the range of 0.5 – 200 μ g/mL for electrophoretic method, respectively. The evaluated parameters of the quantitative analyses are presented in Table II for liquid chromatography and in Table III for capillary electrophoresis.

Table II. Parameters of the Calibration Curves for Liquid Chromatography-Tandem Mass Spectrometry Method

<i>Compound</i>	<i>Slope</i> \pm <i>SD</i>	<i>Intercept</i> \pm <i>SD</i>	<i>p-Value</i> (<i>intercept</i>)	<i>R</i> ²	<i>LOD</i> (ng/mL)	<i>Linearity</i> (ng/mL)
Gallic acid	$8.04 \cdot 10^5 \pm 6.10 \cdot 10^3$	$1.41 \cdot 10^4 \pm 2.59 \cdot 10^4$	0.608	0.9997	4.55	$5 \cdot 1 \cdot 10^4$
Neochlorogenic acid	$2.64 \cdot 10^5 \pm 5.03 \cdot 10^3$	$2.85 \cdot 10^3 \pm 2.14 \cdot 10^4$	0.899	0.9982	2.38	$5 \cdot 1 \cdot 10^4$
<i>p</i> -Hydroxybenzoic acid	$8.11 \cdot 10^5 \pm 3.11 \cdot 10^4$	$2.11 \cdot 10^5 \pm 1.56 \cdot 10^5$	0.270	0.9956	49.77	$1 \cdot 10^2 \cdot 1 \cdot 10^4$
Chlorogenic acid	$5.39 \cdot 10^5 \pm 5.69 \cdot 10^3$	$7.72 \cdot 10^2 \pm 2.42 \cdot 10^4$	0.976	0.9994	1.32	$5 \cdot 1 \cdot 10^4$
Cryptochlorogenic acid	$4.16 \cdot 10^5 \pm 1.03 \cdot 10^4$	$4.28 \cdot 10^4 \pm 4.10 \cdot 10^4$	0.337	0.9963	0.76	$5 \cdot 1 \cdot 10^4$
Caffeic acid	$1.39 \cdot 10^6 \pm 3.58 \cdot 10^4$	$2.86 \cdot 10^4 \pm 1.52 \cdot 10^4$	0.119	0.9999	5.99	$5 \cdot 1 \cdot 10^4$
<i>p</i> -Coumaric acid	$1.51 \cdot 10^6 \pm 3.50 \cdot 10^4$	$1.75 \cdot 10^5 \pm 1.31 \cdot 10^5$	0.224	0.9962	0.55	$1 \cdot 1 \cdot 10^4$
Ferulic acid	$4.43 \cdot 10^4 \pm 1.78 \cdot 10^3$	$1.53 \cdot 10^3 \pm 3.45 \cdot 10^3$	0.676	0.9920	1.50	$0.5 \cdot 1 \cdot 10^3$
Isoquercitrin	$3.44 \cdot 10^5 \pm 2.20 \cdot 10^3$	$9.56 \cdot 10^3 \pm 9.33 \cdot 10^3$	0.353	0.9998	0.08	$5 \cdot 1 \cdot 10^4$
Rutin	$4.78 \cdot 10^5 \pm 4.91 \cdot 10^3$	$6.57 \cdot 10^3 \pm 1.84 \cdot 10^4$	0.732	0.9993	0.05	$0.5 \cdot 1 \cdot 10^4$
Hesperidin	$6.39 \cdot 10^5 \pm 6.14 \cdot 10^3$	$1.29 \cdot 10^5 \pm 2.18 \cdot 10^4$	0.001	0.9993	0.22	$0.5 \cdot 1 \cdot 10^4$
Kaempferol-3- <i>O</i> -rutinoside	$6.55 \cdot 10^5 \pm 1.16 \cdot 10^4$	$6.91 \cdot 10^4 \pm 4.34 \cdot 10^4$	0.155	0.9978	0.04	$1 \cdot 1 \cdot 10^4$
Isorhamnetin-3- <i>O</i> -glucoside	$3.95 \cdot 10^5 \pm 5.14 \cdot 10^3$	$-9.68 \cdot 10^2 \pm 2.04 \cdot 10^4$	0.964	0.9990	0.07	$1 \cdot 1 \cdot 10^4$
Isorhamnetin-3- <i>O</i> -rutinoside	$6.41 \cdot 10^5 \pm 9.26 \cdot 10^3$	$4.80 \cdot 10^4 \pm 3.47 \cdot 10^4$	0.209	0.9985	0.07	$1 \cdot 1 \cdot 10^4$
Quercetin	$1.51 \cdot 10^6 \pm 3.33 \cdot 10^4$	$-8.50 \cdot 10^3 \pm 1.32 \cdot 10^4$	0.544	0.9971	0.19	$0.5 \cdot 1 \cdot 10^3$
Naringenin	$2.09 \cdot 10^6 \pm 6.80 \cdot 10^4$	$2.48 \cdot 10^5 \pm 1.23 \cdot 10^5$	0.091	0.9937	0.09	$0.5 \cdot 1 \cdot 10^4$

<i>Compound</i>	<i>Slope ± SD</i>	<i>Intercept ± SD</i>	<i>p-Value (intercept)</i>	<i>R²</i>	<i>LOD (ng/mL)</i>	<i>Linearity (ng/mL)</i>
Hesperetin	$1.77 \cdot 10^6 \pm 1.62 \cdot 10^4$	$2.22 \cdot 10^4 \pm 6.86 \cdot 10^3$	0.023	0.9996	0.04	$0.5-1 \cdot 10^3$
Kaempferol	$2.91 \cdot 10^5 \pm 7.19 \cdot 10^3$	$8.16 \cdot 10^3 \pm 2.86 \cdot 10^3$	0.029	0.9963	0.07	$0.5-1 \cdot 10^3$

Table III. Parameters of the Calibration Curves for Capillary Electrophoretic Method

<i>Compound</i>	<i>Slope ± SD</i>	<i>Intercept ± SD</i>	<i>p-Value (intercept)</i>	<i>R²</i>	<i>LOD (ng/mL)</i>	<i>Linearity (µg/mL)</i>
Gallic acid	34.41 ± 0.36	-0.29 ± 15.47	0.986	0.9995	211.3	0.5-1·10 ²
Neochlorogenic acid ^a	6.18 ± 0.05	4.04 ± 2.28	0.137	0.9996	223.9	0.5-1·10 ²
<i>p</i> -Hydroxybenzoic acid	19.94 ± 0.38	2.32 ± 16.34	0.893	0.9982	92.6	0.5-1·10 ²
Chlorogenic acid	5.67 ± 0.07	7.77 ± 2.85	0.042	0.9993	141.5	0.5-1·10 ²
Cryptochlorogenic acid ^a	6.54 ± 0.09	-4.32 ± 4.10	0.340	0.9990	241.9	0.5-1·10 ²
Caffeic acid	25.36 ± 0.21	14.17 ± 8.86	0.171	0.9997	111.9	0.5-1·10 ²
<i>p</i> -Coumaric acid	17.21 ± 0.32	-15.11 ± 13.85	0.325	0.9983	80.6	0.5-1·10 ²
Ferulic acid	14.77 ± 0.17	7.92 ± 7.12	0.317	0.9994	138.9	0.5-1·10 ²
Isoquercitrin	12.05 ± 0.10	-0.21 ± 4.75	0.967	0.9997	252.1	1-1·10 ²
Rutin	6.48 ± 0.09	16.95 ± 8.04	0.073	0.9987	118.1	0.5-2·10 ²
Hesperidin	6.52 ± 0.22	13.20 ± 10.35	0.271	0.9954	405.4	0.5-1·10 ²
Kaempferol-3- <i>O</i> -rutinoside, isorhamnetin-3- <i>O</i> -rutinoside ^a	7.41 ± 0.14	-10.72 ± 11.88	0.408	0.9983	133.3	1-1·10 ²
Isorhamnetin-3- <i>O</i> -glucoside	9.07 ± 0.12	7.80 ± 5.19	0.193	0.9991	76.9	0.5-1·10 ²
Quercetin	16.56 ± 2.90	-28.73 ± 29.80	0.406	0.9155	319.1	0.5-20
Naringenin	14.30 ± 0.16	5.36 ± 6.98	0.477	0.9994	53.8	0.5-1·10 ²

<i>Compound</i>	<i>Slope ± SD</i>	<i>Intercept ± SD</i>	<i>p-Value (intercept)</i>	<i>R²</i>	<i>LOD (ng/ mL)</i>	<i>Linearity (µg/mL)</i>
Hesperetin	15.94 ± 0.24	13.62 ± 10.19	0.239	0.9989	66.1	0.5-1 · 10 ²
Kaempferol	22.37 ± 0.62	-61.92 ± 26.93	0.070	0.9961	428.6	0.5-1 · 10 ²

^a The compounds are not resolved under applied conditions.

Table IV. Results of the Quantitative Analysis of Sambucus nigra L. Infusions

<i>Compound</i>	<i>Sample series</i>	<i>Average concentration, (mg/g)</i>		<i>Repeatability of analysis (n = 3) and infusions (n = 5), SD (mg/g)</i>			
		<i>LC/MS</i>	<i>CE</i>	<i>Analysis, LC/MS</i>	<i>Analysis, CE</i>	<i>Infusion, LC/MS</i>	<i>Infusion, CE</i>
Gallic acid	1.	0.10	0.19	0.01	0.08	0.01	0.04
	2.	0.09	0.06	0.01	0.06	0.02	0.04
	3.	0.07	- ^a	0.01	- ^a	0.01	- ^a
Neochlorogenic acid	1.	4.73	5.15 ^b	0.47	0.10 ^b	0.47	0.33 ^b
	2.	3.97	5.21 ^b	0.33	0.14 ^b	0.80	0.62 ^b
	3.	5.05	4.02 ^b	0.44	0.19 ^b	0.51	0.31 ^b
<i>p</i> -Hydroxybenzoic acid	1.	0.19	0.32	0.03	0.07	0.02	0.05
	2.	0.28	0.46	0.03	0.14	0.05	0.06
	3.	0.07	0.18	0.01	0.02	0.01	0.10
Chlorogenic acid	1.	26.91	11.04	1.87	0.18	3.35	0.58
	2.	25.50	12.42	1.61	0.19	4.57	1.37
	3.	14.32	6.50	1.10	0.07	1.17	0.66
Cryptochlorogenic acid	1.	2.96	- ^b	0.36	- ^b	0.17	- ^a
	2.	2.53	- ^b	0.29	- ^b	0.52	- ^a
	3.	1.81	- ^b	0.23	- ^b	0.31	- ^a

<i>Compound</i>	<i>Sample series</i>	<i>Average concentration, (mg/g)</i>		<i>Repeatability of analysis (n = 3) and infusions (n = 5), SD (mg/g)</i>			
		<i>LC/MS</i>	<i>CE</i>	<i>Analysis, LC/MS</i>	<i>Analysis, CE</i>	<i>Infusion, LC/MS</i>	<i>Infusion, CE</i>
Caffeic acid	1.	0.23	0.28	0.02	0.04	0.02	0.06
	2.	0.39	0.32	0.03	0.08	0.08	0.04
	3.	0.15	0.20	0.01	0.01	0.02	0.10
p-Coumaric acid	1.	0.11	- ^a	0.02	- ^a	0.02	- ^a
	2.	0.15	- ^a	0.01	- ^a	0.03	- ^a
	3.	0.04	- ^a	0.01	- ^a	0.01	- ^a
Ferulic acid	1.	0.19	0.33	0.02	0.04	0.02	0.05
	2.	0.22	0.43	0.03	0.04	0.04	0.25
	3.	0.08	0.18	0.02	0.05	0.01	0.07
Isoquercitrin	1.	1.14	1.64	0.03	0.03	0.19	0.16
	2.	1.15	1.80	0.05	0.25	0.22	0.30
	3.	0.41	0.66	0.01	0.03	0.29	0.31
Rutin	1.	26.38	17.46	0.65	0.65	3.24	1.01
	2.	25.65	21.59	0.42	0.27	4.84	1.95
	3.	16.56	12.83	0.72	0.27	1.47	0.74

Continued on next page.

Table IV. (Continued). Results of the Quantitative Analysis of Sambucus nigra L. Infusions

Compound	Sample series	Average concentration, (mg/g)		Repeatability of analysis (n = 3) and infusions (n = 5), SD (mg/g)			
		LC/MS	CE	Analysis, LC/MS	Analysis, CE	Infusion, LC/MS	Infusion, CE
Hesperidin	1.	10.15	- ^a	0.53	- ^a	1.55	- ^a
	2.	10.24	- ^a	0.56	- ^a	1.85	- ^a
	3.	6.56	- ^a	0.54	- ^a	0.59	- ^a
Kaempferol-3- <i>O</i> -rutinoside	1.	0.78	3.21 ^c	0.04	0.04 ^c	0.13	0.18 ^c
	2.	0.83	4.20 ^c	0.04	0.07 ^c	0.17	0.30 ^c
	3.	0.36	3.28 ^c	0.03	0.04 ^c	0.04	0.21 ^c
Isorhamnetin-3- <i>O</i> -glucoside	1.	1.03	0.89	0.01	0.02	0.19	0.09
	2.	1.15	1.34	0.03	0.07	0.23	0.29
	3.	0.59	0.69	0.02	0.07	0.12	0.20
Isorhamnetin-3- <i>O</i> -rutinoside	1.	2.52	- ^c	0.06	- ^c	0.40	- ^c
	2.	2.95	- ^c	0.05	- ^c	0.61	- ^c
	3.	2.71	- ^c	0.15	- ^c	0.38	- ^c
Naringenin	1.	0.83	0.92	0.05	0.04	0.17	0.07
	2.	1.00	1.08	0.05	0.06	0.20	0.09
	3.	0.50	0.61	0.03	0.04	0.08	0.11

^a The concentration of the compound is below the detection limit of the method. ^b The sum of the crypto- and neochlorogenic acid was determined. ^c The sum of the kaempferol-3-*O*-rutinoside and isorhamnetin-3-*O*-rutinoside was determined.

For the liquid chromatography-tandem mass spectrometry method, the calibration data can be considered linear for most of the compounds, at least in the range of three orders of concentration. The coefficients of determination of the linear regression of the data are higher than 0.99 for all compounds. The hypothesis that the intercepts of the calibration curves are statistically insignificant was tested using Student's *t*-test. The calibration curves can be reasonably assumed to pass through zero for almost all tested compounds as the statistical *p*-values of the intercepts at the 95 % significance level is higher than 0.05. The intercepts are statistically significant only for hesperidin, hesperetin and kaempferol. The limits of detection calculated as the concentration yielding signal-to-noise ratio equal to three are between 0.04 and 50 ng/mL. The sensitivity of the method, i.e. the slope of the calibration equations is slightly higher for the phenolic acids and flavonoid aglycones than for flavonoid glycosides. It can be probably attributed to the facile ionization of the carboxylic groups of the acids and hydroxyl-groups presented on the flavonoid skeleton, rather than the hydroxyls in the sugar moieties.

The developed capillary electrophoretic method uses the UV detection, which has narrower linearity range in comparison to the mass spectrometric detection. The utilization of the separation capillary with extended light path detection cell, however, improves the detection sensitivity and increases the linear dynamic range in comparison to the ordinary fused silica capillaries. The electrophoretic calibration data can be considered linear in the range of two-orders of the concentrations (generally in the range of 0.5 – 100 µg/mL) and the limits of detection are in the range of tenths of µg/mL (Table III). The limits of detection for the developed method are slightly lower and the sensitivity (i.e. the slope of the calibration curves) is approximately four times higher in comparison to the values presented for our recently published electrophoretic method employing 25 µm i.d. capillary with detection cell extended to 125 µm (28). The lower limits of detection and higher sensitivity of current method can be probably attributed to the higher injected sample volume and also to the increased internal diameter of the separation capillary including detection cell diameter in current method (50 µm i.d. extended to 150 µm in the cell compared to 25 µm i.d. extended to 125 µm). The coefficients of determination were higher than 0.995 for most of the compounds. Among the tested compounds, the intercept of the linear calibration equation was statistically significant only for chlorogenic acid, which was indicated with the *p*-value of 0.042 lower than critical value 0.05.

The three series of the *Sambucus nigra* L. infusions were quantitatively analyzed using developed methods. Using these results, we have studied the effects of the preparation of infusion and sample type on the content of polyphenolic compounds. Moreover, we have compared both methods developed for quantitative analysis of polyphenolic compounds in terms of the determined concentrations and repeatability of the analyses. Thus three series of the elderflower infusions were prepared. The first and the second series of infusions were prepared from the same batch of herbal tea. In the first series, the infusions were prepared from the adjusted tea bags, while in the second series twenty tea bags were opened and mixed together and the appropriate amount of the elderflower was taken for the preparation of infusion. The third series of

infusions was prepared from air-dried wild growing elderflower. The results of the quantitative analysis are presented in Table IV. The determined concentrations of the polyphenolic compounds were related to the 1 g of the dry elderflower.

The polyphenolic profile of the *Sambucus nigra* L. infusions determined by both methods is consistent with the literature (2, 18). In particular, the highest content of chlorogenic acid and rutin were observed followed with the other polyphenolic compounds, but the exact concentrations are strongly dependent on the extraneous influences (e.g. cultivar, place of origin, treatment of the sample) (6). For example, the concentrations of flavonoids and their glycosides determined in inflorescence samples of *Sambucus nigra* L. presented by Barros et al. are in agreement with our presented results, however, the concentration levels of phenolic acids (especially isomers of chlorogenic acid) determined in our work are significantly higher (2). For both methods, the repeatability of the analyses represented by the relative standard deviations of concentrations is lower than 5 % for the most of the compounds. The deviations between the infusions are significantly higher, ranging from 5 % to 25 % for liquid chromatographic method and up to 50 % for electrophoretic method. To reveal the significant differences between the analyses of infusions and the method used, a two-way ANOVA was performed for each analyte. The results of the analysis of variance showed that in most cases the differences between the consecutive analyses of each infusion are not statistically significant. Also the differences between the infusions within the series of elderflower samples were not significant for the most of the compounds, however, the standard deviations are higher, than for the consecutive analyses of each infusion. The most important differences were however discovered between the applied methods, especially for the compounds with higher abundance in the samples (chlorogenic acid, rutin).

To further compare the results obtained using both liquid chromatographic and capillary electrophoretic methods, the correlation plots of the determined concentrations were constructed. The plots are shown in Figure 3. As can be seen from the higher part of the figure, the coefficient of determination 0.89 indicated, that the concentrations determined using both methods are correlated. The slope of the regression line is however significantly lower than one, which would be expected if both methods provided the same results. The bottom part of Figure 3 represents the regression line fitted to the concentration data of less abundant polyphenolic compounds. The slope of the regression line for less abundant compounds is not significantly different from one and the correlation coefficient is higher than in the previous case. One of the possible sources of the differences between the concentrations of the most abundant polyphenols (rutin, chlorogenic acid) presented in elderflower samples determined using liquid chromatography and capillary electrophoresis can be attributed to ionization suppression in the mass spectrometric detection (29, 30). These matrix effects can play a significant role, especially when the compounds of interest coelute with other compounds, which is the case for rutin, isoquercitrin and hesperidin. To confirm the accuracy of the presented methods, analysis of certified reference material is required, which is not readily available for the herb matrices.

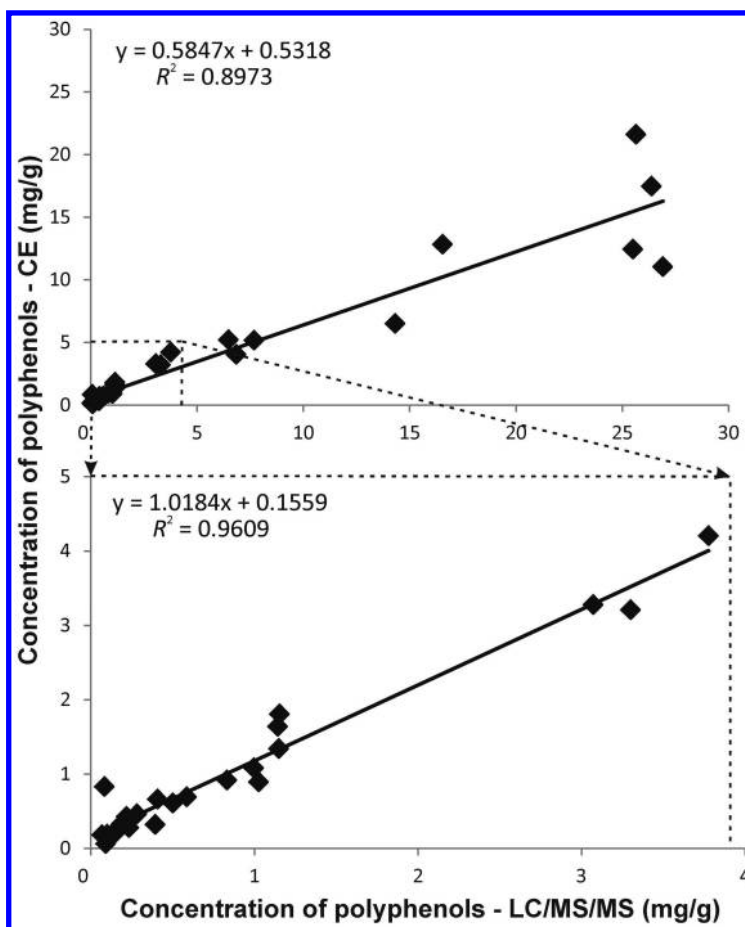


Figure 3. Correlation of the concentrations of polyphenolic compounds in *Sambucus nigra* L. infusions determined by liquid chromatography-tandem mass spectrometry method and capillary electrophoretic method.

Conclusions

In the present work, two methods for the characterization of *Sambucus nigra* L. infusions have been developed. Liquid chromatography-tandem mass spectrometry and capillary electrophoresis with UV detection have been used for the separation and quantification of 18 polyphenolic compounds including phenolic acids, flavonoid aglycones and glycosides. The quantitative results of both methods were compared and the effects of the samples' nature and sample preparation were evaluated. Statistically significant differences were found between the concentrations of the most abundant polyphenolic compounds

determined using both methods, however, a high correlation between the results was obtained for the compounds presented in elderflower infusions at lower concentration levels.

References

1. Kite, G. C.; Larsson, S.; Veitch, N. C.; Porter, E. A.; Ding, N.; Simmonds, M. S. *J. Agric. Food Chem.* **2013**, *61*, 3501–3508.
2. Barros, L.; Duenas, M.; Carvalho, A. M.; Ferreira, I. C. F. R.; Santos-Buelga, C. *Food Chem. Toxicol.* **2012**, *50*, 1576–1582.
3. Scopel, M.; Mentz, L. A.; Henriques, A. T. *Planta Med.* **2010**, *76*, 1026–1031.
4. Huck, C. W.; Buchmeiser, M. R.; Bonn, G. K. *J. Chromatogr. A* **2001**, *943*, 33–38.
5. Rieger, G.; Müller, M.; Guttenberger, H.; Bucar, F. *J. Agric. Food Chem.* **2008**, *56*, 9080–9086.
6. Christensen, L. P.; Kaack, K.; Fretté, X. C. *Eur. Food Res. Technol.* **2008**, *227*, 293–305.
7. Dawidowicz, A. L.; Wianowska, D.; Gawdzik, J.; Smolarz, D. H. *J. Liq. Chromatogr. Relat. Technol.* **2003**, *26*, 2381–2397.
8. Dawidowicz, A. L.; Wianowska, D.; Baraniak, B. *LWT* **2006**, *39*, 308–315.
9. Pietta, P.; Bruno, A.; Mauri, P.; Rava, A. *J. Chromatogr.* **1992**, *593*, 165–170.
10. Gouveia, S. C.; Castilho, P. C. *Rapid Commun. Mass Spectrom.* **2010**, *24*, 1851–1868.
11. Gouveia, S. C.; Goncalves, J.; Castilho, P. C. *Ind. Crop. Prod.* **2013**, *42*, 573–582.
12. Chrubasik, C.; Maier, T.; Dawid, C.; Torda, T.; Schieber, A.; Hofmann, T.; Chrubasik, S. *Phytother. Res.* **2008**, *22*, 913–918.
13. Lin, L. Z.; Harnly, J. M. *J. Agric. Food Chem.* **2007**, *55*, 1084–1096.
14. Celik, S. E.; Özyürek, M.; Güclü, K.; Capanoglu, E.; Apak, R. *Phytochem. Anal.* **2014**, *25*, 147–154.
15. Barros, L.; Cabrita, L.; Vilas Boas, M.; Carvalho, A. M.; Ferreira, I. C. F. R. *Food Chem.* **2011**, *127*, 1600–1608.
16. Seitz, U.; Bonn, G.; Oefner, P.; Popp, M. *J. Chromatogr.* **1991**, *559*, 499–504.
17. Seitz, U.; Oefner, P. J.; Nathakarnkitkool, S.; Popp, M.; Bonn, G. K. *Electrophoresis* **1992**, *13*, 35–38.
18. Urbánek, M.; Pospíšilová, M.; Polášek, M. *Electrophoresis* **2002**, *23*, 1045–1052.
19. Česla, P.; Hájek, T.; Jandera, P. *J. Chromatogr. A* **2009**, *1216*, 3443–3457.
20. Tranchida, P. Q.; Donato, P.; Cacciola, F.; Beccaria, M.; Dugo, P.; Mondello, L. *TRAC-Trends Anal. Chem.* **2013**, *52*, 186–205.
21. Jandera, P.; Hájek, T.; Staňková, M.; Vyňuchalová, K.; Česla, P. *J. Chromatogr. A* **2012**, *1268*, 91–101.
22. Willemse, C. M.; Stander, M. A.; de Villiers, A. *J. Chromatogr. A* **2013**, *1319*, 127–140.
23. Česla, P.; Fischer, J.; Jandera, P. *Electrophoresis* **2010**, *31*, 2200–2210.

24. Guiochon, G.; Gritti, F. *J. Chromatogr. A* **2011**, *1218*, 1915–1938.
25. March, R. E.; Miao, X. S. *Int. J. Mass Spectrom.* **2004**, *231*, 157–167.
26. Váňová, J. M.S. Thesis, University of Pardubice, Pardubice, Czech Republic, 2012.
27. Váňová, J.; Česla, P.; Fischer, J.; Jandera, P. In *CECE 2012 9th International Interdisciplinary Meeting on Bioanalysis*; Foret, F., Křenková, J., Guttman, A., Klepárník, K., Boček, P., Eds.; Publisher: Brno, Czech Republic, 2012; pp 193–199.
28. Česla, P.; Fischer, J.; Jandera, P. *Electrophoresis* **2012**, *33*, 2464–2473.
29. Taylor, P. J. *Clin. Biochem.* **2005**, *38*, 328–334.
30. Gosetti, F.; Mazzucco, E.; Zampieri, D.; Gennaro, M. C. *J. Chromatogr. A* **2010**, *1217*, 3929–3937.

Chapter 9

Flavonoid C-glycosides in *Citrus* Juices from Southern Italy: Distribution and Influence on the Antioxidant Activity

Davide Barreca, Ersilia Bellocco, Ugo Leuzzi, and Giuseppe Gattuso*

Dipartimento di Scienze Chimiche, Università di Messina,
Viale F. Stagno d'Alcontres 31, 98166 Messina, Italy

*E-mail: ggattuso@unime.it.

Flavonoid C-glycosides are key constituents of the flavonoid fraction of *Citrus* juices. By drawing on the results presented over the past few years by our research group, a survey on the presence of these derivatives in the juices from eleven different *Citrus* species cultivated in Southern Italy shows that, so far, 12 individual derivatives have been identified and quantified, in variable amounts ranging from traces to 30–60 mg/L in the richer juices (*C. sinensis*, *C. bergamia* and *C. medica*). In addition, and in-depth study on *C. reticulata* × *C. paradisi* juice led to a critical analysis of the role these flavone derivatives play in the antioxidant activity of fresh *Citrus* juices.

Introduction

Der Mensch ist, was er ißt, or man is what he eats (L. A. Feuerbach (1)). Over the past few years, growing consumer awareness about the beneficial effects of a healthy diet has determined a very fast market expansion for dietary supplements and functional foods. Research on nutraceuticals has been the driving force behind this boom, providing evidence on the health-improving action of nutritious food, as well as relentlessly pursuing hitherto unexploited dietary sources.

Many supplements and functional foods have been prepared taking advantage, as the key ingredient, of citrus or citrus-derived products, being *Citrus* species among the best-known natural sources of health-beneficial compounds (2–6). In particular, aside from ascorbic acids, citrus fruits are extremely rich in flavonoids, a broad group of polyphenolic compounds whose radical scavenging

(7), chronic diseases-preventing (8, 9) abilities and biological activity (10–12) have been largely demonstrated. Furthermore, many studies highlighted their antiviral (13), antimicrobial (14, 15), and anti-inflammatory (16), antiulcer (17) and antiallergenic (18) properties.

Citrus juices are generally characterized by the presence of several flavonoid components, belonging to the flavanone, flavone, flavonol, flavanol and dihydrochalcone subclasses. However, the general trend observed showed that flavanone derivatives are usually the most abundant individual components, whereas flavones are the ones that are seen with the largest variability.

Flavonoids in *Citrus* juices are seldom found as their aglycones. Being the juice an aqueous environment, they often occur as glycosylated derivatives, whereas the less polar aglycones, along with the equally lipophilic polymethoxyflavones, are located in the essential oil vesicles in the flavedo layer of the peel. So far, the vast majority of the glycosylated flavonoids identified in the juices bear, as saccharide substituents, only a very limited set of hexoses, namely D-glucose and L-rhamnose, either as monosaccharides or as the disaccharides rutinose and neohesperidose (α -(1→6)-L-rhamnopyranosyl- β -D-glucopyranose and α -(1→2)-L-rhamnopyranosyl- β -D-glucopyranose, respectively), both composed of glucose and rhamnose, but differing in the position of the interglycosidic linkage.

Furthermore, the saccharide substituents may be found linked to the aglycone skeleton either as *O*-glycosides or as the less conventional *C*-glycosides. The latter derivatives possess significantly different chemical properties than their *O*-linked counterparts, especially (*vide infra*) in terms of their resistance to acidic hydrolysis. Interestingly, with very few notable exceptions, in *Citrus* *C*-glycosyl substituents are found only on flavone aglycones.

Even though *C*-glycosides are the main flavonoid components in other plant species (e.g., millet), they have enjoyed less attention than the better-known *O*-glycosides. Different classes of flavonoids (and their derivatives) have often a different functions, and *C*-glycosyl flavonoids have been shown to play, *in vivo*, the role of insect feeding attractants, antimicrobial agents and UV-protective pigments (19). *In vitro*, on the other hand, they can prevent tissue oxidation, and cancer development, but they have been also suspected of preventing thyroidal iodine uptake (19).

Within this frame, there is surely still room for further investigations, both on the natural plant sources of *C*-glycosyl flavonoids, and the activity of these interesting compounds.

Results and Discussion

C-Glycosyl Flavonoids in *Citrus* Juices

We have been involved, in the past decade, in a long-term project aimed at characterizing the flavonoid and furocoumarin fraction of the juice of fruits from *Citrus* species grown in Southern Italy (Sicily and Calabria regions (20)). To this end, we have optimized a reverse-phase HPLC-DAD-ESI-MS-MS analytical protocol that allows us to identify and quantify flavonoid components

in a single chromatographic course (21). Fresh juice samples are prepared by hand-squeezing fruits that were preliminary peeled to avoid contamination by the lipophilic components present in the flavedo and albedo sections. The juice is then centrifuged, and the supernatant is diluted with DMF (1:1) prior to injection, thus avoiding any preliminary extraction procedure. Analytes separation, carried out on a C-18 column with a water/acetonitrile gradient, takes advantage of simultaneous DAD detection at 278, 310 and 325 nm, that allows for a first discrimination between flavones, flavanones and furocoumarins. In fact, at 278 nm both flavones and flavanones have a strong – and comparable in intensity – absorption band (the so-called ‘band II’), while at 325 nm flavones have a much stronger ‘band I’ absorption than the one observed for flavanones. In such a manner, comparison of the two chromatograms provides immediate indication on the nature of the aglycone of the various flavonoid derivatives. In addition, detection at 310 nm helps in identifying the possible presence of furocoumarins components.

The nature of the glycosidic linkage can be assessed by parallel acidic digestion of the juice (22). Treatment of the juice sample with 6M HCl in methanol/water mixture at 90°C for two hours results in the complete hydrolysis of the *O*-linked saccharide substituent, whereas *C*-linked saccharides do not react under these experimental conditions. Inspection of the hydrolyzed juice by HPLC, and comparison of the resulting chromatogram with the one obtained for the fresh sample, allows for the unambiguous assignment of a *C*-glycosidic bond to those compounds whose peak has not disappeared.

Definitive structural elucidation is carried out by means of ESI-MS-MS. MS² techniques have proved to be a powerful and convenient technique in flavonoid identification. Careful analysis of the fragmentation pattern of the analytes provides evidence on the nature of the aglycone, the nature and number of saccharides bound to the aglycone, the position of the substituents on the aglycone core. Moreover, it provides unambiguous evidence on whether the sugar units are present as mono- or disaccharides and, in the latter case, the position of interglycosidic bond. This subject has been discussed in detail in previous publications by our group (3), and has been extensively reviewed (23). Quantification of the flavonoid component is obtained by means of selected reaction monitoring (SRM) (24).

In the course of our studies, we carried out in-depth investigation on eleven different *Citrus* species (Table I). Flavonoid *C*-glycosides have been found in all the species investigated (collectively shown in Figure 1) and with the exception of phloretin 3',5'-di-*C*-glucoside **12** – which is a dihydrochalcone – they were assigned a flavone skeleton. On reverse-phase columns, they generally elute with shorter retention times than their corresponding *O*-glycosides. Furthermore, as it may be expected di-*C*-glycosyl flavones elutes earlier than the corresponding mono-*C*-glycosyl flavones. As for the latter, 8-*C*-glycosyl flavones have usually shorter retention times than the corresponding 6-*C*-glycosyl derivatives.

Of all the species investigated, *C. bergamia* (27, 28), *C. sinensis* (21, 25), *C. limon* (22) and *C. medica* (22) were found to be the richest in *C*-glucosyl flavones, with bergamot presenting also the highest variety of individual compounds (Table II). In addition, at first glance two compounds stand out

as being the main *C*-glucosides in most of the species investigated, namely, apigenin-6,8-di-*C*-glucoside (vicenin-2, **2**) and diosmetin-6,8-di-*C*-glucoside (lucenin-2 4'-*O*-methyl ether, **3**).

C. bergamia was found to be very rich in both vicenin-2 **2** and lucenin-2 4'-*O*-methyl ether **3**, containing in the three cultivars examined, variable amounts of 38.0–58.4 mg/L for the former, and 22.1–66.8 mg/L for the latter, with the "Femminello" variety being the one with the highest content. The other components are present in lower amount, ranging from the remarkable 5.1–10.1 mg/L determined for scoparin **6** to the small amounts observed for stellarin-2 (chrysoeriol 6,8-di-*C*-glucoside, **4**, 0.5–1.3 mg/L).

Table I. *Citrus species* Investigated

<i>Binomial name</i>	<i>Cultivar(s)</i>	<i>Common name(s)</i>	<i>Ref.</i>
<i>C. sinensis</i>	Moro Tarocco	blood orange	(21, 25)
<i>C. reticulata</i> × <i>C. paradisi</i>		tangelo, mapo	(26)
<i>C. bergamia</i>	Femminello Fantastico Castagnaro	bergamot	(27, 28)
<i>C. limetta</i>		Mediterranean sweet lemon, limetta	(29)
<i>C. japonica</i>		kumquat	(30)
<i>C. aurantium</i>		sour orange, bitter orange	(24)
<i>C. myrtifolia</i>		myrtle-leaved orange, chinotto	(31)
<i>C. limon</i>	Femminello Interdonato Monachello	lemon	(22)
<i>C. medica</i>	Diamante	citron	(22)
<i>C. reticulata</i>		tangerine	(22)
<i>C. deliciosa</i>		clementine	(22)

A fairly different picture emerges for *C. sinensis* (Moro and Tarocco varieties) (21, 25). In this case, along with vicenin-2 **2** (37.0–53.0 mg/L), stellarin-2 **4** was found to be present in high amount (22.13±0.88 mg/L), with lucenin-2 **1** (10.48±0.56 mg/L) and scoparin **6** (7.14±0.88 mg/L) following closely.

	R ₁	R ₂	R ₃	R ₄	R ₅	Compound name
1	H	Glu	Glu	OH	OH	Luteolin 6,8-di- <i>C</i> -glucoside (Lucenin-2)
2	H	Glu	Glu	H	OH	Apigenin 6,8-di- <i>C</i> -glucoside (Vicenin-2)
3	H	Glu	Glu	OH	OMe	Diosmetin 6,8-di- <i>C</i> -glucoside (Lucenin-2 4'-methyl ether)
4	H	Glu	Glu	OMe	OH	Chrysoeriol 6,8-di- <i>C</i> -glucoside (Stellarin-2)
5	H	Glu	H	H	OH	Apigenin 6- <i>C</i> -glucoside (Isovitexin)
6	H	H	Glu	OMe	OH	Chrysoeriol 8- <i>C</i> -glucoside (Scoparin)
7	H	H	Glu	OH	OMe	Diosmetin 8- <i>C</i> -glucoside (Orientin 4'-methyl ether)
8	Glu	Glu	H	H	OMe	Acacetin 3,6-di- <i>C</i> -glucoside
9	H	H	Nh [†]	H	OH	Apigenin 8- <i>C</i> -neohesperidoside
10	H	H	Nh [†]	H	OMe	Acacetin 8- <i>C</i> -neohesperidoside (2"- <i>O</i> -rhamnosyl cytisoside)
11	H	Nh [†]	H	H	OMe	Acacetin 6- <i>C</i> -neohesperidoside (2"- <i>O</i> -rhamnosyl isocytisoside)

†Neohesperidosyl

12 Phloretin 3',5'-di-*C*-glucoside

Figure 1. Flavone-*C*-glycosides found in the juice of *Citrus* spp. investigated. Trivial names are indicated in parentheses.

In the case of *C. medica* and *C. limon* (citron and lemon (22)), lucenin-2 4'-*O*-methyl ether **3** by far surpasses vicenin-2 **2**, with 36–60 mg/L vs. 9–16 mg/L in lemon, and 61–68 mg/L vs. 6–8 mg/L in citron. On the contrary, in the juice of *C. reticulata* and *C. clementina* it is vicenin-2 **2** that is more abundant than lucenin-2 4'-*O*-methyl ether **3**, with 23–27 mg/L vs. 6–8 mg/L for the former, and 4–6 mg/L vs. 1–3 mg/L for the latter.

Table II. C-Glycosyl flavonoids (1–12, Figure 1) found in the juice of investigated *Citrus* spp. (mg/L)

	<i>C. sinensis</i>	<i>C. reticulata</i> × <i>C. paradisi</i>	<i>C. limetta</i>	<i>C. japonica</i>	<i>C. aurantium</i>	<i>C. myrtifolia</i>	<i>C. bergamia</i>	<i>C. limon</i>	<i>C. medica</i>	<i>C. reticulata</i>	<i>C. clementina</i>
1	10.48±0.56	0.10±0.012	n.o.	n.o.	0.12±0.05	n.o.	2.1–3.5 ^(b)	–	–	–	–
2	37.0–53.0 ^(a)	3.89±0.111	0.37±0.02	tr.	1.54±0.21	0.58±0.04	38.0–58.4 ^(b)	9–16 ^(c)	6–8	23–27	4–6
3	2.0–11.7 ^(a)	n.o.	0.75±0.05	tr.	0.45±0.03	0.20±0.02	22.1–66.8 ^(b)	36–60 ^(c)	61–68	6–8	1–3
4	22.13±2.27	n.o.	n.o.	n.o.	n.o.	n.o.	0.5–1.3 ^(b)	–	–	–	–
5	n.o.	n.o.	n.o.	n.o.	n.o.	n.o.	2.1–3.2 ^(b)	–	–	–	–
6	7.14±0.88	n.o.	0.10±0.03	n.o.	n.o.	n.o.	5.1–10.1 ^(b)	–	–	–	–
7	n.o.	n.o.	0.10±0.04	n.o.	n.o.	n.o.	1.3–4.8 ^(b)	–	–	–	–
8	n.o.	n.o.	n.o.	tr.	n.o.	n.o.	n.o.	–	–	–	–
9	n.o.	n.o.	n.o.	0.26±0.01	n.o.	n.o.	n.o.	–	–	–	–
10	n.o.	n.o.	n.o.	0.60±0.03	n.o.	n.o.	n.o.	–	–	–	–
11	n.o.	n.o.	n.o.	0.70±0.05	n.o.	n.o.	n.o.	–	–	–	–
12	n.o.	n.o.	n.o.	19.94±0.40	n.o.	n.o.	n.o.	–	–	–	–

^(a) Range determined for Tarocco and Moro cultivars. ^(b) Range determined for Femminello, Fantastico and Castagnaro cultivars. ^(c) Range determined for Femminello comune, Inerdonato and Monachello cultivars. n.o.: not observed; fields marked as "–" refer to compounds not investigated.

Data in our hands lend themselves to critical analysis. It has been often stressed that the flavonoid chromatographic profile of a given *Citrus* juice can be used both as a fingerprint to identify the species from which it originates and/or potential adulteration, and as a tool to reveal (or confirm) taxonomical relations between different species. It is interesting to observe that, even restricting the analysis to the *C*-glucosyl flavones, few clear connections become evident.

Lemon and citron, which are known to be related (32), share a similar profile, with the diosmetin derivative lucenin-2 4'-*O*-methyl ether **3** as the main compound. *C. limetta* (29), which is also related to these two species, has a similar profile, albeit the amount of *C*-glucosyl flavones present in the juice is so much lower that it is not safe to speculate – basing only on these data – on its taxonomic connection.

In a similar fashion, orange, tangerine (22) and clementine (22) all display the apigenin derivative vicenin-2 **2** as their main flavone *C*-glucoside component. Bergamot, which is a hybrid of citron and sour orange, presents – even if in larger amount than in the parent species – both the *C*-glucosides that characterize the two species, lucenin-2 4'-*O*-methyl ether **3** and vicenin-2 **2**, respectively. Myrtle-leaved orange, which is a mutation of sour orange, possesses a *C*-glucosyl flavone profile that is almost superimposable to that of its parent species, *C. aurantium*.

C. japonica (kumquat (30, 33)) possesses a totally different set of *C*-glycosyl derivatives. The most prominent compound is not a flavone, but rather a dihydrochalcone, namely phloretin 3',5'-di-*C*-glucoside. This is a rather unique compound in the *Citrus* genus, setting kumquat apart from the rest of the commonly grown species. In addition, a wide variety of mono- and di-*C*-glucosyl flavones was detected in kumquat juice, albeit in low amount (typically, < 1 mg/L). Among these, derivatives that seldom are seen in the *Citrus* genus were identified, such as the acacetin 6- or 8-*C*-neohesperidosides. In light of its peculiarity, it is not surprising that for about a century kumquat varieties had been allotted a separate genus, *Fortunella* (34).

Antioxidant Activity Studies

The antioxidant activity of *Citrus* juices descends from the concerted action of a wide variety of compounds able to quench 'free radicals' with different mechanism and efficiency. Best known among these are vitamin C and the broad family of the flavonoids.

As mentioned above, *C*-glucosyl flavones have not been studied intensively for their antioxidant activity. In order to shed light on the contribution this subclass of compounds provides to the radical scavenging and reducing activity of the juice, we decided to turn to preparative HPLC to separate the various flavonoid subclasses. Tangelo (*C. reticulata* × *C. paradisi*) juice (26) was selected as a good candidate, owing to the good variety displayed by its juice. In fact, it was shown to contain *C*-glucosyl flavones (lucenin-2 **1** and vicenin-2 **2**), an *O*-rutosyl flavonol (rutin), a number of di- and tri-*O*-glycosyl flavanones (neoriocitrin, narirutin, neohesperidin, didymin and narirutin 4'-*O*-glucoside) and polymethoxyflavones (sinensetin, nobiletin and tangeretin), thus allowing to collect a significant set of representative compounds.

Six broad fractions were collected (Figure 2): the first one containing all the flavonoids (henceforth referred to as FP, flavonoid pool fraction), and five additional ones containing each all the members of a single flavonoid subclass, that is di-*C*-glucosyl flavones (fraction I), *O*-triglycosyl flavanones (II), *O*-diglycosyl flavonols (III), *O*-diglycosyl flavanones (IV) and polymethoxyflavones (V) (26).

The fractions were collected, evaporated to dryness, and then redissolved in the stipulated amount of solvent needed to restore the original concentration the analytes had in fresh juice.

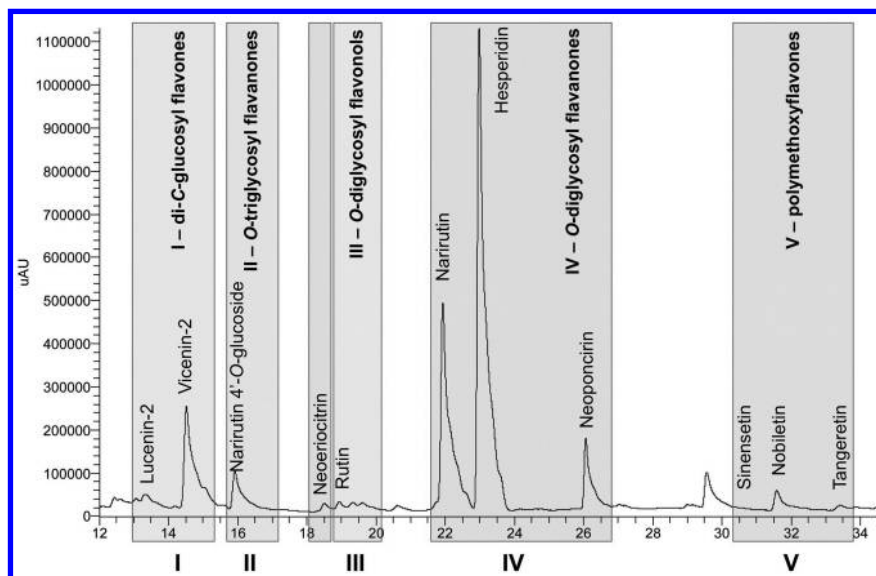


Figure 2. Fractions collected from tangelo juice by preparative RP-HPLC.

The six fractions were subjected to DPPH[•] (2,2-diphenyl-1-picrylhydrazyl), ABTS^{•+} (2,2'-azino-bis(3-ethylbenzothiazoline-6-sulphonic acid)) and HO[•] radical scavenging assays, as well as to ferric reducing antioxidant power (FRAP) assessment, and compared to the results obtained for the crude juice (Figure 3). It is evident, from the data presented, that the different subclasses contribute to different extents to the activity of the juice. In the case of DPPH[•] quenching, the flavonoid pool accounts for *ca.* 50% percent of the activity of crude juice (CJ, 5.85 μM Trolox [6-hydroxy-2,5,7,8-tetramethylchroman-2-carboxylic acid] Equivalents). Within the flavonoid pool, the *C*-glucosyl flavones (fraction I), the *O*-diglycosyl flavonols (III) and the *O*-diglycosyl flavanones (IV) were the subclasses responsible for the activity, whereas the remaining two (i.e., II and V) displayed little or no activity at all (26).

A similar trend was observed for the ABTS^{•+} radical cation quenching, although in this case most of the activity of the crude juice (14.80 mM TE) could be ascribed to the flavonoid pool (*ca.* 80%). Again, it was fractions I, III and IV that contributed the most to the activity measured for the FB fraction (26).

Tangelo juice turned out also an excellent hydroxyl radical scavenger (17.20 mM TE). In this latter case, the FP fraction was found to be responsible for two thirds of the activity (*ca.* 65%), with again the same trend observed for the different subclasses (i.e., I, III, IV >> II, V). As for the reducing activity, the juice was found to be very efficient in the FRAP assay, but the flavonoid pool appeared not to play a key role in this process (FP = *ca.* 25% of CJ). Still, the C-glycosyl flavones were found to be the most active among the five subclass fractions (*ca.* 50% of CJ) (26).

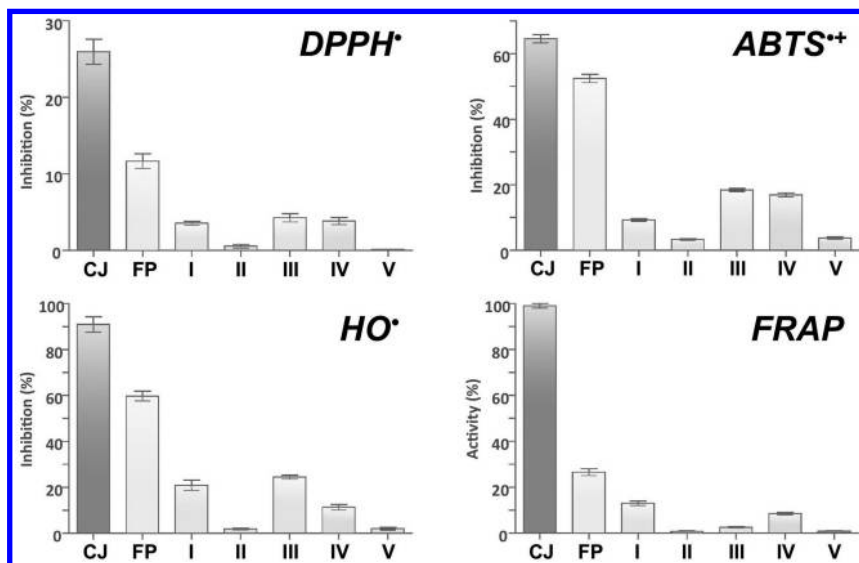


Figure 3. Radical scavenging and reducing activity of the fraction from tangelo juice (data from ref. (26)). CJ: crude juice; FP: flavonoid pool; I: di-C-glycosyl flavones; II: O-triglycosyl flavanones; III: O-diglycosyl flavonols; IV: O-diglycosyl flavanones; V: polymethoxyflavones.

These results allowed us to draw some conclusions. Firstly, it was made evident the polymethoxyflavones and O-triglycosyl flavanones possess a fairly limited efficiency in the *in vitro* radical scavenging processes employed in this study. This should not come as a surprise, given that DPPH•, ABTS•+ and HO• radical quenching rely on H• radical transfer (HAT mechanism (35)), and both these subclasses do not possess highly reactive free phenolic OH groups. A second interesting point came from the analysis of the activity of the other three classes as a function of their abundance in tangelo juice (I+III: ~4 mg/L and IV ~30 mg/L, respectively (26)). The evidence that even though O-diglycosyl flavanones are significantly more abundant than the flavones and the flavonols but display an overall similar activity, demonstrates that the derivatives that bear a double bond in the 2,3-position of the central pyrone C ring of the aglycone are the ones that exert the highest antioxidant activity. In fact, the presence of such double bond

determines a very high degree of conjugation within the flavonoid skeleton, with the consequence that the ArO• radicals generated upon H• transfer enjoy a much higher delocalization and therefore stabilization.

Conclusions

The consumption of fresh and processed *Citrus* products has been shown time and again to be a staple of healthy diets, owing to the abundance in compounds that positively influence well-being and disease prevention. Among the many derivatives that play such a role (i.e. ascorbic acid, flavonoids, anthocyanins, carotenoids, etc.), flavonoid C-glycosides are being studied for their remarkable antioxidant activity. Data discussed in the present chapter, collected over the years on *Citrus* species grown in Southern Italy, demonstrate that indeed they are among the most efficient radical scavengers within the flavonoid family, deserving more attention and further investigation in light of their potential exploitation in food and food supplement industry.

References

1. Arndt, A.; Jaeschke, W. *Materialismus und Spiritualismus: Philosophie und Wissenschaften nach 1848*; Verlag Felix Meiner: Hamburg, 2000.
2. Patil, B. S.; Jayaprakasha, G. K.; Murthy, K. N. C.; Vikram, A. Bioactive Compounds: Historical Perspectives, Opportunities, and Challenges. *J. Agric. Food Chem.* **2009**, *57*, 8142–8160.
3. Berhow, M.; Tisserat, B.; Kanes, K.; Vandercook, C. *Survey of phenolic compounds produced in Citrus*; USDA ARS Technical Bulletin; USDA, ARS, National Center for Agricultural Utilization Research: Peoria, IL, 1998, 1856, 1–154.
4. Gattuso, G.; Barreca, D.; Gargiulli, C.; Leuzzi, U.; Caristi, C. Flavonoid composition of *Citrus* juices. *Molecules* **2007**, *12*, 1641–1673.
5. Ghafar, M. F. A.; Prasad, K. N.; Weng, K. K.; Ismail, A. Flavonoid, hesperidine, total phenolic contents and antioxidant activities from *Citrus* species. *Afr. J. Biotechnol.* **2010**, *9*, 326–330.
6. Barreca, D.; Bellocco, E.; Caristi, C.; Leuzzi, U.; Gattuso, G. Flavonoids and furocoumarins in bergamot, myrtle-leaved orange, and sour orange juices: distribution and properties. In *Emerging Trends in Dietary Components for Preventing and Combating Disease*; Patil, B. S., Jayaprakasha, G. K., Murthy, K. N. C., Seeram, N. P., Eds.; ACS Symposium Series 1093; American Chemical Society: Washington, DC, 2012; pp 17–35.
7. Burda, S.; Oleszek, W. Antioxidant and Antiradical Activities of Flavonoids. *J. Agric. Food Chem.* **2001**, *49*, 2774–2779.
8. Nichenametla, S. N.; Taruscio, T. G.; Barney, D. L.; Exon, J. H. A review of the effects and mechanism of polyphenolics in cancer. *Crit. Rev. Food Sci.* **2006**, *46*, 161–183.
9. Kris-Etherton, P. M.; Hecker, K. D.; Bonanome, A.; Coval, S. M.; Binkoski, A. E.; Hilpert, K. F.; Etherton, T. D. Bioactive compounds in

- foods: Their role in the prevention of cardiovascular disease and cancer. *Am. J. Med.* **2002**, *113*, 71–88.
10. Barreca, D.; Laganà, G.; Bruno, G.; Magazù, S.; Bellocco, E. Diosmin binding to human serum albumin and its preventive action against degradation due to oxidative injuries. *Biochimie* **2013**, *95*, 2042–2049.
 11. Barreca, D.; Laganà, G.; Tellone, E.; Ficarra, S.; Leuzzi, U.; Galtieri, A.; Bellocco, E. Influences of flavonoids on erythrocyte membrane and metabolic implication through anionic exchange modulation. *J. Membrane Biol.* **2009**, *230*, 163–171.
 12. Bellocco, E.; Barreca, D.; Laganà, G.; Leuzzi, U.; Tellone, E.; Kotyk, A.; Galtieri, A. Influence of L-rhamnosyl-D-glucosyl derivatives on properties and biological interaction of flavonoids. *Mol. Cell. Biochem.* **2009**, *321*, 165–171.
 13. Asres, K.; Seyoum, A.; Veeresham, C.; Bucar, F.; Gibbons, S. Naturally derived anti-HIV agents. *Phytother. Res.* **2005**, *19*, 557–581.
 14. Cushnie, T. P. T.; Lamb, A. J. Antimicrobial activity of flavonoids. *Int. J. Antimicrob. Agent.* **2005**, *26*, 343–356.
 15. Barreca, D.; Bellocco, E.; Laganà, G.; Ginestra, G.; Bisignano, C. Biochemical and antimicrobial activity of phloretin and its glycosilated derivatives present in apple and kumquat. *Food Chem.* **2014**, *160*, 292–297.
 16. Kim, H. P.; Son, K. H.; Chang, H. W.; Kang, S. S. Anti-inflammatory plant flavonoids and cellular action mechanisms. *J. Pharmacol. Sci.* **2004**, *96*, 229–245.
 17. Borrelli, F.; Izzo, A. A. The plant kingdom as a source of anti-ulcer remedies. *Phytother. Res.* **2000**, *14*, 581–591.
 18. Middleton, E.; Kandaswami, C. Effects of flavonoids on immune and inflammatory cell functions. *Biochem. Pharmacol.* **1992**, *43*, 1167–1179.
 19. Brazier-Hicks, M.; Evans, K. M.; Gershater, M. C.; Puschmann, H.; Steel, P. G.; Edwards, R. The C-glycosylation of flavonoids in cereals. *J. Biol. Chem.* **2009**, *284*, 17926–17934.
 20. Barreca, D.; Bellocco, E.; Caristi, C.; Leuzzi, U.; Gattuso, G. Flavonoid distribution in neglected citrus species grown in the Mediterranean basin. In *Handbook on Flavonoids: Dietary Sources, Properties and Health Benefits*; Yamane, K., Kato, Y., Eds.; Nova Science Publishers: New York, 2012; pp 491–509.
 21. Caristi, C.; Bellocco, E.; Panzera, V.; Toscano, G.; Vadalà, R.; Leuzzi, U. Flavonoids Detection by HPLC-DAD-MS-MS in Lemon Juices from Sicilian Cultivars. *J. Agric. Food Chem.* **2003**, *51*, 3528–3534.
 22. Caristi, C.; Bellocco, E.; Gargiulli, C.; Toscano, G.; Leuzzi, U. Flavone-di-C-glycosides in *Citrus* juices from Southern Italy. *Food. Chem.* **2006**, *95*, 431–437.
 23. Cuykens, F.; Claeys, M. Mass spectrometry in the structural analysis of flavonoids. *J. Mass Spectrom.* **2004**, *39*, 1–15.
 24. Barreca, D.; Bellocco, E.; Caristi, C.; Leuzzi, U.; Gattuso, G. Distribution of C- and O-glycosyl flavonoids, (3-hydroxy-3-methylglutaryl)glycosyl flavanones and furocoumarins in *Citrus aurantium* L. juice. *Food Chem.* **2011**, *124*, 576–582.

25. Barreca, D.; Bellocco, E.; Leuzzi, U.; Gattuso, G. First evidence of C- and O-glycosyl flavone in blood orange (*Citrus sinensis* (L.) Osbeck) juice and their influence on antioxidant properties. *Food Chem.* **2014**, *149*, 244–252.
26. Barreca, D.; Bisignano, C.; Ginestra, G.; Bisignano, G.; Bellocco, E.; Leuzzi, U.; Gattuso, G. Polymethoxylated, C- and O-glycosyl flavonoids in tangelo (*C. reticulata* × *C. paradisi*) juice and their influence on antioxidant properties. *Food Chem.* **2013**, *141*, 1481–1488.
27. Gattuso, G.; Caristi, C.; Gargiulli, C.; Bellocco, E.; Toscano, G.; Leuzzi, U. Flavonoid Glycosides in Bergamot Juice (*Citrus bergamia* Risso). *J. Agric. Food Chem.* **2006**, *54*, 3929–3935.
28. Gattuso, G.; Barreca, D.; Caristi, C.; Gargiulli, C.; Leuzzi, U. Distribution of Flavonoids and Furocoumarins in Juices from Cultivars of *Citrus bergamia* Risso. *J. Agric. Food Chem.* **2007**, *55*, 9921–9927.
29. Barreca, D.; Bellocco, E.; Caristi, C.; Leuzzi, U.; Gattuso, G. Flavonoid profile and radical scavenging activity of Mediterranean sweet lemon (*Citrus limetta* Risso) juice. *Food Chem.* **2011**, *129*, 417–422.
30. Barreca, D.; Laganà, G.; Ficarra, S.; Tellone, E.; Leuzzi, U.; Galtieri, A.; Bellocco, E. Kumquat (*Fortunella japonica* Swingle) juice: flavonoid distribution and antioxidant properties. *Food Res. Int.* **2011**, *44*, 2302–2310.
31. Barreca, D.; Bellocco, E.; Caristi, C.; Leuzzi, U.; Gattuso, G. Flavonoid Composition and Antioxidant Activity of Juices from Chinotto (*Citrus* × *myrtifolia* Raf.) Fruits at Different Ripening Stages. *J. Agric. Food Chem.* **2010**, *58*, 3031–3036.
32. Gulsen, O.; Roose, M. L. Lemons: diversity and relationships with selected *Citrus* genotypes as measured with nuclear genome markers. *J. Amer. Soc. Hort. Sci.* **2001**, *126*, 309–317.
33. Barreca, D.; Bellocco, E.; Caristi, C.; Leuzzi, U.; Gattuso, G. Flavonoid and antioxidant properties of fruits belonging to the annona and citrus genera. In *Tropical and Subtropical Fruits: Flavors, Color, and Health Benefits*; Patil, B. S., Jayaprakasha, G. K., Roa, C. O., Mahattanatawee, K., Eds.; ACS Symposium Series 1129; American Chemical Society: Washington, DC, 2013; pp 103–119.
34. Zhang, D.-X.; Mabberley, D. J. *Citrus*. In *Flora of China*; Wu, Z. Y., Raven, P. H., Hong, D. Y., Eds.; Science Press: Beijing, 2008; Vol. 11, pp 51–97.
35. Liu, Z.-Q. Chemical methods to evaluate antioxidant ability. *Chem. Rev.* **2010**, *110*, 5675–5691.

Chapter 10

Characterization of Pomegranate's Health Benefiting Bioactive Compounds, Taste, Color, and Post-Harvest Fruit Quality by Studying a Wide Collection of Diverse Accessions

Lior Rubinovich,¹ Doron Holland,² and Rachel Amir*,¹

¹Migal Galilee Technology Center, P.O. Box 831,
Kiryat Shmona 11016, Israel

²Institute of Plant Sciences, Agricultural Research Organization,
Newe Ya'ar Research Center, Ramat Yishay 30095, Israel

*E-mail: rachel@migal.org.il.

Pomegranate (*Punica granatum* L.) is known to be one of the healthiest fruits and its traditional importance as a medicinal plant is supported by modern science. The health beneficial properties of the fruit are attributed to its high levels of antioxidant compounds, mainly hydrolysable tannins (HTs) and anthocyanins. This review focuses on our recent analyses of a wide, bio-diverse pomegranate collection composed of 29 different accessions. Our aim was to compose a wide-scope picture of the various factors that contribute to the health benefits, and to the marketability of the fruit, in particular antioxidant compounds, taste and color. For that purpose we have examined the concentration and localization of HTs, anthocyanins, total phenols, organic acids and total soluble sugars (TSS) in the fruit sections. We have also examined how these factors are affected by environmental conditions. In addition, we have investigated the factors that help maintain fruit quality during prolonged storage and how they may be utilized to control storage diseases and reduce the use of synthetic fungicides. The usage of a large pomegranate collection rich in trait variation is a valuable and powerful resource to increase our knowledge on the biodiversity that can be found in pomegranates. It can also give us insights on

pomegranate biology and help us to determine which bioactive compounds and factors regulate the fruits taste. Besides the obvious benefits to basic science, the overall collected data can assist breeders and growers to respond to consumer and industrial preferences.

Introduction

Fruits and vegetables contain high levels of antioxidant compounds that protect against harmful free radicals. The antioxidant activity is attributed mainly to high total phenols content (TPC). Phenols, in addition to their ability to serve as scavengers of free radicals and reactive oxygen species (ROS), have been associated with the reduction of stress-related chronic diseases and age-related disorders, such as cardiovascular diseases, carcinogenesis, neurodegeneration, skin deterioration as well as other health benefits (1).

Pomegranates (*Punica granatum* L.) have high TPC (2, 3) and strong antioxidant activities (4–6). It was shown that pomegranate juice (PJ) possess a 3-fold higher antioxidant activity than that of red wine or green tea (3), and two-, six- and eight-fold higher levels than those detected in grape/cranberry, grapefruit, and orange juice, respectively (6, 7). Moreover, the pomegranate fruit is known to be one of the healthiest fruits and its traditional importance as a medicinal plant (8) is now supported by data obtained from modern science showing that the fruit contains anti-carcinogenic (9, 10), anti-microbial (11), antifungal (12) and anti-viral compounds (13) as well as many other health beneficial activities. Recent biological studies have also proven that certain compounds contained in PJ reduce blood pressure, are anti-atherosclerotic and significantly reduce low density lipoprotein (LDL) oxidation (2, 4, 5, 14, 15).

Chemical analyses have shown that the phenol fraction of PJ contains a high level of hydrolysable tannins (HTs) as well as anthocyanins, which exhibit high antioxidant activities (3, 16). Anthocyanins are water-soluble pigments primarily responsible for the attractive red-purple color of many fruits, including PJ, and are well known for their antioxidant activity (17). An analysis of PJ prepared by hydrostatic pressure applied to the whole fruit showed that the predominant type of phenolic compounds extracted from the peels during the process are water-soluble HTs; these compounds account for 92% of the fruit antioxidant activity (3). HTs are found in the peel (husk, rind, or pericarp), carpellary membranes, and piths of the fruit (18). The main compounds in this group are the punicalagin isomers, which were suggested as being responsible for about half of the total antioxidant capacity of the juice. In addition, ellagic acid, gallagic acid, and punicalin were also suggested to play a significant role in this activity (3).

The goal of this review is to demonstrate how studies conducted with a large collection of diverse accessions, can help to elucidate different factors that contribute to the health benefits and the marketing of the fruit. Collections of wild and domesticated pomegranates accessions are available in Asia, Europe, North Africa, and North America (19–21). This review is mainly based on our

recent studies performed on 29 pomegranate accessions that were chosen out of several hundred accessions from a collection in the Newe Ya'ar research center, ARO [registered in the Israel Gene Bank for Agriculture Crops (IBG, Website: <http://igb.agri.gov.il>)] (22) (Figure 1) that differ in their size, taste, color, aril hardness and ripening date. This review concentrates on: (i) Measurement and elucidation of the bioactive compounds, and defining their localization in the fruits sections; (ii) Analysis of the effect of two distinct growing habitats on pomegranate health-promoting components; (iii) Elucidation of factors that influence the pomegranate taste; (iv) assessment of the parameters affecting pomegranate color and (v) Studying factors that keep the fruit and especially the peel quality during prolonged storage conditions.



Figure 1. The 29 pomegranate accessions used in this study. Reprinted with permission from Tzulker, R.; Glazer, I.; Bar-Ilan, I.; Holland, D.; Aviram, M.; Amir, R. *J. Agric. Food Chem.* 2007, 55, 9559–9570. Copyright 2007 American Chemical Society. (see color insert)

Table 1. Correlation Matrix between Antioxidant Activities Measured by Different Methods, Total Polyphenols, Total Anthocyanins and the Level of the Four Hydrolysable Tannins in Juice Prepared from the Arils of the 29 Pomegranate Accessions According to the Pearson Test.

	<i>Antioxidant Activity FRAP</i>	<i>Antioxidant Activity DPPH</i>	<i>Total Polyphenols</i>	<i>Total Anthocyanins</i>	<i>Punicalagin</i>	<i>Punicalin</i>	<i>Gallagic Acid</i>
Antioxidant Activity FRAP	1	0.83**	0.86**	0.68**	0.16	-0.02	0.1
Antioxidant Activity DPPH		1	0.62**	0.265	0.48**	0.12	0.39*
Total Polyphenols			1	0.71**	-0.1	0.01	-0.06
Total Anthocyanins				1	-0.34	-0.14	-0.31
Punicalagin					1	0.14	0.45*
Punicalin						1	0.79**
Gallagic Acid							1

The r value of the correlation is given and its significance ($p < 0.05$) is identified by one asterisk, while ($p < 0.01$) is identified by two asterisks. The table is modified from Tzulker et al., 2007.

Table 2. Correlation Matrix (Pearson Test) Conducted on the Data Obtained from Homogenates Prepared from the Peels Alone of 29 Pomegranate Accessions. The r Value of the Correlation Is Given and Its Significance ($p < 0.05$) Is Identified by One Asterisk, while ($p < 0.01$) Is Identified by Two Asterisks.

	<i>Antioxidant Activity FRAP</i>	<i>Antioxidant Activity DPPH</i>	<i>Total Polyphenols</i>	<i>Total Anthocyanins</i>	<i>Punicalagin</i>	<i>Ellagic Acid</i>	<i>Punicalin</i>	<i>Gallagic Acid</i>
Antioxidant Activity FRAP	1	0.51**	0.95**	0.29	0.63**	0.70**	0.85**	0.94**
Antioxidant Activity DPPH		1	0.55**	0.11	0.29	0.33	0.31	0.43**
Total Polyphenols			1	0.28	0.63**	0.77**	0.87**	0.93**
Anthocyanins				1	0.07	0.41*	0.27	0.41*
Punicalagin					1	0.27	0.6**	0.68**
Ellagic Acid						1	0.70**	0.72**
Punicalin							1	0.85**
Gallagic Acid								1

^aThe r value of the correlation is given and its significance ($p < 0.05$) is identified by one asterisk, while ($p < 0.01$) is identified by two asterisks. The table is modified from Tzulker et al., 2007.

Elucidation of the Bioactive Compounds That Contribute to the Antioxidant Activity and Their Localization in the Fruits Sections

In order to define the major bioactive compounds that contribute to the antioxidant activity, and to reveal where they are localized in the fruits sections (peels, arils, seeds, carpellary membranes), we have used 29 unique accessions (23). Arils and peels were separated from the fruits, arils juice was prepared by squeezing the arils and separating them from their seeds, while the peels were homogenized with water. We also obtained juice which contained the aril juices with compounds extracted from the inner peels using a fruit juice extractor.

The results demonstrate that in arils juice, the range of antioxidant activity is about 3 fold and the range of TPC between accessions is about 2.5 fold from the lowest to the highest (23, 24). However, the range of the total anthocyanins contents was about 33-fold difference between the accessions. The antioxidant activity in aril juice correlated significantly to TPC and to the total anthocyanin contents, but not to the levels of four members of HTs (punicalagin, punicalin, gallagic and ellagic acids, Table 1) (23, 25). Anthocyanins are well known to contribute to the antioxidant activity (17). Therefore, when consuming only the arils, the accessions with the highest health benefiting properties are those that have red or darker colored arils, since these have higher total anthocyanins content. It is worth mentioning that the correlation value between the total anthocyanin content and antioxidant activity was significant, but quite low ($r=0.68$). This implies that anthocyanins are only one of the contributors to the antioxidant activity, and that other yet unknown compounds also contribute to this activity.

Measurements of the antioxidant activities of juice prepared by juice extractor and of peels homogenates, have shown that the activity levels were approximately 5-fold and 40-fold higher than that measured in aril juice, respectively (23). This demonstrates that the peels contain compounds that have high antioxidant activity, as previously suggested (3, 26). We have also found that in peels, the ranges of antioxidant activity and TPC within the 29 accessions were about 5 fold and 3 fold respectively.

To assess the levels of HTs that were previously suggested to contribute to the antioxidant activity (17), the contents of four members of this group (punicalagin, punicalin, gallagic and ellagic acids), were measured in the peels homogenates (23). Their levels were significantly correlated to the antioxidant activity ($r=0.63$, $r=0.85$, respectively), suggesting that they are major contributors to this activity in the peels homogenates (Table 2). The levels of punicalagins isomers were about 5×10^3 fold higher in the peels compared to the arils. No correlation was found between the level of anthocyanins to the antioxidant activities of the peels homogenates (23).

All in all, the results of this study have shown that juice prepared from the arils alone exhibit relatively poor antioxidant activity and low TPC, as well as low content of the four HTs, relative to homogenates prepared from the peels. Therefore, in order to achieve maximal health benefits from pomegranate consumption, PJ should be prepared with the proper means which can also extract

the peels along with the arils, since peels contain significantly higher levels of compounds that contribute to the antioxidant activity and human health. A recent study that was carried out on Wonderful accession, has shown that the inner peels have higher levels of antioxidant capacity and higher levels of the examined HTs than the external peels (27). Thus, future studies may be carried out to determine to which level the peels should be extracted along with the arils and to examine the effect of this process on the sensory properties of PJ. Moreover, it would be beneficial to inspect the range and nature of variation in the above mentioned properties of already commercialized pomegranate products in order to elevate its quality.

The Effect of the Habitat on Health-Promoting Compounds

Due to the extensive knowledge about the pomegranate's health attributes noted above and increasing public awareness of functional foods, the demand for pomegranate fruit and its by-products has increased tremendously in the Western world. As a result, the land area devoted to pomegranate orchards has increased significantly, including plantations in different geographic regions having diverse growth condition. In order to gain more knowledge of how environmental conditions affect the antioxidant activity and the levels of HTs, we compared the properties of pomegranates grown in two different habitats for two consecutive years. The habitats compared were a Mediterranean temperate and a hot dry desert climate (24). Eleven out of the 29 accessions were chosen for the study (Figure 2). Our findings revealed that in most of the accessions, the aril juice obtained from fruits grown in Mediterranean temperate had a higher antioxidant activity than those grown in hot and dry desert climate, with some exceptions. Consistent with these findings, it was found that the level of total anthocyanins was significantly higher in aril juice of fruits obtained from Mediterranean climate compared to those from desert climate (up to 40-fold). Anthocyanins level highly correlated to the antioxidant levels and to TPC in Mediterranean climate ($r=0.84$; $r=0.70$, respectively), but less in desert climate ($r=0.34$; $r=0.61$, respectively). Temperature is an important factor that affects anthocyanin accumulation in plants and it was shown that the expression of anthocyanin biosynthetic genes has been induced by low temperature and repressed by high temperature in various plants (28–33). The higher level of anthocyanins in Mediterranean climate fruits could be attributed to the relatively lower temperatures in this habitat compared to desert climate.

In contrast, examination of juices obtained using a juice extractor, which include in addition to the aril juice the extract of the inner parts of the peels, as well as peel homogenates, show that antioxidant activity and TPC were significantly higher in fruits obtained from desert climate (up to 4-fold). The antioxidant capacity in the peels significantly correlated to the levels of punicalagin and punicalin in both habitats (Mediterranean climate: $r=0.33$, $r=0.68$; desert climate: $r=0.64$, $r=0.34$ respectively). The reasons for the higher TPC in the peels of pomegranates grown in desert climate are not clear but could

be attributed to the higher temperatures and radiation found in desert climate compared to Mediterranean climate. The higher phenolic compounds content might protect the fruits and seeds against oxidative stress occurring under the prevailing climatic conditions. In summary, the study of eleven accessions indicates that environmental conditions significantly affect the concentration of pomegranate fruit health beneficial compounds. In addition, the high content of health-promoting components in the peels of fruits grown in a desert climate may be advantageous to the byproduct nutraceuticals industry. A comprehensive study consisting a wider diversity of germplasm may be carried out in order to construct a more complete picture on the effect of environmental conditions on pomegranate fruits parameters.

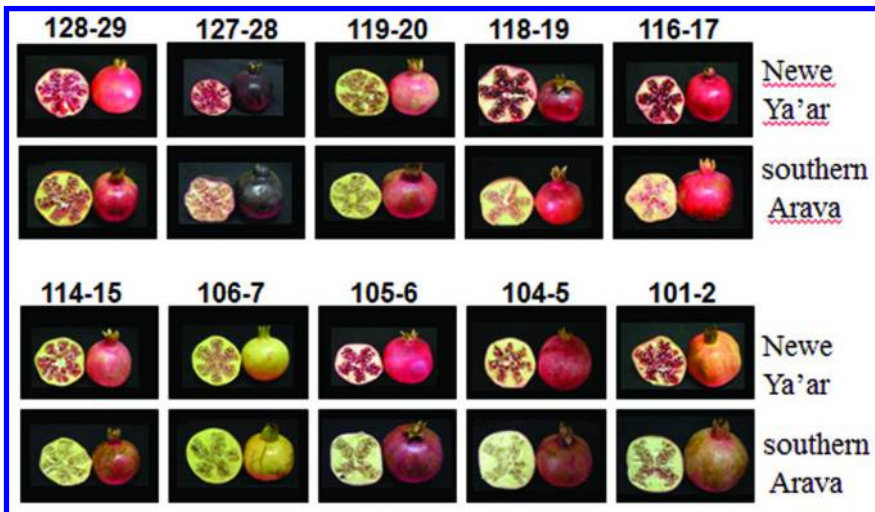


Figure 2. Fruits of the 11 pomegranate accessions grown in two different habitats as photographed in the 2006 and 2007 seasons. The figure is modified from Schwartz et al., 2009. (see color insert)

Parameters Affecting Pomegranate Taste

Analysis of a large collection can also shed more light on the compounds that are responsible and contribute to the taste of PJs. As for many fruit species, pomegranate varieties differ in their taste, ranging from sweet to sour (22). This is related directly to the quality and quantity of the organic acids and sugars found in the fruit, and indeed a great diversity in these components and their contents

has been detected in different pomegranate juices collected from several regions around the world (34–37). The desired pomegranate taste varies, however, in different countries and regions. In North Africa, for example, almost all commercialized pomegranate belong to the sweet varieties (38), while in Russia and other northern countries more sour accessions are commercialized (39). Total soluble solids (TSS) and titratable acidity (TA) are two parameters who's ratio define the taste of PJ. Determination of TSS is important not only to establish the organoleptic quality of the juice, but also because TSS content is the major parameter determining the accessions that can be used for wine preparation. Acidity can play an important role in the perception of fruit quality. It not only affects the fruit's sour taste but also its sweetness by masking the taste of the sugars. Thus, ratio between TSS and TA is commonly used to define the “taste” of a fruit, and overall consumer appreciation is related more to TSS/TA ratio than to soluble sugars content alone (40).

To determine the compounds that contribute to the taste of the aril juices, the levels of TSS and TA were measured in arils juice of the 29 accessions (41). The results showed that in arils juice: (i) There is no significant difference in the TSS and the sugars among the 29 accessions (15 to 18.5% TSS), implying that they are not the main contributors to taste; (ii) The levels of TA and citric acid do differ significantly among these accessions (by 15-fold and 25-fold, respectively), suggesting that they play a major role in determining juice taste; and (iii) Citric acid is predominant in the sour accessions, while oxalic and succinic acids are major in sweet accessions. These results suggest that since the level of sugars and TSS do not alter significantly between the different accessions, TA and citric acid are the main contributors to the taste, which as mentioned above, is determined by the ratio between TSS and TA. This ratio ranged significantly (from 6.1 to 64.6) between the different accessions.

We have also studied the levels of these taste parameters in the peels of the different accessions. Although pomegranate peels are inedible due to their bitter taste and tough dry texture, some pomegranate juice industries squeeze the fruits in such a way that in addition to the arils, the compounds found in the peels are also extracted (3). Therefore, it is important to study the contents of sugars and organic acids in the peels whose ratio defines the taste of PJ. The peel homogenates exhibited lower levels of TSS compared to the aril juice (by about 2-3 folds). In addition to glucose and fructose, which were also found in arils juice, the homogenates contained also maltose (whose concentration differs among the accessions by about 50-fold), sucrose that was found in only six accessions, and mannitol whose concentration differs between the accessions by about 8-fold. The levels of TA were within the range found in aril juices and the concentration range of TA and citric acid within the different accessions was about 3 and 30 fold, respectively. Oxalic acid was detected only in a few accessions.

Exploring the relationship of TA and TSS values between the arils and the peels could lead to better understanding of the factors regulating pomegranate juice qualities, and to gain more information about the regulation of these parameters. For that, we have performed a correlation matrix and found that the levels of TA and citric acid are significantly positively correlated, but no correlations were found in the levels of TSS and soluble sugars (Table 3).

Table 3. Correlation Matrix (Spearman Test) Conducted on Data Obtained from the Peels and Aril Juices of 29 Accessions

	<i>Peels</i>					
<i>Arils</i>	<i>TA</i>	<i>TSS</i>	<i>citric acid</i>	<i>glucose</i>	<i>fructose</i>	<i>Anthocyanin</i>
TA	0.62**	-0.21	0.78**	-0.1	-0.08	-0.28
TSS	0.75**	0.22	0.61**	-0.08	-0.08	0.36
citric acid	0.67**	-0.33	0.88**	-0.19	-0.15	-0.36
glucose	0.53**	0.26	0.32	-0.15	-0.16	0.37*
fructose	0.52**	0.26	0.31	-0.15	-0.15	0.37*
Anthocyanin	0.41**	0.07	0.39*	0.24	0.17	0.26

The *r* value of the correlation is given and its significance ($p < 0.05$) is identified by one asterisk, while ($p < 0.01$) is identified by two asterisks. The table is modified from Dafny-Yalin et al., 2010.

We have also used 11 accessions from that collection to determine the influence of environmental conditions on TSS and TA levels. To this end, eleven accessions grown in Mediterranean temperate region and in the hot and dry desert climate were examined. It was shown that the TSS and TA are largely dependent on the environmental conditions. The TSS was found to be higher in fruits obtained from Mediterranean climate in both seasons examined (by up to 4%) (24). TA level was also determined in fruits obtained from both habitats and found, with one exception, to be higher in accessions grown in Mediterranean climate. The levels of the organic acids (citric, malic, oxalic and succinic acids) were significantly higher in the Mediterranean climate in most of the accessions. The reason for these changes is not yet clear.

The results of this studies lay the foundations for the study of the diversity of different accessions in parameters relating to taste, demonstrating the effect of environmental conditions on the taste that may help industries to produce better pomegranate juices according to consumers' demands. The results also show how studying a collection composed of different accession can indicate which are the factors that contribute to the taste and how these parameters are altered in two different habitats.

Parameters Affecting Pomegranate Color

In addition to taste, the colors of the peel and aril are important traits affecting consumer choices. Therefore, we have determined the parameters which determine color in 29 different pomegranate accessions. We have found that the fruit's skin color gives some indication about aril color in most of the 29 pomegranate accessions which were chosen for this study. The results also showed that the fruit's skin and aril color as examined by a colorimeter are significantly correlated to the levels of anthocyanins, suggesting that anthocyanins are the main contributors to the color of pomegranates (41). As we have previously reported, the color parameters and total anthocyanins content of the peels cannot predict the maturation stage of the pomegranates fruit (42), the aril quality, and the levels of TA, TSS, organic acids and sugars of the aril juices (41).

In order to determine whether the main factor regulating color is genetic or an environmental one, we have performed color analysis in the two distinct habitats. We have found that the habitat significantly affect pomegranate color (42) (Figure 2). The aril juices from fruits grown in the hot and dry desert climate had a lighter color than those from Mediterranean climate. The color of aril juices prepared from trees grown in Mediterranean climate was more intense and had more of the magenta-red and yellow color components. Moreover, principal component analysis (PCA) of parameters measured in aril juice colors indicated that fruits grown in Mediterranean climate can achieve their full colors and, thus, have more uniform aril color, while fruits grown in the desert have major differences among them. In contrast, growth conditions in desert climate lead to similarity in peel color of the fruits which had more of the yellow color component in their peel,

while growth conditions in Mediterranean climate lead to greater variations among the accessions which had more of the magenta-red color component. This indicates that growth conditions in a certain habitat can expose more the genetic differences between accessions in terms of aril and peel color. Moreover, similarly to the results obtained for aril juice, total anthocyanins measured in the peel homogenates clearly demonstrated that their levels were higher in the peels of fruits obtained from Mediterranean climate (up to 45-fold). This could be due to the higher temperatures in desert climate, which negatively affects anthocyanin content and consequently affect the color in both the peels and arils.

Factors That Help Maintain Fruit Quality during Prolonged Periods in Storage Conditions

Due to higher demand to pomegranate products, there is a growing number of industries producing pomegranates, PJ, and pomegranate by-products as well as pharmaceutical companies, which extract health beneficial compounds from the fruit (16). However, the harvest season of the pomegranate is relatively short (lasting about 3 weeks for each accession and usually totaling less than 3 months during autumn). Thus the researchers search for storage conditions that maintain fruit quality. This is important for two reasons: to extend the marketing season of fresh fruit and to prolong the time of its availability to the processing industry. Although several storage protocols have been used commercially to store pomegranates for several months (reviewed by (43, 44)); the stored fruit exhibit significant quality loss. The main factors limiting prolonged storage of pomegranates are shrinkage due to weight loss, decay caused by pathogenic fungi, husk scald and chilling injury symptoms (45, 46). Since these symptoms develop with time, they significantly reduce the period that the fruit can be stored. These disorders are phenotypically present on the husks and customers avoid purchasing visually defective fruit, even though the arils may be of good quality.

To gain better knowledge on processes occurring in the husk during the storage of pomegranates fruits, we have selected seven accessions out of the 29 which differ in the antioxidant capacity and their TPC in their husks. Previously it was suggested that the appearance of husk scald is related to reduction in the TPC and antioxidant activity of the peels (47). By measuring the antioxidant activity during fruit development and maturation, we revealed that this activity is reduced over time. The post-harvest fruits were stored for 5 months and the husk disorders were measured in the day of harvest and then every month (48). The results showed that the antioxidant activity which was consistent with TPC, increased slightly but significantly during storage of most accessions. The level of punicalagin was significantly reduced during storage in all accessions, while punicalin remained relatively unchanged in four accessions and declined in the other three during storage. Our findings indicate that fruits having a high antioxidant capacity, high TPC and high levels of punicalin in their husks (up to 2, 3 and 6 fold respectively), have a better ability to resist fungal decay and weight loss, in addition to being less

sensitive to husk scald. On the other hand, our results suggest that the development of most husk disorders is not correlated to the content of TSS, TA, punicalagin, anthocyanin, or husk color. Nonetheless, poorly colored accessions were relatively more sensitive to chilling injury expressed as surface pitting, compared with the more colored accessions.

The correlation between punicalin and a better ability to resist fungal decay is interesting, since we have previously identified antifungal compounds in pomegranate peels (12). It was shown that aqueous extracts of pomegranate peels inhibit the growth rate of three out of six rot fungi that cause fruit and vegetable decay during storage. The growth rates were negatively correlated (up to 4 fold) with the levels of total polyphenolic compounds in the extract and particularly with punicalagin. These results suggest that punicalagin, which is the dominant compound in pomegranate peels, may be used as a control agent of storage diseases.

Summery and Future Aspects

In this review we focused on our recent studies which were performed across a wide, bio-diverse collection composed of a large number of different pomegranate accessions rich in trait variation. The power of exploring a large collection composed of many different accessions, in comparison to working on single accession, is the ability to apprehend the amplitude of the various phytochemicals contained in the fruits. In particular, our data provides us with a broad picture about the natural variation and the biodiversity that contribute to the antioxidant activity, TPC and total anthocyanin contents in two different fruit parts (arils and peels) among various pomegranate accessions. In addition, it can lead to a wide-scope understanding of factors regulating the taste and color of the fruits, as well as factors that maintain fruit quality during the post-harvest period. The comprehensive data gives strength to deduced trends of different characteristics, for instance, significant correlations between antioxidant capacity and the levels of punicalagin and punicalin were consistent in studies conducted with a wide range of accessions and with different growing conditions. Another example is the significant correlations between citric acid levels and TA which were also found in the our different studies. Besides the obvious benefits to basic science, this data can assist growers, breeders and industries producing pomegranates and their by-products to develop and produce healthier and tastier fruits in order to answer consumer and industrial preferences. In the future, it will be worthwhile to enlarge the database by examining more pomegranate accessions in order to market the fruit as a tasty and attractive functional food with long shelf life, extended marketing period and the best nutritional value and health properties.

References

1. Quideau, S.; Deffieux, D.; Douat-Casassus, C.; Pouységu, L. *Angew. Chem. Int. Ed.* **2011**, *50*, 586–621.
2. Aviram, M.; Dornfeld, L.; Rosenblat, M.; Volkova, N.; Kaplan, M.; Coleman, R.; Hayek, T.; Presser, D.; Fuhrman, B. *Am. J. Clin. Nutr.* **2000**, *71*, 1062–1076.
3. Gil, M. I.; Tomás-Barberán, F. A.; Hess-Pierce, B.; Holcroft, D. M.; Kader, A. *A. J. Agric. Food Chem.* **2000**, *48*, 4581–4589.
4. Aviram, M.; Rosenblat, M.; Gaitini, D.; Nitecki, S.; Hoffman, A.; Dornfeld, L.; Volkova, N.; Presser, D.; Attias, J.; Liker, H.; Hayek, T. *Clin. Nutr.* **2004**, *23*, 423–433.
5. Aviram, M.; Volkova, N.; Coleman, R.; Dreher, M.; Reddy, M. K.; Ferreira, D.; Rosenblat, M. *J. Agric. Food Chem.* **2008**, *56*, 1148–1157.
6. Rosenblat, M.; Aviram, M. In *Pomegranates: Ancient Roots to Modern Medicine*; Seeram, N. P., Heber, D., Eds.; Taylor and Francis Group: New York, 2006; pp 31–43.
7. Azadzoï, K. M.; Schulman, R. N.; Aviram, M.; Siroky, M. B. *J. Urol.* **2005**, *174*, 386–393.
8. Al-Maiman, S. A.; Ahmad, D. *Food Chem.* **2002**, *76*, 437–441.
9. Adhami, V. M.; Mukhtar, H. *Free Radic. Res.* **2006**, *40*, 1095–1104.
10. Bell, C.; Hawthorne, S. *J. Pharm. Pharmacol.* **2008**, *60*, 139–144.
11. Reddy, M. K.; Gupta, S. K.; Jacob, M. R.; Khan, S. I.; Ferreira, D. *Planta Med.* **2007**, *73*, 461–467.
12. Glazer, I.; Masaphy, S.; Marciano, P.; Bar-Ilan, I.; Holland, D.; Kerem, Z.; Amir, R. *J. Agric. Food Chem.* **2012**, *60*, 4841–4848.
13. Kotwal, G. J. *Vaccine* **2008**, *26*, 3055–3058.
14. Kaplan, M.; Hayek, T.; Raz, A.; Coleman, R.; Dornfeld, L.; Vaya, J.; Aviram, M. *J. Nutr.* **2001**, *131*, 2082–2089.
15. Aviram, M.; Dornfeld, L. *Atherosclerosis* **2001**, *158*, 195–198.
16. Seeram, N. P.; Zhang, Y.; Reed, J. D.; Krueger, C. G.; Vaya, J. In *Pomegranates: Ancient Roots to Modern Medicine*; Seeram, N. P., Heber, D., Ed.; Taylor and Francis Group: New York, 2006; pp 3–29.
17. Seeram, N. P.; Nair, M. G. *J. Agric. Food Chem.* **2002**, *50*, 5308–5312.
18. Kulkarni, A. P.; Aradhya, S. M.; Divakar, S. *Food Chem.* **2004**, *87*, 551–557.
19. Still, D. In *Pomegranates ancient roots to modern medicine*; Seeram, N. P., Heber, D., Ed.; Taylor and Francis Group: New York, 2006; pp 199–210.
20. Frison, E. A.; Servinsky, J. *Directory of European institutions holding crop genetic resources collections*, 4th ed.; Int. Plant Genetic Resources Inst.; www.ecpgr.cgiar.org/publications/directories/direct95.htm, 1995; Vol. 1, Ho.
21. Mars, M. *Options Méditerr, Sér A Sémin Méditerr* **2000**, *62*, 55–62.
22. Holland, D.; Hatib, K.; Bar-Ya'akov, I. In *Horticultural Reviews*; Janick, J., Ed.; John Wiley & Sons, Inc.: Hoboken, NJ, 2008; pp 127–191.
23. Tzulker, R.; Glazer, I.; Bar-Ilan, I.; Holland, D.; Aviram, M.; Amir, R. *J. Agric. Food Chem.* **2007**, *55*, 9559–9570.

24. Schwartz, E.; Tzulker, R.; Glazer, I.; Bar-Ya'akov, I.; Wiesman, Z.; Tripler, E.; Bar-Ilan, I.; Fromm, H.; Borochoy-Neori, H.; Holland, D.; Amir, R. *J. Agric. Food Chem.* **2009**, *57*, 9197–9209.
25. Borochoy-Neori, H.; Judeinstein, S.; Tripler, E.; Harari, M.; Greenberg, A.; Shomer, I.; Holland, D. *J. Food Compos. Anal.* **2009**, *22*, 189–195.
26. Li, Y.; Guo, C.; Yang, J.; Wei, J.; Xu, J.; Cheng, S. *Food Chem.* **2006**, *96*, 254–260.
27. Orgil, O.; Schwartz, E.; Baruch, L.; Matityahu, I.; Mahajna, J.; Amir, R. *LWT - Food Sci. Technol.* **2014**, 1–7.
28. Ubi, B. E.; Honda, C.; Bessho, H.; Kondo, S.; Wada, M.; Kobayashi, S.; Moriguchi, T. *Plant Sci.* **2006**, *170*, 571–578.
29. Leyva, A.; Jarillo, J. A.; Salinas, J.; Martinez-Zapater, J. M. *Plant Physiol.* **1995**, *108*, 39–46.
30. Mori, K.; Goto-Yamamoto, N.; Kitayama, M.; Hashizume, K. *J. Exp. Bot.* **2007**, *58*, 1935–1945.
31. Spayd, S. E.; Tarara, J. M.; Mee, D. L.; Ferguson, J. C. *Am. J. Enol. Vitic.* **2002**, *53*, 171–182.
32. Lo Piero, A. R.; Puglisi, I.; Rapisarda, P.; Petrone, G. *J. Agric. Food Chem.* **2005**, *53*, 9083–9088.
33. Dela, G.; Or, E.; Ovadia, R.; Nissim-Levi, A.; Weiss, D.; Oren-Shamir, M. *Plant Sci.* **2003**, *164*, 333–340.
34. Poyrazoğlu, E.; Gökmen, V.; Artık, N. *J. Food Compos. Anal.* **2002**, *15*, 567–575.
35. Melgarejo, P.; Salazar, D. M.; Artés, F. *Eur. Food Res. Technol.* **2000**, *211*, 185–190.
36. Cemeroglu, B.; Artık, N.; Erbas, S. *Fluess. Obst* **1992**, *59*, 335–340.
37. Unal, C.; Velioglu, S.; Cemeroglu, B. *Gida* **1995**, *20*, 339–345.
38. Al-Kahtani, H. A. *J. Am. Soc. Hort. Sci.* **1992**, *117*, 100–104.
39. Gabbasova, L. B.; Abdurazakova, S. K. *Izv. Vyssh. Uchebn. Zaved., Pishch. Tekhnol.* **1969**, *4*, 30–31.
40. Lobit, P.; Génard, M.; Wu, B. H.; Soing, P.; Habib, R. *J. Exp. Bot.* **2003**, *54*, 2489–2501.
41. Dafny-Yalin, M.; Glazer, I.; Bar-Ilan, I.; Kerem, Z.; Holland, D.; Amir, R. *J. Agric. Food Chem.* **2010**, *58*, 4342–4352.
42. Schwartz, E.; Glazer, I.; Bar-Ya'akov, I.; Matityahu, I.; Bar-Ilan, I.; Holland, D.; Amir, R. *Food Chem.* **2009**, *115*, 965–973.
43. Kader, A. A. In *Pomegranates Ancient Roots to Modern Medicine*; Seeram, N. P., Heber, D., Eds.; Taylor and Francis Group: New York, 2006; pp 211–222.
44. Caleb, O. J.; Opara, U. L.; Witthuhn, C. R. *Food Bioprocess Technol.* **2011**, *5*, 15–30.
45. Ben-Arie, R.; Segal, N.; Guelfat-Reich, S. *J. Am. Soc. Hortic. Sci.* **1984**, *109*, 898–902.
46. Ben-Arie, R.; Or, E. *J. Am. Soc. Hortic. Sci.* **1986**, *111*, 395–399.
47. Defilippi, B. G.; Whitaker, B. D.; Hess-Pierce, B. M.; Kader, A. A. *Postharvest Biol. Technol.* **2006**, *41*, 234–243.
48. Matityahu, I.; Glazer, I.; Holland, D.; Bar-Ya'akov, I.; Ben-Arie, R.; Amir, R. *Food Bioprocess Technol.* **2013**, 1–12.

Chapter 11

Application of HPLC–SPE–NMR in Characterization of Bioactive Natural Compounds

Chia-Chuan Chang and Shoei-Sheng Lee*

School of Pharmacy, National Taiwan University, Taipei 10050, Taiwan

*E-mail: shoeilee@ntu.edu.tw.

HPLC hyphenated instrumentations are powerful tools for separation and structure identification of non-crystalline organic compounds on an analytical scale. Prominent among these is the high performance liquid chromatography–solid phase extraction–nuclear magnetic resonance (HPLC–SPE–NMR) hyphenation, which combines the strength of analytical resolution (HPLC), multiple peak trapping and single deuterated solvent used for NMR sampling (SPE), providing definitive information for structural elucidation (NMR, 1D and 2D). Our laboratory has utilized this technique in combination with HPLC–HRESIMS and HPLC–microfractionation–bioassay to explore the bioactive natural products and metabolites of bioactive compounds successfully. It should be addressed that appropriate sample pretreatment is very helpful to facilitate the subsequent optimization of HPLC conditions for well-resolved separation, which is critical to achieve successful application of HPLC–SPE–NMR analysis. In this chapter, the application of HPLC–SPE–NMR in characterization of polyphenols from *Phyllanthus reticulatus*, labile acylated flavonol monorhamnosides from *Machilus philippinensis*, lignans from *P. myrtifolius* and *P. uriaria*, stilbenoids from *Syagrus romanzoffiana*, and Amaryllidaceous alkaloids from *Crinum asiaticum* var. *sinicum* is described. These studies demonstrate that HPLC–SPE–NMR is very useful for thorough chemical investigation with the advantages of saving time, plant materials, and consumables over general methods.

Introduction

HPLC–NMR, which couples high performance liquid chromatography (HPLC) to nuclear magnetic resonance (NMR), is one of the most powerful and versatile hyphenation for the separation and structural elucidation of chemical compositions in mixtures or plant extracts (1–3) on an analytic scale. However, the ^1H NMR spectra acquired by the early applications of sample storage for on-line HPLC–NMR such as on-flow, stop-flow, and loop-transfer modes always encounter the problems of solvent interference and low sensitivity in common. HPLC–SPE–NMR, which hyphenates HPLC and NMR by solid phase extraction (SPE) for peak trapping, vehicle removal, and interface manipulation for subsequent NMR data acquisition of the separated compounds, has overcome solvent effect and greatly improves the sensitivity suffered in LC–NMR. This hyphenation has become a powerful facility for speeding up structural elucidation of compounds in complex mixtures of natural products (4–8) and is especially useful when the mixtures are with limited availability. Furthermore, for natural products chemists, this hyphenation is very helpful to deal with a full scanning of a specific plant, leading to the disclosure of its chemical profile or potential for further development. In this chapter, the background, material and methods with optimization tricks, precautions, and our experiences in HPLC–SPE–NMR are introduced.

An HPLC–SPE–NMR is composed of an HPLC, a flow-probe, and a solid phase extraction (SPE) interface for sample trapping, solvent removal, and sample transferring. The SPE interface consists of an SPE resin tray with 96 cartridges, an automatic trapping system composed of controlling software (HyStar, Bruker BioSpin, Germany), an automatic cartridge exchanger, a high pressure dispenser, and an auxiliary pump. Figure 1 is a photo of the “first generation” of HPLC–SPE–NMR (400 MHz) instrument in our school. Insertion of SPE between HPLC and NMR for sample trapping and concentration has made great progress for sensitivity enhancement and removal of signal interference caused by the eluents of online LC–NMR (9–16). Up to now, several successful applications of HPLC–SPE–NMR in the identification of natural products have been reported (9, 16–27).

Application of SPE for trapping compounds separated by HPLC shows the following advantages over the LC–NMR with a loop interface. First, the delivery system using non-deuterated solvents (and buffer solutions) is the same as in a general HPLC analysis. Second, the HPLC eluents retaining in the SPE cartridges are removed on-line by flushing with dry nitrogen. The compound-loaded cartridges are washed by a deuterated solvent into an inverse NMR flow probe (30 to 120 μL), where the 1D and 2D NMR data are acquired. Such a design avoids massive consumption of deuterated solvents and the huge solvent signals arising from the non-deuterated eluents, both of which being the major concerns in LC–NMR. Third, multiple trapping of one HPLC peak to the same cartridge is allowed, enabling the accumulation of the compound amount and therefore enhancing the sensitivity of NMR measurement. Taking the advantage of such a design in this instrument, only small amount of dried plant material (< 5 g) are required for a thorough chemical investigation.



Figure 1. Photo of the HPLC–SPE–NMR (400 MHz) in School of Pharmacy, College of Medicine, National Taiwan University. (Photo taken by SS Lee.)

In the past decade, HPLC–SPE–NMR has been successfully applied in the identification of flavonol glycosides from *Phyllanthus reticulatus* (10), acylated flavonol monorhamnosides from *Machilus philippinensis* (28), aryl naphthalene-type lignans from *P. myrtifolius* (29), diary butane-type lignans from *P. urinaria* (30), minor stilbenoids from *Syagrus romanzoffiana* (29), alkaloids from *Crinum asiaticum* var. *sinicum* (31), and isoquinoline alkaloids and flavonoid glycosides from *Neolitsea sericea* var. *aurata* (16) by our lab. Through appropriate fractionation of the plant extracts, including bioassay guided fractionation, these studies characterized bioactive components, including those structurally similar or chemically labile ones, on analytical scales. The procedures for these studies are organized as follows. First, pretreatment of the plant extracts was performed according to their properties and complexity in order to concentrate the components of interest and reduce the number of components for higher resolution in HPLC. Next, HPLC separation of the fractions, selected on the basis of bioassay or chromophore (UV absorption), was undertaken. To achieve baseline separation, reverse phase HPLC conditions were optimized by adjusting solvent pairs, polarity, and pH value. Third, the samples were analyzed under the optimized conditions and each HPLC peak was trapped by respective SPE cartridge. Finally, each compound-loaded cartridge after drying by flushing inert gas (N_2) was eluted by a deuterated solvent (usually CD_3OD or CD_3CN) into the NMR flow probe to measure 1D or 2D NMR spectra for structure identification.

Accumulative application and recent advance of HPLC–SPE–NMR resulted in three characteristics. First, the amounts of the pretreated samples used in the HPLC–SPE–NMR analysis were in the ranges between 1.6 to 2.7 mg, generally equivalent to less than 5 g of dried plant material such as leaves. That is this approach requires only about one hundredth of sample amounts

comparing to the general isolation work, therefore environmentally friendly. Second, the geometrical and/ or positional isomers, e.g. the *E*- and *Z*- form of coumaroyl groups on the 2'' to 4'' positions of flavonol α -L-rhamnosides (28) and C-2/C-3 stereomers of dihydroquercetin 3-*O*-rhamnopyranosides, were identified after HPLC–SPE–NMR analysis, indicating the superiority of this hyphenated technique in isomer clarification relative to LC–MS. Third, one of the most recent advances in hyphenation of SPE and NMR is to use a tube transfer (TT) unit. This unit transfers loaded compounds from SPE cartridges to 2-mm or 3-mm NMR tubes by deuterated solvents, then these tubes are placed on an autosampler for NMR measurement by a dual cryoprobe in a Bruker NMR spectrometer such as Avance III 600 MHz NMR, instead of flow probe. This device avoids the uncertainty of compound location in the flow injection and wash-out steps, and the compounds are kept in the NMR tubes safely, making them more accessible to run 2D NMR experiments and easily recovered for bioassay. We have applied this device to analyze the metabolites of pterisin A in rat (32).

Procedure

Materials and Reagents

The selected seven plants whose chemical constituents were analyzed by HPLC–SPE–NMR in this chapter were collected in India and Taiwan (Table I).

Table I. Seven Plants Analyzed by HPLC–SPE–NMR

<i>Family</i>	<i>Binomial name</i>	<i>Place of collection</i>	<i>Reference</i>
Euphorbiaceae	<i>Phyllanthus reticulatus</i> (PR)	India	(9)
Lauraceae	<i>Machilus philippinensis</i> (MP)	Taiwan	(28)
Euphorbiaceae	<i>Phyllanthus myrtifolius</i> (PM)	Taiwan	(29)
Euphorbiaceae	<i>Phyllanthus urinaria</i> (PU)	Taiwan	(30)
Arecaceae	<i>Syagrus romanzoffiana</i> (SR)	Taiwan	(29)
Amoryllidaceae	<i>Crinum asiaticum</i> var. <i>sinicum</i> (CA)	Taiwan	(31)
Lauraceae	<i>Neolitsea sericea</i> var. <i>aurata</i> (NS)	Taiwan	(16)

Appropriate pretreatment of the crude extracts plays a key role for increasing the resolution of subsequent HPLC analysis. Theoretically, any proper method capable of focusing the wanted compounds or reducing the complexity of the mixture in a single fraction (e.g. compound number) can be used. Liquid-liquid partitioning of the ethanolic extract into fractions soluble in nonpolar (hexanes), moderate polar (CHCl₃ or EtOAc), and polar solvents (*n*-BuOH, H₂O), followed by Sephadex LH-20 fractionation, was found to be very useful in focusing and

analyzing the polyphenolics or aromatic compounds-containing fractions. This approach has been applied to six of our seven studies as listed in the column entitled "Fraction analyzed" in Table II. Another study applied centrifugal partition chromatography (CPC) for fractionation of alkaloids in *C. asiaticum* var. *sinicum*.

Table II. Fractions and Methods of Pretreatment for the Seven Plants Studied by HPLC–SPE–NMR

<i>Plant</i>	<i>Fraction analyzed</i>	<i>Chromatographic method</i>	<i>Mobile phase</i>
<i>PR</i>	BuOH	Sephadex LH-20 (470 g)	MeOH
<i>MP</i>	CH ₂ Cl ₂	Sephadex LH-20 (2.6 L)	MeOH
<i>PM</i>	MeCN	Sephadex LH-20 (70 mL)	MeOH–CHCl ₃ (1:0 – 1:1)
<i>PU</i>	CHCl ₃	Sephadex LH-20 (240 mL)	MeOH–CHCl ₃ (1:0 – 7:3)
<i>SR</i>	BuOH	Sephadex LH-20 (20 g)	MeOH–H ₂ O (7:3)
<i>CA</i>	Free base	CPC (flow rate 3 mL/min, 700 rpm, 14 mL fraction)	CHCl ₃ –MeOH– 0.5%HOAc _(aq) (5:5:3)
<i>NS</i>	Polar compounds in EtOH extract	Sephadex LH-20 (192 g)	MeOH

Compounds with aromatic rings are UV detectable and with high affinity to common SPE materials such as Resin GP. Although the fraction of interest up to 20 g level was used both for chromatographic isolation and HPLC–SPE–NMR analysis, the latter generally consumes less than 1 g. This hyphenation makes "one-injection to get all compounds analyzed, separated, and all structural information acquired" possible. What emphasized here is that only very small amount of the pretreated samples, generally in the range between 0.5 mg and 2.0 mg, is needed. For samples with limited amount, the HPLC–SPE–NMR experiments consume only a small part. The remainder can be used for bioassays and semi-preparative separation, using the HPLC conditions adjusted from LC–SPE–NMR. For tracing the bioactive components in a specific fraction, this hyphenation is powerful since full compound screening is accomplished in one separation. In addition, only small amount of a deuterated solvent is used to elute a trapped compound (about 270 μ L from the SPE cartridge to the 30 μ L-flow probe in our equipment). The amount of deuterated solvent used in SPE–NMR for each compound is about half of that used in routine NMR measurement. Computer-controlled injection of SPE-trapped compounds made all the processing steps working automatically and the superior design of SPE–NMR made such a small amount of compound enough for measuring various NMR spectra sequentially.

Table III. HPLC Conditions Utilized to Analyze the Selected Fractions of Seven Plants

<i>Plant</i>	<i>Flow rate (mL/min)</i>	<i>Sample conc. (mg/mL)</i>	<i>Injection (μ, mg)</i>	<i>Mobile phase</i>	<i>Column^c</i>	<i>Detector</i>
<i>PR</i>	0.5	10	20, 0.2	MeOH-H ₂ O (40:60-44:56, v/v) in 20 min, to 47% in 40 min (linear gradient)	A	UV 280 nm
<i>MP</i>	0.5	50	20, 1.0	MeOH-H ₂ O (40:60-44:56, v/v) in 20 min, to 47% in 40 min (linear gradient)	A	UV 280 nm
<i>PM</i>	0.5	40	20, 0.8	MeCN-H ₂ O (30:70-54:46, v/v) in 30 min (linear gradient)	B	UV 254, 320 nm
<i>PU</i>	0.6-0.9	100	20, 2.0	THF-H ₂ O (3:7)-MeCN (100:0 at 20 min, ^a 100:0 at 50 min ^b (isocratic), 60:40 at 65 min, ^b 100:0 at 67 min, v/v) in 67 min ^b	C	UV 225 nm
<i>SR</i>	0.6	20.8	20, 4.2	MeCN-H ₂ O (30:70-54:46, v/v) in 30 min (linear gradient)	A	UV 254, 320 nm
<i>CA</i>	0.7	–	5	0.1% (v/v) TFA in water-MeOH or MeCN (linear gradient)	A	UV 280 nm
<i>NS</i>	0.5	50	10, 0.5	water (A)-MeOH (B) 11:9 (23 min), 45% B to 68% B in 9 min, to 72% B in 3 min, and to 90% B in 5 min (latter three linear gradients)	A	UV 215, 280, 365 nm

^a flow rate 0.6 mL/min; ^b flow rate 0.9 mL/min; ^c A, Phenomenex Prodigy ODS-3 250 × 4.6 mm, 5 μ m; B, Merck LiChrospher 100 RP-18e 250 × 4.0 mm 5 μ m; C, Agilent Zorbax Eclipse XDB-C8 150 × 4.6 mm 5 μ m.

HPLC Method Development

Table III shows the RP-HPLC condition used to separate the components in the fractions of interest. The flow rate was set between 0.5 and 0.9 mL/min to avoid overpressure in the HPLC system. To get more amount of each compound trapped in respective SPE cartridge, the sample concentration for HPLC separation from 10 to 100 mg/mL was prepared. To perform actual collection works, the highest amount of sample should be loaded for each HPLC run unless it might affect resolution. In our cases, sample amounts between 0.2 mg and 2 mg were injected for each run. If the sample is a mixture of ten compounds with equal concentration, triple SPE trappings will provide 60 μg for each compound at least, enough for obtaining decent ^1H NMR signals and ^1H -detected 2D NMR spectra. To avoid tedious and time-consuming trial and error, method development of HPLC was carried out according to our previous research outcomes, the reported literatures, or modifications of the aforementioned conditions to obtain optimized resolution. For compounds with moderate to high polarity, MeCN–H₂O or MeOH–H₂O isocratic mobile phases or linear gradient with ascending ratios of organic solvents with maximum ratio lower than 60% (e.g. MeCN–H₂O from 30:70 to 54:46 in the case of *S. romanzoffiana*) were chosen with the flow rate ratio of HPLC to make-up pump (H₂O) in the range of 1:2 to 1:3. For alkaloids, 0.1% of trifluoroacetic acid (TFA) was utilized to improve separation. For the less polar compounds such as lignans in *P. urinaria*, a reported condition was applied first, however, co-elution of compounds was observed. Under optimized conditions, using 30% aqueous THF as eluent at a flow rate of 0.6 mL/min, nearly baseline separation was finally achieved.

Solid Phase Extraction (SPE)

To collect and concentrate the analytes after HPLC separation, a Prospekt II (Spark, Holland) solid-phase extraction (SPE) unit equipped with a total of 192 HySphere Resin GP cartridges (10 × 2 mm, 10–12 μm) and an automatic cartridge exchanger was used. The SPE methods and conditions were listed in Table IV. The amounts used were in the ranges between 0.2 to 4.0 mg (column 4, Table III). HPLC flow rate lower than 1.0 mL/min (0.5 to 0.9 mL/min) was selected to avoid overpressure and possible damage to the cartridges in the SPE system. Prior to compound trapping by the SPE cartridges, the effluent was mixed with water, supplied by a post-column pump at a flow rate about two to three times as that of HPLC to decrease the ratio of organic solvent for higher SPE cartridge capacity. The compound loaded cartridges were then flushed with dry nitrogen. Once all the cartridges were dried (each around 30 min), each loaded compound was washed with a deuterated solvent (CD₃OD or CD₃CN) into the NMR flow probe. The sample volume should match the volume of flow cell to avoid dilution in transfer process.

Table IV. SPE Conditions for Trapping of the HPLC Peaks in the Selected Fractions of Seven Plants

<i>Plant</i>	<i>SPE</i>	<i>HPLC flow rate (mL/min)</i>	<i>Make-up pump flow (mL/min)</i>	<i>Trapping times</i>	<i>Drying time (min)</i>	<i>Solvent of elution</i>	<i>NMR probe^b</i>
<i>PR</i>	GP	0.5	1.0	3	30	CD ₃ CN	A
<i>MP</i>	GP	0.5	1.0	3	30	CD ₃ CN	A
<i>PM</i>	GP	0.5	1.5	1	40	CD ₃ CN	B
<i>PU</i>	GP	0.6–0.9	–	1	118	CD ₃ CN	B
<i>SR</i>	GP	0.6	2.4	1	40	CD ₃ OD and CD ₃ CN ^a	C
<i>CA</i>	GP	0.7	1.51.8	3	–	CD ₃ OD	A
<i>NS</i>	GP	0.5	1.2	3	–	CD ₃ CN	A

^a CD₃OD for compounds **SR-1** to **SR-7** and CD₃CN for compound **SR-8** ^b A, 30 μ L inverted probe; B, 120 μ L inverted probe; C, 60 μ L inverted probe.

Table V. Instrument and Settings for Measuring NMR Spectra of the HPLC-Separated Compounds from Seven Plants

<i>Plant</i>	<i>Frequency of magnet (MHz)</i>	<i>NMR Probe^a</i>	<i>Solvent suppression pulse</i>	<i>Temp (K)</i>	<i>Number of scan</i>	<i>Data acquired</i>
<i>PR</i>	400	A	LC1DWTDC	300	256-2048	¹ H, COSY, NOESY
<i>MP</i>	400	B	LC1DWTDC	300	256-2048	¹ H, COSY, NOESY
<i>PM</i>	400	A	LC1DWTDC	300	256-1024	¹ H, COSY, NOESY
<i>PU</i>	400	A	LC1DWTDC	-	2048	¹ H
<i>SR</i>	600	C	LC1DWTDC	300	256-1024	¹ H, COSY, NOESY
<i>CA</i>	400	B	LC1DWTDC	298	256-1024	¹ H
<i>NS</i>	400	B	LC1D12	300	256-2048	¹ H

^a A, 120 μ L inverse; B, 30 μ L inverse; C, 60 μ L inverse.

Table VI. LC-MS Parameters for Analysis of Chemical Constituents from Seven Plants

<i>Plant</i>	<i>Instrument</i>	<i>ESI interface temperature (°C)</i>	<i>Nebulizer gas pressure (psi)</i>	<i>Dry gas flow (L/min)</i>	<i>Spray voltage (kV)</i>	<i>Nitrogen dry temperature (°C)</i>
<i>PR</i>	Esquire-2000 Ion Trap	300	15	5	–	–
<i>MP</i>	Esquire-2000 Ion Trap	–	15	–	–	300
<i>PM</i>	Finnigan MAT TSQ7000	–	–	–	–	–
<i>PU</i>	–	–	–	–	–	–
<i>SR</i>	Esquire-3000 or MicrOTOF	–	–	–	3.0	–
<i>CA</i>	Esquire-2000 Ion Trap	28	9	4.0	325	
<i>NS</i>	Esquire-2000 Ion Trap	300	15	6	–	–

Nuclear Magnetic Resonance (NMR)

The NMR experiments were conducted on Bruker NMR instruments (400 MHz or 600 MHz), equipped with a 30, 60 or 120 μL inverse flow probe (see Table V) at 298 or 300K. To ensure the completion of each signal acquisition, the number of scan was set among 256 and 2048. For 2D NMR experiments, only homo-nuclear experiments such as COSY and NOESY were undergone. 1D NOESY and TOCSY spectra would be recorded if necessary. Some ^1H -detected hetero-2D NMR data such as HMBC and HSQC could be obtained for the major compounds.

LC-MS

Table VI shows the parameters for LC-MS analysis of chemical constituents from these seven plants. In principle, these experiments shared most of parameters in common or in a close range. The instruments used to analyze the MS data included Bruker Esquire-2000, Esquire-3000, and Finnigan MAT TSQ7000. The scan mode and range were set to positive mode and between 50 to 1000 Da, respectively, and the LC-MS splitter was set to a ratio of 1:20. The other parameters were set as follows: ESI interface temperature, 300°C; nebulizer gas pressure, about 15 psi; dry gas flow, 5 or 9 L/min; spray voltage, 3.0 to 4.0 kV; nitrogen dry temperature, 300 or 325 °C.

Results and Discussion

Brief Description on the Analytic Results of the Seven Plants by HPLC-SPE-NMR

Phyllanthus reticulatus (9)

A polyphenol-rich fraction from the methanolic extract of the *P. reticulatus* leaf was studied using HPLC-SPE-NMR, leading to the characterization of six compounds (**PR-1**, $t_{\text{R}} = 11.36$ min; **PR-2**, $t_{\text{R}} = 18.68$ min; **PR-3**, $t_{\text{R}} = 20.27$ min; **PR-4**, $t_{\text{R}} = 21.32$ min; **PR-5**, $t_{\text{R}} = 23.02$ min; **PR-6**, $t_{\text{R}} = 23.36$ min) (Figure 2). Among them, three flavonoid glycosides (**PR-4-6**) were not isolated by a parallel study using general chromatographic method. This study demonstrates that, with appropriate pretreatment, HPLC-SPE-NMR is very powerful and useful for thorough chemical investigation of natural products and shows the advantages such as time-saving and minimal sample consumption over general methods.

Machilus philippinensis (28)

Bioassay-guided fractionation and separation of the *M. philippinensis* leaf led to the characterization of two active compounds, **MP-1** and **MP-2**, against α -glucosidase with the IC_{50} values of 6.10 and 1.00 μM , respectively. Application

of HPLC–SPE–NMR in the active fraction resulted in the identification of 10 compounds, including luteolin (**MP-3**, $t_R = 40.8$ min) and seven additional 3-*O*-(coumaroyl-rhamnopyranosyl)-flavonols (**MP-4–10**) with the structures shown in Figure 3. These additional identified compounds were found labile and interchangeable while stored in HPLC eluent overnight. Their structures were elucidated by ^1H NMR spectroscopic analyses. Compounds **MP-2**, **MP-4**, **MP-5**, and **MP-7** were new natural products.

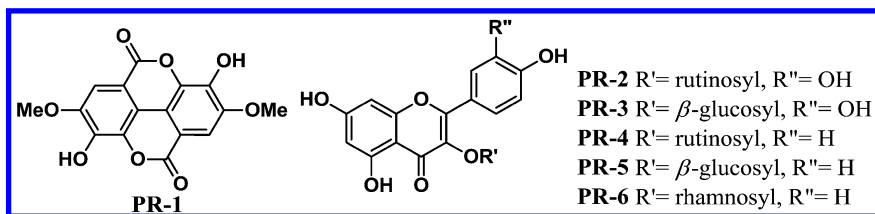


Figure 2. Structures of compounds **PR-1–6**.

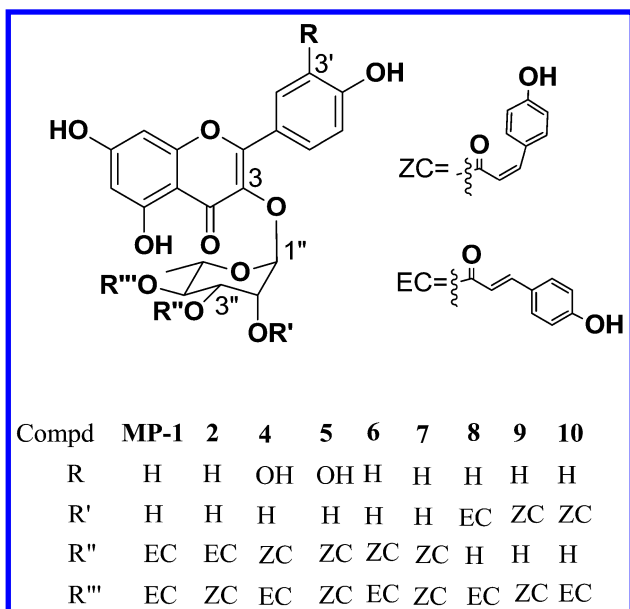


Figure 3. Structures of compounds **MP-1**, **MP-2**, and **MP-4–10**.

This study demonstrates the powerfulness of HPLC–SPE–NMR in thorough exploration of bioactive labile natural products. In addition, these compounds are geometric and/ or positional isomers, which cannot be distinguished by LC-MS/MS.

Phyllanthus myrtifolius (29)

HPLC–SPE–NMR in association with HR-ESI/MS resulted in rapid characterization of the aryl naphthalene-type lignans present in a lignan-rich fraction of *P. myrtifolius*. Seven lignans (**PM-1–7**, Figure 4) with highly structural similarity were identified by these hyphenated instruments and consumed only 1.6 mg of partially purified mixtures. This study demonstrates that HPLC–SPE–NMR associated with HR-ESI/MS is a very powerful tool for rapid screening of known and/ or poorly separated natural products. Emphasis should be laid that appropriate sample pretreatment and concentration, such as liquid–liquid partitioning and subsequent Sephadex LH-20 fractionation, were found very helpful to facilitate the focusing and analysis of the lignan fraction.

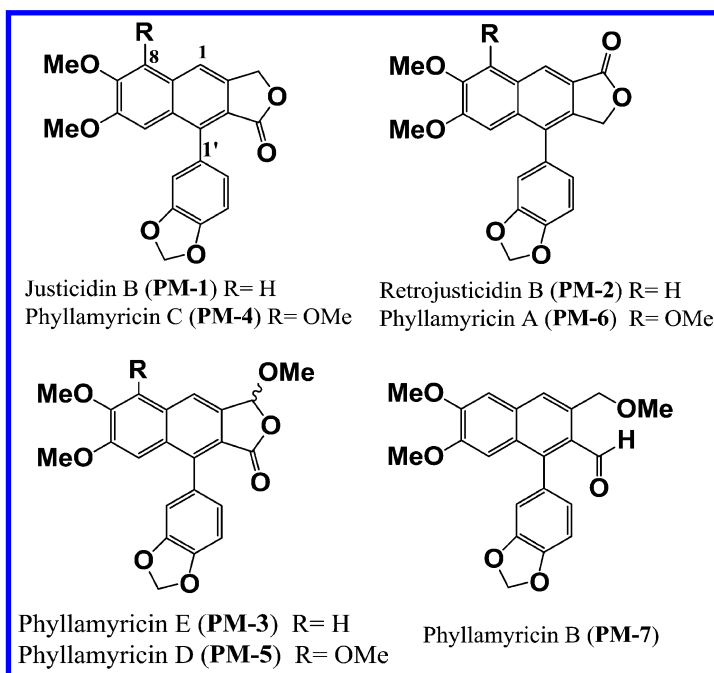


Figure 4. Structures of compounds **PM-1–7**.

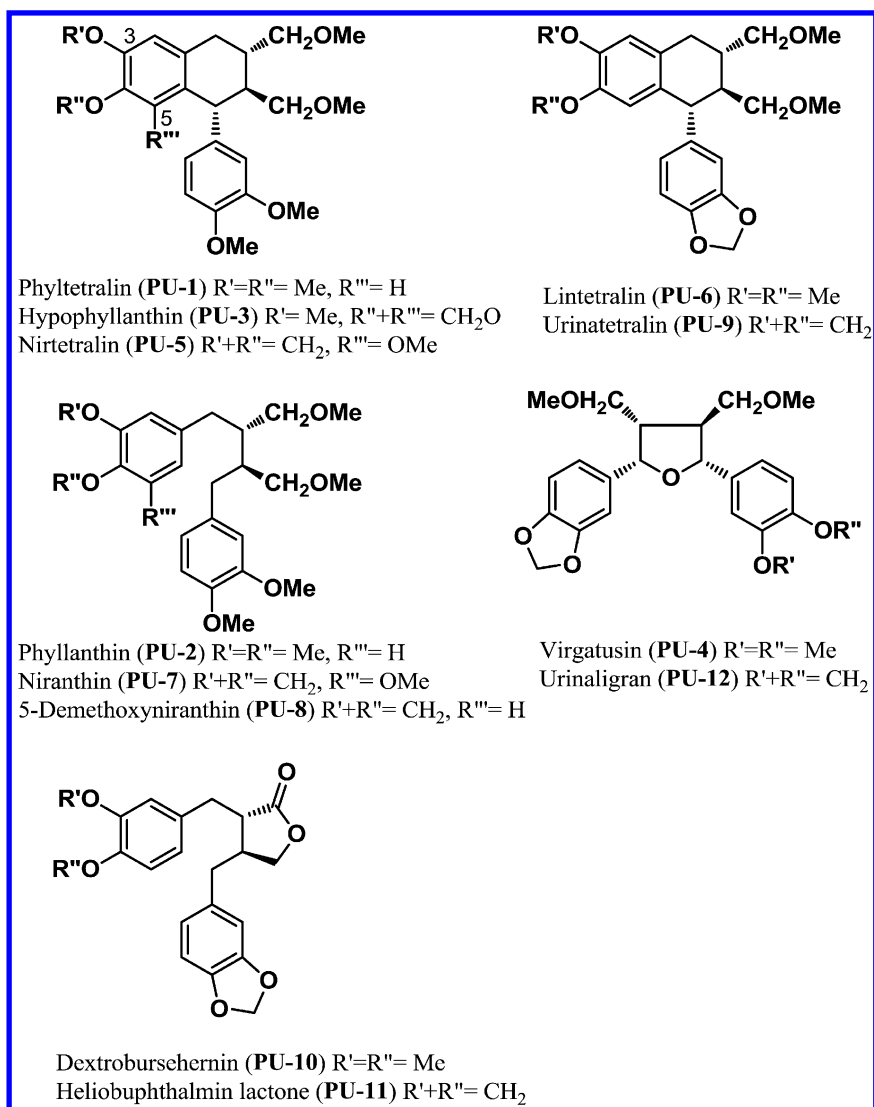


Figure 5. Structures of compounds **PU-1–12**.

Phyllanthus urinaria (30)

HPLC–SPE–NMR was applied to analyze a number of structurally similar lignans (**PU-1–12**) present in *P. urinaria*. By using a previously optimized HPLC condition that gave good resolution for seven lignans (**PU-1–7**) from *P. urinaria*, the SPE–NMR system trapped the individual peaks and provided clean 1H NMR spectra for nine lignans (**PU-1–9**) (Figure 5), present in a lignan-rich fraction. This study demonstrates that the NMR spectral data obtained from

HPLC–SPE–NMR provided much more detailed structural information than those from other hyphenated methods such as LC–MS. In addition, only 4 mg of the lignan-rich fraction was consumed for structural identification of nine lignans. Because the potential of HPLC–SPE–NMR, as shown in this work, the trend of applications of this hyphenation shall spread dramatically in the near future, especially for the identification of known natural products.

Syagrus romanzoffiana (29)

HPLC analysis of a polyphenol-rich fraction from the ethanolic extract of *S. romanzoffiana* seeds was carried out using an Agilent 1100 liquid chromatography. Characterization of this polyphenol-rich fraction by HPLC–DAD(MS)–SPE–NMR gave four additional compounds, including one unusual rearranged bisstilbene, syagrusin C (**SR-1**, $t_R = 27.0$ min) and three bisstilbenes, scirpusins E (**SR-5**), B (**SR-6**, $t_R = 51.5$ min), and A (**SR-7**, $t_R = 62.3$ min), besides four having been isolated stilbenoids, syagrusin A (**SR-2**, $t_R = 42.8$ min), scirpusin C (**SR-3**, $t_R = 20.9$ min), scirpusin D (**SR-4**, $t_R = 25.8$ min), and 5-hydroxyaiphanol (**SR-8**, $t_R = 60.3$ min), characterized by ^1H NMR spectroscopic analysis and HR-ESI-MS data. Among these, syagrusin C (**SR-1**) and scirpusin E (**SR-5**) were new compounds (Figure 6).

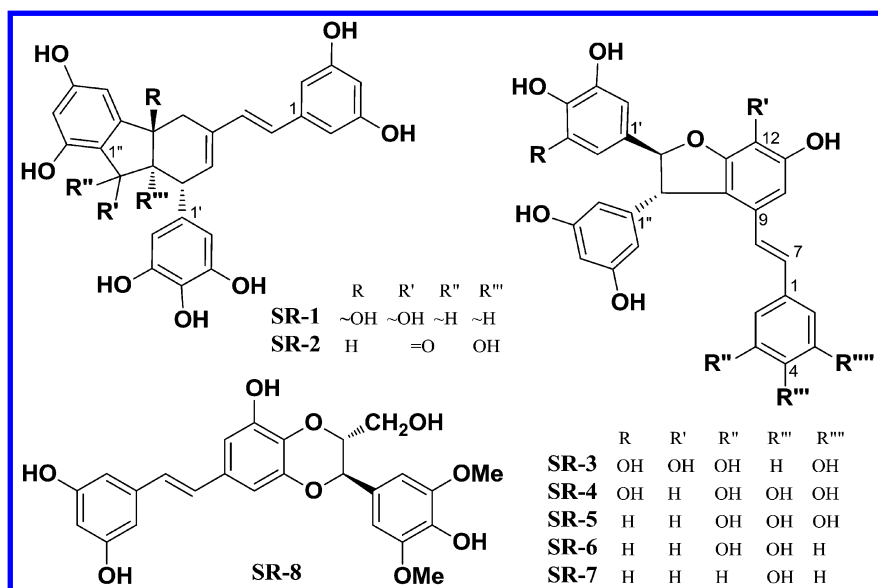


Figure 6. Structures of compounds **SR-1–8**.

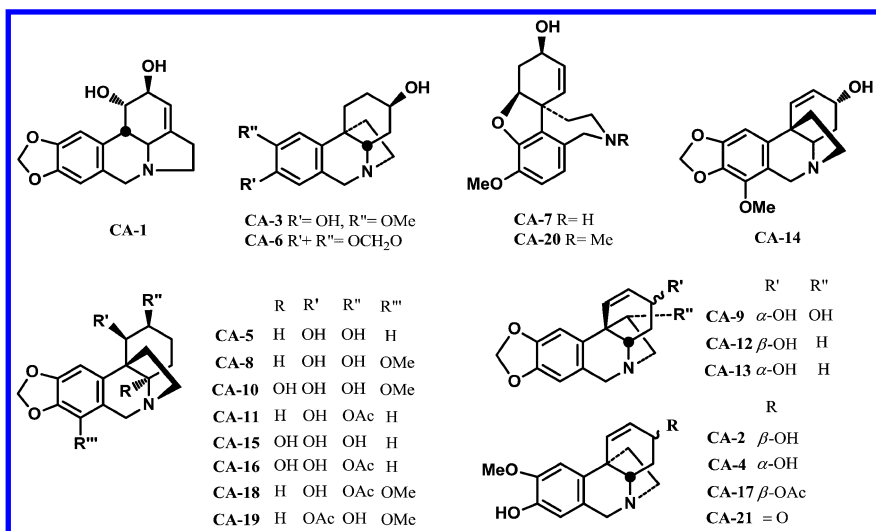


Figure 7. Structures of compounds CA-1–21.

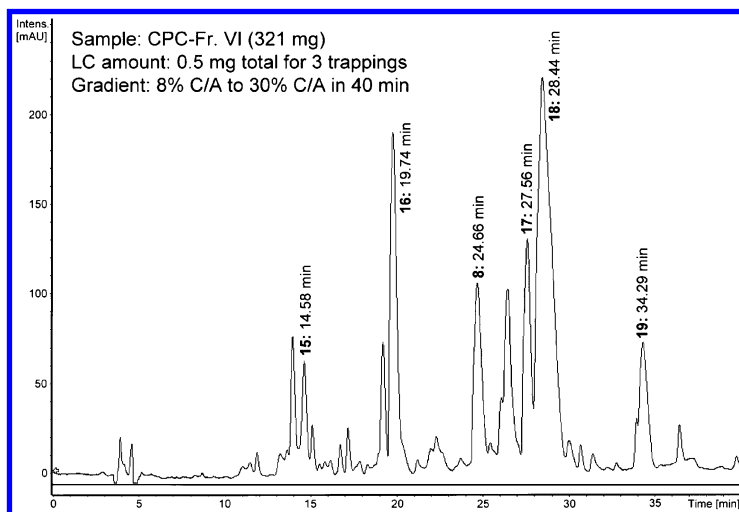


Figure 8. HPLC chromatogram of CPC fraction VI from *C. asiaticum* var. *sinicum* extracts. (Reproduced from reference (20). Copyright 2011, ACS publications.)

Prior to HPLC–SPE–NMR analysis, liquid-liquid partitioning, followed by Sephadex LH-20, were undertaken to facilitate the focusing and analysis of the polyphenolic fraction. The full process ended up with the consumption of 1.25 mg of partially purified mixtures, equivalent to ca. 0.68 g of dry seeds.

Crinum asiaticum var. *sinicum* (31)

Analysis on the free bases fraction of *C. asiaticum* var. *sinicum* leaf, assisted by HPLC–SPE–NMR, resulted in the identification of 21 alkaloids (Figure 7) with similar polarity on an analytical scale. A typical HPLC profile (Figure 8) and ^1H NMR spectra of six separated alkaloids (Figure 9), adopted from HPLC–SPE–NMR are shown.

This study led to the elucidation of seven new compounds, including (+)-siculine (CA-4), 1-epijosephinine (CA-11), 7-methoxycrinamabine (CA-10), 2-*O*-acetylcrinamabine (CA-16), 3-*O*-acetyl-8-*O*-demethylmaritidine (CA-17), 2-*O*-acetylbulbisine (CA-18), and 1-*O*-acetylbulbisine (CA-19). Furthermore, dihydrovittatine (CA-6) and 8-*O*-demethyloxomaritidine (CA-21) were isolated for the first time from Nature. Before this study, only four alkaloids had been identified from this plant because of difficult separation due to the great similarity of their structures.

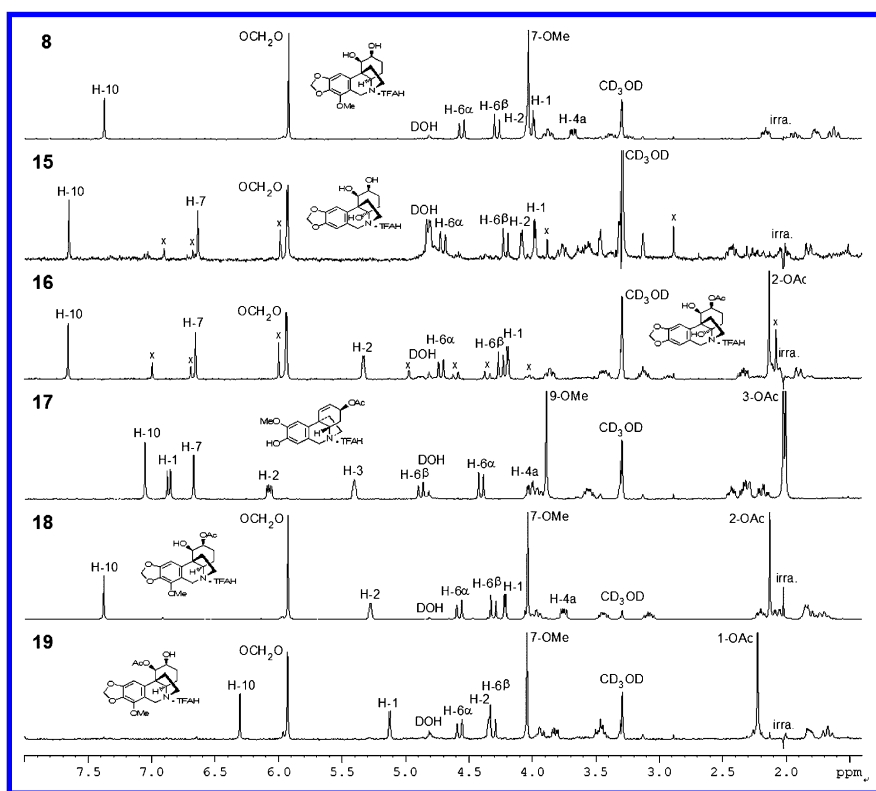


Figure 9. On-line ^1H NMR spectra of compounds CA-8 and CA-15–19 from *Crinum asiaticum* var. *sinicum* from HPLC–SPE–NMR (CD_3OD , 400 MHz). (Reproduced from reference (20). Copyright 2011, ACS publications.)

Figure 9 shows the high cleanness (without observable minor impurities) of the ^1H NMR signals of **CA-8** and **CA-15-19**, obtained by SPE-trapping, flow injection and then measurement on a 30 μL inverted NMR probe. A chromatographic pretreatment of the fractions of interest by CPC fractionation of the non-phenolic alkaloids delivered by buffer-containing mobile phase is very helpful to facilitate the subsequent optimization of HPLC separation conditions. Combination of HPLC-SPE-NMR with ESI-MS or CD is very powerful for a thorough investigation of natural chemical constituents in a complicated mixture.

Neolitsea sericea var. *aurata* (16)

Six flavonol rhamnosides (**NS-1**, $t_{\text{R}} = 16.95$ min; **NS-2**, $t_{\text{R}} = 18.12$ min; **NS-4**, $t_{\text{R}} = 23.50$ min; **NS-5**, $t_{\text{R}} = 25.50$ min; **NS-6**, $t_{\text{R}} = 30.63$ min; **NS-7**, $t_{\text{R}} = 36.95$ min) and one glucoside (**NS-3**, $t_{\text{R}} = 21.67$ min) (Figure 10) were identified from a flavonoid-rich fraction of the EtOH extract of the leaves of *N. sericea* var. *aurata* by application of HPLC-SPE-NMR. Among them, **NS-1-2** and **NS-4-5** are diastereomeric dihydroquercetin 3-*O*-rhamnosides at the C-2 and C-3 positions, characterized by ^1H NMR spectroscopic analysis and CD data. This study overcomes the weakness of LC-MS for distinguishing the diastereomers.

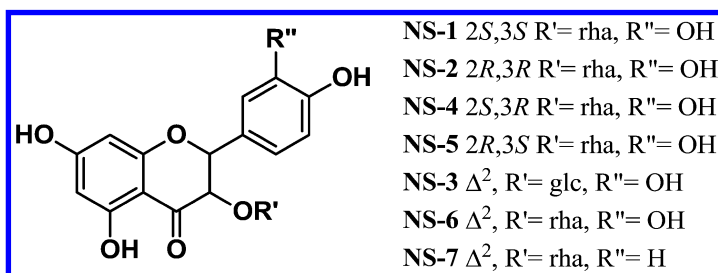


Figure 10. Structures of compounds **NS-1-7**.

This work took only 1.5 mg of the flavonoid-rich fraction and less than one month to accomplish the whole work. It is noted that the S/N (signal to noise) ratios of the ^1H NMR spectra of compounds **NS-1-2** and **NS-4-5** obtained from the HPLC-SPE-NMR were more than 150, with number of scans between 1024 and 2048, suggesting the high trapping ability of the SPE cartridges and high sensitivity of the inverse NMR flow probe. The achievement of such high S/N ratios demonstrated the importance of sample pretreatment for establishment of a baseline-separated HPLC condition, ensuring the powerfulness of HPLC-SPE-NMR for the identification of the containing natural products.

HPLC Method Development

The HPLC profiles for partially purified fractions of the seven plants had been optimized for good resolution of the major compounds. The optimized conditions were shown in Table III. These conditions were used for both LC–SPE–NMR and LC–MS analyses. Table VII showed compound classification, peak number in the HPLC chromatograms, and the number of peaks trapped for NMR analysis. The peak number in the HPLC chromatograms was obtained by calculating all observable peaks after solvent front. Figure 4 illustrated the resolution-optimized HPLC chromatogram of an *n*-BuOH-soluble fraction of *S. romanzoffiana*, monitored at UV 320 nm, in which a baseline separation for the ingredients in this fraction was achieved, and the same fraction was analyzed by SPE–NMR.

Table VII. Compound Classification, Peak No., Peaks Trapped, and Compounds Identified, New Compound No. from Seven Plants by HPLC–SPE–NMR

<i>Plant</i>	<i>Compound classification</i>	<i>Peak No.</i>	<i>Peaks trapped</i>	<i>Compds identified</i>	<i>New compds</i>
<i>PR</i>	Flavonol glycosides	15	12	12	0
<i>MP</i>	Acylated flavonol monorhamnosides	22	10	10	4
<i>PM</i>	Lignans	13	7	7	0
<i>PU</i>	Lignans	23	9	7	0
<i>SR</i>	Stilbenoids	23	9	9	1
<i>CA</i>	Alkaloids	34	21	21	7
<i>NS</i>	Flavonol glycosides	15	7	7	0

As shown in Table III, among the HPLC conditions for the seven plants, the percentage of organic solvents for *P. reticulatus*, *M. philippinensis*, *P. myrtifolius*, and *S. romanzoffiana* are between 30–50% MeOH or MeCN. For *P. urinaria*, appropriate amounts of tetrahydrofuran (THF) (30%) were added for better resolution. For *N. sericea* var. *aurata*, the amount of MeOH shall be more than 70% to elute kaempferol 3-*O*-rhamnoside (**NS-7**).

HPLC analyses on the two lignan-containing plants resulted in similar conditions for separation after optimization. For *P. urinaria*, the optimized HPLC condition for twelve lignans of great structural similarity present in the lignan-rich CHCl₃-soluble subfraction had been established before (30). HPLC–SPE–NMR was used to analyze the lignans contained in *P. urinaria*. To increase the resolution and thus enhancing the purity of the compounds trapped by the SPE cartridges, the HPLC condition was modified by increasing the retention time. This condition was not only utilized to identify a mixture of these isolated lignans but also to a partially purified lignan-rich fraction in high efficiency and accuracy.

For identification of the lignans in *P. myrtifolius*, the HPLC system used in *P. urinaria* was modified to a certain extent (Table III).

Preliminary HPLC analysis on the alkaloids of *C. asiaticum* var. *sinicum* showed that far more than the reported number of alkaloids (33) was observed. Three alkaloid-rich fractions after CPC fractionation were separated by an analytic HPLC column with the mobile phase of MeCN–H₂O (containing 0.1% TFA) in linear gradient to give 21 alkaloids (**CA-1–21**) in total. They were separated and identified by HPLC–SPE–NMR. Addition of TFA to the mobile phase was found to improve the separation of these alkaloids in RP-HPLC, although the protonation on the basic nitrogen atom affected the chemical shifts of the adjacent protons.

SPE

The use of SPE makes sequential and automatic trapping and concentration of the separated compounds possible. In addition, it also eliminates the elution solvents and buffers. The S/N ratio of the obtained ¹H NMR spectra represented the trapping ability. The higher the S/N ratio is, the more the trapping amount/ability stands for. Compounds with low affinity to SPE cartridges will not be trapped efficiently, therefore little or no ¹H NMR signals will be observed. For major peaks in HPLC chromatogram, such as **SR-3** (Figure 6), only partial peak volume was trapped by reducing the trapping time from 30 seconds to 10 seconds because of the limited SPE capacity. For the major peak co-eluted with minor one, this approach was used to improve the purity. It's noted that for online SPE–NMR, an optimized transfer volume from the SPE cartridge to the cell of the flow probe is critical to ensure the decent measurement of the ¹H NMR spectra and the advantage of SPE. To reduce the solvent interference, the SPE cartridge must be thoroughly dried (29). In general, the drying time for each SPE cartridge is 30–40 min.

NMR

Table VII summarizes the type and number of compounds isolated from the seven plants. The automation work of NMR measurement was accomplished under the control of the software ICON-NMR (Bruker BioSpin, Rheinstetten, Germany). By using this software, the pulse program, number of scan and solvent can be set for automatic experiment running. Comparing to the on-line LC–NMR with stop-flow and loop storage mode, the eluate containing separated compounds will not diffuse using HPLC–SPE–NMR during the signal acquisition, therefore higher S/N such as 258 for **NS-1** (ns = 2048), 823 for **NS-2** (ns = 1024), 325 for **NS-4** (ns = 1024), and 228 for **NS-5** (ns = 2048) (Figure 9) (16) will be obtained (10, 29). Although automatic structural identification via NMR spectral database analysis remains to be established, the achievements of the aforementioned works do recognize the powerfulness of HPLC–SPE–NMR. Within a few days of instrumental analysis and structural elucidation, an overview on the chemical profile for one mixture of interest can be obtained from analytical amount of the partially purified products of the alcoholic extract.

Conclusions

Application of HPLC–SPE–NMR in characterization of bioactive natural compounds is proven to be an extremely powerful tool. This hyphenation provides detailed structural information of interested compounds from a mixture on an analytical scale with short total processing time. As shown in this chapter, a total of seventy-five compounds, including twelve new compounds, were identified from seven plants using HPLC–SPE–NMR. For HPLC–SPE–NMR, the quality of HPLC analysis serves as a key for the overall performance. Partial purification of the extracts via appropriate pretreatment and fractionation is important for HPLC optimization. Sephadex LH-20 and CPC fractionation are of value for such purpose. The use of SPE as an interface between HPLC and NMR for automatic compound trapping, vehicle removal, and compound transferring has been demonstrated its great contribution for rapid chemical investigation of natural products. The HySphere Resin GP cartridge was selected for trapping of the compounds of interest in these seven plants for its good affinity toward the analytes including polyphenols, flavonoids, lignans, stilbenoids, and alkaloids and for its good desorption property by appropriate deuterated solvents. By using high resolution NMR (600 MHz) equipped with a cryoprobe, the ^1H NMR spectra of these 75 compounds were obtained with high S/N and structures of the regio- and positional isomers can be solved directly, overcoming the weakness of LC–MS in this point of view. Although so many strengths for HPLC–SPE–NMR have been noted, some limitations, especially for the nonpolar and highly polar compounds, are still present. The use of normal phase HPLC columns is still not feasible in practical cases because of the intolerable HPLC tubing and SPE cartridge to the organic solvents such as chloroform.

Future Works

Current works demonstrate that hyphenation of HPLC and NMR with SPE to identify the chemical constituents of natural mixtures are highly powerful, in particular for the minor compounds that are not easily isolated by general chromatographic methods. Although the pure compounds obtained after HPLC–SPE–NMR experiments are in micro-gram scale, further spectroscopic analysis (such as CD, $[\alpha]_D$ and UV) and bioassay (α -glucosidase and anti-acetylcholinesterase assays in 96-well plates) can be undertaken. If automatic signal process, structural elucidation and database matching are available, the ^1H NMR spectrum of a specific compound can be labeled, baseline-flatten, and integrated automatically. These data while compared automatically with an internal database will enable the structural elucidation of this compound and the day of "finding novel drugs from natural products automatically" will not be so far. In addition, the development of UPLC–SPE–NMR will be another concern since UPLC has better resolution than HPLC but NMR sensitivity needs to be considered due to less amounts of sample used for UPLC separation.

Acknowledgments

Dr. Li-Hong Tseng at the Bruker BioSpin (Germany) provided technical supports and helpful suggestions with the HPLC–SPE–NMR spectroscopy. The National Science Council (NSC) of Taiwan, R.O.C., provided the financial supports for these studies.

References

1. Albert, K.; Dachtler, M.; Glasser, T.; Handel, H.; Lacker, G.; Schlotterbeck, G.; Strohschein, S.; Tseng, L. H. *J. High Resolut. Chromatogr.* **1999**, *22*, 135–143.
2. Hansen, S. H.; Jensen, A. G.; Cornett, C.; Bjørnsdottir, I.; Taylor, S.; Wright, B.; Wilson, I. D. *Anal. Chem.* **1999**, *71*, 5235–5241.
3. Lommen, A.; Godejohann, M.; Venema, D. P.; Hollman, P. C. H.; Spraul, M. *Anal. Chem.* **2000**, *72*, 1793–1797.
4. Bobzin, S. C.; Yang, S. T.; Kasten, T. P. *J. Chromatogr. B* **2000**, *748*, 259–267.
5. Sandvoss, M.; Weltring, A.; Preiss, A.; Levsen, K.; Wuensch, G. *J. Chromatogr. A* **2001**, *917*, 75–86.
6. Exarchou, V.; Godejohann, M.; van Beek, T. A.; Gerotheranassis, I. P.; Vervoort, J. *Anal. Chem.* **2003**, *75*, 6288–6294.
7. Lin, H. C.; Lee, S. S. *J. Nat. Prod.* **2012**, *75*, 1735–1743.
8. Grosso, C.; Jäger, A. K.; Staerk, D. *Phytochem. Anal.* **2013**, *24*, 141–147.
9. Lee, S. S.; Lai, Y. C.; Chen, C. K.; Tseng, L. H.; Wang, C. Y. *J. Nat. Prod.* **2007**, *70*, 637–642.
10. Lam, S. H.; Wang, C. Y.; Chen, C. K.; Lee, S. S. *Phytochem. Anal.* **2007**, *18*, 251–255.
11. Tatsis, E. C.; Boeren, S.; Exarchou, V.; Troganis, A. N.; Vervoort, J.; Gerotheranassis, I. P. *Phytochemistry* **2007**, *68*, 383–393.
12. Xu, F.; Alexander, A. J. *Magn. Reson. Chem.* **2005**, *43*, 776–782.
13. Christophoridou, S.; Dais, P.; Tseng, L. H.; Spraul, M. *J. Agric. Food Chem.* **2005**, *53*, 4667–4679.
14. Godejohann, M.; Tseng, L. H.; Braumann, U.; Fuchser, J.; Spraul, M. *J. Chromatogr. A* **2004**, *1058*, 191–196.
15. Simpson, A. J.; Tseng, L. H.; Simpson, M. J.; Spraul, M.; Braumann, U.; Kingery, W. L.; Kelleher, B. P.; Hayes, M. H. *The Analyst* **2004**, *129*, 1216–1222.
16. Lam, S. H.; Chen, C. K.; Wang, J. S.; Lee, S. S. *J. Chin. Chem. Soc.* **2008**, *55*, 449–455.
17. Wiese, S.; Wubshet, S. G.; Nielsen, J.; Staerk, D. *Food Chem.* **2013**, *141*, 4010–4018.
18. Johansen, K. T.; Wubshet, S. G.; Nyberg, N. T. *Anal. Chem.* **2013**, *85*, 3183–3189.
19. Goulas, V.; Exarchou, V.; Kanetis, L.; Gerotheranassis, I. P. *J. Funct. Foods* **2014**, *6*, 248–258.

20. Wubshet, S. G.; Schmidt, J. S.; Wiese, S.; Staerk, D. *J. Agric. Food Chem.* **2013**, *61*, 8616–8623.
21. Wubshet, S. G.; Nyberg, N. T.; Tejesvi, M. V.; Pirttilä, A. M.; Kajula, M.; Mattila, S.; Staerk, D. *J. Chromatogr. A* **2013**, *1302*, 34–39.
22. Silva, L. M. A.; Filho, E. G. A.; Thomasi, S. S.; Silva, B. F.; Ferreira, A. G.; Venâncio, T. *Magnet. Reson. Chem.* **2013**, *51*, 541–548.
23. Johansen, K. T.; Ebild, S. J.; Christensen, S. B.; Godejohann, M.; Jaroszewski, J. W. *J. Chromatogr. A* **2012**, *1270*, 171–177.
24. Agnolet, S.; Wiese, S.; Verpoorte, R.; Staerk, D. *J. Chromatogr. A* **2012**, *1262*, 130–137.
25. Schmidt, J. S.; Lauridsen, M. B.; Dragsted, L. O.; Nielsen, J.; Staerk, D. *Food Chem.* **2012**, *135*, 1692–1699.
26. Gao, H.; Zehl, M.; Kaehlig, H.; Schneider, P.; Stuppner, H.; Moreno, Y.; Banuls, L.; Kiss, R.; Kopp, B. *J. Nat. Prod.* **2010**, *73*, 603–608.
27. Yang, Y. L.; Liao, W. Y.; Liu, W. Y.; Liaw, C. C.; Shen, C. N.; Huang, Z. Y.; Wu, S. H. *Chem. Eur. J.* **2009**, *15*, 11573–11580.
28. Lee, S. S.; Lin, H. C.; Chen, C. K. *Phytochemistry* **2008**, *69*, 2347–2353.
29. Wang, C. Y.; Lam, S. H.; Tseng, L. H.; Lee, S. S. *Phytochem. Anal.* **2011**, *22*, 352–360.
30. Wang, C. Y.; Lee, S. S. *Phytochem. Anal.* **2005**, *16*, 120–126.
31. Chen, C. K.; Lin, F. H.; Tseng, L. H.; Jiang, C. L.; Lee, S. S. *J. Nat. Prod.* **2011**, *74*, 411–419.
32. Lee, Y. P.; Hsu, F. L.; Kang, J. J.; Chen, C. K.; Lee, S. S. *Drug Metab. Dispos.* **2012**, *40*, 1566–1574.
33. Corcoran, O.; Spraul, M. *Drug Discovery Today* **2003**, *8*, 624–631.

Chapter 12

Headspace and Solid-Phase Microextraction Methods for the Identification of Volatile Flavor Compounds in Citrus Fruits

**Priyanka R. Chaudhary, G. K. Jayaprakasha,
and Bhimanagouda S. Patil***

**Vegetable and Fruit Improvement Center, Department of Horticultural
Sciences, Texas A&M University, College Station, Texas 77845-2119**

***E-mail: b-patil@tamu.edu.**

Analysis of volatiles using headspace (HS) is a fast, simple and sensitive method, which does not alter the original volatile chemical composition. Headspace solid-phase micro-extraction (HS-SPME) is also commonly used for analysis of volatiles in wide range of samples from food, soil, air and water. SPME is used by either immersing the fiber in the sample or by placing the fiber in headspace of the sample. Both the methods are convenient for sample preparation, fast, sensitive, reproducible, solventless, and prevent the degradation of aroma / volatile compounds during heating at higher temperature. In addition to clevenger distillation and solvent extraction techniques, HS and HS-SPME methods are gaining popularity due to several advantages. Citrus fruits are commonly consumed as fresh and processed juice due to their appealing flavor, aroma and health benefits. Therefore, citrus volatile oils have been widely used for their flavor and aroma and are commonly isolated using distillation techniques. However low boiling volatiles are degraded due to distillation and aroma molecules form artifacts. To overcome such challenges, HS and HS-SPME methods are most commonly used in recent years.

Introduction

The use of volatile oil dates back to thousands of years in Egypt, China and India (1). The Indian Ayurveda system of medicine and the traditional Chinese medicine used volatile oils for treating various diseases (2, 3). In the current age of fragrance, use of volatile oils has increased tremendously. It is used not only in perfume and cosmetic industry but also in food industry. In addition, aromatherapy is emerging as a new potential market for volatile oils (4).

Citrus fruits are used for both fresh consumption and juice processing. They are known for their unique aroma and flavor and are rich source of volatile oils; with more than 200 volatile oil components being reported (5). In citrus fruits, volatiles accumulate in oil glands present in flavedo (peels) as well as in oil bodies present in juice vesicles (6, 7). Citrus peels obtained as byproducts from citrus juice industry are commercially used for volatile oil extraction. Citrus oils are widely used in cosmetic industry, perfumes, cleaning products, air fresheners, medicines, insect repellents, desserts, confectionaries, juices and carbonated drinks. Apart from their aesthetic value, citrus volatile oils are widely studied for their health benefits such as anti-microbial, anti-proliferative, anti-inflammatory and anti-oxidant activity (8–12). D-limonene is a major component of citrus volatiles and accounts for nearly 50-90% of the volatile oil composition.

Various techniques have been developed to study the composition of volatile oils. Gas chromatography (GC) and GC-mass spectrometry (GC-MS) are commonly used to analyze volatile components. Volatile oils are isolated using different methods which are employed in industrial processes as well as in laboratories. Most common techniques used are hydro-distillation, steam distillation, simultaneous distillation-extraction (SDE), solvent extraction, supercritical fluid extraction, microwave assisted extraction, and direct sampling techniques such as headspace and solid phase micro-extraction (13). Clevenger apparatus and Likens Nickerson apparatus are commonly used for distillation and SDE process respectively (14, 15). Hydro-distillation, steam distillation and SDE methods require heat energy and longer extraction time which can destroy the thermally labile volatiles. To overcome these problems techniques such as static or dynamic headspace (HS) and solid phase micro-extraction (SPME) are used in analyzing the volatiles. Both these techniques are simple, solvent free, sensitive and rapid.

Headspace Analysis

Headspace analysis is generally defined as a vapor-phase extraction, involving the partitioning of analytes between a non-volatile liquid or solid phase and the vapor phase above the liquid or solid. The first reported method on static headspace with GC was developed in 1958 (16). The widely-read use of dynamic headspace (purge and trap) with GC was reported in the 1970s (17). Headspace sampling is divided into static (vapor-phase extraction), dynamic (purge and trap)

and solid-phase microextraction (18). In static headspace analysis, the liquid or solid samples are usually placed in a sealed vial forming two distinct phases, namely the gas phase, commonly referred to as the headspace and the sample phase containing the liquid or solid sample (19, 20). The volatile compounds diffuse from the sample into the headspace and reach equilibrium state after certain time. Further with help of a gas tight syringe an aliquot of the sample from headspace is taken and analyzed using gas chromatography (19, 20). However, the analytes present in minor quantities are difficult to detect using static HS resulting into low recovery of the volatiles (21, 22). In dynamic HS continuous flow of inert gas above the sample or through the sample (purge) is used to remove analytes and concentrated in a trap (adsorbent cartridge) (18). The trapped compounds are thermally desorbed and analyzed using GC. Dynamic HS can be used when analytes need to be concentrated due to their very low concentration in the sample (21, 23).

Headspace Solid-Phase Microextraction

SPME method was developed in 1990 by Pawliszyn and co-workers (24, 25). In SPME, pre-concentration and sample introduction are completed in one step. The analyte in the sample is isolated and concentrated (adsorbed / absorbed) on the fused-silica fiber coated with suitable polymeric sorbent or immobilized liquid which increases the sensitivity. Partitioning principle is used to extract analytes from gaseous or liquid phases (26). After the analytes are concentrated on the fiber and the equilibrium is reached, the analytes are thermally desorbed in the injection port of a gas chromatograph (GC) or in high performance liquid chromatography injection valve (27).

SPME technique is further classified into headspace (HS) –SPME and direct immersion (DI)-SPME. In HS-SPME fiber is injected in the headspace above the samples (gaseous, liquid or solid), while in DI-SPME fiber is directly immersed in the liquid samples and analyzed. Different SPME fibers are available commercially namely, polydimethylsiloxane (PDMS), polyacrylate (PA), divinylbenzene (DVB), carboxen (CAR), carbowax/divinylbenzene (CW/DVB), polydimethylsiloxane/divinylbenzene (PDMS/DVB), polydimethylsiloxane /carboxen (PDMS/CAR), divinylbenzene/carboxen/polydimethylsiloxane (DVB/CAR/PDMS) (28, 29). These coatings can be further classified according to their extraction mechanisms namely absorption (liquid coatings) or adsorption (solid coatings). Selection can be done on basis of the polarity of fibers and the volatile compounds. A list of commercially available HS-SPME-GC fibers is given in Table 1

Table 1. List of Commercially Available HS-SPME Fibers for GC and GC-MS Analysis

<i>Coating type</i>	<i>Polarity</i>	<i>Use</i>	<i>Ref.</i>
Polydimethylsiloxane (PDMS)	non-polar	Volatile organic compounds	(28, 30)
Polyacrylate (PA)	polar	Phenols and alcohols	(28, 30)
Carbowax (polyethyleneglycol, PEG)	polar	Polar alcohols	(30)
Carbowax/divinylbenzene (CW/DVB)	polar	Used for alcohols, ketones, ethers, volatile amines and polar compounds	(28)
Polydimethylsiloxane /divinylbenzene (PDMS/DVB)	polar	Low molecular weight volatile and polar analytes, amines, and nitroaromatic compounds	(31)
Polydimethylsiloxane/ carboxen (PDMS/CAR)	polar	Volatile organic compounds, volatile, small analytes, hydrocarbons	(30)
Divinylbenzene/carboxen/ polydimethylsiloxane (DVB/CAR/PDMS)	bi-polar	Volatiles and semi-volatiles	(30, 32)
Carboxen/divinylbenzene (CAR/DVB)	bi-polar	Low molecular weight volatile and polar analytes	(30, 31)

Factors Affecting SPME Extraction

Fiber Polarity

Depending on the polarity of the analytes fibers can be selected to increase adsorption/absorption of the target volatile compounds. PDMS which is non-polar and thermally stable is commonly used for extracting non-polar volatile organic compounds, while PA which is polar and has moderate thermal stability is used for polar compounds (30).

Fiber Thickness

Thicker polymer coat on the fiber helps in adsorption/absorption of volatile compounds while thin coat helps in extraction of semi-volatile compounds (28, 30). Retention and separation is better for thicker film coats resulting in higher sensitivity as more analytes can be detected (28, 30). However, they require longer equilibration time for adsorption.

Extraction Time

Since SPME is an equilibrium extraction method, pre-concentration of analyte is required. Extraction time should be determined when analyte concentration is in equilibrium in the sample, vapor phase and the fiber coating (33).

Extraction Temperature

Temperature controls the diffusion rates of the analytes into the fiber coating. Extraction yield can be increased by increasing the extraction temperature (30). In addition, elevated temperature helps to reach the equilibrium state quickly. However, temperature should be optimized based on the sample to achieve satisfactory sensitivity (34). Higher temperature affects the fiber adsorption ability due to decreased distribution constant at equilibrium (34).

Sample Volume

Headspace volume should be kept small to reduce equilibrium time and to increase sensitivity (27). Sample volume can be optimized on basis of the analyte concentration in the sample and the headspace of the vial.

Agitation

Agitation of sample assists in extraction of analytes and reduces the time of equilibrium (31). Use of magnetic stirrer is a common technique for agitation of samples. The main aim of agitating samples is to maintain the concentration of the analytes in the headspace and reduce their depletion (27).

Adjusting pH

The sensitivity for acidic and basic analytes can be improved by adjusting the pH of the aqueous samples. The pH can be adjusted in accordance to the sample pH to increase extraction efficiency. Sample pH can be adjusted in the range of 2 to 10 (27).

Salt Addition

Salts such as NaCl, NaSO₄, NaHCO₃, K₂CO₃ and (NH₄)₂SO₄ are commonly used for extraction to increase ionic strength of sample and improve sensitivity (27, 31, 35). Increasing ionic strength decreases the solubility of analytes and increases their concentration in the headspace (35). Salting out is helpful in case of analytes with greater solubility in aqueous phase. Extraction efficiency of polar compounds and volatiles can be increased by addition of salts in the aqueous samples (36). In a study done by Reinhard et al (37) saturated solution of sodium chloride (0.5 ml/1.5 ml sample) was used to optimize adsorption of analytes.

Table 2. Comparison of HS-SPME Conditions and Fibers Used in Different Citrus Fruit and Juice Analysis

<i>Samples used for analysis</i>	<i>SPME fiber and GC conditions</i>	<i>Identified major compounds</i>	<i>Ref.</i>
Marsh grapefruit (<i>Citrus paradisi</i>) fresh and canned juice	75 µm CAR/PDMS, 50/30 µm DVB/CAR/PDMS, 65 µm PDMS/DVB. Adsorption at 40 °C for 30 min.	13 Volatile sulphur compounds identified. Main compounds $i_C^{1/2}$ hydrogen sulphide, methanethiol, 1-p-menthene-8-thiol	(45)
Powell Navel Late sweet orange (<i>Citrus sinensis</i> (L.) Osb.), Clemenules (<i>Citrus clementine</i> Hort. ex Tan.), and two Citrus hybrids: Fortune (<i>C. clementine</i> x <i>C. tangerine</i>) and Chandler pummelo (<i>C. grandis</i> x <i>C. grandis</i>) fruit juices	50/30 µm DVB/CAR/PDMS fibers. Sample equilibrated at 50 °C for 10 min. Adsorption at 50 °C for 20 min. Desorption at 250 °C for 1 min.	109 compounds identified	(46)
Orange juice	100 µm PDMS fiber. Absorption at 20 °C for 60 min. Desorption at 220 °C for 2 min.	5 compounds namely D-limonene, α -pinene, ethyl butyrate, octanal and decanal identified.	(47)
Orange juice	CAR/PDMS and DVB/CAR/PDMS fibers. CAR/PDMS fiber conditioned at 300 °C for 2h, DVB/CAR/PDMS at 270 °C for 4h. Sample equilibrated at 40 °C for 5-30 min. Adsorption at 40 °C for 1 to 15 min.	32 components identified. Main compounds- D-limonene, ethyl butanoate and myrcene	(48)
Orange juice	100 µm PDMS and 85 µm PA. Sample equilibrated at 22 °C for 15 min. Absorption at 22 °C for 45 and 60 min for PDMS and PA respectively. Desorption at 250 °C for 5 min.	48 components identified.	(49)

<i>Samples used for analysis</i>	<i>SPME fiber and GC conditions</i>	<i>Identified major compounds</i>	<i>Ref.</i>
Moro, Tarocco, Washington navel and Valencia late oranges (<i>Citrus sinensis</i>) hand-squeezed juices.	50/30 μm DVB/CAR/PDMS fiber. Fiber conditioned at 250 $^{\circ}\text{C}$ for 5 min and then at room temperature for 2 min. Sample equilibrated at 40 $^{\circ}\text{C}$ for 30 min with constant stirring. Adsorption at 40 $^{\circ}\text{C}$ for 5 min. Desorption at 250 $^{\circ}\text{C}$ for 5 min.	22 components identified. Main compounds-D-Limonene, β -myrcene, methyl butanoate, α -pinene and ethyl hexanoate.	(50)
Commercial orange juices	100 μm PDMS fibre. Sample equilibrated at 60 $^{\circ}\text{C}$ under agitation for 15 min. Absorption at 60 $^{\circ}\text{C}$ for 30 min.	Principal component analysis.	(51)
Citrus juices	100 μm PDMS, 65 μm PDMS/ DVB, 50/30 μm DVB/CAR/ PDMS, 85 μm PA, 75 μm CAR/PDMS and 65 μm CW /DVB fibers. Best fit - DVB/CAR/PDMS. Sample equilibrated at 80 $^{\circ}\text{C}$ for 30 min under agitation. Absorption/adsorption at 80 $^{\circ}\text{C}$ for 10 min. Desorption at 250 $^{\circ}\text{C}$ for 5 min	Principal component analysis.	(37)
Citrus juices	PDMS, CW/DVB, CAR/PDMS, PDMS/DVB, DVB/CAR/PDMS fibers. Best fit - DVB/CAR/PDMS. Absorption/adsorption at 40 $^{\circ}\text{C}$ for 120 min. Desorption at 260 $^{\circ}\text{C}$ for 5 min	44 components identified. Main compounds- D-limonene and γ -terpinene.	(43)
Lemon (<i>Citrus limon</i> Burn) hand squeezed juices	50/30 μm DVB/CAR/PDMS fiber. Sample equilibrated at 40 $^{\circ}\text{C}$ for 60 min with constant stirring. Absorption at 40 $^{\circ}\text{C}$ for 30 min. Desorption at 250 $^{\circ}\text{C}$ for 2 min.	35 components identified. Main compounds-D-limonene, α -thujene, α -pinene, camphene, β -pinene, β -myrcene, α -terpinene, β -ocimene, γ -terpinene, and terpinolene	(52)

Continued on next page.

Table 2. (Continued). Comparison of HS-SPME Conditions and Fibers Used in Different Citrus Fruit and Juice Analysis

<i>Samples used for analysis</i>	<i>SPME fiber and GC conditions</i>	<i>Identified major compounds</i>	<i>Ref.</i>
Hallabong (<i>Citrus sphaerocarpa</i> Tan.), lemon (<i>Citrus limonum</i>), orange (<i>Citrus aurantium</i> (Linn.) var. <i>dulcis</i>) and grapefruit (<i>Citrus paradisi</i>) peel	50/30 μ m DVB/CAR/PDMS, 100 μ m PDMS, 30 μ m PDMS and 75 μ m CAR/PDMS fibers were used. Best fit - 50/30 μ m DVB/CAR/PDMS. Fibers conditioned 250-320 °C for 30-240 min. Adsorption /adsorption at 20 °C or 40 °C for 60 min. Desorption at 250 °C for 1 min.	24 components identified. Main compounds - D-limonene, β -pinene, γ -terpinene, terpinolene and linalool	(44)
<i>Citrus madurensis</i> Lour varieties Taiwan calamondin and Philippine calamansi fruit juice	65 μ m CW/DVB fiber. Adsorption at 25 \pm 1 °C for 20 min. Desorption at 250 °C for 3 min.	58 components identified.	(53)
Jinchen sweet orange fruit (<i>Citrus sinensis</i> (L.) Osbeck) fruit juice and peel oil	50/30 μ m DVB/CAR/PDMS fiber. Fiber conditioned at 270 °C for 1 h. Sample equilibrated at 40 °C \pm 1 °C for 15 min. Adsorption at 40 °C for 40 min. Desorption at 270 °C for 5 min.	Main compounds: 1/2 D-limonene, linalool, terpinen-4-ol, β -myrcene, α -terpineol, octanal, and γ -terpinene	(54)
<i>C. sinensis</i> cv. <i>Valencia</i>	100 μ m PDMS fiber. Desorption at 250 °C for 3 min.	Main compounds- D- limonene, myrcene, sabinene, α -pinene.	(55)
Indonesian Pontianak orange (<i>Citrus nobilis</i> Lour. var. <i>microcarpa</i> Hassk.), Indian Mosambi (<i>Citrus sinensis</i> Osbeck) and Philippine Dalandan (<i>Citrus reticulate</i> Blanco) fresh juices	50/30 μ m DVB/CAR/PDMS fiber. Adsorption at 50 °C for 30 min	51 components detected in Pontianak orange, 50 in Mosambi and 41 in Dalandan juice. Main compounds- D-limonene, valencene, γ -terpinene.	(56)
Grapefruit (<i>Citrus paradisi</i>) different plant parts	100 μ m PDMS fiber. Sample equilibrated at room temperature for 20 min. Adsorption at room temperature for 15 min.	Main compounds- D-limonene, linalool, sabinene, myrcene and β -caryophyllene.	(57)

Citrus Volatile Oil

Citrus volatile oil mainly consists of terpenoids formed from isoprene units (C₅). They are classified as monoterpenes (C₁₀) and sesquiterpenes (C₁₅). These are further classified as hydrocarbons and oxygenated hydrocarbons. Monoterpene hydrocarbons are main group of compounds present in citrus volatile oils accounting for nearly 70-90 % of the volatile oil composition (38). D-limonene, a monoterpene hydrocarbon, is major component of citrus volatiles (38). Other major volatile components reported in citrus are α -pinene, β -pinene, β -myrcene, γ -terpinene, *p*-cymene, linalool, β -caryophyllene (5, 39). However, each citrus crop has few minor components which impart the characteristic aroma to the fruits such as in grapefruit the aroma is mainly due to nootkatone (40) and p-1-menthene-8-thiol (41). In addition, nootkatone is also considered as senescence indicator with its levels increasing during postharvest storage in grapefruit (42).

Several different fibers and methods have been used for HS-SPME extraction of volatile oil components from different citrus fruits and juices including grapefruit (Table 2). DVB/CAR/PDMS is commonly used due to its adsorption efficiency of volatile oil components in citrus fruits. It was reported to be more suitable as compared to PDMS, PDMS/ DVB, PA, CAR/PDMS and CW/DVB fibers (37, 43, 44).

Health Benefits of Citrus Volatile Oil

Citrus volatile oil has been in use for their antimicrobial activity (38, 58). Grapefruit volatile oil showed antifungal activity and was especially most effective against *Penicillium chrysogenum* and *Penicillium verrucosum* (59). In addition, volatile oil components of citrus fruits have several other health beneficial activities. D-limonene the major component of citrus volatile oil has been reported to possess chemopreventive and therapeutic properties against different types of cancers (60–62). In a previous study conducted in our lab D-limonene present in blood orange inhibited angiogenesis, metastasis and cell death in human colon cancer cells (11). Inhibition of inflammation and activation of apoptosis in human SW480 colon cancer cells was observed after the treatment with volatile oil from palestine sweet lime (*Citrus limettioides*) (63). Furthermore, D-limonene has showed anti-tumor activity against prostate (64), mammary (65), forestomach (66); and increased apoptosis and decreased cell proliferation in gastric cancer (67). D-limonene is reported to induce phase I and phase II enzymes (60). These enzymes help to remove the carcinogens formed in our body. Glutathione S-transferase interacts with pro-carcinogens to form conjugated products which are excreted from our body. In some clinical studies D-limonene was found effective in dissolving gallstones in gallbladder and alleviating heart burn and gastroesophageal reflux disorder (68). Linalool is another compound which is reported to possess anti-proliferative activity against nine carcinoma cells namely - carcinoma of the cervix, stomach, skin, lung and bone (69). In addition, α -terpinene, nootkatone, citronellal, citral, γ -terpinene, terpinolene, and geraniol are reported to possess good antioxidant activity (70).

Conclusion

It is essential to study the volatile compounds in citrus juices which have several health beneficial properties. HS-SPME is a convenient and easy technique which can be used for analyzing citrus volatiles. Overall DVB/CAR/PDMS fiber was found to be most suitable in several citrus volatile oil studies. However several factors need to be optimized while developing HS-SPME method according to the nature sample matrix to obtain best separation.

Acknowledgments

This research was supported by Research Grant Award No. TB- 8056 - 08 from the Texas Department of Agriculture, Texas Israel Exchange and the United States – Israel Binational Agricultural Research and Development Fund, and State funding 2013-121277 VFIC-TX State appropriation”.

References

1. Vinatoru, M.; Toma, M.; Radu, O.; Filip, P. I.; Lazurca, D.; Mason, T. J. The use of ultrasound for the extraction of bioactive principles from plant materials. *Ultrason. Sonochem.* **1997**, *4*, 135–139.
2. Schnaubelt, K. Essential oil therapy according to traditional Chinese medical concepts. *Int. J. Aromather.* **2005**, *15*, 98–105.
3. Frawley, D. Oil therapy, aroma therapy and incense. In *Ayurvedic Healing: A Comprehensive Guide*; Frawley, D., Ed.; Lotus Press: Twin Lakes, WI, 2000; pp 393–396.
4. Cooke, B.; Ernst, E. Aromatherapy: a systemic review. *Br. J. Gen. Pract.* **2000**, *50*, 493–496.
5. Shaw, P. E. Review of Quantitative Analyses of Citrus Essential Oils. *J. Agric. Food Chem.* **1979**, *27*, 246–257.
6. Iglesias, D. J.; Cercós, M.; Colmenero-Flores, J. M.; Naranjo, M. A.; Ríos, G.; Carrera, E.; Ruiz-Rivero, O.; Lliso, I.; Morillon, R.; Tadeo, F. R.; Talon, M. Physiology of citrus fruiting. *Braz. J. Plant Physiol.* **2007**, *19*, 333–362.
7. Jayaprakasha, G. K.; Kumar, C. K.; Priyanka, C.; Murthy, K. N. C.; Bhimanagouda, S. P. Identification of Volatiles from Kumquats and Their Biological Activities. In *Tropical and Subtropical Fruits: Flavors, Color, and Health Benefits*; American Chemical Society: Washington, DC, 2013; Vol. 1129, pp 63–92.
8. Patil, J. R.; Jayaprakasha, G. K.; Chidambara Murthy, K. N.; Tichy, S. E.; Chetti, M. B.; Patil, B. S. Apoptosis-mediated proliferation inhibition of human colon cancer cells by volatile principles of *Citrus aurantifolia*. *Food Chem.* **2009**, *114*, 1351–1358.
9. Dabbah, R.; Edwards, V. M.; Moats, W. A. Antimicrobial Action of Some Citrus Fruit Oils on Selected Food-Borne Bacteria. *Appl. Microbiol.* **1970**, *19*, 27–31.

10. Kotamballi, N. C. M.; Jayaprakasha, G. K.; Shivappa, M. M.; Bhimanagouda, S. P. Citrus Monoterpenes: Potential Source of Phytochemicals for Cancer Prevention. In *Emerging Trends in Dietary Components for Preventing and Combating Disease*; American Chemical Society: Washington, DC, 2012; Vol. 1093, pp 545–558.
11. Murthy, K. N. C.; Jayaprakasha, G. K.; Patil, B. S. D-limonene rich volatile oil from blood oranges inhibits angiogenesis, metastasis and cell death in human colon cancer cells. *Life Sci.* **2012**, *91*, 429–439 PMID: 22935404.
12. Jayaprakasha, G.; Murthy, K.; Patil, B. Inhibition of pancreatic cancer cells by furocoumarins from *Poncirus trifoliata*. *Planta Med.* **2012**, *78*, PI175.
13. Huie, C. A review of modern sample-preparation techniques for the extraction and analysis of medicinal plants. *Anal. Bioanal. Chem.* **2002**, *373*, 23–30.
14. Chaintreau, A. Simultaneous distillation–extraction: from birth to maturity—review. *Flavour Fragrance J.* **2001**, *16*, 136–148.
15. Ferhat, M. A.; Meklati, B. Y.; Smadja, J.; Chemat, F. An improved microwave Clevenger apparatus for distillation of essential oils from orange peel. *J. Chromatogr. A* **2006**, *1112*, 121–126.
16. Bovijn, L.; Piroette, J.; Berger, A. In *Gas Chromatography 1958 (Amsterdam Symposium)*. Desty, D. H., Ed.; Butterworths: London, 1958; p 310.
17. Zlatkis, A.; Lichtenstein, H.; Tishbee, A. Concentration and analysis of trace volatile organics in gases and biological fluids with a new solid adsorbent. *Chromatographia* **1973**, *6*, 67–70.
18. Kolb, B. Headspace sampling with capillary columns. *J. Chromatogr. A* **1999**, *842*, 163–205.
19. Kolb, B.; Ettre, L. S. Theoretical Background of HS-GC and Its Applications. In *Static Headspace–Gas Chromatography*; John Wiley & Sons, Inc.: New York, 2006; pp 19–50.
20. Kolb, B.; Ettre, L. S. General Introduction. In *Static Headspace–Gas Chromatography*; John Wiley & Sons, Inc.: New York, 2006; pp 1–18.
21. Miller, M. E.; Stuart, J. D. Comparison of Gas-Sampled and SPME-Sampled Static Headspace for the Determination of Volatile Flavor Components. *Anal. Chem.* **1998**, *71*, 23–27.
22. Núñez, A. J.; Maarse, H. Headspace methods for volatile components of grapefruit juice. *Chromatographia* **1986**, *21*, 44–48.
23. Snow, N. H.; Slack, G. C. Head-space analysis in modern gas chromatography. *TrAC, Trends Anal. Chem.* **2002**, *21*, 608–617.
24. Berlardi, R.; Pawliszyn, J. The application of chemically modified fused silica fibers in the extraction of organics from water matrix samples and their rapid transfer to capillary columns. *Water Pollut. Res. J. Can.* **1989**, *24*.
25. Arthur, C. L.; Pawliszyn, J. Solid Phase Microextraction with Thermal Desorption Using Fused Silica Optical Fibers. *Anal. Chem.* **1990**, *62*, 2145–2148.
26. Pawliszyn, J. In *Solid Phase Microextraction: Theory and Practice*; Wiley-VCH, Inc.: New York, 1997; p 61.
27. Eisert, R.; Pawliszyn, J. New trends in Solid-Phase Microextraction. *Crit. Rev. Anal. Chem.* **1997**, *27*, 103–135.

28. Spietelun, A.; Pilarczyk, M.; Kloskowski, A.; Namiesnik, J. Current trends in solid-phase microextraction (SPME) fibre coatings. *Chem. Soc. Rev.* **2010**, *39*, 4524–4537.
29. Kumar, A.; Gaurav, ; Malik, A. K.; Tewary, D. K.; Singh, B. A review on development of solid phase microextraction fibers by sol–gel methods and their applications. *Anal. Chim. Acta* **2008**, *610*, 1–14.
30. Shirey, R. E., SPME commercial devices and fibre coatings. In *Handbook of Solid Phase Microextraction*; Pawliszyn, J., Ed.; Elsevier: Oxford, 2012; pp 99–133.
31. Kataoka, H.; Lord, H. L.; Pawliszyn, J. Applications of solid-phase microextraction in food analysis. *J. Chromatogr. A* **2000**, *880*, 35–62.
32. *Solid phase microextraction application guide*, 5th ed.; Supelco Bulletin 925D; Sigma-Aldrich.
33. Pawliszyn, J. Theory of Solid-Phase Microextraction. In *Handbook of Solid Phase Microextraction*; Pawliszyn, J., Ed.; Elsevier: Oxford, 2012; pp 13–59.
34. Kudlejova, L.; Risticvic, S.; Vuckovic, D. Solid-Phase Microextraction Method Development. In *Handbook of Solid Phase Microextraction*; Pawliszyn, J., Ed.; Elsevier: Oxford, 2012; pp 201–249.
35. Lambropoulou, D. A.; Albanis, T. A. Optimization of headspace solid-phase microextraction conditions for the determination of organophosphorus insecticides in natural waters. *J. Chromatogr. A* **2001**, *922*, 243–255.
36. King, A. J.; Readman, J. W.; Zhou, J. L. The application of solid-phase microextraction (SPME) to the analysis of polycyclic aromatic hydrocarbons (PAHs). *Environ. Geochem. Health* **2003**, *25*, 69–75.
37. Reinhard, H.; Sager, F.; Zoller, O. Citrus juice classification by SPME-GC-MS and electronic nose measurements. *LWT - Food Sci. Technol.* **2008**, *41*, 1906–1912.
38. Espina, L.; Somolinos, M.; Lorán, S.; Conchello, P.; García, D.; Pagán, R. Chemical composition of commercial citrus fruit essential oils and evaluation of their antimicrobial activity acting alone or in combined processes. *Food Control* **2011**, *22*, 896–902.
39. Steffen, A.; Pawliszyn, J. Analysis of Flavor Volatiles Using Headspace Solid-Phase Microextraction. *J. Agric. Food Chem.* **1996**, *44*, 2187–2193.
40. MacLeod, W. D.; Buigues, N. M. Sesquiterpenes. I. Nootkatone, A New Grapefruit Flavor Constituent. *J. Food Sci.* **1964**, *29*, 565–568.
41. Demole, E.; Enggist, P.; Ohloff, G. 1-p-Menthene-8-thiol: a powerful flavor impact constituent of grapefruit juice (*Citrus paradisi* Macfayden). *Helv. Chim. Acta* **1982**, *65*, 1785–1794.
42. Biolatto, A.; Sancho, A. M.; Cantet, R. J. C.; Güemes, D. R.; Pensel, N. A. Use of Nootkatone as a Senescence Indicator for Rouge La Toma Cv. Grapefruit (*Citrus paradisi* Macf.). *J. Agric. Food Chem.* **2002**, *50*, 4816–4819.
43. Barboni, T.; Luro, F.; Chiamonti, N.; Desjobert, J.-M.; Muselli, A.; Costa, J. Volatile composition of hybrids Citrus juices by headspace solid-phase micro extraction/gas chromatography/mass spectrometry. *Food Chem.* **2009**, *116*, 382–390.

44. Yoo, Z. W.; Kim, N. S.; Lee, D. S. Comparative analyses of the flavors from Hallabong (*Citrus sphaerocarpa*) with lemon, orange and grapefruit by SPTE and HS-SPME combined with GC-MS. *Bull. Korean Chem. Soc.* **2004**, *25*, 271–279.
45. Jabalpurwala, F.; Gurbuz, O.; Rouseff, R. Analysis of grapefruit sulphur volatiles using SPME and pulsed flame photometric detection. *Food Chem.* **2010**, *120*, 296–303.
46. González-Mas, M. C.; Rambla, J. L.; Alamar, M. C.; Gutiérrez, A.; Granell, A. Comparative analysis of the volatile fraction of fruit juice from different *Citrus* species. *PLoS ONE* **2011**, *6*, e22016.
47. Jia, M.; Zhang, Q. H.; Min, D. B. Optimization of Solid-Phase Microextraction Analysis for Headspace Flavor Compounds of Orange Juice. *J. Agric. Food Chem.* **1998**, *46*, 2744–2747.
48. Rega, B.; Fournier, N.; Guichard, E. Solid Phase Microextraction (SPME) of Orange Juice Flavor: Odor Representativeness by Direct Gas Chromatography Olfactometry (D-GC-O). *J. Agric. Food Chem.* **2003**, *51*, 7092–7099.
49. Jordán, M. J.; Goodner, K. L.; Castillo, M.; Laencina, J. Comparison of two headspace solid phase microextraction fibres for the detection of volatile chemical concentration changes due to industrial processing of orange juice. *J. Sci. Food Agric.* **2005**, *85*, 1065–1071.
50. Arena, E.; Guarrera, N.; Campisi, S.; Nicolosi Asmundo, C. Comparison of odour active compounds detected by gas-chromatography–olfactometry between hand-squeezed juices from different orange varieties. *Food Chem.* **2006**, *98*, 59–63.
51. Winne, A. D.; Dirinck, P., HS-SPME GC-MS analysis of fresh and reconstituted orange juices. In *Expression of Multidisciplinary Flavour Science*; Yeretian, C., Blank, I., Wüst, M., Eds.; Zürcher Hochschule für Angewandte: Wissenschaften, Winterthur, Switzerland, 2010; pp 223–226.
52. Allegrone, G.; Belliardo, F.; Cabella, P. Comparison of Volatile Concentrations in Hand-Squeezed Juices of Four Different Lemon Varieties. *J. Agric. Food Chem.* **2006**, *54*, 1844–1848.
53. Yo, S. P.; Lin, C. H. Qualitative and quantitative composition of the flavour components of Taiwan calamondin and Philippine calamansi fruit. *Eur. J. Hort. Sci.* **2004**, *69*, 117–124.
54. Qiao, Y.; Xie, B.; Zhang, Y.; Zhang, Y.; Fan, G.; Yao, X.; Pan, S. Characterization of aroma active compounds in fruit juice and peel oil of Jincheng Sweet Orange fruit (*Citrus sinensis* (L.) Osbeck) by GC-MS and GC-O. *Molecules* **2008**, *13*, 1333–1344.
55. Azar, P. A.; Nekoei, M.; Larijani, K.; Bahraminasab, S. Chemical composition of the essential oils of *Citrus sinensis* cv. Valencia and a quantitative structure–retention relationship study for the prediction of retention indices by multiple linear regression. *J. Serb. Chem. Soc.* **2011**, *76*, 1627–1637.
56. Dharmawan, J.; Kasapis, S.; Curran, P.; Johnson, J. R. Characterization of volatile compounds in selected citrus fruits from Asia. Part I: freshly-squeezed juice. *Flavour Fragrance J.* **2007**, *22*, 228–232.

57. Flamini, G.; Cioni, P. L. Odour gradients and patterns in volatile emission of different plant parts and developing fruits of grapefruit (*Citrus paradisi* L.). *Food Chem.* **2010**, *120*, 984–992.
58. Vasudeva, N.; Sharma, T. Chemical Composition and Antimicrobial Activity of Essential Oil of Citrus limettioides Tanaka. *J. Pharm. Technol. Drug Res.* **2012**, *1*.
59. Viuda-Martos, M.; Ruiz-Navajas, Y.; Fernández-López, J.; Pérez-Álvarez, J. Antifungal activity of lemon (*Citrus lemon* L.), mandarin (*Citrus reticulata* L.), grapefruit (*Citrus paradisi* L.) and orange (*Citrus sinensis* L.) essential oils. *Food Control* **2008**, *19*, 1130–1138.
60. Crowell, P. L. Prevention and Therapy of Cancer by Dietary Monoterpenes. *J. Nutr.* **1999**, *129*, 775.
61. Gould, M. N. Prevention and therapy of mammary cancer by monoterpenes. *J. Cell. Biochem.* **1995**, *59*, 139–144.
62. Wattenberg, L. W.; Coccia, J. B. Inhibition of 4-(methylnitrosamino)-1-(3-pyridyl)-1-butanone carcinogenesis in mice by D-limonene and citrus fruit oils. *Carcinogenesis* **1991**, *12*, 115–117.
63. Jayaprakasha, G. K.; Murthy, K. N. C.; Uckoo, R. M.; Patil, B. S. Chemical composition of volatile oil from Citrus limettioides and their inhibition of colon cancer cell proliferation. *Ind. Crops Prod.* **2013**, *45*, 200–207.
64. Rabi, T.; Bishayee, A. D. -Limonene sensitizes docetaxel-induced cytotoxicity in human prostate cancer cells: Generation of reactive oxygen species and induction of apoptosis. *J. Carcinog.* **2009**, *8*, 9–9.
65. Jayaprakasha, G. K.; Murthy, K. N. C.; Demarais, R.; Patil, B. S. Inhibition of Prostate Cancer (LNCaP) Cell Proliferation by Volatile Components from Nagami Kumquats. *Planta Med.* **2012**, *78*, 974–980.
66. Wattenberg, L. W.; Spornins, V. L.; Barany, G. Inhibition of N-Nitrosodiethylamine Carcinogenesis in Mice by Naturally Occurring Organosulfur Compounds and Monoterpenes. *Cancer Res.* **1989**, *49*, 2689–2692.
67. Uedo, N.; Tatsuta, M.; Iishi, H.; Baba, M.; Sakai, N.; Yano, H.; Otani, T. Inhibition by D-limonene of gastric carcinogenesis induced by N-methyl-N'-nitro-N-nitrosoguanidine in Wistar rats. *Cancer Lett.* **1999**, *137*, 131–136.
68. Wilkins, J. Method for treating gastrointestinal disorder. U.S. Patent 642045, 2002.
69. Cherng, J.-M.; Shieh, D.-E.; Chiang, W.; Chang, M.-Y.; Chiang, L.-C. Chemopreventive Effects of Minor Dietary Constituents in Common Foods on Human Cancer Cells. *Biosci., Biotechnol., Biochem.* **2007**, *71*, 1500–1504.
70. Choi, H.-S.; Song, H. S.; Ukeda, H.; Sawamura, M. Radical-Scavenging Activities of Citrus Essential Oils and Their Components: Detection Using 1,1-Diphenyl-2-picrylhydrazyl. *J. Agric. Food Chem.* **2000**, *48*, 4156–4161.

Chapter 13

GC and On-line LC-GC: Useful Tools for the Qualitative and Quantitative Analysis of Phytosterols and Their Esters

Rebecca Esche, Birgit Scholz, and Karl-Heinz Engel*

Technische Universität München, Lehrstuhl für Allgemeine Lebensmitteltechnologie, Maximus-von-Imhof-Forum 2, D-85350 Freising-Weihenstephan, Germany

*E-Mail: k.h.engel@wzw.tum.de.

Phytosterols/-stanols and their esters possess several health-benefits such as cholesterol-lowering and anti-oxidative properties. For the qualitative and quantitative analysis of individual free sterols/stanols and intact steryl/stanyl esters in various food matrices different approaches were established. A combination of GC-based analysis and fractionation via solid-phase extraction was applied to investigate the natural variability of these compounds in cereal grains. On-line LC-GC was demonstrated to be a useful tool for the rapid analysis of stanyl fatty acid esters in enriched dairy foods as well as for the simultaneous analysis of free sterols/stanols, steryl/stanyl fatty acid esters, and other minor lipids in edible plant oils and nuts.

Introduction

Phytosterols/-stanols are bioactive secondary plant metabolites occurring in free form, esterified with fatty acids or phenolic acids (Figure 1), and as glycosides or acylated glycosides (1). The nutritional interest in these compounds mainly arises from their cholesterol-lowering properties (2, 3). A total intake of 2 g plant sterols/stanols per day can reduce the levels of low-density lipoprotein cholesterol in hypercholesterolemic patients by up to 10 % (4). For this purpose, a broad spectrum of foods such as spread, margarine, yogurt, or milk

is currently enriched with mixtures of plant steryl/stanyl fatty acid esters. In the European Union, these mixtures are specified concerning the distributions of esterified sterols/stanols and fatty acids (5–7). Vegetable oils can be used as sources to provide phytosterols/-stanols and the fatty acid mixtures used for the esterification; tall oil is also a possible source to obtain sterols/-stanols. The following profile of free or esterified sterols/stanols is considered as acceptable in general for the incorporation into enriched food products in the European Union: up to 80% β -sitosterol, 40% campesterol, 30% stigmasterol, 15% sitostanol, 5% campestanol, 3% brassicasterol and 3% other phytosterols (6). Among natural foods, cereals, nuts, and edible plant oils are particularly rich sources of free sterols/stanols and steryl/stanyl esters (1).

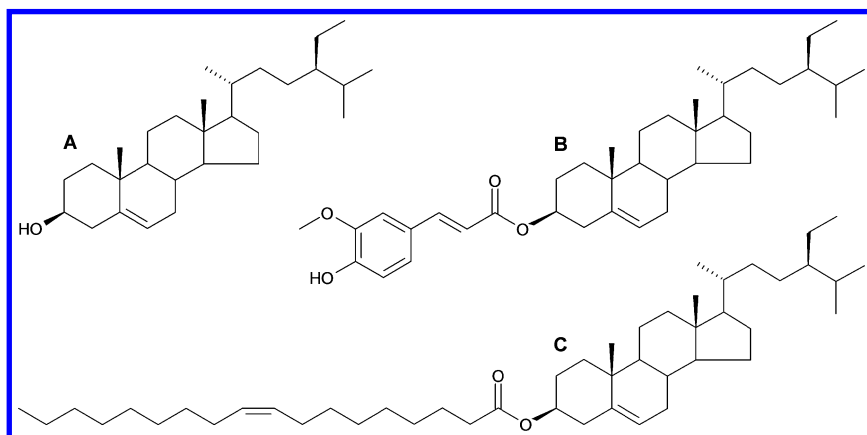


Figure 1. Representative structures of a free sterol and steryl esters: (A) sitosterol, (B) *trans*-sitosteryl ferulate, and (C) sitosteryl oleate.

Previously, qualitative and quantitative investigations have been mainly based on the analysis of total sterols/stanols determined after alkaline hydrolysis of the lipids. As a result, information on the contents and compositions particularly of individual intact steryl/stanyl fatty acid esters is rare. Therefore, analytical approaches are needed allowing both the authentication of foods enriched with steryl/stanyl fatty acid esters as well as the determination of naturally occurring free sterols/stanols and their intact esters. Recently, high temperature capillary gas chromatography was demonstrated to be suitable for the analysis of complex mixtures of steryl/stanyl fatty acid esters (8, 9). On this basis, three methodologies were established enabling the analysis of stanyl fatty acid esters in enriched dairy foods as well as the comprehensive analysis of free sterols/stanols and individual steryl/stanyl fatty acid and phenolic acid esters in cereals, edible plant oils, and nuts.

Experimental Section

Materials and Chemicals

The cereal grains, edible vegetable oils, and nuts were obtained in local stores (Freising, Germany). The cheese-based spread enriched with stanyl fatty acid esters (“Benecol naturalny-krem kanapkowy” produced by Raisio Sp. Z o.o/Bahca Polska Sp z o.o, Warszawa, Poland) was purchased in a supermarket in Poland.

A mixture of plant stanyl fatty acid esters (“plant stanol ester, STAEST 115”) was provided by Raisio Group (Raisio, Finland). Reference compounds of steryl/stanyl fatty acid esters and steryl/stanyl phenolic acid esters were synthesized according to previously described procedures (8, 10). All other chemicals and solvents were obtained from Sigma Aldrich (Steinheim, Germany), VWR International (Darmstadt, Germany), Evonik Industries AG (Essen, Germany) or Acros Organics (Morris Plains, NJ, U.S.A.).

Sample Preparation

Enriched Dairy Foods

After homogenization and addition of the internal standard (IS, cholesteryl-16:0), the samples were subjected to an acid digestion step with hydrochloric acid (25 %) at 130 °C for 45 min. The lipids were extracted with a mixture of *n*-hexane/methyl *tert*-butyl ether (MTBE; 3:2, v/v), and the extracts were directly used for on-line LC-GC analysis (11).

Cereal Grains

Lipids were extracted from ground and freeze-dried cereal grains after the addition of the internal standards (5α -cholestan- 3β -ol, cholesteryl-16:0, and cholestanyl *p*-coumarate) with of a mixture of *n*-hexane/dichloromethane (1:1, v/v) under stirring for 1 h at room temperature. The solvent was removed by rotary evaporation and 100 mg of the obtained oil was dissolved in 10 mL of *n*-hexane; 1 mL of that solution was used for SPE (10).

Edible Plant Oils and Nuts

The commercially obtained edible plant oils were spiked with the internal standards C17:0, 5α -cholestan- 3β -ol, cholesteryl-16:0, and *trans*-cholestanyl ferulate. The nut samples were ground to a fine powder and lipids were extracted after the addition of the internal standards (5α -cholestan- 3β -ol and cholesteryl-16:0) with of a mixture of *n*-hexane/dichloromethane (1:1, v/v) under stirring for 1 h at room temperature. The solvent was removed by rotary evaporation (12).

Fifty milligrams of the edible plant oils and of the obtained nut oils, respectively, were dissolved in 5 mL of *n*-hexane. An aliquot (250 μ L) of the solution was dried by a gentle stream of nitrogen, and the residue was silylated with 75 μ L of pyridine and 150 μ L of *N,O*-bis(trimethylsilyl)trifluoroacetamide/trimethyl-chlorosilane (99:1, v/v) at 80 °C for 20 min. After removal of the reagents, the residue was dissolved in 250 μ L of *n*-hexane/MTBE/2-propanol (96:4:0.1, v/v/v) and used for on-line LC-GC analysis (12).

Gas Chromatography-Flame Ionization Detection (GC-FID) and Gas Chromatography-Mass Spectrometry (GC-MS)

Separations were performed using a gas chromatograph equipped with an FID (Agilent Technologies Instrument 6890N, Böblingen, Germany). The sample solutions (1 μ L) were injected onto a 30 m \times 0.25 mm i.d., 0.1 μ m film, trifluoropropylmethyl polysiloxane capillary column (Rtx-200MS, Restek, Bad Homburg, Germany). The temperature of the injector was set to 280 °C. Hydrogen was used as carrier gas with constant flow (1.5 mL/min) and the split flow was set to 11.2 mL/min. The oven temperature program was as follows: initial temperature 100 °C, 15 °C/min to 310 °C (2 min), 1.5 °C/min to 315 °C, and 15 °C/min to 340 °C (2 min). The detector temperature was set to 360 °C.

GC-MS analyses and identifications of individual compounds were performed on a Finnigan Trace gas chromatograph ultra coupled with a Finnigan Trace DSO mass spectrometer (Thermo Electro Corp., Austin, TX, U.S.A.) as previously described (8–10).

Solid-Phase Extraction (SPE)

Lipid extracts of cereal grains were separated into fractions of free sterols/stanols, steryl/stanyl fatty acid esters, and steryl/stanyl phenolic acid esters via SPE (Strata NH₂, 55 μ m, 70 Å, 1 g/6 mL, Phenomenex, Germany) as previously described (10).

On-line Liquid Chromatography-Gas Chromatography (On-line LC-GC)

The applied on-line LC-GC system consisted of a 1220 Infinity liquid chromatograph, which was coupled to a 7890A gas chromatograph equipped with an FID via a 1200 Infinity Series 2-position/6-port switching valve (Agilent Technologies, Waldbronn, Germany). The valve was fitted with a 200 μ L sample loop. LC analyses were carried out on a 250 \times 2 mm, 5 μ m, Eurospher-100 Si column (Knauer, Berlin, Germany) at 27 °C using *n*-hexane/MTBE (96:4, v/v) as eluent for enriched dairy foods and *n*-hexane/MTBE/*iso*-propanol (96:4:0.1, v/v/v) as eluent for nuts and edible plant oils. Detection was performed with an ultraviolet (UV)-detector set to 205 nm for free sterols/stanols and steryl/stanyl esters, and set to 325 nm for *trans*-steryl/stanyl ferulic acid esters. LC fractions were transferred on-line by switching the valve and the evaporation of the solvent was performed via a programmable multimode inlet in the solvent vent mode. GC separations were carried out on a 30 m \times 0.25 mm i.d., 0.1 μ m film,

trifluoropropylmethyl polysiloxane capillary column (Rtx-200MS, Restek GmbH, Bad Homburg, Germany). Detailed LC, GC, and interface conditions have been described elsewhere (11, 12).

Identification was carried out using an on-line LC-GC-MS system. The gas chromatograph was coupled via a transfer line to an inert 5975C mass spectrometer (MS) with triple axis detector (Agilent Technologies, Waldbronn, Germany) and analyses were performed at conditions previously described (12).

Results and Discussion

GC Analysis of Intact Steryl/Stanyl Fatty Acid Esters

GC analysis of intact steryl/stanyl fatty acid esters is a challenge due to their structural similarities and high boiling points. Previous studies using non-polar stationary phases (e.g. DB-1 and DB-5) resulted in only insufficient separations regarding the degree of saturation of the esterified fatty acid moieties (13–15). Recently, the suitability of an intermediately polar stationary phase for the efficient separation of complex mixtures of steryl/stanyl fatty acid esters was demonstrated (8, 9, 16). The esters were separated according to the sterol/stanol moiety as well as according to the carbon number and degree of unsaturation of the esterified fatty acid moiety. The GC analysis is exemplarily shown for a commercially obtained plant stanyl fatty acid ester mixture in Figure 2. Only saturated and mono-unsaturated fatty acid esters of the same chain length eluted at the same time.

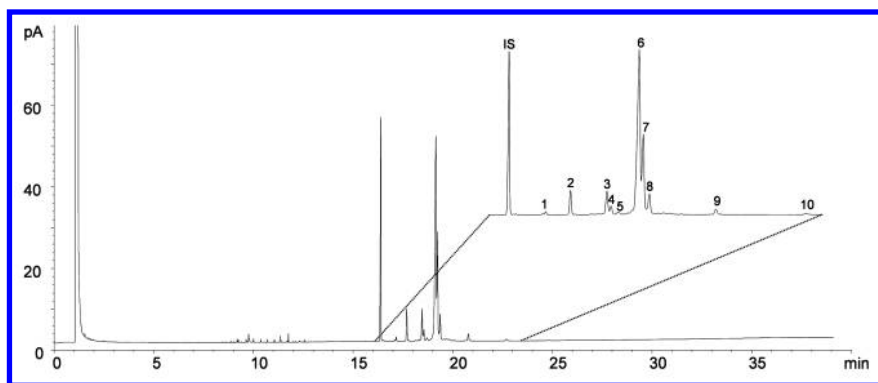


Figure 2. GC analysis of a plant stanyl fatty acid ester mixture. Peak numbering according to Table I; (IS) cholesteryl-16:0.

Taking into account the thermal instability of intact steryl/stanyl fatty acid esters during high temperature GC analysis, response factors were determined for individual esters to compensate for degradation processes (9, 16).

The employed intermediately polar stationary phase was also shown to be effective in the detection and separation of free sterols/stanols and intact steryl/stanyl phenolic acid esters (10).

SPE-Based Approach for the Fractionation of Plant Lipids

For the separation of plant lipids into fractions containing free sterols/stanols and steryl/stanyl esters an approach based on SPE was established (10). Figure 3 illustrates the main steps of the methodology from lipid extraction to GC analysis.

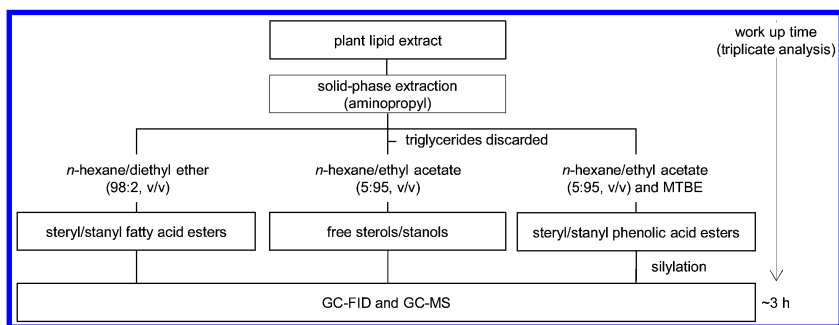


Figure 3. SPE-based approach for the separation of free sterols/stanols and steryl/stanyl esters from plant lipid extracts.

The lipids were extracted from the ground plant material and further separated on an aminopropyl-modified silica gel phase. This type of phase was more efficient in the removal of triglycerides than normal silica phases. The resulting GC analyses are exemplarily shown for the fractions of free sterols/stanols, steryl/stanyl fatty acid esters, and steryl/stanyl phenolic acid esters extracted from whole corn kernels in Figure 4.

On-line LC-GC-Based Approach for the Analysis of Steryl/Stanyl Fatty Acid Esters

The on-line coupling of LC and GC is an efficient and elegant alternative to laborious off-line techniques such as SPE, column chromatography or thin layer chromatography. Fractionation, pre-concentration, and analysis take place in a closed and fully automated system, whereby the risks of sample loss and contamination are reduced. A schematic representation of an on-line LC-GC system with a programmable temperature vaporizer as interface for the evaporation of the solvent, which is transferred from LC to GC, is shown in Figure 5.

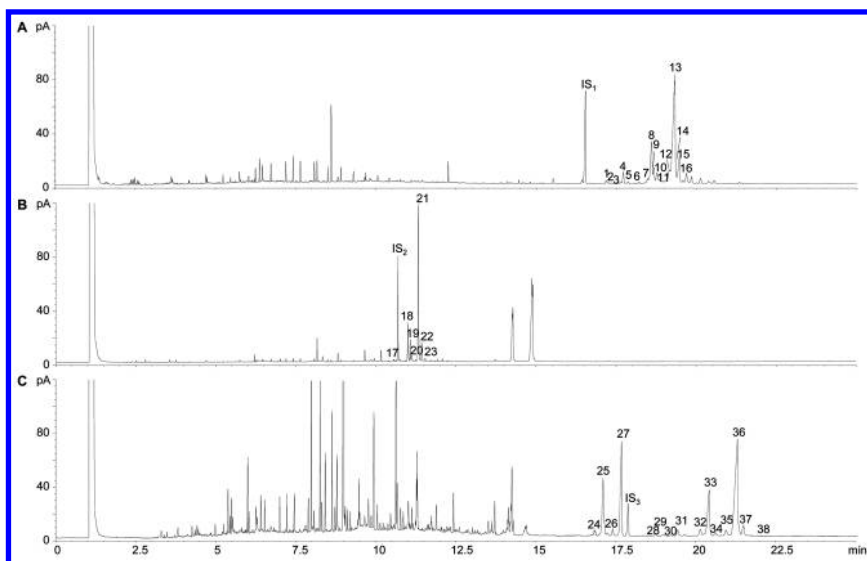


Figure 4. GC analysis of (A) free sterols/stanols, (B) steryl/stanyl fatty acid esters, and (C) steryl/stanyl phenolic acid esters extracted from whole corn kernels: (1) cholesterol, (2) campesterol, (3) stigmasterol, (4) campestanol, (5) sitosterol, (6) sitostanol, (7) unknown sterol, (8) campesteryl-16:0/16:1, (9) stigmasteryl-16:0/16:1, (10) campestanyl-16:0/16:1, (11) sitosteryl-16:0/16:1, (12) sitostanyl-16:0/16:1, (13) Δ^7 sitosteryl-16:0/16:1, (14) campesteryl-18:0/18:1 (15) campesteryl-18:2+stigmasteryl-18:0/18:1, (16) campestanyl-18:0/18:1+stigmasteryl-18:2, (17) campestanyl-18:2, (18) Δ^7 campesteryl-18:2, (19) sitosteryl-18:0/18:1, (20) sitosteryl-18:2, (21) sitostanyl-18:0/18:1, (22) sitostanyl-18:2, (23) Δ^7 sitosteryl-18:2, (24) *cis*-campesteryl ferulate, (25) *cis*-campestanyl ferulate, (26) *cis*-sitosteryl ferulate, (27) *cis*-sitostanyl ferulate, (28) *trans*-campesteryl *p*-coumarate, (29) *trans*-campestanyl *p*-coumarate, (30) *trans*-sitosteryl *p*-coumarate, (31) *trans*-sitostanyl *p*-coumarate, (32) *trans*-campesteryl ferulate, (33) *trans*-campestanyl ferulate, (34) *trans*- Δ^7 campesteryl ferulate, (35) *trans*-sitosteryl ferulate, (36) *trans*-sitostanyl ferulate, (37) *trans*- Δ^7 sitosteryl ferulate, (38) *trans*-24-methylene cycloartanyl ferulate, (IS₁) cholesteryl-16:0, (IS₂) 5 α -cholestan-3 β -ol, and (IS₃) *trans*-cholestanyl ferulate.

The lipids were fractionated on a normal silica gel phase, which has been shown to be effective for the retention of triglycerides (9, 17, 18). The fraction of steryl/stanyl fatty acid esters could then be transferred on-line to the GC, which enabled the analysis of the individual composition of the transferred LC fraction. Compared to methods commonly used for the determination of sterols/stanols and steryl/stanyl esters in enriched foods or natural foods, the advantage of the presented on-line LC-GC-based approaches is in particular the far less complex sample preparation. The work up time is strikingly decreased and compared to

methods involving saponification and purification steps, less solvent amount is needed. Detailed information on the validation of the on-line LC-GC approach, including the limits of detection, has been provided (11, 12, 17). Figure 6 illustrates the on-line LC-GC analysis of a mixture of plant stanyl fatty acid esters.

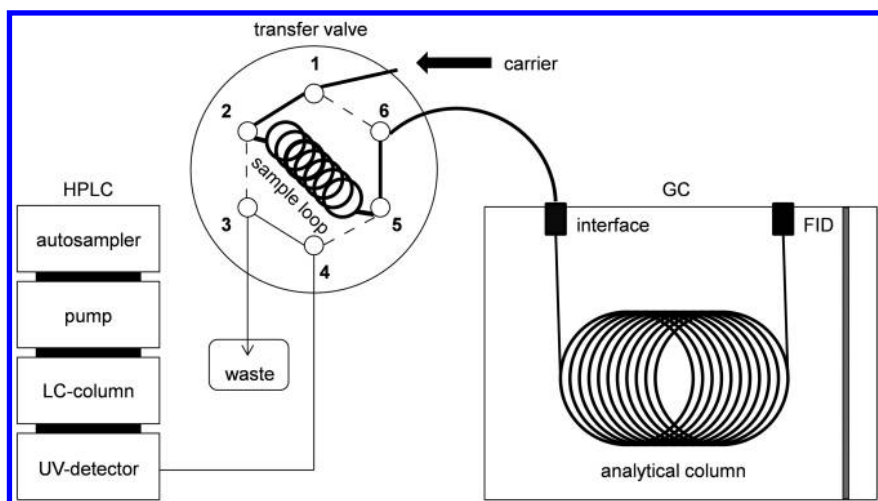


Figure 5. Schematic presentation of an on-line LC-GC system with programmable temperature interface (transfer mode).

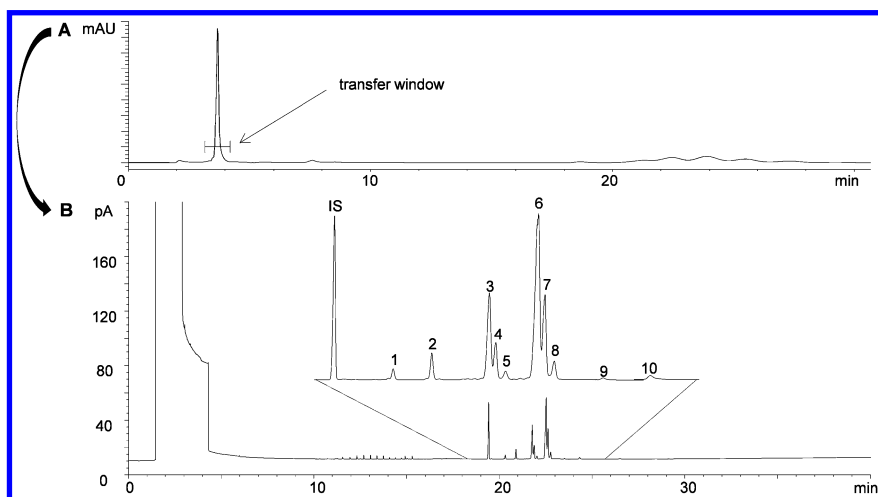


Figure 6. On-line LC-GC analysis of a stanyl fatty acid ester mixture extracted from an enriched cheese-based spread: (A) LC-UV chromatogram at 205 nm and (B) GC-FID chromatogram of the transferred LC fraction. Peak numbering according to Table I; (IS) cholesteryl-16:0.

Application of the Analytical Approaches to Enriched Dairy Foods and Important Natural Sources

Investigation of Free Sterols/Stanols and Steryl/Stanyl Esters in Cereal Grains

The SPE-based approach was applied to the qualitative and quantitative analysis of free sterols/stanols, steryl/stanyl fatty acid esters, and steryl/stanyl phenolic acid esters in corn, rye, wheat, and spelt (10). The methodology provided detailed data on the contents and the distributions of individual members of these compound classes. The distribution patterns of corn, particularly of steryl/stanyl fatty acid and phenolic acid esters, exhibited distinct differences compared to those of rye, wheat, and spelt. In corn, esters of sitosterol and campesterol were predominant and these sterols were mainly esterified to unsaturated fatty acids. Linoleic and oleic acid esters represented more than 90% of total steryl/stanyl fatty acid esters (Figure 7A). Sitosteryl and campesteryl esters were also predominant in rye, wheat, and spelt, but linoleic and oleic acid esters made up only approximately 50% of total esters. The other half was represented by esters of C16-fatty acids, mainly palmitic acid esters (Figure 7A).

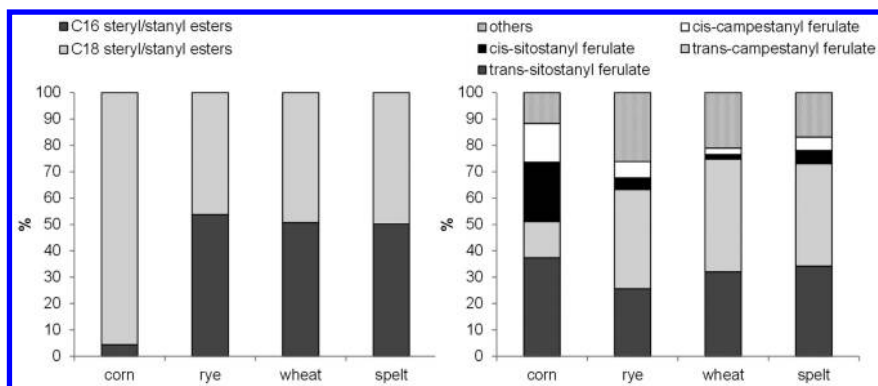


Figure 7. Distributions of (A) steryl/stanyl fatty acid esters and (B) steryl/stanyl phenolic acid esters in cereals.

Regarding the distributions of free sterols/stanols, the observed differences were not as pronounced. Sitosterol accounted for 55-62% and was the dominating free sterol in all four investigated cereal grains, followed by either campesterol or stigmasterol. Sitostanol and campestanol made up between 10 and 16%. Within the fraction of steryl/stanyl phenolic acid esters, the *trans*-derivatives of sitostanyl and campestanyl ferulate were predominant. Coumaric acid esters represented less than 3.4% of total phenolic acid esters. Whereas in corn sitostanyl and sitosteryl esters were more abundant than campestanyl and campesteryl esters, the phenolic acid esters extracted from rye, wheat, and spelt showed an inverse distribution (Figure 7B).

Table I. Analysis of Stanyl Fatty Acid Esters in Enriched Cheese-Based Spread

<i>stanyl esters</i> [g/100 g] ^a		<i>esterified stanols</i> [%] ^{a,c}	
(1) campestanol-16:0/16:1	0.11 ± 0.00	campestanol	29.1 ± 0.4
(2) sitostanol-16:0/16:1	0.20 ± 0.00	sitostanol	70.5 ± 0.4
(3) campestanol-18:0/18:1	1.00 ± 0.03	others	0.5 ± 0.0
(4) campestanol-18:2	0.33 ± 0.01		
(5) campestanol-18:3	0.12 ± 0.01	<i>esterified fatty acids</i> [%] ^{a,c}	
(6) sitostanol-18:0/18:1	2.36 ± 0.05		
(7) sitostanol-18:2	0.83 ± 0.02	16:0/16:1	5.8 ± 0.1
(8) sitostanol-18:3	0.28 ± 0.02	18:0/18:1	63.0 ± 0.4
(9) sitostanol-20:0/20:1	0.08 ± 0.01	18:2	21.7 ± 0.2
(10) sitostanol-22:0/22:1	0.03 ± 0.01	18:3	7.5 ± 0.4
others ^b	0.03 ± 0.00	20:0/20:1	1.5 ± 0.1
total stanyl esters	5.36 ± 0.12	22:0/22:1	0.5 ± 0.1
calculated as stanols ^c	3.28 ± 0.07		

^a Values represent the mean × standard deviation of a triplicate analysis. ^b Calculated with a response factor of 1, relative to cholesteryl-16:0. ^c Calculated on the basis of intact stanyl esters.

Investigation of Stanyl Fatty Acid Esters in Fat-Based Enriched Dairy Foods

On-line LC-GC was successfully applied to the analysis of intact steryl/stanyl esters in enriched dairy products with substantial amounts of protein and fat (11). The samples were subjected to an acid digestion step with hydrochloric acid to release the lipids from the protein matrix, followed by the extraction of the lipids using a mixture of *n*-hexane and MTBE. The lipid extracts were further subjected to on-line LC-GC analysis for the determination of the contents and compositions of the added stanyl fatty acid esters. Possibly interfering neutral lipids such as triglycerides could be effectively removed using a normal silica gel phase as stationary LC-phase and *n*-hexane/MTBE (96:4, v/v) as eluent. Hence, no further purification step was needed and the extracts could directly be analyzed with the on-line LC-GC system. Table I shows qualitative and quantitative data on total and individual stanyl fatty acid esters obtained by the investigation of an enriched cheese-based spread. Oleic acid esters were predominant, followed by linoleic, linolenic, and palmitic acid esters. The determined amounts were in agreement with the declaration on the package (3.3 g stanols/100 g), and the calculated profile of the esterified fatty acids indicates rapeseed oil being the source of the fatty acid mixture used for the esterification of the stanols.

Investigation of Free Sterols/Stanols, Steryl/Stanyl Esters, and Other Minor Lipids in Edible Plant Oils and Nuts

The sample preparation for the analysis of free sterols/stanols, steryl/stanyl esters, and other minor lipids in edible plant oils and nut lipids only required a silylation of the oils. Owing to the silylation step, the trimethyl silyl (TMS)-derivatives of free sterols/stanols and the steryl/stanyl fatty acid esters as well as the TMS-derivatives of other minor lipids such as tocopherols and free fatty acids exhibited similar polarities and thus eluted at the same time in a merged peak under the employed LC conditions; this enabled the transfer in a single fraction to the GC (12). *Trans*-derivatives of steryl/stanyl ferulic acid esters could be analyzed via a second transfer. The simultaneous analysis of free fatty acids, tocopherols, free sterols, and steryl fatty acid esters by on-line LC-GC is exemplarily shown for rapeseed oil in Figure 8.

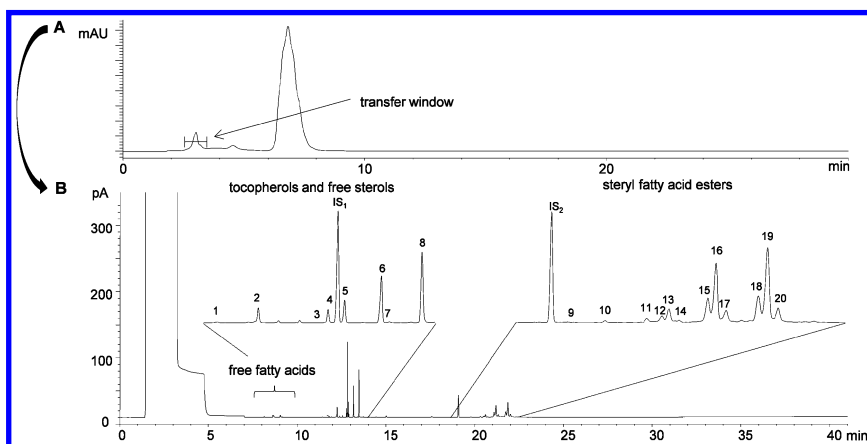


Figure 8. On-line LC-GC analysis of free fatty acids, tocopherols, free sterols, and steryl fatty acid esters in rapeseed oil: (A) LC-UV chromatogram at 205 nm and (B) GC-FID chromatogram of transferred LC fraction: (1) δ -tocopherol, (2) γ -tocopherol, (3) cholesterol, (4) α -tocopherol, (5) brassicasterol, (6) campesterol, (7) stigmasterol, (8) sitosterol, (9) brassicasteryl-16:0/16:1, (10) campesteryl-16:0/16:1, (11) sitosteryl-16:0/16:1, (12) brassicasteryl-18:0/18:1, (13) brassicasteryl-18:2, (14) brassicasteryl-18:3, (15) campesteryl-18:0/18:1, (16) campesteryl-18:2, (17) campesteryl-18:3, (18) sitosteryl-18:0/18:1, (19) sitosteryl-18:2, (20) sitosteryl-18:3, (IS₁) 5 α -cholestan-3 β -ol, and (IS₂) cholesteryl-16:0.

The analysis of several commercially available oils revealed corn germ oil and rapeseed oil as the richest sources of, in particular, steryl/stanyl fatty acid esters. The average total amounts of steryl/stanyl fatty acid esters ranged from 0.07 to 0.96 mg/100 mg oil; those of free sterols/stanols from 0.14 to 2.34 mg/100 mg oil (Figure 9). Ferulic acid esters could only be detected in corn germ oil,

accounting for 0.1 mg/100 mg oil. The majority of the sterols/stanols in most of the investigated plant oils occurred in form of their fatty acid esters, except for the native sunflower oils, safflower oil, soybean oil and olive oils, where the amounts of free sterols/stanols and steryl/stanyl fatty acid esters were either equal or free sterols/stanols were predominant. Regarding the distribution patterns of free sterols/stanols and steryl/stanyl esters, considerable differences were observed between the various oils. The applied on-line LC-GC-based approach enabled the fast and robust analysis of these lipid compounds, which could thus be a useful tool for authenticity assessments of plant oils.

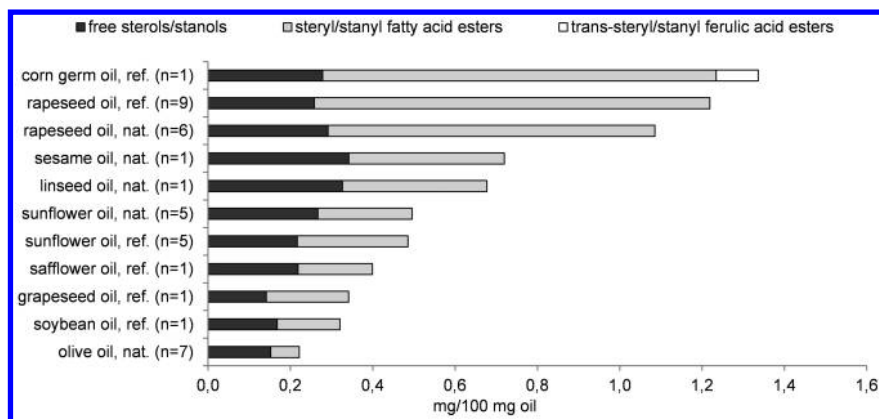


Figure 9. Mean total contents of free sterols/stanols and steryl esters in edible plant oils.

Additionally, three batches of ten different commercially important nut types were studied regarding their contents and compositions of free sterols/stanols and steryl/stanyl fatty acid esters (Figure 10).

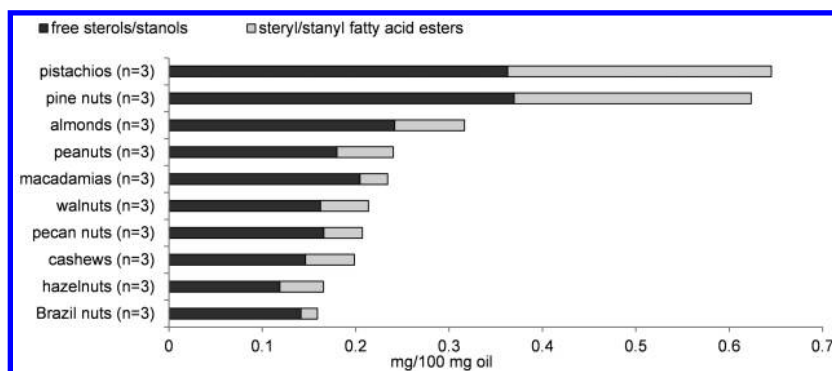


Figure 10. Mean total contents of free sterols/stanols and steryl/stanyl esters in oils extracted from nuts.

The main part of the sterols/stanols in the investigated nuts occurred in free form, followed by fatty acid esters; *trans*-steryl/stanyl ferulic acid esters could not be detected. The total amounts of steryl/stanyl fatty acid esters in the extracted nut oils ranged from 0.02 to 0.28 mg/100 mg, those of free sterols/stanols from 0.12 to 0.37 mg/100 mg; they were both by far the highest in pistachios and pine nuts (12).

Conclusion

Capillary gas chromatography on an intermediately polar stationary phase was shown to be suitable for the detection and separation of individual free sterols/stanols and intact steryl/stanyl esters. On this basis, analytical approaches for the qualitative and quantitative analysis of free sterols/stanols and steryl/stanyl esters were established. The authentication of steryl/stanyl fatty acid esters in enriched fat-based dairy foods can be performed via a combination of acid digestion, lipid extraction, and on-line LC-GC analysis. For the determination of naturally occurring free sterols/stanols and steryl/stanyl esters, an approach based on solid-phase extraction and GC analysis was developed; the applicability was shown for the investigation of cereal grains. The suitability of on-line LC-GC for the analysis of free sterols/stanols and steryl/stanyl esters in plant lipids was demonstrated using edible plant oils and nuts as examples. The established methodologies show distinct advantages compared to methods commonly used for the determination of sterols/stanols and steryl/stanyl esters in enriched as well as natural foods. They allow the simultaneous analysis of various sterol/stanol substance classes, and especially the achieved GC separation enables a detailed qualitative and quantitative analysis of individual intact steryl/stanyl esters. Thus, the presented methodologies can be applied as useful tools for the analytical characterization of functional foods and of naturally occurring bioactive food constituents.

References

1. Piironen, V.; Lindsay, D. G.; Miettinen, T. A.; Toivo, J.; Lampi, A.-M. *J. Sci. Food Agric.* **2000**, *80*, 939–966.
2. Demonty, I.; Ras, R. T.; van der Knaap, H. C. M.; Duchateau, G. S. M. J. E.; Meijer, L.; Zock, P. L.; Geleijnse, J. M.; Trautwein, E. A. *J. Nutr.* **2009**, *139*, 271–284.
3. Plat, J.; Mensink, R. P. *Am. J. Cardiol.* **2005**, *96*, 15D–22D.
4. Katan Martijn, B.; Grundy Scott, M.; Jones, P.; Law, M.; Miettinen, T.; Paoletti, R. *Mayo Clin. Proc.* **2003**, *78*, 965–78.
5. SCF (Scientific Committee on Food) SCF/CS/NF/DOS/1 FINAL. 2000.
6. SCF (Scientific Committee on Food) SCF/CS/NF/DOS/15 ADD 2 FINAL. 2003.
7. SCF (Scientific Committee on Food) SCF/CS/NF/DOS/23 ADD 2 FINAL. 2003.

8. Barnsteiner, A.; Esche, R.; di Gianvito, A.; Chiavaro, E.; Schmid, W.; Engel, K.-H. *Food Control* **2012**, *27*, 275–283.
9. Barnsteiner, A.; Lubinus, T.; di Gianvito, A.; Schmid, W.; Engel, K.-H. *J. Agric. Food Chem.* **2011**, *59*, 5204–5214.
10. Esche, R.; Barnsteiner, A.; Scholz, B.; Engel, K.-H. *J. Agric. Food Chem.* **2012**, *60*, 5330–5339.
11. Esche, R.; Carcelli, A.; Barnsteiner, A.; Sforza, S.; Engel, K.-H. *Eur. Food Res. Technol.* **2013**, *236*, 999–1007.
12. Esche, R.; Müller, L.; Engel, K.-H. *J. Agric. Food Chem.* **2013**, *61*, 11636–11644.
13. Evershed, R. P.; Male, V. L.; Goad, L. J. *J. Chromatogr., A* **1987**, *400*, 187–205.
14. Gunawan, S.; Melwita, E.; Ju, Y.-H. *Food Chem.* **2010**, *121*, 752–757.
15. Kamm, W.; Dionisi, F.; Fay, L. B.; Hischenhuber, C.; Schmarr, H. G.; Engel, K. H. *J. Chromatogr., A* **2001**, *918*, 341–349.
16. Engel, K.-H.; Barnsteiner, A. In *Progress in Authentication of Food and Wine*; Ebeler, S. E., Takeoka, G. R., Winterhalter, P., Eds.; ACS Symposium Series 1081; American Chemical Society: Washington, DC, 2011; pp 177–187.
17. Esche, R.; Scholz, B.; Engel, K.-H. *J. Agric. Food Chem.* **2013**, *61*, 10932–10939.
18. Grob, K.; Kaelin, I.; Artho, A. *J. High Resolut. Chromatogr.* **1991**, *14*, 373–376.

Chapter 14

Unraveling Food Aroma: Methods for Odor Active Compounds Analysis

Henryk Jeleń*

Poznań University of Life Sciences, Faculty of Food Science and Nutrition,
Wojska Polskiego 31, 60-624 Poznań, Poland

*E-mail: henrykj@up.poznan.pl.

Odorants in food represents various chemical classes and include compounds of different volatility, polarity, chemical character, stability and reactivity. Moreover, food is a complex matrix to extract aroma compounds from, which makes their analysis a challenging task. In this chapter different approaches to the analysis of food odorants are discussed. Emphasis is put on their proper extraction methods, specificity of gas chromatography – olfactometry and multidimensional chromatography. Identification methods based on chromatography and mass spectrometry and quantitation approaches to food odorants are summarized.

Introduction

Aroma of food is one of the main attribute which is taken into consideration by consumers when choosing or rejecting food. Odoriferous compounds often indicate biochemical, chemical or microbial changes that take place during food processing and storage. Some odoriferous compounds, being the cause of off-odors and taints can be markers of these processes. Aroma compounds are formed also in a result of physiological processes in fruit and vegetables, are produced by microorganisms in fermentation processes, and also in a result of thermal treatment of food products or raw materials. Heat generated flavors form the most abundant group of volatile compounds in food.

Among thousands of volatile compounds isolated from foods only a small fraction (few %) is responsible for food aroma (1). Aroma compounds despite being extremely diverse in character are present in food in very broad concentration ranges. They can contribute to flavor in concentrations as low as ng/L range, moreover, their impact on food aroma is dependent on their concentration, as well as on their odor thresholds (OT), which also is often in a ng/L range. This poses a special challenge for analysts, making aroma compounds analysis challenging and specific task, as methods developed are often verified by human smell perception. As a result for the investigation of aroma compounds in food several factors have to be considered for a successful qualitative and quantitative analysis. These factors include:

- the complex nature and diversity of food odorants to be determined often in a single run,
- different concentrations of aroma compounds and other volatiles,
- matrix complexity and influence on aroma compounds release,
- extraction specificity guaranteeing maximum compounds recovery and protecting analytes from decomposition,
- matrix and aroma compounds stability,
- method performance - competitive to human nose in terms of limits of detection (LOD) and quantitation (LOQ)

For the successful analysis of aroma compounds, bearing in mind their low odor thresholds, all steps should be optimized: compounds isolation and pre-concentration, separation, detection and quantitation. There are many review papers and other sources on the specificity of flavor compounds analysis, focused either on specific foods, compounds or mainly, techniques (2–6). There are also specific guidelines regarding mainly the aroma compounds identification and quantitation procedures (7–9).

Strategies for aroma compounds analysis in food can be divided roughly into three approaches:

- i) target analysis of specific odorants,
- ii) sensory guided analysis of key odorants,
- iii) fingerprinting/profiling of volatile compounds.

Target analysis of specific compounds is often used for identification of known odoriferous compounds related to specific odor note or aroma of particular food. The example of such approach is the determination of compounds responsible for a known off-flavors or taints. Earthy – musty off-odors of some foods can be caused by several suspects: haloanisoles, geosmin, 2-methylisoborneol, 2-methoxy-3,5-dimethylpyrazine (MDMP), 2-methoxy-3-isopropylpyrazine (IPMP), or 1-octene-3-one. The type of off-odor can provide a hint in selection of compounds for screening and the analysis is directed to the search for known suspects. When it is impossible to deduce the possible source of an odor or off-odor, sensory guided analysis is usually performed.

Sensory guided analysis of key odorants is the approach that focuses on pinpointing compounds responsible for the aroma of a given product (i.e. key odorants). In a result of sensory profile analysis of investigated food descriptors of the main odor notes can be elucidated and a sensory profile of the product is revealed. Then, chromatographical methods are used to find key odorants. Modern separation techniques allow separation of hundreds of volatile compounds isolated from food. In case of multidimensional gas chromatography the number of possible compounds separated increases substantially compared to one dimensional gas chromatography. As only a small portion of compounds is responsible for the aroma, to select these compounds methods based on the use of human nose as a detector emerged (10, 11). Gas chromatography-olfactometry (GC-O) allows identification of odoriferous fractions in the chromatogram and methods such as AEDA (Aroma Extract Dilution Analysis)(1) allow quantitation of odor sensation. Key odorants are then identified and quantified using usually GC/MS. Reconstitution or aroma from identified key odorants should resemble the smell of investigated product.

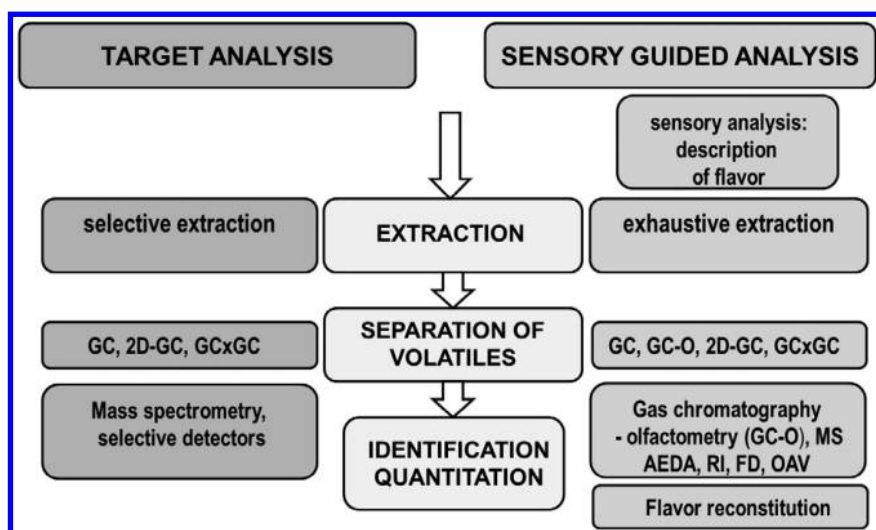


Figure 1. Scheme of the analytical approaches to aroma compounds determination in food.

Volatile compounds fingerprinting/profiling is usually not targeted at aroma compounds analysis, but is often used for the comparison of products, treatments, processes and storage conditions. One of the most important field of application of volatile compounds profiling is their use in the authenticity and traceability investigation of foods. It is used to determine botanical, regional origin, differentiation of varieties of beers, honeys, wines, spirits, coffee, olive oil, cheese to name the most frequently investigated products (12). Chemometric approach is used to process data and multivariate statistical methods, such as cluster analysis (CA), principal component analysis (PCA), linear discriminant analysis (LDA) are used to differentiate, groups of objects and identify compounds responsible for the differences between groups. PCA is usually utilized as a first step to visualize differences between samples and their classification patterns. Both CA and PCA represent an unsupervised learning methods. To obtain a statistical tool for both sample classification and prediction supervised learnind methods are used, such as LDA. In this approach a model is built in which data is divided into training set of samples of known origin, and validation set of the same sample type. Once the model is validated unknown samples can be analyzed predicting the belonging of unknowns to particular class. Another perspective for profiling volatile compounds is in the development of metabolomic approach to the analysis of large sets of data to focus on sensory relevant compounds (13). Figure 1. shows the main approaches and steps in the analysis of aroma compounds in foods.

Compounds that are perceived by human sense of smell exist in food in their free form i.e. they are released from food into the headspace and then sniffed. To be analyzed they have to be extracted, eventually preconcentrated and transferred to a gas chromatograph. Release of flavor compounds from the matrix is highly dependent on the matrix-analyte interaction - partition of analyte and the eventual interactions of analyte with food macromolecules such as proteins, carbohydrates and lipids. Three main macroconstituents of food – lipids, carbohydrates and proteins influence the behavior of flavor compounds and their interaction with matrix. Aroma compounds are usually hydrophobic and lipids act as solvents for lipophilic compounds. Hydrophobicity is one of the main factors that governs the interactions of volatiles with liquid phase. Partition coefficients will therefore be dependent on fat contents changes (i.e. in milk products). In emulsions proportions of oil/water will influence partition of flavor compounds between air and emulsion. When carbohydrates form the marix type of saccharide influences partition of volatiles as polysaccharides influence viscosity – gelatinized starch increases flavor retention by minimizing diffusion rates, in starch solutions competitive binding can take place. Dry starch granules can act as porous adsorbent. When proteins are main matrix constituents their sensitivity to heat treatment and pH changes influence their aroma binding capacities. Binding to protein process can be reversible and irreversible and the binding sites and constants are protein type dependent. The complexity of matrix – volatiles interactions has been discussed in books and numerous papers (14–18) and the analyte matrix interaction are one of crucial issues in food flavor analysis.

Extraction Methods

Extraction methods used for analysis of odor active compounds can be roughly divided into exhaustive and non-exhaustive extractions.

Exhaustive extraction allows total transfer of aroma compounds from matrix into the extracting solvent. Liquid/liquid extraction can be an example of such methods. Because flavor compounds are in great part compounds of low polarity (ie lipophilic) they can be co-extracted from food products with fat when extraction is performed using nonpolar solvents. Aroma compounds are often mixtures of compounds of different polarities, therefore mixtures of solvents are used (ie pentane/diethylether) for their extraction. To get rid of co-extracted impurities distillation methods have been developed. The most appropriate for labile aroma compounds extraction are methods using vacuum to minimize formation of artefacts and compounds decomposition. Among methods used for key odorants isolation, where preservation of aroma of the product as intact as possible is important SAFE (Solvent Assisted Flavor Evaporation) is widely used (19). It allows separation (distillation) of volatile fraction from the matrix. SAFE is the basic method used for gas chromatography-olfactometry methods. For compounds that are thermally stable simultaneous distillation-extraction methods are used, such as in Likens-Nikerson distillation apparatus (5).

Non-exhaustive extraction comprise methods that are based on partition of the analyte between matrix and the headspace. As aroma compounds are volatile, headspace analysis methods are widely used in their analysis. Headspace analysis in its simplest form is a static headspace method, where a certain volume of headspace is transferred from vial, which was equilibrated (at certain temperature and time) into injection port of gas chromatograph using different transfer methods (using syringe or a loop transfer). The drawback of static headspace is its relatively low sensitivity (usually high $\mu\text{g}/\text{kg}$), which sometimes limits its use for trace analysis. Because many of odorants need to be quantified at very low (ng/L) levels preconcentration step is a crucial element of sample preparation. Method based on the headspace analysis but using sorbents or solvents for analyte preconcentration were developed within last decades. Of microextraction methods providing high preconcentration of analytes SPME dominates in flavor compounds analysis. Majority of SPME applications are in the field of wine analysis, followed by fruit/vegetables, dairy, beverages, meat, spices, cereals, fats and oils to name the most explored applications. The success of SPME in volatile-flavor compounds analysis is related to its sensitivity, robustness and ease of use. SPME extraction can be done manually maintaining high reproducibility. Apart from being very sensitive SPME is also extraction technique that offers high selectivity. The selectivity is based on the fiber coating materials that are used. The coatings are available in different types and polarities and sorption mechanisms are typical for liquid phases (absorption in polydimethylsiloxane (PDMS), polyacrylate (PA) fibers), or for polymers (adsorption in Carboxene/Divinylbenzene or carboxene fibers). Though very simple to perform SPME methods to be used properly for quantitative purposes require multistep method parameters optimization procedure. Other microextraction methods used for flavor analysis encompasses stir bar sorptive

extraction (SBSE), single drop microextraction (SDME) and also liquid/liquid microextraction (LLME)(6). Microextraction methods offer frequently very low limits of detection, which makes them an attractive tool for trace compounds analysis.

In nonexhaustive extraction methods partition coefficient of analyte is dependent on the nature of matrix, therefore it is of a special importance to explore matrix influence on extraction in the method development process. Figure 2 illustrates the influence of matrix type on the partition of analyte: 2-(Z)-heptenal spiked into mayonnaise of different fat contents yields different peak areas when sampled using static headspace. It indicates the necessity of careful calibration of the compounds using specific matrix. Food products are matrices which are homogenous, but can also be non-homogenous. Extraction of aroma compounds from homogenous matrices simplifies sample preparation, especially calibration process. However in many instances for non-homogenous matrices, solid matrices or non-Newtonian liquids, calibration process is more laborious and sophisticated. For solid matrices spiking standard compounds to construct calibration curves does not always reflects the interactions, which exist in naturally occurring compounds. Solid matrices are often homogenized with water and such pre-prepared matrix is spiked with analytes for calibration purposes. In case of hydrophobic compounds water addition can ease their migration into headspace. Such preparation of potato chips to facilitate volatile lipid oxidation products partition into headspace is shown on Figure 3. The water addition to chips influences the peak area of 2-(Z)-heptenal and shows the possibilities of increasing sensitivity of the method using this approach. Manipulation with matrix by water addition is used often for solid foods (20).

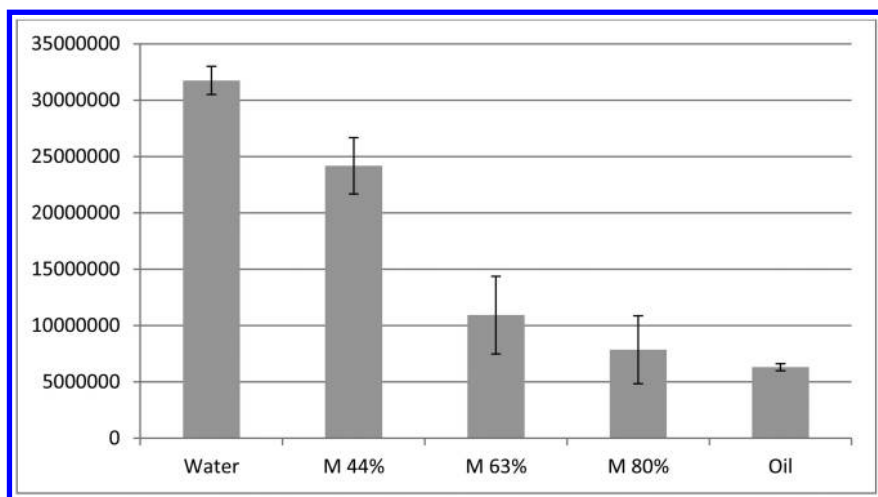


Figure 2. Peak area of 2-(Z)-heptenal spiked at 10mg/L and then extracted by static headspace technique from mayonnaise of different oil contents (44 – 80%). For a comparison peak areas of 2-(Z)-heptenal from spiked water and rapeseed oil are shown.

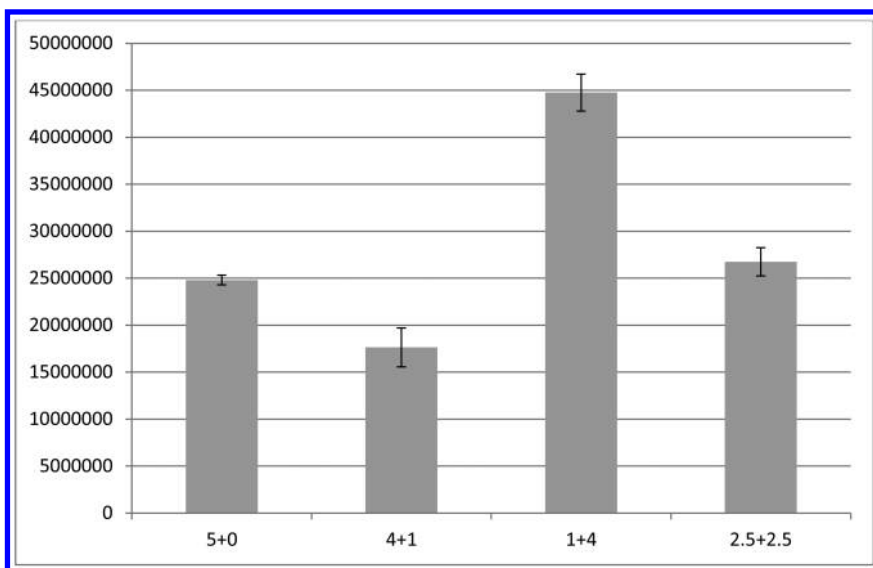


Figure 3. Peak area of 2-(Z)-heptenal spiked at 10mg/L and then extracted by static headspace technique from potato chips prepared in a different way: (5+0) – 5g of chips, no water added; (4+1) – 4g of chips, 1g of water, vortexed; (1+4) – 1g of chips, 4g of water, vortexed; (2.5+2.5) – equal amounts on chips and water (2.5g), vortexed.

Separation Methods

As the aroma compounds are volatile, capillary gas chromatography is a separation method of a choice with a long tradition. Capillary gas chromatography when performed on a single column allows separation of few hundred compounds per analysis. The main obstacle in analyses using single dimensional chromatography is the coelution of compounds. To overcome this problem and increase peak capacity of chromatographic system, multidimensional chromatography was developed. It is performed on a two dimensional (2D GC) systems, using a method called heart cutting that facilitates transfer of a peak (or chromatographical fraction of interest) using a special valve or pneumatic system onto another column, where different separation mechanism is applied. The other column is connected to a different detector than the first one. 2D GC has been used to separate complex mixtures, also to provide chiral separation of odor active isomers in mixtures. Developments in gas chromatography leading to comprehensive gas chromatography (GCxGC) opened a possibility to separate few thousand compounds mixtures in a single run. Orthogonal

separation mechanism is usually performed on nonpolar-polar, or polar non-polar columns setup. All compounds eluting from the first column enter second column after being refocused usually by crioccentration performed in a modulator. All compounds are transferred into the detector, which is in most cases mass spectrometer able to acquire spectra in a fast rate, as the second column is usually a narrowbore, producing very narrow peaks. Such approach is used mainly for target analysis, where selectivity of the chromatographical system achieved by physical separation of peaks allows their better identification using mass spectrometry. As an example Figure 4 shows region of GCxGC chromatogram of white wine, where 2,4,6-tribromoanisole (TBA) appears (highlighted on chromatogram, 10ng/L, spiked into white wine). Tribromoanisole is a compound originating from microbial methylation of bromophenols that are used as wood preservatives (fungicides) or flame retardants. TBA is responsible for a musty-corky taint in wine, though its main source is 2,4,6-trichloroanisole (TCA). Similarly to TCA, TBA has low odor threshold of 4-8ng/L. The upper TIC chromatogram shows the complexity of the region, where TBA elutes. The peak due to the low amount of TCA is practically non visible in TIC mode. It can be seen that analyzing it on a single dimensional chromatography on DB5 column there are several compounds that can coelute with it in the same time. When ion $m/z=329$, characteristic for TBA is extracted, the compound is visible on the lower chromatogram, however also for the selected mass, there is a noticeable coelution on DB-5 column with another compound sharing the same ion. TBA is separated from the potential coeluting compounds on Supelcowax-10 used in the setup as a secondary column, which improves its separation and signal/noise ratio.

Comprehensive gas chromatography (GCxGC) as well as two dimensional chromatography (2D-GC) are also very helpful in the separation of coeluting compounds and an unequivocal identification of odor active molecules often present besides peak of volatiles with lesser or none sensory importance (21–23).

Identification and Quantitation Methods

Identification and quantitation of odor active molecules in flavor research is based on two main hyphenated techniques: gas chromatography olfactometry (GC-O) and gas chromatography – mass spectrometry (GC-MS).

Gas chromatography – olfactometry enables identification of odor active regions in chromatogram, where key odorants are present. Sniffing effluent from a capillary column and parallel detection using mass spectrometry enables identification of compounds that interact with receptors in human olfactory bulbs inducing certain aroma. Screening techniques based on analysis of serially diluted flavor extract, such as AEDA (1, 10) enable selection of key odorants of particular food. Figure 5 shows the aromagram of main odorants in fried tempeh (23). FD (flavor dilution) factors illustrate how many times diluted was the extract in which a particular compound was still detectable using GC-O. On the figure compound number 10 (2-acetyl-1-pyrroline, FD 1024) was the predominant key odorant, followed by 4 detectable ones at a 1:512 dilution (compounds 2, 12, 13, 14), and more compounds of lower FD factors.

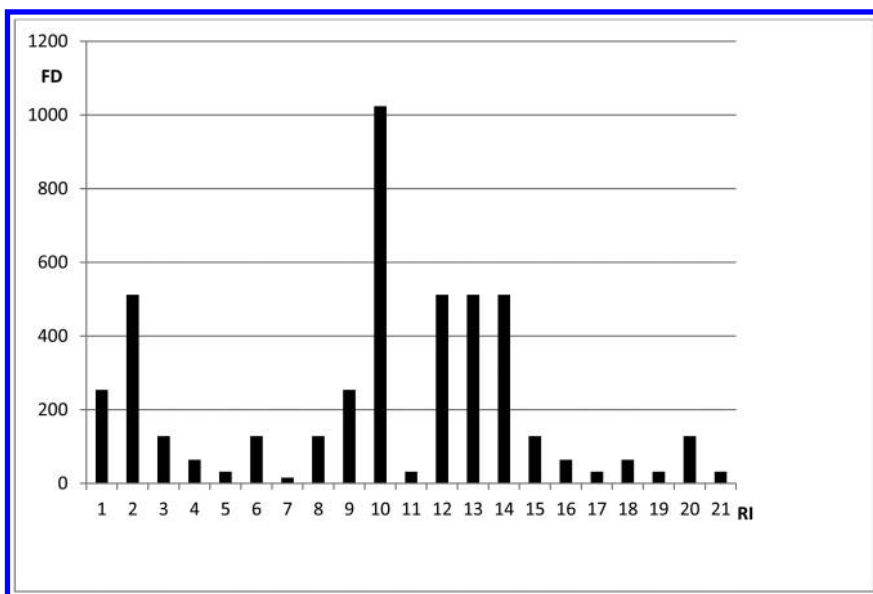


Figure 4. Flavor dilution factors (FD) vs. peak numbers of main odoriferous fractions of tempeh fermented for 5 days and fried. Bar numbers correspond to peaks of: 1) dimethyl sulfide; 2) 2-methylpropanal; 3) 2 and 3-methyl butanal; 4) 2,3-butanedione; 5) butanol; 6) hexanal; 7) 3-methyl butanol; 8) (Z)-4-heptenal; 9) 1-octene-3-one; 10) 2-acetyl-1-pyrroline; 11) (Z)-1,5-octadienone; 12) dimethyl trisulfide; 13) 2-ethyl-3,5-dimethylpyrazine; 14) 3-(methylthio)propanal; 15) 2,3-diethyl-5-methylpyrazine; 16) (E)-2-nonenal; 17) (E,Z)-2,6-nonadienal; 18) phenylacetaldehyde; 19) unknown; 20) (E,E)-2,4-decadienal; 21) 2-methoxy phenol. Based on (17).

Mass spectrometry is a method of choice in the identification of odor active molecules. Hyphenation of gas chromatography with mass spectrometry provides a universal tool for the identification of aroma compounds based on their EI spectra and comparison with commercially available libraries and also provides a tool for quantitation of even unresolved compounds. Apart from “standard” EI mass spectra libraries, such as NIST or Wiley, there are more specific libraries for particular groups of compounds (i.e. pesticides, terpenes). As the quality of spectra is of substantial importance in proper identification of compounds the best available separation of volatiles using state of art GC is required. For the unresolved compounds deconvolution software can be used to identify compounds from overlapping mass spectra. Such software is either an add-on to the mass spectra library (Amdis) or is incorporated into instrument’s data processing software.

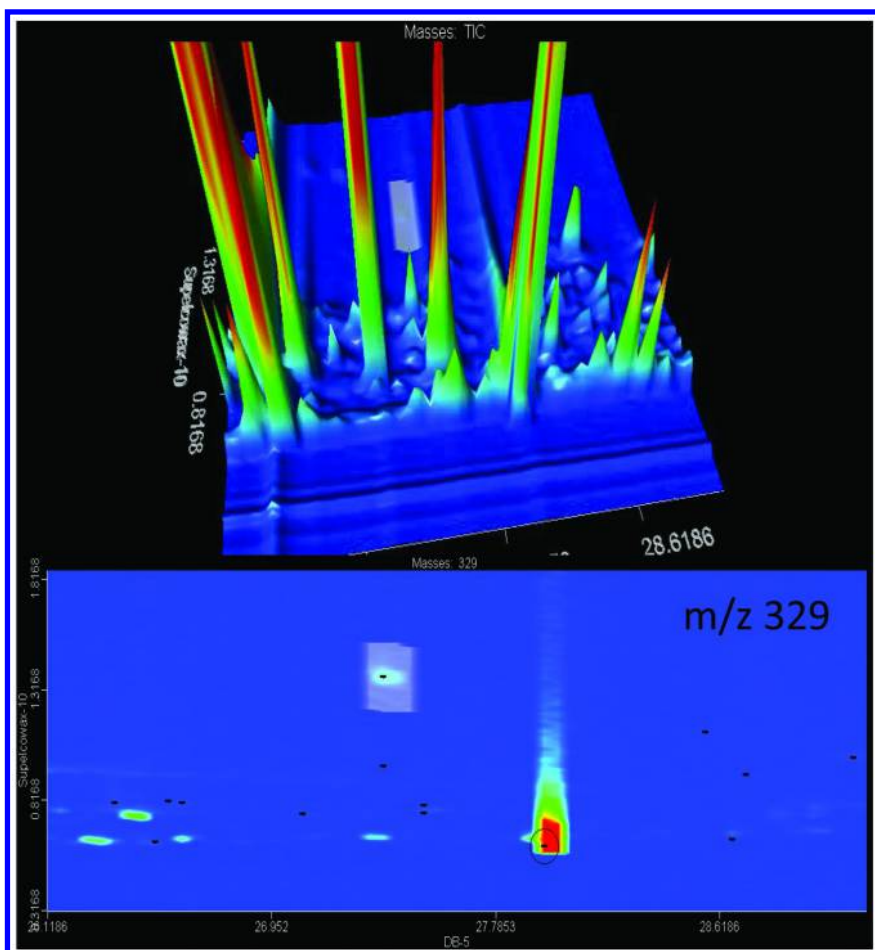


Figure 5. Total ion current (TIC) of a GCxGC chromatogram with eluting TBA (10ng/L) highlighted. Lower graph shows extracted ion chromatogram ($m/z=329$) for TBA.

Identification of aroma compounds present in food is usually a complex task. Despite the abilities of two dimensional chromatography to resolve a complex mixtures, single dimensional chromatography is still a prevailing separation tool in these analyses. As a standard approach analysis of odorants should be

performed on two columns of different polarities (usually nonpolar ones, such as DB-1 or DB-5 type, and a polar ones based on Carbowax type phase). For identification purposes retention times are replaced by retention indices that are calculated usually based on a series of *n*-alkanes homologues. There is a substantial literature data on retention indices of flavor compounds, which provide useful information for compounds identification. Combination of separation of a compound on two columns and the mass spectrum gives strong evidences for compound identity, though is not always sufficient. Retention data and mass spectra of tentatively identified compounds should be compared with authentic standards. If not commercially available the compounds should be preferably synthesized. For additional confirmation gas chromatography – olfactometry (GC-O) should be performed to compare the odor of analyzed compound with the authentic standard. For chiral compounds their retention data should be obtained on chiral columns. For novel compounds identified, their spectral characteristics should be provided (HRMS, NMR, IR) (7).

After GC-O and GC-MS analyses a list of key odorants (based on FD factors) is obtained with a sensory characteristic (by GC-O) of particular compound and compounds identity obtained by GC/MS. The next step after identification of key odorants is their quantitation. It is usually done using mass spectrometry, as it is a method that allows the use of isotopically labelled internal standards for quantitation (SIDA), and also in many cases enables quantitation of unresolved compounds based on extracted ions or tandem mass spectrometry.

Quantitation of aroma compounds is the most demanding part of analysis, bearing in mind the complex character of food as a matrix, and often very low concentrations in which odorants are present. As it is very hard to obtain analyte-free matrices standard addition method is a preferred one, if SIDA is not possible. Proper calibration is especially important in such extraction methods as SPME (24), and can standard addition method, apart from SPME be used in other isolation methods, such as SAFE, though it requires several analyses for a compound. Guidelines for the quantitative gas chromatography of flavor compounds are provided in the literature (8).

Stable isotope dilution analysis (SIDA) is the preferred method of quantitation as the physico-chemical behavior of analyte and its isotopically labelled analogue are identical, therefore extraction errors are minimized. In Table 1 identified key odorants of tempeh are listed, with their odor characteristics, retention indices on two different columns, odor thresholds (literature data) and concentration. 11 out of 19 compounds were quantified using SIDA, the remaining ones using standard addition. Figure 6 shows one of the tempeh key odorants – 1-octene-3-one quantified using $^2\text{H}_3$ -1-octene-3-one as a deuterated analogue. For quantitative purposes ions m/z 70 and 73 were selected and analysis was performed by GCxGC-ToFMS. The last step in quantitative analysis of odorants is the calculation of OAV (Odor Activity Values), which is a ratio of compounds concentration to its odor threshold. It indicates the true impact of the compound on the overall aroma of a particular food. Odor thresholds for the OAV calculation should be preferably determined in investigated food as a matrix, however usually OT values for water are used for calculations. Compounds of the highest OAV have the strongest influence on food aroma.

Table 1. Main Aroma Fractions of Fried Tempeh Prepared from Soy Fermented for 5 Days (Based on (17))

	<i>Compound</i>	<i>Odor</i>	<i>RI^b Wax/DB5</i>	<i>OT^c [$\mu\text{g/L}$]</i>	<i>Conc^d [$\mu\text{g/kg}$]</i>	<i>OAV^e</i>
1.	dimethyl sulfide	cabbage	718/502	7,6	145	19
2.	2-methylpropanal	rancid	870/562	0,7	218	311
3.	2 and 3-methyl butanal	malty	920/651	0,4	224	560
4.	2,3-butanedione	buttery	980/593	15	118	8
5.	2-butanol	spoilage	1012/552	17000	3150	<1
6.	hexanal	grass	1079/801	10	3386	339
7.	3-methyl butanol	rancid	1215/732	29930	13488	<1
8.	(Z)-4-heptenal	rancid	1267/901	0,06	18	300
9.	1-octen-3-one	mushroom	1296/980	0,04	21	525
10	2-acetyl-1-pyrroline	popcorn	1325/931	0,1	138	1380
11	(Z)-1,5-octadienone	geranium	1353/983	0,0012	Nd	Nd
12	dimethyl trisulfide	cabbage	1369/963	0,01	9	900
13	2-ethyl-3,5-dimethylpyrazine	roasted	1445/1081	0,16	54	338
14	3-(methylthio)propanal	boiled potato	1449/908	0,2	186	930
15	2,3-diethyl-5methyl pyrazine	earthy, roasted	1490/1087	0.09	4,4	49
16	(E)-2-nonenal	soap, fatty	1531/1156	0,69	26	38
17	(E,Z)-2,6-nonandienal	cucumber	1585/1135	0,03	Nd	Nd
18	phenylacetaldehyde	honey	1641/1038	6,3	624	99

	<i>Compound</i>	<i>Odor</i>	<i>RI^b Wax/DB5</i>	<i>OT^c [µg/L]</i>	<i>Conc^d [µg/kg]</i>	<i>OAV^e</i>
19	unknown	spicy	1688/unkn	-	Nd	Nd
20	(E,E)-2,4-decadienal	fatty, fried	1798/1321	0,2	91	455
21	2-methoxy phenol	smoke	1859/1089	1	5	5

^a–Odor perceived at the sniffing port ^b - Retention Indices determined on Supelcowax-10 and DB-5 columns ^c – odor thresholds in water ^d - mean values based on three replicates ^e - odor activity values (OAV) calculated by dividing the concentration of analyte by its odor threshold value.

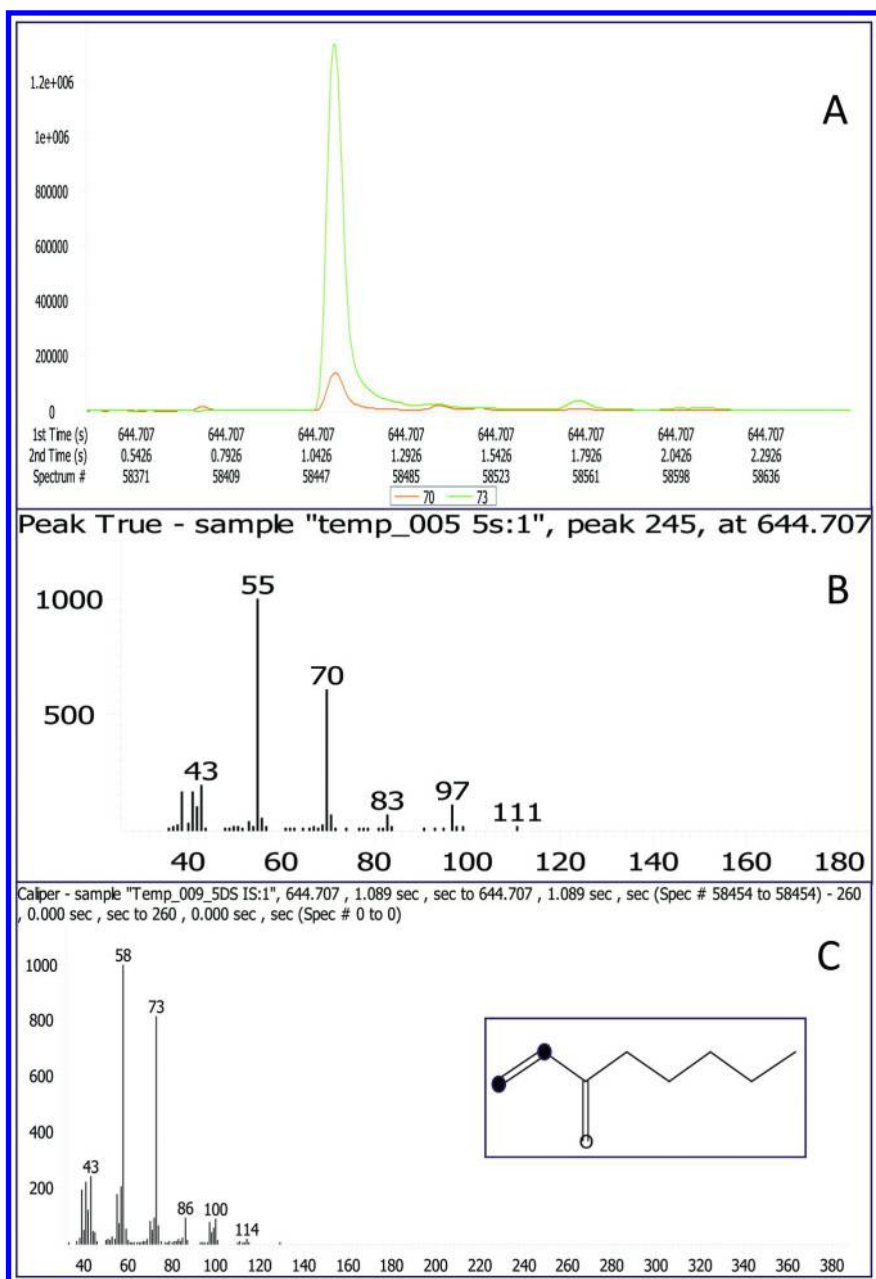


Figure 6. (A) - Extracted ion chromatogram (EIC) of ions ($m/z=70$ and $m/z=73$) used for quantitation of 1-octene-1-one in tempeh using SIDA; (B) - mass spectrum of 1-octene-3-one from tempeh sample; (C) - mass spectrum of 2H₃-1-octen-3-one used as a standard for 1-octene-3-on determination. Carbon atoms with deuterium substituted are shown on formula

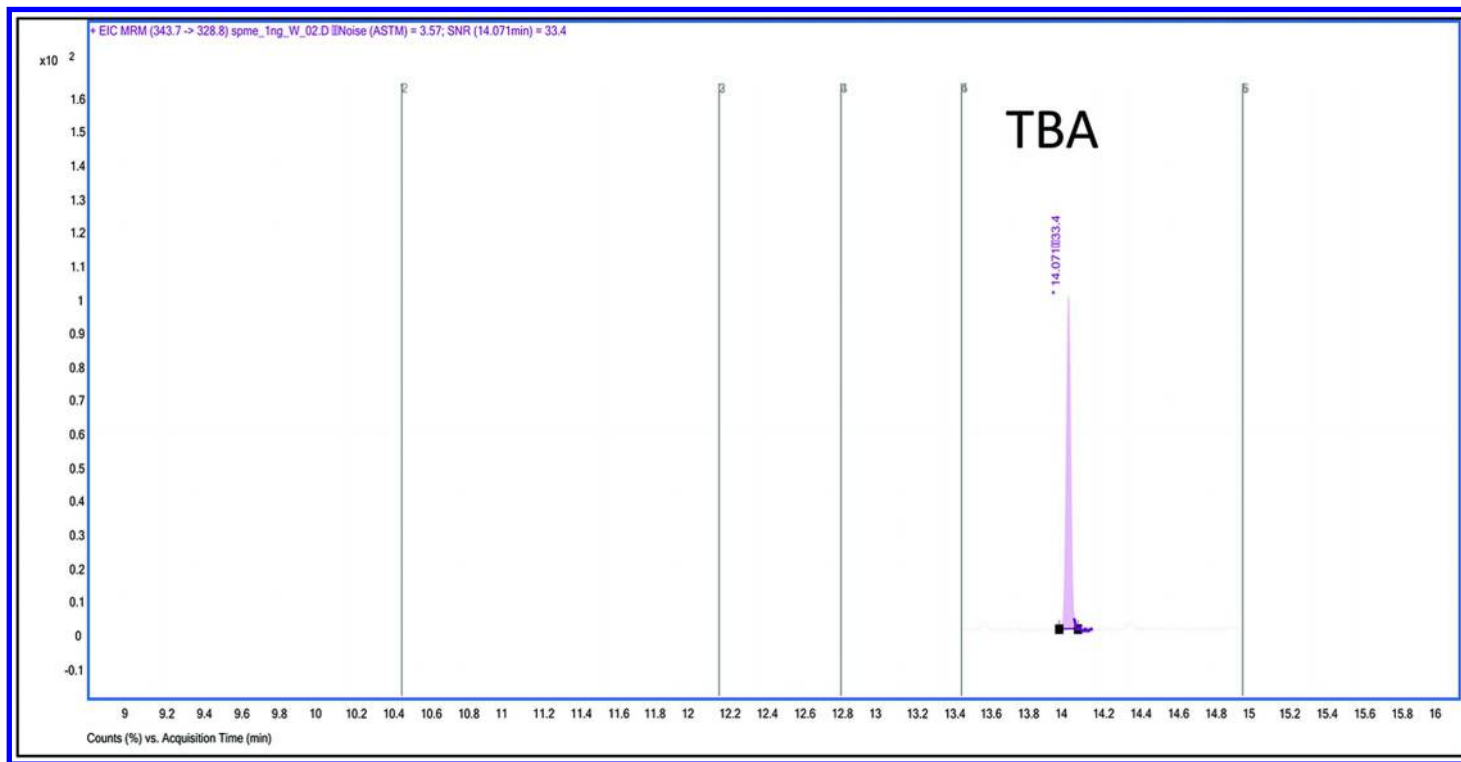


Figure 7. Single reaction monitoring (m/z 343.7 \rightarrow 328.8) peak for 1ng of TBA spiked into dry white wine.

Quantitation using mass spectrometry is usually performed on selected ions obtained either by extraction from total ion current, or obtained using SIM (Selected Ion Monitoring) mode of quadrupole mass spectrometers. SIM analysis is usually more sensitive than that run in SCAN mode, however it can be used only for quantitative purposes. The drawback of SIM approach in aroma compounds analysis is the complexity of food as a matrix. As volatile compounds are usually low molecular compounds, often with a low abundance molecular ions their intense EI fragments are frequently in a low mass region. This results often in a noisy baseline, which make the quantitation of odor active compounds difficult. Therefore selection of ions for SIM and their evaluation must be done very cautiously (25). Solution for this is the quantitation of compounds based on CI spectra, which yield much less fragments and abundant protonated or deprotonated molecular ion. It is also better for SIDA quantitation as molecular ion contains all the isotope substitutions. Other solution for this problem is the use of tandem mass spectrometry, which for complex matrices provide unrivaled selectivity, eliminating the influence of ions from the matrix, and though in the most frequently used mode (Multiple Reaction Monitoring, MRM) the signal is much lower, the matrix background drops substantially increasing signal to noise ratio. Figure 7 shows the chromatogram of 1ng of 2,4,6-TBA spiked into dry white wine and obtained using SPME extraction and tandem mass spectrometry (triple quadrupole) quantitation of this compound in targeted haloanisoles analysis in wines (26). Signal to noise obtained for TBA (33:1) allowed its reliable quantitation in concentrations lower than the odor threshold of this compound.

Conclusions

Analysis of aroma compounds in food nowadays benefits from the developments in chromatographical techniques, where comprehensive gas chromatography enables separation of up to thousands volatiles per run. Analysis of aroma compounds should be related to sensory analysis, and sensory guided approach to the food aroma analysis is the most rationalized but also a challenging one. Due to the nature of aroma compounds their analysis requires carefully performed extraction to preserve the flavor of specific product, efficient separation to avoid coelution problems and reliable quantitation, preferably using stable isotope analogues to provide reliable results.

Acknowledgments

Research partially financed within project POIG 01.01.02-00.061/09

References

1. Grosch, W. *Chem. Senses*. **2001**, *26*, 533–545.
2. Nongonierma, A.; Cayot, P.; Le Querre, J. L.; Springett, M; Voilley, A. *Food Rev. Int.* **2006**, *22*, 51–94.

3. Chaintreau, A. *Flavour Fragrance J.* **2001**, *16*, 136–148.
4. Snow, N. H. *Trends Anal. Chem.* **2002**, *21*, 608–617.
5. Jeleń, H. H.; Majcher, M.; Dziadas, M. In *Comprehensive Sampling and Sample Preparation*; Pawliszyn, J., Mondello, L., Dugo, P., Eds.; Elsevier Academic Press: Oxford U.K., 2012; Volume 4, pp 119–145.
6. Jeleń, H. H.; Dziadas, M.; Majcher, M. *Anal Chim. Acta.* **2012**, *738*, 13–26.
7. Molyneux, R. J.; Schieberle, P. *J. Agric. Food Chem.* **2007**, *55*, 4625–4629.
8. IOFI Working Group of Methods of Analysis. *Flavor Fragrance J.* **2011**, *26*, 297–299.
9. Schieberle, P.; Molyneux, R. J. *J. Agric. Food Chem.* **2012**, *60*, 24040–2408.
10. van Ruth, S. M. *Biomol. Eng.* **2001**, *17*, 121–128.
11. Zellner, B. D.; Dugo, P.; Dugo, G.; Mondello, L. *J. Chromatogr., A.* **2008**, *1186*, 123–143.
12. Cajka, T.; Hajslova, J. In *Food Flavors. Chemical, Sensory and Technological Properties*; Jeleń, H., Ed.; CTC Taylor & Francis: Boca Raton, FL, 2012; pp 355–411.
13. Kiefl, J.; Pollner, G.; Schieberle, P. *J. Agric. Food Chem.* **2013**, *61*, 5226–5235.
14. *Flavor Release*; Roberts, D. D., Taylor, A. J., Eds.; ACS Symposium Series 763; American Chemical Society: Washington, DC, 2000.
15. Guichard, E. *Biotechnol. Adv.* **2006**, *24*, 226–229.
16. Druaux, C.; Voilley, A. *Trends Food Sci. Technol.* **1997**, *8*, 364–368.
17. Nongonierma, A. B.; Springett, M.; Le Quéré, J. L.; Cayot, P.; Voilley, A. *Int. Dairy J.* **2006**, *16*, 102–110.
18. Harrison, M.; Hills, B. P. *J. Agric. Food Chem.* **1997**, *45*, 1883–1890.
19. Mandić, A. I.; Sedej, I. J.; Sakač, M. B.; Mišan, A.Č. *Food Anal Methods.* **2013**, *6*, 61–68.
20. Engel, W.; Bahr, W.; Schieberle, P. *Eur. Food Res. Technol.* **1999**, *209*, 237–242.
21. Ochiai, N.; Sasamoto, K. *J. Chromatogr., A* **2011**, *1218*, 3180–3185.
22. Schmarr, H.-G.; Koschinski, S.; Sang, W.; Slabizki, P. *J. Chromatogr., A.* **2012**, *1226*, 96–102.
23. Jeleń, H.; Majcher, M.; Ginja, A.; Kuligowski, M. *Food Chem.* **2013**, *141*, 459–465.
24. IOFI Working Group of Methods of Analysis. *Flavor Fragrance J.* **2012**, *27*, 224–226.
25. IOFI Working Group of Methods of Analysis. *Flavor Fragrance J.* **2010**, *25*, 406–406.
26. Jeleń, H. H.; Dziadas, M.; Majcher, M. *J. Chromatogr., A.* **2013**, *1313*, 185–193.

Chapter 15

Quantification of Health-Promoting Compounds by Quantitative ^1H NMR Spectroscopy

G. K. Jayaprakasha* and Bhimanagouda S. Patil

Vegetable and Fruit Improvement Center, Department of Horticultural Sciences, Texas A&M University, 1500 Research Parkway, A120, College Station, Texas 77845-2119

*E-mail: gjayaprakasha@ag.tamu.edu.

Nuclear magnetic resonance (NMR) spectroscopy is a well-known analytical technique for simultaneous quantitation and structural elucidation of small molecules and macromolecules. In natural products research, quantitative NMR (qNMR) gives valuable information on metabolites. qNMR is robust with high precision, good reproducibility and is non-destructive, compared to traditional analytical methods. It has proven to be rapid, highly reliable for the determination of purity, examination of impurities, metabolic profiling, and for the quantitation of single entities in complex mixtures without fractionation or isolation. Therefore, qNMR can be used to simultaneously identify and quantify multiple metabolites. This chapter discusses current challenges in quantitation, metabolomics, and sample preparation, as well as the selection of references for quantitation of health-promoting compounds.

Introduction

Nuclear magnetic resonance (NMR) spectroscopy is a well-known analytical technique for elucidating the structure of small molecules and macromolecules (*1*). NMR spectroscopy uses the application of strong magnetic fields and radio frequency pulses to the nuclei of atoms. For atoms with odd atomic number (^1H) or odd mass number (^{13}C), the magnetic field will cause the nucleus to possess spin, which is known as nuclear spin. Absorption of radio frequency energy then

allows the nuclei to be promoted from low-energy to high-energy spin states, and the emission of radiation during the subsequent relaxation process is detected. ^1H NMR spectroscopy has been used for quantitative analysis during 1963 for determining the intra-molecular proton ratios (2). In the ^1H NMR spectrum, the chemical shift and coupling constants give valuable information about the quantitative relationship between intramolecular and inter-molecular resonances. Also, as long as the analytes contain protons, NMR can analyze any class of compound. Figure 1 depicts the ^1H NMR spectrum of L-citrulline in D_2O recorded at 400 MHz JEOL ECS spectrometer. The chemical shifts of each signal have been assigned to the respective protons in the L-citrulline molecule. The integral values in each signal denote the number of protons present in molecule.

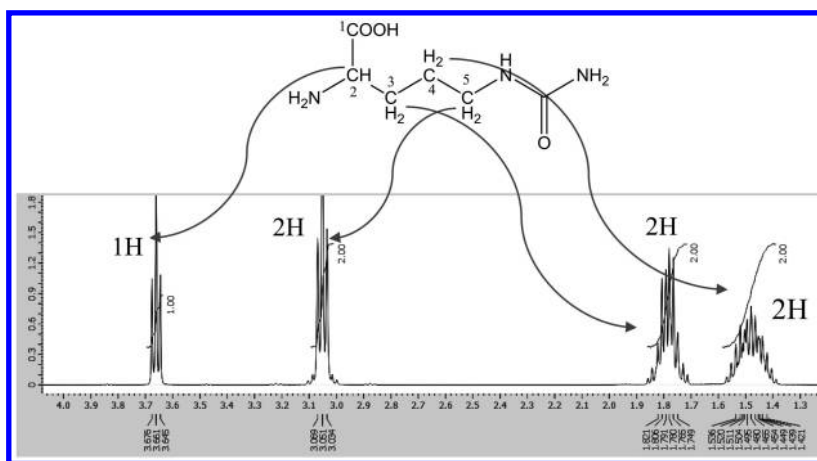


Figure 1. Structure of L-citrulline and its proton NMR spectrum shows the relative integrals and chemical shifts of intra –molecular resonances. The integral values depends on the number of nuclei per resonance.

In natural products research, quantitative proton nuclear magnetic resonance (q ^1H NMR) has emerged as one of the most reliable, and suitable techniques for comprehensive qualitative and quantitative analysis. The main advantage of q ^1H NMR compared to other analytical methods is the primary ratio measurement, since the peak area in q ^1H NMR is proportional to the number of nuclei (CH , CH_2 and CH_3) giving rise to the signal. With q ^1H NMR, the quantitation of the compounds present in a complex sample can be performed in a single, rapid, non-destructive measurement. Sample preparation for q ^1H NMR is simple and non-tedious and the uncertainty in quantification is minimal (3). NMR spectroscopy has additional advantages, such as the ability to determine molecular structures, the lack of a requirement for individual experimental setup for authentication, validation, and calibration, rapid, and non-destructive measurements. It is also possible to quantitatively analyze multiple metabolites simultaneously from a mixture.

The applicability and ease of use of qNMR has increased due to availability of high-sensitivity detection methods, sample changers with good homogeneity, and modern software packages that allow accurate and precise data processing for large numbers of samples. In the last decade, researchers have reported intensive studies using qNMR for the analysis of individual components in complex mixtures without prior LC separation (4, 5). qNMR does not require a particular reference standard, but quantification can also be performed using an internal standard. Various internal standards have been used in qNMR (Table 1), usually co-dissolved with the sample or introduced in a separate coaxial insert tube.

qNMR and Metabolomics

Metabolomics involves the study of small molecules from cells, plants, foods, tissues, organisms or other biological tissues. These small molecules include primary and intermediary metabolites, as well as exogenous compounds, such as secondary metabolites, drugs, and other compounds. Metabolic fingerprinting compares patterns, signatures or fingerprints of metabolites that change in response to external stimuli either in different plant varieties or species, or in response to adulteration, toxins, drug exposure, environmental or genetic alterations (6, 7). Metabolomics fingerprinting is a promising tool in clinical diagnosis, drug screening and toxicology studies (8–12).

One of the main problems in metabolomics is the lack of standardized methods, especially for global metabolomics analysis. In analytical chemistry, applications of qNMR include the identification and quantification of targeted and non-targeted metabolites. More recently, qNMR has been used to provide an unbiased view of sample composition, and, simultaneously, to quantify multiple compounds. qNMR has become the method of choice for metabolome studies and quality control of complex natural samples such as foods, plants, herbal remedies, and biofluids (10). Metabolomics is often deemed more discriminating than transcriptomics and proteomics, possibly because there are fewer chemical metabolites than genes and proteins. The main advantages for metabolic profiling using qNMR is faster than proteome and transcriptome analyses, as well as less expensive. Thus, qNMR-based metabolomics presents an ideal choice for systems biology studies on interactions at different molecular levels (13).

Challenges in Metabolomics Analysis

The main challenge in metabolomics involves the extraction of metabolites (targeted and non-targeted), detection, identification, and quantification of huge numbers of compounds present in a wide range of concentrations. To address this complex challenge, integration of various analytical platforms including gas chromatography-mass spectrometry (GC-MS), ultra-high performance liquid chromatography combined with MS (UHPLC-MS) and nuclear magnetic resonance (NMR) have been explored to improve metabolite coverage and expand the categories of metabolite identification (14). Moreover, improved

detection techniques (NMR and LC-MS) have been discussed recently for the identification of various metabolites (1, 15). Evident demand exists for the development of robust strategies for preparation of biological samples (16). Due to the heterogeneity of target samples in metabolomics experiments, selection of solvents for the extraction of targeted metabolites and preparation of samples are key steps (17, 18). For example, quantitation of non-polar or mid-polar metabolites requires extraction with deuterated solvents such as CDCl_3 , CD_2Cl_2 whereas polar metabolites can be extracted with various solvents such as deuterated water (D_2O), CD_3OD , CD_3CN and DMSO-d_6 . The liquid samples can be analyzed by lyophilization, followed by extraction with appropriate NMR grade solvents.

Selection of Samples, Storage, and Processing

Sampling and sample preparation are critical and valuable steps in metabolite analysis. The sampling time, method of sampling, diurnal, and dietary influences can greatly affect the reproducibility (19, 20) and have major effects on the composition of the metabolome (21, 22). The storage of biological samples is important, as freeze/thaw cycles may have detrimental effects on the stability and composition of the sample (23–25). All these factors will influence the precision, accuracy and reproducibility of results. It seems that the biological variability is always greater than analytical variability, even in studies that use controlled sampling and sample preparation (26). Extra-cellular metabolite samples such as urine, depict a period of metabolic activity and are easy to acquire. Intra-cellular metabolite samples provide a snapshot of the metabolome, but can be time-consuming and difficult to acquire, depending on the accessibility of the tissue. Metabolic processes occur rapidly in biological systems, so both types of samples require quick inhibition of enzymatic processes, generally by freeze-clamping or freezing in liquid nitrogen after harvesting, and subsequent storage at -80°C . However, freezing of biological samples has been reported to cause loss of certain intracellular metabolites (27). To prevent changes in the composition of the samples during storage, the number of cycles of freezing and thawing should be minimized. Acidic treatments (perchloric or nitric acid) may cause severe reduction or degradation of certain metabolites. Physical and chemical disruption of the cells generally involves extraction with polar or non-polar solvents, and distribution of metabolites in polar (methanol/water) and non-polar (chloroform) solvents is also commonly used. Figure 2 shows the extraction efficiency of curcuminoids extracted using CDCl_3 , acetone- d_6 and DMSO-d_6 . Since curcumin is lipophilic in nature, thus CDCl_3 showed selective extraction of curcumin as compared to acetone- d_6 and DMSO-d_6 . The NMR spectra of polar solvents showed other polar compounds signals along with curcumin. All signals were assigned, confirmed and quantitatively determined as curcumin. In case of Figure 2B and 2C, many minor signals denotes the presence of more compounds extracted in these solvents. Thus selection of solvent is more critical to isolate certain targeted metabolites.

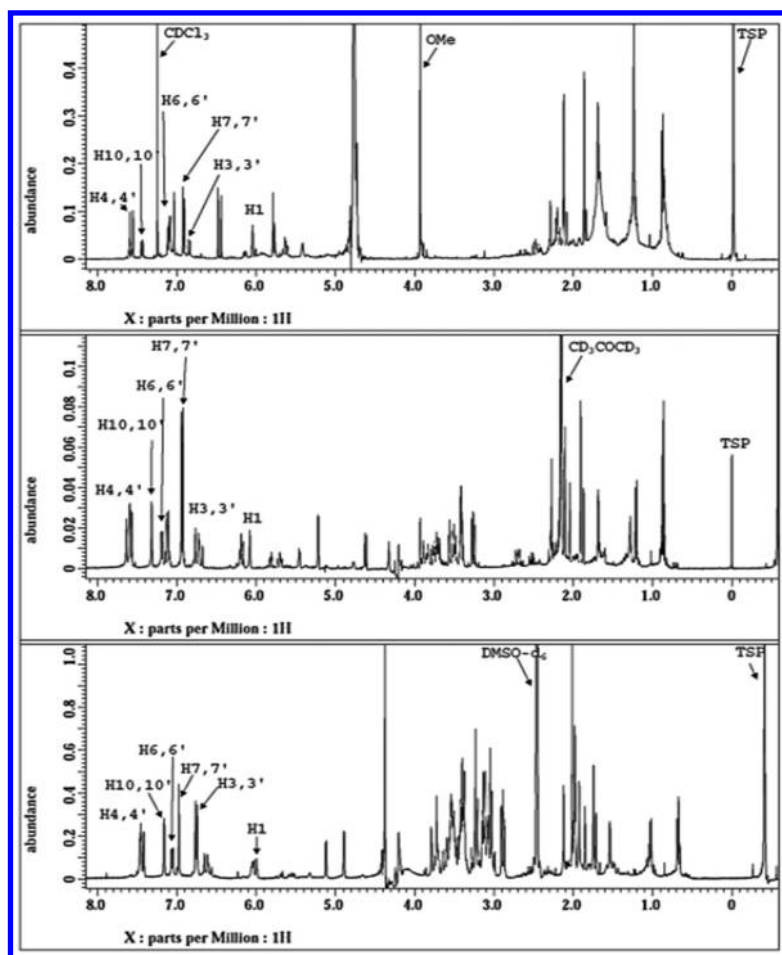


Figure 2. Extraction efficiency of curcuminoids in various solvents such as (A). CDCl_3 (B). Acetone – d_6 and (C). $\text{DMSO-}d_6$. Sample ($525\mu\text{L}$) was transferred to an NMR tube and coaxial glass tube containing $60\mu\text{L}$ 0.012% 3-(trimethylsilyl) propionic-(2,2,3,3- d_4) acid sodium salt in D_2O and was inserted into the 5 mm NMR tube. TSP- d_4 in reusable external tube served as a quantitative reference. The major compound curcumin signals were assigned.

In some cases, the loss of metabolites occurs due to non-specific binding or adsorption to the container surface; this can be prevented by post-addition of reagents such as bovine serum albumin or Tween-80 (28). Sample collection should be non-invasive and randomized. The choice of sample type and method of sample preparation are critical aspects in metabolomics studies. These aspects directly affect the data quality, accuracy and interpretation of the results.

Sample Preparation

Optimization of metabolites isolation without degradation is a critical step in analytical chemistry. To get satisfactory results, sample preparation should be simple and rapid to prevent metabolite loss, and it should be high-throughput to enable processing of large numbers of samples in short time span. Furthermore, the sample preparation method should be reproducible and include a metabolism-quenching step to represent the true metabolome composition at the time of sampling. One more challenge is that the extraction of metabolites from various matrices, including plants, food, tissues, and organisms, will vary because of the differences in each matrix; thus, extraction procedures need to be optimized. The first step in preparation of biological samples is to freeze at -80°C or in liquid nitrogen, because the pattern of the metabolites may change prior to analysis. Methanol cooling of samples has often been used as a simple and rapid method to terminate metabolism and rupture cells, promoting the release of intracellular metabolites.

As the polarity of the solvent increases, the range of metabolites extraction is also increases. Moreover, extractions should be performed at suitable pH, which leads to a maximum recovery of metabolites with minimal extraction interfering materials. The extraction methods must be highly efficient, nonselective, and reproducible, and should not cause degradation of the metabolites. However, the analysis of targeted metabolites or the construction of metabolic profiles requires a selective method of sample preparation to decrease other compounds that may interfere with the analysis.

Reference and Calibration Standards.

As similar to any analytical method, qNMR requires calibration. Most quantitative NMR experiments require referencing of chemical shifts (δ ppm) and quantitation of NMR signals by calibrating sample and standard signals. Table 1 shows the most commonly used standards in qNMR, while TMS and DSS are the IUPAC-approved NMR standards. The referencing and calibration of chemical shifts are often done externally, that is with a separate sample rather than with an internal standard. Chemical shifts can also be calibrated using the residual solvent signal. qNMR requires a well-defined standard material, which is often termed the reference standard. The primary standard should be highly pure, have good solubility, be stable and not be volatile (e.g. TMS). Moreover, it should be a well-characterized material and does not chemically interact with the analyte. In the case of biological samples (e.g., serum, plasma, and other biological fluids), which have abundant proteins, lipoproteins and fatty acids, the selection of internal standard is critical.

Table 1. Structures of Compounds Used for Determination of Concentrations by qNMR and Their Molecular Weights and Chemical Shifts

Name of the compound (Molecular weight)	Structures	Chemical shift
3(Trimethylsilyl) propanoic - 2,2,3,3-D ₄ acid sodium salt (172.08)		0
Tetra methyl silane (88.07)		0
Hexamethylcyclotrisiloxane (222.06)		0.1
Sodium acetate (82)		1.9
1,3,5 Trioxane (90.03)		5.1
Maleic acid (116.01)		6.4, 10.5
Fumaric acid-2,3-d ₂ (118.02)		10.05

Quantitation of Health-Promoting Compounds in Food

qHNMR has a growing application in analysis of food, because it has numerous advantages over currently used routine analytical methods (29). Current chromatographic methods require method development, optimization of sample preparation, relatively longer analysis times (15-60 min), frequent

calibrations using identical reference materials. The simplicity and swiftness of qNMR-based methods have been demonstrated to advance food science and technology in the study of metabolic and fermentation processes, composition of foods, or controlling manufacturing stages (29–33). The following two examples were demonstrated for the quantitation of certain health beneficial compounds using qNMR.

Quantitation of Curcumin in Turmeric Samples.

Recently, optimized a quantitative proton NMR for the determination of purity of curcuminoids is reported (29). Curcuminoids are yellow pigments with many pharmacological properties including antimicrobial, antiviral, antifungal, anticancer, and anti-inflammatory activities (34). A variety of methods have been reported for the quantification of the curcuminoids, and most of these are spectrophotometric methods, which measure the total color content of the sample (35). Commercial turmeric products contain mixtures of curcumin, demethoxycurcumin, and bisdemethoxycurcumin. However, spectrophotometric methods cannot quantify individual curcuminoids. While HPLC method for the determination of curcuminoids in turmeric was reported (36–38). This HPLC method requires 20 min run time and uses authenticated standards for calibration and quantification. While recently developed qNMR method needed less than 5 min, which can be used for quantitation of large numbers of samples.

As an example of the utility of this method, a turmeric powder (50 mg) was extracted in 1 mL of DMSO- d_6 for 30 min by sonication at 40 °C. The sample was filtered through 0.45 micron filter and analyzed by NMR at a frequency of 400 MHz using 5 mm multinuclear inverse probe. A 525 μ L DMSO- d_6 extracted sample was transferred to a NMR tube. An external coaxial glass tube (Wildmad-LabGlass, Vineland, NJ) containing 60 μ L 0.012% 3-(trimethylsilyl) propionic-(2,2,3,3- d_4) acid sodium salt (TSP) solution in D_2O was inserted into the NMR sample tube as a quantitative reference. The TSP concentration in the tube was pre-calibrated using a separate standard solution. A sufficiently long (16 s) relaxation delay was used to ensure full recovery of magnetization from both sample and internal reference (TSP) for accurate quantization. 1H NMR spectra obtained from the single pulse sequence were used to determine the curcumin content in turmeric sample. The purity of the curcumin in turmeric sample was determined by comparing the peak integrals of the compounds and the reference, taking into account the volume of the sample, the number of protons that contribute to the peak area and the molecular weights of curcumin and the reference standard. Figure 3A shows the 1HNMR spectra of the turmeric sample along with TSP. The TSP signal displayed at δ -0.55 ppm in the sample due to the presence of two solvents in one NMR tube (525 μ L of turmeric sample in DMSO- d_6 and 60 μ L of TSP in D_2O). The arrow indicates the signals for curcumin and the rest of the signal for other, minor curcuminoids. Further, the selectivity of each signal was confirmed by spiking a known amount of pure curcumin into the turmeric sample and recording the spectra as described above (Figure 3B). This spectrum clearly shows that the assigned

proton signal intensity is enhanced after spiking with the standard curcumin, which confirms the selectivity of the signal. Using these signal integral values, the purity of compounds was determined using the following formula (39).

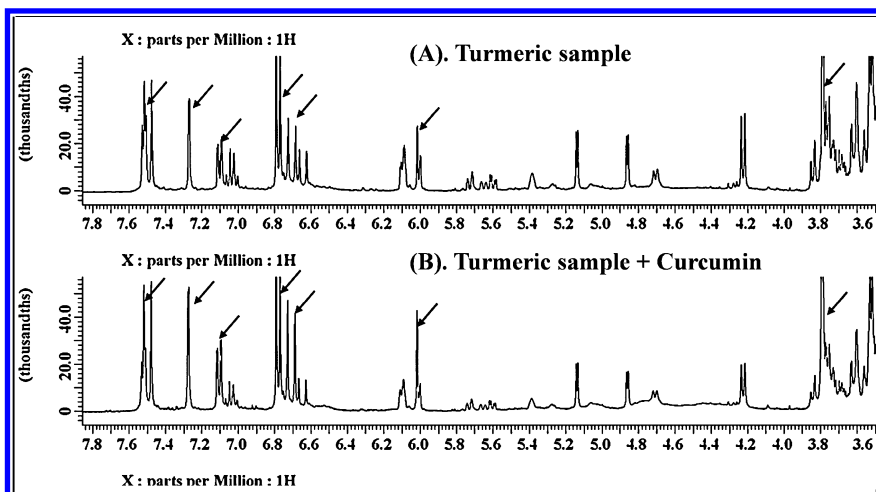


Figure 3. ^1H NMR signal enhancement by spiking with a known standard and recorded at 400 MHz: (A). Turmeric sample (50 mg) was extracted with 1 mL of DMSO-d_6 and 600 μL was used, (B). Turmeric sample (400 μL) was spiked with 10 mM curcumin (200 μL). The arrows indicates the enhanced curcumin signals.

$$\text{Purity} = \frac{I_A / H_A \cdot M_A / C_A}{I_{\text{Ref}} / H_{\text{Ref}} \cdot M_{\text{Ref}} / C_{\text{Ref}}} \times 100$$

I_A and I_{Ref} are the signal integral values of analyte and reference (e.g. TSP), respectively.

H_A and H_{Ref} are the number of protons in analyte and reference, respectively

M_A and M_{Ref} are the molecular weights of analyte and reference, respectively

C_A is the concentration of analyte or weight of sample and C_{Ref} is the concentration of the reference used for the assay.

The purity of curcumin (3.8%) was found to be comparable to HPLC analysis with <5% CV.

Quantitative Measurement of Purity of Phytochemical-Loaded Nanoparticles.

Citrus limonoids are a class of secondary metabolites known as triterpenoids, and act as defense agents against insects. Limonoids constitute one of the major phytochemicals in citrus, along with flavonoids, coumarins, and carotenoids. However, recent research has discovered the various health benefits and

pharmacological uses of limonoids, such as antibacterial, antifungal, antiviral, antioxidant, and anticancer activities (40–42). Limonoids also exhibited anti-HIV, moderate radical scavenging, and anti-oxidant activities (43, 44). For the first time, our group reported that certain citrus limonoids inhibit bacterial cell-cell signaling and biofilm formation (45). Specially, obacunone functioned as the most potent inhibitor of *Escherichia coli* O157:H7 biofilm formation (45). Understanding the structure-function relationship of limonoids plays a vital role in understanding their biological action. The structure-activity relationships of limonoids on antifeedant activity was demonstrated. The highest activity was speculated to furan ring and the epoxide group against insects (46). Furthermore, the A ring of the limonoid nucleus may be a key regulator for antineoplastic activity and cancer chemopreventive activity (47, 48), whereas the D ring may not be associated with biological activity (49, 50). Lipophilic compounds are emerging as important ingredients of functional foods and prophylactic formulations due to their ability to inhibit chronic diseases, including cancer.

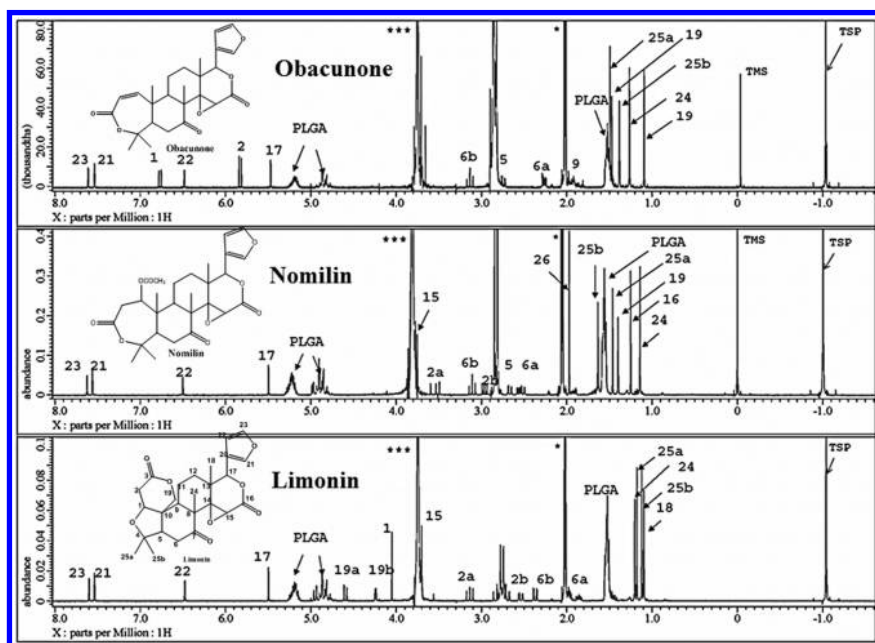


Figure 4. Phytochemical loaded PLGA nanoparticles of obacunone, nomilin and limonin were analyzed for purity and identity by quantitative proton NMR spectra. The spectra was recorded on a JEOL ECS NMR spectrometer at 400 MHz in acetone d_6 . Each sample 525 μ L was taken in 5mm NMR tubes, a coaxial glass tube (OD 2 mm) containing 65 μ L of 0.012% 3-(trimethylsilyl) propionic-(2,2,3,3- d_4) acid sodium salt (TSP- d_4) in D_2O was inserted into the NMR tube. TSP- d_4 in reusable external tube served as a quantitative reference. The numbering of proton signals corresponds to the numbering in the structures. * denotes residual signal from acetone- d_6 and ** denotes residual water from D_2O in the coaxial tube containing TSP- d_4 reference.

Recently, nanotechnology has emerged as a promising field of interdisciplinary research that has opened up a wide array of opportunities in various fields like agriculture, medicine, health and electronics (51). Nanoencapsulation-based enhancement of delivery of health beneficial compounds from agricultural byproducts may also help to improve human health by preventing chronic diseases (52–55). In this direction, emulsion diffusion technique (56, 57) was used to formulate nano-biomaterials (poly lactic-co-glycolic acid, PLGA) loaded with phytochemicals such as limonin, nomilin and obacunone separately. The purity of the nanoparticles were determined by qNMR as described earlier (29). A known quantity (2 mg) of phytochemical-loaded nano-biomaterials was dispersed in 525 μL of acetone d_6 and spectra were recorded at 400 MHz. Figure 4 depicts the chemical shifts of all proton signals to the structures of obacunone, nomilin and limonin. The phytochemical entrapment (w/w) or purity of limonin, nomilin and obacunone in nano-biomaterial was found to be 47.35 ± 0.79 , $52.85 \pm 1.02\%$ and 51.72 ± 1.25 respectively.

Conclusions

Quantitative NMR provides a rapid, robust, and relatively simple method to analyze natural products and biological samples. The main advantages of this technique are: (a) data can be used to derive molecular structure, (b) short measuring times, (c) samples are non-destructive and can be used for other analyses, (d) multiple components can be determined quantitatively using single reference compound, (e) no specific reference standard are needed, (f) qNMR has better reproducibility, accuracy, and precision. Thus, qNMR can be used for quality control for large numbers of samples, standardization of various plant extracts and their commercially available products and can also be applied for fingerprinting of other plant-based products with high reproducibility without specific marker standards.

Acknowledgments

This project is based upon work supported by the USDA-NIFA # 2010-34402-20875 “Designing Foods for Health” through the VFIC and State funding – 2013-121277 Vegetable & Fruit Improvement Center-TX State Appropriation.

References

1. Wishart, D. S. *TrAC, Trends Anal. Chem.* **2008**, 27 (3), 228–237.
2. Jungnickel, J.; Forbes, J. *Anal. Chem.* **1963**, 35 (8), 938–942.
3. Malz, F.; Jancke, H. *J. Pharm. Biomed. Anal.* **2005**, 38 (5), 813–823.
4. Sumner, L. W.; Mendes, P.; Dixon, R. A. *Phytochemistry* **2003**, 62 (6), 817–836.
5. Zhang, S.; Nagana Gowda, G. A.; Asiago, V.; Shanaiah, N.; Barbas, C.; Raftery, D. *Anal. Biochem.* **2008**, 383 (1), 76–84.

6. Fiehn, O.; Kopka, J.; Dormann, P.; Altmann, T.; Trethewey, R. N.; Willmitzer, L. *Nat. Biotechnol.* **2000**, *18* (11), 1157–1161.
7. Wilson, I. D.; Plumb, R.; Granger, J.; Major, H.; Williams, R.; Lenz, E. M. *J. Chromatogr., B* **2005**, *817* (1), 67–76.
8. González-Domínguez, R.; García-Barrera, T.; Gómez-Ariza, J. L. *J. Pharm. Biomed. Anal.* **2014**, *98* (0), 321–326.
9. Heus, F.; Vonk, F.; Otvos, R. A.; Bruyneel, B.; Smit, A. B.; Lingeman, H.; Richardson, M.; Niessen, W. M. A.; Kool, J. *Toxicol.* **2013**, *61* (0), 112–124.
10. Frank, T.; Engel, K. H., 8 - Metabolomic analysis of plants and crops. In *Metabolomics in Food and Nutrition*; Weimer, B. C., Slupsky, C., Eds.; Woodhead Publishing: Cambridge, 2013; pp 148–191.
11. Beger, R. D.; Sun, J.; Schnackenberg, L. K. *Toxicol. Appl. Pharm.* **2010**, *243* (2), 154–166.
12. Shyur, L.-F.; Yang, N.-S. *Curr. Opin. Chem. Biol.* **2008**, *12* (1), 66–71.
13. Fiehn, O. *Plant Mol. Biol.* **2002**, *48* (1-2), 155–171.
14. Winder, C. L.; Dunn, W. B.; Schuler, S.; Broadhurst, D.; Jarvis, R.; Stephens, G. M.; Goodacre, R. *Anal. Chem.* **2008**, *80* (8), 2939–2948.
15. Bedair, M.; Sumner, L. W. *TrAC, Trends Anal. Chem.* **2008**, *27* (3), 238–250.
16. Naganagowda, G.; Gururaja, T.; Satyanarayana, J.; Levine, M. *J. Pept. Res.* **1999**, *54* (4), 290–310.
17. Dunn, W. B.; Ellis, D. I. *TrAC, Trends Anal. Chem.* **2005**, *24* (4), 285–294.
18. Want, E. J.; Wilson, I. D.; Gika, H.; Theodoridis, G.; Plumb, R. S.; Shockcor, J.; Holmes, E.; Nicholson, J. K. *Nat. Protoc.* **2010**, *5* (6), 1005–1018.
19. Luthria, D. L.; Biswas, R.; Natarajan, S. *Food Chem.* **2007**, *105* (1), 325–333.
20. Mukhopadhyay, S.; Luthria, D. L.; Robbins, R. J. *J. Sci. Food Agric.* **2006**, *86* (1), 156–162.
21. Goodspeed, D.; Liu, J. D.; Chehab, E. W.; Sheng, Z.; Francisco, M.; Kliebenstein, D. J.; Braam, J. *Curr. Biol.* **2013**, *23* (13), 1235–1241.
22. Sharma, M.; Bhatt, D. *Mol. Plant Pathol.* **2014** DOI: 10.1111/mpp.12178.
23. Al-Jowder, O.; Kemsley, E.; Wilson, R. *Food Chemistry* **1997**, *59* (2), 195–201.
24. Berry, M.; Fletcher, J.; McClure, P.; Wilkinson, J. *Frozen Food Sci. Technol.* **2008**, *26*.
25. Berry, M.; Fletcher, J.; McClure, P.; Wilkinson, J. *Frozen Food Sci. Technol.* **2008**, *26*.
26. Roessner, U.; Wagner, C.; Kopka, J.; Trethewey, R. N.; Willmitzer, L. *Plant J.* **2000**, *23* (1), 131–142.
27. Wittmann, C.; Krömer, J. O.; Kiefer, P.; Binz, T.; Heinzle, E. *Anal. Biochem.* **2004**, (1), 135–139.
28. Li, W.; Luo, S.; Smith, H. T.; Tse, F. L. S. *J. Chromatogr., B* **2010**, *878* (5–6), 583–589.
29. Jayaprakasha, G. K.; Nagana Gowda, G. A.; Marquez, S.; Patil, B. S. *J. Chromatogr., B* **2013**, *937* (0), 25–32 PMID: 24013126.
30. Skov, T.; Honoré, A. H.; Jensen, H. M.; Næs, T.; Engelsen, S. B. *TrAC, Trends Anal. Chem.* **2014**, *60* (0), 71–79.

31. Tarachiwin, L.; Masako, O.; Fukusaki, E. *J. Agric. Food Chem.* **2008**, *56* (14), 5827–5835.
32. Hills, B. P.; Clark, C. J.; G. A. W., Quality Assessment of Horticultural Products by NMR. In *Annual Reports on NMR Spectroscopy*; Academic Press: New York, 2003; Vol. 50, pp 75–120.
33. Cox, D. G.; Oh, J.; Keasling, A.; Colson, K.; Hamann, M. T. *Biochim. Biophys. Acta, Gen. Subj.* **2014**, *1840* (12), 3460–3474.
34. Jayaprakasha, G.; Jagan Mohan Rao, L.; Sakariah, K. *Trends Food Sci. Tech.* **2005**, *16* (12), 533–548.
35. Method, A.
36. Jayaprakasha, G. K.; Rao, L. J. M.; Sakariah, K. K. *J. Agric. Food Chem.* **2002**, *50* (13), 3668–3672.
37. Jain, V.; Prasad, V.; Pal, R.; Singh, S. *J. Pharm. Biomed. Anal.* **2007**, *44* (5), 1079–1086.
38. Jang, H.-D.; Chang, K.-S.; Huang, Y.-S.; Hsu, C.-L.; Lee, S.-H.; Su, M.-S. *Food Chem.* **2007**, (3), 749–756.
39. Shen, S.; Yao, J.; Shi, Y. *J. Pharm. Biomed. Anal.* **2014**, *89*, 118–121.
40. Roy, A.; Saraf, S. *Biol. Pharm. Bull.* **2006**, *29* (2), 191–201.
41. Patil, B. S.; Brodbelt, J. S.; Miller, E. G.; Turner, N. D., Potential health benefits of citrus: an overview. In *Potential Health benefits of citrus*, Patil, B. S., Turner, N. D., Miller, E. G., Brodbelt, J. S., Ed. American Chemical Society, Washington, DC: 2006; Vol. 936, pp 1-16.
42. Manners, G.; Jacob, R.; Breksa, A., III; Schoch, T.; Hasegawa, S. *J. Agric. Food Chem.* **2003**, (14), 4156–4161.
43. Battinelli, L.; Mengoni, F.; Lichtner, M.; Mazzanti, G.; Saija, A.; Mastroianni, C. M.; Vullo, V. *Planta Med.* **2003**, *69* (10), 910–3.
44. Poulouse, S. M.; Harris, E. D.; Patil, B. S. *J. Nutr.* **2005**, *135* (4), 870.
45. Vikram, A.; Jesudhasan, P. R.; Jayaprakasha, G.; Pillai, B.; Patil, B. S. *Int. J. Food Microbiol.* **2010**, *140* (2-3), 109–116.
46. Bentley, M. D.; Rajab, M. S.; Randall Alford, A.; Mendel, M. J.; Hassanali, A. *Entomol. Exp. Appl.* **1988**, *49* (3), 189–193.
47. Lam, L. K. T.; Li, Y.; Hasegawa, S. *J. Agric. Food Chem.* **1989**, *37* (4), 878–880.
48. Perez, J. L.; Jayaprakasha, G. K.; Cadena, A.; Martinez, E.; Ahmad, H.; Patil, B. S. *BMC Complementary Altern. Med.* **2010**, *10* (1), 51.
49. Miller, E. G.; Taylor, S. E.; Berry, C. W.; Zimmerman, J. A.; Hasegawa, S. Citrus limonoids: increasing importance as anticancer agents. In *Citrus Limonoids: Functional Chemicals in Agriculture and Foods*; Berhow, M., Hasegawa, S., Manners, G. D., , Eds.; ACS Symposium Series 758; American Chemical Society: Washington, DC, 2000; pp 132–144.
50. Miller, E. G.; Porter, J. L.; Binnie, W. H.; Guo, I. Y.; Hasegawa, S. *J. Agric. Food Chem.* **2004**, *52* (15), 4908–4912.
51. Cattaneo, A. G.; Gornati, R.; Sabbioni, E.; Chiriva-Internati, M.; Cobos, E.; Jenkins, M. R.; Bernardini, G. *J. Appl. Toxicol.* **2010**, *30* (8), 730–744.
52. Sahoo, S.; Parveen, S.; Panda, J. *Nanomed.: Nanotechnol., Biol. Med.* **2007**, *3* (1), 20–31.
53. Augustin, M. A.; Hemar, Y. *Chem. Soc. Rev.* **2009**, *38* (4), 902–912.

54. Meyer, O. *Angiology* **1994**, *45* (6) (Pt 2), 579.
55. Lyseng-Williamson, K. A.; Perry, C. M. *Drugs* **2003**, *63* (1), 71–100.
56. D'Aurizio, E.; van Nostrum, C. F.; van Steenbergen, M. J.; Sozio, P.; Siepmann, F.; Siepmann, J.; Hennink, W. E.; Di Stefano, A. *Int. J. Pharm.* **2011**, *409* (1-2), 289–296.
57. Govender, T.; Stolnik, S.; Garnett, M. C.; Illum, L.; Davis, S. S. *J. Controlled Release* **1999**, *57* (2), 171–185.

Chapter 16

Meat Freshness: Peroxynitrite's Oxidative Role, Its Natural Scavengers, and New Measuring Tools

Alina Vasilescu,¹ Alis Vezeanu,¹ Ying Liu,² Ioana S. Hosu,³
R. Mark Worden,² and Serban F. Peteu^{*,2,3}

¹International Centre for Biodynamics 1B Intrarea Portocalelor,
S6, 060101 Bucharest, Romania

²Department of Chemical Engineering and Material Science,
Michigan State University, 428 S. Shaw Lane,
East Lansing, Michigan 48824-1226, United States

³National Institute for R & D in Chemistry & Petrochemistry,
NemsBio Laboratory, 202 Splaiul Independentei,
S6, 060021 Bucharest, Romania

*E-mail: peteu@egr.msu.edu; serbanfpeteu@gmail.com.

Typically, about \$1 billion/year is lost when red meat loses freshness on the shelf. Consumer purchasing decisions depend on meat color and flavor, which are strongly influenced by complex nitro-oxidative events within meat muscle tissue. One goal of this chapter is to explain the loss in meat freshness linked to the action of peroxynitrite anion ONOO⁻, a strong nitro-oxidative agent. The toxicity of abnormally high ONOO⁻ levels *in vivo* has been proven, and ONOO⁻ is also suspected of accelerating meat spoilage by two principal mechanisms: (1) oxidation of iron atoms in heme-containing globin proteins, leading to a color change from red to brown, and (2) peroxidation of unsaturated lipids, leading to flavor degradation. A second goal is to review electrochemical quantification methods for ONOO⁻ and its oxidative effects on biologically relevant molecules, including unsaturated phospholipids within biological membranes and heme-containing molecules. A third goal is to examine the natural polyphenols that protect against peroxynitrite-induced oxidative damage. The final goal is to

assess research advances and remaining research challenges related to ONOO–induced oxidative processes that reduce meat’s shelf life.

1. Introduction: Peroxynitrite’s Formation and Fate In Vivo

The color, flavor and texture of food are critical freshness factors in the consumer’s decision to purchase muscle foods, especially red meat, such as beef. Recent studies show that 15% of retail beef is typically discounted in price due of surface discoloration, resulting in annual revenue losses of \$1 billion (1). Color and flavor are primary indicators of freshness and wholesomeness, so extending the meat-color lifetime could yield significant economic benefits. Loss of red meat color is largely due to oxidative processes whose rate depends on conditions before and after harvesting, the so-called *pre-* and *postmortem* stages of meat.

Recent work in food science hypothesized the role of peroxynitrite (PON) as a strong promoter and modulator of the myoglobin oxidation, which contributes to discoloration of the muscle foods (3, 4, 10, 11). Furthermore, it is known that PON and its associated radicals induce lipid peroxidation *via* the abstraction of a hydrogen atom from unsaturated fatty acids, which are components of lipoproteins and phospholipids that compose bilayer lipid membranes (BLM) and liposomes (8, 12). PON’s role in the oxidative degradation of lipids contained in muscle foods can be studied by monitoring PON-induced damage to synthetic bilayer lipid membranes (BLM) that mimic cell membranes (13–15). PON-induced degradation of lipids could potentially be prevented *via* natural antioxidants (e.g., polyphenolic compounds) that scavenge radicals or catalyze decomposition of PON (16–18).

Lipids are important components of muscle tissue and known to enhance the flavor, tenderness and juiciness of fresh meat (2–4). In addition, PON is a reactive oxygen species (ROS) and powerful cytotoxic agent *in vivo* (5–7). Biochemical and medical research of the last two decades has confirmed the involvement of PON and its associated radicals in many major degenerative patho-physiological processes (8, 9).

The PON anion ONOO[–] is formed by the reaction of two precursors: the nitric oxide free radical (NO[•]) and the superoxide anion (O₂^{•–}) (5–8). The PON reaction pathway is coupled with reactions involving other reactive nitrogen and oxygen species (RNS; ROS), as shown in Figure 1.

One precursor, NO[•] nitric oxide derives from a 2-step catalytic oxidation of L-arginine by nitric oxide synthases. Superoxide can be leaked by respiratory chain enzymes, generated by several oxidases, or produced by inflammatory processes (8, 12). The O₂^{•–} and NO[•] precursors are combined (rates 3 - 20 x 10⁹ M⁻¹s⁻¹) in diffusion-controlled reactions whose rates exceed those of most other cellular events. This high reaction rate ensures PON formation virtually whenever the precursors are in close proximity (5–7). When CO₂ is present, it will react with PON to form nitrosoperoxy-carbonate (ONOOCO₂[–]) as the predominant product. (8, 12). A controlled level of PON within normal limits has a protective role in homeostasis of healthy cells and organisms. For example, PON participates in

redox regulation of critical signaling pathways by triggering protective signals against ischemia-reperfusion injury (8). However, an excessively high PON level is correlated with cytotoxicity and pathological conditions including stroke, cancer, diabetes complications, chronic inflammation, and several devastating neurodegenerative conditions (7, 8, 12).

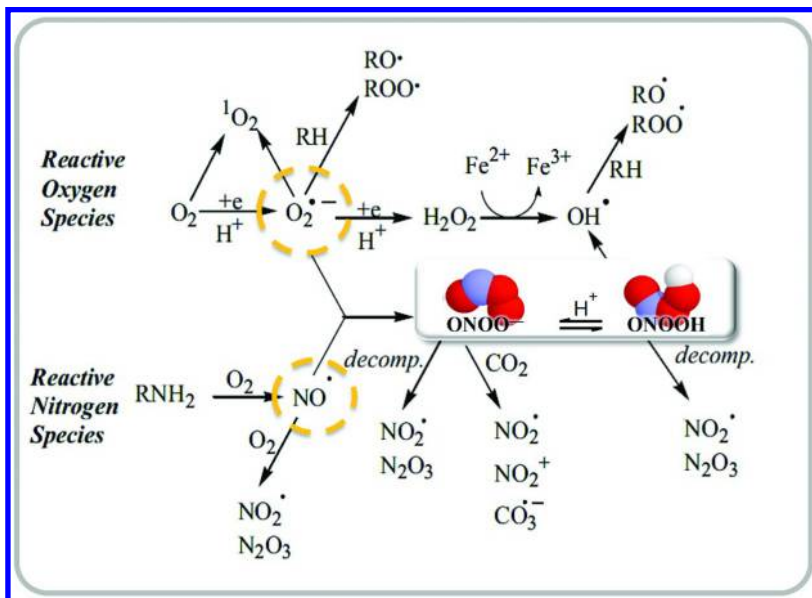


Figure 1. The formation of $ONOO^-$ anion from superoxide $O_2^{\cdot-}$ and nitric oxide (NO^{\cdot}), with the conjugate peroxynitrous acid ($ONOOH$). The reaction pathway illustrates the formation of the other reactive oxygen species and reactive nitrogen species (ROS, RNS). Reproduced with permission from reference (22) copyright 2008 American Chemical Society. See text for more details.

This chapter outlines advances in PON detection with electrochemical methods, typically preferred over the chemiluminescence and fluorescence optical analytical techniques (20, 21), especially when *in situ* measuring speed is critical. Broadly defined, electrochemistry investigates the redox processes of electron transfer at polarized interfaces, typically with a three-electrode setup: working (WE), auxiliary or counter (Aux), and reference (Ref). Two very basic electrochemical methods used in solution are the cyclic voltammetry (CV) and the amperometry (CA). During CV, the electric potential is cycled between two set values, while the current is measured. For CA, the WE is polarized at a fixed potential and the current is measured continuously in time, while different aliquots of analyte are added sequentially to the solution. Changes in current are correlated with analyte concentration, in calibration graphs showing the linear response. The PON electrochemical sensing was recently reviewed (101, 102) and recent developments are critically discussed in the Section 4 of this chapter.

2. Peroxynitrite Interaction with Lipid Membranes

PON with its related radical products is known to induce peroxidation of membrane phospholipids. The established methods to detect lipid oxidation include the measurement of one or more of the following types: absorption of oxygen, loss of initial substrates, formation of free radicals, or formation of primary and/or secondary radicals (94). The individual physical and chemical tests totaled about thirty different methods, ranging from sensory analysis by a trained panel, to using antioxidant activity (ready-to-use) kits, differential scale calorimetry (DSC), or more complex equipment such as Fourier transform infrared spectroscopy (FTIR) or electron spin resonance (ESR) (94). By looking at the total number of lipid oxidation tests, the authors' opinion is that this diversity of methods on several levels (analysis time, technical complexity, operational cost) could bring too much experimental variability, due to differences in the results obtained by different operators, using different methods, on different brands of equipment, to test food samples having inherent differences.

One way in which PON induces toxicity *in vivo* is by degrading cell membranes. The degradation may be mediated either by ONOO^- or its conjugate peroxynitrous acid ONOOH . (8, 9). A simplified conceptual model of lipid peroxidation by PON in a BLM is illustrated in Figure 2. This figure only considers select ROS reactions. The action of PON as a nitrating agent is well documented, but these actions will not be discussed here.

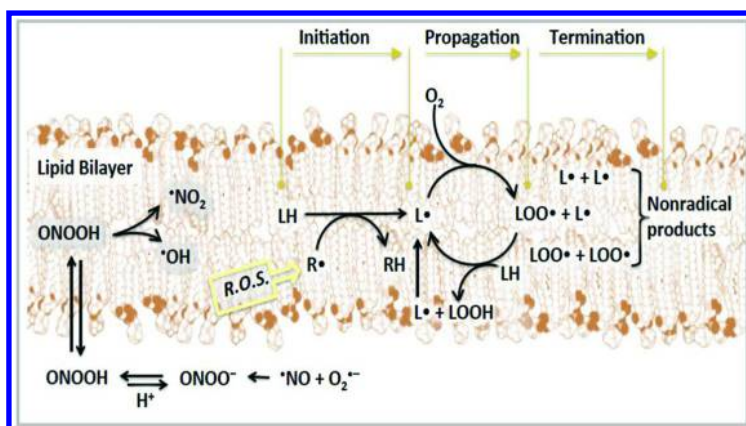


Figure 2. Conceptual model of lipid peroxidation in a BLM that takes into account the ROS illustrated in Figure 1. Legend: ONOOH , peroxynitrous acid; LH , unsaturated lipid; LOO^\bullet , lipid peroxyl radical; LOOH , lipid hydroxyl peroxide. Modified with elements reproduced with permission from reference (32) copyright 2014 Wikipedia and from references (34) copyright 2006 Brazilian Society of Chemistry. See text for more details.

PON and its associated radical products are known to induce peroxidation of phospholipids in BLM, liposomes, and lipoproteins *via* abstraction of a hydrogen atom from unsaturated fatty acids (8, 9). The resulting products from reactions

of unsaturated lipid peroxidation (ULP), as well as nitration reactions, have the potential to influence membrane integrity, fluidity, and other physiological properties of the BLM.

Numerous *in vivo* and *in vitro* studies of effects of oxidative processes on meat quality have demonstrated that PON and associated oxidative species, including hydroxyl and peroxy radicals are capable of inducing biochemical changes. These biochemical changes may be associated in part with BLM phenomena (16). Hydroxyl and peroxy radicals resulting from lipid peroxidation can cause significant biological consequences including an increase in membrane viscosity and permeability, a decrease in membrane electrical resistance and fluidity, as well as enhanced lipid exchange between upper and lower leaflet of the BLM (23–26).

A primary function of cell membranes is to provide a selective permeability barrier to ions. The BLM's resistance to ion transport can be measured using EIS and other methods that have the potential to be adapted to high throughput operation (13–15). In addition, electrochemical assays provide real-time, label-free, direct PON quantification of peroxyxynitrite (20, 21). Thus, BLM-based electrochemical methods offer the potential of simultaneously measuring the PON local concentration and other reactive nitrogen oxide species (RNOS), as well as the resulting changes in biomembrane impedance resulting from lipid peroxidation and nitration.

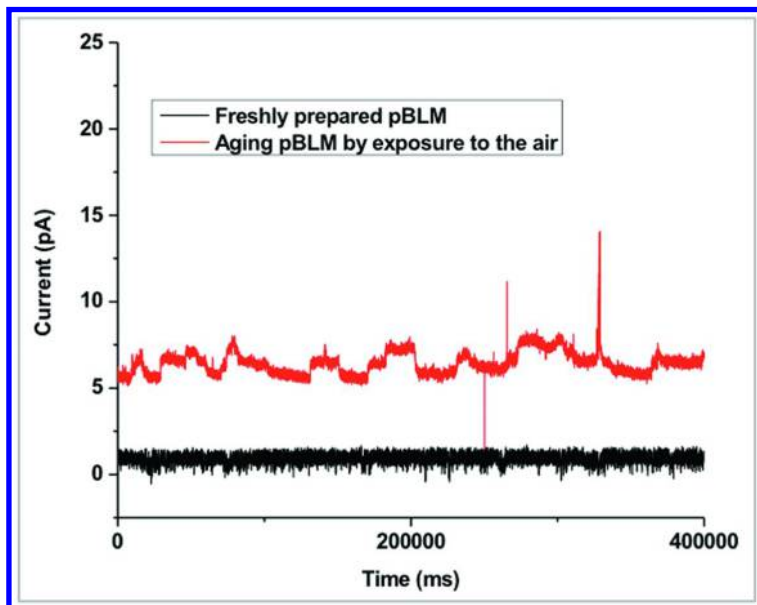


Figure 3. Current profiles of pBLM composed of 1,2-diphytanoyl-*sn*-glycero-3-phosphocholine(DPhPC). Lower curve: immediately after BLM formation. Upper curve: after 24 h exposure to air. Experiments performed in HEPES buffer (20 mM HEPES, 20 KCl, pH7.4) at a sampling frequency of 1000 Hz and applied potential of +100 mV.

Characterization of the effect of RNOS on lipid bilayers is challenging when using intact cell membranes, because the RNOS may influence many different molecules within the membrane, including a broad spectrum of membrane proteins. To isolate the effects of RNOS on the lipids, synthetic BLM may be used as a biomimetic substitute for intact biological membranes. A variety of model synthetic BLMs have been used for electrochemical studies, including the planar (pBLM) and tethered BLM (tBLM). The composition of the synthetic BLM can be customized to test hypotheses and meet experimental objectives. These two methodologies have been widely used to study channel peptides/proteins, toxins, and engineered nanomaterials because of their easy setup, high resolution and high sensitivity (13).

The pBLM method provides extremely high ion-current sensitivity, on the order of pA, and can measure dynamics of a single transient pore with time resolution on the order of ms (19, 27). BLM lipid degradation can trigger transient current spikes, extended integral conductance, and increased baseline current. Some of these effects are shown in Figure 3, which contrasts the ion currents for a single pBLM formed across a 760 nm pore immediately after formation and after the pBLM was aged by 24h of air exposure. Immediately after formation with fresh lipids, the pBLM exhibited a stable baseline current of about 1 pA. However, after exposure to the air for 24 h, the baseline current was three-fold higher, and both current spikes and integral conductance (i.e., extended periods of increased current) were observed. This evidence of impaired membrane impedance due to oxidized lipids was obtained using saturated diphytanoyl lipids, which are less susceptible to oxidative damage than phospholipids containing unsaturated fatty acids (e.g., oleoyl).

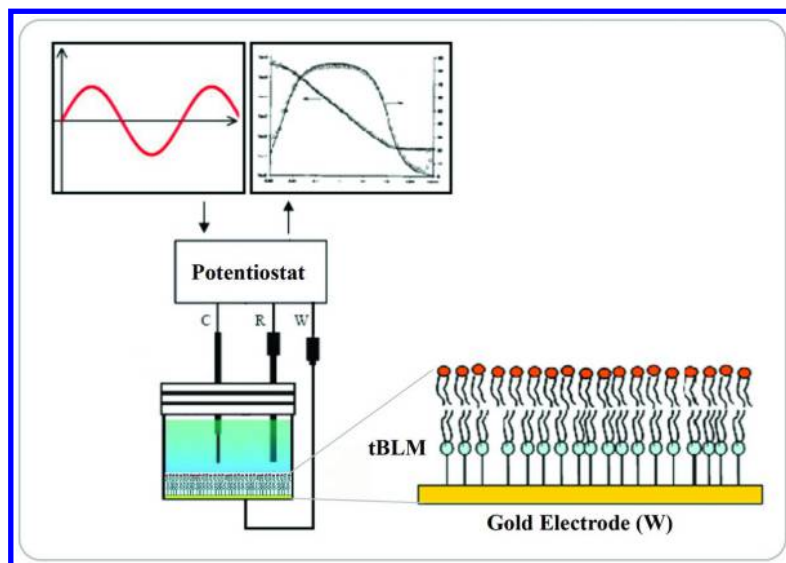


Figure 4. Schematic diagram of EIS characterization of interaction between tBLM and peroxynitrite. C, R and W represent counter, reference and working electrode, respectively.

The tBLM method offers the advantage of a more stable membrane than a pBLM. Electrochemical impedance spectroscopy (28) (Figure 4) is commonly used to measure changes in membrane resistance due to agents that create membrane pores (e.g., channel-forming proteins (14)) or disrupt membranes, (e.g., engineered nanomaterials (13)). In preliminary studies, we observed that the resistance of a tBLM composed of 1, 2-dipalmitoyl-*sn*-glycero-phosphothioethanol (DPPTe) lower leaflet and 1, 2-dioleoyl-*sn*-glycero-phosphocholine (DOPC) upper leaflet increased during exposure to 30 mM from a PON donor, 3-morpholino-sydnonimine (SIN-1), which generated about 300 μM PON. However, this increase in impedance was prevented by the addition of an iron porphyrin that catalyzes PON decomposition. Because DOPC is commonly found in cell membranes and each molecule of DOPC has two unsaturated lipid chains, this finding suggests that electrochemical characterization of a DOPC BLM (either pBLM or tBLM) following PON exposure represents a potentially valuable model system to characterize PON-induced ULP reactions.

3. Oxidative Processes in the Muscle Tissue

The freshness of raw meat is indicated by its color, texture and olfactory cues. Reduced ferrous Fe (II) myoglobin (Mb) imparts the purple-red color associated with fresh meat. Oxidation of Mb's iron atom to the ferric Fe (III) oxidation state results in a color transition to brown, visually indicating a loss of freshness. The rate of this oxidation process thus plays a significant role in raw meat's shelf life. Food chemistry research has shown that PON promotes and modulates oxidation of Mb to metmyoglobin (metMb) (29, 34), and is thus involved in the discoloration of muscle foods. Moreover, experimental evidence (30, 31) indicates a possible link between ULP and the heme-containing globin oxidation (HGO), suggesting that PON plays a central role for both classes of meat degradation reactions.

In living muscle, the metmyoglobin (metMb) concentration is extremely small, due to the presence of the enzyme metmyoglobin reductase (MMR). This enzyme, in the presence of the cofactor NADH and co-enzyme cytochrome b4 reduces the Fe(III) from the heme prosthetic group of metMb back to Fe(II) of reduced myoglobin (33, 34). By contrast, in raw meat, metabolic processes responsible for NADH regeneration and metmyoglobin reduction are unavailable, so metmyoglobin accumulates, leading the color change associated with meat aging.

The PON interaction with meat myoglobin will be considered next. Its precursors NO^\cdot and $\text{O}_2^{\cdot-}$ are both present in fresh meat. The inorganic chemistry of meat, including PON interactions with Mb, has been explored by a number of authors. (29, 34). Research (35, 36) indicated that, by analogy to the oxidation of oxymyoglobin with hydrogen peroxide, the myoglobin should react with peroxynitrous acid *ONOOH* via 2-electron oxidation of myoglobin *MbFe(II)* in equilibrium with oxymyoglobin *MbFe(II)O_2*: $\text{MbFe(II)O}_2 \rightleftharpoons \text{O}_2 + \text{MbFe(II)}$.

In addition, fast-scan UV-Vis spectroscopy data revealed that *ONOOH* mediates the oxidation of *MbFe(II)* in a 2 steps reaction. First, *MbFe(II)* is rapidly oxidized to ferrylmyoglobin *MbFe(IV) = O*, which reacts next with PON to form the metmyoglobin *MbFe(III)OH₂* as illustrated in **Equations 1-2**. According with *ab initio* calculations (29), the *ONOO•* radical is unstable and thus prone to dissociation into *NO•* and *O₂* as shown in **Equation 3**:

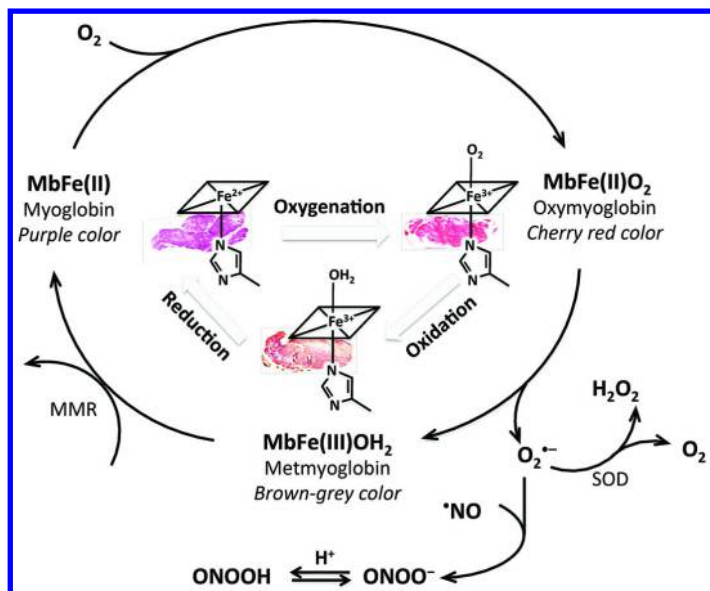
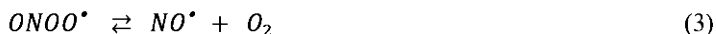
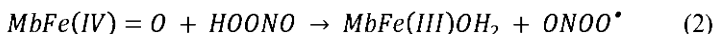
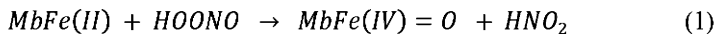


Figure 5. The meat color cycle. See text for more details.

The “meat color cycle” is illustrated in Figure 5 as the interconversion between myoglobin’s different forms. The purple, cherry-red color oxymyoglobin is oxidized into the grey-brown color metmyoglobin and the *O₂⁻* is generated in an uncatalyzed reaction. Next, the metMb is reduced to Mb by the MMR.

This reduced form readily binds molecular oxygen to yield oxymyoglobin. The same pathway illustrates how the $O_2^{\cdot-}$ dismutates to H_2O_2 and O_2 in the presence of superoxide dismutase (SOD). Significantly, $O_2^{\cdot-}$ will react with the NO^{\cdot} to produce the PON coupled with its conjugate peroxyntitrous acid ONOOH. This creates an avenue of interaction between the processes of ULP and HGO. In regards to the meat color cycle, the MMR enzyme is reported to be still partially effective in freshly harvested muscle tissue (38, 39). The color stability of meat throughout processing, storage and display is a complex process that depends on multiple factors, including *post mortem* pH, storage temperature, addition of salt, O_2 and light exposure during display or packaging.

Next, the coupling between lipid oxidation and meat myoglobin oxidation. The ULP generates off-flavors, much as the HGO results in meat discoloration (31, 37). Both of these processes decrease the value of meat products, and thus research has explored their interaction. Amino acids in meat protein were shown to be vulnerable to products of lipid oxidation, in fact more prone to damage by lipid oxidation secondary products (*i.e.*, aldehydes) than primary products of lipid oxidation (*i.e.*, hydroperoxides). On the other hand, these secondary products can interact with the amino acid residues of proteins regulating the proteins' structure and function (40). Fatty acid (lipid) oxidation was shown to promote protein (meat) oxidation, in animals fed with fatty acids having different degrees of unsaturation (41). Also, it was discovered that feeding animals with oxidized oil induced a higher level of protein carbonyl groups, a marker of oxidative stress (42). Some proteins in muscle foods, especially myoglobin, can act as pro-oxidants that initiate and accelerate lipid oxidation (43). Also, higher levels of oxygen in packaged beef were associated with increased lipid oxidation, accelerating color degradation in the meat (44).

These results support the hypothesis that protein oxidation products enhance the rate of lipid oxidation and *vice versa* (31). Several reviews have cited evidence that myoglobin and lipid (per)oxidation and underlying mechanisms are in fact linked (31, 43, 45). Because oxidative reactions involving lipids and proteins can influence meat quality during *post mortem* aging, strategies involving antioxidants have been proposed to extend shelf life. Such strategies, including addition of antioxidants such as addition of vitamin E to the animal's diet have been reviewed by Lund et al. (46).

A body of published inquiries seems to indicate that PON can accelerate oxidative degradation of muscle foods by generating free radicals that initiate lipid peroxidation and by reacting with cellular components to decrease the anti-oxidative capacity (3, 4, 15, 34, 47, 48). Moreover, fresh meat is a complex and gradually changing milieu, whose properties are influenced by environmental, health, and nutritional factors acting both before and after the animal meat is harvested, including a) the composition of the animal's diet; b) the animal's physiological state, which is influenced by the animal's age and general health; c) pre-harvesting animal handling procedures, including low water availability or exposure to extreme temperatures, that might induce nitro-oxidative stress; d) meat-harvesting practices, including rough handling during transportation to, or processing at the abattoir site; and e) the meat storage conditions the first few days *post-mortem* (49, 50).

3.3. Scavengers of the Peroxynitrite Caused Injury: Natural Polyphenols from Grapes and Grape Products

Natural antioxidants from fruits and vegetables are powerful scavengers of radical species, including PON (17). Although these antioxidants may be present in somewhat limited amounts in the organism due to bioavailability and transformation, they can protect against nitro-oxidative stress. The huge potential of natural antioxidants is indicated by several ongoing clinical trials assessing antioxidant effects of natural substances for alleviating a number of medical conditions (18).

In this section we will focus on a special class of natural PON scavengers, namely polyphenolic compounds from grapes and wine (Figure 6), which are often natural companions of meat during meals. Recent studies have shown that consumption of partially oxidized meat increases lipid peroxidation in the stomach, increasing absorption of cytotoxic lipid peroxidation products in the body. When meals included red wine polyphenols in addition to meat, the level of malondialdehyde (MDA, an indicator of biological oxidative stress) in plasma was significantly lower (51, 52). Moreover, natural polyphenols seem to modulate the endogenous antioxidant system while lowering the risk of death from some diseases, including cardiovascular, neurodegenerative diseases, diabetes, or some types of cancer (18). Consumption of red wine is believed to lower the risk of death from coronary heart disease (53) by preventing the oxidation of LDL, or bad cholesterol (54). Resveratrol, the famous wine polyphenol, was reported to possess anti-cancer (55), anti-inflammatory (56), and anti-aging activity (57). Its role in cardiovascular, cerebral and metabolic diseases was recently reviewed (18).

Grapes contain high amounts of polyphenolic compounds distributed in the grape skin, seeds and pulp. A glass of red wine is estimated to contain about 100 mg polyphenols (58) which contribute to its high antioxidant capacity. Polyphenols from wine are classified in two categories (Figure 6) flavonoid and nonflavonoid compounds (stilbenes, phenolic acids, and tannins). These natural antioxidants were shown to intervene and alleviate all transformations induced by PON such as protein nitration and oxidation, DNA damage, or lipid peroxidation (59–61).

To give a few examples, phenolic compounds like gallic acid, tyrosol, caffeic acid, resveratrol and epicatechin protected various cell cultures (primary cortical neurons, bovine aortic endothelial cells etc) against PON-induced injury (62, 64, 65) as illustrated in Figure 7. Epicatechin prevented the nitration of fibrinogen (59) (Figure 7A). Resveratrol minimised the intracellular depletion of glutathione (the endogenous antioxidant), caused by PON (62) (Figure 7B). Ellagic acid protected against single strand breaks produced by incubating DNA with PON (63) (Figure 7C).

The scavenging activity of red wines against PON was found to be correlated with their polyphenolic content (66). On the other hand, individual polyphenols from grapes and wines exert their protective effect against PON-induced transformations through different mechanisms. To complicate things further, for the same compound (e.g resveratrol), the protective action corresponds to

different reaction pathways at various concentrations levels (62). Also, synergies and antagonisms between various antioxidants influence the global antioxidant effect in mixtures.

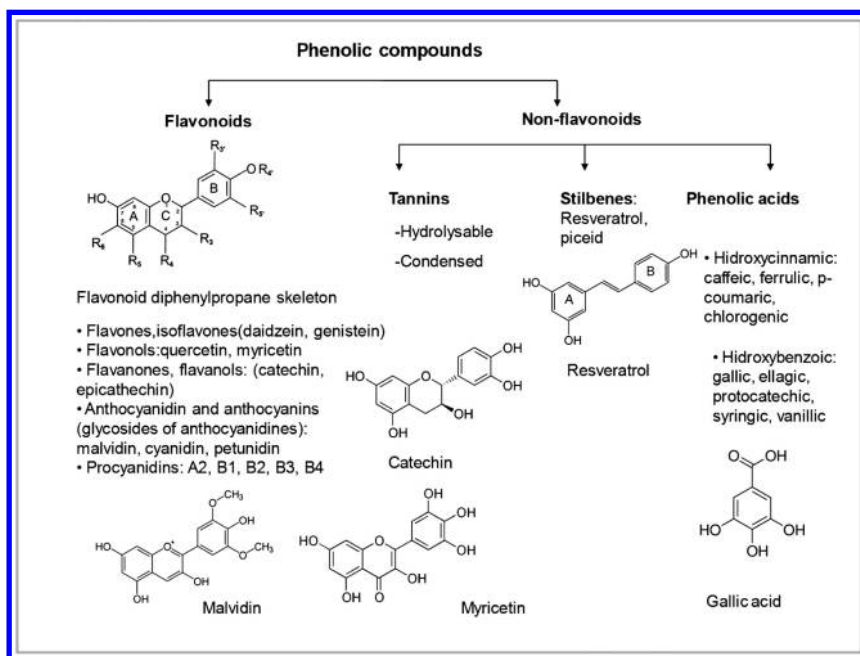


Figure 6. Phenolic compounds from grapes and wine.

Mechanisms by which natural compounds from grapes and wines exert their antioxidant effect range from direct scavenging of PON and PON-derived radicals to activation of transcription factors (67) or inhibition of radical-producing enzymes (68). For example, a 50 μM concentration of resveratrol upregulated the intracellular content of glutathione, minimizing the depletion due to PON (62). Procyanidins from grape seeds prevented PON attack to vascular cells by binding to the surface of coronary endothelial cells (69). Flavonoids exert their protective effect against PON-induced DNA damage most likely indirectly, by scavenging free radicals produced by PON (nitrogen dioxide, carbonate and hydroxyl radicals) (70, 71).

The PON scavenging activity of polyphenols is related to their chemical structure. For flavonoids (Figure 6), the presence of the 3', 5'-dihydroxy structure in the B ring, a catechol moiety, offers a higher stability and provides scavenging activity (72). The presence of 3- and 5-hydroxy groups with 4-oxo function in the A and a C rings ensures a maximum scavenging activity. Compared with the aglycone antioxidants, glycosylation decreases the radical scavenger activity (72). For the stilbene resveratrol (structure also in Figure 6), the 4-hydroxyl group in its ring B and the m-hydroxyl configuration in ring A are critical for its scavenging activity (73–75). Methods used to study the PON antioxidant effect of

polyphenolic compounds in grape extracts and wines include direct quantitative measurement of PON levels and indirect assessment of protective effects on PON-tyrosine (PON-Tyr) interaction (i) and PON-induced DNA damage (ii).

Direct detection of PON by chemiluminescence and fluorescence methods proved helpful to rank the scavenging activity of several polyphenols (+)-catechin, (-)-epicatechin, and myricitrin (76) or to emphasize for example reduced plasma PON levels in diabetic rats whose diets were supplemented with resveratrol (77).

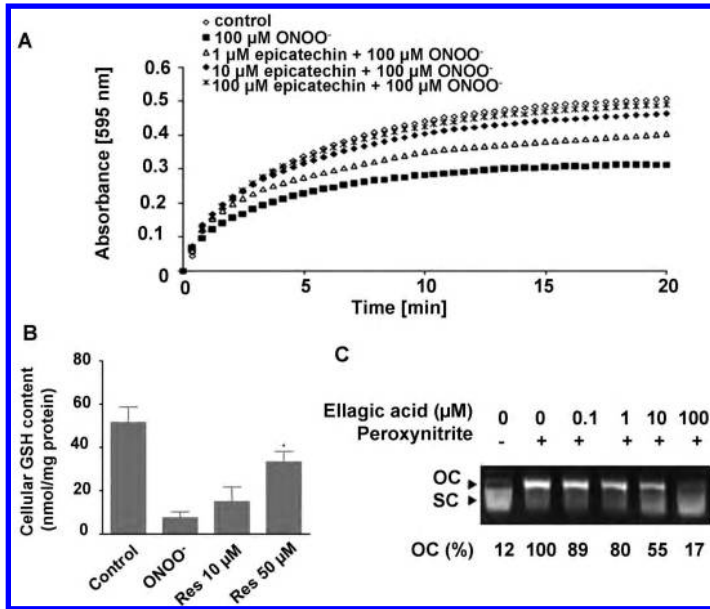


Figure 7. *A*: The effect of epicatechin on PON-induced changes in fibrinogen clotting. *B*: Cellular glutathione content in bovine aortic endothelial cells treated with 500 µM PON after pre-incubation with resveratrol. *C*: Protection by ellagic acid against PON-mediated strand breaks in DNA. The relative intensity of open circular and supercoiled DNA in the PON-untreated sample (lane 1), the ellagic acid-treated samples (lanes 3–6), versus the sample treated with PON only (lane 2). Reproduced with permission from references (62) copyright 2006, from reference (63) copyright 2009 and from reference (88) copyright 2012, all Elsevier.

3.3.1. Antioxidant Effect of Polyphenols on PON-Tyrosine Interaction

Formation of nitrogen dioxide radical from PON as result of its fast reaction with carbon dioxide in biological media triggers further attack on biomolecules, leading to nitrated compounds (70). It has been demonstrated both *in vivo*

and in animal models that increased levels of 3-nitro-Tyr are associated with cardiovascular disease, atherosclerosis, ischemia–reperfusion, and stroke (78–81). In all, more than 50 human diseases are associated with increased levels of nitrated proteins (82).

Tyr is a non-essential amino acid with a polar side group. Most Tyr residues in proteins are surface-exposed and, as a consequence, are available for nitration by PON (83, 84). Besides Tyr, tryptophan (Trp) is another amino acid that can be nitrated by PON in proteins, leading to 6-nitro-Trp as a major product (85, 86).

The nitrating effect of PON has been exploited for screening various radical scavenging compounds and for studying the precise modifications induced in proteins upon attack by PON. Scavenger screening studies relied on the PON-induced nitration of either free tyr or of proteins such as collagen (87) bovine serum albumin (63) and fibrinogen (61, 88). Among these, fibrinogen is particularly sensitive to the toxic action of PON. Fibrinogen is a glycoprotein representing 4% of the total plasma proteins. PON produces both structural and functional changes in this protein (89, 90), as nitration of fibrinogen by PON translates further into changes in its clotting ability (88). Cardiovascular diseases are associated with an increase of nitrated fibrinogen (8).

Several methods have been described for evaluating the nitration of Tyr and Trp residues in proteins: HPLC (with coulometric, UV or mass spectrometry detection), ELISA or Western blotting. Specificity of the detection in complex biological samples was ensured by using either chromatographic separation (73, 91–93) or by using specific antibodies against 6-nitro-Trp and 3-nitro-Tyr (59, 85, 86, 94, 95) In studies aimed at identifying nitration sites the two approaches were usually combined. Detection limits for 3-NO₂-Tyr were in some cases less than 1 nM (92).

Several natural antioxidants such as sinapinic acid, ellagic acid, epicatechin, catechin, rutin, quercetin and resveratrol (59, 61, 63, 73, 87), as well as grape seed (59) and grape extracts (73) were found to inhibit the PON-induced formation of 3-nitro-Tyr.

The antiradical effect of grape extracts, pure antioxidants and mixtures of phenolic compounds from grapes (catechin, rutin, epicatechin, quercetin and resveratrol) (73) was expressed as the amount of polyphenolic compounds necessary to inhibit 50% of nitration of free Tyr induced by PON. One study compared the interactions between pure compounds observed via the inhibition of PON-induced Tyr nitration with those emphasized by a classic test of antioxidant capacity, 2,2-diphenylpicrylhydrazyl (DPPH) and found differences between the results and trends gathered via these two methods (73). Different results between antioxidant assays are however a common occurrence, due to the different underlying principles and different radical species involved (73).

For some polyphenols (ellagic acid, epicatechin, shown in Figure 6), the magnitude of their protective effect *in vitro* was concentration-dependent (59, 63), while for others like resveratrol no such dependence was found (61).

3.3.2. Effect on DNA Damage

PON reacts with DNA, causing mutations and structural damage. Antibodies generated against PON-treated DNA appear to bind DNA from patients suffering of various types of cancer but not DNA from healthy individuals, suggesting that peroxynitrate-induced stress plays a role in cancer etiopathology (60). PON can damage DNA by attacking either the sugar-phosphate backbone (leading to DNA single strand breaks (96) or DNA bases, with guanine being the most susceptible to oxidation and nitration by PON (97).

Some flavonoids with an ortho-trihydroxyl group were shown to inhibit the PON-mediated formation of 8-nitroguanine in calf-thymus DNA (98) while other dietary antioxidants (epigallocatechin-gallate, quercetin, and rutin) protected against PON-induced DNA damage manifested through the formation of 8-hydroxy-2'-deoxyguanosine (99). Single strand breaks due to PON attack were either minimised or totally abolished by ellagic acid (63) and various flavonoids (myricetin, myricitrin, epigallocatechingallate, quercetin, rutin etc (71, 98–100). The protective effect of ellagic acid against single strand breaks damage (produced by incubating DNA with PON) was proportional to antioxidant concentration in the range 0.1–100 μM (63).

A simple and fast colorimetric method allowed the protective effects of various antioxidants such as gallic acid, caffeic acid and ascorbic acid against ONOO⁻-induced DNA damage to be compared (100). The method relies on single strand DNA adsorbed on gold nanoparticles. Upon attack by PON, the strands are cleaved to smaller fragments that can no longer prevent the electrostatic attraction between particles. The resulting aggregation determines a color change of the nanoparticle dispersion from red to blue.

4. Peroxynitrite Detection: Focus on Electrochemical Sensors

PON has also been shown to have cytoprotective roles in the redox regulation of critical signaling pathways. Specifically, PON is modulating the protective signals against ischemia-reperfusion injury and neural apoptosis (8, 12, 101). Thus, the dynamic concentration of PON generated in tissues under various conditions, and the balance to local concentrations of other species such as NO[•], seem to modulate its role in many vital cellular functions. Efforts by biochemists and physiologists to clarify both PON's negative and positive physiological roles require the ability to measure PON accurately *in vivo* in real time (21, 101). This section outlines recent research on ONOO⁻ electrochemical sensing. Other detection methods, such as the fluorescent or (bio)luminescent probes have been recently presented in detail elsewhere (102) and will not be covered here.

4.1. Preparation Methods for Peroxynitrite

Maintaining a controllable, stable PON concentration during experiments is important but challenging, due to PON's fast reaction kinetics. Challenges and approaches used to provide a stable PON supply are briefly reviewed below.

Two practical approaches used to provide PON are (i) adding aliquots of chemically synthesized, stable alkaline solutions of PON and (ii) *in situ* generation of PON from various donors. Chemical synthesis of PON was achieved by various pathways, including use of ozone and sodium azide (103–105) hydroxylamine oxidation (106), reaction of hydrogen peroxide with alkyl nitrite (107, 108) or sodium nitrite (109, 110). Fresh chemically synthesized PON in alkaline solutions can be aliquoted and kept at -80°C for several months. The PON concentration is typically derived from the absorbance at 302 nm using the molar extinction coefficient (molar absorptivity) $\epsilon = 1670\text{ L mol}^{-1}\text{ cm}^{-1}$ (111).

Peroxynitrite can be generated *in situ* at physiological pH using various donors (112, 113), including SIN-1 (114–117). SIN-1 decomposes spontaneously and liberates NO^{\bullet} and $\text{O}_2^{\bullet-}$ and with a 1:1 stoichiometry, thereby generating ONOO^- continuously for a period of time (118). A solution of 1mM SIN-1 is known to release PON at a rate of $1\mu\text{M}/\text{min}$ (114). However the decomposition kinetics are influenced by the composition of the medium (119). The peak concentration of peroxynitrite is linearly correlated with SIN-1 concentration. Most authors have reported a PON concentration of 1.2–3.6% of the added SIN-1 (114–117). Electron spin resonance spectroscopy (ESR) was used to derive the PON formation rate at a rate of $1\mu\text{M min}^{-1}$ PON from 1 mM SIN-1 in phosphate buffer solution (PBS).

4.2. Electrochemical Quantification of Peroxynitrite

Several recent reviews have appraised methods for PON detection, mainly by electrochemical techniques (22, 121) and optical (fluorescence and luminescence) methods (21, 101, 102). This section describes the state of the art PON-sensitive electrochemical sensing *via* hybrid films, their quantification mechanism and response performance: detection limit, sensitivity and measuring range, where available. Advantages, drawbacks and challenges of the various methods are also analyzed. Table 1 outlines several recent significant contributions.

The group of Amatore has developed several innovative methods (122–128) supported by both theoretical and experimental models. Among these, one technique involved the concurrent quantification of NO , $\text{O}_2^{\bullet-}$ and ONOO^- in the vicinity of a single cell (123, 126). The amperometric studies performed on fibroblast cells at different oxidative potentials have shown a complex response that apparently incorporated multiple electroactive species. Indeed, the *in vivo* experimental data involved several oxidative waves, successively confirmed by *in vitro* experiments with platinized carbon microfiber electrodes (Pt-C μFEs) for stable solutions. The inset (A) in Table 1 illustrates the species H_2O_2 , ONOO^- , NO , NO_2^- being directly oxidized by Pt-C μFEs at their distinct potentials *vs.* a standard saturated calomel electrode (SSCE). In addition, the same concept was applied to nano-electrodes placed inside macrophages to detect these RNOS *in vivo* under relevant conditions (129). The integration of the reconstructed fluxes of the RNOS allowed the calculation of an average total amount of each species, detected as shown in inset (B) same table (126). This intriguing assay procedure allowed the exploration of a carefully controlled biological environment; however its merits still remain to be fully appreciated for unknown, complex *in vivo* configurations.

Bedioui and colleagues reported a number of PON-sensitive films and methods (130–132), including ONOO⁻ detection on bare gold (Au) microelectrodes (μ Es) by amperometry at -0.1 V vs. Ag/AgCl in PBS (132). The simultaneous detection of ONOO⁻ and NO was also revealed. The NO detection involved using a polyeugenol–polyphenol film at +0.8 V vs. Ag/AgCl. This method was developed for an on-chip electrochemical sensor array (ESA) platform with individually addressable Au μ Es for simultaneous screening of NO[•] and PON, as shown in insets (C) and (D). The ESA was interfaced with cell culture wells (132).

Notably, several synthetic manganese complexes were employed as components in ONOO⁻ sensitive electroactive films on electrodes. For instance, Koh and colleagues (133) synthesized a manganese–polymer complex film with the polydithienyl-pyrrole-benzoic acid (pDPB) by electrodeposition onto a Platinum (Pt) μ Es. This (Mn-pDPB) film was decorated with electrodeposited Au nanoparticles that reportedly enhanced the PON reduction, according to the reaction scheme from inset (E) and calibration graph from (F). Moreover, an increase in selectivity was reported by using an outer layer of polyethyleneimine (PEI). The interferents tested included several electroactive species and PON decomposition molecules (133). The selectivity was reported as satisfactory, allowing these Mn-pDPB-PEI μ Es to be employed for the PON determination *in vitro* on glioma tumor cells. To further validate this work, it would be useful to repeat the same experiments with the “genuine” synthetic PON freshly prepared.

The group of Malinski (134) used a manganese(III) [2-2]paracyclophenylporphyrin (MnPCP) film electrodeposited on carbon microfiber electrodes (C μ FE) for PON detection in the presence of NO and O₂^{-•}. The chronoamperometry was conducted with the three working electrodes poised at different potentials, namely 0.67 V for NO, 0.35 V for O₂^{-•} and -0.35 V for ONOO⁻. Carbon μ FEs were modified with a MnPCP film. Detection was based on the reduction of ONOO⁻. The concentration ratio [NO] / [ONOO⁻] was reported as a potentially useful marker to diagnose cardiovascular disease. (134). The same group quantified PON after release upon stimulation by a beta-blocker medication, Nebivolol (135) as illustrated in inset (G).

L.T. Jin and colleagues used Mn(III) tetraamino-phthalocyanine (MnTAPC) (136) as films electropolymerized onto C μ FEs. Quantum chemistry predicted the outermost **oxygen** atom from ONOO⁻ would provide the lone-pair electron to the center of the Mn atom of the MnTAPC, with formation of an axial coordination complex with the reaction scheme as in inset (J). This reaction shows that PON was oxidized to nitric dioxygen and nitrite (136). Differential pulse amperometry (DPA) current was recorded as the difference between the values at the potentials 0.20 V and 0.0 V vs Ag/AgCl. In addition, a poly(4-vinylpyridine) positively charged film was placed on the MnTAPC microsensors, and its cation-repulsive barrier functioned as a diffusional screen for larger molecules. The selectivity was tested against a list of electroactive interfering agents from biological media. (136). This microsensors was utilized with DPA to quantify PON at the surface of single myocardial cells as shown in inset (K). The improvement in selectivity is noteworthy; however the addition of a selective membrane typically comes at the expense of the response time, which is a drawback when fast detection is needed.

Table 1. ONOO⁻ Sensitive Electrochemical Methods (More Details in Text)

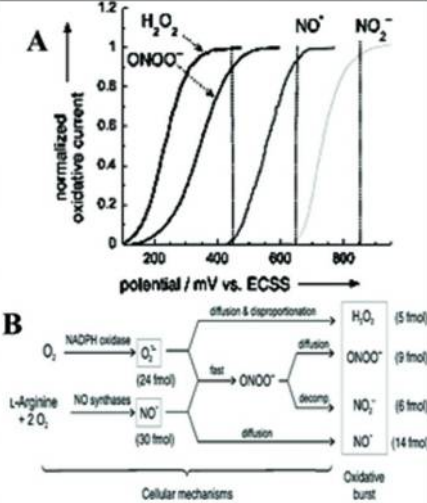
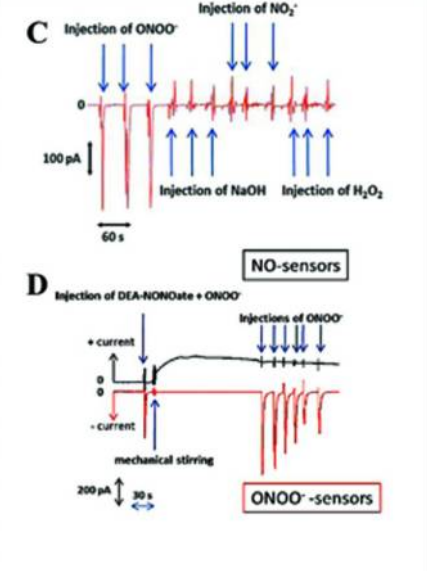
Method and References. Detection Limit (LoD), Sensitivity (S), Linear Range (LR)	Reaction Mechanism and Response to Peroxynitrite
<p>(A). Response of platinized carbon μEs sited close to single cells. Cell's oxidative burst was detected and deconstructed to reveal the RNOS separate waves. (123, 124, 126). Same technique was applied to nanoelec-trodes placed inside macrophages to detect RNOS <i>in vivo</i>. (129)</p> <p>(B). Schematic with the RNOS pathway and the amount of each species detected. (124)</p> <p>Selective by design.</p>	 <p>A</p> <p>B</p>
<p>(C). PON detection on bare Au μEs by amperometry at -0.1 V in PBS. Injection of 50 μM ONOO⁻; 1700 μM NaOH; 200 μM NO₂⁻; 500 μM H₂O₂. (132)</p> <p>(D). Parallel detection of ONOO⁻ and NO with aliquots of (10 μM NO donor in alkaline solution + 50 μM ONOO⁻) and 5 min. later, aliquot of 50 μM ONOO⁻ alkaline solution. NO detected on seven Au μEs coated with the complex poly(eugenol) /poly(phenol) at +0.8 V (132). The ONOO⁻ injections were the same as in (C). All potentials vs. Ag/AgCl.</p> <p><input type="checkbox"/> Selective to NO, NO₂⁻, H₂O₂.</p>	 <p>C</p> <p>D</p>

Table 1. (Continued) ONOO⁻ Sensitive Electrochemical Methods (More Details in Text)

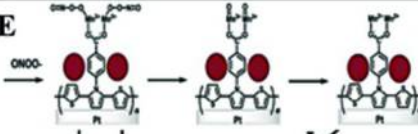
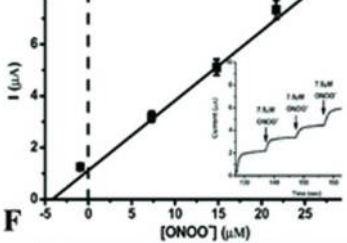
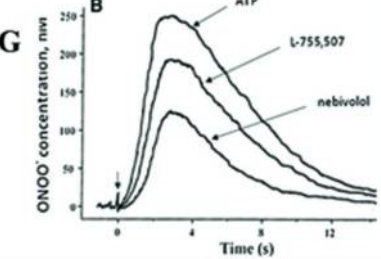
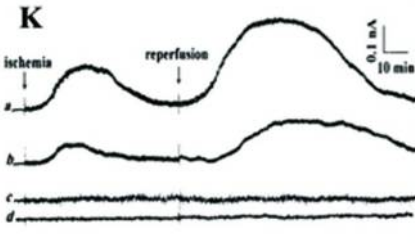
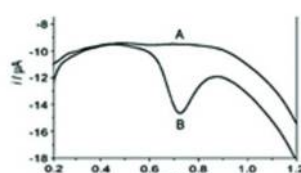
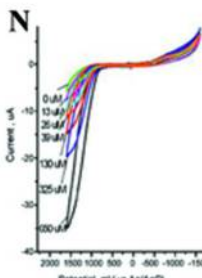
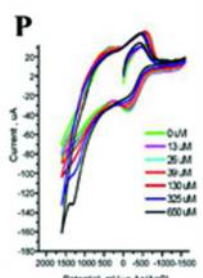
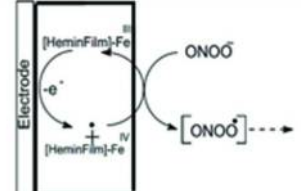
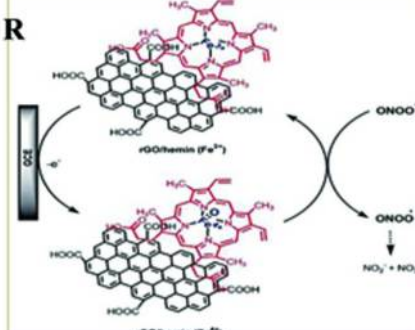
<p>(E). Pt μEs modified with Mn ion and poly- di-thienyl-pyrrole-benzoic acid (Mn-pDPB), providing binding sites for Mn²⁺ for PON interaction</p> <p>(F). Calibration graph for the Mn-pDPB microsensor with 7.5 μM PON (133).</p> <p>□ LoD = 1.9 nM; □ LR = (2×10^{-8} ÷ 3×10^{-5}) M</p>	<p>E</p>  <p>F</p> 
<p>(G). Carbon μFEs modified with Mn(III)-2-para cyclophenylporphyrin film. The PON reduction (134) was detected after upon stimulation by a beta-blocker Nebivolol medication for hypertension (135).</p> <p>□ LoD = 1 nM</p>	<p>G</p> 
<p>(J). Carbon μFEs modified with Mn(III) tetraaminophthalocyanine Mn(TAPC) complex. One of PON lone pair electrons filled the empty orbital of poly Mn(TAPC) creating an axial coordination complex. PON was catalytically oxidized to NO₂ and NO₂⁻.</p> <p>(K). Differential pulse amperometry in single myocardial cells spiked with 100 μM PON (a); 100 μM melatonin (b; c); cell free HBSS buffer with 100 μM melatonin (d). (136)</p> <p>□ LoD = 18 nM; S = 2.4×10^{-3} nA nM⁻¹ □ Selectivity studied <i>in vitro</i></p>	<p>J</p> $\text{poly-(TAPc)Mn}^{\text{III}}(\text{H}_2\text{O}) + \text{O}=\text{N}-\text{O}-\text{O}^- \rightarrow [\text{poly-(TAPc)Mn}^{\text{III}}\text{-OONO}]^- + \text{H}_2\text{O}$ $2[\text{poly-(TAPc)Mn}^{\text{III}}\text{-OONO}]^- \rightarrow 2\text{poly-(TAPc)Mn}^{\text{IV}} = \text{O} + \text{NO}_2^- + \text{NO}_2$ $\text{poly-(TAPc)Mn}^{\text{IV}} = \text{O} + 2e + 2\text{H}^+ \rightarrow \text{poly-(TAPc)Mn}^{\text{III}}(\text{H}_2\text{O})$ <p>K</p> 

Table 1. (Continued) ONOO⁻ Sensitive Electrochemical Methods (More Details in Text)

<p>(L). Poly(cyanocobalamin)-based GCE catalyzed PON oxidation.</p> <p>(M). Differential pulse voltammetry with 40 μM PON spiked in serum (trace B) compared with a blank (trace A). PDA pulse amplitude of 50 mV, with 0.1 s, at 9.2 pH. (137).</p> <p>□ LoD=10⁻⁷ M; LR= (2x10⁻⁶ ÷ 3x10⁻⁴) M</p>	<p>poly-Cbl(III) + O=N-O-O^{•-} → poly-Cbl(II)-OONO[•]</p> <p>L poly-Cbl(II)-OONO[•] - e → poly-Cbl(III) + ONO₂[•]</p> <p>2ONO₂[•] → O₂ + 2NO₂</p> <p>M</p> 
<p>Carbon μFes modified with hemin and hemin-PEDOT films. Redox current increased with PON concentration (145). Response sensitivity of hemin-PEDOT film (P) was 13 nA μM⁻¹, or 50 times higher than for hemin alone (N). This seems to result of an enhanced interaction between the PEDOT nanostructured matrix and the hemin catalyst.</p> <p>□ LoD = 200 nM; S = 13 nA μM⁻¹</p>	<p>N</p>  <p>P</p> 
<p>(Q). Hemin-based c μFEs catalyzed PON oxidation (138). Reaction mechanism shows the Fe atom to mediate the e⁻ transfer from PON substrate to oxidizing porphyrin ring.</p> <p>□ Selective vs. NO, NO₂⁻ and NO₃⁻</p>	<p>Q</p> 
<p>(R). GCEs modified with (hemin-reduced graphene oxide) complex. (141). The PON electrocatalytic reaction occurred at +1.1 V vs. Ag/AgCl.</p> <p>LoD = 5 nM; S = 7.5 nA nM⁻¹</p>	<p>R</p> 

The cobalt compound cyanocobalamin (vitamin B12) was used by Wang and Chen (137) to functionalize glassy carbon electrodes (GCEs). The electropolymerized film displayed electrocatalytic activity for PON oxidation. The reaction mechanism in inset (L) indicated that the redox-active cobalt center in poly(cyanocobalamin) film catalyzed ONOO⁻ decomposition through the formation of intermediates. The DPA allowed detection of PON spiked in serum as seen in inset (M). The authors declared PON selectivity in the presence of potentially interfering molecules (137), however no data were provided to support this claim.

The group of Bayachou (145), used the electroactive, intrinsically conductive polymer polyethylenedioxythiophene (PEDOT) together with hemin electro-assembled on C_μFEs for the detection of ONOO⁻. The response of the hemin film to PON was compared, with and without PEDOT by CV and CA. When PEDOT was copolymerized in the hemin film (inset N) the sensitivity was strongly enhanced, as compared to just the hemin film (P) or the PEDOT film. Significantly, the typical “nano-cauliflower” tortuous and porous matrix of the hemin-PEDOT hybrid seemed to provide a very high specific area/volume, as ascertained by SEM imaging (145). This testing has suggested that synergy occurs between the PEDOT and the hemin macrocycle molecules; this hypothesis was supported by a decrease of the oxidation potential for the nano-hybrid material (146), as compared with the responses from either of the two components employed separately

In a follow up investigation, Peteu and colleagues electro-polymerized hemin thin films on either GCEs or C μFEs (138) and assessed the resulting sensors’ oxidative detection of PON in stirred solution or in a flow-cell. The advantages of using a flow-cell include the convective transport of analyte, resulting in less noise and faster response times. The catalytic efficiency (calculated as the ratio of the catalytic peak current in the PON presence and absence, respectively) decreased as the scan rate increased, and the peak potential of the catalytic oxidation was found to depend on pH. The analyte tests indicated a fast catalytic oxidation of PON specific for hemin, and not for protoporphyrin-only films where iron was absent. This finding suggests a fundamental role of the bound iron center atom to ensure the oxidative catalytic turnover of PON (Q). In separate tests, related species such as NO•, nitrite, or nitrate did not interfere with electrocatalytic detection of PON (138).

The group of Szunerits built on their earlier published method (140, 141) to prepare a hemin-functionalized reduced graphene oxide to prepare PON-sensitive electrodes with Peteu and collaborators. The graphene surface is supporting electron-donating organic molecules. Porphyrins, for instance, were shown to allow at same time a reduction of GO to reduced GO (or rGO) and the insertion of organic aromatic molecules *via* π-π stacking interaction (139, 141–144) and this has spawned a high interest to study the PON activity of GO decorated with hemin. The meaning of the expression “graphene oxide (GO)” is “a single or few layer graphene” prepared by the oxidation of graphite. Thus, oxygenated functionalities are introduced in the structure, expanding the layer separation and also making the material dispersible in water, *i.e.* by sonication. The hemin-functionalized graphene nanosheets have revealed PON activity (141,

142). Hence, a hemin-rGO complex was prepared from a graphene oxide aqueous solution mixed with hemin with subsequent sonication for several hours and freshly drop-cast onto GCEs. Addition of ONOO⁻ from SIN-1 to the hemin-rGO modified GCE has shown an oxidative wave at 1.17 V that was ascribed to the electrochemical oxidation of hemin on the rGO platform. In the presence of ONOO⁻, an electrocatalytic oxidation mediated by hemin centers seems to occur, as illustrated by the reaction mechanism (inset **R**). The Fe³⁺ center of hemin in the rGO-hemin film was oxidized to a high valent iron form such as [Fe^{4+=O}] iron oxo intermediate, electrochemically at the electrode interface. In the PON presence, this iron oxo intermediate is reduced back to Fe³⁺ for further turnovers (141). The resulting current scaled linearly with the PON concentration, and a detection limit of 5±0.5 nM was recorded in PBS with a sensitivity of 7.5 nA nM⁻¹ (141).

The reasons for this apparent increased sensitivity brought by graphene need to be elucidated. Firstly, graphene provides a two-dimensional support with large open accessible surface with high area per volume ratio, where the catalyst-PON interaction seems to be enhanced, which could be beneficial for the surface-driven electrocatalytic activity. Secondly, the graphene-supported hemin could prevent hemin molecules from self-polymerization and thus increase the available iron-hemin catalytic active sites. Thirdly, the amount of hemin present on the electrodes seems to be important; the amount incorporated into the new rGO/hemin matrix is 2.5 times larger than that on rGO that is post-modified with hemin. Ongoing research seeks a better understanding of the catalytic mechanisms of graphene supported hemin for PON oxidation and to potentially develop highly sensitive sensor platforms (141).

4.3. Challenges to Develop Electrochemical PON Sensors

Quantitative determination of short-lived reactive species, such as PON in complex analytical matrices (biological samples, meat etc) require a sensitive, selective and accurate detection method with fast response time. A variety of sensor architectures and analytical strategies have been designed to improve measurement quality. As examples, experimental conditions (e.g operating potential) have been customized to favor selective detection of specific RNOS analytes, semipermeable membranes have been used to screen out interferents, and (micro)electrodes have been fabricated from a variety of materials (21, 22, 102). Results of these studies were summarized in Table 1.

The choice of electrochemical detection method is typically determined by the requirements of time resolution, sensitivity and selectivity. For example, differential pulse voltammetry offers good sensitivity, as the contribution of the background current to overall signal is drastically reduced. Moreover, the sensors miniaturization is desirable. The ultra-small sensors can afford fast response times in non-stirred soft solid matrices, high spatial resolution (146) and are potentially integrated in biosensor arrays (147).

In cases when temporal resolution is most important, (e.g monitoring in real-time oxidative bursts) amperometry and fast-scan cyclic voltammetry are more appropriate. The impedance methods monitor changes in cell membrane resistance due to PON-induced membrane-lipid oxidation.

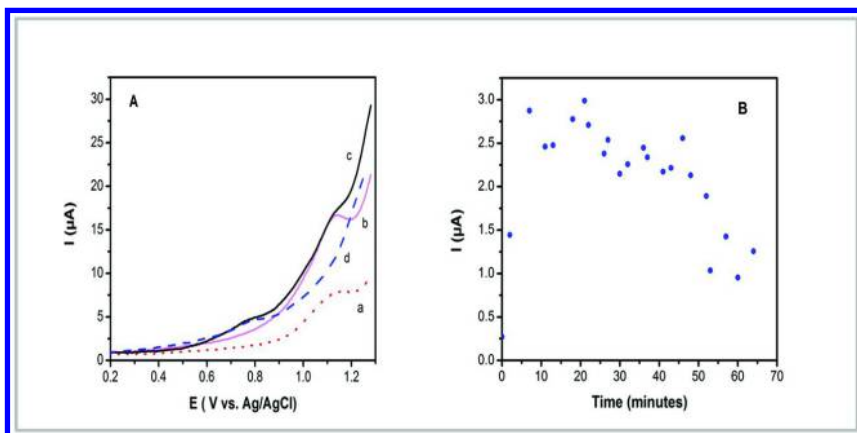


Figure 8. A: Square wave voltammograms (SWV) recorded for a solution of 100 μM SIN-1 (a, fresh solution, red dotted line, b, after 20 minutes, pink, and c, after 100 minutes, black line) and for a 10 μM sodium nitrite solution in PBS pH 7.4 (d, blue dashed line). The potential was scanned in the range from -0.25 V to 1.3 V, with a step potential 5 mV, step amplitude 25 mV (scan rate: 250 mV/s). The electrode was poised at -0.25 V for 10 s before starting the scan. B: Evolution of the anodic peak current at 1.1 V recorded for SIN-1 solutions at different times after preparation). The height of the anodic peak current was resolved from the SWV with the Origin 8 program. See text for more details.

Figure 8A presents the square wave voltammograms recorded for a 50 μM solution of SIN-1 following dissolution in PBS buffer pH 7.4. The 3-electrode electrochemical cell had a GCE working, a Pt counter and Ag/AgCl (KCl, 3M) reference. At time zero, one anodic peak due to PON oxidation was observed at 1.1 V (trace a). The peak height increased with time up to 20-30 min (b), then decreased slowly. After 45-50 minutes, the decrease as abrupt. A second peak appeared at 0.74 V (c). This second peak could be attributed to nitrite oxidation (d).

The time evolution of the anodic peak current at 1.1 V (Figure 8B) suggests a working window of 25-30 minutes where PON concentration is relatively stable, allowing for accurate electrochemical measurements. This finding is in agreement with profiles of PON generation from SIN-1 obtained by other authors through fluorescence experiments based on the quenching effect of PON on NADH fluorescence (120).

5. Discussion, Conclusions, and Future Research Needs

Consumers' awareness of nutritious foods and increased attention to healthy eating are strong drivers for the food market, including meat products. As such, color and flavor are meat wholesomeness indicators. Thus, improving the meat color and flavor shelf life will result in substantial economic benefits.

Consequently, significant research efforts have been directed toward methods to quantify meat freshness and elucidate mechanisms of oxidative processes causing degradation of meat quality. As described in this paper, electrochemical methods, especially micro-sensing approaches, provide outstanding potential for label free, in situ, fast measurement of PON's concentration and effects. Technological progress has been significant, but there are still no widely accepted, commercial bio/sensors available to detect the freshness of meat using simple and user-friendly procedures.

This chapter has focused on two key reaction agents: ULP, which contributes to *off-flavors* and HGO, which contributes to *discoloration*. Within each of these classes, model molecules have been identified for in-depth study of PON's role in meat spoilage: DOPC, a model ULP commonly found in biological membranes, and myoglobin, an HGO whose oxidation modulates the meat discoloration.

As critically discussed herein, the characterization of oxidative meat degradation is complicated for several reasons. First, multiple methods have been developed to characterize various aspects of PON-related food degradation, but no method has been adopted as a gold standard. Thus, the state-of-the art in characterizing meat quality and degradation rate may be considered to be early-stage and evolving. Second, there is substantial variability among fresh meat samples. Samples of animal muscle tissue harvested *post mortem* should be viewed as inherently complex and a continually changing milieu. Multiple factors can influence the concentrations of PON and other RNOS, as well the natural antioxidants and radical scavengers that modulate slow oxidative meat spoilage. These factors include the animal's age, health, environment, nutrition, access to water, and even its handling and physiological state just before meat harvesting.

The complexity of meat's structure and chemistry, combined with the difficulty in quantitatively measuring the highly reactive RNOS suggest that it is unlikely a single bio/chemical test will be developed that satisfactorily measures meat quality and spoilage rate. However, widespread acceptance of key classes of chemical reactions (HGO and ULP) and robust, reproducible assays involving representative molecules within each class (myoglobin and DOPC) would provide a framework on which to advance fundamental understanding of oxidative key processes in meat spoilage and to develop useful, cost-effective, and standardized meat-quality assays.

Such assays would supplement existing currently used commercial food test kits that use enzyme-linked immunosorbent assays to measure the presence of specific analytes. These ELISA assays have several inherent disadvantages, including one-time use, large coefficient of variation, low precision, the need for antibodies that are highly specific for the target analyte, and an inability to monitor temporal changes in the analyte's concentration. These disadvantages are not

shared by the electrochemical methods reviewed in this chapter, which are better suited to monitor rapidly evolving changes due to small, rapidly reacting oxidative species for which antibodies are not available.

However, development of commercially viable electrochemical sensors for specific analytes offers significant challenges. Despite large investments of time and research, few electrochemical sensor systems for biochemical analytes are widely used commercially. One noteworthy success story is glucose biosensors, providing simple, accurate, reproducible, inexpensive home blood glucose measurements for diabetics. However, several decades of research and an overall investment of hundreds of millions of dollars were required to develop, validate, and bring to these biosensors to market. No other commercial electrochemical biosensor offers similar cost-performance features, although some are in various stages of development.

Recent experience in commercial biosensor development suggests that significant investments of research funds and time will be required to develop an electrochemical biosensor platform for meat freshness that is suitable for cost-effective use by farmers, meat processors, and retailers. Development of the commercial biosensor systems to monitor key biochemical processes, such as oxidation of myoglobin and DOPC, will likely follow the glucose biosensor model, in which a permanent portable electronic device is used with disposable interfaces that are placed into contact with the meat samples.

Efforts to develop such systems will be facilitated by recent advances in the speed of microdevices, whose computing power can be leveraged to carry out advanced processing algorithms needed for electrochemical techniques (EIS, DPA, etc.) in real time. In addition, telemetry technologies will allow wireless data communication from remote sensors to central processing units. These advancements could accelerate the timeline from bench research to commercial implementation and reduce the ultimate cost per measurement. In addition, ongoing research may develop correlations between indicators of PON-related oxidative degradation (e.g., rate of myoglobin oxidation) and traditional indicators of spoiled meat (e.g., rate of color change). Such correlations would facilitate development of widely accepted standards for high-quality meat products.

Because the oxidative processes described in this chapter require oxygen, which diffuses into the meat from the surface, significant spatial gradients of oxygen and oxidation rate within the meat sample would be expected. Development of needle-type electrochemical sensors would allow indicators of PON oxidation rate to be measured as a function of depth within the product. Such measurements would provide a more complete assessment of product quality than is possible with surface techniques, such as most optical methods. The three-dimensional measurements would also allow validation of mechanistic mathematical models of the simultaneous transport, chemistry, and reaction kinetics that govern the rate of meat spoilage. Such models, together with the electrochemical sensor platforms, would provide a framework with which to elucidate mechanisms of meat spoilage and to optimize meat-processing methods that maximize product shelf life.

Acknowledgments

The authors kindly acknowledge funding support. The financial support for RMW and YL was provided by NIH grant 5RC2ES018756-02. AV1 and AV2 acknowledge financial support from the MEN-UEFISCDI grant PNII-PCCA-2011-3.1-1809. SFP and ISH were funded from the MEN-UEFISCDI grant PNII-ID-PCE-2011-3-1076.

References

1. Smith, G. C.; Belk, K. E.; Sofos, J. N.; Tatum, J. D.; Williams, S. N. In *Antioxidants in Muscle Foods: Nutritional Strategies To Improve Quality*; Wiley Interscience: Hoboken NJ, 2000; pp 397–426.
2. Min, B.; Ahn, D. U. *Food Sci. Biotechnol* **2005**, *14*, 152–163.
3. Connolly, B. J.; Decker, E. A. *Meat Sci.* **2004**, *66*, 499–505.
4. Connolly, B. J.; Brannan, R. G.; Decker, E. A. *J. Agric. Food Chem.* **2002**, *50*, 5220–5223.
5. Beckman, J. S.; Carson, M.; Smith, C. D.; Koppenol, W. H. *Nature* **1993**, *364*, 584.
6. Beckman, J. S.; Beckman, T. W.; Chen, J.; Marshall, P. A.; Freeman, B. A. *Proc. Natl. Acad. Sci. U.S.A.* **1990**, *87*, 1620–1624.
7. Beckman, J. S.; Koppenol, W. H. *Am. J. Physiol.* **1996**, *271*, C1424–1437.
8. Pacher, P.; Beckman, J. S.; Liaudet, L. *Physiol. Rev.* **2007**, *87*, 315–424.
9. Radi, R.; Beckman, J. S.; Bush, K. M.; Freeman, B. A. *Arch. Biochem. Biophys.* **1991**, *288*, 481–487.
10. Møller, J. K. S.; Skibsted, L. H. *Quim. Nova* **2006**, *29*, 1270–1278.
11. Carlsen, C. U.; Møller, J. K. S.; Skibsted, L. H. *Coord. Chem. Rev.* **2005**, *249*, 485–498.
12. Szabó, C.; Ischiropoulos, H.; Radi, R. *Nat. Rev. Drug Discov.* **2007**, *6*, 662–680.
13. Negoda, A.; Liu, Y.; Hou, W. C.; Corredor, C.; Moghadam, B. Y.; Musolff, C.; Li, L.; Walker, W.; Westerhoff, P.; Mason, A. J.; Duxbury, P.; Posner, J. D.; Worden, R. M. *Int. J. Biomed. Nanosci. Nanotechnol.* **2013**, *3*, 52–83.
14. Yue, H.; Ying, L.; Hassler, B. L.; Worden, R. M.; Mason, A. J. *IEEE. Trans. Biomed. Circuits Syst.* **2013**, *7*, 43–51.
15. Liu, Y.; Zhang, Z.; Zhang, Q.; Baker, G. L.; Worden, R. M. *Biochim. Biophys. Acta* **2014**, *1*, 429–37.
16. Bekhit, A. E.-D. A.; Hopkins, D. L.; Fahri, F. T.; Ponnampalam, E. N. *Compr. Rev. Food Sci. Food Saf.* **2013**, *12*, 565–597.
17. Kaur, C.; Kapoor, H. C. *Int. J. Food Sci. Technol.* **2001**, *36*, 703–725.
18. Carrizzo, A.; Forte, M.; Damato, A.; Trimarco, V.; Salzano, F.; Bartolo, M.; Maciag, A.; Puca, A. A.; Vecchione, C. *Food Chem. Toxicol.* **2013**, *61*, 215–226.
19. Kresak, S.; Hianik, T.; Naumann, R. L. C. *Soft Matter* **2009**, *5*, 4021–4032.
20. Quinton, D.; Griveau, S.; Bedioui, F. *Electrochem. Commun.* **2010**, *12*, 1446–1449.

21. Peteu, S. F.; Szunerits, S. Peroxynitrite Electrochemical Quantification: Recent Advances and Challenges. In *Detection Challenges in Clinical Diagnostics*; Vadgama, P., Peteu, S., Eds.; Royal Society of Chemistry: Cambridge, U.K., 2013; pp 156–181.
22. Amatore, C.; Arbault, S.; Guille, M.; Lemaître, F. *Chem. Rev.* **2008**, *108*, 2585–2621.
23. Rubbo, H.; Trostchansky, A.; O'Donnell, V. B. *Arch. Biochem. Biophys.* **2009**, *484*, 167–172.
24. Richter, C. *Chem. Phys. Lipids* **1987**, *44*, 175–189.
25. Hogg, N.; Kalyanaraman, B. *Biochim. Biophys. Acta, Bioenerg.* **1999**, *1411*, 378–384.
26. De Lima, V. R.; Morfim, M. P.; Teixeira, A.; Creczynski-Pasa, T. B. *Chem. Phys. Lipids* **2004**, *132*, 197–208.
27. Trojanowicz, M.; Mulchandani, A. *Anal. Bioanal. Chem.* **2004**, *379*, 347–350.
28. Rossi, C.; Chopineau, J. *Eur. Biophys. J.* **2007**, *36*, 955–65.
29. Exner, M.; Herold, S. *Chem. Res. Toxicol.* **2000**, *13*, 287–293.
30. O'Grady, M. N.; Monahan, F. J.; Brunton, N. P. *J. Food Sci.* **2001**, *66*, 386–392.
31. Faustman, C.; Sun, Q.; Mancini, R.; Suman, S. P. *Meat Sci.* **2010**, *86*, 86–94.
32. Wikipedia, wikipedia.org/wiki/Lipid_bilayer; accessed February 2014.
33. Britannica online, britannica.com/ebchecked/topic/378707/myoglobin; accessed February 2014.
34. Moller, J. K. S.; Skibsted, L. H. *Quim. Nova* **2006**, *29*, 1270–1278.
35. Yusa, K.; Shikama, K. *Biochemistry* **1987**, *26*, 6684–6688.
36. Wan, L.; Twitchett, M. B.; Eltis, L. D.; Mauk, A. G.; Smith, M. *Proc. Natl. Acad. Sci. U.S.A.* **1998**, *95*, 12825–12831.
37. McKee, M. L. *J. Am. Chem. Soc.* **1995**, *117*, 1629–1637.
38. Mikkelsen, A.; Juncher, D.; Skibsted, L. H. *Meat Sci.* **1999**, *51*, 155–167.
39. Mikkelsen, A.; Skibsted, L. H. *Z. Lebensm.-Unters. Forsch.* **1992**, *9*, 134–150.
40. Hidalgo, F. J.; Alaiz, M.; Zamora, R., *Anal. Biochem.* **1998**, *262*, 129–136.
41. Nute, G. R.; Richardson, R. I.; Wood, J. D.; Hughes, S. I.; Wilkinson, R. G.; Cooper, S. L.; Sinclair, L. A. *Meat Sci.* **2007**, *77*, 547–555.
42. Zhang, W. G.; Xiao, S.; Lee, E. J.; Ahn, D. U. *J. Agric. Food Chem.* **2011**, *59*, 969–974.
43. Baron, C. P.; Andersen, H. J. *J. Agric. Food Chem.* **2002**, *50*, 3887–3897.
44. Zakrys, P. I.; Hogan, S. A.; O'Sullivan, M. G.; Allen, P.; Kerry, J. P. *Meat Sci.* **2008**, *79*, 648–655.
45. Zhang, WG; Xiao, S; Ahn, DU *Crit. Rev. Food Sci. Nutr.* **2013**, *53*, 1191–1203.
46. Lund, M. M.; Hviid, M. S.; Skibsted, L. H. *Meat Sci.* **2007**, *76*, 226–233.
47. Carlsen, C. U.; Moller, J. K. S.; Skibsted, L. H. *Coord. Chem. Rev.* **2005**, *249*, 485–498.
48. Min, B.; Ahn, D. U. *Food Sci. Biotechnol.* **2005**, *14*, 152–163.
49. Skibsted, L. H. In *Oxidation in Foods and Beverages and Antioxidant Applications*; Decker, E. A. Elias, R. J., McClements, D. J., Eds.; Series in

- Food Science, Technology and Nutrition No. 199; Woodhead Publishing: Oxford, 2010; Vol. 1, pp 3–35.
50. R. G. Brannan, Ph.D. Thesis, University of Massachusetts Amherst, Amherst, MA, 2002.
 51. Gorelik, S.; Ligumsky, M.; Kohen, R.; Kanner, J. *J. Agric. Food Chem.* **2008**, *56*, 5002–5007.
 52. Gorelik, S.; Ligumsky, M.; Kohen, R.; Kanner, J. *FASEB J.* **2008**, *22*, 41–46.
 53. Levantesi, G.; Marfisi, R.; Mozaffarian, D.; Franzosi, M. G.; Maggioni, A.; Nicolosi, G. L.; Schweiger, C.; Silletta, M.; Tavazzi, L.; Tognoni, G.; Marchioli, R. *Int. J. Cardiol.* **2013**, *163*, 282–287.
 54. Arranz, S.; Chiva-Blanch, G.; Lamuela-Raventos, R. M.; Estruch, R. In *Polyphenols in Human Health and Disease*; Watson, R. R., Preedy, V. R., Zibadi, S., Eds.; Academic Press: San Diego, 2014; pp 993–1006.
 55. Schneider, Y.; Vincent, F.; Durantou, B.; Badolo, L.; Gossé, F.; Bergmann, C.; Seiler, N.; Raul, F. *Cancer Lett.* **2000**, *158*, 85–91.
 56. Vang, O.; Ahmad, N.; Baile, C. A.; Baur, J. A.; Brown, K.; Csiszar, A.; Das, D. K.; Delmas, D.; Gottfried, C.; Lin, H.-Y.; Ma, Q.-Y.; Mukhopadhyay, P.; Nalini, N.; Pezzuto, J. M.; Richard, T.; Shukla, Y.; Surh, Y.-J.; Szekeres, T.; Szkudelski, T.; Walle, T.; Wu, J. M. *PLoS ONE* **2011**, *6*, e19881.
 57. Jeong, J.-H.; Jung, H.; Lee, S.-R.; Lee, H.-J.; Hwang, K. T.; Kim, T.-Y. *Food Chem.* **2010**, *123*, 338–344.
 58. Pandey, K. B.; Rizvi, S. I. *Appl. Physiol. Nutr. Metab.* **2009**, *34*, 1093–1097.
 59. Bijak, M.; Kolodziejczyk-Czepas, J.; Ponczek, M. B.; Saluk, J.; Nowak, P. *Intl. J. Biol. Macromol.* **2012**, *51*, 183–187.
 60. Habib, S.; Ahmad, S.; Dixit, K.; Moinuddin, din; Ali, A. *Hum. Immunol.* **2013**, *74*, 1239–1243.
 61. Olas, B.; Nowak, P. *J. Nutr. Biochem.* **2006**, *17* (2), 96–102.
 62. Brito, P. M.; Mariano, A.; Almeida, L. M.; Dinis, T. C. P. *Chem.-Biol. Interact.* **2006**, *164*, 157–166.
 63. Ippoushi, K.; Takeuchi, A.; Azuma, K. *Food Chem.* **2009**, *112*, 185–188.
 64. Vauzour, D.; Vafeiadou, K.; Corona, G.; Pollard, S. E.; Tzounis, X.; Spencer, J. P. E. *J. Agric. Food Chem.* **2007**, *55*, 2854–2860.
 65. Klotz, L.-O.; Sies, H. *Toxicol. Lett.* **2003**, *140-141*, 125–132.
 66. Valdez, L. B.; Alvarez, S.; Zaobornyj, T.; Boveris, A. *Biol. Res.* **2004**, *37*, 279–286.
 67. Ferk, F.; Chakraborty, A.; Jäger, W.; Kundi, M.; Bichler, J.; Mišík, M.; Wagner, K.-H.; Grasl-Kraupp, B.; Sagmeister, S.; Haidinger, G.; Hoelzl, C.; Nersesyan, A.; Dušinská, M.; Simić, T.; Knasmüller, S. *Mutat. Res.* **2011**, *715*, 61–71.
 68. Paquay, J. B. G.; Haenen, G. R. M. M.; Korthouwer, R. E. M.; Bast, A. *J. Agric. Food Chem.* **1997**, *45*, 3357–3358.
 69. Aldini, G.; Carini, M.; Piccoli, A.; Rossoni, G.; Facino, R. M. *Life Sci.* **2003**, *73*, 2883–2898.
 70. McCarty, M. F. *Med. Hypotheses* **2008**, *70*, 170–181..
 71. Chen, W.; Li, Y.; Li, J.; Han, Q.; Ye, L.; Li, A. *Food Chem. Toxicol.* **2011**, *49*, 2439–2444.

72. Pereira, R. B.; Sousa, C.; Costa, A.; Andrade, P. B.; Valentão, P. *Molecules* **2013**, *18*, 8858–8872.
73. Iacopini, P.; Baldi, M.; Storchi, P.; Sebastiani, L. *J. Food Compos. Anal.* **2008**, *21*, 589–598.
74. Kang, K. S.; Tanaka, T.; Cho, E. J.; Yokozawa, T. *J. Med. Food* **2009**, *12*, 124–130.
75. Choi, C.-W.; Jung, H. A.; Kang, S. S.; Choi, J. S. *Arch. Pharm. Res.* **2007**, *30*, 1–7.
76. Alvarez, S.; Zaobornyj, T.; Actis-Goretta, L.; Fraga, C. G.; Boveris, A. *Ann. N. Y. Acad. Sci.* **2002**, *957* (1), 271–273.
77. Kumar, A.; Kaundal, R. K.; Iyer, S.; Sharma, S. S. *Life Sci.* **2007**, *80*, 1236–1244.
78. Isobe, C.; Abe, T.; Terayama, Y. *Brain Res.* **2009**, *1305*, 132–136.
79. Liu, B.; Tewari, A. K.; Zhang, L.; Green-Church, K. B.; Zweier, J. L.; Chen, Y.-R.; He, G. *Biochim. Biophys. Acta* **2009**, *1794*, 476–485.
80. Turko, I. V.; Li, L.; Aulak, K. S.; Stuehr, D. J.; Chang, J.-Y.; Murad, F. J. *Biol. Chem.* **2003**, *278*, 33972–33977.
81. Zhang, R.; Brennan, M. L.; Fu, X.; Aviles, R. J.; Pearce, G. L.; Penn, M. S.; Topol, E. J.; Sprecher, D. L.; Hazen, S. L. *JAMA, J. Am. Med. Assoc.* **2001**, *286*, 2136–2142.
82. Alvarez, B.; Radi, R. *Amino Acids* **2003**, *25*, 295–311.
83. Abello, N.; Kerstjens, H. A. M.; Postma, D. S.; Bischoff, R. *J. Proteome Res.* **2009**, *8*, 3222–3238.
84. Pfeiffer, S.; Schmidt, K.; Mayer, B. *J. Biol. Chem.* **2000**, *275*, 6346–6352.
85. Yamakura, F.; Ikeda, K.; Matsumoto, T.; Taka, H.; Kaga, N. *Int. Congr. Ser.* **2007**, *1304*, 22–32.
86. Vaz, S. M.; Prado, F. M.; Di Mascio, P.; Augusto, O. *Arch. Biochem. Biophys.* **2009**, *484*, 127–133.
87. Niwa, T.; Doi, U.; Kato, Y.; Osawa, T. *FEBS Lett.* **1999**, *459*, 43–46.
88. Bijak, M.; Nowak, P.; Borowiecka, M.; Ponczek, M. B.; Żbikowska, H. M.; Wachowicz, B. *Thromb. Res.* **2012**, *130*, e123–e128.
89. Nowak, P.; Zbikowska, H. M.; Ponczek, M.; Kolodziejczyk, J.; Wachowicz, B. *Thromb. Res.* **2007**, *121*, 163–174.
90. Selmeçi, L.; Székely, M.; Soós, P.; Seres, L.; Klinga, N.; Geiger, A.; Acsády, G. *Free Radical Res.* **2006**, *40*, 952–958.
91. Richards, D. A.; Silva, M. A.; Devall, A. *J. Anal. Biochem.* **2006**, *351*, 77–83.
92. Kawasaki, H.; Ikeda, K.; Shigenaga, A.; Baba, T.; Takamori, K.; Ogawa, H.; Yamakura, F. *Free Radicals Biol. Med.* **2011**, *50*, 419–427.
93. Pennathur, S.; Jackson-Lewis, V.; Przedborski, S.; Heinecke, J. W. *J. Biol. Chem.* **1999**, *274*, 34621–34628.
94. Shahidi, F.; Zhong, Y. *Bailey's Industrial Oil and Fat Products*, 6th ed.; Shahidi, F., Ed.; John Wiley & Sons Inc.: Hoboken, NJ, 2005; pp 357–385.
95. Zanardi, C.; Terzi, F.; Seeber, R. *Anal. Bioanal. Chem.* **2013**, *405*, 509–531.
96. Duncan, M. W. *Amino Acids* **2003**, *25*, 351–361.
97. Szabó, C. *Toxicol. Lett.* **2003**, *140-141*, 105–112.

98. Ohshima, H.; Yoshie, Y.; Auriol, S.; Gilibert, I. *Free Radicals Biol. Med.* **1998**, *25*, 1057–1065.
99. Moon, H. K.; Yang, E. S.; Park, J. W. *Arch. Pharm. Res.* **2006**, *29*, 213–217.
100. Chen, W.; Zhuang, J.; Li, Y.; Shen, Y.; Zheng, X. *Food Chem.* **2013**, *141*, 927–933.
101. Peteu, S. F.; Banihani, S.; Gunsekera, M. M.; Peiris, P.; Siciua, O. A.; Bayachou, M. *Oxidative Stress: Diagnostics, Prevention, and Therapy*; ACS Symposium Series 1083; American Chemical Society: Washington, DC, 2011; pp 311–339.
102. Peteu S.F., S. F.; Boukherroub, R.; Szunerits, S. *Biosens. Bioelectron.* **2014**, *58*, 359–373.
103. Pryor, W. A.; Cueto, R.; Jin, X.; Koppenol, W. H.; Ngu-Schwemlein, M.; Squadrito, G. L.; Uppu, P. L.; Uppu, R. M. *Free Radicals Biol. Med.* **1995**, *18*, 75–83.
104. Salgo, M. G.; Bermúdez, E.; Squadrito, G. L.; Pryor, W. A. *Arch. Biochem. Biophys.* **1995**, *322*, 500–505.
105. Uppu, R. M.; Squadrito, G. L.; Cueto, R.; Pryor, W. A. In *Nitric Oxide Part B: Physiological and Pathological Processes*; Packer, L., Ed.; Methods in Enzymology; Academic Press: San Diego, 1996; Vol. 269, pp 311–321.
106. Hughes, M. N.; Nicklin, H. G. *J. Chem. Soc. A* **1971**, 164–168.
107. Leis, J. R.; Pea, M. E.; Ríos, A. *Chem. Commun.* **1993**, 1298–1299.
108. Uppu, R. M.; Pryor, W. A. *Anal. Biochem.* **1996**, *236*, 242–249.
109. Saha, A.; Goldstein, S.; Cabelli, D.; Czapski, G. *Free Radicals Biol. Med.* **1998**, *24*, 653–659.
110. Plumb, R. C.; Edwards, J. O. *J. Phys. Chem.* **1992**, *96*, 3245–3247.
111. Hughes, M. N.; Nicklin, H. G. *J. Chem. Soc. A* **1968**, 450–452.
112. Ieda, N.; Nakagawa, H.; Horinouchi, T.; Peng, T.; Yang, D.; Tsumoto, H.; Suzuki, T.; Fukuhara, K.; Miyata, N. *Chem. Commun.* **2011**, *47*, 6449–6451.
113. Griveau, S.; Dumézy, C.; Goldner, P.; Bedioui, F. *Electrochem. Commun.* **2007**, *9*, 2551–2556.
114. De la Fuente, E.; Villagra, G.; Bollo, S. *Electroanalysis* **2007**, *19*, 1518–1523.
115. Gramsbergen, J. B.; Larsen, T. R.; Rossen, S. P.; Roepstorff, P. *J. Neurochem.* **2007**, *101*, 21–682007.
116. Konishi, K.; Watanabe, N.; Arai, T. *Nitric Oxide* **2009**, *20*, 270–278.
117. Trackey, J. L.; Uliasz, T. F.; Hewett, S. J. *J. Neurochem.* **2001**, *79*, 445–455.
118. Feelisch, M.; Ostrowski, J.; Noack, E. *J. Cardiovasc. Pharmacol.* **1989**, *14*.
119. Lomonosova, E. E.; Kirsch, M.; Rauen, U.; De Groot, H. *Free Radicals Biol. Med.* **1998**, *24*, 522–528.
120. Martin-Romero, F. J.; Gutiérrez-Martin, Y.; Henao, F.; Gutiérrez-Merino, C. *J. Fluoresc.* **2004**, *14*, 17–23.
121. Borgmann, S. *Anal. Bioanal. Chem* **2009**, *394*, 95–105.
122. Amatore, C.; Arbault, S.; Bruce, D.; De Oliveira, P.; Erard, M.; Vuillaume, M. *Faraday Discuss.* **2000**, 319–333, 335–351d.
123. Amatore, C.; Arbault, S.; Bruce, D.; De Oliveira, P.; Erard, L. M.; Vuillaume, M. *Chem. Eur. J.* **2001**, *7*, 4171–4179.
124. Amatore, C.; Arbault, S.; Bouton, C.; Coffi, K.; Drapier, J.-C.; Ghandour, H.; Tong, Y. *ChemBioChem* **2006**, *7*, 653–661.

125. Amatore, C.; Arbault, S.; Chen, Y.; Crozatier, C.; Tapsoba, I. *Lab Chip* **2007**, *7*, 233–238.
126. Amatore, C.; Arbault, S.; Bouton, C.; Drapier, J.-C.; Ghandour, H.; Koh, A. C. W. *ChemBioChem* **2008**, *9*, 1472–1480.
127. Amatore, C.; Arbault, S.; Koh, A. C. W. *Anal. Chem.* **2010**, *82*, 1411–1419.
128. Filipović, M. R.; Koh, A. C. W.; Arbault, S.; Niketić, V.; Debus, A.; Schleicher, U.; Bogdan, C.; Guille, M.; Lemaître, F.; Amatore, C.; Ivanović-Burmazović, I. *Angew. Chem., Intl. Ed.* **2010**, *49*, 4228–4232.
129. Wang, Y.; Noël, J.-M.; Velmurugan, J.; Nogala, W.; Mirkin, M. V.; Lu, C.; Collignon, M. G.; Lemaître, F.; Amatore, C. *Proc. Natl. Acad. U.S.A.* **2012**, *109*, 11534–11539.
130. Cortés, J. S.; Granados, S. G.; Ordaz, A. A.; Jiménez, J. A. L.; Griveau, S.; Bedioui, F. *Electroanalysis* **2007**, *19*, 61–64.
131. Bedioui, F.; Quinton, D.; Griveau, S.; Nyokong, T. *Phys. Chem. Chem. Phys.* **2010**, *12*, 9976–9988.
132. Quinton, D.; Girard, A.; Thi Kim, L. T.; Raimbault, V.; Griscom, L.; Razan, F.; Griveau, S.; Bedioui, F. *Lab Chip* **2011**, *11*, 1342–1350.
133. Koh, W. C. A.; Son, J. I.; Choe, E. S.; Shim, Y.-B. *Anal. Chem.* **2010**, *82*, 10075–10082.
134. Kubant, R.; Malinski, C.; Burewicz, A.; Malinski, T. *Electroanalysis* **2006**, *18*, 410–416.
135. Mason, R. P.; Jacob, R. F.; Corbalan, J. J.; Szczesny, D.; Matysiak, K.; Malinski, T. *BMC Pharmacol. Toxicol.* **2013**, *14*, 48.
136. Xue, J.; Ying, X.; Chen, J.; Xian, Y.; Jin, L.; Jin J. *Anal. Chem.* **2000**, *72*, 5313–5321.
137. Wang, Y.; Chen, Z. *Talanta* **2010**, *82*, 534–539.
138. Peteu, S. F.; Bose, T.; Bayachou, M. *Anal. Chim. Acta* **2013**, *780*, 81–88.
139. Kaminska, I.; Das, M. R.; Coffinier, Y.; Niedziolka-Jonsson, J.; Sobczak, J.; Woisel, P.; Lyskawa, J.; Opallo, M.; Boukherroub, R.; Szunerits, S. *ACS Appl. Mater. Interfaces* **2012**, *4*, 1016–1020.
140. Kaminska, I.; Das, M. R.; Coffinier, Y.; Niedziolka-Jonsson, J.; Woisel, P.; Opallo, M.; Szunerits, S.; Boukherroub, R. *Chem. Commun.* **2012**, *48*, 1221–1223.
141. Oprea, R.; Peteu, S. F.; Subramanian, P.; Qi, W.; Pichonat, E.; Happy, H.; Bayachou, M.; Boukherroub, R.; Szunerits, S. *Analyst* **2013**, *138*, 4345–4352.
142. Vernekar, A. A.; Muges, G. *Chem.–Eur. J.* **2012**, *18*, 15122–15132.
143. Xue, T.; Jiang, S.; Qu, Y.; Su, Q.; Cheng, R.; Dubin, S.; Chiu, C.-Y.; Kaner, R.; Huang, Y.; Duan, X. *Angew. Chem., Int. Ed.* **2012**, *51*, 3822–3825.
144. Guo, Y.; Deng, L.; Li, J.; Guo, S.; Wang, E.; Dong, S. *ACS Nano* **2011**, *5*, 1282–1290.
145. Peteu S.F., S. F.; Peiris, P.; Gebremichael, E.; Bayachou, M. *Biosens. Bioelectron.* **2010**, *25*, 1914–1921.
146. D., ; Peteu, S. F.; Worden, R. M. *Biotechnol. Tech.* **1996**, *10*, 673–678.
147. C., ; Huang, Y.; Hassler, B. L.; Worden, R. M.; Mason, A. J. *IEEE Trans. Biomed. Circuits Syst.* **2009**, *3*, 160–168.

Chapter 17

Measurement of Resistant Starches in Rat Cecal Contents using Fourier Transform Infrared Photoacoustic Spectroscopy

**Timothy J. Anderson,^{1,2,5} Yongfeng Ai,³ Roger W. Jones,^{*,2,4}
Robert S. Houk,^{1,2} Jay-lin Jane,³ Yinsheng Zhao,³ Diane F. Birt,³
and John F. McClelland^{2,4}**

¹Department of Chemistry,

²Ames Laboratory–USDOE,

³Department of Food Science and Human Nutrition, and

⁴Department of Biochemistry, Biophysics, and Molecular Biology,
Iowa State University, Ames, IA 50011

⁵Current address: POET, LLC, 4615 N. Lewis Avenue,
Sioux Falls, South Dakota 57104.

*E-mail: rwjones@iastate.edu.

Including resistant starch in the diet has potential health benefits, but studies of the digestion of resistant starch are hampered by the complexity of having to isolate the starch from digesta or fecal material before measuring it. We examined whether Fourier transform infrared photoacoustic spectroscopy (FTIR-PAS) would provide a method of measuring resistant starch without separating it from the biological matrix. FTIR-PAS was used to quantitatively measure the amount of resistant starch present in the contents of rat ceca. Rats were fed four diets that were identical except for the starch they contained. The four different starches were ordinary cornstarch (non-resistant control), HA7 high-amylose starch, HA7 modified with octenyl succinate anhydride, and HA7 modified with stearic acid. A partial least-squares model was used to correlate the spectra of the cecal contents from all of these diets with the amount of resistant starch present as determined by enzymatic assay. The cross validation for the

model had an R^2 of 0.997, demonstrating an excellent fit of the model to the resistant starch content. The amount of resistant starch present varied from 0.3% to 50.1% (by weight, dry basis). In addition, principal component analysis of the spectra showed that the cecal contents could easily be differentiated according to diet.

Introduction

Starch is the major energy-storage component of most plants used as food by humans and is an important energy source in fodder for domesticated animals. Starch content in food and feed and its fate during digestion are therefore intensively studied. Starch is divided into three categories depending on the speed and location of its digestion (1)—rapidly digestible starch (RDS), slowly digestible starch (SDS), and resistant starch (RS). RS is that fraction of starch that is not digested in the small intestine and reaches the colon, where it may be fermented by microorganisms (2) or pass through and be excreted. RS has received attention for its potential to prevent colon cancer and inflammatory bowel disease and to reduce fluctuations of postprandial blood-glucose concentration and prevent the development of diabetes (3, 4).

The resistance of starch to digestion is dependent on several factors, including the physical accessibility of the starch, the type of crystalline structure, and any chemical modifications to it. RS is divided into five types. Englyst et al. (1) identified the first three, naturally occurring types in 1992 and described methods for their measurement, and two chemically or physically modified types have been added since. Type 1 (RS1) is physically inaccessible starch. In grains and seeds, starch granules are surrounded by a protein matrix and cell walls. These structures hinder digestibility. Type 2 (RS2) is B-type crystalline starch. The B-type crystalline structure resists enzyme hydrolysis. It occurs in uncooked starches, such as raw potato and green banana starch, but it gelatinizes and becomes highly digestible when cooked. Another RS2 is high-amylose maize starch, produced from an amylose-extender gene mutation (*ae* mutant), which possesses substantially longer branch-chains of amylopectin and a larger proportion of amylose (5). It has a high gelatinization temperature and resists disruption of the crystalline structure during cooking. Type 3 (RS3) is retrograded starch. Amylose molecules are linear chains, and they tend to form double helices at lower temperatures, such as room temperature. The double helices cannot be bound by amylases, so they are not hydrolyzed. Type 4 (RS4) is chemically modified starch, either with additives or by cross-linking. Highly cross-linked starch does not swell during cooking and therefore cannot be hydrolyzed by amylases. The appropriate additive, such as octenyl succinic anhydride (6), alters the structure of the starch and hinders enzyme hydrolysis. Lastly, Type 5 (RS5) is starch modified with lipids. Amylose and long branches of amylopectin form single-helix complexes with fatty acids (7) and consequently cannot be hydrolyzed by amylases.

Analysis for RS has been accomplished through modification of methods developed for the analysis of dietary fiber (DF). Both RS and DF are broadly defined as polysaccharides that escape digestion in the small intestine and pass into the colon. DF analysis methods, however, frequently do not accommodate all types of RS, so RS determinations using DF-analysis methods often differ, depending on the RS type present. The method of Englyst et al. (8) for DF determination has been widely used, and AOAC has developed several official methods similar to that of Englyst et al. (9–12). All of these use enzyme digestion to remove starch from DF, but some forms of RS can also resist the digestion. AOAC Method 991.43 (9) uses a thermostable α -amylase at 95 °C for the digestion, so only RS stable at that temperature survives. AOAC Methods 2009.01 and 2011.25 (11, 12) determine DF including RS, but the RS is lumped together with DF and not determined separately; the methods use α -amylase and amyloglucosidase for digestion, but only at 37 °C, which removes ordinary starch but not RS. These methods can therefore determine RS if there is no DF present. Englyst et al. (1) have also developed a method to indirectly measure RS in food by determining total starch, RDS, and SDS, and then finding RS by the difference ($RS = \text{total starch} - RDS - SDS$). The method imitates *in vivo* digestion by using a mincer and shaking bath to physically breakdown the sample and then using amyloglucosidase and pancreatin at 37 °C to digest it. AOAC Method 2002.02 (13) for determining RS uses a similar digestion to isolate RS, but then the solid RS is dissolved using 2M KOH and digested with amyloglucosidase, and the resulting glucose is measured to determine the RS content. AACC International has also issued a similar method for measuring RS (14).

Such wet chemical methods are rather cumbersome and expensive, so spectroscopic methods have long been of interest as an efficient alternative. Near infrared reflectance spectroscopy (NIRS) has become a standard method for analyzing food, fodder, and forage (15–18). NIRS first gained acceptance for nondestructive analysis of grain in the 1970s (19, 20), and soon thereafter it was applied to the analysis of animal feed (21). That study successfully determined numerous feed properties using NIRS, including acid detergent fiber and neutral detergent fiber, by correlating the spectra with the properties via multiple linear regression involving the reflectance at selected wavelengths. Of course, these early studies did not involve RS, which was not recognized until the 1990s (1), but even the later handbooks and reviews cited above say little about RS.

Most analyses for RS in food and fodder have used the AOAC, AACC, or Englyst methods, or variations of them (22). Hódsági et al. (23) recently demonstrated qualitatively that NIRS could be used to determine the amount of RS present in mixtures of starches, but it does not appear that NIRS has been applied to measuring RS quantitatively in food or fodder. Mid-infrared spectroscopy has been used to measure the amount of short-range structure in starch (24), which would indicate the level of RS2 or RS3.

Of course, knowing the RS content of food or feed is only half of the requirement. The starch content of digesta within humans and animals at a specific point or the starch content of feces must be known to determine the fate of RS and the role it plays in nutrition.

Analysis of starch digestibility in humans may be the ideal approach for measuring RS, but such studies are relatively few (25–27) and are costly to implement. In such studies, human ileostomates are typically the test subjects, so that there is ready access to the digesta at the terminus of the small intestine. Mid-infrared spectroscopy has been used to measure the degree of short-range order in starch in digesta from human ileostomates (25).

Starch analysis of digesta from animals via NIRS has been done on several occasions. Starch in the jejunal digesta of cannulated pigs was determined with NIRS (28). The digesta was freeze dried, ground, and then oven dried before analysis. NIRS has been used to determine not only starch but numerous other chemical properties in freeze-dried chicken excreta as part of studies to increase the efficiency of feed use by chickens (29, 30). None of these studies, however, analyzed for RS.

Fecal analysis is much more common than digesta analysis, and NIRS has been used for this purpose as well, but analysis for starch is not common because so little starch is present in the feces of healthy subjects not on diets high in RS. NIRS was used, however, to measure fiber and other constituents in fecal matter from pen-fed cattle (31).

Medical application of NIRS fecal analysis has been explored. Fecal carbohydrate (i.e., starch and sugar combined) levels, indicative of several gastrointestinal diseases, can be determined by NIRS (32). Another study examined sugar and starch content separately in children's stools by NIRS and was able to quantify sugar but not starch (33). In both of these studies, the feces were homogenized but not otherwise processed. They were not dried.

NIRS has usually been the form of optical spectroscopy applied to food, feed, digesta, and feces because the spectroscopic absorptions in the near-infrared region are relatively weak. This weakness allows the undiluted samples to be analyzed by NIRS without excessive optical saturation. Unfortunately, the absorption features in the near infrared are broad and overlapping, which can make determination of details, such as the differentiation between normal starch and RS, difficult. Absorption features in the mid-infrared are generally much sharper, so more detailed analyses are possible, but the features are also much stronger, so mid-infrared spectroscopy is much more susceptible to saturation. We have chosen to use photoacoustic spectroscopy (PAS) for the present study because of this. PAS can analyze undiluted and largely unprocessed samples in the mid-infrared region without succumbing to saturation.

PAS is a technique based on the acoustic response produced when a gaseous or condensed-phase sample absorbs radiation. When modulated or pulsed radiation is absorbed, the deposited energy produces a thermal expansion that results in an acoustic signal. This photoacoustic effect was discovered by Alexander Graham Bell (34). He not only demonstrated wireless communication via his "photophone," which was based on the photoacoustic effect, but also performed PAS using his "spectrophone" (34, 35). Despite this, a century would pass before PAS gained popularity. When the Fourier transform infrared (FTIR) spectrometer became widespread in the 1980s, its high throughput and multiplex advantage made infrared PAS practical. In addition, its innate modulation of the infrared beam made FTIR and PAS a natural pairing.

PAS has the advantage that it can be applied to nearly every type of solid or semisolid material (36). Usually the sample can be analyzed with little or no sample preparation, so PAS is nondestructive. In addition, it is applicable to dark, opaque, and highly light scattering materials. Conventional spectroscopy measures the radiation that either passes through or is reflected off the sample. This places limits on the surface morphology, the transparency of the sample, or both, so substantial sample preparation is often needed. PAS, on the other hand, measures the absorption directly by detecting the heat deposited when radiation is absorbed near the sample surface.

The concept behind PAS is illustrated in Figure 1. The sample is placed in a sealed chamber with a microphone and a window that lets an intensity-modulated beam enter and strike the sample. The sample is heated if it absorbs the radiation, and the heat diffuses to the surface of the sample, where it transfers to the surrounding gas. Because the incident radiation is modulated, the temperature of the gas is also modulated, and the pressure inside the chamber oscillates, which the microphone detects as sound. The detailed theory behind the generation of the photoacoustic signal has been developed (36), but roughly speaking, only the energy deposited within a thermal diffusion length, μ , of the sample surface is close enough to the surface to diffuse out of the sample in time to contribute to the photoacoustic signal. The thermal diffusion length depends on the modulation frequency of the incoming radiation, f :

$$L = \frac{1}{a} = \left(\frac{D}{\pi f} \right)^{1/2}$$

where a is the thermal diffusion coefficient of the sample, D is the thermal diffusivity of the sample, and $D = k/\rho C$, where k is the thermal conductivity of the sample, C is the heat capacity of the sample, and ρ is the density of the sample. Thanks to its dependence on f , μ is user adjustable. If α is the absorption coefficient of the sample, and f is high enough (i.e., the FTIR spectrometer scanning speed is high enough) that $\mu \ll 1/\alpha$, as shown in Figure 1, then the amount of radiation absorbed within a distance μ of the surface is proportional to α , and the photoacoustic spectrum is equivalent to a conventionally acquired spectrum. This is true even if the physical thickness of the sample makes it opaque. In the study reported here, the spectra were recorded at a 2.5 kHz spectrometer scanning speed. This results in the modulation frequency of the spectrometer infrared beam varying linearly with wavenumber from 63 Hz at 400 cm^{-1} to 633 Hz at 4000 cm^{-1} . Dry fecal matter has a thermal diffusivity of very roughly 0.0011 cm^2/s (37), so the above equation yields a thermal diffusion length of 7 μm at 4000 cm^{-1} , rising to 23 μm at 400 cm^{-1} . Although not used in the present study, the dependence of μ on f allows sample depth profiling (38, 39). There are numerous reviews of PAS in the literature that will provide the reader with further detail (38–42).

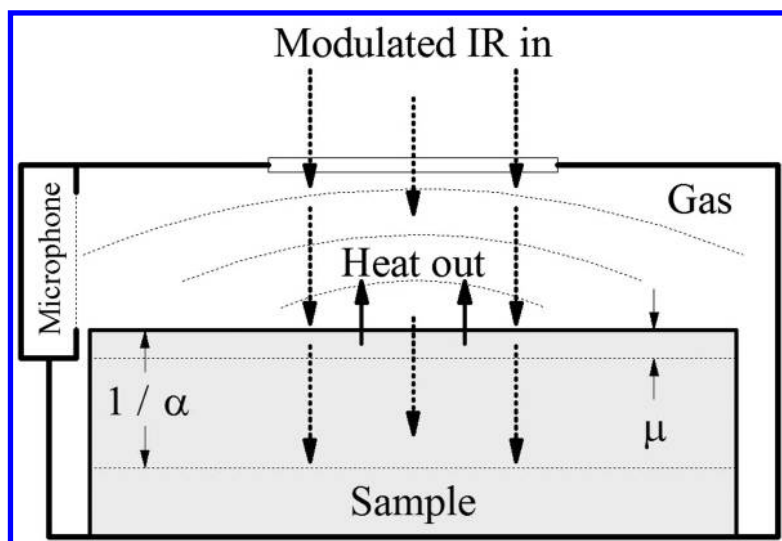


Figure 1. Schematic of the photoacoustic process. Intensity-modulated light incident on a sample within a sealed cell is absorbed principally within a distance $1/\alpha$ of the sample surface, where α is the absorption coefficient. The absorbed energy degrades to heat and diffuses to the sample surface, where it transfers to and warms the gas in the cell. Because the light was intensity modulated, the temperature of the gas is also modulated, and so the pressure in the sealed cell is modulated, which the microphone detects as sound. Only the light absorbed within approximately a thermal diffusion length, μ , of the sample surface can diffuse to the surface in time to contribute to the signal.

The biological application of photoacoustics with the greatest research activity is microscopic imaging, where photoacoustics is a complement to MRI (43–45). Applications of mid-infrared FTIR-PAS to food and feed, however, have been wide ranging. It has been used to analyze intact (i.e., not ground) beef and pork (46). It has been used to analyze both cheddar cheese and its wrapping (47). Depth profiling them both showed the near-surface loss of moisture in the cheese and migration of fat and protein from the cheese into the packaging. FTIR-PAS analysis of roasted, ground coffee was able to differentiate organic and conventionally grown varieties (48). The amount of fat in chocolate was quantitatively measured using FTIR-PAS (49). Monitoring the oxidation of fat with FTIR-PAS has been used to assess degradation during storage of potato chips (50) and of lard, peanut butter, and mayonnaise (51). It has also been used to study storage degradation of intact wheat kernels (52). Depth profiling showed minor structural and morphological changes in the wheat over time. PAS can analyze very small amounts of material. One study used FTIR-PAS to examine ground material from individual peas (53). The amount of material taken was small enough that the peas were still viable, yet the researchers quantitatively determined both total starch and amylose, as well as total protein, total lipids, and some individual fatty acids.

By virtue of its sample-surface sensitivity, FTIR-PAS has proven to be very good for detecting microorganisms on food and fodder. It has been used to detect infections on the skin of apples, and applying canonical variate analysis to the spectra successfully differentiated between pathogenic and non-pathogenic strains of *E. coli* (54). FTIR-PAS has been used to detect and categorize microorganism contamination on intact corn kernels (55, 56).

The ability of FTIR-PAS to detect and measure so many different factors in such a wide variety of biological materials makes it a natural choice for analysis of digesta and fecal material in dietary and disease studies, but our recent work reported here and elsewhere (57, 58) appears to be the first such uses. The results reported here have also been discussed in our previous publication (57). Our principal goal in this work is to develop FTIR-PAS as a practical alternative to the enzymatic assay normally used to measure starch content and demonstrate its use for multiple forms of RS.

Materials and Methods

Rat Diet and Treatment

Fischer 344 rats were housed as described in Zhao et al. (59). The trial started with a total of 90 rats (two rats died before sacrifice), which were randomly assigned to four diet regimens described below. Each diet involved a different starch—cornstarch (control diet), HA7, OS-HA7, and RS5-HA7. The animals were on the feeding regimens for eight weeks prior to sacrifice. For purposes important to companion studies (58, 60, 61) that used this same diet trial, each diet group was further split up into two or four treatment subgroups. The control and RS5-HA7 diet groups each contained 29 rats that were split up among four subgroups according to whether or not the rats were given injections of the carcinogen azoxymethane (AOM) and whether or not they were treated with an antibiotic. The rats were given two injections of either saline or AOM (Midwest Research Institute, Kansas City, MO) administered as described in Zhao et al. (59), and some were fed an antibiotic treatment mixture of vancomycin and imipenem. The treatments resulted in four subgroups within the control and RS5-HA7 diets consisting of rats given both AOM and antibiotic, given AOM but not antibiotic, given saline and antibiotic, and given only saline. The HA7 and OS-HA7 diet groups each contained 15 rats and were divided into only two subgroups. They were given either AOM or saline. None were given antibiotic. The AOM and antibiotic treatments were given immediately before the rats were placed on the four different eight-week diet regimens. For purposes of the tests reported here, data for AOM and antibiotic treated rats are included with data for the other rats for a specific diet if these treatments were administered to animals on that diet, unless otherwise noted. The animal studies were approved by and performed in compliance with the guidelines of The Institutional Animal Care and Use Committee of Iowa State University.

Four starch varieties were utilized for the feeding study: cornstarch for the control diet (Cargill Gel 03420; Cargill Inc., Minneapolis, MN); high-amylose starch HA7 (AmyloGel 03003; Cargill Inc.), which is a Type 2 resistant starch;

HA7 bound to octenyl succinate (OS-HA7, produced in the Department of Food Science and Human Nutrition, Iowa State University), a Type 4 resistant starch; and HA7 processed with stearic acid (RS5-HA7, produced by the Department of Food Science and Human Nutrition), a Type 5 resistant starch (6, 62). The starches were cooked before inclusion in the diets according to Zhao et al. (59). The diets were formulated on the basis of the standard diet recommended by the American Society for Nutritional Sciences for mature rats (AIN-93M) (63). Starch diets were prepared every other day and served fresh to the rats.

Rat Cecal Samples

The cecal contents were collected from the sacrificed rats and placed in Corning centrifuge tubes (Tewksbury, MA) on dry ice, which were then transferred to -80 °C storage. The companion studies made use of the collected material prior to the present experiment, so many of the samples were no longer available at the time of this study. Adequate material from 28 samples, seven from each of the four feeding groups, was obtained. The wet cecal samples were placed in aluminum weighing pans and dried at 105 °C for three hours. The dried cecal material formed dry wafers, which were ground using mortar and pestle. The ground cecal material was then placed in 1.7-mL microcentrifuge tubes (Marsh Bio Products, Rochester, NY) and stored sealed at room temperature prior to analysis.

Reference Assay for Starch Content

The starch content of the cecal material was measured using the Total Starch Assay Kit (Megazyme International Ireland Ltd., Co. Wicklow, Ireland) following AACC Method 76-13 (64).

FTIR-PAS

The FTIR-PAS analysis was performed using an MTEC Photoacoustics PAC300 detector installed in a Digilab FTS 7000 FTIR spectrometer. The detector has a 1-cm interior-diameter chamber for the sample with a window at the top for the infrared beam to enter and illuminate the sample. The dry, ground cecal material was placed in a disposable aluminum cup, which was fully illuminated by the infrared beam. Immediately before analysis the detector was purged with helium to remove atmospheric water vapor and carbon dioxide, which have strong mid-infrared absorptions. Helium also increases the photoacoustic signal by a factor of two to three compared to air because of its superior thermal properties. Magnesium perchlorate, a desiccant, was placed beneath the sample to remove any moisture that might evolve from the sample during analysis. Spectra were taken at 8 cm⁻¹ resolution and a 2.5 kHz scan speed, with the co-addition of 256 scans. The carbon-black-covered polymer-film sample provided with the detector was used as the (100% absorption) reference.

PLS and PCA

The spectra were correlated with starch levels determined by the enzymatic assay via partial least-squares analysis (PLS) (65–67) using commercial software (Thermo Galactic GRAMS/AI PLSplus IQ, Version 5.1). PLS utilizes a training set of spectra from samples whose relevant properties are known and span the range of interest. In the present case, the relevant property is the amount of starch, as determined by the enzymatic assay. PLS modeling breaks the training-set spectra down into a weighted sum of basis-vector spectra, called factors. The factors with the smallest weightings consist mostly of noise and are dropped from the model. PLS then performs a multiple linear regression correlating the factor weightings with the known values of the property being predicted. Once the PLS model is built, the correlated property can be determined for unknown samples directly from the model, as long as the properties of the unknowns fall within the range of those covered by the original training set.

Because the starch level was determined for only 28 samples (seven per diet), the sample set was not split into separate training and validation sets. Instead, all samples were used in the training set, and a single-elimination cross validation was used to assess model quality. In such a cross validation, one member of the training set is removed, and a model is built from the remaining members. The removed spectrum is then analyzed as an unknown. The removed spectrum is returned to the training set, a different spectrum is removed, and the process is repeated. This is done until all training set members have been removed and analyzed as unknowns. A cross-validation plot comparing known starch content and the model-predicted values is included in Results. The standard error of cross validation (SECV) is a measure of model quality. It is the root-mean-square difference between these model-predicted values and the known starch contents.

The model with the lowest prediction residual error sum of squares (PRESS) value was selected as the most accurate model and the appropriate number of factors to include in the model. PRESS is given by

$$\text{PRESS} = \sum_{i=1}^N (k_i - p_i)^2$$

where there are N samples in the training set, and k_i and p_i are the known and predicted values for the i^{th} sample. A variety of models were tested to find the optimum one. In the most-accurate model, the 4000–397 cm^{-1} range of the spectra was used, the spectra were preprocessed using multiplicative scatter correction (MSC) (68), and they were converted to first derivatives (19-point Savitsky-Golay). The model had ten factors.

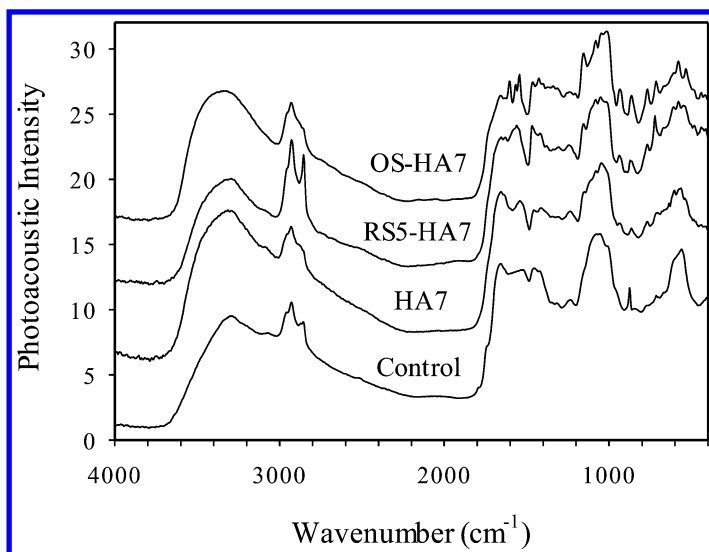


Figure 2. FTIR-PAS spectra of rat cecal contents. The spectra are from single, representative rats from each of the diet groups. (Reproduced from reference 57. Copyright 2013 American Chemical Society.)

Classification of the spectra according to diet was done using principal component analysis (PCA) (69, 70). The same 4000-397 cm^{-1} range and the same first derivative and MSC preprocessing were applied to the data as in the PLS modeling. This was sufficient to cleanly separate the samples into clusters according to diet.

Results

Enzymatic Assay for Starch Content

The starch content of the cecal material was highly dependent on the starch included in the diet. Starch content was lowest for the control (cornstarch) diet, where it varied from 0.3 to 1.1 wt. % (dry basis). It ranged from 12.7 to 21.3 wt. % for the HA7 diet, and from 13.3 to 30.5 wt. % for the RS5-HA7 diet. The cecal contents from the rats fed the OS-HA7 diet had the highest starch concentration, ranging from 47.1 to 50.1 wt. %. These results suggest that the OS-HA7 has the highest resistance to *in vivo* digestion, and normal cornstarch has the least. There was no significant differences among food disappearance (used to estimate intake but includes losses) for the rats fed the different diets (data not shown).

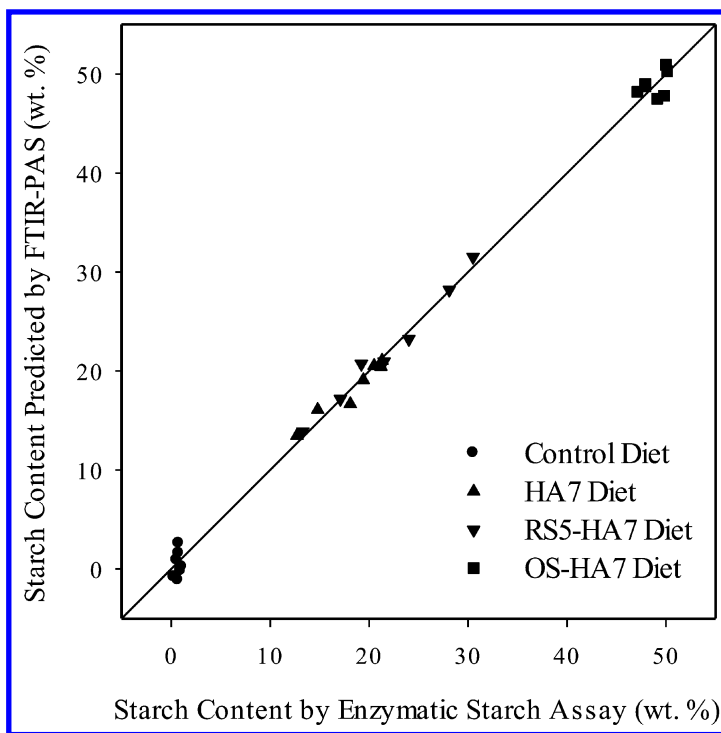


Figure 3. Cross-validation plot for starch content from PLS model correlating photoacoustic spectra with enzymatic starch assay. (Reproduced from reference 57. Copyright 2013 American Chemical Society.)

Infrared Spectra and Chemometric Analysis

FTIR-PAS spectra were acquired for 4000–397 cm^{-1} . Spectra from all four diets are shown in Figure 2. The spectra have many bands in common, but in the fingerprint region (1800 to 397 cm^{-1}) there are visible differences among the cecal samples from different diets. Irudayaraj and Yang (71) identified individual bands in FTIR-PAS spectra of pure starch. Some of the bands they identified, such as the 1054 cm^{-1} C–O–C bend and the 930 cm^{-1} and 857 cm^{-1} C–H bends, are apparent in all of the spectra in Figure 2 except that of the control-diet sample, which contains very little starch. However, the cecal material is highly complex, resulting in substantial peak overlap, so determination of starch content based on manual measurement of the heights of one or a few peaks is not reliable. Chemometric modeling was used instead.

PLS successfully modelled the relation between the enzymatic-assay-determined starch content and the FTIR-PAS spectra of the rat cecal contents. Figure 3 shows the cross validation for the best fitting model. The plot correlates

the known starch content (dry basis) with the starch content predicted by the PLS model. The diagonal line is the ideal (i.e., predicted = known), and the fit of the data to that line has R^2 equal to 0.997 and SECV is 1.055 wt. %. SECV is only 2% of the total starch-content range of the sample set (0.3 to 50.1 wt. %), so the fit is quite good. Because the model accurately fits all of the samples, the model should be useful for analyzing unknown samples from any of the four starch diets tested.

Besides the quantitative starch information, qualitative information concerning which starch is involved could be useful. The data were analyzed using PCA to see if the specific starch in the diet could be identified from the spectra. The first two principal components from the PCA of the spectra separated the samples according to diet well, as shown in Figure 4. These two components account for 83.5% of the variance in the data. The PCA analysis gives a simple and visibly clear means to match the samples to specific diets.

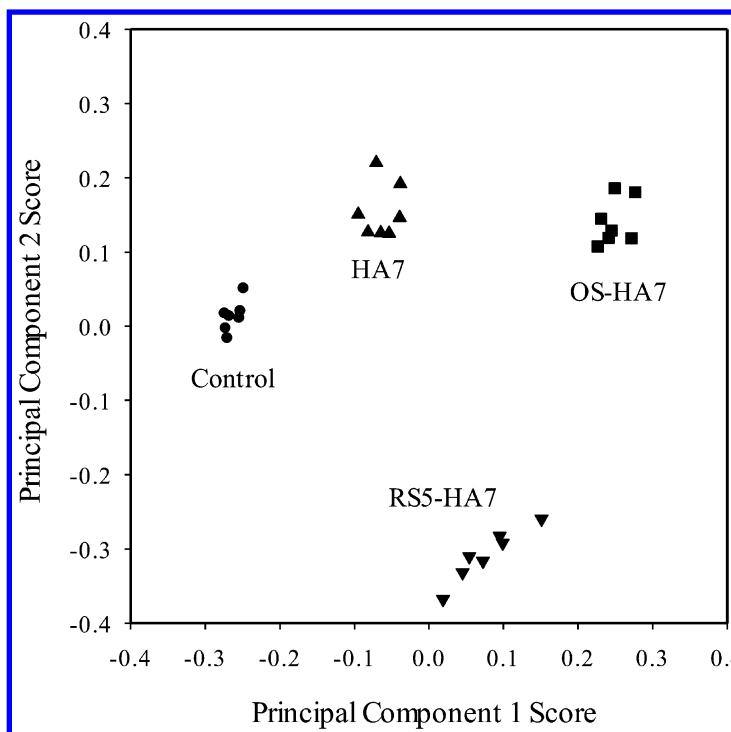


Figure 4. Scores for the first two principal components in the PCA model separate the cecal-content samples according to the RS diets fed to the rats. (Reproduced from reference 57. Copyright 2013 American Chemical Society.)

Conclusions

Despite the similarity of the spectra, the chemometric analysis was able to determine both the content and identity of the starch in the cecal material. The FTIR-PAS data coupled with the enzyme starch assay results clearly were able to produce a cross-validation plot that gave high-quality quantitative results. The PCA analysis cleanly separated the samples according to diet but showed no clustering related to the antibiotic- and AOM-treated subgroups. This demonstrates that FTIR-PAS data can see through minor variations even within complex matrix materials.

Once the samples were prepared, the 256-scan photoacoustic spectra gathered in this study required approximately five minutes each. This study was proof of concept that FTIR-PAS analysis could be a faster and less expensive substitute for the enzymatic-assay analysis.

References

1. Englyst, H. N.; Kingman, S. M.; Cummings, J. H. Classification and Measurement of Nutritionally Important Starch Fractions. *Eur. J. Clin. Nutr.* **1992**, *46* (Suppl. 2), S33–S50.
2. Englyst, H. N.; Cummings, J. H. Digestion of the Polysaccharides of Some Cereal Foods in the Human Small Intestine. *Am. J. Clin. Nutr.* **1985**, *42*, 778–787.
3. Higgins, J. A.; Brown, I. L. Resistant Starch: A Promising Dietary Agent for the Prevention/Treatment of Inflammatory Bowel Disease and Bowel Cancer. *Curr. Opin. Gastroenterol.* **2013**, *29*, 190–194.
4. Robertson, M. D. Dietary-Resistant Starch and Glucose Metabolism. *Curr. Opin. Clin. Nutr. Metab. Care* **2012**, *15*, 362–367.
5. Li, L.; Jiang, H.; Campbell, M.; Blanco, M.; Jane, J. Characterization of Maize Amylose-Extender (ae) Mutant Starches. Part I: Relationship Between Resistant Starch Contents and Molecular Structures. *Carbohydr. Polym.* **2008**, *74*, 396–404.
6. Zhang, B.; Huang, Q.; Luo, F.; Fu, X.; Jiang, H.; Jane, J. Effects of Octenylsuccinylation on the Structure and Properties of High-Amylose Maize Starch. *Carbohydr. Polym.* **2011**, *84*, 1276–1281.
7. Ai, Y.; Hasjim, J.; Jane, J. Effects of Lipids on Enzymatic Hydrolysis and Physical Properties of Starch. *Carbohydr. Polym.* **2013**, *92*, 120–127.
8. Englyst, H. N.; Quigley, M. E.; Hudson, G. J. Determination of Dietary Fibre as Non-starch Polysaccharides with Gas-Liquid Chromatographic, High-performance Liquid Chromatographic or Spectrophotometric Measurement of Constituent Sugars. *Analyst* **1994**, *119*, 1497–509.
9. AOAC Official Method 991.43. Total, Soluble, and Insoluble Dietary Fiber in Foods. *Official Methods of Analysis of AOAC International*; <http://www.aoac.org> (accessed October 29, 2013).
10. AOAC Official Method 2001.03. Dietary Fiber Containing Supplemented Resistant Maltodextrin (RMD). *Official Methods of Analysis of AOAC International*; <http://www.aoac.org> (accessed October 29, 2013).

11. AOAC Official Method 2009.01. Total Dietary Fiber in Foods. *Official Methods of Analysis of AOAC International*; <http://www.aoac.org> (accessed October 29, 2013).
12. AOAC Official Method 2011.25. Insoluble, Soluble, and Total Dietary Fiber in Foods. *Official Methods of Analysis of AOAC International*; <http://www.aoac.org> (accessed October 29, 2013).
13. AOAC Official Method 2002.02. Resistant Starch in Starch and Plant Materials. *Official Methods of Analysis of AOAC International*; <http://www.aoac.org> (accessed October 29, 2013).
14. AACCI Method 32-40.01. Resistant Starch in Starch Samples and Plant Materials. *Approved Methods of Analysis*, <http://dx.doi.org/10.1094/AACCIntMethod-32-40.01> (accessed November 29, 2013).
15. Landau, S.; Glasser, T.; Dvash, L. Monitoring Nutrition in Small Ruminants with the Aid of Near Infrared Reflectance Spectroscopy (NIRS) Technology: A Review. *Small Ruminant Res.* **2006**, *61*, 1–11.
16. *Near Infrared Reflectance Spectroscopy (NIRS): Analysis of Forage Quality*; Marten, G. C., Shenk, J. S., Barton, F. E., II, Eds.; Agriculture Handbook No. 643; U.S. Department of Agriculture, U.S. Government Printing Office: Washington, DC, 1985.
17. Stuth, J.; Jama, A.; Tolleson, D. Direct and Indirect Means of Predicting Forage Quality through Near Infrared Reflectance Spectroscopy. *Field Crops Res.* **2003**, *84*, 45–56.
18. *Near-Infrared Technology in the Agricultural and Food Industries*, 2nd ed.; Williams, P., Norris, K., Eds.; American Association of Cereal Chemists: St. Paul, MN, 2001.
19. Hymowitz, T.; Dudley, J. W.; Collins, F. I.; Brown, C. M. Estimations of Protein and Oil Concentration in Corn, Soybean, and Oat Seed by Near-Infrared Light Reflectance. *Crop Sci.* **1974**, *14*, 713–715.
20. Williams, P. C. Application of Near Infrared Reflectance Spectroscopy to Analysis of Cereal Grains and Oilseeds. *Cereal Chem.* **1975**, *52*, 561–576.
21. Norris, K. H.; Barnes, R. F.; Moore, J. E.; Shenk, J. S. Predicting Forage Quality by Infrared Reflectance Spectroscopy. *J. Anim. Sci.* **1976**, *43*, 889–897.
22. Perera, A.; Meda, V.; Tyler, R. T. Resistant Starch: A Review of Analytical Protocols for Determining Resistant Starch and of Factors Affecting the Resistant Starch Content of Foods. *Food Res. Int.* **2010**, *43*, 1959–1974.
23. Hódsági, M.; Gergely, S.; Gelencsér, T.; Salgó, A. Investigations of Native and Resistant Starches and their Mixtures Using Near-Infrared Spectroscopy. *Food Bioprocess Technol.* **2012**, *5*, 401–407.
24. van Soest, J. J. G.; Tounois, H.; de Wit, D.; Vliegthart, J. F. G. Short-Range Structure in (Partially) Crystalline Potato Starch Determined with Attenuated Total Reflectance Fourier-Transform IR Spectroscopy. *Carbohydr. Res.* **1995**, *279*, 201–214.
25. Zhou, Z.; Topping, D. L.; Morell, M. K.; Bird, A. R. Changes in Starch Physical Characteristics following Digestion of Foods in the Human Small Intestine. *Br. J. Nutr.* **2010**, *104*, 573–581.

26. Langkilde, A. M.; Champ, M.; Andersson, H. Effects of High-Resistant-Starch Banana Flour (RS²) on *in vitro* Fermentation and the Small-Bowel Excretion of Energy, Nutrients, and Sterols: An Ileostomy Study. *Am. J. Clin. Nutr.* **2002**, *75*, 104–111.
27. Englyst, H. N.; Kingman, S. H.; Hudson, G. J.; Cummings, J. H. Measurement of Resistant Starch *in vitro* and *in vivo*. *Br. J. Nutr.* **1996**, *75*, 749–755.
28. Noah, L.; Robert, P.; Millar, S.; Champ, M. Near-Infrared Spectroscopy as Applied to Starch Analysis of Digestive Contents. *J. Agric. Food Chem.* **1997**, *45*, 2593–2597.
29. Mignon-Grasteau, S.; Muley, N.; Bastianelli, D.; Gomez, J.; Péron, A.; Sellier, N.; Millet, N.; Besnard, J.; Hallouis, J.-M.; Carré, B. Heritability of Digestibilities and Divergent Selection for Digestion Ability in Growing Chicks Fed a Wheat Diet. *Poultry Sci.* **2004**, *83*, 860–867.
30. Bastianelli, D.; Bonnal, L.; Juin, H.; Mignon-Grasteau, S.; Davrieux, F.; Carré, B. Prediction of the Chemical Composition of Poultry Excreta by Near Infrared Spectroscopy. *J. Near Infrared Spectrosc.* **2010**, *18*, 69–77.
31. Boval, M.; Coates, D. B.; Lecomte, P.; Decruyenaere, V.; Archimède, H. Faecal Near Infrared Reflectance Spectroscopy (NIRS) to Assess Chemical Co H. Faecal Near Infrared Reflectance Spectroscopy (NIRS) to Assess Chemical Composition, *in vivo* Digestibility and Intake of Tropical Grass by Creole Cattle. *Anim. Feed Sci. Technol.* **2004**, *114*, 19–29.
32. Stein, J.; Purschian, B.; Zeuzem, S.; Lembcke, B.; Caspary, W. F. Quantification of Fecal Carbohydrates by Near-Infrared Reflectance Analysis. *Clin. Chem.* **1996**, *42*, 309–312.
33. Rivero-Marcotegui, A.; Olivera-Olmedo, J. E.; Valverde-Visus, F. S.; Palacios-Sarrasqueta, M.; Grijalba-Uche, A.; García-Merlo, S. Water, Fat, Nitrogen, and Sugar Content in Feces: Reference Intervals in Children. *Clin. Chem.* **1998**, *44*, 1540–1544.
34. Bell, A. G. On the Production and Reproduction of Sound by Light. *Am. J. Sci. (Series 3)* **1880**, *20*, 305–324.
35. Bell, A. G. Upon the Production of Sound by Radiant Energy. *Phil. Mag. (Series 5)* **1881**, *11*, 510–528.
36. Rosenzweig, A.; Gersho, A. Theory of the Photoacoustic Effect with Solids. *J. Appl. Phys.* **1976**, *47*, 64–69.
37. Iwabuchi, K.; Kimura, T.; Otten, L. Effect of Volumetric Water Content on Thermal Properties of Dairy Cattle Feces Mixed with Sawdust. *Bioresour. Technol.* **1999**, *70*, 293–297.
38. Michaelian, K. H. *Photoacoustic Infrared Spectroscopy*; Wiley-Interscience: New York, 2003.
39. McClelland, J. F.; Bajic, S. J.; Jones, R. W.; Seaverson, L. M. Photoacoustic spectroscopy. In *Modern Techniques in Applied Molecular Spectroscopy*; Mirabella, F. M., Ed.; Wiley-Interscience: New York, 1998; pp 221–265.
40. McClelland, J. F. Photoacoustic Spectroscopy. *Anal. Chem.* **1983**, *55*, 89A–105A.
41. McClelland, J. F.; Jones, R. W.; Luo, S.; Seaverson, L. M. A Practical Guide to FT-IR Photoacoustic Spectroscopy. In *Practical Sampling Techniques for*

- Infrared Analysis*; Coleman, P. B., Ed.; CRC Press: Boca Raton, FL, 1993; pp 107–144.
42. Schmid, T. Photoacoustic Spectroscopy for Process Analysis. *Anal. Bioanal. Chem.* **2006**, *384*, 1071–1086.
 43. *Photoacoustic Imaging and Spectroscopy*; Wang, L. V., Ed.; CRC Press: Boca Raton, FL, 2009.
 44. Cox, B.; Laufer, J. G.; Arridge, S. R.; Beard, P. C. Quantitative Spectroscopic Photoacoustic Imaging: A Review. *J. Biomed. Opt.* **2012**, *17* No. 061202.
 45. Hu, S.; Wang, L. V. Optical-Resolution Photoacoustic Microscopy: Auscultation of Biological Systems at the Cellular Level. *Biophys. J.* **2013**, *105*, 841–847.
 46. Yang, H.; Irudayaraj, J. Characterization of Beef and Pork using Fourier-Transform Infrared Photoacoustic Spectroscopy. *Lebensm.-Wiss. Technol.* **2001**, *34*, 402–409.
 47. Irudayaraj, J.; Yang, H. Analysis of Cheese Using Step-Scan Fourier Transform Infrared Photoacoustic Spectroscopy. *Appl. Spectrosc.* **2000**, *54*, 595–600.
 48. Gordillo-Delgado, F.; Marín, E.; Cortés-Hernández, D. M.; Mejía-Morales, C.; García-Salcedo, A. J. Discrimination of Organic Coffee via Fourier Transform Infrared–Photoacoustic Spectroscopy. *J. Sci. Food Agric.* **2012**, *92*, 2316–2319.
 49. Belton, P. S.; Saffa, A. M.; Wilson, R. H. The Potential of Fourier Transform Infrared Spectroscopy for the Analysis of Confectionery Products. *Food Chem.* **1988**, *28*, 53–61.
 50. Sivakesava, S.; Irudayaraj, J. Analysis of Potato Chips using FTIR Photoacoustic Spectroscopy. *J. Sci. Food Agric.* **2000**, *80*, 1805–1810.
 51. Irudayaraj, J.; Sivakesava, S.; Kamath, S.; Yang, H. Monitoring Chemical Changes in Some Foods Using Fourier Transform Photoacoustic Spectroscopy. *J. Food Sci.* **2001**, *66*, 1416–1421.
 52. Mohamed, A.; Rayas-Duarte, P.; Gordon, S. H.; Xu, J. Y. Estimation of HRW Wheat Heat Dama J. Y. Estimation of HRW Wheat Heat Damage by DSC, Capillary Zone Electrophoresis, Photoacoustic Spectroscopy and Rheometry. *Food Chem.* **2004**, *87*, 195–203.
 53. Letzelter, N. S.; Wilson, R. H.; Jones, A. D.; Sinnaeve, G. Quantitative Determination of the Composition of Individual Pea Seeds by Fourier Transform Infrared Photoacoustic Spectroscopy. *J. Sci. Food Agric.* **1995**, *67*, 239–245.
 54. Irudayaraj, J.; Yang, H.; ; Sakhamuri, S. Differentiation of Detection of Microorganisms using Fourier Transform Infrared Photoacoustic Spectroscopy. *J. Molec. Struct.* **2002**, *606*, 181–188.
 55. Gordon, S. H.; Schudy, R. B.; Wheeler, B. C.; Wicklow, D. T.; Greene, R. V. Identification of Fourier Transform Infrared Photoacoustic Spectral Features for Detection of *Aspergillus flavus* Infection in Corn. *Int. J. Food Microbiol.* **1997**, *35*, 179–186.
 56. Greene, R. V.; Gordon, S. H.; Jackson, M. A.; Bennett, G. A.; McClelland, J. F.; Jones, R. W. Detection of Fungal Contamination in Corn: Potential of FTIR–PAS and –DRS. *J. Agric. Food Chem.* **1992**, *40*, 1144–1149.

57. Anderson, T. J.; Ai, Y.; Jones, R. W.; Houk, R. S.; Jane, J.; Zhao, Y.; Birt, D. F.; McClelland, J. F. Analysis of Resistant Starches in Rat Cecal Contents Using Fourier Transform Infrared Photoacoustic Spectroscopy. *J. Agric. Food Chem.* **2013**, *61*, 1818–1822.
58. Anderson, T. J.; Jones, R. W.; Ai, Y.; Houk, R. S.; Jane, J.; Zhao, Y.; Birt, D. F.; McClelland, J. F. High-Resolution Time-of-Flight Mass Spectrometry Fingerprinting of Metabolites from Cecum and Distal Colon Contents of Rats Fed Resistant Starch. *Anal. Bioanal. Chem.* **2014**, *406*, 745–756.
59. Zhao, Y.; Hasjim, J.; Li, L.; Jane, J.; Hendrich, S.; Birt, D. F. Inhibition of Azoxymethane-Induced Preneoplastic Lesions in the Rat Colon by a Cooked Stearic Acid Complexed High-Amylose Cornstarch. *J. Agric. Food Chem.* **2011**, *59*, 9700–9708.
60. Birt, D. F.; Phillips, G. J. Diet, Genes, and Microbes: Complexities of Colon Cancer Prevention. *Toxicol. Pathol.* **2014**, *42*, 182–188.
61. Ai, Y.; Nelson, B.; Birt, D. F.; Jane, J. *In vitro* and *in vivo* Digestion of Octenyl Succinic Starch. *Carbohydr. Polym.* **2013**, *98*, 1266–1271.
62. Hasjim, J.; Lee, S.-O.; Hendrich, S.; Setiawan, S.; Ai, Y.; Jane, J. Characterization of a Novel Resistant-Starch and Its Effects on Postprandial Plasma-Glucose and Insulin Responses. *Cereal Chem.* **2010**, *87*, 257–262.
63. Reeves, P. G. Components of the AIN-93 Diets as Improvements in the AIN-76A Diet. *J. Nutr.* **1997**, *127* (Suppl. 5), 838S–841S.
64. AACC International. *Approved Methods of the American Association of Cereal Chemists*, 10th ed., Method 76-13; The Association: St. Paul, MN, 2000.
65. Haaland, D. M.; Thomas, E. V. Partial Least-Squares Methods for Spectral Analyses. 1. Relation to Other Quantitative Calibration Methods and the Extraction of Qualitative Information. *Anal. Chem.* **1988**, *60*, 1193–1202.
66. Fredstrom, S. B.; Jung, H.-J. G.; Halgerson, J. L.; Eyden, C. A.; Slavin, J. L. Trial of Near-Infrared Reflectance Spectroscopy in a Human Fiber Digestibility Study. *J. Agric. Food Chem.* **1994**, *42*, 735–738.
67. Franck, P. F.; Sallerin, J.-L.; Schroeder, H.; Gelot, M.-A.; Nabet, P. Rapid Determination of Fecal Fat by Fourier Transform Infrared Analysis (FTIR) with Partial Least-Squares Regression and an Attenuated Total Reflectance Accessory. *Clin. Chem.* **1996**, *42*, 2015–2020.
68. Geladi, P.; MacDougall, D.; Martens, H. Linearization and Scatter-Correction for Near-Infrared Reflectance Spectra of Meat. *Appl. Spectrosc.* **1985**, *39*, 491–500.
69. Leardi, R. Chemometrics in Data Analysis. In *Food Authenticity and Traceability*; Lees, M., Ed.; Woodhead Publishing: Cambridge, U.K., 2003; pp 299–320.
70. Roldán-Marín, E.; Jensen, R. I.; Krath, B. N.; Kristensen, M.; Poulsen, M.; Cano, M. P.; Sánchez-Moreno, C.; Dragsted, L. O. An Onion Byproduct Affects Plasma Lipids in Healthy Rats. *J. Agric. Food Chem.* **2010**, *58*, 5308–5314.
71. Irudayaraj, J.; Yang, H. Depth Profiling of a Heterogeneous Food-Packaging Model using Step-Scan Fourier Transform Infrared Photoacoustic Spectroscopy. *J. Food Eng.* **2002**, *55*, 25–33.

Chapter 18

Metabolic Fingerprinting of the Lycopodiales Species for Chemotaxonomy and Quality Control

Chee-Yan Choo,^{*,1} NorShahidah Sahidan,¹ and A. Latiff²

¹MedChem Herbal Research Group, Faculty of Pharmacy,
Universiti Teknologi MARA, 42300 Puncak Alam, Selangor, Malaysia
²Faculty of Sciences and Technology, Universiti Kebangsaan Malaysia,
Bangi, Selangor, Malaysia
*E-mail: choo715@puncakalam.uitm.edu.my.

Herbs are used either singly or in combination as an alternative to drugs for the treatment of a variety of diseases. The advancement of technology has enabled more stringent quality control of herbs. For example, (-) Huperzine A is an alkaloid originally isolated from *Huperzia serrata* and has been found to be a potent, reversible and selective acetylcholinesterase inhibitor. (-) Huperzine A is found in other Lycopodiales species. The aim of this study is to develop chemical profiles of Lycopodiales species with the hplc-pda system. Chemical profiles are analyzed with the chemometrics software. Species from the Lycopodiales order were collected throughout Peninsular Malaysia. Methanolic extracts of dried club mosses were dissolved in methanol and subjected to hplc analysis. The chemical profile was acquired with a hplc-pda connected to a 250 x 4.6mm ODS-3, 3 μ m column maintained at 35 °C. A gradient system was used for the separation of (-) huperzine A. Data were collected from 200-500nm. The chemical profiles were exported to the UnScramblerX software. Using the unsupervised principal component analysis, the species were clustered into two families, namely the Huperziaceae and Lycopodiaceae families. The species can be chemically

discriminated using the principal component analysis. This methodology is useful for both the chemotaxonomic discrimination of species from the Lycopodiales order and quality control of plant material.

Keywords: Lycopodiales; metabolic fingerprint; chemotaxonomy

Introduction

Alzheimer's disease is a neurodegenerative disorder of the central nervous system, characterized by loss of cognitive ability and severe behavior abnormalities, which ultimately results in degradation of intellectual and mental activities (1). It is associated with a selective loss of cholinergic neurons and reduced levels of acetylcholine neurotransmitter. Breakdown of acetylcholine causes decreased activity in the cerebral synapses and is a cause of cognitive impairment in the course of Alzheimer's disease. Huperzine A (Figure 1) is an alkaloid originally isolated from *H. serrata* and has been found to be a potent, reversible and selective acetylcholinesterase inhibitor (2, 3). Clinically it was proven useful for Alzheimer's disease in China and approved for mild-to-moderate stages (4, 5) and marketed in the United States as a dietary supplement (6).

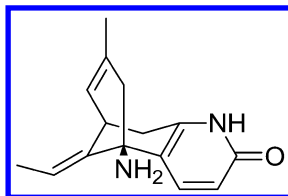


Figure 1. Structure of (-) Huperzine A.

There are more than 500 Lycopodiales species yet only fewer than 40 species have been studied on its alkaloidal content (7–12). Lycopodiales species is a large group of species that are commonly known as club mosses. These species are characterized by low, evergreen, coarsely moss-like and club-shaped strobili at the tips of mosslike branches. The club mosses are the oldest extant terrestrial vascular plants with origin from the late Silurian to early Devonian era. The taxonomy of the genus is still not fixed. There are more than 500 species in Lycopodiales belonging to the two main families Lycopodiaceae and Huperziaceae. Nevertheless, these plants are not abundant, grow very slowly and are only found in very specialized habitats.

Since the discovery of (-) huperzine A as a potent anticholinesterase, various groups have reported the distribution of huperzine A or anticholinesterase activity in club mosses from various regions, namely Europe (13), China (14–16), Australasia and Southeast Asia (17, 18), Peninsular Malaysia (19, 20), Panama (21), Iceland (22) and northeastern India (23).

The objective of this study was to use the metabolite profile to discriminate the species into clusters. The Principal Component Analysis (PCA) model can be further used to classify the species or quality control of finished pharmaceutical products containing Lycopodiales species.

Methodology

Sample Preparation

The club mosses were collected from the Peninsular Malaysia and authenticated by Emeritus Prof. Dr. A. Latiff from the Universiti Kebangsaan Malaysia. The collected club mosses were dried at 40 °C for 24 hours or until constant weight. The process of drying, grinding and extraction is according to earlier method (20). Briefly, the powdered club mosses were extracted with methanol at 40 °C. Every hour, the extract is decanted and fresh methanol is refilled in for the next cycle of extraction. This process is repeated five cycles. The combined extracts were dried under reduced pressure with a rotary evaporator (Buchi, Switzerland) at 40 °C and further freeze dried (Labconco, USA). Stock solution of 5 mg/mL was prepared by dissolving in methanol.

Chromatographic Condition

The method developed with a HPLC-PDA (Waters, USA) was used for the analysis of club mosses samples (20). The oven temperature was maintained at 35 °C and the column used was a 250 x 4.6 mm ODS-3, 3µm, column (Inertsil, Japan). A gradient method was used with increasing amount of acetonitrile from 20 % to 70 % in deionised water with 0.01 % TFA and the flow rate was maintained at 1 mL/min. The photodiode array detector wavelength was set to monitor from 200-500 nm. Triplicate samples were used. (-) Huperzine A (Sigma, USA) was used as an internal standard.

Principal Component Analysis (PCA)

Chromatogram data extracted at 308 nm were exported to the multivariate software (UnScramblerX (Camo, Norway)). Peak areas of the dataset were normalized without further treatment of the dataset. The dataset was analysed with the unsupervised pattern recognition method, Principal component analysis (PCA). PCA is a mathematical method using orthogonal transformation to change a set of possibly correlated variables to a set of values of uncorrelated variables named principal components (PCs). PCA can highlight both similar and independent information. Dataset were subjected to the multivariate software, UnScramblerX, v10.1 (Camo, Norway).

Result

The Lycopodiales species were collected from Peninsular Malaysia (Table 1). A total of 23 species were collected from the mountain.

Table 1. Lycopodiales species from Peninsular Malaysia

<i>Sample No.</i>	<i>Name</i>	<i>Collected location</i>
1	<i>Huperzia pinifolia</i> Trevis	Taman negara
2	<i>Huperzia c.f. pinifolia</i> Trevis	Taman negara
3	<i>Huperzia pinifolia</i> Trevis	Perak/Pahang border
4	<i>Huperzia pinifolia</i> Trevis	Cameron Highlands
5	<i>Huperzia phlegmaria</i> (L.) Rothm	Perak/Pahang border
6	<i>Huperzia phlegmaria</i> (L.) Rothm	Cameron Highlands
7	<i>Huperzia phlegmaria</i> (L.) Rothm	Pahang border
8	<i>Huperzia phyllantha</i> (Hook.f.&Arn.) Hulob	Kelantan
9	<i>Huperzia carinata</i> (Desv. Ex poir) Trevis.	Cameron Highlands
10	<i>Huperzia nummulariifolia</i> (Blume) Jermy in T.C. Chambers & Crabbe	Pahang
11	<i>Huperzia nummulariifolia</i> (Blume) Jermy in T.C. Chambers & Crabbe	Perak/Pahang border
12	<i>Huperzia tetrasticha</i> (Kunze ex Aldrew.) Hulob	Pahang
13	<i>Huperzia squarrosa</i> (G. Frost) Trevis	Perlis
14	<i>Lycopodium platyrhizoma</i> Wilce	Cameron Highlands
15	<i>Lycopodium platyrhizoma</i> Wilce	Frasers Hill
16	<i>Lycopodium casuarinoides</i> Spring	Cameron Highlands
17	<i>Lycopodium casuarinoides</i> Spring	Pahang
18	<i>Lycopodium casuarinoides</i> Spring	Frasers Hill
19	<i>Lycopodium clavatum</i> L.	Pahang
20	<i>Lycopodium clavatum</i> L.	Cameron Highlands
21	<i>Lycopodiella cernua</i> (L.) Pic. Serm.	Langkawi
22	<i>Lycopodiella cernua</i> (L.) Pic. Serm.	Selangor
23	<i>Lycopodiella cernua</i> (L.) Pic. Serm.	Frasers Hill

The chromatogram dataset was integrated at 308 nm with 73 peaks (C1-C73) for all the species were used (Figure 2). The dataset was normalized with the UnScramblerX software and all the 73 peaks were used for the chemometric analysis. (-) Huperzine A was eluted as peak number C39. All the peaks were overlaid on the similar line plot.

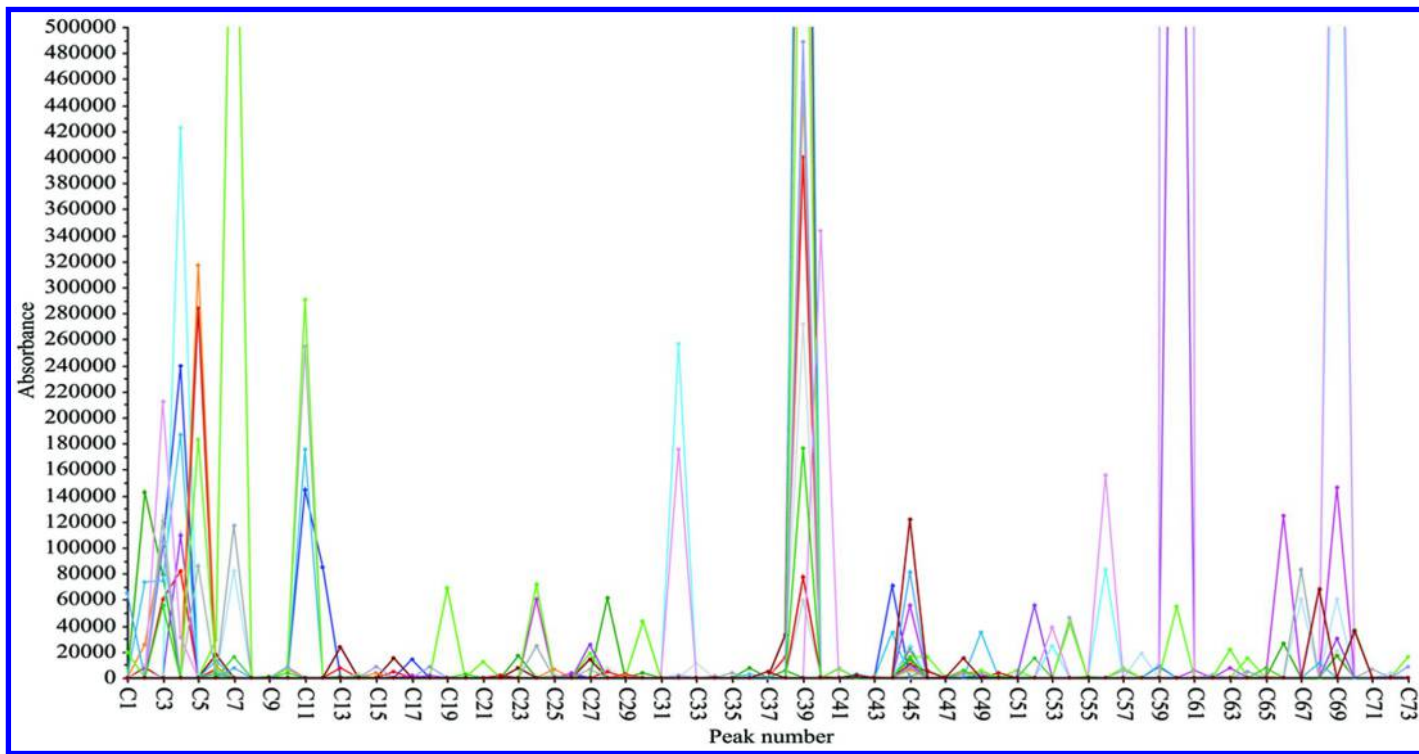


Figure 2. Line plot of normalized dataset.

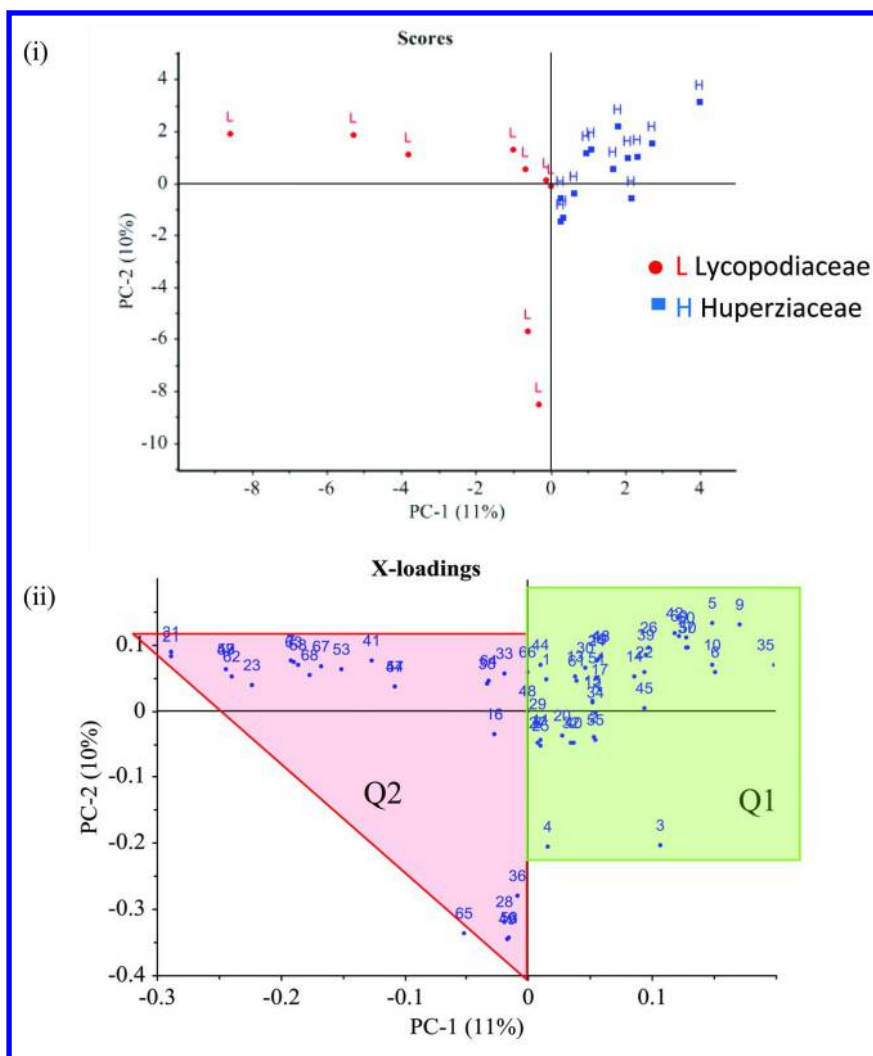


Figure 3. PCA (i) score plot and (ii) loadings analysis of *Lycopodiaceae* species.

The normalized dataset subjected to PCA analysis projected two clusters (Figure 3i). All the species from the genera *Lycopodium* and *Lycopodiella* were clustered into one cluster (Figure 3i). Species from the genus *Huperzia* were clustered into the second cluster. Since the 73 peaks were used for the PCA analysis, both Principal component (PC) 1 and 2 were only able to explained 21% of the variations. Nonetheless, the species were discriminated into two clusters, namely, Lycopodiaceae and Huperziaceae families, respectively. The metabolite profile used for the principal component analysis (PCA) showed similarity to the taxonomy classification by Ching (24) and Holub (25). Both have classified the species from Lycopodiales order into two families, namely Huperziaceae and Lycopodiaceae. However, Ollgaard (26) have combined both the families

with four genera, namely, *Huperzia*, *Lycopodiella*, *Lycopodium* and . Thus, the chemical profiles acquired with a high performance liquid chromatography coupled to the photo-diode array detector was congruent will the earlier taxonomy by Ching (24) and Holub (25).

From the loading plot (Figure 3ii), influential peaks contributing to the clustering of the species were identified. All the peaks in the quadrant Q1 of the loading plot were influential peaks in the Huperzeaceae family clustering. While all the peaks on the quadrant Q2 of the loading plot were influential peaks for the clustering of the Lycopodiaceae family. No outliers were detected with the Hotelling T² statistics with a significance of 99 % (Figure 4).

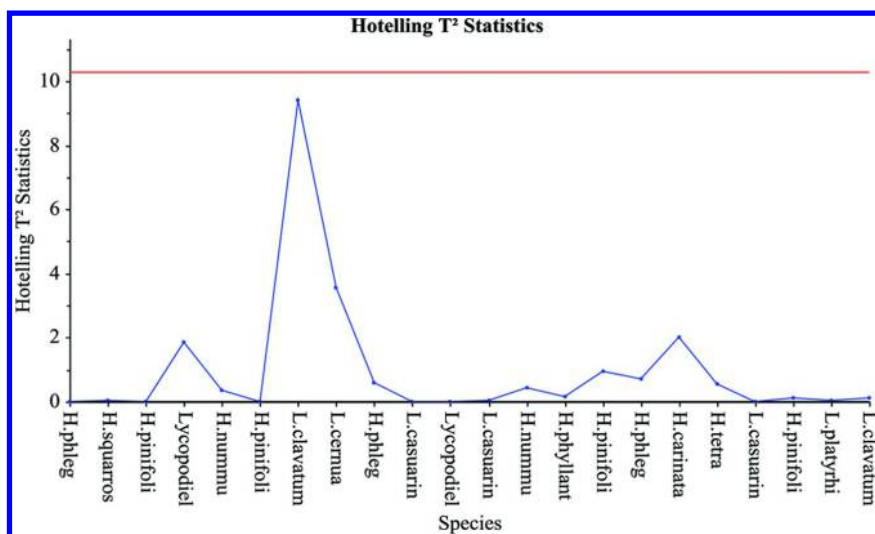


Figure 4. Hotelling T² Statistics.

Conclusion

The metabolite profiles from the high performance liquid chromatography coupled to a photodiode array detector were clustered into two clusters, namely the Lycopodiaceae and Huperzeaceae families. Influential peaks were identified contributing to the clusters. No outliers were detected. The PCA model maybe applied for the quality control of pharmaceutical supplements containing Lycopodiales species.

Acknowledgments

The author is grateful to the Ministry of Science and Technology and Innovation for funding this study under the eScience grant, the university's internal RIF grant and a postgraduate scholarship from MOHE.

References

1. Jia, P.; Sheng, R.; Zhang, J.; Fang, L.; He, Q.; Yang, B.; Hu, Y. *Eur. J. Med. Chem.* **2008**, *2008*, 1–13.
2. Tang, X. C.; Han, Y. F. *CNS Drug Rev.* **1999**, *5*, 281–300.
3. Tang, X. C.; Han, Y. F.; Chen, X. P.; Zhu, X. D. *Acta Pharmacol. Sin.* **1986**, *7*, 501–511.
4. Wang, B. S.; Wang, H.; Wei, Z. H.; Song, Y. Y.; Zhang, L.; Chen, H. Z. *J. Neural Transm* **2009**, *116*, 457–465.
5. Ha, G. T., *Chem. Biodiversity* **2011**, *8*, 1189–1204.
6. Yue, P.; Tao, T.; Zhao, Y.; Ren, J.; Chai, X. *Int. J. Pharm.* **2007**, *337*, 127–132.
7. MacLean, D. B. The Lycopodium Alkaloids. *Alkaloids* **1968**, *10*, 305.
8. MacLean, D. B. The Lycopodium Alkaloids. *Alkaloids* **1973**, *14*, 348.
9. MacLean, D. B. In *The Alkaloids*; Brossi, A., Ed.; Academic Press: New York, 1985; Vol. 26, p 241.
10. Ayer, W. A. The Lycopodium alkaloids. *Nat. Prod. Rep.* **1991**, 455–463.
11. Ayer, W. A.; Trifonov, L. S. In *The Alkaloids*; Cordell, G. A., Brossi, A., Ed.; Academic Press: San Diego, 1994; Vol.45, p 233.
12. Kobayashi, J.; Morita, H. The Lycopodium Alkaloids. In *Alkaloids*; Cordell, G. A., Ed.; Academic: New York, 2005.
13. Borloz, A.; Marston, A.; Hostettmann, K. *Phytochem. Anal.* **2006**, *17* (5), 332–6.
14. Ma, X. Q.; Jiang, S. H.; Zhu, D. Y. *Biochem. Syst. Ecol.* **1998**, *26*, 723–728.
15. Ma, X.; Tan, C.; Zhu, D.; Gang, D. R. *J. Ethnopharmacol.* **2006**, *104*, 54–67.
16. Wu, Q.; Gu, Y. *J. Pharm. Biomed. Anal.* **2006**, *40*, 993–998.
17. Goodger, J. Q. D.; Whincup, A. L.; Field, A. R.; Holtum, J. A. M.; Woodrow, I. E. *Biochem. Syst. Ecol.* **2008**, *36*, 612–618.
18. Lim, W. H.; Goodger, J. Q. D.; Field, A. R.; Holtum, J. A. M.; Woodrow, I. E. *Pharm. Biol.* **2010**, *48* (9), 1073–8.
19. Choo, C. Y.; Hazni, H.; Sahidan, N. S.; Latiff, A.; Jaman, R. *Planta Med.* **2009**, *75*, PJ181.
20. Sahidan, N. S.; Choo, C. Y.; Latiff, A.; Jaman, R. *Chin. J. Nat. Med.* **2012**, *10*, 125–8.
21. Calderon, A. I.; Simithy-Williams, J.; Sanchez, R.; Espinosa, A.; Valdespino, I.; Gupta, M. P. *Nat. Prod. Res.* **2013**, *27*, 500–5.
22. Halldorsdottir, E. S.; Jaroszewski, J. W.; Olafsdottir, E. S. *Phytochemistry* **2010**, *71*, 149–57.
23. Singh, H. B.; Singh, M. K. *NeBIO* **2010**, *1* (1), 27–34.
24. Ching, R. C. *Acta Phytotaxon. Sin.* **1978**, *16*, 19.
25. Holub, J. *Folia Geobot Phytotaxon.* **1985**, *20*, 67–80.
26. Ollgaard, V. *Opera Bot.* **1987**, *92*, 153–178.

Chapter 19

New Approaches in Metabolic Fingerprinting: Improved Extraction Method and Automatic Reduction of NMR Spectra to Essential Data

**Jan Schripsema,^{*,1} Marianna A. Lemos,¹ Marcilene F. V. Dianin,^{1,2}
Dalessandro S. Vianna,² and Denise S. Dagnino³**

¹Grupo Metabolômica, Laboratório de Ciências Químicas, Universidade Estadual do Norte Fluminense, Av. Alberto Lamego, 2000, Campos dos Goytacazes, RJ-28013-602, Brazil

²Instituto de Ciência e Tecnologia, Universidade Federal Fluminense, Rua Recife s/n, Rio das Ostras, RJ-28809-000, Brazil

³Grupo Metabolômica, Laboratório de Biotecnologia, Universidade Estadual do Norte Fluminense, Av. Alberto Lamego, 2000, Campos dos Goytacazes, RJ-28013-602, Brazil

*E-mail: jan@uenf.br or jan.schripsema@gmail.com.

Because metabolomics is still a recent area of research, continuous development takes place leading to further improvements and adaptations of experimental protocols. In this chapter an overview is given of the sequence of experimental procedures of typical metabolomic experiments. The focus is on NMR based metabolomics, but many aspects apply to other techniques that can be used in metabolomics such as MS or HPLC. Major holdbacks are pointed out and improved protocols are suggested for the extraction of the samples and for the conversion of NMR spectra to data, which can be analyzed by multivariate analysis. For an improved coverage of the extracted metabolites a single two-phase (using immiscible solvents) extraction procedure is proposed. To minimize the overlooking of minor components in the extract a procedure for automatic reduction of NMR spectra to essential data is proposed.

Metabolomics

Genomics, transcriptomics, proteomics and metabolomics are the most important –omics. Genomics studies the genes, the genetical foundations of life. The genes furnish the blackprint of the living organisms and much information of these organisms can be obtained through the genes. However, cells can develop completely different with the same genes. All cells in the human body contain in principle the same genes, but each cell is different due to interactions with its environment and consequent differences in the activation of genes. In transcriptomics the mRNA is studied, which shows which genes are activated at certain moments. Through time the transcriptomic profile changes and the presence of mRNA indicates the activation of genes but if this leads to functional proteins is only revealed by proteomics, where the protein profile is studied. Proteins include the enzymes and entities which enable the biochemical reactions to occur. But once again the presence of an enzyme is not a guarantee for its activity. This depends, among others, on the availability of substrates and often co-factors. Only when the micromolecules are studied an effective and complete image is obtained, which shows the characteristics of phenotypes or of individual cells. This is the purpose of metabolomics. Often it has been described as the area of research which tries to analyze all micro-molecules in a cell, tissue or organism (1, 2), but as will be shown below, this definition is much too limited.

The objective of metabolomics is not limited to the analysis of all molecules present in a given system. It also includes the interpretation of the changes in metabolite levels. Therefore a better definition of metabolomics has been given (1): Metabolomics is the area of research which strives to obtain complete metabolic fingerprints, to detect differences between them and to provide hypothesis to explain those differences. From this definition it is clear that another important part of metabolomics is the comparison of metabolic fingerprints. What are the differences, what molecules are responsible for those differences and what factors cause the differences? The usefulness of the measurement of metabolite levels to investigate the status of an organism is illustrated by tests used routinely for diagnosis. For example measuring metabolites such as glucose and cholesterol in human blood samples will detect diseases such as diabetes or predict the chances of a future heart disease.

This area of research is still rapidly developing. Each year the number of papers on metabolomics increases and metabolomics has become a powerful tool in the study of all types of organisms (1).

In contrast to the other –omics mentioned, metabolomics does not have well established experimental procedures. This is the result of the enormous variety of metabolites which exist and which can be encountered in a given system. Actually, it is not known how many metabolites exist in a single cell or in a plant or in any other organism. Estimates have been made on the basis of the number of genes or by extrapolation of known metabolites and the quantities are generally in the range of thousands (3, 4).

The tools of metabolomics are in contrast to the other -omics not well defined. In literature mainly two techniques are used: NMR or MS; the last generally coupled to LC or GC. All techniques have their specific advantages

and disadvantages. In the review by Schripsema (2010) many factors have been pointed out (5). In the present chapter, some specific points are highlighted, i.e. the extraction of the sample and the processing of the data.

Procedures Used in Metabolomics

As is clear from the foregoing, in metabolomic studies a series of phases exist. Already from the definition presented above three phases are apparent: the obtaining of complete metabolic fingerprints, the detection of differences between them and the generation of hypothesis to explain those differences.

But in fact many more stages can be discerned. Schripsema and Dagnino (*1*) discerned the following stages in a metabolomic experiment:

1. Proposing the Questions To Be Answered and the Objectives of the Study

This was considered the most important and often sub-estimated part of a metabolomic experiment (*1*). Only when the initial questions are well defined the experiment can be properly designed.

2. Experimental Design

The experimental design involves the choice of the analytical technique(s) to be used in the experiment, the planning of the sample preparation, with or without extraction, and the procedures for compound quantification.

3. Sampling of the Material To Be Analyzed

When comparing sample populations, it is essential that for correct sampling the homogeneity of the populations is considered. The variation between samples within the population should be known. Preferably, different populations should only differ in the factor under investigation.

4. Measurement of Spectra and/or Chromatograms

In the measurements the best possible results should be obtained from the equipment. Much care should be taken with the adjustment of the apparatus and the measurement conditions. The reproducibility of the results is also essential.

5. Data Pretreatment

For the analysis of the data of a metabolomic experiment the data from each analysis need to be converted to a format suitable to be processed with multivariate analysis.

6. Multivariate Analysis

The most common ways of multivariate analysis are PCA (Principal Component Analysis) and PLS (Partial Least Squares Analysis). Much care should be taken with the results, and adequate tests should be performed to check for the validity of the conclusions.

7. Interpretation of Factors

When differences are detected between data sets, those differences should be linked to specific metabolites. To identify those compounds might be the most elaborate part of a metabolomic study.

It was emphasized by Schripsema & Dagnino (1) that the first two stages are extremely important for the success of metabolomic experiments, because any errors made in the sample collection, preparation and measurement cannot be corrected afterwards and might seriously damage the outcome of metabolomic experiments, or even completely invalidate them (1).

The choice of the analytical technique to be used is also very important for the way how the experiment is conducted. In most metabolomic experiments, which have been published up till now, one of the techniques GC-MS, LC-MS or NMR was used, because these techniques provide metabolic fingerprints, containing information about a large quantity of metabolites (6). Considering the number of metabolites which can be detected GC-MS and LC-MS are superior to NMR, but NMR is superior when quantitative aspects are taken in consideration (7, 8). With NMR the signal intensity is directly related to the quantity of the compound, and hardly influenced by compound specific response factors. This fact also turns the sample preparation for NMR based metabolomics less exigent.

However, whatever the analytical technique chosen, it should be realized that a complete analysis of the metabolome is not feasible, due to the large differences which exist between the different metabolites. Some occur in large quantities (up to tens of percent of dry mass), while others only occur as traces (in pmol quantities or less). Some are extremely hydrophilic (e.g. sugars), while other are lipophilic (e.g. fats), turning the extraction of both in a single extract practically impossible.

The analytical technique produces a large amount of data for each sample. For the adequate analysis of these data multivariate data analysis is essential. This means the data should be transformed to an adequate format to permit the analysis. For the subsequent multivariate data analysis, many different programs are available, both free or commercial. An extensive discussion of available software was published by Blekherman et al. (9).

As final stage of the metabolomic experiment the discriminating factors between data sets should be analyzed, and the molecules responsible for these differences have to be identified. Often this stage is the most elaborate and complex, because compounds might be present in minute quantities and the data obtained in the metabolomic experiments are generally too limited to obtain a 100% certain identification, making it necessary to perform additional experiments. In some cases this can be done by obtaining ^{13}C NMR and 2D NMR from the same samples as used in the metabolomic experiments. But,

more common the sample does not contain the compound in sufficient quantity or there is too much interference in the spectrum from other compounds. Then, the compound should be isolated in a quantity sufficient to permit the recording of the additional data.

Areas of Metabolomics Needing Further Developments

In metabolomics the objective is to obtain quantitative and qualitative information of all metabolites present. Considering the present state-of-the-art further advances are required in both the quantitative and qualitative aspects (5).

The number of metabolites detected should be increased further. Especially for NMR this is important, because the detection of metabolites is limited by several factors, including the following:

- It is not possible to extract all metabolites with one single solvent or solvent mixture.
- When concentration differences are very big (> 100-1000), the minor components are not detectable.
- Superposition of signals is frequent due to the limited spectral range of ^1H NMR. Especially smaller signals close to larger signals are difficult to detect.

Many metabolomic studies have been devoted to the search of the best solvent (10). What solvent or solvent mixture is most suitable and extracts more compounds from a biological matrix? Dependent on the solvent or solvent mixture large differences are found in the extracted metabolites (11, 12). Figure 1 shows NMR spectra obtained after extraction of plant material from *Baccharis trimera* with different deuterated solvents. The differences in the spectra are caused by differences in the metabolites extracted by the different solvents and also because different solvents result in different spectra for the same compound. This makes the direct comparison of spectra in different solvents nearly impossible.

In general the evaluation of the extraction efficiency by NMR is done by counting the number of peaks in the spectrum (13). However some remarks should be made on this evaluation procedure: a single compound, dependent on its structure, can show a single peak (e.g. acetic acid) or hundreds of peaks (e.g. triterpenes), and the number of peaks detected depends on the resolution of the spectrum, which also depends for a certain part on the solvent used.

Superposition of signals is also a serious problem, especially when the process of binning or bucketing is used (5). This process is generally used to avoid interference of incidental slight changes of chemical shift values. But at the same time this process leads to a tremendous loss of resolution which turns the observation of minor signals close to bigger signals impossible.

In the following some new approaches are proposed to diminish the above mentioned problems.

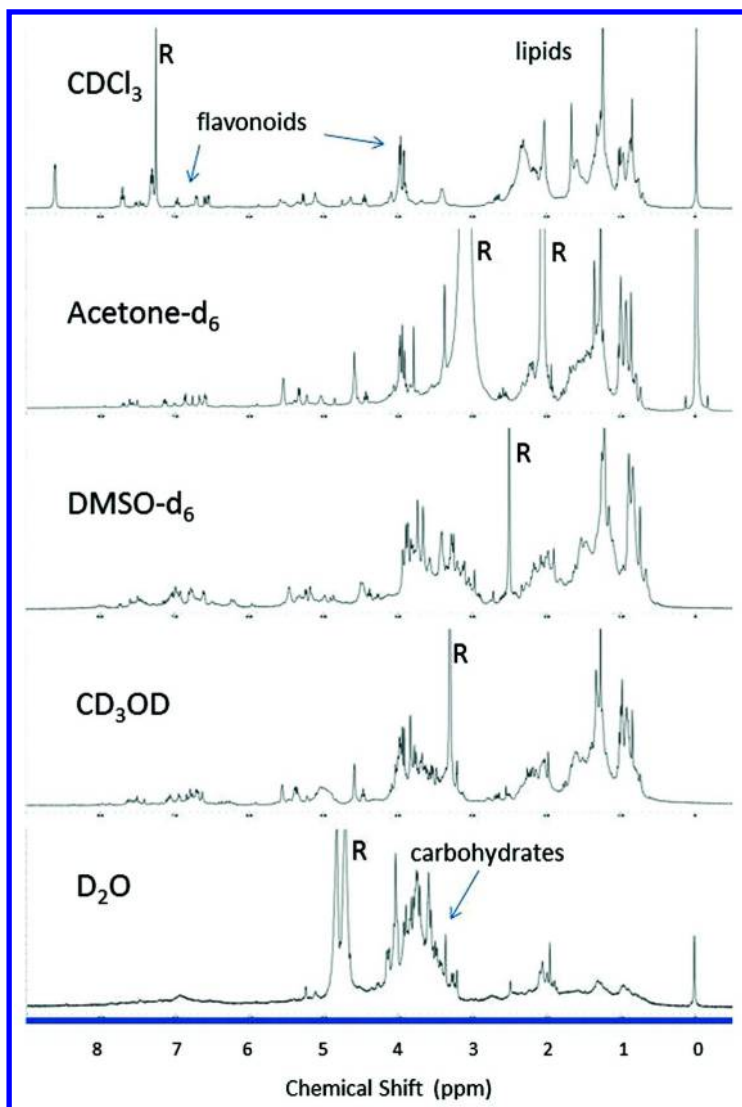


Figure 1. ^1H NMR spectra of extracts from the medicinal plant *Baccharis trimera* (Less.) DC. Extracts were prepared by direct extraction of plant material (100 mg) with the deuterated solvent (1.00 ml). The spectra were obtained at 400 MHz. (R = residual solvent signal).

Two-Phase Extraction

In metabolomic experiments large amounts of samples are processed. This means that the procedures should be kept as simple and reproducible as possible. Any additional step in a procedure introduces an additional source of variation.

For example, in the extraction procedure for NMR based metabolomics the use of deuterated solvents for extraction will eliminate the evaporation and redissolution steps.

As stated above, in an ideal situation, all metabolites of a sample should be extracted to allow their quantification. But it is clear that the extraction of a sample with a single solvent only extracts a part of all metabolites (see Figure 1). Mixtures of solvents have been used in an attempt to expand the number of metabolites extracted (14, 15). Most common in metabolomics is the extraction with a mixture of water and methanol but the most lipophilic metabolites are not extracted with this mixture

A further major disadvantage of the use of a solvent mixture for the extraction is the fact that the NMR data of individual compounds, i.e. the chemical shifts, are dependent on the solvent in which the spectrum is recorded (16). Therefore, if the spectrum has been obtained in a mixture of water and methanol, the chemical shifts will be different than those obtained in pure water or in pure methanol. Because, the data published for isolated compounds are nearly always published using a single solvent, most generally CDCl_3 for apolar compounds and D_2O for polar compounds, the obtained chemical shifts with solvent mixtures cannot be related directly to the databases which have been constructed over the decades that NMR has been developing. Consequently, when using a solvent mixture, a specific spectrum database needs to be generated, corresponding to the specific solvent system.

Considering these facts we investigated the possibility of using multiple, sequential extracts of the same sample. If different solvents are used for the extraction, every solvent provides a specific fingerprint (see Figure 1). The difficulty in generating extracts with different solvents for metabolomic samples in a sequential way lies in the fact that some of the previous solvent will stay in the material and influence the next extraction. As a consequence, as outlined above, this solvent mixture will influence the spectrum obtained. Furthermore extreme care should be taken not to lose biomass in the extraction process.

For the quantification of compounds in the sample extracted by multiple sequential solvents a further difficulty is expected: quantification of individual compounds will become more difficult, because compounds can appear in several extracts each of them giving a different spectrum (see above).

Therefore we analyzed the possibility to extract samples with a two-phase system of deuterated water and chloroform. In this way two separate extracts are obtained, which have the following advantages:

1. The spectra can be obtained directly in the solvents that are the most common solvents used in NMR for natural products. Therefore the resulting NMR spectra can be compared directly to existing data.
2. The two extracts are completely complementary. Extracted individual compounds dissolve in one or both of the two solvents.
3. In the case of plant material or microbial material, by using water, the compounds dissociate better from the matrix.

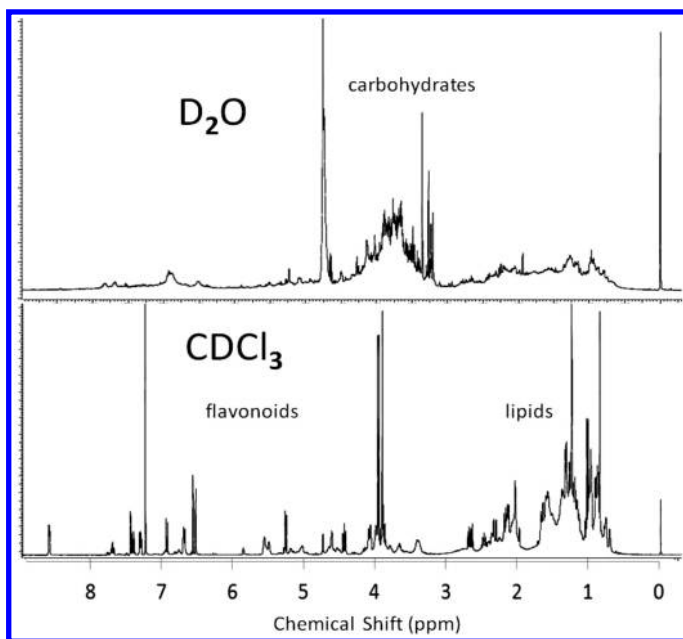


Figure 2. ^1H NMR spectra (400 Mhz) of extracts from the medicinal plant *Baccharis trimera* (Less.) DC., obtained by the two-phase extraction outlined in the text. 100 mg of plant material was extracted with 0.80 ml of D_2O and 0.80 ml of CDCl_3 . The D_2O extract shows the signals from carbohydrates, while the CDCl_3 extract shows signals from flavonoids and lipids.

In our experience with this two phase solvent system we rarely observed that the same compound was found in both of the solvents. We have applied it for extraction of numerous plant species, microbial biomass and different food products, e.g. butter (17). With the two extracts two spectra are obtained, which means that superposition of signals will be less. Furthermore, compounds across the whole polarity range are extracted. In Figure 2 the spectra of the medicinal plant *Baccharis trimera*, obtained with this two phase system are shown. A similar sample was used as for Figure 1 and it is seen that both solvents extract specific compound classes.

In Figure 3 another example is shown, i.e. the spectra of black tea obtained with this two phase system. Caffeine is only encountered in the CDCl_3 layer, while theanine is only observed in the D_2O layer. It is remarkable that caffeine is not present in the water extract, because it is easily extracted with water, e.g. in regular coffee or tea (18). Not only for NMR analysis the two phase extraction is useful, because the extracts can also be used for subsequent analysis by HPLC or LC-MS.

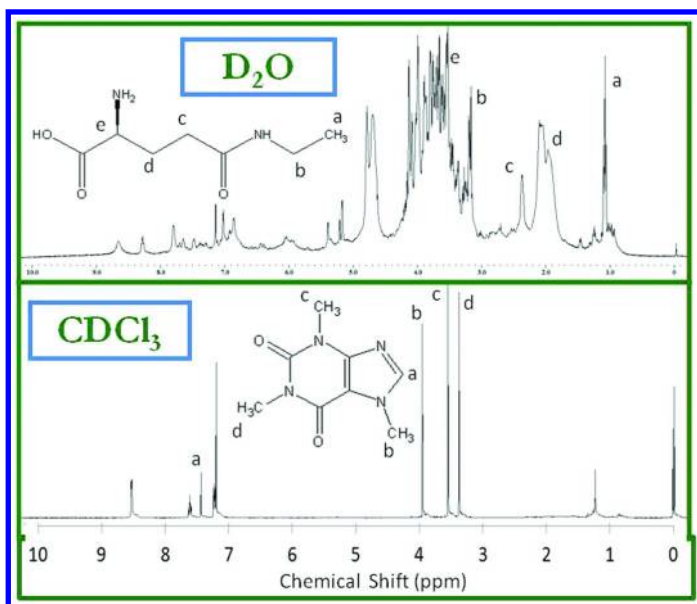


Figure 3. ¹H NMR spectra (400 MHz) of extracts of black tea (*Camellia sinensis*) obtained by the two-phase extraction outlined above. 100 mg of plant material was extracted with 0.80 ml of D₂O and 0.80 ml of CDCl₃. The D₂O extract shows the signals from theanine, while the CDCl₃ extract shows signals from caffeine.

Automatic Reduction of NMR Spectra to Essential Data (ARNSED)

Once the samples have been extracted adequately and representative spectra are obtained they should be compared so as to verify eventual differences in the samples. This is carried out by multivariate data analysis after transformation of the NMR data to a suitable format. This transformation is usually done by binning (also known as bucketing), however this method leads to significant loss of information (19). In the process of binning the total intensity of regions of the spectrum is determined instead of using all available data points. Normally a spectrum containing about 16000 data points is converted by binning to about 400 data points. This means that a tremendous loss of resolution is obtained and consequently much information is lost.

The process of binning is used to avoid that small variations in the chemical shifts of signals lead to problems in the multivariate data analysis. Those variations can occur due to differences in pH, temperature, analyte concentration or salt concentration. Alternatively alignment procedures could be used, but because signals can move to both directions this is not a straight forward process (20).

In fact the best way of processing spectra is the deconvolution of the spectrum in the spectra of the individual components of the mixture of metabolites. But this is only possible if the components are known, e.g. as it has been described for the analysis of urine samples (19, 21).

Another factor which might negatively influence the analysis of series of spectra are problems in the shimming of samples, leading to peak distortions. To avoid those distortions the process of reference deconvolution has been described (22–24). In this process the FID is corrected leading to a near perfect peak shape for all signals, leading to an improved resolution and enhanced possibility to recognize minor signals near to larger ones.

We here propose an alternative approach, in which a standard peak in the spectrum is used to correct the whole spectrum. In this way the spectrum is in fact transformed to a series of single lines that correspond to the peaks, each characterized by a chemical shift and intensity. In a next step the peaks are analyzed to recognize signal shapes, such as doublets, triplets or more complex shapes. Based on the intensities signals can be joined as belonging to the same compound.

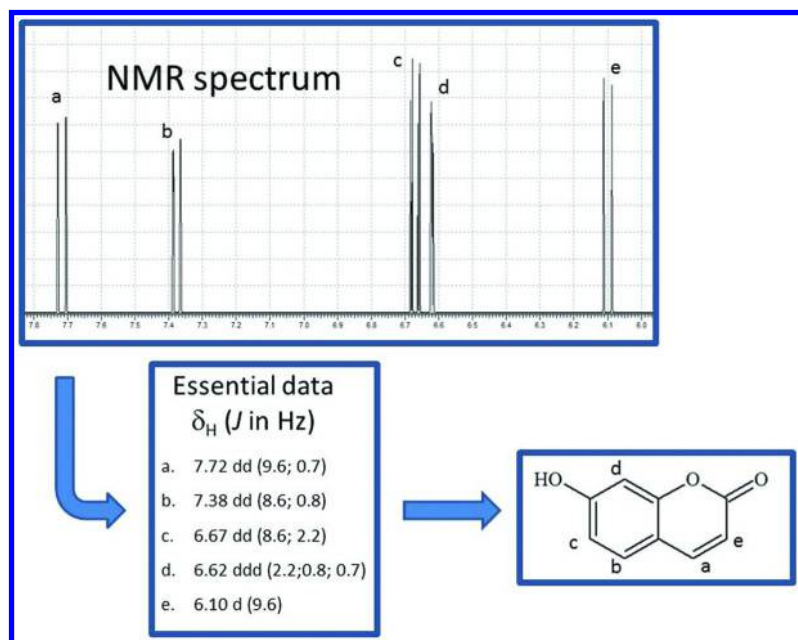


Figure 4. Illustration of the principle of ARNSED (Automatic Reduction of NMR Spectra to Essential Data). The ^1H NMR spectrum is converted to a series of lines, taking into consideration the peak shape of the spectrum. The series of lines is resumed in the listing of essential data. Those data permit a rapid identification of metabolites by consulting data bases.

In this way a spectrum can be automatically reduced to the so-called essential data, since each signal in an NMR spectrum is characterized by the following three parameters: chemical shift, signal form and intensity. The process is illustrated in Figure 4.

The essential data, the chemical shift, coupling constants and intensity of the signals are independent of the apparatus and permit the search in databases with the purpose to achieve the identification of the compound or compounds.

A special software is being developed to extract the essential data from the NMR spectra (ARNSED – Automatic Reduction of NMR Spectra to Essential Data). In this program a standard peak is indicated (usually TMS) and its peak shape is used to reduce the other peaks to single lines. The usefulness of this approach is illustrated in Figure 5.

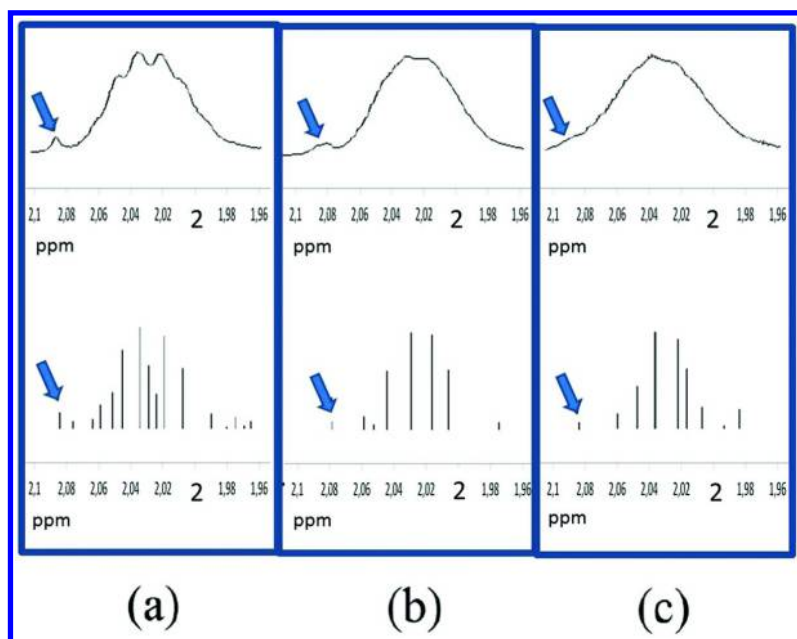


Figure 5. Visualization of a small region of the spectrum from Cashew Nut Shell Liquid obtained at 400 MHz on a Jeol Eclipse+ NMR spectrometer (a). A small signal next to the large complex signal is highlighted by an arrow. In b and c spectra were obtained, by on purpose, using incorrect shimming, causing in this way progressive broadening of the peaks. In the lower panels are displayed the peaks that are recognized by the program ARNSED.

Next to a large signal in the spectrum (caused by superposition of methylene group signals) a small signal is present, which can be observed if the resolution of the spectrum is good (Figure 5a). The ARNSED routine clearly recognizes the peak and quantifies it. Even when the spectrum is deteriorated, by on purpose

introducing inhomogeneity in the magnetic field (wrong shimming) the small peak remains detectable (Figure 5b). Even with an extreme broadening and even duplication of the standard signal the small peak is recognized (Figure 5c). It should be pointed out that some variation occurs in the attribution of the peaks composing the large signal. This is because in large broad peaks, multiple solutions exist. This problem can only be addressed by spectral interpretation and database comparison of data. The ARNSED program is now further developed to detect signal shapes (doublet, triplet or more complex), and combining signals on the basis of integration values. As a last step in the development of the program the integration with spectral databases is envisaged.

Conclusions

It was shown that with a single extraction with a two-phase solvent system using D₂O and CDCl₃ both polar and apolar metabolites can be extracted, increasing the number of compounds that can be analyzed. This also offers great advantages in the analysis of the spectral data, because standard solvents for NMR are used. The extraction with this two phase system is an adequate method to be applied in metabolomics: matrix effects are reduced, both hydrophilic and lipophilic compounds are extracted from the sample and the quantification of the compounds is facilitated since only two, complementary spectra are obtained.

A procedure for extraction of essential data is described for the adequate and most effective analysis of NMR data in metabolomics experiments. The initial experiments with the ARNSED program illustrate its feasibility. Even the detection of small not resolved peaks is possible. The processing of spectra with the ARNSED program will increase the amount of data available for metabolomic experiments, adding information about minor components that are not detected by the current methods.

References

1. Schripsema, J.; Dagnino, D. In *Handbook of Chemical and Biological Plant Analytical Methods*; Hostettmann, K., Stuppner, H., Marston, A., Chen, S., Eds.; John Wiley & Sons, Ltd.: Hoboken, NJ, 2014; pp 885–902.
2. Dettmer, K.; Aronov, P. A.; Hammock, B. D. *Mass Spectrom. Rev.* **2007**, *26*, 51–78.
3. Bino, R. J.; Hall, R. D.; Fiehn, O.; Kopka, J.; Saito, K.; Draper, J.; Nikolau, B. J.; Mendes, P.; Roessner-Tunali, U.; Beale, M. H.; Trethewey, R. N.; Lange, B. M.; Wurtele, E. S.; Sumner, L. W. *Trends Plant Sci.* **2004**, *9*, 418–425.
4. Schwab, W. *Phytochemistry* **2003**, *62*, 837–849.
5. Schripsema, J. *Phytochem. Anal.* **2010**, *21*, 14–21.
6. Xiao, J. F.; Zhou, B.; Ransom, H. W. *Trends Anal. Chem.* **2012**, *32*, 1–14.
7. Pauli, G. F.; Goedecke, T.; Jaki, B. U.; Lankin, D. C. *J. Nat. Prod.* **2012**, *75*, 834–851.

8. Simmler, C.; Napolitano, J. G.; McAlpine, J. B.; Chen, S.-N.; Pauli, G. F. *Curr. Opin. Biotechnol.* **2014**, *25*, 51–59.
9. Blekherman, G.; Laubenbacher, R.; Cortes, D. F.; Mendes, P.; Torti, F. M.; Akman, S.; Torti, S. V.; Shulaev, V. *Metabolomics* **2011**, *7*, 329–343.
10. Verpoorte, R.; Choi, Y. H.; Mustafa, N. R.; Kim, H. K. *Phytochem. Rev.* **2008**, *7*, 525–537.
11. Naz, S.; Garcia, A.; Barbas, C. *Anal. Chem.* **2013**, *85*, 10941–10948.
12. Kim, H. K.; Choi, Y. H.; Verpoorte, R. *Nat. Protoc.* **2010**, *5*, 536–549.
13. Beltran, A.; Suarez, M.; Rodríguez, M. A.; Vinaixa, M.; Samino, S.; Arola, L.; Correig, X.; Yanes, O. *Anal. Chem.* **2012**, *84*, 5838–5844.
14. Wu, H.; Southam, A. D.; Hines, A.; Viant, M. R. *Anal. Biochem.* **2008**, *372*, 204–212.
15. Kim, H. K.; Choi, Y. H.; Verpoorte, R. *Trends Biotechnol.* **2011**, *29*, 267–275.
16. Gottlieb, H. E.; Kotlyar, V.; Nudelman, V. *J. Org. Chem.* **1997**, *62*, 7512–7515.
17. Schripsema, J. *J. Agric. Food Chem.* **2008**, *56*, 2547–2552.
18. Tavares, L. A.; Ferreira, A. G. *Quím. Nova* **2006**, *29*, 911–915.
19. Wishart, D. S. *Trends Anal. Chem.* **2008**, *27*, 228–237.
20. Forshed, J.; Schuppe-Koistinen, I.; Jacobsson, S. P. *Anal. Chim. Acta* **2003**, *487*, 189–199.
21. MacKinnon, N.; Somashekar, B. S.; Tripathi, P.; Ge, W. C.; Rajendiran, T. M.; Chinnaiyan, A. M.; Ramamoorthy, A. *J. Magn. Reson.* **2013**, *226*, 93–99.
22. Morris, G. A. *J. Magn. Reson.* **1988**, *80*, 547–552.
23. Gibbs, A.; Morris, G. A. *J. Magn. Reson.* **1991**, *91*, 77–81.
24. Morris, G. A.; Barjat, H. In *Methods for Structure Elucidation by High-Resolution NMR*; Batta, G., Kover, K. E., Szantay, C., Eds.; Elsevier Science B.V.: Amsterdam, 1997; pp 303–316.

Subject Index

A

- Analysis of phenolic phytochemicals
 - factors influencing
 - extraction, 12
 - extraction techniques, 13
 - postharvest and storage, 5
 - processing, 16
 - sampling, 4
 - influence of extraction methods, 8*t*
 - influence of postharvest processing and storage, 6*t*
 - influence of secondary processing, 17*t*
 - introduction to phenolics, 3
 - qualitative and quantitative analysis,
 - analytical techniques used, 24
 - chromatographic techniques, 25
 - electrochemical detection (ECD), 25
 - fingerprinting, 26
 - MS and NMR detections, 25
 - techniques used, 20*t*
 - UV irradiation, 23

B

- Bilayer lipid membranes (BLM), 304
- Bioactive compounds, fast analysis, 79
 - chromatographic conditions, 92
 - column temperature, 93
 - elution order of isoflavones, effect of
 - column temperature, 94*f*
 - flow rate and mobile phase linear velocity, 96
 - hypothetical gradient example, 97*t*
 - mobile phase composition, 95
 - separation performed, system pressure profile, 97*f*
 - column characteristics, 86
 - dimensions, 88
 - experimental HEPT (μm) plots of columns, 87*f*
 - operating conditions, 88
 - sub-2 μm particles columns, 87
 - ultra-high performance liquid chromatography (UHPLC), 88
 - columns, design, 92
 - columns packed with partially porous (fused-core) particles, 90
 - conventional HPLC, system pressure using different types of columns, 89*f*

- conventional particles, comparison, 91*f*
- fast LC separations, 81
- fast LC strategies, selection of recent applications, 82*t*
- improve and speed-up LC separations, strategies used, 81*f*
- introduction, 80
- monolithic columns, 91
 - chromatographic characteristic, 92
- Bitter melon, cucurbitane-type triterpenoids
 - additional CTMs reported from
 - Momordica charantia*
 - fruits, 71
 - leaves, 72
 - stems, 73
 - ^{13}C NMR of compounds A-K^a isolated, 61*t*
 - ^{13}C NMR of nonglycosylated compounds L-U^a isolated, 64*t*
 - identification of CTMs, 57
 - pressurized extractions, 53
 - purification techniques
 - flash chromatography, 56
 - open column chromatography, 54
 - preparative HPLC, 55
 - reported CTMs, 66
 - solvent extractions, 52
 - sterols from *Momordica charantia*, 73
 - structures of selected CTM aglycones, 60*f*
 - structures of triterpenoid glucosides, 58*f*
 - various triterpenoids reported, 66*t*
- BLM. *See* Bilayer lipid membranes (BLM)

C

- Characterization of bioactive natural compounds
 - application of HPLC-SPE-NMR, 217
 - brief description on analytic results by HPLC -SPE-NMR
 - compound classification, 235*t*
 - Crinum asiaticum* var. *sinicum*, 233
 - HPLC chromatogram of CPC fraction VI, 232*f*
 - HPLC method development, 235
 - Machilus philippinensis*, 227
 - Neolitsea sericea* var. *aurata*, 234
 - NMR, 236

- on-line ^1H NMR spectra of compounds, 233*f*
- Phyllanthus myrtifolius*, 229
- Phyllanthus reticulatus*, 227
- Phyllanthus urinaria*, 230
- SPE, 236
- structures of compounds, 228*f*, 230*f*, 231*f*, 232*f*, 234*f*
- Syagrus romanzoffiana*, 231
- photo of HPLC-SPE-NMR, 219*f*
- procedure
 - analysis of chemical constituents, LC-MS parameters, 226*t*
 - analyze selected fractions of seven plants, HPLC conditions, 222*t*
 - fractions and methods of pretreatment, 221*t*
 - HPLC method development, 223
 - LC-MS, 227
 - materials and reagents, 220
 - measuring NMR spectra of HPLC-separated compounds, 225*t*
 - nuclear magnetic resonance (NMR), 227
 - solid phase extraction (SPE), 223
 - trapping of HPLC peaks, 224*t*
- Characterization of pomegranate's health benefiting bioactive compounds, 201
 - 29 pomegranate accessions, 203*f*
 - correlation matrix between antioxidant activities, 204*t*
 - data obtained from homogenates, correlation matrix (Pearson test), 205*t*
 - effect of habitat on health-promoting compounds, 207
 - elucidation of bioactive compounds, 206
 - fruit quality during prolonged periods in storage conditions, 212
 - fruits of 11 pomegranate accessions, 208*f*
 - parameters affecting pomegranate color, 211
 - parameters affecting pomegranate taste, 208
 - data obtained from peels and aril juices, Spearman test, 210*t*
 - titratable acidity (TA), 208
 - total soluble solids (TSS), 208
 - taste of aril juices, 209
- Characterization of *Sambucus nigra* L. infusions, 165
 - capillary electrophoresis method, 168, 175
 - parameters of calibration curves, 178*t*
 - UV detection, 183
- chemicals, 167
- comparison of quantitative results, 175
- conditions of liquid chromatography/tandem mass spectrometric detection, 169*t*
- correlation of concentrations of polyphenolic compounds, 185*f*
- liquid chromatographic and capillary electrophoretic methods, comparison, 184
- liquid chromatography-tandem mass spectrometry method, 168, 173
 - calibration data, 183
 - parameters of calibration curves, 176*t*
- polyphenolic profile, 184
- results of quantitative analysis, 180*t*
- sample preparation, 167
- separation of elderflower infusion, 172*f*
- series analysis, 183
- statistical evaluation of data, 173
- tandem mass spectra and fragmentation, 174*f*
- Chromatography combined with bioassays and other hyphenations, 101
 - bioassay detection, protocol improvement, 108
 - biochemical assays for effect-directed detections, 115
 - challenges for hyphenation less critical for HPTLC-EDA, 105
 - drawbacks for hyphenation of bioassays with HPLC, 103
 - effect-directed analysis (EDA), 102
 - effect-directed analysis, HPTLC hyphenations, 106*f*
 - HPTLC-EDA, direct link to effective compound, 112
 - algae assays, 114
 - bacterial detection of antibiotic compounds, 114
 - bioactive Salvia sample, 115*f*
 - effect-directed detections, biological assays, 113
 - fungi assays, 114
 - TLC/HPTLC-EDA and some examples, categorization, 113*f*
 - visualization via tetrazolium, 114
 - identification and structure elucidation, hyphenations, 105
 - Alivbriofischeri* bioassay, 109
 - elution and desorption based HPTLC-MS approaches, 107*f*
 - FLD/UV/Vis inspection, 110*f*
 - HPTLC plate with two different propolis samples, 110*f*
 - HPTLC-EDA, performance, 109

HPTLC-ESI-MS of unknown bioactive *Salvia* sample zone, 111*f*
streamlined analytical approach, 106
microchemical effect-directed detections, 116
planar yeast estrogen screen (pYES), substantial improvement, 108*f*
sharply-bounded zones and optimal detectabilities, 108
Chromatography directly combined with bioassays, 102

F

Flavonoid C-glycosides in *Citrus* juices from Southern Italy
in-depth investigation, 191
results and discussion
antioxidant activity studies, 195
C-glycosyl flavonoids in *Citrus* juices, 190
Citrus species investigated, 192*t*
flavone-C-glycosides found in juice of *Citrus* spp. investigated, 193*f*, 194*t*
fractions collected from tangelo juice by preparative RP-HPLC, 196*f*
glycosidic linkage, 191
radical scavenging and reducing activity, 197*f*
structural elucidation, 191

H

Health-promoting compounds
quantification
determination of concentrations, structures of compounds used, 295*t*
extraction efficiency of curcuminoids, 293*f*
metabolomics analysis, challenges, 291
qNMR and metabolomics, 291
quantitation of health-promoting compounds in food, 295
¹H NMR signal enhancement, 297*f*
phytochemical loaded PLGA nanoparticles, 298*f*
purity of phytochemical-loaded nanoparticles, quantitative measurement, 297
quantitation of curcumin in turmeric samples, 296
reference and calibration standards, 294
sample preparation, 294

selection of samples, storage, and processing, 292
structure of L-citrulline and its proton NMR spectrum, 290*f*
HHP. *See* High hydrostatic pressure (HHP)
High hydrostatic pressure (HHP), 16, 23
Honey bee products, extraction and chromatographic analysis. *See* Propolis polyphenols
analysis of polyphenols in raw propolis samples, 45
fragmentation pathways
caffeic acid benzyl and cinnamyl esters, 37*f*
caffeic acid phenylethyl and prenyl esters, 37*f*
p-coumaric acid benzyl, cinnamyl and prenyl esters, 38*f*
fragmentation pathways of propolis flavonoids
negative ion mode, 41*f*
positive ion mode, 41*f*
main classes of volatile compounds in Italian samples, 47*f*
polyphenolic compounds extracted from raw propolis *versus* solvent composition, 44*f*
polyphenols extraction methods, 43
central composite design (CCD), 43
propolis polyphenols
propolis volatile compounds, HS-SPME-GC-MS analysis, 45
representative total ion current (TIC) chromatogram, 46*f*
structures of flavanones and dihydroflavonols, 40*t*
structures of flavones and flavonols, 39*t*
HPLC in flow with bioassay detection, intrinsic drawbacks, 104

I

Identification of volatile flavor compounds in citrus fruits, 243
citrus volatile oil, health benefits, 251
comparison of HS-SPME conditions and fibers used, 248*t*
factors affecting SPME extraction
adjusting pH, 247
agitation, 247
extraction temperature, 247
extraction time, 247
fiber polarity, 246
fiber thickness, 246

- salt addition, 247
- sample volume, 247
- headspace analysis, 244
- headspace solid-phase microextraction, 245
- list of commercially available HS-SPME fibers, 246*t*

L

- Lycopodiales species, metabolic fingerprinting, 355
- hotelling T² statistics, 359*f*
- line plot of normalized dataset, 357*f*
- methodology
 - chromatographic condition, 355
 - principal component analysis (PCA), 355
 - sample preparation, 355
- PCA score plot and loadings analysis, 358*f*
- Peninsular Malaysia, lycopodiales species, 356*t*

M

- MAE. *See* Microwave-assisted extraction (MAE)
- Meat freshness, 303
 - antiradical effect of grape extracts, 315
 - conceptual model of lipid peroxidation, 306*f*
 - current profiles of pBLM composed, 307*f*
 - effect of epicatechin on PON-induced changes, 314*f*
 - effect on DNA damage, 316
 - formation of ONOO⁻ anion, 305*f*
 - interaction between tBLM and peroxynitrite, 308*f*
 - lipid and meat myoglobin oxidations, coupling, 311
 - meat color cycle, 310*f*
 - nitrating effect of PON, 315
 - nitration of Tyr and Trp residues, 315
 - O₂^{•-} dismutation, 310
 - oxidative degradation, 311
 - oxidative processes in muscle tissue, 309
 - oxidative reactions, 311
 - pBLM method, 308
 - peroxynitrite detection
 - develop electrochemical PON sensors, challenges, 323

- electrocatalytic activity for PON oxidation, 322
- electrochemical quantification, 317
- electro-polymerized hemin thin films, 322
- hemin-functionalized reduced graphene oxide, 322
- Mn(III) tetraamino-phthalocyanine (MnTAPC), 318
- ONOO⁻ sensitive electrochemical methods, 319*t*
- polyethylenedioxythiophene (PEDOT), 322
- preparation methods, 316
- square wave voltammograms (SWV) recorded, 324*f*
- synthetic manganese complexes, 318
- peroxynitrite interaction with lipid membranes, 306
- peroxynitrite's formation and fate in vivo, 304
- phenolic compounds from grapes and wine, 313*f*
- PON scavenging activity of polyphenols, 313
- PON-tyrosine interaction, antioxidant effect of polyphenols, 314
- scavengers of peroxynitrite caused injury, 312
- Melia azedarach* extracts, Biofunctional properties
 - agricultural uses/controlling pest organisms and pathogens, 156
 - antibacterial activity and inhibition, 154
 - antimalarial activity, 154
 - crude extracts, 154
 - general extraction methods and chemical composition analysis, 159
 - medicinal uses/controlling diseases, 152
 - medicinal uses/controlling insects vectors of diseases and animal parasites, 155
 - methanolic leaf extract, 153
 - physiological functions of cells, 154
 - some of most active compounds isolated, 158*t*
 - synthesis of nanoparticles (NPs), 153
- Microwave-assisted extraction (MAE), 13

N

- New approaches in metabolic fingerprinting, 361

areas of metabolomics needing further developments, 365
automatic reduction of NMR spectra to essential data (ARNSED), 369
principle, 370*f*
extracts from medicinal plant *Baccharis trimera*, 368*f*
extracts of black tea (*Camellia sinensis*), 369*f*
metabolomics, 362
procedures used in metabolomics
data pretreatment, 363
experimental design, 363
interpretation of factors, 364
measurement of spectra and/or chromatograms, 363
multivariate analysis, 364
proposing questions to be answered and objectives of study, 363
sampling of material to be analyzed, 363
two-phase extraction, 366
visualization of small region of spectrum from cashew nut shell liquid, 371*f*

P

PEF. *See* Pulsed electric field (PEF)
PLE. *See* Pressurized liquid extraction (PLE)
Pressurized liquid extraction (PLE), 14
Propolis polyphenols
conventional fully-porous stationary phase, 34
representative HPLC-UV/DAD chromatogram, 35*f*
structures of phenolic acids and derivatives, 36*t*
fused-core stationary phase, 42
Pulsed electric field (PEF), 23
Purity assessment of small molecules in drug discovery, 125
Atlantis dC18 column, 133
chromatographic methods, 129
comparison of peak capacity *versus* gradient time, 132*f*
comparison of UV and MS response for standard gradient, 132*f*
gradient time, 129
physico-chemical properties of columns used, 131*t*
common approaches, 127
comparative study on Gemini NX C18 and Atlantis dC18 columns, 135*f*, 135*t*

comparison of gradients on Atlantis dC18 column, 136*f*
error estimation, 145
estimation of error or confidence interval
function of specific RS %, 145*t*
function of total RS %, 145*t*
Gemini-NX phase, 133
global validation, 143
instrumentation, 128
Kinetex core-shell column, 133
peak capacity comparison, 134*f*
peak capacity comparison of Gemini NX C18 and XBridge C18, 137*f*
quality control of bioactive compounds from natural sources, 146
reagents and columns, 129
results of TRS at low and high pH, 144*t*
XTerra MS C18 column, 133

Q

Quality control of bioactive compounds from natural sources, 146

R

Rat cecal contents, measurement of resistant starches, 333
analysis of dietary fiber (DF), 335
cross-validation plot for starch content, 343*f*
FTIR-PAS, 340
analysis, 338
spectra, 342*f*
infrared spectra and chemometric analysis, 343
near infrared reflectance spectroscopy (NIRS), 335
photoacoustic process, 338*f*
photoacoustic spectroscopy (PAS), 336
PLS and PCA, 341
principal components in PCA model, 344*f*
rapidly digestible starch (RDS), 334
rat cecal samples, 340
rat diet and treatment, 339
resistant starch (RS), 333
slowly digestible starch (SDS), 334
spectroscopic methods, 335
starch content, enzymatic assay, 342
starch content, reference assay, 340

S

SFE. *See* Supercritical fluid extraction (SFE)
Supercritical fluid extraction (SFE), 15

U

UAE. *See* Ultrasonic-assisted extraction (UAE)
UHPLC. *See* Ultra-high performance liquid chromatography (UHPLC)
Ultra-high performance liquid chromatography (UHPLC), 86
Ultrasonic-assisted extraction (UAE), 14
Unraveling food aroma analysis
 factors, 272
 strategies, 272
analytical approaches, 273*f*
chemometric approach, 274
extracted ion chromatogram (EIC) of ions, 284*f*
extraction by static headspace technique
 mayonnaise, 276*f*
 potato chips, 277*f*
extraction methods, 275
GC-O and GC-MS analyses, 281
identification and quantitation methods, 278
macroconstituents of food, 274
main aroma fractions of fried tempeh, 282*t*
odoriferous fractions, flavor dilution
 factors vs peak numbers, 279*f*
quantitation of aroma compounds, 281
separation methods, 277
single reaction monitoring, 285*f*
stable isotope dilution analysis (SIDA), 281
total ion current (TIC) of GCxGC chromatogram, 280*f*
volatile compounds fingerprinting/profiling, 274
Useful tools for qualitative and quantitative analysis of phytosterols and their esters
analysis of steryl/stanyl fatty acid esters, on-line LC-GC-based approach, 262
enriched dairy foods and important natural sources
 cheese-based spread, analysis of stanyl fatty acid esters, 266*t*
 distributions of steryl/stanyl fatty and phenolic acid esters in cereals, 265*f*

 edible plant oils and nuts, free sterols/stanols, 267
 fat-based enriched dairy foods, stanyl fatty acid esters, 266
 free sterols/stanols and steryl esters, mean total contents, 268*f*
 free sterols/stanols and steryl/stanyl esters in cereal grains, 265
 on-line LC-GC analysis of free fatty acids, 267*f*
fractionation of plant lipids, SPE-based approach, 262
free sterol and steryl esters, representative structures, 258*f*
gas chromatography-flame ionization detection (GC-FID), 260
gas chromatography-mass spectrometry (GC-MS), 260
GC analysis, 263*f*
intact steryl/stanyl fatty acid esters, GC analysis, 261
materials and chemicals, 259
on-line LC-GC system with programmable temperature interface, 264*f*
on-line liquid chromatography-gas chromatography (On-line LC-GC), 260
plant stanyl fatty acid ester mixture, GC analysis, 261*f*
sample preparation
 cereal grains, 259
 edible plant oils and nuts, 259
 enriched dairy foods, 259
separation of free sterols/stanols and steryl/stanyl esters, 262*f*
solid-phase extraction (SPE), 260
stanyl fatty acid ester mixture extracted, on-line LC-GC analysis, 264*f*

V

Variability in methods and procedures for purity assessment in drug discovery, 137
optimization of analytical method
 analysis of different fractions of inhomogeneous sample, 143*f*
 importance of 8 min gradient for TRS, 141*f*
 integration parameters, 140, 141*t*
 other considerations, 142
 percentages of TRS at low and high pH, 139*t*

sample preparation, influence of
acetonitrile percentage, 142*t*
selection of UV Wavelength, 138
solvent and sample concentration, 141
standard open access analysis, 141

TRS analysis, 142
UV spectrum and λ_{max} chosen for
compounds at low and high pH,
140*f*